Geology of the Blue Mountains Region of Oregon, Idaho, and Washington:

Stratigraphy, Physiography, and Mineral Resources of the Blue Mountains Region

U.S. GEOLOGICAL SURVEY PROFESSIONAL PAPER 1439

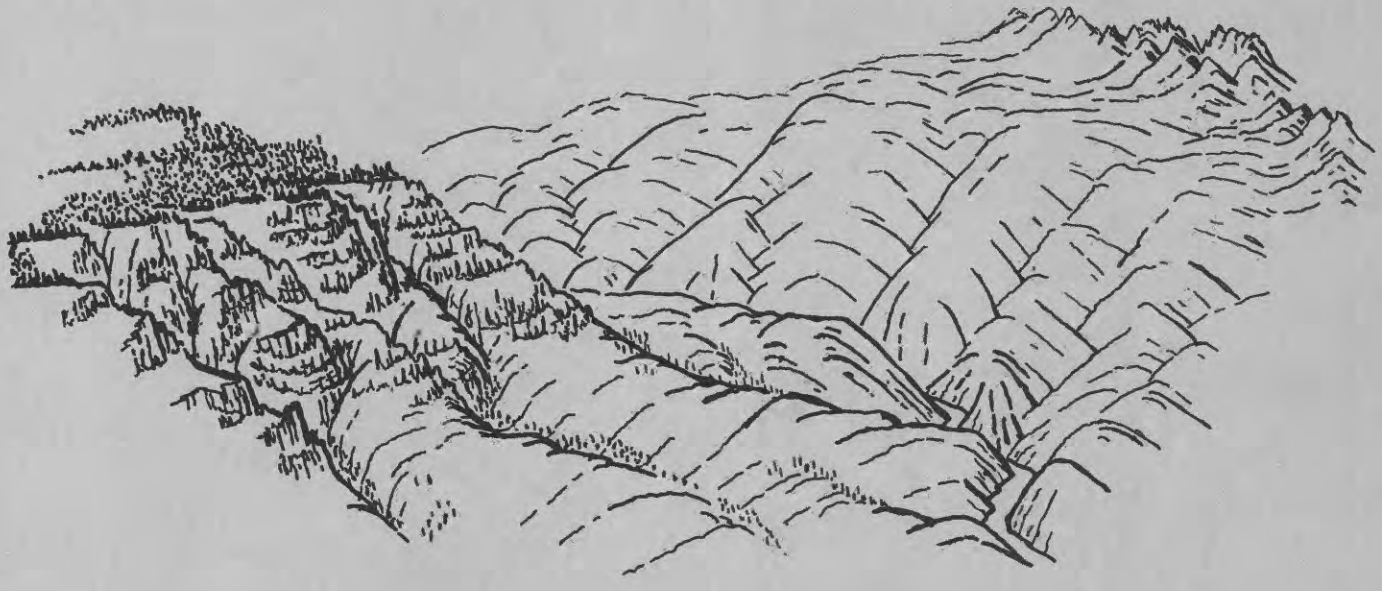

AVAILABILITY OF BOOKS AND MAPS OF THE U.S. GEOLOGICAL SURVEY

Instructions on ordering publications of the U.S. Geological Survey, along with prices of the last offerings, are given in the current-year issues of the monthly catalog "New Publications of the U.S. Geological Survey." Prices of available U.S. Geological Survey publications released prior to the current year are listed in the most recent annual "Price and Availability List." Publications that are listed in various U.S. Geological Survey catalogs (**see back inside cover**) but not listed in the most recent annual "Price and Availability List" are no longer available.

Reports released through the NTIS may be obtained by writing to the National Technical Information Service, U.S. Department of Commerce, Springfield, VA 22161; please include NTIS report number with inquiry.

Order U.S. Geological Survey publications **by mail** or **over the counter** from the offices given below.

BY MAIL

Books

Professional Papers, Bulletins, Water-Supply Papers, Techniques of Water-Resources Investigations, Circulars, publications of general interest (such as leaflets, pamphlets, booklets), single copies of Earthquakes & Volcanoes, Preliminary Determination of Epicenters, and some miscellaneous reports, including some of the foregoing series that have gone out of print at the Superintendent of Documents, are obtainable by mail from

U.S. Geological Survey, Map Distribution
Box 25286, MS 306, Federal Center
Denver, CO 80225

Subscriptions to periodicals (Earthquakes & Volcanoes and Preliminary Determination of Epicenters) can be obtained ONLY from the

Superintendent of Documents
Government Printing Office
Washington, DC 20402

(Check or money order must be payable to Superintendent of Documents.)

Maps

For maps, address mail orders to

U.S. Geological Survey, Map Distribution
Box 25286, Bldg. 810, Federal Center
Denver, CO 80225

Residents of Alaska may order maps from

U.S. Geological Survey, Earth Science Information Center
101 Twelfth Ave., Box 12
Fairbanks, AK 99701

OVER THE COUNTER

Books and Maps

Books and maps of the U.S. Geological Survey are available over the counter at the following U.S. Geological Survey offices, all of which are authorized agents of the Superintendent of Documents.

- **ANCHORAGE, Alaska**—4230 University Dr., Rm. 101
- **LAKEWOOD, Colorado**—Federal Center, Bldg. 810
- **MENLO PARK, California**—Bldg. 3, Rm. 3128, 345 Middlefield Rd.
- **RESTON, Virginia**—National Center, Rm. 1C402, 12201 Sunrise Valley Dr.
- **SALT LAKE CITY, Utah**—Federal Bldg., Rm. 8105, 125 South State St.
- **SPOKANE, Washington**—U.S. Post Office Bldg., Rm. 135, W. 904 Riverside Ave.
- **WASHINGTON, D.C.**—Main Interior Bldg., Rm. 2650, 18th and C Sts., NW.

Maps Only

Maps may be purchased over the counter at the U.S. Geological Survey offices:

- **FAIRBANKS, Alaska**—New Federal Building, 101 Twelfth Ave.
- **ROLLA, Missouri**—1400 Independence Rd.
- **STENNIS SPACE CENTER, Mississippi**—Bldg. 3101

Geology of the Blue Mountains Region of Oregon, Idaho, and Washington:

Stratigraphy, Physiography, and Mineral Resources of the Blue Mountains Region

TRACY L. VALLIER *and* HOWARD C. BROOKS, *editors*

U.S. GEOLOGICAL SURVEY PROFESSIONAL PAPER 1439

UNITED STATES GOVERNMENT PRINTING OFFICE, WASHINGTON : 1994

DEPARTMENT OF THE INTERIOR

BRUCE BABBITT, *Secretary*

U.S. GEOLOGICAL SURVEY

Robert M. Hirsch, *Acting Director*

Library of Congress Cataloging-in-Publication Data

Stratigraphy, phsiography, and mineral resources of the Blue Mountains region / Tracy L. Vallier and Howard C. Brooks, editors.

p. cm.—(Geology of the Blue Mountains region of Oregon, Idaho, and Washington) (U.S. Geological Survey professional paper ; 1439)

Includes bibliographical references.

Supt. of Docs. no.: I 19.16:1439

1. Geology—Blue Mountains Region (Or. and Wash.) 2. Geology—Idaho. 3. Geology, Stratigraphic. 4. Island arcs—Pacific, Northwest. I. Vallier, T.L. (Tracy L.) II. Brooks, Howard C. III. Series. IV. Series: U.S. Geological Survey professional paper ; 1439.

QE156.B57S77 1992

557.95'7—dc20 93-19340

CIP

For sale by the Book and Open-File Report Sales, U.S. Geological Survey,
Federal Center, Box 25286, Denver, CO 80225

PREFACE

U.S. Geological Survey Professional Paper 1439 is one volume of a five-volume series on the geology, paleontology, and mineral resources of the Blue Mountains region in eastern Oregon, western Idaho, and southeastern Washington. This professional paper deals specifically with stratigraphy, physiography, and mineral resources. Other professional papers in the series are professional paper 1435 on paleontology and biostratigraphy, professional paper 1436 on the Idaho Batholith and its border zone, professional paper 1437 on Cenozoic geology, and professional paper 1438 on petrology and tectonics. The purpose of these volumes is to familiarize readers with work that has been completed in the Blue Mountains region and to emphasize the region's importance for understanding island-arc processes and the accretion of an allochthonous terrane to a continent. These professional papers provide current interpretations of a complex island-arc terrane that was accreted to ancient North America in the late Mesozoic Era, of a large batholith that was intruded after accretion, and of overlying Cenozoic volcanic rocks that were subsequently uplifted and partly stripped off the older rocks by erosion.

Modern island arcs are not well understood, and even less so are ancient arcs that have been deformed, metamorphosed, and subsequently accreted to continents. We have learned that characteristics of modern arcs change significantly both along and across the arcs' axes and that studies of arc fragments are less than satisfactory because they generally do not characterize an entire arc. For example, the landward trench slopes of arcs can differ greatly, depending on whether materials from the descending slab are being accreted or the slope is being tectonically eroded; which process dominates apparently is related to the volume of sediment in the adjacent trench and the vector of plate convergence. In addition, some arcs (Aleutian) have broad, long, and sediment-filled forearc basins, whereas in others (Tonga-Kermadec) the forearc insular slopes descend precipitously to trench depths and are only interrupted in places by narrow fault-bounded terraces. Moreover, some arcs have erupted primarily tholeiitic igneous products throughout their histories (Tonga-Kermadec) and others (Aleutian) have a long history of both calc-alkaline and tholeiitic eruptive activity. Ridge axes of island arcs may be narrow or broad, and in some arcs (Solomons and Vanuatu), the axial regions have extended to form deep bathymetric and sedimentary basins. Even back-arc basins have different origins and histories of development. Some (Mariana Trough and Lau Basin) have active spreading ridges whereas others (Aleutian basin) are floored by ancient oceanic crust that was trapped behind the arc.

Because our knowledge of the diverse processes within modern arcs is limited, it becomes even more important to study ancient analogs. By the very nature of their on-land exposures, ancient arcs can provide insights into sedimentary facies, magmatic evolution, and deep crustal processes that can only be studied in modern arcs by geophysical methods, dredging, and drilling. Few ancient island arcs have exposures as well developed and as extensive as those in the Blue Mountains province. Particularly spectacular and helpful are outcrops provided by intensive stream erosion, which has left some canyon walls more than 2 km deep (Snake River canyon west of the Seven Devils Mountains).

Most earth scientists who have worked in the Blue Mountains region agree that pre-Tertiary rocks there form one or more allochthonous terranes. The importance of such terranes in the evolution of circum-Pacific continental margins has been recognized for more than a decade, but many complex questions remain. For example, how, when, and where did most of the circum-Pacific allochthonous terranes form? How did they accrete to continents? What are the mechanisms of amalgamation processes during terrane formation and transport? And, perhaps most importantly, what are the effects of these processes on mineral and hydrocarbon resources? While these volumes provide some answers, the data and interpretations contained in them will no doubt raise new and equally intriguing questions for future generations of earth scientists.

CONTENTS

[Numbers indicate chapters]

1. SEDIMENTOLOGY AND STRATIGRAPHY OF THE MARTIN BRIDGE LIMESTONE AND HURWAL FORMATION (UPPER TRIASSIC TO LOWER JURASSIC) FROM THE WALLOWA TERRANE, OREGON

By MICHAEL F. FOLLO[1]

CONTENTS

ABSTRACT

Stratigraphic and sedimentological analysis of sedimentary sequences from the Wallowa terrane of northeastern Oregon has provided a unique insight into the paleogeography and depositional history of the terrane, as well as establishing important constraints on its tectonic evolution and accretionary history. Its Late Triassic history is considered here by examining the two most important sedimentary units in the Wallowa terrane—the Martin Bridge Limestone and the Hurwal Formation.

Conformably overlying epiclastic volcanic rocks of the Seven Devils Group, the Martin Bridge Limestone comprises shallow-water platform carbonate rocks and deeper water, off-platform slope and basin facies. Regional stratigraphic and tectonic relations suggest that the Martin Bridge was deposited in a narrow, carbonate-dominated (forearc?) basin during a lull in volcanic activity. The northern Wallowa platform was a narrow, rimmed shelf delineated by carbonate sand shoals. Interior parts of the shelf were characterized by supratidal to shallow subtidal carbonates and evaporites, which were deposited in a restricted basin. In the southern Wallowa Mountains, lithofacies of the Martin Bridge are primarily carbonate turbidites and debris flow deposits, which accumulated on a carbonate slope apron adjacent to the northern Wallowa rimmed shelf from which they were derived.

Drowning of the platform in the latest Triassic, coupled with a renewed influx of volcanically derived sediments, resulted in the progradation of fine-grained turbidites of the Hurwal Formation over the carbonate platform. Within the Hurwal, Norian conglomerates of the Excelsior Gulch unit contain exotic clasts of radiolarian chert, which were probably derived from the Baker terrane. Such a provenance provides evidence of a tectonic link between the Baker and Wallowa terranes as early as the Late Triassic, and offers support for the theory that both terranes were part of a more extensive and complex Blue Mountains island-arc terrane.

INTRODUCTION

The Wallowa terrane of northeastern Oregon and western Idaho consists of a thick sequence of Permian to Triassic volcanic-arc rocks and their overlying cover of Upper Triassic and Jurassic marine sedimentary rocks. Rocks of the terrane crop out as a series of erosional inliers within the regional cover of the Miocene Columbia River Basalt Group (see fig. 1.3). The best exposures are found in the Snake River canyon along the Oregon-Idaho border, and to the west in the Wallowa Mountains, from which the terrane draws its name.

On the basis of similar stratigraphy, faunal assemblages, and paleomagnetism, the Wallowa terrane

[1]Department of Geology, University of North Carolina, Chapel Hill, NC 27599-3315

Manuscript approved for publication February 26, 1993.

has been correlated with other displaced terranes in the Cordillera—most significantly the Wrangellia terrane, which crops out on Vancouver Island, the Queen Charlotte Islands, and in the Wrangell Mountains of Alaska (Jones and others, 1977; Silberling and Jones, 1984). More recent paleontological data from both the Wallowa and Wrangellia terranes has proved to be somewhat equivocal regarding both their relation to one another and their original paleolatitudes (Newton, 1983, 1986, 1987; Silberling, 1986; and Stanley, 1986). Some workers have challenged the correlation of the Wallowa terrane with the Wrangellia terrane on the basis of differences between the faunas (Whalen and Stanley, 1985) and the volcanic rock units of the two terranes (Sarewitz, 1983).

The Upper Triassic and Jurassic sedimentary sequences of the Wallowa terrane were studied to better understand the paleogeography and depositional history of this "suspect" terrane (Follo, 1986). These sedimentary rocks also establish important constraints on the tectonic evolution and accretionary history of the Wallowa terrane, and they provide another basis for terrane comparison. This report summarizes some results from that research.

The Wallowa Mountains and adjoining areas, as well as significant geographic localities and features referred to in the text are shown in figure 1.1. All directional references in this report correspond to present geographic coordinates. Paleomagnetic studies (Simpson and Cox, 1977; Wilson and Cox, 1980; Hillhouse and others, 1982) indicate that the Wallowa terrane (together with the rest of the Blue Mountains) has undergone a clockwise rotation of approximately 65° relative to the stable craton since the latest Jurassic. A comparable amount of counterclockwise rotation would be required to restore all Martin Bridge and Hurwal paleogeographic directions to their proper (pre-rotational) orientation.

ACKNOWLEDGMENTS

This research was part of a doctoral dissertation completed at Harvard University under the direction of Professor Raymond Siever. Financial support for the dissertation research was provided by the National Science Foundation (Grant EAR 83-13262), the Geological Society of America, and the Department of Geological Sciences, Harvard University. Continued research on Martin Bridge platform lithofacies from the northern Wallowa Mountains has been supported by the University Research Council of the University of North Carolina. This manuscript benefited from careful reviews by Tracy Vallier, Howard Brooks, Catherine Newton, and George Stanley. Their help is greatly appreciated, but responsibility for the conclusions and opinions expressed herein ultimately rest with the author.

GEOLOGY

The Wallowa terrane is made up of approximately 5 km of volcanic and sedimentary rocks ranging in age from Early Permian to Late Jurassic (fig. 1.2). The lower part of the stratigraphic sequence is composed of intermediate and silicic volcanic and volcaniclastic rocks of the Seven Devils Group. These range in age from Early Permian and Middle and Late Triassic (Karnian) in age and are at least partially correlative with the Clover Creek Greenstone and "Lower Sedimentary Series" of Prostka (1962) in the Wallowa Mountains.

Conformably overlying the uppermost volcaniclastic sedimentary rocks is the (Karnian to Norian) Martin Bridge Limestone, which contains platform as well as slope and basin lithofacies. The Martin Bridge interfingers laterally with, and is overlain by, basinal volcanic argillites and minor carbonate rocks and conglomerate of the Hurwal Formation. In the northern part of the Wallowa terrane, the Hurwal records discontinuous sedimentation from the Norian into the Toarcian (Early Jurassic). The youngest pre-Tertiary sedimentary rocks in the Wallowa terrane are found in the Middle and Upper Jurassic (Callovian and Oxfordian) Coon Hollow Formation, which crops out at two isolated localities in Hells Canyon. The Coon Hollow rests with angular unconformity upon rocks of the Seven Devils Group; both the Martin Bridge and the Hurwal are missing at the contact.

The Wallowa terrane was intruded during the Late Jurassic and Early Cretaceous by the Wallowa batholith and its satellites, including the Cornucopia and Sawtooth stocks. These and other contemporaneous intrusions postdate suturing of the Wallowa terrane to other terranes of the Blue Mountains. This sedimentological study resulted in the conclusion that rocks of the Wallowa terrane were in tectonic contact with other terranes in Oregon—in particular, the Baker terrane—at least as early as the Late Triassic.

PREVIOUS WORK

A detailed listing of all previous geologic work in the Wallowa terrane can be found in Follo (1986). Mention is made here only of those investigations that provided the stratigraphic framework for this

study of the sedimentology and depositional history of the entire terrane. Vallier's work (1974, 1977) on the Permian and Triassic Seven Devils Group in Hells Canyon established a workable stratigraphy for the volcanic rocks that make up the lower part of the Wallowa terrane. Nolf (1966) conducted a detailed structural and stratigraphic study of the rocks of the Wallowa terrane exposed in the northern Wallowa Mountains. His unpublished dissertation has proved to be a remarkably accurate and invaluable resource for this report. A regional study of the southern Wallowa Mountains was done by Ross (1938), but it was Prostka's report on the geology of the Sparta 15-minute quadrangle (1962, 1963) that has proved most valuable in providing a basis for understanding the complex structure and stratigraphy of the southern Wallowa terrane.

The geographically restricted scope of the above mentioned studies has contributed to the persistence of a somewhat arbitrary division between the northern and southern Wallowa Mountains. However, this division does correspond to a more fundamental difference in tectonic setting and depositional environments across the Wallowa terrane.

MARTIN BRIDGE LIMESTONE

The Martin Bridge Limestone is the most distinctive and widely distributed sedimentary unit in the Wallowa terrane (fig. 1.3). As such, it has been used by numerous workers as a convenient stratigraphic marker. The Martin Bridge was first studied by J.P. Smith (1912, 1927), who identified much of its Late

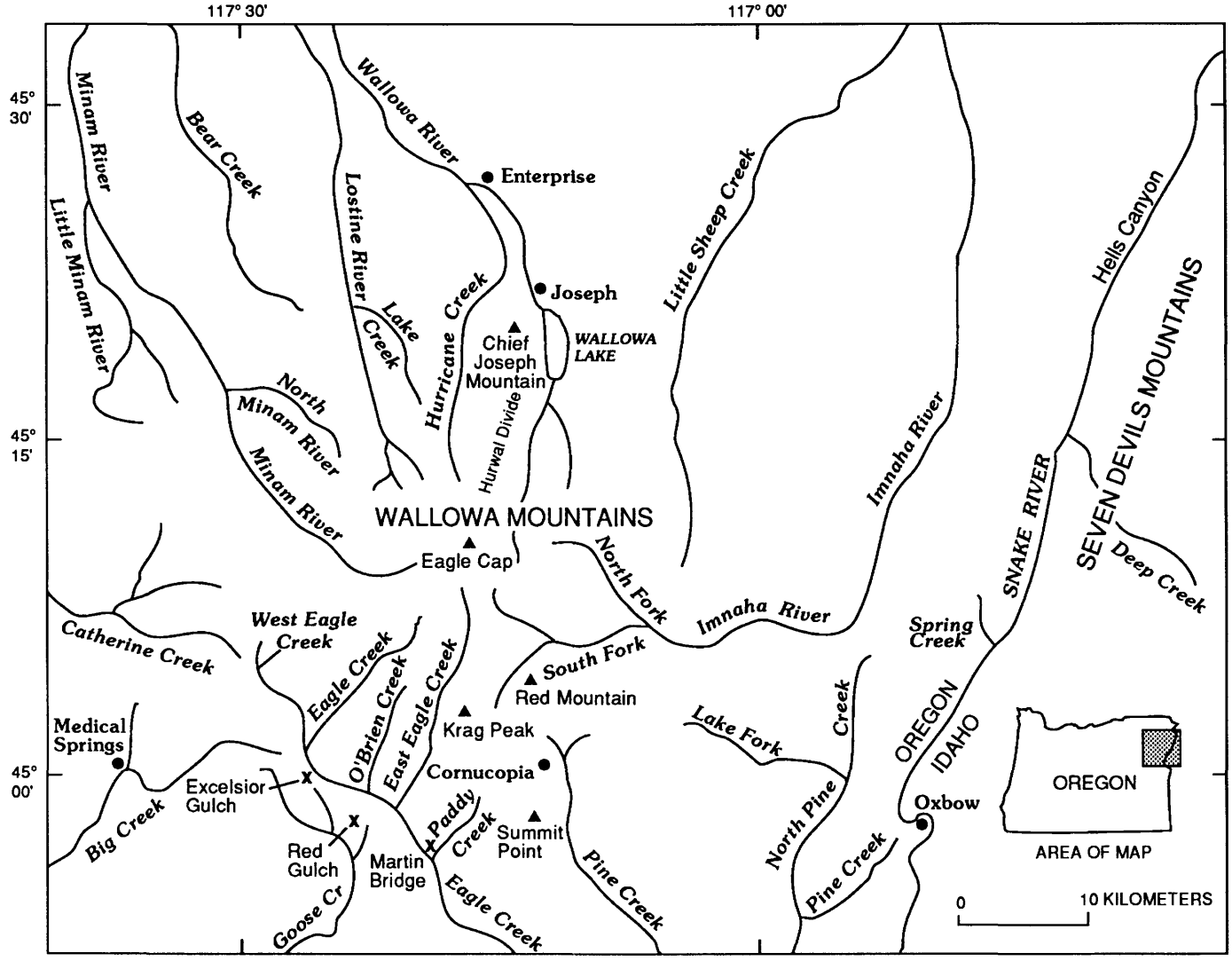

FIGURE 1.1.—Index map of Wallowa Mountains and surrounding area, northeastern Oregon and western Idaho.

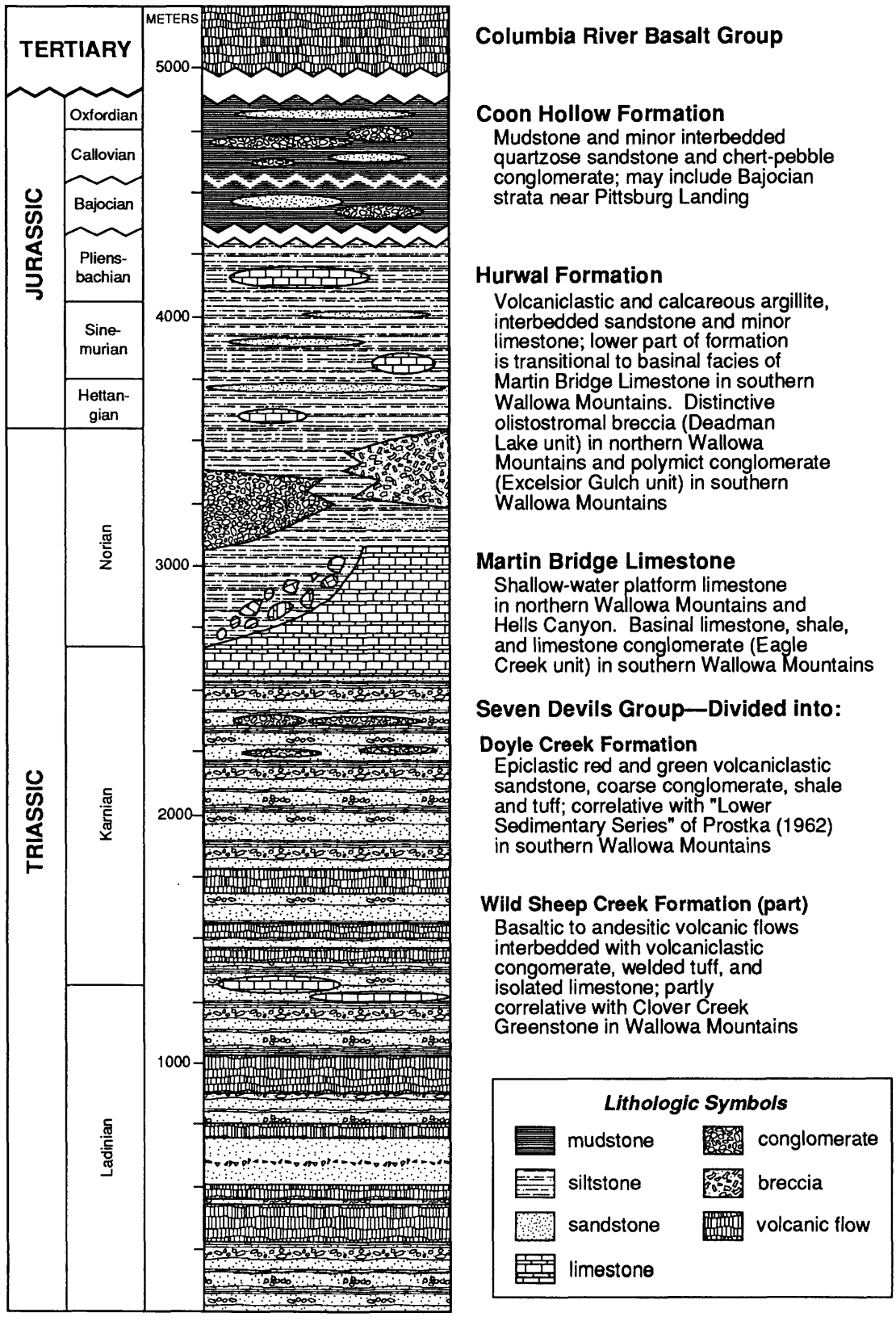

FIGURE 1.2.—Generalized stratigraphic column of Upper Triassic and younger rocks of Wallowa terrane, northeastern Oregon. Wavy lines indicate known unconformities or intervals of missing time.

Triassic fauna and measured a section of massive and bedded limestones and calcareous shales near the confluence of Paddy Creek and Main Eagle Creek in the southern Wallowa Mountains. Ross (1938) named this unit the Martin Bridge Formation, after the bridge that formerly crossed Eagle Creek at the site of Smith's measured section. This unit was later renamed the Martin Bridge Limestone by Hamilton (1963), who was working in the Riggins area of western Idaho.

The exposure and preservation of limestone strata of the Martin Bridge vary considerably across the

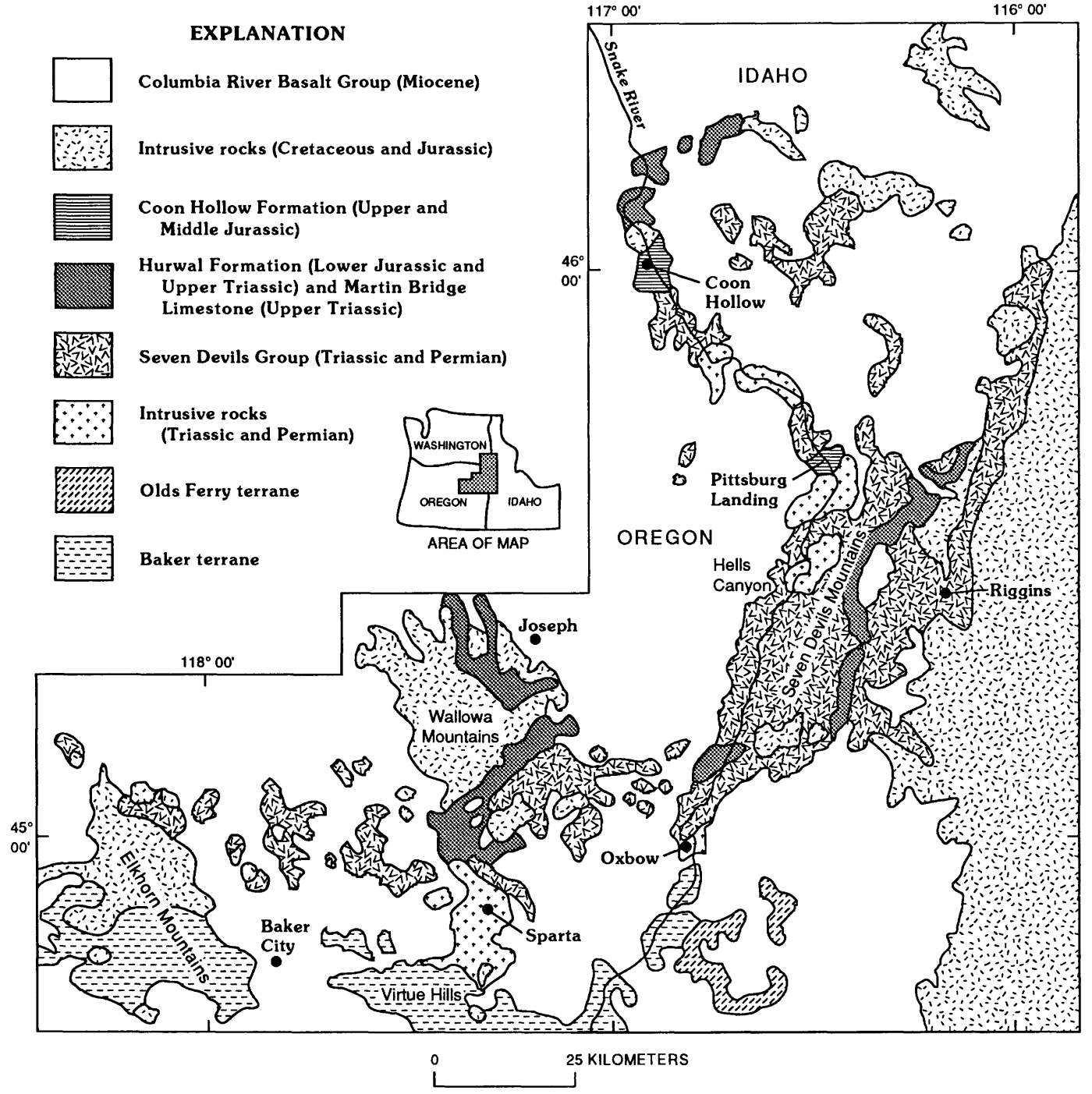

FIGURE 1.3.—Geologic map of Wallowa and adjacent terranes, northeastern Oregon and western Idaho. Modified from Walker, 1977; Bond, 1978; and Weiss and others, 1976.

Wallowa terrane. These differences are a function of the original carbonate lithologies, which record deposition in very different platform and basinal environments, as well as the postdepositional structural and metamorphic history of the unit. In the eastern Seven Devils Mountains near Riggins, Idaho, limestones correlated with the Martin Bridge are penetratively sheared and recrystallized near the suture of the Wallowa terrane with the North American continent (Hamilton, 1963; Lund and others, 1985; Lund, in press). At the mouth of the Grande Ronde River, beds of the Martin Bridge Limestone are also intensely deformed, whereas farther south in the Snake River canyon platform limestones at Kinney Creek are well exposed and only slightly recrystallized. In the northern Wallowa Mountains, exposures are consistently excellent owing to the high relief and lack of vegetation. However, extensive metamorphic recrystallization and ductile flow of the Martin Bridge near the Wallowa batholith has obscured most sedimentary structures and textures. This is in marked contrast to the southern part of the range, where relatively pristine Martin Bridge carbonate rocks are common, but poorly exposed. Here, subdued topography and thick vegetation has developed in an area underlain by less resistant basinal (off-platform) carbonate lithologies.

AGE AND STRATIGRAPHIC RELATIONS

The age of the Martin Bridge Limestone is early Norian (*Mojsisovicsites kerri* Zone). The *M. kerri* Zone is indicated by a bivalve fauna including *Halobia halorica* and *H. dilatata* from calcareous shales at the type locality in the southern Wallowa Mountains (Smith, 1927), and the cephalopod *Tropiceltites columbianus* from limestone beds in the northern Wallowa Mountains (Silberling and Tozer, 1968) and Hells Canyon (Vallier, 1967). Recent work on ammonite and halobiid bivalve faunas from the Martin Bridge on Eagle Creek suggests that these lowermost Martin Bridge strata may actually span the Karnian-Norian boundary (Stanley, 1986). Fossiliferous limestones from Mission Creek, near Lewiston, Idaho, have been correlated with the Martin Bridge, but their late Norian age (Stanley, 1986) and uncertain stratigraphic and structural relations make this correlation somewhat tenuous.

In the Wallowa Mountains, the Martin Bridge Limestone conformably overlies epiclastic sedimentary rocks of the Clover Creek Greenstone and "Lower Sedimentary Series" (Follo, 1986; Laudon, 1956). These volcanic units are in part correlative with the Wild Sheep Creek and Doyle Creek Formations of the Seven Devils Group, which underlies the Martin Bridge Limestone in the Snake River canyon (Vallier, 1977). The contact between the limestones and underlying volcaniclastic rocks is very often a zone of significant structural dislocation, and this dislocation accounts for many previous workers viewing the contact as unconformable. The best exposures of the undisturbed contact are in the Wallowa Mountains on the southwest flank of Chief Joseph Mountain and along the west side of East Eagle Valley south of Krag Peak (Follo, 1986). At both localities, the transition from volcaniclastic to carbonate rocks is gradational vertically over approximately 10 m of section and is characterized by distinctive gray-green calcareous siltstone and sandstone. Locally, lithologies above and below this contact are highly variable, and the transition is possibly diachronous across the Wallowa terrane. However, given the limited biostratigraphic data from both the "Lower Sedimentary Series" (correlative of Doyle Creek Formation) and the Martin Bridge Limestone, this diachronism cannot be conclusively demonstrated.

The onset of regionally extensive carbonate sedimentation appears to have been contingent primarily upon decreased volcaniclastic sediment supply. The epiclastic volcanic rocks of the "Lower Sedimentary Series" represent the lag time between the end of Seven Devils volcanism and the deposition of Martin Bridge Limestone. It was only after the volcanic sediment supply—both primary and eroded—was greatly reduced that conditions were favorable for regionally extensive carbonate deposition. Immediately following any interruption of volcanic activity, the increased supply of epiclastic material continued to inhibit carbonate production for a time, and thereby masked most short-lived periods of volcanic quiescence. However, the presence of carbonates does not necessarily imply an absence of volcanic activity within the arc terrane because local conditions of a basin may strongly influence the erosion, transport, and deposition of clastic sediments. The irregular basal contact of the Martin Bridge supports this observation, as does the presence of isolated limestone units within the underlying Seven Devils Group (Vallier, 1977; Grant, 1980).

Estimates of the total thickness of the Martin Bridge Limestone in the Wallowa terrane vary considerably. Vallier (1977) measured a section 530 m thick at Kinney Creek in Hells Canyon. Although the top of the Martin Bridge is eroded at this locality, Vallier's figure may be somewhat high because numerous small-scale bedding-plane thrusts ramp through the carbonate section and cause some repetition of beds. In the northern Wallowa Mountains, a

continuous section of the Martin Bridge Limestone is exposed on the west side of Hurricane Creek canyon. Here, approximately 350 m of section can be measured between the basal contact with the underlying volcanic rocks and the upper gradational contact with the Hurwal Formation. Anomalously thick sections of the Martin Bridge Limestone, such as the 1,150-m-thick section along Snow Creek in East Eagle valley, are typically the result of isoclinal folding and pervasive ductile flow of the recrystallized limestones.

Measuring the thickness of the Martin Bridge Limestone in the southern Wallowa Mountains is even more difficult owing to its structural complications, limited exposures, and ambiguous facies relations with the Hurwal Formation. Prostka (1962) and Carnahan (1962) estimated thicknesses of 450 to 600 m, but these estimates were based on aerial photos and correlations with sections in the northern Wallowa Mountains and are undoubtedly high. Based on measurements and observations from throughout the southern Wallowa Mountains (Follo, 1986), the thickness of the Martin Bridge slope and basin facies is estimated to be approximately 250 to 300 m, no more than 200 m of which is actually limestone. This contrasts with the most reliable estimate of 350 to 450 m for the thickness of the platform limestones of the Martin Bridge in the northern Wallowa Mountains and Hells Canyon.

LITHOFACIES

Carbonate facies of the Martin Bridge Limestone in the Wallowa Mountains and the Snake River canyon are products of the diverse depositional processes that characterize carbonate-platform and basin environments (Follo and Siever, 1985; Follo, 1986; Newton, 1986; Read, 1985; Stanley, 1986; Whalen, 1985). Intense structural deformation of the Wallowa terrane in the Late Jurassic that disrupted the Martin Bridge carbonate platform makes any regional paleogeographic reconstruction extremely difficult. It is impossible to observe a continuous transition from platform to basin facies, and there is very little lateral facies control along the platform margin. Although transitional facies such as platform-margin shoals or fringing reefs are poorly preserved or missing altogether, it is possible to reconstruct (or at least infer) the nature of the original platform margin by studying both the platform lithologies in the northern Wallowa Mountains and the depositionally displaced slope and basin facies in the southern Wallowa Mountains. Sedimentological data regarding depositional processes and environments for individual Martin Bridge lithofacies are summarized and compared in table 1.1.

NORTHERN WALLOWA MOUNTAINS

Many of the carbonate outcrops in the high country of the northern Wallowa Mountains are thoroughly recrystallized marbles, which have been intensely deformed and metamorphosed. In less deformed sections of the Martin Bridge Limestone, Nolf (1966) identified three informal stratigraphic units: the Hurricane Creek, BC Creek, and Scotch Creek units. These unit names are used herein to distinguish Martin Bridge carbonate lithofacies in the northern Wallowa Mountains (table 1.1). However, the interpretations presented here regarding original stratigraphic relations and depositional environments are different from those of Nolf. Formal designation of these and other stratigraphic units from the Wallowa terrane is outside the scope of this report, but it will be undertaken elsewhere (Follo, unpub. data).

Hurricane Creek Unit

The Hurricane Creek unit consists of approximately 150 to 175 m of white to light gray limestone directly overlying volcaniclastic rocks (Clover Creek Greenstone) lithologically equivalent to the Seven Devils Group. The limestone grades upward into deeper water carbonate rocks of the Scotch Creek unit. Limestones of the Hurricane Creek unit are extremely pure—they contain little or no interbedded argillaceous sedimentary material. They are usually coarse grained, saccharoidal, massive to irregularly bedded, and show small-scale foliation. Beds, where present, are highly variable in thickness and frequently contain oblique surfaces that Nolf (1966) interpreted as large-scale crossbedding. Although no crossbedded intervals were observed during this study, their presence is certainly compatible with the facies interpretation presented here.

The overall massive nature of the Hurricane Creek unit led Nolf to propose that it represents a barrier reef. However, no fossils have ever been recovered from the unit, and so this interpretation is somewhat suspect. Pervasive recrystallization has obscured diagnostic microfacies characteristics, but metamorphism was not so intense that it would have obliterated all textural and biological evidence for a reef. The Hurricane Creek unit more likely represents carbonate sand shoals and other shallow-water

TABLE 1.1.—*Comparative summary of carbonate lithologies of the Martin Bridge Limestone in the northern and southern Wallowa Mountains, northeastern Oregon and western Idaho*

	Northern Wallowa Mountains			Southern Wallowa Mountains		
	Hurricane Creek unit	BC Creek unit	Scotch Creek unit	Eagle Creek facies A	Eagle Creek facies B	Eagle Creek facies C
Lithology	White to light-gray pure limestone; uniform texture and composition.	Red to buff or white lithographic limestone; often laminated or nodular; rarely dolomitic; chert present as nodules and irregular beds.	Dark-gray carbonaceous limestone with bioclastic layers and argillaceous interbeds; minor intraformational breccias.	Organic-rich silty to micritic limestone and calcareous shale; diagenetic pyrite common.	Carbonate grainstones and packstones interbedded with limestones and shales of facies A and conglomerates of facies C.	Limestone conglomerate; clasts entirely platform-derived (especially oolitic and bioclastic grainstones and packstones).
Bedding	Massive, irregular beds 0.5 to 5 m thick; laterally discontinuous.	Well-bedded (1 cm – 2 m thick); laterally continuous; irregular base often stylolitic.	Impure limestone beds (1 cm – 1 m thick); laterally continuous; coarser, shelly layers are channelized.	Limestone beds (0.25 – 1 m thick) are internally laminated (1 mm - 1 cm); laterally continuous except where truncated by slumps.	Well-bedded (5 cm – 2 m thick); laterally continuous beds often with scoured and channeled base; amalgamation of individual carbonate beds common.	Massively bedded (0.5 – 10 m); uniform thickness, but susceptible to structural thickening and lensing.
Texture	Coarse-grained foliated saccharoidal marble; pervasive recrystallization obscures original composition and texture.	Very fine grained, dense recrystallized limestone; pseudo-evaporitic texture in limestone and chert after nodular and bedded anhydrite.	Silty, impure carbonate and coarse, poorly sorted bioclastic layers are moderately recrystallized.	Very fine grained; well sorted.	Fine to coarse grained; moderately well sorted.	Clast size 1 cm to 1 m; well-rounded, poorly sorted; usually clast-supported with common pressure solution between clasts.
Sedimentary structure	Oblique partings may be large-scale crossbedding.	Rare crossbedding and rip-up clasts indicate only minor current activity; cryptalgal laminations indicate lack of bioturbation.	Graded bedding and scour and fill structures common in coarse bioclastic layers; large-scale slump folds, pinch and swell bedding also common.	Graded laminations; common slump folds; rare crossbedding.	Crossbedding, rip-up clasts, graded bedding, load casts, some channel cut and fill; Bouma sequences common but poorly developed.	Zone of inverse grading at base (10 – 20 percent of total bed thickness) includes rip-ups up underlying strata; no clast imbrication.
Fossils	No fossils preserved	Rare: gastropods, bivalves, and some corals recognized.	Whole fossils and fragments of ammonites, gastropods, corals, bryozoans, bivalves, spongiomorphs, and echinoderms.	Pelagic fauna (bivalves and ammonites) ubiquitous on many bedding-plane surfaces.	Bioclastic beds common; usually broken and abraded shallow-water fossils: gastropods, sponge spicules, echinoderms, and ostracodes.	Often richly bioclastic; whole fossils and large fragments; corals, bryozoans, spongiomorphs, and bivalves common.
Other	150 to 175 m thick; conformably overlies Seven Devils Group and grades upward into Scotch Creek unit.	150 m thick; conformably overlies Seven Devils Group; overlain by Columbia River Basalt Group; lateral facies relation with Hurricane Creek unit uncertain.	150 to 200 m thick; gradational contacts with underlying Hurricane Creek unit and overlying Hurwal Formation.	Laterally equivalent to fine-grained basinal facies of Hurwal Formation in southern Wallowa Mountains.	Proximal and distal facies distinguished on the basis of 1) limestone: shale ratio 2) bed thickness 3) grain size of allochemical components.	Abundant secondary silicification postdates redeposition and is usually localized within individual carbonate clasts.
Interpretation	High-energy shoal deposits of platform interior and shelf margin; possible barrier relation with shallow-water sediments of BC Creek unit lying farther north.	Shallow subtidal to supratidal carbonates;sparse fauna, cryptalgal laminites and evaporites suggest deposition in shallow, restricted basin.	Argillaceous and bioclastic carbonate turbidites deposited in deep-water environment; records incipient drowning of Wallowa carbonate platform and northward migration of shallow-water facies.	Hemipelagic facies records normal or "background" sedimentation on carbonate slopes.	Proximal and distal carbonate turbidites derived from off-shelf transport of unconsolidated shelf edge and platform-interior sediments.	Debris sheets produced by erosion and gravity-flow transport of lithified high-energy platform-margin shoal facies; fossil debris derived from localized patch reefs.

deposits of the open platform and shelf edge. Accumulation of these sediments in a high-energy environment could account for both the massive bedding and the paucity of intermixed argillaceous material. Carbonate sand shoals of the Hurricane Creek unit could have occupied a barrier position relative to the BC Creek unit.

BC Creek Unit

This unit consists of 150 m of well-bedded, finely crystalline limestones conformably overlying volcanic rocks of the Clover Creek Greenstone on Chief Joseph Mountain (fig. 1.4*A*). Strata of the Hurricane Creek unit appear to overlie the BC Creek unit on the north side of Hurwal Divide. However, because both the BC Creek and Hurricane Creek units conformably overlie the Clover Creek Greenstone in their so-called "type" localities, there is probably some degree of lateral facies equivalency between these two informal units and (or) the contact between the Clover Creek and Martin Bridge is more diachronous than previously recognized.

Carbonate lithologies within the BC Creek unit are slightly recrystallized but, in most cases, original sedimentary structures and textures can still be discerned. Beds range in thickness from 1 cm to 2 m, with an average thickness of 5 to 25 cm. Most are laterally continuous over hundreds of meters. Bedding planes are often irregular, with stylolites and other evidence of pressure solution. Some beds are internally laminated, whereas others are crossbedded and contain rip-up clasts. Several distinctive lithologies are recognized (fig. 1.4), all of which suggest shallow subtidal to supratidal depositional environments in a shallow, restricted basin.

Laminated limestones are present in beds ranging from 5 cm to 1 m in thickness and are interspersed with thinly bedded and fine-grained packstones and grainstones. Individual laminations are often silty and (or) dolomitic and are laterally continuous over several meters. The laminations frequently show small-scale domal structures with relief of as much as 1 cm above the bedding plane (fig. 1.4*B*). These appear to be algally mediated and are very similar to cryptalgal laminites from the Martin Bridge Limestone in Hells Canyon. Fossils are rare in the BC Creek unit, but irregularly distributed gastropods, bivalves, and some corals have been recognized.

Nodular limestones are also common in this unit (fig. 1.4*C*). They typically occur in beds, which range from 50 cm to slightly more than 2 m in thickness. The white to light gray carbonate nodules are 0.5 to 4 cm in maximum diameter, very well rounded, and surrounded by a matrix of red, iron-rich carbonate. Randomly interpenetrating grain boundaries between adjacent nodules probably reflect displacive growth of *in situ* nodules, rather than compaction-related pressure solution. Later dissolution of some nodules is indicated by quartz-lined cavities of the same size and shape as the original nodules.

Replacement chert is another distinctive feature of limestones in the BC Creek unit. This chert is pure white, coarsely crystalline, and occurs both as irregularly distributed beds and as isolated cauliflower-textured nodules aligned parallel to bedding planes. The layered cherts are interbedded with limestones and have a unique "chickenwire" texture. Individual chert layers are 2 to 10 cm thick and laterally continuous over several tens of meters.

Near the base of the BC Creek unit, limestone beds are locally characterized by networks of remnant salt casts, which indicate the former presence of evaporites (fig. 1.4*D*). Further evidence supporting this interpretation includes the occurrence of isolated intraformational breccias, which are probably the product of karstic solution collapse. These observations, together with the bedding sequences, lithologic associations, and sedimentary textures described above, suggest that many limestones of the BC Creek unit represent calcitized and silicified evaporites. Features such as dissolved nodules, remnant anhydrite crystals, salt casts, and diagenetic strontium minerals (Nolf, 1966, p. 48) are all similar to those described by West (1964) in altered evaporites from the Upper Jurassic Purbeck Formation in Great Britain. The nodular limestones and chickenwire replacement cherts are remarkably similar in appearance to nodular and bedded anhydrite, respectively. Both carbonate and chert are common replacement products of anhydrite in evaporite sequences.

Thinly bedded and laterally extensive limestones, as well as the altered evaporites, dolomites, cryptalgal laminites, and karstic solution-collapse breccias in the BC Creek unit indicate deposition in shallow subtidal to supratidal environments within a restricted basin. The sparse fauna, cryptalgal laminations, clastic textures, and current structures also support this interpretation. The Hurricane Creek unit was probably located seaward of the BC Creek depositional basin and acted as a partial barrier to wave action and normal marine currents. Coarser, current-bedded layers within the BC Creek unit may record occasional storm washover deposits. However, the paucity of fossil debris in these beds is further evidence that the Hurricane Creek unit does not represent a reef.

Scotch Creek Unit

The Scotch Creek unit is the uppermost lithofacies of the Martin Bridge Limestone in the northern Wallowa Mountains. It is exposed along the west side of Hurricane Creek Canyon, where it ranges from 150 to 250 m in thickness and grades upward into argillaceous strata of the Hurwal Formation. The Scotch Creek unit is composed of silty, carbonaceous limestones, which can be classified as poorly sorted calcareous grainstones. They are typically recrystallized and contain a substantial amount of silt-size and finer clastic material. Individual beds range from 1 cm up to 1 m in thickness and can be followed along strike for hundreds of meters. Minor variations in bed thickness are the result of differential compaction and (or) erosional channeling. Other sedimentary structures include graded beds, scour and fill structures, slump folds, and minor crossbedding.

Coarse bioclastic layers ranging from 10 cm to 1 m in thickness are also very common within the Scotch Creek unit. They are richly fossiliferous and occur in both channeled and laterally continuous beds. These bioclastic beds are poorly sorted and composed of

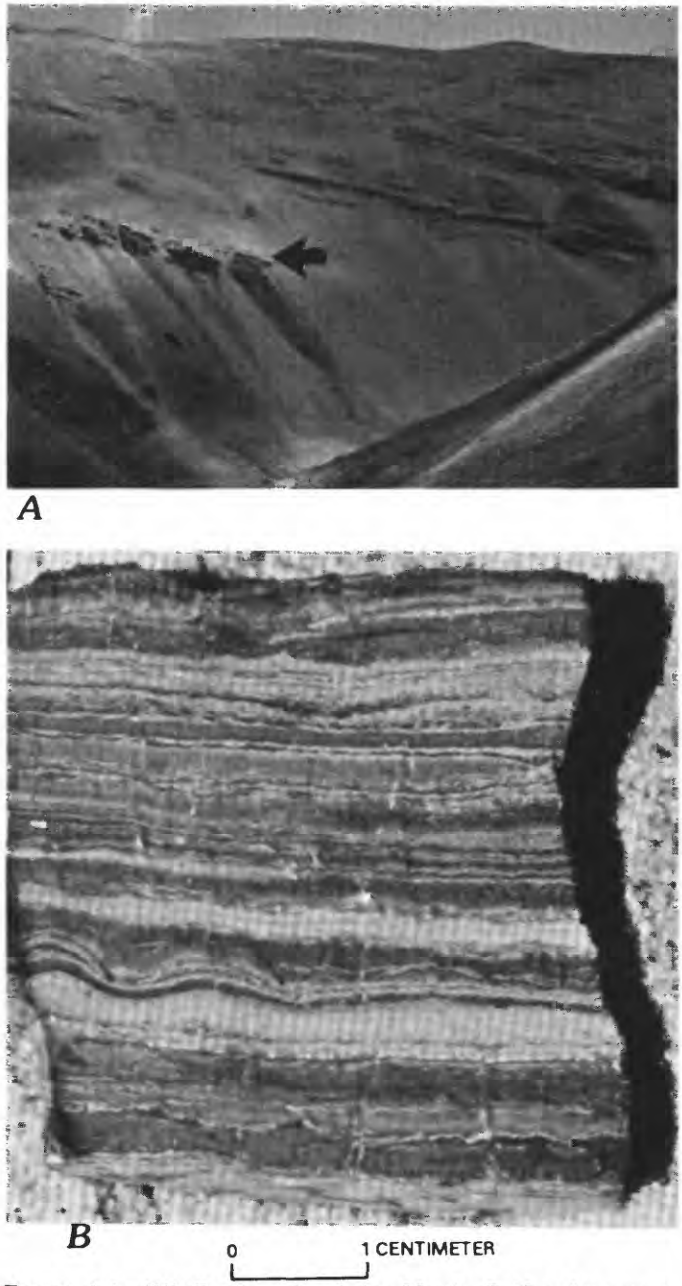

FIGURE 1.4.—BC Creek unit of the Martin Bridge Limestone, northern Wallowa Mountains, northeastern Oregon. *A*, View of stratigraphic section (approximately 150 m thick) on south flank of Chief Joseph Mountain. Arrow marks conformable contact between the BC Creek unit and underlying volcaniclastic rocks of the Seven Devils Group (Clover Creek Greenstone). *B*, Cryptalgal laminite that includes light-colored dolomitic laminae; scale in centimeters. *C*, Nodular limestone that may be the product of calcitization of original nodular anhydrite (see text for discussion); scale in centimeters. *D*, Salt casts preserved in limestone from lower part of BC Creek unit.

both inversely and normally graded fossil debris in a matrix of dark-gray silty carbonate. Fossil material in these beds of the Scotch Creek unit consists of fragments of ammonites, gastropods, corals, bryozoans, bivalves, spongiomorphs, and echinoderms (Nolf, 1966).

The Scotch Creek unit records incipient drowning of the Martin Bridge carbonate platform and northward migration of the shallow-water facies described above. The interbedding of graded carbonate intervals, many of which contain abundant broken and abraded shallow-water fossils, with thinly bedded calcareous argillites suggests downslope transport by turbidity currents. The depositional slope had a low profile with no marginal escarpment, as indicated by the thin, uniform bedding of the turbidites and the absence of laterally extensive carbonate clast conglomerates. The rare limestone breccias that are present in the Scotch Creek unit are intraformational and were probably derived from local slumping of lithified slope sediments. Bioclastic debris concentrated in some turbidite beds was transported downslope as unconsolidated sediment derived primarily from isolated shallow-water bioherms.

SOUTHERN WALLOWA MOUNTAINS

In the drainage basin of Eagle Creek in the southern Wallowa Mountains, the Martin Bridge Limestone can be divided into three end-member lithofacies (table 1.1). Unlike the three informal units of the Martin Bridge Limestone in the northern Wallowa Mountains, these Eagle Creek rocks are true lithofacies, which are irregularly interbedded and have no consistent stratigraphic order. The first lithofacies (facies A) is composed of fine-grained laminated carbonate rocks and shales, which represent the normal, or "background," sedimentation on the slope. These periplatform carbonate deposits are interbedded with two depositionally (not structurally) displaced facies. These allochthonous sediments include well-bedded carbonate grainstones (facies B) and massive limestone conglomerates (facies C) interpreted as carbonate turbidites and debris sheets, respectively.

Eagle Creek Facies A: Laminated Limestones

In the southern Wallowa Mountains, fine-grained lithologies in the Martin Bridge Limestone are assigned to Eagle Creek facies A. These include calcareous and noncalcareous shales and argillites, as well as thinly bedded to laminated organic-rich limestones (fig. 1.5). Facies A is best exposed at the Martin Bridge type locality near the intersection of Paddy and Eagle Creeks (fig. 1.1), where thin beds of black, petroliferous shales containing abundant remains of pelagic bivalves and ammonites are interbedded with 0.25- to 1-m-thick beds of fine-grained limestone. These individual limestone beds consist of numerous laminae ranging from 1 mm to 1 cm in thickness (fig. 1.5*A*). The typically graded laminae consist of well-sorted, partially recrystallized silt-sized and finer carbonate grains but also contain diagenetic pyrite and almost 10 percent subrounded, silt-sized quartz and plagioclase grains.

The carbonate rocks of facies A were derived primarily from calcareous muds and fine-grained sands originally deposited on a carbonate platform and subsequently transported off the platform into a deeper water basinal environment. Rare crossbedding and scoured bases in some beds are evidence of current deposition. Ubiquitous graded laminae suggest that each layer was actually the product of a single depositional event—probably a small-scale gravity flow. Slump folds are common and consistently overturned to the south; such evidence indicates that

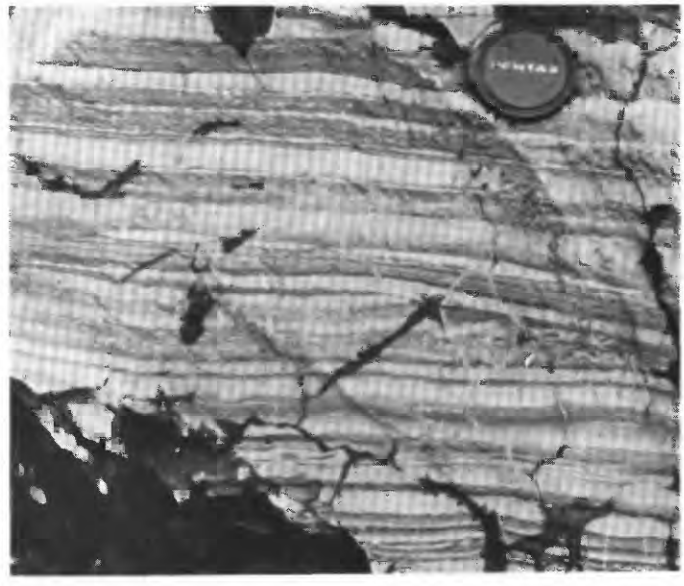

A

FIGURE 1.5.—Slope and basin lithofacies of the Martin Bridge Limestone from the southern Wallowa Mountains, northeastern Oregon. Called Eagle Creek facies on table 1.1 and in text. *A*, Laminated hemipelagic limestone (facies A) from the Martin Bridge locality on Eagle Creek. *B*, Carbonate turbidites consisting of interbedded calcareous grainstones (facies B) and shales. *C*, Limestone clast conglomerate (facies C). *D*, Massive 2- to 3-m-thick debris flow channel (facies C) interbedded with hemipelagic limestones and carbonate turbidites (facies A and B) along Eagle Creek; divisions on staff are 25 cm.

these sediments were deposited on a gentle, south-directed paleoslope. Nodular textures observed in some limestone beds of the Martin Bridge are analogous to similar textures formed through incomplete submarine cementation on modern carbonate slopes (Mullins, 1983). The lack of benthic fauna, preservation of delicate laminations on a microscopic scale, high organic content, and diagenetic pyrite all suggest that the slope environment was at least locally anaerobic.

Eagle Creek Facies B: Carbonate Grainstones

Much of the Martin Bridge Limestone in the southern Wallowa Mountains consists of well-bedded carbonate grainstones and packstones that make up facies B. These are moderately well sorted, are fine- to coarse-grained, and have a highly variable terrigenous sand and silt content. The primary allochemical components are peloids, bioclastic debris, and carbonate extraclasts. Most of the bioclastic material consists of broken and abraded fragments of shallow-water fossils, especially gastropods, echinoderms, ostracodes, and sponge spicules. These grainstones (fig. 1.5*B*) are interbedded with shales and laminated carbonate rocks of facies A, as well as with limestone conglomerates of facies C. The thickness of individual beds ranges from 5 cm to 2 m and, in most places, is typically inversely proportional to the thickness of the interbedded shaly limestone intervals.

Sedimentary structures are common in this facies. They include scoured and channeled bases, load casts, rip-up clasts, graded bedding, and small-scale crossbedding. Often, individual beds show a vertical succession of sedimentary structures resembling the classic Bouma sequence of siliciclastic turbidites. Proximal and distal facies relations can be recognized on the basis of (1) limestone : shale ratio, (2) thickness of individual carbonate grainstone beds, and (3) the grain size of allochemical components. All three criteria increase northward with proximity to the platform source of the carbonate sediment.

B

FIGURE 1.5.—Continued.

Lithology, bedding sequences, and sedimentary structures all support the theory that carbonate grainstones of facies B were reworked on a shallow-water carbonate platform and transported downslope by turbidity currents. The interbedding of calcareous sediment containing a diverse shallow-water fauna (including fragments of corals, calcareous sponges, bivalves, and echinoids) with deep-water shales and thinly bedded basinal limestones (facies A) also implies downslope transport and mixing of carbonate sediments from diverse environments. Sedimentary structures, including graded beds with erosionally scoured bases, plastically deformed rip-up clasts, and poorly developed crossbedding, can best be explained by deposition from turbidity currents. Although these carbonate grainstones are often recrystallized and not necessarily diagnostic of a particular sedimentary provenance, they were probably derived at least in part from unconsolidated high-energy shoals. The absence of continuous fringing reefs along the shelf edge would have also allowed platform-interior sediments to bypass marginal shoals and be transported into deeper water by turbidity currents.

Eagle Creek Facies C: Conglomeratic Limestone

Carbonate clast conglomerates are a distinctive Martin Bridge lithofacies, which is found exclusively in the southern Wallowa Mountains (fig. 1.5*C*). Ross (1938) described this lithology, but he considered it to be the result of intraformational fracture:

> Above [the argillaceous member] is a massive blue limestone. The lower part of this is a breccia which on weathered surfaces, looks like a conglomerate. On polished surfaces, however, the structure is clearly seen to result from the fracturing of the blue limestone. The resemblance to a conglomerate is increased by the fact that shaly beds are unfractured, so that the seeming conglomerate locally appears to be interbedded with shale. (Ross, 1938, p. 32)

Ross correctly noted that this "seeming conglomerate" is interbedded with thinly bedded shales and limestones, and that the conglomeratic texture is best expressed on weathered surfaces. Diagenetic and low-grade metamorphic recrystallization of carbonate clasts and matrix obscures the textural differences between them, except where these differences have

been highlighted by differential weathering and (or) silicification. Pressure-solution contacts between limestone clasts could be misconstrued as "fractures," but the diverse clast lithologies, as well as depositional textures and abundant rip-up fragments within individual beds, support a conglomeratic interpretation for this unit.

The conglomerate is poorly sorted, massively bedded, and may be either clast or matrix supported. It is typically interbedded with thinly bedded shales and limestones of facies A and B. Individual beds range from less than 0.5 m up to 10 m in thickness. Most beds appear to be laterally continuous, but the thickest beds are typically lens shaped and discontinuous (fig. 1.5*D*); characteristics of these thick beds suggest erosional channeling during deposition. Some of the more massive limestone knobs, which can be seen in the southern Wallowa Mountains (especially on the hillsides above Eagle Creek between East Eagle and Basin Creek), appear to be debris flow channels similar to those described in Devonian carbonate rocks near Alberta, Canada (Cook, 1983; Cook and others, 1972).

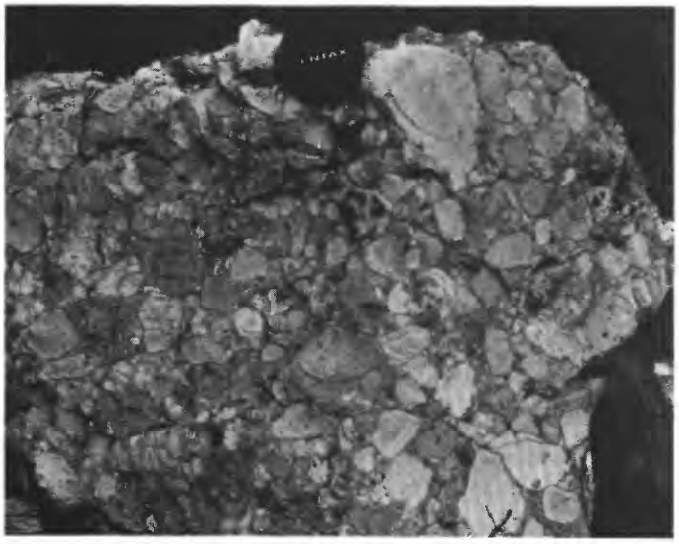

C

D

FIGURE 1.5.—Continued.

Limestone clasts in these conglomerates range from 1 cm to over 1 m in diameter and are almost exclusively derived from shallow-water carbonate-platform environments. Bioclastic and oolitic grainstones and packstones are the most common clast types, and they are typical of platform margin high-energy shoal facies. Fine-grained slope facies are present only as plastically deformed rip-up clasts. These are especially common in a zone of inverse grading that distinguishes the lower parts of many of the conglomerate beds. Reef material, including corals, calcareous sponges, tabulozoans, spongiomorphs, bivalves, echinoid fragments, and crinoids, is locally abundant in this conglomeratic facies and suggests derivation from isolated patch reefs on the slope and (or) shelf edge.

DEPOSITIONAL MODEL

Read (1985), in his classification of carbonate platforms, makes a primary distinction between ramps, which may be homoclinal or distally steepened, and rimmed shelves, which are characterized by a marked break in slope at the high-energy shallow shelf edge. At different stages in its evolution, the Martin Bridge platform showed characteristics of each of these depositional profiles.

Paleogeographic reconstruction of the northern Wallowa platform during deposition of the lower part of the Martin Bridge Limestone indicates that it was a narrow, south-facing rimmed shelf dominated by carbonate sand shoals (Hurricane Creek unit). Landward (north) of these marginal shoals, shallow subtidal to supratidal limestones and evaporites of the BC Creek unit were deposited in a restricted basin (fig. 1.6). The shoals likely served as a barrier that isolated the shelf interior from open-platform circulation and wave action.

Limestones of the Martin Bridge in the southern Wallowa Mountains include carbonate turbidites and debris flow deposits, which accumulated on a carbonate slope apron (Mullins and Cook, 1986) adjacent to the northern Wallowa rimmed shelf. Provenance analysis of these slope facies supports the conclusion that the platform from which they were derived was rimmed by high-energy oolitic sand shoals, rather

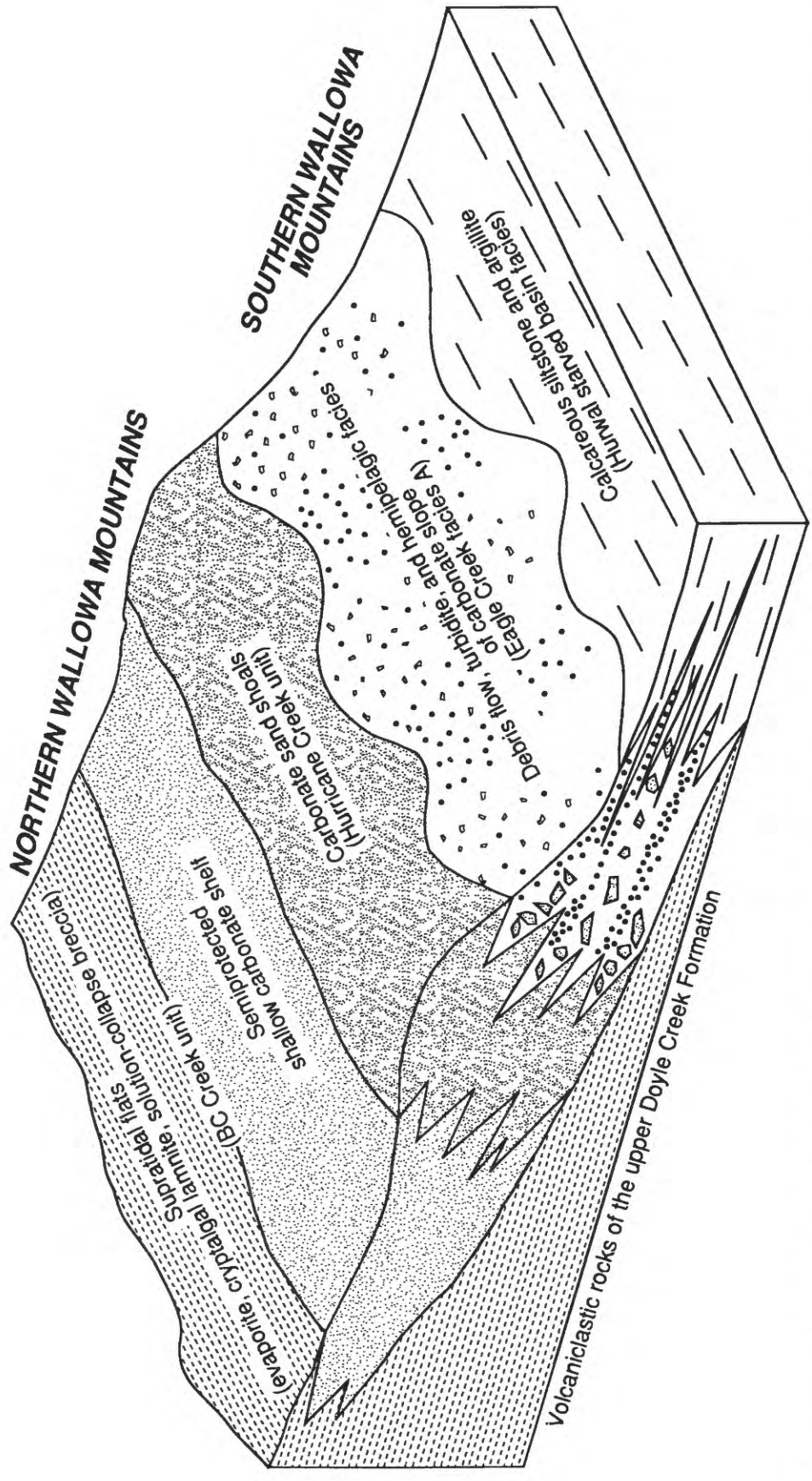

FIGURE 1.6.—Paleogeographic model for evolution of carbonate platform, slope, and basin of the Martin Bridge Limestone during Late Triassic (early Norian) time. Martin Bridge lithofacies from the northern Wallowa Mountains were deposited on a lime-sand dominated rimmed shelf. BC Creek unit consists of both shallow platform and supratidal facies. In the southern Wallowa Mountains, carbonate slope apron facies were transitional to starved basin lithologies of the Hurwal Formation. Later deposition of Scotch Creek unit (not shown here) reflects incipient drowning of the carbonate platform.

than fringing reef complexes. Small, isolated patch reefs such as the one described at Summit Point in the southern Wallowa Mountains (Stanley and Senowbari-Daryan, 1986) were present, however, and could be considered a separate and unique Martin Bridge lithofacies. Forereef slumping near these buildups probably generated the coarse bioclastic debris that is associated with Martin Bridge slope deposits.

Drowning of the carbonate platform in Norian time resulted in a major landward shift of the shallow-water facies. This shift is suggested by stratigraphic relations in the northern Wallowa Mountains, where intertidal facies of the BC Creek unit and shoal deposits of the Hurricane Creek unit are both overlain by deeper water gravity-flow facies of the Scotch Creek unit. The landward shift in shallow carbonate environments established a new carbonate ramp, which was distally steepened at the old shelf edge. The Scotch Creek unit is the youngest Martin Bridge unit, and it represents the deep-water ramp facies deposited on the incipiently drowned platform. This deepening of the depositional basin in the Late Triassic is recorded in the southern Wallowa Mountains by the diminished influence of carbonate sedimentation and the transition to basinal facies of the Hurwal Formation.

HURWAL FORMATION

The Hurwal Formation was originally defined by Smith and Allen (1941) as the thick sequence of well-indurated calcareous and noncalcareous argillites and graywackes that conformably overlies the Martin Bridge Limestone in the northern Wallowa Mountains. The unit was named for outcrops on Hurwal Divide, a prominent (>2,500 m) ridge in the northern Wallowa Mountains. In the southern Wallowa Mountains, similar argillaceous strata not only overlie, but also interfinger laterally with, basinal carbonate rocks of the Martin Bridge Limestone. These strata in the southern Wallowa Mountains have also been assigned to the Hurwal Formation (Prostka, 1962), although paleontological data indicates that they may be only partly equivalent to Hurwal strata from the type locality.

In the Snake River canyon, the only rocks that resemble the Hurwal Formation are a series of metamorphosed shales and calcareous argillites of unknown age, which crop out locally near the mouth of the Grande Ronde River (Glerup, 1960). The one sedimentary unit in Hells Canyon demonstrably younger than the Martin Bridge Limestone is the Jurassic (Callovian and Oxfordian) Coon Hollow Formation, which unconformably overlies volcanic rocks of the Seven Devils Group at Coon Hollow. The Coon Hollow Formation consists primarily of mudstones and siltstones, but it also contains interbedded quartzose sandstones and chert-pebble conglomerates in its upper part (Follo, 1986; Goldstrand, chap. 2, this volume). Rocks of Bajocian and Callovian age that crop out at Pittsburg Landing (Ash, 1991; Stanley and Beauvais, 1990) may be in part correlative with the Coon Hollow Formation. These strata have been described by White and Vallier (chap. 3, this volume) and by White (chap. 4, this volume).

North of Riggins in western Idaho, dark-gray calcareous slates of the Lucile Slate have been correlated with the Hurwal (Brooks and Vallier, 1978). Locally, however, the Lucile stratigraphically underlies limestones of the Martin Bridge and is in gradational contact with volcanic rocks of the Seven Devils Group. Lund and others (1983) suggested that rocks of the Lucile stratigraphically interfinger and are facies equivalent with the Martin Bridge. This hypothesis is supported by observations of unmetamorphosed strata from the Martin Bridge locality in the southern Wallowa Mountains (Follo, 1986). There, lithologies and stratigraphic relations of basinal carbonate facies in the Martin Bridge Limestone are remarkably similar to calcareous rocks of the Lucile Slate.

AGE AND STRATIGRAPHIC RELATIONS

Paleontological samples collected by Nolf in the northern Wallowa Mountains (Nolf, 1966) indicate an overall latest Triassic (Norian) to latest Early Jurassic (Toarcian) age for strata assigned to the Hurwal Formation in the Wallowa terrane. Most of the formation, however, including the entire Hurwal in the southern Wallowa Mountains, is Norian in age. Outcrops of the Lower Jurassic part of the Hurwal occur only in the northern Wallowa Mountains, where they are structurally and stratigraphically isolated from the thick Upper Triassic section.

In the northern Wallowa Mountains, the lower contact of the Hurwal Formation is marked by a gradational transition from fine-grained carbonate rocks of the Martin Bridge Limestone. On the north face of Hurwal Divide, impure limestones of the Scotch Creek unit (of the Martin Bridge) grade upward over 10 to 15 m of section through argillaceous carbonate to calcareous argillite and ultimately to volcaniclastic argillite and fine-grained graywacke of the Hurwal Formation (fig. 1.7*A*). On the basis of measured sections from Hurwal Divide and the west side of Hurricane Canyon,

a minimum of 1,600 m can be estimated for the thickness of the Hurwal Formation. Elsewhere in the northern Wallowa Mountains, such as on Traverse Ridge and Sheep Ridge, isolated outcrops of the Hurwal containing Jurassic fossils could add as much as 300 to 400 m of section to the total thickness (Nolf, 1966). At its upper contact, the Hurwal is either unconformably overlain by basalts of the Columbia River Basalt Group or truncated by intrusive rocks of the Wallowa batholith.

Limited exposure and structural complexities in the southern Wallowa Mountains make determination of the thickness and stratigraphic relations there extremely difficult. Determinations are further complicated because the Hurwal appears to be at least in part laterally equivalent to basinal facies of the Martin Bridge Limestone (Follo and Siever, 1985). Early Norian fossils are present in both formations. Whereas physically tracing Martin Bridge strata into noncalcareous Hurwal beds is impossible, indirect evidence strongly supports their correlation. Much of the Martin Bridge as originally mapped by Ross (1938) and Prostka (1963) contains noncalcareous shales, which are indistinguishable from fine-grained Hurwal sedimentary rocks. Also, characteristic carbonate debris sheets composed entirely of platform-derived Martin Bridge lithologies are present in the southern Wallowa Mountains interbedded with basinal strata of both the Martin Bridge and Hurwal.

The total thickness of Hurwal strata in the southern Wallowa Mountains appears to be much less than that to the north. Prostka estimated a total thickness of 1,200 m for the Hurwal Formation near Sparta (fig. 1.2), but that estimate was based primarily on correlations with the northern Wallowa Mountains. Using direct measurements from throughout the southern Wallowa Mountains, a maximum of 350 to 450 m is probably a more reasonable estimate for the total thickness of the Hurwal in that area (Follo, 1986). A 360-m-thick, continuous section of the Hurwal measured on the south wall of Eagle Creek Canyon near Excelsior Gulch supports this estimate. Conglomeratic limestone at the base of this section is lithologically identical to debris sheets within the Martin Bridge. The uppermost 80 m of the section is composed of a distinctive limestone-greenstone-chert conglomerate, which is herein referred to as the Excelsior Gulch unit of the Hurwal Formation. The Excelsior Gulch unit is early Norian in age, as evidenced by well-preserved fossils (including the early Norian bivalve *Halobia* cf. *H. cordillerana* and the Norian belemnoid *Aulacoceras*) collected from a calcareous siltstone interbed lying 5 m above the base of the unit. This conglomeratic unit is restricted to the southern Wallowa Mountains, and it is consistently the uppermost stratigraphic interval in the Hurwal section. As discussed in the next section, the absence of younger, uppermost Triassic and Lower Jurassic strata in the southern Wallowa Mountains is probably, at least in part, the result of local uplift and erosion along the southern margin of the Wallowa terrane during the Late Triassic.

LITHOFACIES

The Hurwal Formation consists of a thick sequence of thinly bedded argillite and fine-grained sandstone (fig. 1.7*B*) that includes varying amounts of interbedded volcanic tuff, limestone, and polymict conglomerate. These sedimentary rocks are typically well indurated, dark gray to brown, and have distinctive rusty surface weathering owing to the oxidation of accessory pyrite. The argillites are often calcareous and contain abundant ammonites and halobiid bivalves concentrated along bedding planes. Well-preserved trace fossils of the genus *Chondrites* (fig. 1.7*C*) probably indicate a lack of oxygen during deposition, but they are not necessarily associated with any particular depositional environment (Bromley and Ekdale, 1984).

Sandstones occur most commonly as 2- to 10-cm-thick units interbedded with the finer grained argillaceous sedimentary rocks. These lithic arenites are composed primarily of volcanic lithic grains and highly altered plagioclase. They contain little or no quartz and are often carbonate cemented. Current-generated sedimentary structures, including graded bedding, crossbedding, channel cut and fill structures, and small rip-up clasts of underlying sedimentary material, are abundant in the sandy interbeds and suggest deposition by low-volume turbidity currents in a distal basin setting. Typical Bouma sequences are very rare within the Hurwal, and no large-scale vertical bedding sequences, which might be associated with a submarine fan system, were observed.

Buff-colored tuffaceous shales are a distinctive Hurwal lithology in the southern Wallowa Mountains. These laminated to thinly bedded (1 mm – 5 cm) tuffaceous intervals are 1 to 5 m thick and usually contain numerous well-preserved bivalves and ammonites. The tuff is fine to medium grained and weathers quickly to a soft, clay-rich shale containing minor amounts of plagioclase and quartz silt. Large diagenetic pyrite cubes (as large as 1 cm) are widely distributed through the tuff; their presence indicates enough organic matter to induce anaerobic conditions after burial. Reworked and waterlain tuff, together

with the more abundant volcaniclastic argillites and sandstones of the Hurwal, suggest deposition in a deep-water marginal basin adjacent to a locally active volcanic source.

Carbonate is present not only as cement and (or) matrix dispersed in the fine-grained clastic rocks but also as massive limestone units 20 cm to 5 m thick interbedded with the Hurwal Formation. In the southern Wallowa Mountains many of these limestones are bioclastic or conglomeratic debris sheets lithologically identical to those in the Martin Bridge Limestone. In the northern Wallowa Mountains calcareous lithologies are especially common within the "middle Hurwal" stratigraphic interval, as originally defined by Nolf (1966). One prominent limestone unit near the top of the "middle Hurwal" is approximately 75 m thick and stands out high on the west wall of Hurricane Creek canyon (fig. 1.7*D*). This limestone is extensively recrystallized, but conglomeratic textures are visible in some beds. The presence of these limestones interbedded with basinal sedimentary material can best be explained by downslope transport of shallow-water carbonate sediments by gravity-flow processes.

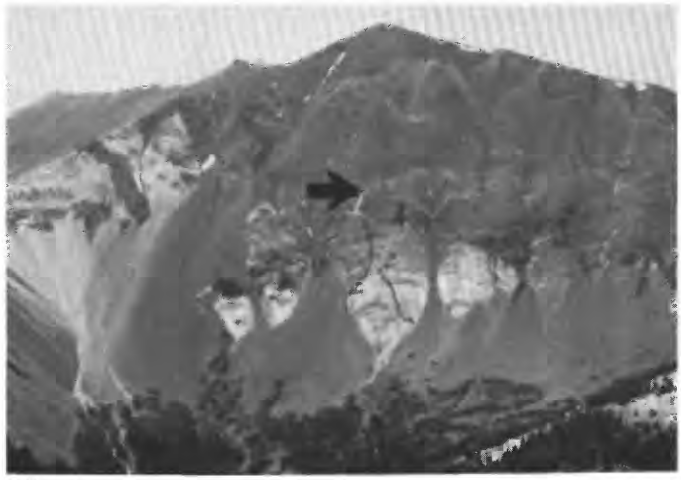

A

B

C

0 1 CENTIMETER

D

FIGURE 1.7.—Outcrop and lithologies of the Hurwal Formation in Wallowa terrane, northeastern Oregon. *A*, North face of Hurwal Divide, northern Wallowa Mountains. Arrow marks approximate location of gradational contact between the Martin Bridge Limestone (Scotch Creek unit) and overlying Hurwal Formation. *B*, Typical thinly bedded argillite of the Hurwal Formation. *C*, Basinal trace fossil Chondrites from calcareous argillite of the Hurwal Formation, southern Wallowa Mountains. *D*, Limestone interval within middle part of the Hurwal Formation, west wall of Hurricane Creek Canyon. Looking south toward Twin Peaks.

TABLE 1.2.—*Sedimentologic comparison of the Deadman Lake and Excelsior Gulch units of the Hurwal Formation from the Wallowa terrane, northeastern Oregon*

	Deadman Lake unit	Excelsior Gulch unit
Age	Early Norian	Early Norian.
Stratigraphic position	Approximately 300 m above Martin Bridge Limestone.	Approximately 300 m above Martin Bridge Limestone.
Thickness	50 to 100 m	50 to 80 m.
Bedding	None	10 cm to 10 m.
Fabric	Matrix supported	Primarily clast supported.
Clast sorting	Poor to chaotic	Moderate to well.
Clast shape	Angular to well rounded	Rounded.
Maximum clast size (long dimension).	300 m	1 m.
Clast composition	Limestone, argillite	Limestone, volcanic rocks, radiolarian chert, and intrusive rocks.
Matrix	Calcareous silt and sand	Coarse sand
Interpretation	Olistostromal megabreccia from large submarine slump.	Resedimented conglomerate from submarine fan or fan delta.
Provenance	Unstable shelf edge	Uplifted accretionary complex.

The transition from Martin Bridge sedimentation to the Hurwal in the Late Triassic resulted in the northward displacement of shallow-water carbonate environments. While Hurwal clastic deposits were accumulating in the Wallowa basin, contemporaneous shallow-water carbonate facies not unlike those of the Martin Bridge Limestone were being deposited somewhere to the north, in an area now covered by volcanic rocks of the Tertiary Columbia River Basalt Group. The only preserved record of these carbonate deposits in the Wallowa terrane is downslope-displaced sedimentary material within the Hurwal Formation.

Polymict conglomerates within the Hurwal Formation are especially important to understanding the nature and tectonic setting of the Wallowa depositional basin during Late Triassic time. The sedimentology and composition of these conglomerates provide critical constraints on depositional processes and provenance, respectively. The two most distinctive of these conglomeratic sequences—the previously mentioned Excelsior Gulch unit and the Deadman Lake unit, an olistostromal megabreccia first identified by Nolf (1966) in the northern Wallowa Mountains—are mappable units of regional extent. Although their composition and sedimentological characteristics are very different, these two conglomerates are remarkably similar in terms of age, thickness, and relative stratigraphic position, as discussed in the following sections and summarized in table 1.2.

DEADMAN LAKE UNIT

"Deadman Lake breccia" is the informal name given by Nolf (1966) to a distinctive sequence of poorly sorted, matrix-supported conglomerates and breccias, which are exposed along the east side of Hurricane Divide in the northern Wallowa Mountains. The unit is 50 to 100 m thick and crops out approximately 300 m above the top of the Martin Bridge Limestone within a continuous sequence of argillites and calcareous shales of the Hurwal Formation. The conglomerate is massively bedded and has an irregular base characterized by as much as 10 m of erosional relief. The presence of clasts, which are also conglomeratic, within the Deadman Lake unit suggests that the unit resulted from more than one depositional event.

Clast and matrix textures in the Deadman Lake unit are extremely heterogeneous, but all textures indicate chaotic mobility during transport and deposition (fig. 1.8*A*). Diverse and poorly sorted clasts of limestone and argillite are randomly dispersed in the silty, sandy, or calcareous matrix. Limestone clasts are bimodally distributed between small (<20 cm) well-rounded cobbles and larger, more angular blocks ranging from 1 m to as much as 300 m in length. No reliable age has yet been determined for these carbonate clasts, as they are usually recrystallized and only rarely fossiliferous. Intermixed with the limestone clasts are argillite blocks of Norian age, which are identical to underlying Hurwal lithologies. These are 20 cm to 10 m in length and usually broken parallel to bedding. Some blocks, especially the smaller ones, have been subject to intense plastic deformation and have wispy, indented, or diffuse margins that suggest erosion and transport in a semiconsolidated state (fig. 1.8*B*). Others clasts are more massive, have well-defined planar boundaries, and appear to have been transported as rigid blocks within a semifluid matrix.

The depositional textures of the Deadman Lake unit suggest transport by subaquaeous slump and (or) debris flow. Many sedimentological characteristics of the unit are identical to those described in olistostromes from the Apennines of northern Italy (Abbate and others, 1970). In the Apennines, individual olistoliths may be as much as 200 to 300 m thick and 1 to 2 km wide. In the Wallowa Mountains, the entire Deadman Lake unit is only 100 m thick, but clasts as large as 40 m thick by 300 m long have been described in the cirque of Deadman Lake and elsewhere (Nolf, 1966). Most larger slide blocks within the Deadman Lake unit are approximately 10 to 25 m in maximum dimension. Although no reliable paleocurrent indicators were observed within the olistostrome, the absence of Deadman Lake lithologies in the southern Wallowa Mountains, together with the thinning of the unit from north to south along Hurricane Divide, indicates that the source of the slide lay somewhere to the north.

A

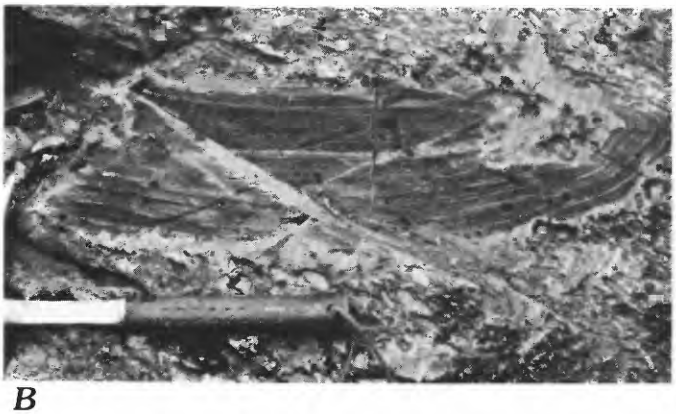

B

FIGURE 1.8.—Breccias from the Deadman Lake unit of the Hurwal Formation, northern Wallowa Mountains, northeastern Oregon. *A*, Chaotic megabreccia from east side of Hurricane Divide (1.5-m staff for scale). *B*, Close-up of same outcrop showing plastically deformed argillite clast; hammer for scale. Note wispy, diffuse margin of larger clast and preferred orientation of stretched limestone pebbles.

Lithologies in the Deadman Lake unit could all have been derived from Martin Bridge and Hurwal units in the Wallowa terrane. The volume of debris generated by the slump indicates a zone of failure, which cut deeply through a lithologically diverse stratigraphic section. The renewal and persistence of Hurwal sedimentation following the deposition of megabreccias of the Deadman Lake unit and the absence of any regionally extensive contemporaneous thrust sheets in the area suggest that the slide was initiated by high-angle faulting along the northern margin of the Hurwal basin. However, the stratigraphic continuity of the Triassic sedimentary section in the Wallowa Mountains and the absence of any large truncation surfaces or synsedimentary normal faults all indicate that the source of the slide lay somewhere outside the outcrop limits of the Wallowa terrane.

EXCELSIOR GULCH UNIT

The Excelsior Gulch unit of the Hurwal Formation is a 50- to 80-m-thick sequence of mixed conglomerates containing limestone, volcanic, and chert clasts, which are exposed in isolated outcrops throughout the southern Wallowa Mountains (fig. 1.9). The Excelsior Gulch is the youngest Hurwal unit in the southern Wallowa Mountains and is exposed approximately 300 m above the top of the Martin Bridge Limestone. Near Excelsior Gulch, the unit is approximately 80 m thick and is directly overlain by basalts of the Columbia River Basalt Group. The Excelsior Gulch unit is composed primarily of coarse, clast-supported conglomerates interbedded with sandstones. Clasts are consistently rounded and range in size from 1 cm to 1 m in maximum diameter. Beds range from 10 cm to several meters in thickness. Most are laterally discontinuous—a characteristic that suggests erosional channeling. The more massive conglomerate intervals are as thick as 10 m and probably represent the amalgamated beds of several depositional events rather than a single depositional event.

Although reliable paleocurrent indicators such as crossbedding and consistent clast imbrication are rare in the Excelsior Gulch unit, texture and bedding trends strongly suggest that its source area lay nearby to the south. There is an overall northward decrease in average clast size and bed thickness from

outcrops near Red Gulch (fig. 1.9*A*) to those along East Eagle Creek (fig. 1.9*B*) and O'Brien Creek. This trend is accompanied by a northward increase in the degree of conglomerate organization—sorting, stratification, and imbrication—across the same area.

Coarse-grained sedimentary rocks of the Excelsior Gulch unit show many characteristics of resedimented deep-water conglomerates such as those described by Walker (1975). Observed facies associations all suggest channel-filling conglomerates in the proximal realm of a rapidly prograding submarine fan. The conglomerates directly overlie fine-grained basinal Hurwal rocks containing pelagic fossils and the trace fossil *Chondrites*. The abundance of limestone clasts as much as 1 m in diameter requires substantial relief over a very short distance between the uplifted source area and the deep marine depositional basin.

A

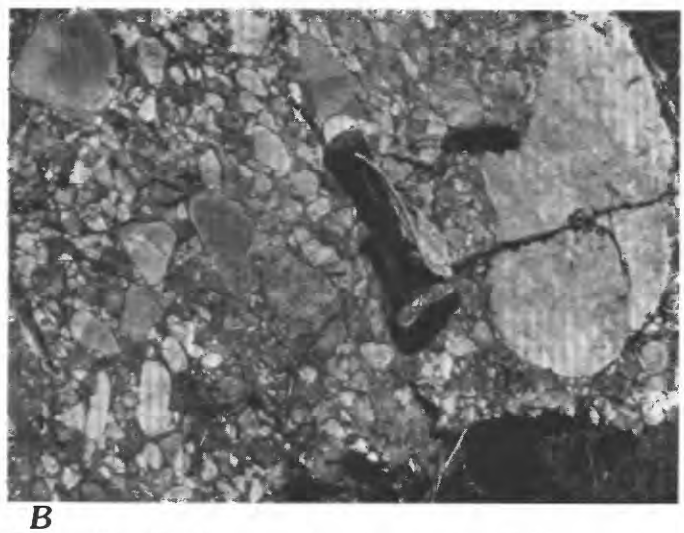

B

FIGURE 1.9.—Conglomerates from the Excelsior Gulch unit of the Hurwal Formation, southern Wallowa Mountains, northeastern Oregon. *A*, Well-sorted, imbricated lithology along East Eagle Creek. *B*, Massive, poorly sorted conglomerate near Red Gulch.

The composition of Excelsior Gulch conglomerates provides valuable information as to their tectonic significance and the exact nature of the source terrane. Clasts are predominantly limestone, altered volcanic rocks, and radiolarian chert but include some coarse-grained intrusive rocks. Numerous cobble count results from conglomerates throughout the southern Wallowa Mountains are shown in figure 1.10*A*. Compositional variation is stratigraphically controlled, as shown by carbonate clasts being especially abundant in the lower part of the section and supplanted by volcanic clasts upward through the section (fig. 1.10*B*). This pattern may represent an unroofing sequence derived from a source terrane where limestones overlay bedded cherts and volcanic rocks.

The unique presence of radiolarian chert clasts within conglomerates of the Excelsior Gulch unit has significant implications for the provenance of this enigmatic unit. Specifically, they are the only constituent of the Excelsior Gulch conglomerates that could not be locally derived from stratigraphic sequences within the Wallowa terrane. Replacement cherts (silicified carbonate and volcanic rocks) are present in both the Martin Bridge Limestone and Clover Creek Greenstone, but no bedded radiolarian cherts are present anywhere in the entire Wallowa terrane. Deformation, uplift, and erosion of deep-water oceanic deposits such as bedded cherts is most often associated with subduction along convergent-plate margins. These distinctive radiolarian chert clasts suggest that conglomerates of the Excelsior Gulch unit were derived from a tectonic source outside the Wallowa terrane, most likely from a nearby subduction complex. Dissolution of radiolarian chert clasts from the Excelsior Gulch unit in an attempt to separate datable radiolarians and further characterize the source terrane has proved unsuccessful, largely because of the pervasive recrystallization.

Although the radiolarian chert is the one clast type in the Excelsior Gulch unit that could only have come from outside the Wallowa terrane, the limestone and volcanic clasts were probably also derived from outside the Wallowa terrane. If the limestone clasts are Martin Bridge lithologies and the volcanic rocks are equivalent to the Clover Creek Greenstone, then one

would also expect to find some clasts from the "Lower Sedimentary Series" or its correlatives, which underlies the Martin Bridge Limestone in the Wallowa terrane. These lithologies—principally coarse-grained red, purple, and green volcaniclastic rocks—are easily recognizable and yet completely missing from Excelsior Gulch conglomerates. Significantly, limestone clasts of the Excelsior Gulch unit are Norian in age and contain much more reef material than typical Martin Bridge carbonate rocks. These limestones probably developed as fringing reef facies associated with an uplifted accretionary prism composed of oceanic sediments and volcanic rocks (Follo, 1986). This would explain the observed unroofing sequence, as well as the inferred subduction complex provenance.

The most likely source for sediments of the Excelsior Gulch unit appears to be the Baker terrane, units of which crop out directly south of the Wallowa Mountains in the Virtue Hills (fig. 1. 11). Strata of the Elkhorn Ridge Argillite in the Baker terrane consist of a lithologically diverse assemblage of bedded cherts, argillites, limestones, and altered greenstones (Coward, 1982; Blome and others, 1986). This compares remarkably well with the hypothesized provenance for the Excelsior Gulch unit, and the paleogeography corresponds with a southern source for the unit.

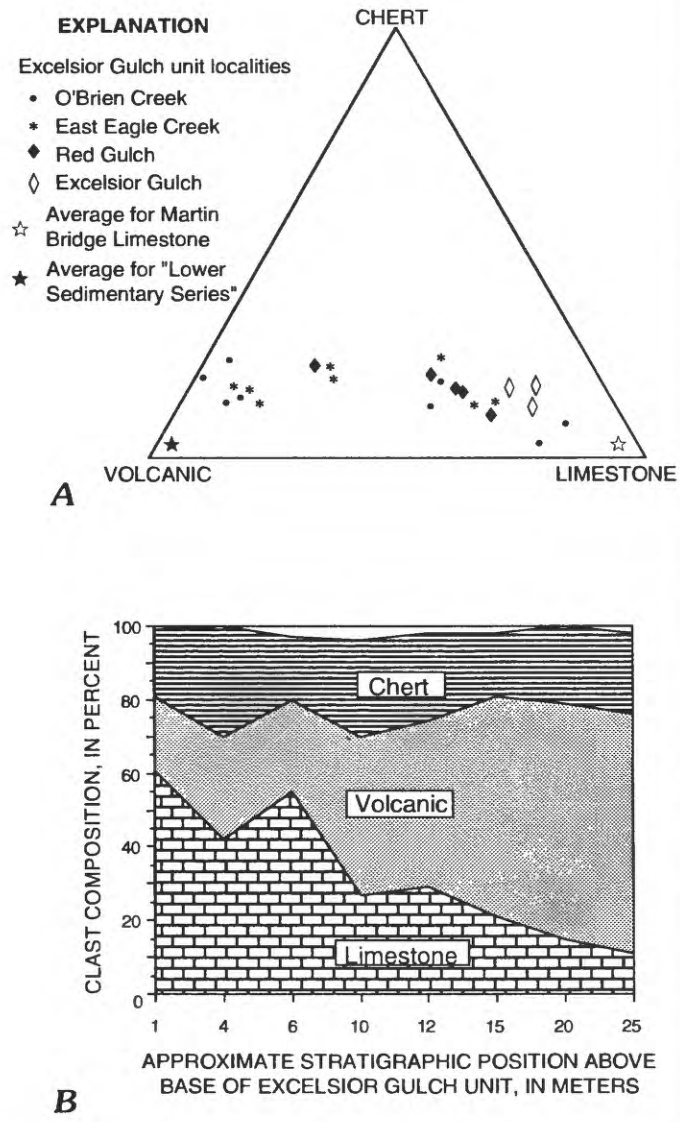

FIGURE 1.10.—Clast counts of conglomerates from Excelsior Gulch unit of the Hurwal Formation. *A*, Triangular plot of compositional data from several localities showing variability between relative proportions of limestone and volcanic clasts. Average composition of conglomerates from the Martin Bridge Limestone and the "Lower Sedimentary Series" of Prostka (1962) provided for comparison. *B*, Area plot of clast counts from stratigraphic section along East Eagle Creek. Stratigraphically controlled inverse relation between limestone and volcanic clasts suggests unroofing sequence.

DEPOSITIONAL AND TECTONIC MODEL

The composition and sedimentology of the Hurwal Formation indicate derivation from a locally active volcanic arc and deposition by turbidity currents in a distal basin setting. One possible source for the volcaniclastic deposits of the Hurwal Formation is the Olds Ferry terrane (Huntington arc) (fig. 1.2), where arc volcanism may have continued through the Early Jurassic (Dickinson, 1979; Silberling, 1983). A more likely source for the Hurwal volcaniclastic material appears to be the Wallowa terrane itself. Although widespread volcanic activity in the area of the Wallowa Mountains had apparently ceased by the end of the Karnian, volcanism may have persisted, or resumed, in other parts of the arc. At Pittsburg Landing in the Snake River canyon, a tuff unit of Callovian age is present at the base of the Coon Hollow Formation (White and Vallier, chap. 3, this volume). On Vancouver Island—which, like the Wallowa Mountains, may be part of the Wrangellia terrane—the Lower Jurassic Bonanza Formation records a period of extensive Early Jurassic volcanism (Muller, 1977). These volcanic rocks are the same age as the Hurwal and overlie Upper Triassic carbonate strata (Quatsino Limestone and Parson Bay Formation), which have been correlated with the Martin Bridge Limestone (Jones and others, 1977). Post-Jurassic strike-slip faulting is presumably responsible for disrupting these formerly contiguous pieces of the Wrangellia terrane.

Upper Triassic conglomerates within the Hurwal Formation reflect the influence of localized tectonism within the Wallowa terrane. The Deadman Lake unit

is an olistostromal megabreccia presumably derived from catastrophic slumping along the northern landward margin of the depositional basin. Its age and stratigraphic position within the Hurwal Formation are very similar to those of the Excelsior Gulch unit, a resedimented conglomerate of turbidite association, which was deposited within the southern part of the basin. The Excelsior Gulch sediments were most likely derived from an uplifted subduction complex represented at least in part by strata of the Baker terrane now exposed in the Virtue Hills. However, the tectonic affinity of that part of the Baker terrane, as well as the ultimate cause of uplift, is enigmatic.

Sediments eroded from uplifted accretionary prisms are typically deposited locally within the forearc or within ponded trench-slope basins (Underwood and Bachman, 1982). A forearc environment seems more likely for the Excelsior Gulch unit because the stratigraphy and structure of the Hurwal basin is not compatible with a trench-slope setting. If, however, Excelsior Gulch sediments were generated as a consequence of normal subduction-related uplift, one would expect that other sedimentary deposits of similar provenance would also be found locally within the Hurwal Formation. No other such sedimentary units are present in the Wallowa terrane, although this could be in part a function of the absence of Lower Jurassic strata in the southern Wallowa Mountains.

The Excelsior Gulch and Deadman Lake units may also record local sedimentary responses to a singular tectonic event. The early Norian age of the units corresponds to metamorphic ages of 228 to 219 Ma ($^{40}Ar/^{39}Ar$) determined by Avé Lallemant and others (1985) from mylonites within a shear zone near Oxbow on the Snake River (fig. 1.1). They suggested that left-lateral strike-slip faulting within the Wallowa terrane occurred in response to oblique convergence with the Huntington arc. According to a theory proposed by Beck (1986), such sympathetic shear zones typically develop either within the arc and forearc regions or within the subduction complex.

Strike-slip faulting in the Oxbow shear zone, or a similar zone, may have resulted in local uplift of forearc basement rocks along the eastern edge of the Wallowa terrane. It is possible that this faulting involved rocks of the arc massif, as well as melange units of the Baker terrane. The Excelsior Gulch unit of the Hurwal Formation consists of synorogenic sedimentary deposits derived from this uplifted fault complex and establishes a provenance link with rocks

FIGURE 1.11.—Melange topography of the Baker terrane in the Virtue Hills, just south of Wallowa Mountains, northeastern Oregon. Knockers of Permian to Triassic limestone (left foreground) and altered greenstone (dark outcrop, center) are enclosed within a sheared matrix of argillite and radiolarian chert. Southern Wallowa Mountains are visible 8 km to the north. Contact between Baker and Wallowa terranes in intervening area covered by the Miocene Columbia River Basalt Group.

of the Baker terrane during the early Norian. This theory implies that the Wallowa terrane and at least part of the Baker terrane had developed as elements of a more extensive arc-trench system associated with west-dipping subduction during the Late Triassic. Another possibility is that the two terranes were not genetically related and were first juxtaposed during Late Triassic time by strike-slip faulting. More detailed structural studies are needed to determine the nature of the contact between these two terranes.

Evidence supporting the theory of west-dipping subduction under the Wallowa terrane is the presence of Upper Triassic tholeiitic volcanic rocks within the presumably correlative Wrangellia terrane. Sarewitz (1983) pointed out that tholeiites such as these are characteristic of oceanic rifts and furthermore suggested that they should not be correlated with intermediate arc volcanic rocks of the Wallowa terrane in eastern Oregon and western Idaho. Despite compositional differences between these Upper Triassic volcanic rocks, paleomagnetic data, faunal assemblages, and stratigraphic sequences within the two terranes are so similar as to suggest a common heritage. One possible scenario is that the Wrangellia terrane, in the strict sense, was part of a rifted backarc basin lying immediately west of an east-facing volcanic island arc. The forearc realm of this arc is now preserved in eastern Oregon as the Wallowa terrane. Western parts of the arc and backarc regions were transported north along large right-lateral strike-slip faults that modified the western North America continental margin during the Cretaceous and Tertiary. These dispersed backarc fragments of the Wrangellia terrane are now found on Vancouver Island and the Queen Charlotte Islands of British Columbia and in the Wrangell Mountains of Alaska.

Regardless of the specific geologic evidence opposing or supporting correlation of the Wallowa terrane with the Wrangellia terrane, the lumping or splitting of individual terranes will remain a difficult, if not futile, exercise until a more accurate model for terranes is developed. Such a model must consider the structural complexity and variability (in terms of lithologies, depositional environments, and faunal assemblages) of modern island-arc terranes in an accretionary tectonic setting such as the southwestern Pacific.

TERRANE SEDIMENTOLOGY AND MODERN ANALOGS

Advances in our understanding of modern subduction-related tectonics in Indonesia and the southwestern Pacific have led to a much greater appreciation of the complexities inherent in ancient accretionary orogenic belts (Hamilton, 1979; Silver and Smith, 1983). And while the recognition of these modern analogues certainly does not make the task of reconstructing a tectonic "collage" such as the Cordillera any simpler, it does help geologists to produce a reasonably accurate description of tectonic and sedimentary processes in complex accretionary settings.

One of the more distinctive characteristics of the Wallowa stratigraphic sequence is the abundance of carbonate sedimentary rocks, both in the Martin Bridge Limestone and Hurwal Formation. Although limestones are a minor component of forearc basins in the geologic record, carbonate sediments are extremely common in modern arc-trench systems of equatorial regions such as Indonesia and the southwestern Pacific. These occurrences indicate that favorable climatic conditions are no less important than clastic sediment supply in controlling carbonate sedimentation within arc-related basins. In the case of the Wallowa terrane, a low equatorial paleolatitude (<20°) is suggested by the abundant carbonate sedimentary deposits and confirmed by paleomagnetic data, as discussed in the following section.

The Mentawai Trough (Sumatra forearc) provides an interesting modern analog of volcanic forearc sedimentation proposed here for the Wallowa terrane in the Late Triassic (fig. 1.12). Depositional environments and sedimentary processes in the Sumatra forearc region are very similar to those observed in the Wallowa terrane. Sedimentation in the Mentawai Trough is dominated by carbonate and arc-derived clastic material (Karig and others, 1980; Beaudry and Moore, 1981; Moore and others, 1982). Clastic sediments in the forearc basin are primarily deep-water turbidites fed by submarine canyons, which emanate from the Sumatra Shelf. During quiescent periods, shallow-water limestones were deposited as part of a carbonate platform, which built out into the forearc region. This platform apparently underwent several episodes of subsidence and drowning as the result of tectonic activity in the arc and subduction complex. Presently, shallow-water carbonate sedimentation is dominant along the shelf except in those areas that receive large quantities of arc-derived terrigenous sediments.

Deformed strata of the Sunda trench subduction complex are exposed on Nias Island, Nicobar Islands, and other islands along the outer-arc high. Extensive uplift of this accretionary prism appears to be related to offscraping of Bengal Fan sediments, which are being subducted as part of the Indian Plate. The outer-arc high is less well developed to the southeast near

Java, where Bengal Fan sediments are not present within the trench. Sediments eroded from this uplifted subduction complex (including recent reef material fringing the outer-arc islands) are deposited both within the outer realm of the forearc basin and within ponded basins on the inner slope of the Sunda trench. Oblique convergence between the Indian Plate and the Asian Plate has resulted in dextral strike-slip faults, which cut across both the accretionary complex and the Sumatra arc massif (Karig and others, 1980). Similar faulting in the Wallowa terrane during late Norian time probably generated coarse conglomerates of the Excelsior Gulch and Deadman Lake units.

Unlike the complex accretionary island-arc setting of the Wallowa terrane, the Sumatra arc is actually a rather simple continental-margin arc built above preexisting Paleozoic and Mesozoic basement rocks.

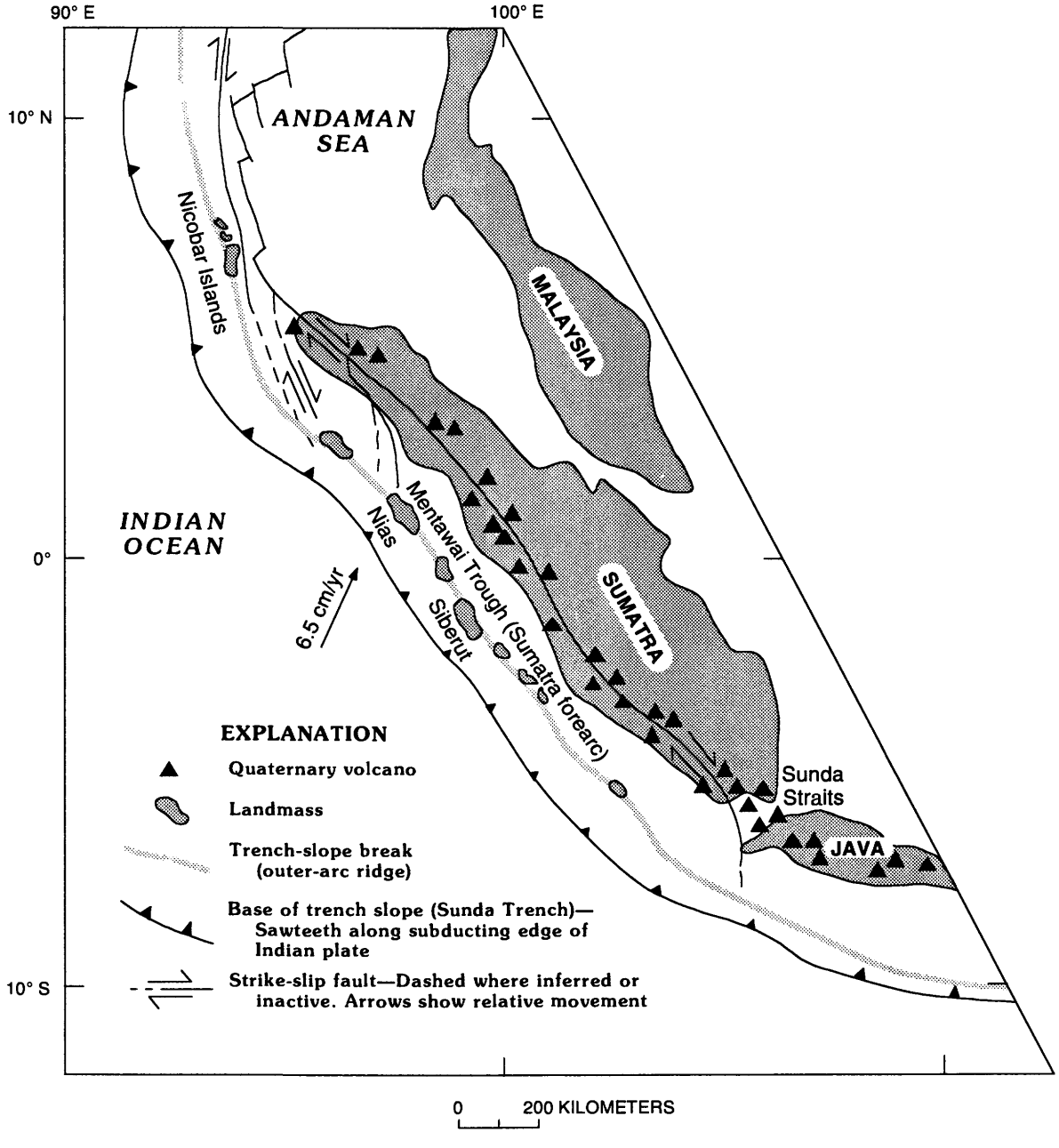

FIGURE 1.12.—Sketch map of the western Sunda arc, Indonesia. Sedimentary tectonics in this arc-trench system are probably analogous to those of the Wallowa terrane in the Late Triassic. Indian Plate is moving NNE at 6.5 cm per year.

Whereas the Mentawai Trough provides a valuable sedimentary analog, subduction- and accretion-related tectonics of the Wallowa terrane are probably more analogous to the modern Solomon Islands arc. The Solomon arc originally developed as a northeast-facing oceanic island arc in the late Eocene (Coulson and Vedder, 1986). Southwest-directed subduction of the Pacific Plate under the Solomon Islands ceased at the end of Miocene time, most likely as a result of tectonic accretion of the Ontong-Java terrane. At that time there appears to have been a reversal in arc polarity, and northeast-directed subduction commenced on the southwest side of the arc. Volcaniclastic and carbonate sedimentation in intra-arc and forearc basins of the Solomon Islands has a very complex history, primarily as a result of this subduction-zone flipping in the late Miocene. It is possible, but at this time not proven, that a similar reversal of arc polarity could have played an important role in the tectonic history of the Wallowa terrane. Unlike Sumatra, there is no evidence in the Solomon Islands of a well-developed accretionary prism, which could have been a local source of forearc sediments. There is no thick accumulation of sediments offshore of the Solomon Islands (such as the Bengal Fan) that might be scraped off the downgoing oceanic plate and incorporated into the suduction complex.

SUMMARY AND CONCLUSIONS

Strata of the Martin Bridge Limestone and Hurwal Formation record carbonate and clastic sedimentation in the Wallowa terrane during the Late Triassic and Early Jurassic. These sedimentary deposits establish important constraints on the tectonic development of the terrane prior to the beginning of accretion-related deformation in the Middle and Late Jurassic. In addition, they provide a critical measure with which to compare sedimentary processes and environments from ancient and modern volcanic arc-trench systems.

Following cessation of volcanic activity in the Karnian, platform and basinal sediments of the Martin Bridge Limestone were deposited in a carbonate-dominated forearc (?) basin. However, carbonate sedimentation in this part of the Wallowa terrane was relatively short lived and was succeeded by clastic sediments of the Hurwal Formation. Stratigraphic relations between the Hurwal and Martin Bridge suggest that they are, at least in part, lateral facies equivalents. Transgression of Hurwal clastic sediments over the subsiding Martin Bridge platform in the Wallowa Mountains was the result of a renewed influx of volcaniclastic sediments and a continued deepening of the depositional basin.

Oblique-slip faulting within the southern part of the Wallowa terrane during the early and middle Norian is indicated by shear zones such as that at Oxbow. Hurwal conglomerates of the same age (Deadman Lake and Excelsior Gulch units) record isolated sedimentary responses to this tectonism and indicate that the Wallowa terrane was structurally coupled to the actively deforming Baker terrane in the Late Triassic. Radiolarian chert clasts within conglomerates of the Excelsior Gulch unit further suggest a provenance link with the Baker terrane.

Certain aspects of the sedimentary tectonic model presented here—in particular, the volcanic provenance of the Hurwal Formation—strengthen proposed correlations of the Wallowa terrane with parts of the Wrangellia terrane. However, questions regarding the original paleolatitude and subsequent displacement history of the terrane(s) remain. Paleomagnetic data from both the Triassic volcanic rocks in the Wallowa and Wrangellia terranes indicate an original paleolatitude of 18±4° (Hillhouse and others, 1982), but this does not allow a unique solution regarding a northern or southern hemisphere origin. A northern hemisphere origin would imply little or no latitudinal displacement (relative to the North American craton) of that part of the terrane preserved in eastern Oregon and western Idaho.

The sedimentological evidence from this study does not support the notion of a distant or exotic (southern hemisphere) origin for the Wallowa terrane (Follo, 1986). The dominance of arc- and accretionary prism-derived sedimentary rocks in the Wallowa Mountains indicates that convergent-plate-margin tectonic processes strongly influenced sedimentation throughout the history of the terrane. Furthermore, an original eastern Pacific location for the Wallowa terrane is suggested by previous paleontological studies of Late Triassic bivalves from the Wallowa and Wrangellia terranes (Newton, 1983; Silberling, 1986). Faunal affinities with the North American craton indicate that these terranes, while not necessarily linked to the continent, originated close enough to the continent to allow faunal exchange. Origin of the Wallowa terrane in the eastern Pacific leaves minimal room for subsequent eastward displacement, and it also implies that very little north-south motion could be accomplished through oblique convergence of the terrane with the continental margin of North America. Furthermore, there is no evidence, either in terms of characteristic strike-slip basin development or distinctive patterns of sedimentary provenance, that significant latitudinal displacements of the Wallowa terrane occurred

during the Late Triassic and Jurassic along continental-margin transform fault systems.

I propose that the Wallowa terrane developed as part of an east-facing volcanic-arc system, which developed at low northerly paleolatitudes, and was separated from the continental margin of North America by a narrow ocean basin. West-dipping oblique subduction under the Wallowa terrane led to the closure of this marginal basin in the Middle Jurassic. Initial accretion of the Wallowa terrane most likely led to tectonic reshuffling of the existing continental-margin sequences. Final accretion of the Wallowa terrane to the North American craton was not complete until the end of the Early Cretaceous (Albian), as indicated by metamorphic ages of 105 to 95 Ma from the Riggins area of western Idaho, where deformed rocks of the Wallowa terrane are juxtaposed with cratonal units along a complex tectonic suture (Lund and others, 1985).

REFERENCES CITED

Abbate, Ernesto, Bortolotti, Valerio, and Passerini, Pietro, 1970, Olistostromes and olistoliths: Sedimentary Geology, v. 4, p. 521–557.

Ash, Sydney, 1991, A new Jurassic Phlebopteris (Plantae, Filicales) from the Wallowa terrane in the Snake River canyon, Oregon and Idaho: Journal of Paleontology, v. 65, p. 322–329.

Avé Lallemant, H.G., Schmidt, W.J., and Kraft, J.L., 1985, Major Late-Triassic strike-slip displacement in the Seven Devils terrane, Oregon and Idaho: A result of left-oblique plate convergence?: Tectonophysics, v. 119, p. 299–328.

Beaudry, Desiree, and Moore, G.F., 1981, Seismic-stratigraphic framework of the forearc off central Sumatra, Sunda Arc: Earth and Planetary Science Letters, v. 54, p. 17–28.

Beck, M.E., Jr., 1986, Model for late Mesozoic-early Tertiary tectonics of coastal California and western Mexico and speculations on the origin of the San Andreas fault: Tectonics, v. 5, p. 49–64.

Blome, C.D., Jones, D.L., Murchey, B.L., and Lienecki, Margaret, 1986, Geologic implications of radiolarian-bearing Paleozoic and Mesozoic rocks from the Blue Mountains province, eastern Oregon, *in* Vallier, T.L., and Brooks, H.C., eds., Geology of the Blue Mountains Region of Oregon, Idaho, and Washington: Biostratigraphy and Paleontology: U.S. Geological Survey Professional Paper 1435.

Bond, J.G., 1978, Geologic map of Idaho: Idaho Bureau of Mines and Geology, scale 1:500,000.

Bromley, R.G., and Ekdale, A.A., 1984, Chondrites: A trace fossil indicator of anoxia in sediments: Science, v. 224, p. 872–874.

Brooks, H.C., and Vallier, T.L., 1978, Mesozoic rocks and tectonic evolution of eastern Oregon and western Idaho, *in* Howell, D.G., and McDougall, K.A., eds., Mesozoic Paleogeography of the Western United States: Society of Economic Paleontologists and Mineralogists Pacific Coast Paleogeography Symposium 2, p. 133–145.

Carnahan, G.L., 1962, Geology of the southwestern part of Eagle Cap quadrangle, Wallowa Mountains, Oregon: Oregon State University, Masters thesis, 108 p.

Cook, H.E., 1983, Ancient carbonate platform margins, slopes, and basins, in Cook and others, eds., Platform Margin and Deep Water Carbonates: Society of Economic Paleontologists and Mineralogists Short Course No. 12, p. 5.1–5.189.

Cook, H.E., McDaniel, P.N., Mountjoy, E.W., and Pray, L.C., 1972, Allochthonous carbonate debris flows at Devonian bank ('reef') margins, Alberta, Canada: Bulletin of Canadian Petroleum Geology, v. 20, p. 439–497.

Coward, R.I., 1982, The Elkhorn Ridge Argillite: A deformed accretionary prism in northeastern Oregon: Geological Society of America Abstracts with Programs, v. 14, p. 157.

Coulson, F.I., and Vedder, J.G., 1986, Geology of the central and western Solomon Islands, *in* Vedder, J.G., Pound, K.S., and Boundy, S.Q., eds., Geology and offshore resources of Pacific island arcs—central and western Solomon Islands: Circum-Pacific Council for Energy and Mineral Resources Earth Science Series, v. 4, p. 59–87.

Dickinson, W.R., 1979, Mesozoic forearc basin in central Oregon: Geology, v. 7, p. 166–170.

Follo, M.F., 1986, Sedimentology of the Wallowa terrane, northeastern Oregon: Cambridge, Massachusetts, Harvard University, Ph.D. dissertation, 292 p.

Follo, M.F., and Siever, Ray, 1985, Carbonate platform margin facies on an evolving suspect terrane: Geological Society of America Abstracts with Program, v. 17, p. 584.

Glerup, M.O., 1960, Economic geology of the Lime Point area, Nez Perce County, Idaho: Moscow, University of Idaho, M.S. thesis, 40 p.

Grant, P.R., 1980, Limestone units within the Triassic Wild Sheep Creek Formation of the Snake River canyon: Pullman, Washington State University, M.S. thesis, 103 p.

Hamilton, Warren, 1963, Metamorphism in the Riggins region, western Idaho: U.S. Geological Survey Professional Paper 436, 95 p.

Hamilton, Warren, 1979, Tectonics of the Indonesian region: U.S. Geological Survey Professional Paper 1078, 345 p.

Hillhouse, J.W., Grommé, C.S., and Vallier, T.L., 1982, Paleomagnetism and Mesozoic tectonics of the Seven Devils volcanic arc in northeastern Oregon: Journal of Geophysical Research, v. 87, p. 3777–3794.

Jones, D.L., Silberling, N.J., and Hillhouse, J.W., 1977, Wrangellia—a displaced terrane in northwestern North America: Canadian Journal of Earth Science, v. 14, p. 2565–2577.

Karig, D.E., Lawrence, M.B., Moore, G.F., and Curray, J.R., 1980, Structural framework of the fore-arc basin, NW Sumatra: Journal of the Geological Society of London, v. 137, p. 77–91.

Laudon, T.S., 1956, The stratigraphy of the Upper Triassic Martin Bridge Formation and Lower Sedimentary Series of the northern Wallowa Mountains, Oregen: Madison, University of Wisconsin, M.S. thesis, 100 p.

Lund, Karen, in press, Metamorphic and structural history of island-arc rocks in the Slate Creek-John Day Creek area, west-central Idaho, *in* Vallier, T.L., and Brooks, H.C., eds., Geology of the Blue Mountains region of Oregon, Idaho, and Washington: Petrology and tectonic evolution of a pre-Tertiary island arc: U.S. Geological Survey Professional Paper 1438.

Lund, Karen, Scholten, Robert, and McCollough, W.F., 1983, Consequences of interfingered lithologies in the Seven Devils island arc: Geological Society of America Abstracts with Program, v. 15, p. 284.

Lund, Karen, Snee, L.W., and Sutter, J.F., 1985, Style and timing of suture-related deformation in island arc rocks of western Idaho: Geological Society of America Abstracts with Program, v. 17, p. 367.

Moore, G.F., Curray, J.R., and Emmel, F.J., 1982, Sedimentation in the Sunda Trench and forearc region, *in* Leggett, J.K., ed., Trench-Forearc Geology: Sedimentation and Tectonics on Modern and Ancient Active Plate Margins: Geological Society of London Special Publication 10, p. 245–258.

Muller, J.E., 1977, Evolution of the Pacific margin, Vancouver Island, and adjacent regions: Canadian Journal of Earth Science, v. 14, p. 2062–2085.

Mullins, H.T., 1983, Modern carbonate slopes and basins of the Bahamas, in Cook, and others, eds., Platform Margin and Deep Water Carbonates: Society of Economic Paleontologists and Mineralogists Short Course No. 12, p. 4.1–4.138.

Mullins, H.T., and Cook, H.E., 1986, Carbonate apron models: Alternatives to the submarine fan model for paleoenvironmental analysis and hydrocarbon exploration: Sedimentary Geology, v. 48, p. 37–79.

Newton, C.R., 1983, Paleozoogeographic affinities of Norian bivalves from the Wrangellian, Peninsular, and Alexander terranes, western North America, *in* Stevens, C.H., ed., Pre-Jurassic rocks in western North American suspect terranes: Pacific Section, Society of Economic Paleontologists and Mineralogists, p. 37–48.

———1986, Late Triassic bivalves of the Martin Bridge Limestone, Hells Canyon, Oregen: Taphonomy, paleoecology, paleozoogeography: U.S. Geological Survey Professional Paper 1435, p. 7–21.

———1987, Biogeographic complexity in Triassic bivalves of the Wallowa terrane, northwestern United States: Oceanic islands, not continents, provide the best analogues: Geology, v. 15, p. 1126–1129.

Nolf, B.O., 1966, Structure and stratigraphy of part of the northern Wallowa Mountains, Oregon: Princeton University, Ph.D. dissertation, 135 p.

Prostka, H.J., 1962, Geology of the Sparta quadrangle, Oregon: State of Oregon, Department of Geology and Mineral Industries Geological Map Series GMS-1, scale 1:62,500.

———1963, The geology of the Sparta quadrangle, Oregon: Johns Hopkins University, Ph.D. dissertation, 245 p.

Read, J.F., 1985, Carbonate platform facies models: American Association of Petroleum Geologists Bulletin, v. 69, p. 1–21.

Ross, C.P., 1938, The geology of part of the Wallowa Mountains: Oregon Department of Geology and Mineral Industries Bulletin no. 3, 74 p.

Sarewitz, Daniel, 1983, Seven Devils terrane: Is it really a piece of Wrangellia?: Geology, v. 11, p. 634–637.

Silberling, N.J., 1983, Stratigraphic comparison of the Wallowa and Huntington terranes, northeast Oregon: Geological Society of America Abstracts with Program, v. 15, p. 372.

———1986, Biogeographic significance of the Upper Triassic bivalve Monotis in circum-Pacific accreted terranes, *in* Howell, D.G., ed., Tectonostratigraphic Terranes of the Circum-Pacific Region: Circum-Pacific Council for Energy and Mineral Resources, Earth Science Series, Number 1, p. 63–70.

Silberling, N.J., and Jones, D.L., 1984, Lithotectonic terrane maps of the North American Cordillera: U.S. Geological Survey Open File Report 84-523, scale 1:250,000.

Silberling, N.J., and Tozer, E.T., 1968, Biostratigraphic classification of the marine Triassic in North America: Geological Society of America Special Paper 110, 63 p.

Silver, E.A., and Smith, R.B., 1983, Comparison of terrane accretion in modern Southeast Asia and the Mesozoic North American Cordillera: Geology, v. 11, p. 198–202.

Simpson, R.W., and Cox, Allan, 1977, Paleomagnetic evidence for tectonic rotation of the Oregon Coast Range: Geology, v. 5, p. 585–589.

Smith, J.P., 1912, The occurrence of coral reefs in the Triassic of North America: American Journal of Science, v. 33, p. 92–96.

———1927, Upper Triassic marine invertebrate faunas of North America: U.S. Geological Survey Professional Paper 141, 262 p.

Smith, W.D., and Allen, J.E., 1941, Geology and physiography of the northern Wallowa Mountains, Oregon: Oregon Department of Geology and Mineral Industries Bulletin, no. 12, 64 p.

Stanley, G.D., Jr., 1986, Late Triassic coelenterate faunas of western Idaho and northeastern oregon: Implications for biostratigraphy and paleogeography: U.S. Geological Survey Professional Paper 1435, p. 23–39.

Stanley, G.D., Jr., and Beauvais, Louise, 1990, Middle Jurassic corals from the Wallowa terrane, west central Idaho: Journal of Paleontology, v. 64, p. 352–362.

Stanley, G.D., Jr., and Senowbari-Daryan, Baba, 1986, Upper Triassic, Dachstein-type reef limestone from the Wallowa Mountains, Oregon: Report of the first occurrence in the United States: Palaios, v. 1. p. 172–177.

Underwood, M.B., and Bachman, S.B., 1982, Sedimentary facies associations within subduction complexes, *in* Leggett, J.K., ed., Trench-Forearc Geology: Sedimentation and Tectonics on Modern and Ancient Active Plate Margins: Geological Society of London Special Publication 10, p. 537–550.

Vallier, T.L., 1967, The geology of part of the Snake River canyon and adjacent areas in northeastern Oregon and western Idaho: Corvallis, Oregon State University, Ph.D. dissertation, 267 p.

———1974, A preliminary report on the geology of part of the Snake River canyon, Oregon and Idaho: Oregon Department of Geology and Mineral Industries Geological Map Series GMS-6, scale 1:125,000.

———1977, The Permian and Triassic Seven Devils Group, western Idaho and northeastern Oregon: U.S. Geological Survey Bulletin 1437, 58 p.

Walker, G.W., 1977, Geologic map of Oregon east of the 121st Meridian: U.S. Geological Survey Miscellaneous Investigations Series Map I-902, scale 1:500,000.

Walker, R.G., 1975, Generalized facies models for resedimented conglomerates of turbidite association: Geological Society of America Bulletin, v. 86, p. 737–748.

Weiss, P.L., Gualtieri, J.L., Cannon, W.F., Tuchek, E.T., McMahan, A.B., and Federspiel, F.E., 1976, Mineral resources of the Eagle Cap Wilderness and adjacent areas, Oregon: U.S. Geological Survey Bulletin 1385-E, 100 p.

West, I.M., 1964, Evaporite diagenesis in the lower Purbeck beds of Dorset: Proceedings of the Yorkshire Geological Society, v. 34, p. 315–330.

Whalen, M.T., 1985, The carbonate petrology and paleoecology of Upper Triassic limestones of the Wallowa terrane, Oregon and Idaho: Missoula, University of Montana, M.S. thesis, 151 p.

Whalen, M.T., and Stanley, G.D., 1985, Triassic stratigraphy and paleontology of the Wrangell Mountains and Hells Canyon: Is the Wallowa terrane really part of Wrangellia?: Proceedings of the Pacific Division, American Association for the Advancement of Science, v. 4, pt. 1, p. 43.

Wilson, Douglas, and Cox, Allan, 1980, Paleomagnetic evidence for tectonic rotation of Jurassic plutons in Blue Mountains, eastern Oregon: Journal of Geophysical Research, v. 85, p. 3681–3689.

2. THE MESOZOIC GEOLOGIC EVOLUTION OF THE NORTHERN WALLOWA TERRANE, NORTHEASTERN OREGON AND WESTERN IDAHO

By PATRICK M. GOLDSTRAND[1]

CONTENTS

ABSTRACT

Mesozoic rocks exposed along the Snake River in the northern Wallowa terrane represent a volcanic island and its associated sedimentary basins within the Blue Mountains island arc of Washington, Oregon, and Idaho. In the northern part of the Wallowa terrane, rock units include the Wild Sheep Creek, Doyle Creek, and Coon Hollow Formations, the (informal) Imnaha intrusion, and the (informal) Dry Creek stock.

The volcanic rocks of the Ladinian to Karnian Wild Sheep Creek Formation show two stages of evolution—an early dacitic phase (lower volcanic facies) and a late mafic phase (upper volcanic facies). The two volcanic facies are separated by eruption-generated turbidites of siliceous argillites and arkosic arenites (argillite-sandstone facies). The two magmatic phases of the Wild Sheep Creek Formation may be recorded by the compositional zoning from older quartz diorite and diorite to younger gabbro in the Imnaha intrusion. Although the Late Triassic Imnaha intrusion is in fault contact with the Wild Sheep Creek Formation, it may be a subduction-related pluton and was the likely magma source for the Wild Sheep Creek Formation.

Interbedded with the upper volcanic facies are eruption-generated turbidite and debris flow deposits (sandstone-breccia facies) and thick carbonate units (limestone facies). The limestone facies consists of two marker units, which may represent carbonate platform environments. Clast imbrication, fossil orientation, and cross-stratification in the Wild Sheep Creek Formation indicate a shoaling to subaerial volcanic island to the south and southeast; sediment was transported to the north and northwest.

The Karnian Doyle Creek Formation consists largely of epiclastic conglomerate, sandstone, and shale that were deposited in well-oxygenated basins. Vitric tuffs interbedded with these sediments suggest shallow or subaerial pyroclastic eruptions. Quartz diorite clasts in this formation may indicate uplift and erosion of part of the Imnaha intrusion related to the later emplacement of the gabbroic part of the intrusion.

The Norian Martin Bridge Limestone and Upper Triassic and Lower Jurassic Hurwal Formation, exposed elsewhere in the region, were either not deposited in the study area (see fig. 2.1) or were subsequently eroded prior to deposition of Jurassic strata.

During the Middle and Late Jurassic, clastic sediments of the Coon Hollow Formation were deposited over the tilted Triassic carbonate and volcanic rocks of the Wild Sheep Creek Formation. The nearshore to offshore deposits of the sandstone-conglomerate facies fine upward from a basal conglomerate to hummocky cross-stratified sandstone into graded sandstone and shale. Crossbedding measurements suggest that the shoreline trended approximately northeast-southwest and that the sea transgressed southeastward onto the terrane. The provenance for the sandstone-conglomerate facies is the Wild Sheep Creek Formation and the Imnaha intrusion. This facies fines upward into the flysch facies, which represents a prograding submarine fan. The flysch facies coarsens and thickens upward from nonchanneled outer fan to channeled mid-fan deposits. The provenance of the flysch facies is the Wild Sheep Creek Formation, the Imnaha intrusion, and a radiolarian chert-metasedimentary source.

The chert-metasedimentary source may delimit the timing of the amalgamation of the Wallowa and Baker terranes to the Oxfordian. Uplift and extension was associated with this collisional event, and hornblende dikes and sills intruded the Wallowa terrane. After this intrusive event, northwest-southeast compression

[1]Environmental Sciences Division, Oak Ridge National Laboratory, Oak Ridge, TN 37831

and regional metamorphism to the greenschist facies occurred during the Late Jurassic. This collisional event may be related to the initial accretion of the Wallowa and Baker terranes to the western margin of North America. Possibly related to this accretion is a pyroxene-hornblende diorite stock (Dry Creek stock), which intruded the Wallowa terrane at shallow depths around 139.5±2.1 Ma.

INTRODUCTION

Rocks of the northern part of the Wallowa terrane (herein referred to as the northern Wallowa terrane) crop out along the Snake River and tributary streams in northeastern Oregon and western Idaho (fig. 2.1). These rocks consist of the Triassic Wild Sheep Creek and Doyle Creek Formations and the Jurassic Coon Hollow Formation. Two intrusions, the (informal) Imnaha intrusion and the (informal) Dry Creek stock, are exposed along the Snake River and its tributaries. These volcanic, plutonic, and sedimentary rocks were studied to determine the volcanic evolution of a volcanic island and the later sedimentary deposition within an intra-arc basin in the Blue Mountains island arc. Pre-Tertiary stratigraphy, petrology, and facies associations were used to interpret the depositional environments, provenances, paleogeography, and tectonic history of the northern Wallowa terrane.

Fieldwork was conducted during the summer of 1986 and consisted of mapping at a scale of 1:24,000, detailed measurements of stratigraphic sections, and paleocurrent analysis. Owing to the steep topography and lack of roads in the study area, access is primarily by boat and foot. Stratigraphic sections were measured with a Jacob's staff, and pebble counts were made on all pebbles 10 cm or larger within a 1 m^2 area. Laboratory studies consisted of petrographic analysis of 60 samples of medium- to coarse-grained sandstone using the Gazzi-Dickinson point-counting method described by Ingersoll and others (1984). Approximately 50 thin sections of the volcanic and plutonic rock suite were studied petrographically. Geochemical analysis and radiometric dating of the volcanic and plutonic rocks were done at the U.S. Geological Survey.

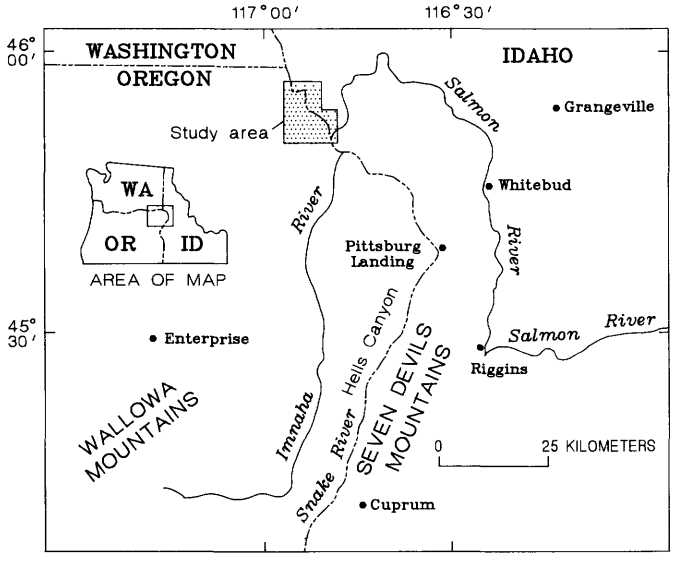

FIGURE 2.1.—Index map of area near Wallowa and Seven Devils Mountains, Oregon and Idaho. Boundary of northern Wallowa terrane not shown. Study area denoted by stipple pattern.

ACKNOWLEDGMENTS

Partial financial support was provided by a grant from the CREST Foundation and a Western Washington University Geology Department Research award. I would like to thank George Stanley for coral identification, Charles Blome for radiolarian identification, L.B.G. Pickthorn for K-Ar analysis, M. Dyslin, D. Vivit, R. Lerner, and N. Elsheimer for geochemical analysis, C.A. Suczek, J. De Chant, D.L. White, J.D.L. White, and T. Vallier for their critical reviews and C. Suczek, R.S. Babcock, and T. Vallier for their helpful discussions and suggestions. I would especially like to thank Myrna and Wally Beamer for boat transportation into and out of the field area, and Tracy Vallier for all his help and time. Without their help, this study could not have been completed.

GEOLOGY

In the study area, the principal lithologic units are the Triassic Wild Sheep Creek and Doyle Creek Formations, Jurassic Coon Hollow Formation, Imnaha intrusion, and Dry Creek stock. Overlying much of the area and separated from the underlying pre-Tertiary strata by a pronounced angular unconformity is the Miocene Columbia River Basalt Group. These younger basalts are not included in this study.

The Wild Sheep Creek Formation consists of more than 1,500 m of volcanic flow rocks, pillow lava, volcaniclastic rocks, and limestone (figs. 2.2 and 2.3). Fossil bivalves delimit the age of the Wild Sheep Creek Formation within the Ladinian and Karnian (Vallier and Hooper, 1976; Vallier, 1977).

The overlying Doyle Creek Formation crops out on the Oregon side of the Snake River and is discontinuous within the study area (fig. 2.2). Its maximum thickness of approximately 200 m of epiclastic rocks and tuff deposits was measured in the Cook Creek

drainage. The Karnian age for the Doyle Creek Formation is based on fossils collected outside the study area (Vallier and Hooper, 1976).

Unconformably overlying the Wild Sheep Creek and Doyle Creek Formations is the Coon Hollow Formation. The Coon Hollow Formation consists of as much as 580 m of shale, sandstone, and conglomerate. The age of the Coon Hollow Formation in the study area is Middle and Late Jurassic (Vallier and Hooper, 1976).

The Imnaha intrusion is exposed in the southern part of the study area (fig. 2.2), where it is structurally juxtaposed against the Wild Sheep Creek Formation. The composition ranges from metagabbro to metaquartz diorite (Morrison, 1963), and it is Middle(?) and Late Triassic in age (Balcer, 1980; Walker, 1986).

The Dry Creek stock is an unmetamorphosed pyroxene-hornblende diorite that is exposed in the Cook Creek and Dry Creek drainage (fig. 2.2). The stock intrudes Upper Triassic and Lower Jurassic volcanic and sedimentary rocks, and its age is 139.5±2.1 Ma, as determined from K-Ar analysis (this report).

Hornblende diorite dikes and sills are abundant throughout the Wild Sheep Creek, Doyle Creek, and Coon Hollow Formations. Pyroxene diorite dikes intrude the northern margin of the Imnaha intrusion and unmetamorphosed diorite dikes are associated with the Dry Creek stock.

Late Jurassic regional metamorphism (to the lower greenschist facies) affected most of the pre-Tertiary rocks (Hamilton, 1963) with the exception of the Dry Creek stock. The sedimentary rocks surrounding this small intrusion are contact metamorphosed. For convenience, the prefix "meta" will be dropped from the terms metavolcanic and metasedimentary, but the rocks described herein (except the Dry Creek stock) are slightly metamorphosed to lower greenschist facies. Common metamorphic minerals include chlorite, epidote, prehnite, calcite, and sericite.

STRATIGRAPHY

WILD SHEEP CREEK FORMATION

Five mappable lithofacies are present in the Wild Sheep Creek Formation of the northern Wallowa terrane. These are, in ascending order, the lower volcanic facies, argillite-sandstone facies, upper volcanic facies, sandstone-breccia facies, and the limestone facies.

LOWER VOLCANIC FACIES

The stratigraphically lowest unit in the study area, with the possible exception of the Imnaha intrusion, is the lower volcanic facies. This facies is exposed along the Snake and Salmon Rivers and at their confluence, and it has a minimum thickness of approximately 500 m. The lower volcanic facies is in fault contact with the upper volcanic facies to the southeast, and to the east and north the upper and lower volcanic facies are separated by the argillite-sandstone facies (fig. 2.2).

The lower volcanic facies consists of massive flows, breccias, tuffs, and some pillow lavas. The flow rocks consist of microcrystalline and porphyritic dacites that range in color from light green and gray to red. Plagioclase (oligoclase and andesine) is the most common phenocryst, and clinopyroxene is the predominant mafic mineral. Flows are medium- to very thickly bedded, but some units are thinly bedded. Poorly developed, rare pillow lavas are associated with breccias. Flow tops are commonly brecciated and grade laterally into massive, unstratified flow breccias. The breccias are angular and clast supported in a matrix of silicified hyaloclastites.

Commonly associated with the breccias and flows are light green siliceous tuffs. These devitrified tuffs contain minor amounts of quartz, andesine, and amphibole. The quartz is clear, subhedral, and embayed, whereas amphiboles occur as euhedral psuedomorphs. Subrounded lithic fragments of crystal-lithic tuffs are locally present within these tuffs.

The lower volcanic facies represents dacitic submarine volcanic eruptions of flows and pyroclastic and autoclastic rocks. The presence of local pillow lavas within this facies as well as its association with the marine argillite-sandstone facies indicate deposition in a subaqueous environment. Autoclastic flow breccia and hyaloclastites formed on the top of flows by the rapid cooling induced by water. Distal parts of the flows were autobrecciated owing to rapid cooling and frictional movement downslope (Lajoie, 1976). The tuffs being interbedded with submarine sediments and the presence of pillow lavas both suggest deposition below sea level. Convolute laminations in the tuffs suggest gravity slumping after deposition.

ARGILLITE-SANDSTONE FACIES

Interbedded with and overlying the lower volcanic facies are volcaniclastic sandstones and argillites of the argillite-sandstone facies. The sedimentary rocks overlying the argillite-sandstone facies are approximately 300 m thick and are well exposed along the Snake River, 3 km northwest of its confluence with the Salmon River (fig. 2.2). Channel fills of arkosic arenites (classification from Dott, 1964) are common near the top of the lower volcanic facies and along

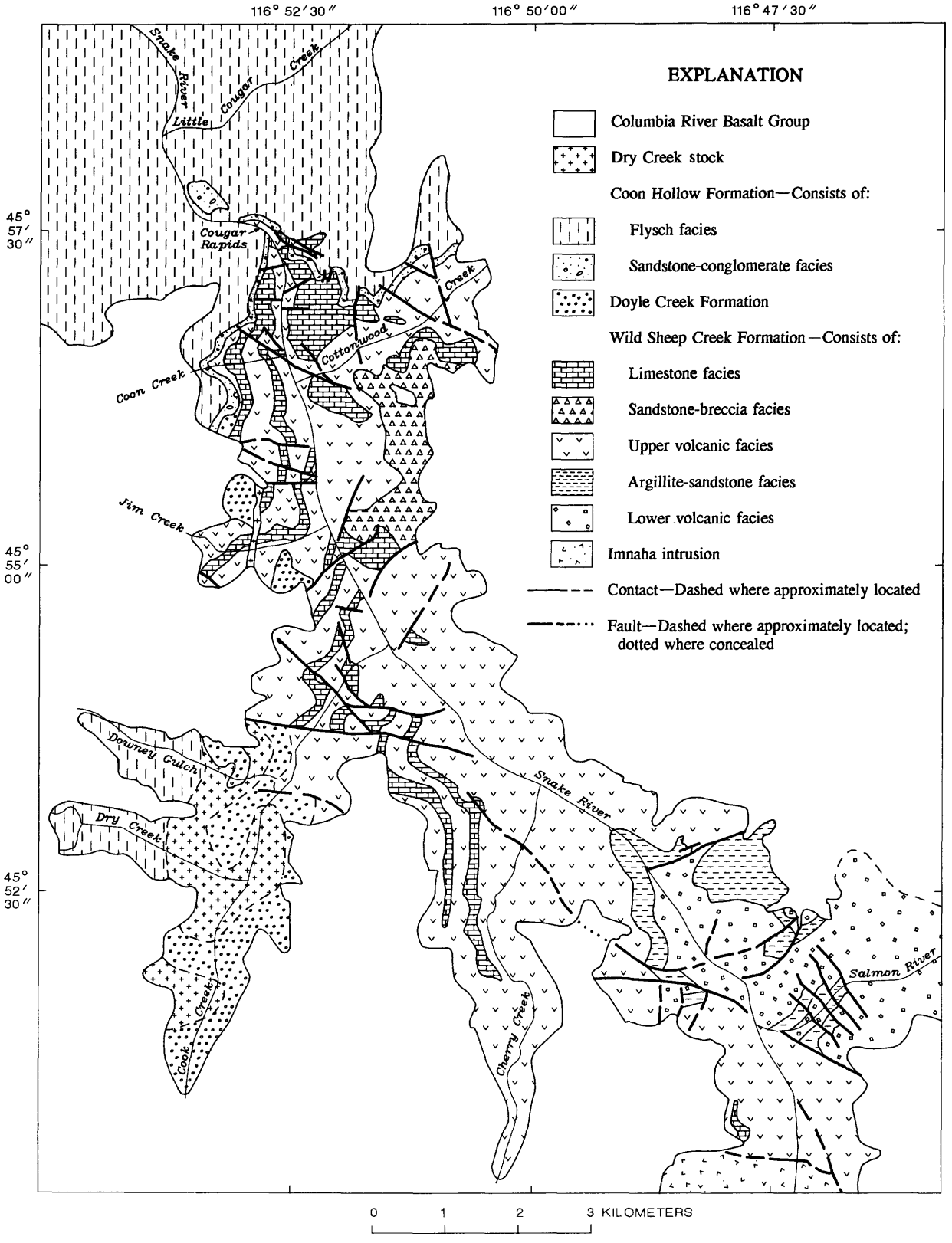

FIGURE 2.2.—Generalized geologic map of northern Wallowa terrane, northern Oregon and western Idaho (from Goldstrand, 1987).

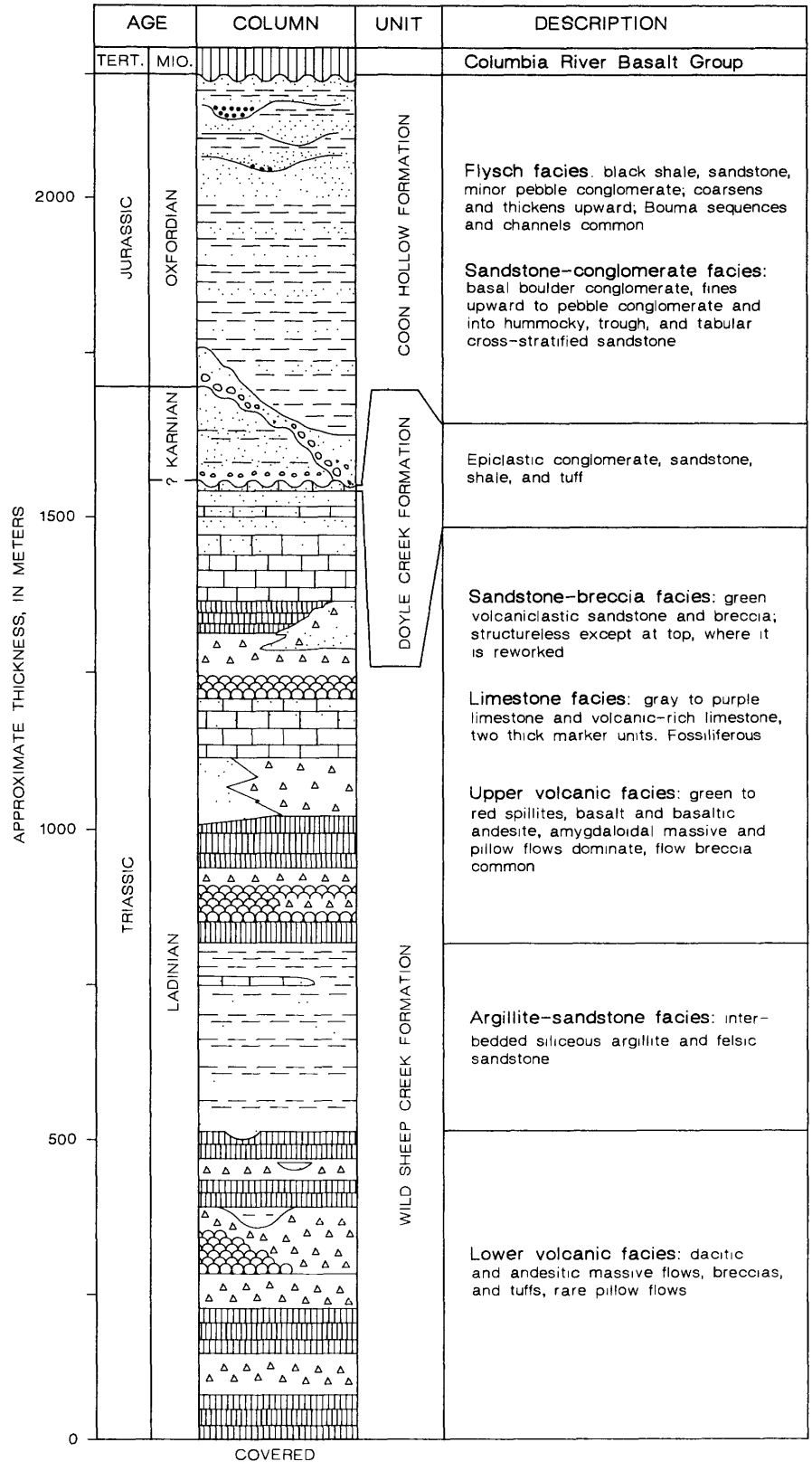

FIGURE 2.3.—Generalized stratigraphic column of geologic units in northern Wallowa terrane, northern Oregon and western Idaho. Wavy line denotes unconformity.

the Salmon River near its confluence with the Snake River; these channel fills are grouped with the argillite-sandstone facies.

Rocks of this facies are gray, thin- to medium-bedded volcaniclastic sandstones and siliceous argillites. Sandstone beds are commonly graded and have sharp basal contacts. Quartz and plagioclase crystals and felsic volcanic lithic fragments are concentrated at the bases of the beds. Several beds grade upward from devitrified ash and pumice into finely laminated siliceous argillite. Rarely, pumice is concentrated near the tops of the beds. Not only are individual beds graded, but sequences of approximately 20 to 40 beds thin and fine upward.

Channels are common in this facies and in the lower volcanic facies. Thick amalgamated sandstones fill channels within the argillite-sandstone facies, and conglomerates at the bases of these channels are derived from the felsic volcanic rocks of the lower volcanic facies. The channels are filled by lenticular volcaniclastic sandstone between 50 and 150 m thick and are increasingly common in the upper part of the lower volcanic facies.

Rare horizontal worm traces, load casts, soft-sediment slump folds, and minor interbeds of fossiliferous limestone suggest marine deposition. Overall, the argillite-sandstone facies fines upward into laminated argillite and minor amounts of impure carbonate lithologies.

The argillite-sandstone facies represents eruption-generated turbidity-current deposits similar to those described by Fiske and Matsuda (1964) and Busby-Spera (1986). During eruptions, pyroclastic debris was either erupted directly into the marine environment or settled to the ocean surface, if the eruption was subaerial. Dense crystal and lithic fragments settled rapidly back to the flanks of the volcano and were sloughed into deeper water as turbidity currents. The finer, less-dense fractions of the eruptive column (ash and pumice) settled out later and were deposited over the denser turbidites. The finely laminated argillites and local bioturbation indicate quiescence between eruptions.

As the lower volcanic facies was building the volcano, topographic lows served as channels for pyroclastic-flow deposits. These early channels filled in with sediment and were eventually covered by lava flows. As volcanic flows migrated to other areas, thick accumulations of volcanic turbidites were deposited in basins on the flanks of the volcano. The abundance of argillite and impure limestone in the upper part of the facies indicates that the basin had filled to the point that turbidity sedimentation had nearly ceased or overflowed into another basin.

UPPER VOLCANIC FACIES

The upper volcanic facies is the most voluminous unit in the study area; it is characterized by abundant mafic, amygdaloidal pillows and massive flows with associated breccias. Breccias and flows are interbedded with limestone and are less abundant in the uppermost part of the Wild Sheep Creek Formation, where carbonate and siliciclastic sedimentation dominated. To the south, the upper volcanic facies is in fault contact with the Imnaha intrusion. In the north, this facies is overlain by the Coon Hollow Formation.

Abrupt lateral and vertical facies changes within this facies make stratigraphic correlation difficult. However, two laterally continuous limestone units that crop out on the Oregon side of the Snake River serve as marker units within the upper volcanic facies (see "Limestone Facies" section). Four stratigraphic sections were measured (fig. 2.4), all on the Oregon side. In the Cook Creek drainage, a 550-m section was measured (fig. 2.4). The upper limestone marker unit is exposed 0.4 km northeast of the measured section, but it is covered by the Columbia River Basalt Group in the measured area. Therefore, approximately 200 more meters of section can be correlated from the second column shown in figure 2.4.

Petrographic analyses suggest that basalt is the most abundant rock type in the upper volcanic facies. Stratigraphically higher in the section, basaltic andesite is more common, but basalt is also present. Colors range between dark green and purple. Textures in these lavas include porphyritic, glomeroporphyritic, amygdaloidal, hyalophitic, hyalopilitic, pilotaxitic, trachytic, and microcrystalline. The flows are either thickly bedded pillows or massive lavas but include some thinly bedded pahoehoe lava.

Massive flows are very thickly bedded or are amalgamations of numerous thinner flows. Amygdules are common near the tops of the massive flows. Some massive flows grade laterally into pillow lavas. Pillows average 1 m in diameter, but larger pillows (2 to 3 m) and welded megapillows (Dimroth and others, 1978) are also common. Smaller pillows are subspherical or ellipsoidal and larger pillows are more elongate. Isolated pillows are commonly amygdaloidal and surrounded by green palagonite. Pillow breccias consist of complete pillows and pillow fragments set in a hyaloclastic matrix. Breccias are common at the tops of flows and where flows intrude sediments (shale or limestone). Massive breccia beds probably represent the distal facies of flows and grade into more proximal pillows and massive flows (Dimroth and others, 1978).

Plagioclase is the most common phenocryst in the porphyritic basalt. Although most plagioclase is albitized, compositions between An_6 and An_{50} were measured either by the Michel-Levy or A-normal method depending on the amount of alteration. Andesine is the most common unaltered plagioclase.

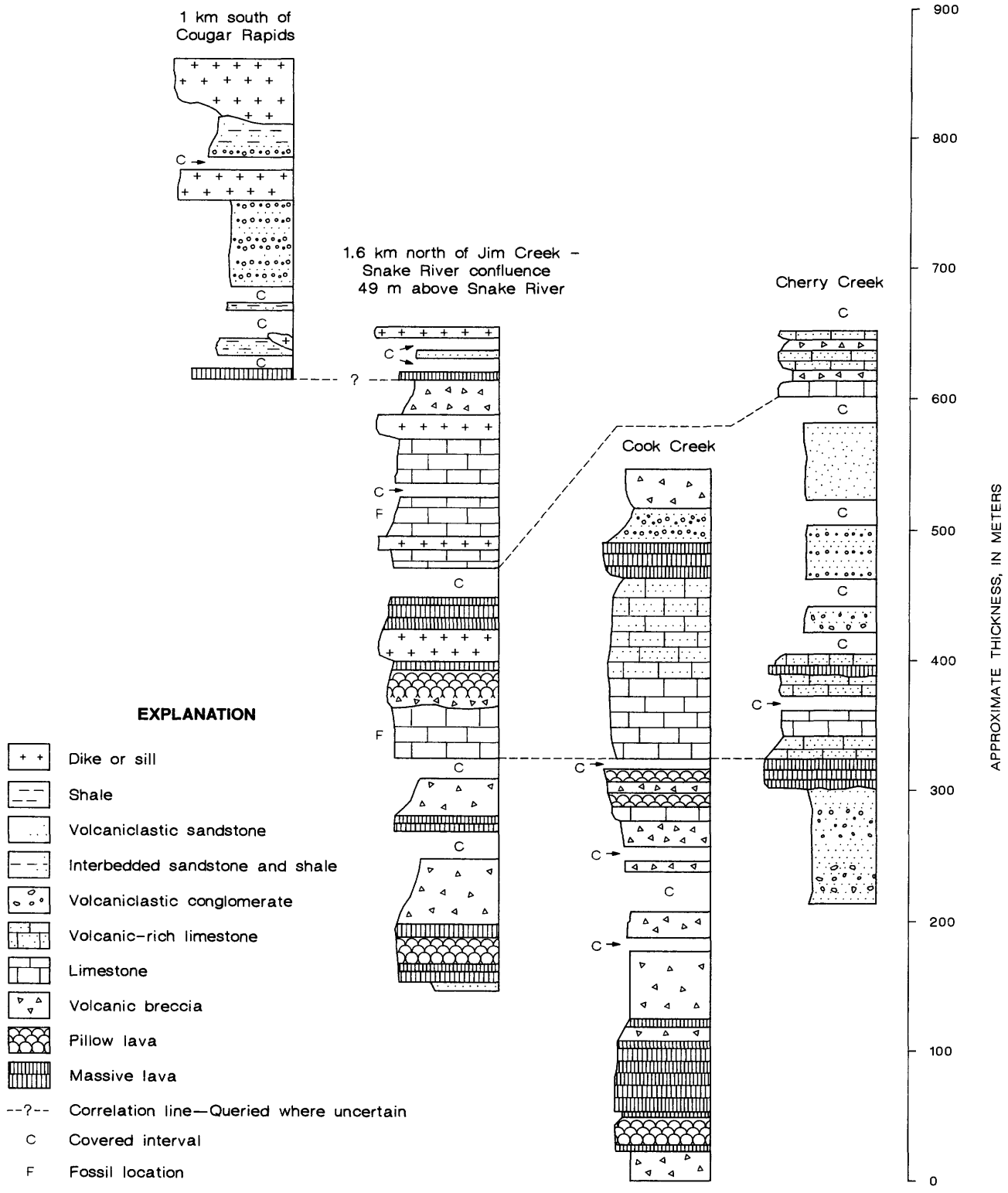

FIGURE 2.4.—Stratigraphic columns of Wild Sheep Creek Formation of northern Wallowa terrane, northern Oregon.

Augite is the dominant mafic mineral in the lower part of the facies but disappears at the transition between basalt and basaltic andesite. In the upper part of the section, amphibole is the major mafic mineral. Hematite is a major component of a large number of the volcanic rocks in the upper volcanic facies, either as an alteration product of mafic minerals or in the groundmass. Rocks with hematite in the groundmass are recognized in the field by their dark purple and red colors.

Nonwelded crystal-lithic tuff is interbedded with flows and breccias of the upper volcanic facies and is more common in the upper sections. The predominant crystal component is andesine; the lithic materials consist of microlitic, hyalopilitic, and pilotaxitic volcanic rock fragments. Scoriaceous lapilli are abundant in these units.

Interbedded with the flows and flow breccias of the upper volcanic facies are numerous epiclastic shale, sandstone, and conglomerate units. The thickest section of epiclastic sedimentary rocks was measured in the Cherry Creek drainage (fig. 2.4). Commonly the epiclastic units are 10 to 20 m thick and structureless to very thickly bedded. Volcanic clasts are round to subangular and are supported in a matrix of poorly sorted sandstone. Scoria clasts are common in these units. Clast imbrication within these units indicates paleocurrent flow to the north and west (fig. 5*A*, diagrams A and B). Rarely, density-current sequences of volcaniclastic sandstone and shale are present. They were deposited in topographic lows formed in the upper volcanic facies.

The upper volcanic facies is a thick series of lava flows and sedimentary deposits that formed on the flanks of a submarine volcano. The transition from pyroxene basalt to amphibole basaltic andesite records increasingly siliceous magma composition. The lateral transition from massive to pillowed lavas indicates the transition from proximal to distal flow facies (Dimroth and others, 1978), and massive pillow breccia may represent the most distal part of these flows.

Epiclastic sediments were deposited throughout the upper volcanic facies in topographic lows along the flanks of the volcanic island. Sediment was transported by density currents resulting from volcanic eruptions or debris flows. Clastic sedimentation continued until the depositional depressions were inundated by lava flows or covered by carbonate sediment. The petrology and northwesterly paleocurrent suggest a volcanic source terrane to the south and east (fig. 2.5*A*, diagrams A and B).

LIMESTONE FACIES

The limestone facies consists of gray to purple, medium- to thickly bedded micrite, pelmicrite, and volcaniclastic-rich limestone. Undifferentiated carbonate rocks crop out on both sides of the Snake River in the upper parts of the Wild Sheep Creek Formation. However, two thick limestone marker units crop out on the Oregon side from Cherry Creek to north of Coon Creek (fig. 2.2) and are the only stratigraphic marker units in the Wild Sheep Creek Formation.

The lower marker unit is between 40 and 130 m thick, and volcaniclastic-rich limestone is concentrated in its upper half. An 8-m-thick, thinly bedded tuff unit is interbedded with limestone in the Cook Creek area and thins laterally. The lower marker unit is thickest in the Cook Creek area and thins to the north and south (fig. 2.4). The upper marker unit is between 50 and 110 m thick and thickens to the north (fig. 2.4). The upper part of the unit grades upward from volcaniclastic-rich limestone into interbedded tuffs and epiclastic rocks. Scoriaceous lapilli are the dominant clasts in the volcaniclastic-rich limestone.

These two limestone marker units are important in delineating the lateral facies changes within the Wild Sheep Creek Formation. Below the lower unit, the upper volcanic facies changes from massive flows in the south (near Cherry Creek) to pillow basalt and pillow breccia (near Cook Creek) to breccia in the north (1 km south of Cook Creek, fig. 2.4). This marker unit is overlain by a thick section of volcaniclastic sediments in the south, which thins to the north. In the northernmost section, these carbonate rocks are overlain by pillow lavas. Blocks of the underlying limestone are locally incorporated into the base of the lava flows. Rare pillowed flows intrude the limestones; their intrusion caused disruption of the bedding and resulted in their brecciation.

The upper marker unit overlies volcaniclastic rocks to the south, breccia in the Cook Creek area, and massive flows to the north. The upper part of this unit generally grades upward from limestone to volcaniclastic sandstones in the south and is overlain by pillow breccia in the north (fig. 2.4).

The limestone facies is the most fossiliferous unit in the Wild Sheep Creek Formation. Crinoids, bivalves, brachiopods, and corals are locally abundant. *In situ* corals(?) were found in several locations, but no reef complexes were recognized. Silicified, branching organisms collected from the upper marker unit are too poorly preserved to be positively identified. If corals, they may be *Retiophyllia* or *Pinnacophyllum*

(George D. Stanley, written commun., 1987). Paleocurrent measurements on solitary coral and crinoid stem orientations indicate a north-south current direction in the limestone facies (fig. 2.5*A*, diagrams C and D). The association with *in situ* framework organisms, shell-lag deposits, and bimodal crosslaminations suggests wave orientation of these fossils rather than unidirectional density-current orientation (Jones and Dennison, 1970).

The presence of branching coral(?) and biogenic debris in a micritic matrix suggests a shallow-marine platform environment (Milliman, 1974; Wilson, 1974) for the limestone facies. The presence of scoriaceous lapilli tuff and vitric tuff interbedded in this facies indicates that the eruptive center was either subaerial or near the surface. Paleocurrent data for the upper volcanic and the limestone facies suggest a landmass to the southeast. The presence of coral, shell-lag deposits, and wave-oriented fossils in this facies indicate a shallow-marine depositional environment, within the photic zone and above the storm-wave base.

Several times during the evolution of the volcanic island, lava flows inundated the fringing carbonate platform. Some flows sank into the unconsolidated carbonate muds, while other lavas flowed over more cohesive limestones, ripped up carbonate blocks, and incorporated the blocks into the bases of the flows. As lava flows migrated to other regions on the volcano, the platform environment was reestablished.

SANDSTONE-BRECCIA FACIES

On the Idaho side of the Snake River is a discontinuous sequence of green volcaniclastic sandstone and breccia. This sedimentary unit overlies both the limestone and upper volcanic facies and, in contrast, is a slope-forming unit. This facies is overlain by undifferentiated, stratified volcaniclastic-rich limestone. Interbedded lava flows are concentrated near the base of this unit. This facies has a maximum thickness of approximately 400 m south of Cottonwood Creek and has been divided into lower, middle, and upper units on the basis of its sedimentary structures.

The lower unit of this facies consists of very poorly sorted sandstone and breccia. Breccia clasts (as much as 0.6 m in diameter) are green, angular to subangular, aphanitic or amygdaloidal pillow lava fragments supported in an epiclastic matrix. These volcanic lithic sandstones weather spheroidally and contain rare limestone clasts. No imbrication or other sedimentary structures were observed in the lower unit of the sandstone-breccia facies.

The lower unit fines upward into the middle unit, a poorly sorted volcanic breccia and sandstone that is stratified into 2-m-thick beds. Higher in this unit, inversely and normally graded sandstones are common. Several thin beds of vitric tuff are present in the middle unit, and scoriaceous rock fragments are common. Imbricated clasts in the middle unit suggest flow to the west (fig. 2.5*A*, diagram E).

The upper unit consists of thinly bedded, green sandstone; pebbly conglomerate; and minor amounts of shale. Trough cross-stratification, small channels, and shell-lag deposits are common. Fossils include bivalves, belemnites, and rare ammonite fragments, all of which show signs of reworking. Belemnite orientation, cross-stratification, and the trends of troughs indicate paleocurrent directions to the northwest, north, and northeast in the upper unit of the sandstone-breccia facies (fig. 2.5*A*, diagrams F, G, and H).

The lower unit of the sandstone-breccia facies may have been deposited as submarine debris flows. The angular, matrix-supported clasts; poor sorting; and the lack of internal structure indicate debris flow deposition (Mitchell, 1970; Pickerill and Pajari, 1981; Tasse and others, 1978). The interbedding of the sandstone-breccia facies with lava flows indicates several different debris flows, possibly generated by eruptive events. The abundance of pillow-basalt clasts in the facies suggests that the debris flows originated below sea level.

The thick beds in the middle unit are inversely graded and poorly sorted; these characteristics indicate deposition as a series of debris flows, although smaller in volume than the flows of the lower unit. These debris flows originated to the east and were transported westward. The absence of wave-generated structures suggests that the middle unit was deposited below storm-wave base.

The abundance and character of sedimentary structures and shell-lag deposits in the upper unit indicates that it was deposited in a shallow-marine environment. Trough cross-stratification, channels, shell debris, and pebbly conglomerates of the upper unit suggest deposition in a nearshore environment (Bourgeois, 1980; Howard and Reineck, 1981; Busby-Spera, 1984), and a landmass source presumably lay to the south.

DOYLE CREEK FORMATION

The Doyle Creek Formation crops out on the Oregon side of the Snake River and discontinuously overlies the Wild Sheep Creek Formation (fig. 2.2).

Approximately 200 m of epiclastic conglomerate, sandstone, shale, and minor amounts of tuff were measured in the Cook Creek drainage (fig. 2.6). The sedimentary rocks are red and purple and thin to medium bedded. Pebble conglomerates grade upward into sandstone and shale. Pumice clasts and shale rip-up clasts are common. Although the provenance of the Doyle Creek Formation is largely volcanic, subrounded to subangular quartz diorite clasts are present.

Concentrated near the base of the formation are several white vitric tuff beds that range in thickness from 0.5 m to multiple beds as much as 4 m thick. Minor amounts of plagioclase and euhedral and embayed quartz are present in these tuffs. Interbedded with red shale and sandstone higher in the formation are several crystal tuff beds 1 to 3 m thick. The crystals consist of plagioclase and anhedral quartz fragments. Rare devitrified pumice fragments are also present in the tuff. A slumped tuff bed is interbedded with other stratified rocks (in the Cook Creek drainage) and suggests gravity movement to the northwest.

The Doyle Creek Formation was deposited in one or more well-oxygenated basins. The lack of primary sedimentary structures in the interbedded tuff beds suggests deposition below storm-wave base. The normal grading, thin to medium bedding, and rip-up clasts indicate turbidity-current transport. The slumped tuff bed suggests a paleoslope dipping to the northwest. The red and purple color of the rocks suggests that the basins were well oxygenated. Ash either settled out of the water column or was transported into the basins by turbidity currents caused by the rapid accumulation and subsequent slumping of volcanic debris during eruptive events. Volcanic quartz in the tuff suggests silicic eruptions. The presence of quartz diorite clasts indicates uplift and erosion of a plutonic terrane by Karnian time. These subangular clasts in-

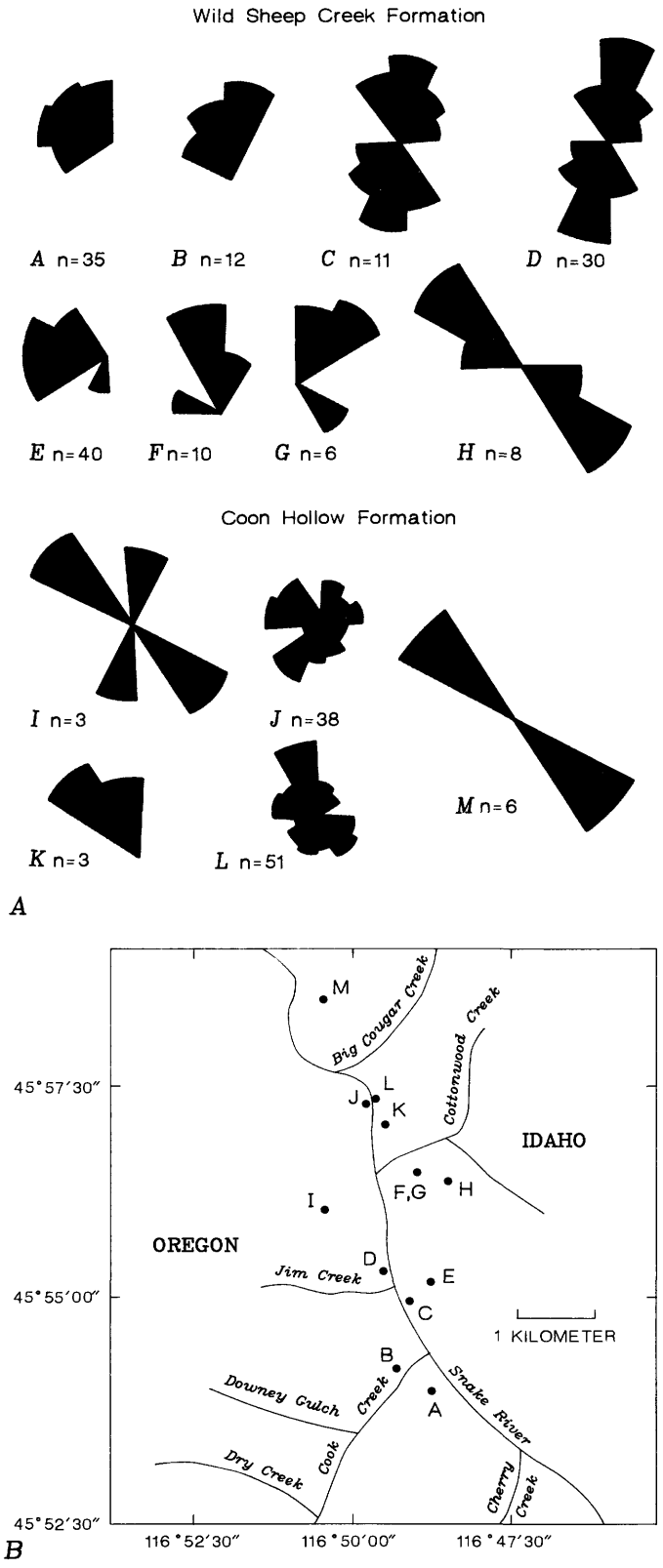

◀ FIGURE 2.5.—Paleocurrent data for Wild Sheep Creek and Coon Hollow Formations of northern Oregon and western Idaho and index map showing data collection locations. *A*, Rose diagrams (in 30° segments) showing paleocurrent for Wild Sheep Creek Formation and Coon Hollow Formation A and B: clast imbrication, upper volcanic facies of Wild Sheep Creek Formation; C and D: fossil orientation, limestone facies of Wild Sheep Creek Formation; E: imbrication; F: trough axes; G: cross-stratification; and H: belemnite orientation, sandstone-breccia facies of Wild Sheep Creek Formation; I: belemnite orientation; J: cross-stratification; K: tabular cross-stratification; and L: cross-stratification, sandstone-conglomerate facies of Coon Hollow Formation; M: groove casts, flysch facies of Coon Hollow Formation. n, number of measurements. Paleocurrent data not corrected for tectonic rotation. *B*, Index map showing data collection locations.

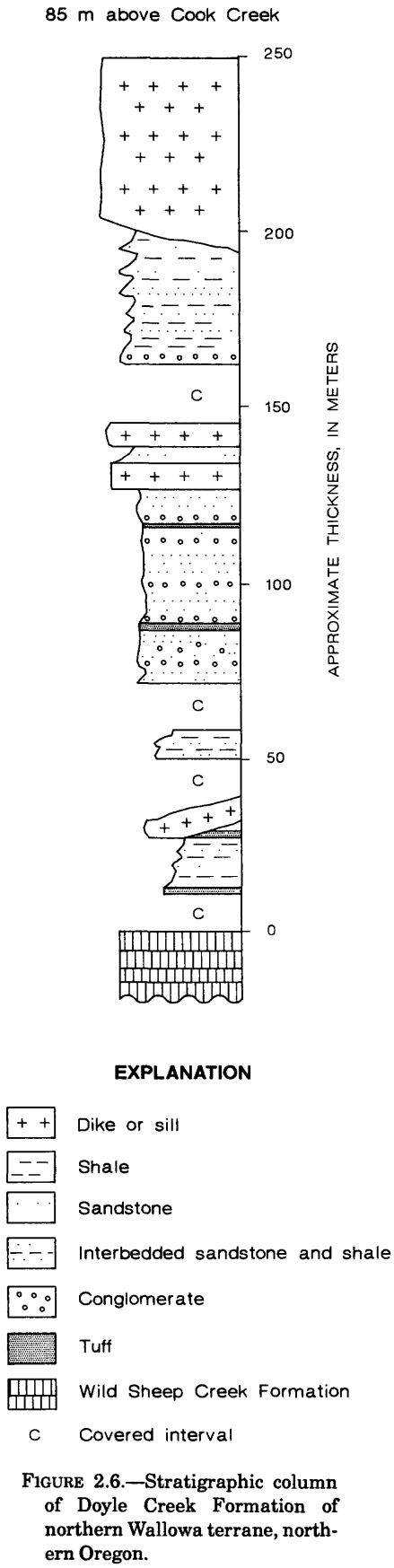

FIGURE 2.6.—Stratigraphic column of Doyle Creek Formation of northern Wallowa terrane, northern Oregon.

dicate little transport (Abbott and Peterson, 1978) and a close spatial relation between the plutonic terrane and the depositional basin.

COON HOLLOW FORMATION

The Coon Hollow Formation crops out between the Washington-Oregon border at Cougar Rapids (Morrison, 1963, 1964; this report) and in the Pittsburg Landing area (White, D.L., 1974; White, J.D.L., 1985; White, J.D.L., chap. 4, this volume). In the Pittsburg Landing area, these rocks are Callovian in age (White and Vallier, chap. 3, this volume) and in the northern Wallowa terrane they are Callovian and Oxfordian in age (T. Vallier, oral commun., 1989). An angular unconformity separates the Middle and Upper Jurassic Coon Hollow Formation from the Middle and Upper Triassic Wild Sheep Creek and Upper Triassic Doyle Creek Formations. In the northern Wallowa terrane, two lithofacies are recognized in the Coon Hollow Formation: a (lower) sandstone-conglomerate facies and an (upper) flysch facies.

SANDSTONE-CONGLOMERATE FACIES

The sandstone-conglomerate facies crops out on both sides of the Snake River near Cougar Rapids, where it is well exposed (fig. 2.2). The facies is typically 20 to 60 m thick but appears to be missing in one section on the Idaho side. Poor exposure and disruption by sills intruding along the contact between the facies and the Wild Sheep Creek Formation probably obscure the facies in this area.

The sandstone-conglomerate facies was deposited on the tilted and irregularly eroded topographic surface of the volcanic and carbonate rocks of the Wild Sheep Creek Formation and on the volcaniclastic sediments of the Doyle Creek Formation. This erosional topographic surface (with tens of meters of relief at the time of deposition) may account for the variable thickness of the facies.

Generally, the sandstone-conglomerate facies fines upward from a basal boulder conglomerate to medium- and fine-grained sandstones and then into the overlying flysch facies. However, lateral facies changes are abrupt in this unit. Although the basal conglomerate is present in most of the exposures, on the Oregon side 1 km north of Coon Creek the sandstone-conglomerate facies consists of sandstone and shale directly overlying the limestone facies of the Wild Sheep Creek Formation (fig. 2.7).

The basal conglomerate consists of poorly sorted boulder and cobble conglomerate derived from the

underlying strata. Limestone clasts are well rounded and as much as 1.5 m in diameter; volcanic clasts are rounded and as much as 1 m in diameter. The conglomeratic beds are between 4 and 10 m thick and are overlain by trough cross-stratified sandstone. The trough cross-stratified sandstone grades upward into medium-grained sandstone with oscillation ripples and hummocky cross stratification. The hummocky cross-stratified sandstone is amalgamated, and erosional surfaces are common. Normal and inversely

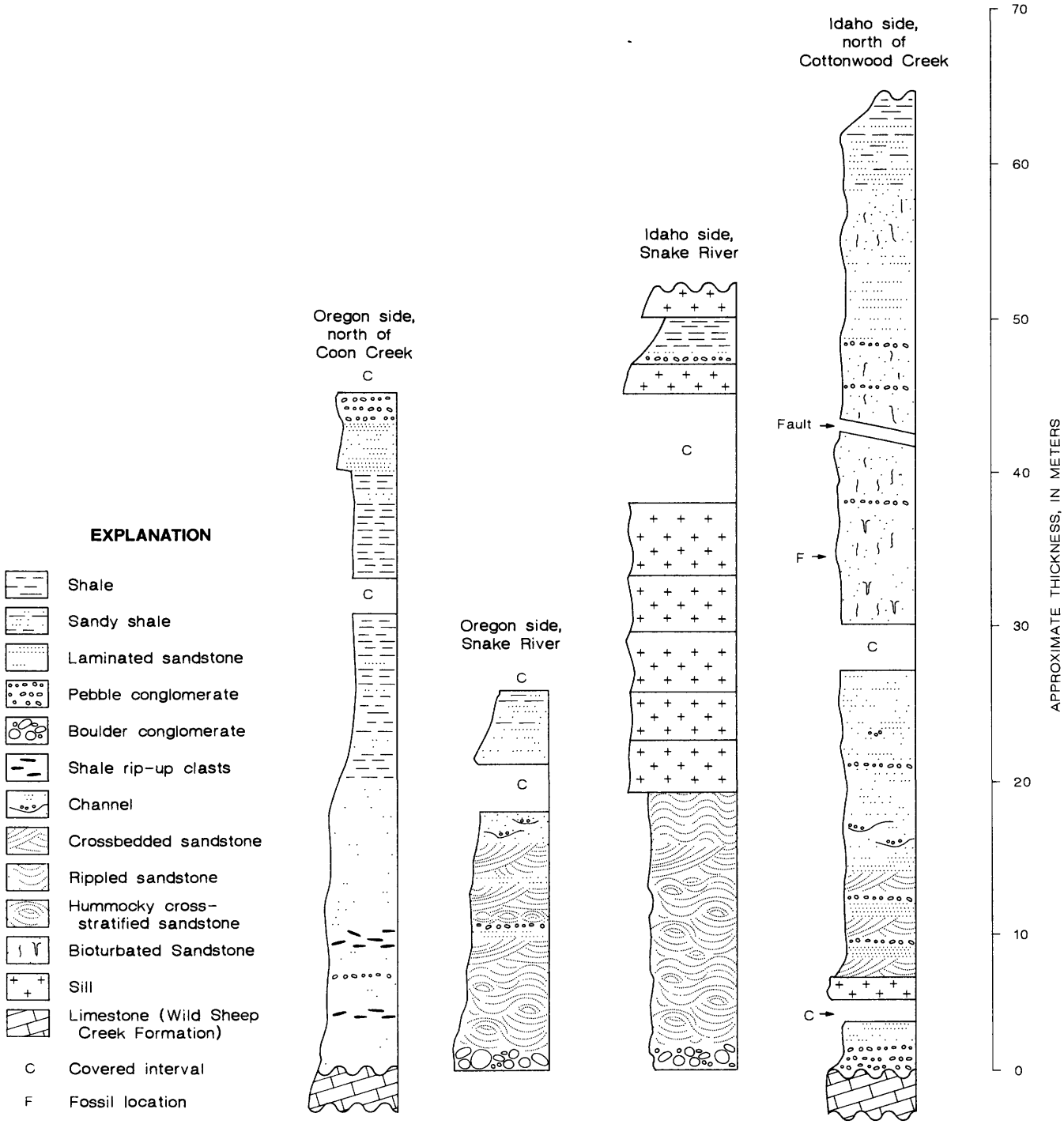

FIGURE 2.7.—Generalized stratigraphic columns of sandstone-conglomerate facies of Coon Hollow Formation, northern Wallowa terrane, northern Oregon and western Idaho.

graded sandstone and minor amounts of laminated shale overlie the cross-stratified sandstone. They grade upward into the shale of the flysch facies.

Oxfordian ammonites previously collected from the Coon Hollow Formation (Morrison, 1963) are from the overlying flysch facies. The upper sandstone of the sandstone-conglomerate facies locally contains bivalve biocenoses. Accordingly, these bivalves were not transported into the basin after death. Other fossils contained in this facies include belemnites and plant fragments. Bioturbation is locally abundant in the bivalve-bearing sandstone. The abundance of horizontal burrows in the well-sorted sandstone suggests a *Skolithos* ichnofacies where these trace fossils occur (Frey and Pemberton, 1984).

Paleocurrent data collected from cross-stratified units, tabular crosslaminations, ripples, and belemnite orientations indicate a general current direction to the northwest and a secondary component to the southwest at Cougar Rapids on the Oregon side of the Snake River (fig. 2.5*A*, diagrams I, J, K, and L).

The petrology of the sandstone-conglomerate facies varies greatly between locations and is related to the different depositional environments, source areas, and amount of transport and reworking. Boulder, cobble, and pebble conglomerates containing volcanic and carbonate clasts dominate. Quartz and hornblende diorite clasts are also abundant. In the sand-size fraction, undulose quartz, plagioclase, and volcanic lithic materials generally dominate. Limestone lithic grains are locally abundant, as are plutonic fragments of undulose quartz and plagioclase. Rarely, plutonic grains show myrmekitic intergrowths.

The sandstone-conglomerate facies represents a transgressive nearshore and offshore (outer shelf), wave-dominated environment. The basal conglomerate and trough cross-stratified sandstones that directly overlie the unconformity formed in a nearshore environment. No beach facies were recognized, but the basal conglomerate and sandstone was probably deposited in relatively shallow water. Directly overlying the basal conglomerate and sandstone are sandstones showing hummocky cross-stratification and oscillation ripples, structures indicative of transitional (inner shelf) environments (Bourgeois, 1980; Howard and Reineck, 1981; Busby-Spera, 1984). These sandstones were deposited below fair-weather wave base during the waning stages of large storms (Hunter and Clifton, 1982).

Hummocky cross-stratified sandstone gives way to locally fossiliferous and bioturbated sandstone (*Skolithos* ichnofacies) and then into graded fine sandstone and shale, which represent an offshore-outer shelf depositional environment (Howard and Reineck, 1981; Frey and Pemberton, 1984). The graded sandstone was deposited on the outer shelf by storm-induced density currents, and the thin shale interbeds were deposited during fair-weather sedimentation (Busby-Spera, 1984).

The distribution of environments and the paleocurrent directions suggest that the coastline trended approximately northeast-southwest and that the landmass was to the southeast. The paleocurrent direction to the southwest (fig. 2.5*A*, diagram J) may have resulted from a longshore current. Because of the different environments of deposition, source areas, transport, and abrasion histories, the petrology of these sandstones varies significantly. Rocks exposed at Cougar Rapids were derived from the underlying volcanic and carbonate rocks of the Wild Sheep Creek Formation. Quartz and hornblende diorite clasts in these rocks indicate a plutonic source as well. Therefore, the source areas for the sandstone-conglomerate facies were the Wild Sheep Creek Formation and a quartz diorite to hornblende diorite terrane to the southeast.

FLYSCH FACIES

The flysch facies consists of more than 520 m of shale, sandstone, minor amounts of conglomerate, and intrusive sills. Two sections were measured on the ridge north of Little Cougar Creek and correlated by walking out small cliff-forming sandstone beds (fig. 2.8). The total combined thickness measured for this report is approximately 460 m. An estimated 60 m of sedimentary rocks stratigraphically overlies the highest measured section. When combined with the maximum thickness of the sandstone-conglomerate facies, the overall thickness of the Coon Hollow Formation is approximately 580 m, which is close to the 610 m Morrison (1964) estimated.

Overall, the facies thickens and coarsens upward. Its base consists of thinly laminated black shale and minor amounts of sandstone. Bouma (1962) divisions B and D are common in the lower sections. Bouma E, if present, is obscured by pencil structures developed in the shales. The sedimentary rocks thicken and coarsen upward into channeled sandstone and conglomerate. Both normally and inversely graded sandstone is present, and Bouma (1962) divisions A through D are common. Channels are between 10 and 50 m deep and 100 m wide, and they are filled with amalgamated sandstone and conglomerate. Beds are thickest near the channel axis and thin laterally to medium- and thinly bedded sandstone.

Petrographic analysis and pebble-count data indicate three sources for this facies: volcanic, plutonic,

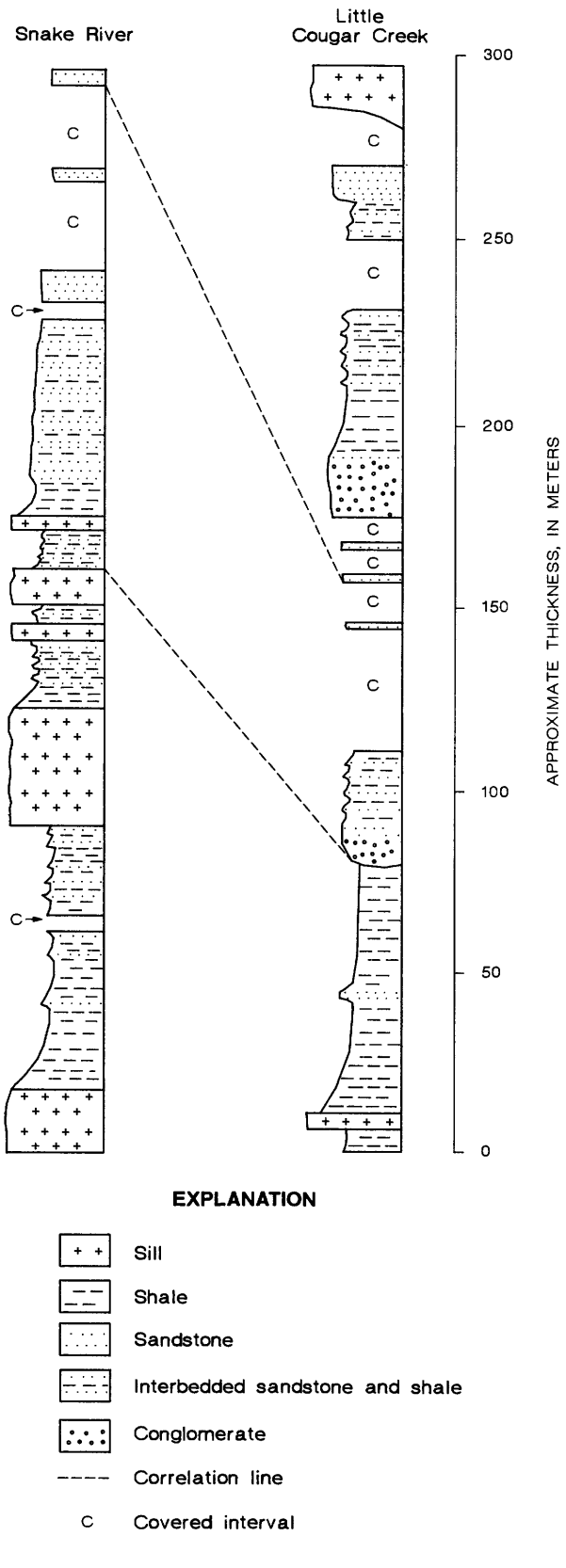

FIGURE 2.8.—Stratigraphic columns of flysch facies of Coon Hollow Formation, northern Wallowa terrane, western Idaho.

and chert-metasedimentary. Volcanic lithic grains are common throughout the facies, and plutonic lithic fragments are rare except in the Downey Gulch area. Approximately 90 m above the base of the facies, radiolarian chert and microcrystalline, siliceous metasedimentary lithic fragments are present, which increase in abundance up-section.

The poor exposure hampers measurements of paleocurrent data in the flysch facies. However, groove casts from two beds suggest a northwest-southeast current direction (fig. 2.5*A*, diagram M). Locations of data shown in diagrams A-M of figure 2.5*A* are shown in figure 2.5*B*.

No fossils were found in this facies during this study, but Oxfordian ammonites were collected by Morrison (1963; 1964) in the lower part of the flysch facies. Radiolarians extracted from the chert clasts in the upper part of the flysch facies were identified by C.D. Blome of the U.S. Geological Survey. Fauna identified include *Canoptum browni* Blome, *Canoptum* sp., *Capnodoce* sp., *Corum speciosum* Blome, *Latium paucum*, *Triassocampe* sp., *Xipha pessagnoi* Nakaseko and Nishimura, and *Xipha striata* Blome. These fauna belong to either the *Xipha striata* or *Latium paucum* subzone (Blome, 1984; Blome, written commun., 1987). These subzones indicate a late Karnian to middle Norian age for the chert source (Blome, 1984; Blome, written commun., 1987).

The flysch facies represents a progradational sequence of turbidity-current deposits in an oxygen-poor basin. The sequence coarsens and thickens upward from outer fan to midfan channeled sandstone and conglomerate. The lower part of the flysch facies consists of abundant shale and minor amounts of fine-grained sandstone (facies D of Mutti and Ricci-Lucchi, 1978), which grade upward into nonchanneled, thinly bedded shale and fine- to medium-grained sandstone (facies D and C of Mutti and Ricci-Lucchi, 1978). These deposits represent distal fan to outer fan turbidites (Mutti and Ricci-Lucchi, 1978). The black shales and lack of bottom-dwelling organisms suggest an oxygen-poor basin. The presence of channel deposits above the nonchanneled shale and sandstone is used as the boundary between outer fan and midfan environments (Mutti and Ricci-Lucchi, 1978; Busby-Spera, 1985). In the upper part of the flysch facies, channeled sandstone and conglomerate belong to facies A, B, and C (Mutti and Ricci-Lucchi, 1978). These channeled deposits are often overlain by shale; this characteristic indicates the abandonment of the channel as a result of lateral migration, and it also suggests midfan deposition (Busby-Spera, 1985). Deposits of inner fan and slope environments are missing because of erosion or are covered by younger rocks.

The northwest-southeast paleocurrent directions when compared with the proposed paleogeography for the underlying sandstone-conglomerate facies suggest that the flysch facies submarine fan prograded to the northwest. The chert-metasedimentary source terrane was probably exposed to the southeast.

The presence of chert and metasedimentary lithic fragments in this facies is important for the interpretation of the tectonic history of the terrane. The sandstone petrology suggests that the provenance of the flysch facies differs significantly from that of the other sedimentary units in the study area. The provenance of the argillite-sandstone and sandstone-conglomerate facies and the Doyle Creek Formation is predominantly volcanic, although the Doyle Creek Formation and sandstone-conglomerate facies have an additional plutonic source (fig. 2.9). The flysch facies is divided into two petrofacies (an upper and lower petrofacies). The lower petrofacies has sandstone compositions similar to the underlying units (fig. 2.9) and was derived from an arc-orogenic source (the Wallowa arc).

The upper petrofacies of the flysch facies contains more polycrystalline quartz (Qp, fig. 2.9) and sedimentary lithic fragments (Ls, fig. 2.9) as a result of the influx of chert and metasedimentary lithic materials from a different provenance than those of the underlying sedimentary rocks. The source for the upper petrofacies may be either a subduction complex or collisional orogenic provenance (fig. 2.9). A collisional orogenic source can be ruled out, because sands derived from collision zones have distinctive signatures (Suczek and Ingersoll, 1985). Cenozoic sands derived from the Himalayan collision zones have plagioclase/feldspar (P/F) ratios of 0.66, volcanic lithic/total lithic (Lv/L) ratios of 0.10, and mean quartz-feldspar-lithic (QFL) percents of 43-30-27 (Suczek and Ingersoll, 1985). The upper petrofacies has a P/F ratio of nearly 1.0, an Lv/L ratio of 0.44, and a QFL mean of 46-13-41 (Goldstrand, 1987). The petrology of the upper petrofacies of the flysch facies is influenced by volcanic detritus from the Wild Sheep Creek Formation, but it may also reflect the uplift and erosion of a subduction complex. Paleocurrent and fossil data indicates that the source is Late Triassic in age and was exposed to the southeast.

DIKES AND SILLS

Dikes and sills are common in the Wild Sheep Creek, Doyle Creek, and Coon Hollow Formations. They are probably Late Jurassic in age, because they intrude the Callovian and Oxfordian sediments of the Coon Hollow Formation and show a slight metamorphism that may be related to Late Jurassic metamorphism.

Sills are common in the Coon Hollow Formation, and their feeder dikes can be followed into the Wild Sheep Creek Formation. The sills occur singularly or in complexes as thick as 35 m. The sills are parallel or subparallel to bedding, and they have chilled margins and baked zones both on their upper and lower contacts. Vertical cooling fractures are common. A thick sill complex intrudes the upper part of the Wild Sheep Creek and Doyle Creek Formations. However, dikes are more common in these formations and range in thickness from 0.5 to 3 m.

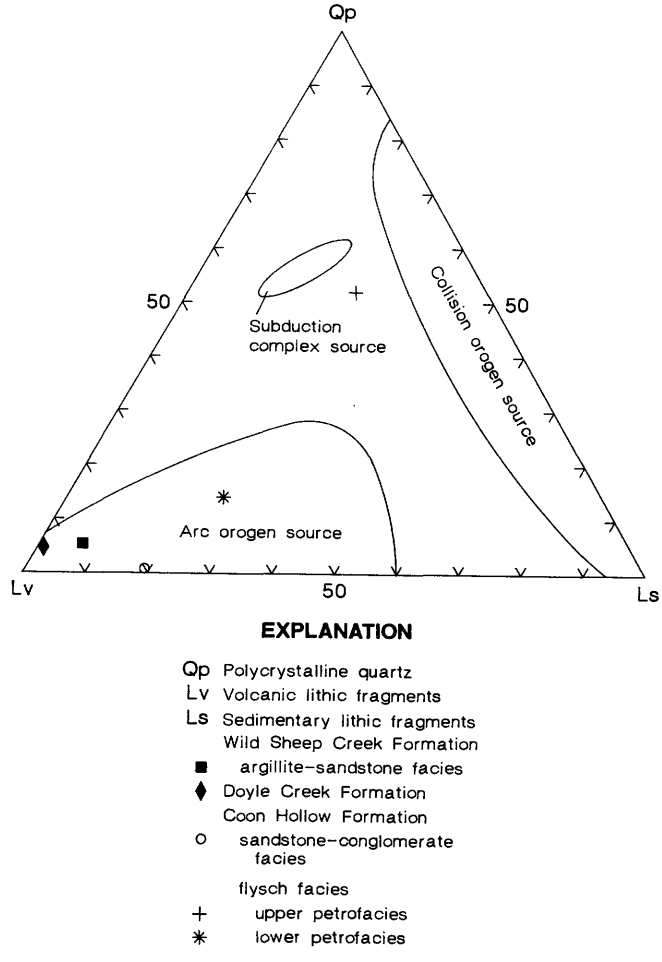

FIGURE 2.9.—Ternary diagram for Coon Hollow, Doyle Creek, and Wild Sheep Creek Formations of northern Wallowa terrane, northern Oregon and western Idaho. Means plotted for upper petrofacies of the flysch facies of Coon Hollow Formation, lower petrofacies of flysch facies of Coon Hollow Formation, sandstone-conglomerate facies of Coon Hollow Formation, Doyle Creek Formation, and argillite-sandstone facies of Wild Sheep Creek Formation. Tectonic source fields from Dickinson and Suczek (1979).

All dikes and sills sampled, except one, are green, porphyritic, and hyalophitic or hyalopilitic diorite. Euhedral hornblende is the dominant mafic phenocryst, and quartz is a minor or trace component. One dike is a white microcrystalline aplite with greater than 20 percent quartz. This aplite cuts the diorite dikes in the upper part of the Wild Sheep Creek Formation and forms a sill in the basal part of the Coon Hollow Formation. Geochemical data from a sill in the Cougar Rapids area indicates that it is calc-alkaline in composition (T. Vallier, written commun., 1987).

Hornblende diorite dikes intruded the Wild Sheep Creek and Doyle Creek Formations during the Late Jurassic. As a result of textural differences between the volcanic rocks of the Wild Sheep Creek Formation and the sedimentary rocks of the Coon Hollow Formation, the dikes intruded across bedding in the Wild Sheep Creek Formation and intruded parallel or subparallel to bedding in the flysch deposits of the Coon Hollow Formation. The crosscutting aplite dike may represent the most differentiated magma that supplied the dike and sill complexes.

PLUTONS

IMNAHA INTRUSION

The (informal) Imnaha intrusion is exposed along the Snake and Imnaha Rivers south of the study area and is in fault contact with the upper volcanic facies of the Wild Sheep Creek Formation 1.9 km south of the Salmon River confluence (fig. 2.2). A minimum age of emplacement of the intrusion is between 226 Ma (Walker, 1986) and 219 Ma (Balcer, 1980). The Imnaha intrusion shows a general zonation from quartz diorite near its northern margin to diorite and gabbro in the Imnaha River drainage. Gabbroic rocks typically contain 71 percent plagioclase (An_{60}), 20 percent pyroxene, 3 percent hornblende, 3 percent quartz, and lesser amounts of accessory minerals and alteration products (Morrison, 1963). Dioritic rocks contain approximately 56 percent plagioclase (An_{53}), 40 percent hornblende, 1 percent pyroxene, and minor amounts of magnetite and quartz (Morrison, 1963). Samples collected near the northern margin of the intrusion are coarse grained, equigranular, holocrystalline leuco-quartz diorites. Plagioclase (65 percent) is sericitized and subhedral, quartz (25 percent) is slightly undulose and anhedral, and hornblende constitutes 5 percent of the rock. Granophyric textures of quartz and potassium feldspar are locally present.

North-south-trending pyroxene diorite dikes are abundant near the northern margin of the Imnaha intrusion. These dikes intrude the quartz diorite and do not appear to continue into the Wild Sheep Creek Formation at its northern boundary; they are probably cut by a fault in this region. The dikes are medium grained and porphyritic. Plagioclase constitutes 70 percent of the rock, and augite and magnetite are present in minor amounts.

The Imnaha intrusion may represent two stages of magmatic evolution during the Middle(?) and Late Triassic. The quartz diorite and hornblende diorite may have been the first magmas and were later intruded by pyroxene diorite dikes. These dikes may have originated from a second magma, the pyroxene gabbro.

DRY CREEK STOCK

The (informal) Dry Creek stock and its associated dikes are exposed in the Cook Creek-Dry Creek drainage. This stock is the only unmetamorphosed pre-Tertiary unit in the study area and has a K-Ar age of 139.5±2.1 Ma, based on biotite. This diorite stock intrudes the Wild Sheep Creek, Doyle Creek, and Coon Hollow Formations (fig. 2.2). The sedimentary units near the stock show varying amounts of contact metamorphism. A sample of the stock collected at the confluence of Cook and Dry Creeks is a medium-grained, hypidiomorphic pyroxene hornblende diorite. Subhedral plagioclase makes up approximately 75 percent of the rock and shows oscillatory and sector zoning. Unzoned plagioclase has a composition of An_{47}. Anhedral hornblende (10 percent) is either intersertal or forms corona textures around clinopyroxenes. The clinopyroxenes (augite) are subhedral, embayed, and constitute 10 percent of the rock. Some clinopyroxenes form corona textures around deeply embayed hypersthene. Anhedral biotite makes up approximately 5 percent of this sample.

Associated with the Dry Creek stock are several large diorite dikes, which have been mapped collectively with the stock. These dikes surround and radiate outward from the stock and differ from other dikes in the study area by their lack of metamorphic alteration. Baked zones within the sedimentary rocks that the dikes intrude are generally less than 1 m thick. The dikes are green hornblende diorite with glomeroporphyritic or porphyritic textures. The plagioclase is slightly sericitized and shows the same zoning patterns (oscillatory and sector zoning) as the stock plagioclases. Plagioclase compositions range from An_{55} near the stock to An_{38} 4 km away from its margin (Jim Creek area, fig. 2.2). Minor quartz phenocrysts increase away from the stock, whereas hornblende phenocrysts decrease.

The Dry Creek stock intruded to shallow depths, as suggested by zoned plagioclase, radial dikes, and contact metamorphism. Corona textures of hornblende surrounding augite indicate an incomplete reaction of augite with the melt. At shallow depths or with low pH_2O, a melt would first crystallize pyroxene and then, as cooling progressed, alter pyroxene to amphibole, which is common in shallow subvolcanic stocks (McBirney, 1984).

STRUCTURE

The most conspicuous structural feature of the study area is the uniform northwest dip of bedding. The oldest stratified rocks in the study area are exposed in the southeast and belong to the lower volcanic facies of the Wild Sheep Creek Formation. Because of the fault contact between the Wild Sheep Creek Formation and the Imnaha intrusion and the lack of precise age control, the age of the Imnaha intrusion relative to the lower volcanic facies is unknown. The angular unconformity between the Triassic formations and the Jurassic Coon Hollow Formation indicates tilting of the northern Wallowa terrane to the northwest between Karnian and Oxfordian time. Syn- or post-Oxfordian tilting also occurred, as indicated by the overall northwest dip and folding of the Coon Hollow strata.

Northeast-southwest-trending folds occur in the Coon Hollow Formation. The fold axes plunge slightly southwest. Carbonate units (limestone facies) of the Wild Sheep Creek Formation also show broad, open folds with similar axial trends, but faulting is more prevalent in the limestone units.

Faults are abundant in the more competent parts of the Wild Sheep Creek Formation. These high-angle faults show little vertical displacement, with the possible exception of the Imnaha boundary fault. Displacements on faults cutting the two limestone marker units suggest horst and graben structures, but rare slickensides indicate some strike-slip movement. Silicification and copper mineralization took place in the thin breccia zones along these faults. Faults generally trend either northwest or northeast. Many of the large dikes radiating outward from the Dry Creek stock trend north or north-northeast and may have intruded along preexisting planes of weakness. A wide shear zone associated with the northern part of the Imnaha intrusion trends about N. 70° W. (Vallier, 1974).

The timing of the structural events in the study area is not well understood. Extensional faulting may be associated with the tilting and uplift of the Wild Sheep Creek Formation during the Karnian to Oxfordian. This extensional deformation is represented by small horst and graben faults that do not displace the sandstone-conglomerate facies of the Coon Hollow Formation. After deposition of the Callovian and Oxfordian Coon Hollow Formation, another extensional event allowed dikes and sills to intrude the terrane. The northern Wallowa terrane subsequently underwent northwest-southeast compression, which folded sills and sedimentary rocks of the Coon Hollow Formation into broad anticlines and synclines. Faults cut dikes of the Early Cretaceous Dry Creek stock; this relation indicates a period of faulting between the Early Cretaceous and the Miocene. In the study area, no faults cut the strata of the Miocene Columbia River Basalt Group. However, in adjacent areas, normal faults that cut these younger basalts indicate post-Miocene deformation (Vallier, 1974).

GEOLOGIC HISTORY

The geology described thus far probably represents only a small part of a single volcano and its associated basins within a much larger island arc complex, the Blue Mountains island arc (Vallier and Brooks, 1986). Modern island arcs, such as the Aleutian arc, are extremely large (440,300 km^2) and complex (Vallier and Brooks, 1986). Therefore, the approximately 130 km^2 mapped during this study in the northern Wallowa terrane represents only a small segment of the Mesozoic history of the Blue Mountains island arc.

A history of intrusive and eruptive events and sedimentation can be constructed from the superposition of rock units, crosscutting relations, and the presence or absence of metamorphic minerals. Because of the fault contact between the Imnaha intrusion and the Wild Sheep Creek Formation, time of emplacement for the intrusion cannot be determined precisely. The U-Pb ages by Walker (1986) and Ar 40/39 ages by Balcer (1980) give minimum ages for emplacement of 226 Ma and 219 Ma, respectively. Quartz diorite clasts within the sandstone-conglomerate facies of the Coon Hollow Formation suggest that the Imnaha intrusion was exposed and deeply eroded by the Late Jurassic. Quartz diorite clasts in the Doyle Creek Formation suggest that at least part of the Imnaha intrusion may have been uplifted during the Karnian. The minimum age of emplacement of the Imnaha intrusion is Late Triassic, but parts of it may be older. Therefore, the Imnaha intrusion may be coeval with the Wild Sheep Creek Formation.

The forceful intrusion of diorite dikes into the quartz diorite of the Imnaha intrusion indicates that

TABLE 2.1.—*Major- and minor-element oxides, in weight percent, of Upper Triassic volcanic flows of the Wild Sheep Creek Formation, and an Early Cretaceous pluton (Dry Creek stock), northeastern Oregon and western Idaho*

[Oxides are adjusted to 100 percent and volatile percents are included to show the amount of alteration]

	Wild Sheep Creek Formation							Dry Creek stock	
Sample ------	G-7-8G	G-7-12B	G-7-19E	G-7-19K2	G-7-21F	G-7-22A	G-7-29F	G-7-18H	G-8-25C
SiO_2 ----------	47.4	46.3	46.9	49.1	50.2	48.1	72.0	58.0	62.5
TiO_2 ----------	.96	1.10	.94	1.18	.96	.81	.35	1.00	.43
Al_2O_3 ---------	15.8	16.3	17.9	15.1	18.1	16.3	11.6	16.7	17.4
Fe_2O_3 --------	1.2	1.2	.9	1.2	.9	.9	.3	.7	.4
FeO ----------	10.2	11.0	8.1	10.4	8.1	7.8	2.5	5.9	3.8
MgO ----------	6.7	5.1	5.5	2.3	3.4	3.9	.85	3.7	2.3
MnO ----------	.18	.18	.21	.14	.11	.22	.09	.10	.07
CaO ----------	8.95	7.83	9.00	9.17	5.72	14.5	3.20	7.13	5.00
Na_2O ---------	3.8	4.2	2.7	5.4	6.0	3.5	4.3	4.4	4.7
K_2O ----------	.72	.98	2.70	.23	1.31	.29	1.13	1.05	.58
P_2O_5 ----------	.17	.19	.15	.24	.26	.12	.10	.47	.19
H_2O^+ ---------	2.23	2.99	2.39	1.82	2.36	2.32	.92	.50	1.74
H_2O^- ----------	.35	.37	.32	.26	.28	.14	.18	.05	.28
CO_2 ----------	.61	2.65	1.64	3.19	1.75	1.08	1.51	.04	.33
FeO/MgO ---	1.75	2.4	1.6	5.0	2.6	2.2	3.2	1.8	1.8

at least the margins of the intrusion had cooled and solidified before the dikes intruded. The mineral assemblages in Imnaha dikes suggest that they are not related to the dikes and sills intruding the Wild Sheep Creek, Doyle Creek, and Coon Hollow Formations. Imnaha dikes lack amphiboles, which are abundant in the other dikes and sills of the study area. However, clinopyroxenes are present and may suggest a relation between these dikes and the volcanic rocks of the lower part of the upper volcanic facies of the Wild Sheep Creek Formation.

Zoning in the Imnaha intrusion, from quartz diorite and diorite to gabbro, may represent two stages of magmatic emplacement, which are related to the lower and upper volcanic facies of the Wild Sheep Creek Formation, respectively. The first and outboard magma was the quartz diorite and diorite, which may have been the magma chamber for the siliceous lower volcanic facies. The second and inboard magma, the gabbro, was injected to the south and caused uplift of the solidified quartz diorite. Quartz and hornblende-diorite clasts in the Doyle Creek Formation may correlate with this uplift. Clinopyroxene-diorite dikes intruded outward across the margin of the quartz diorite and extruded lava for the lower part of the pyroxene-rich upper volcanic facies.

The Imnaha intrusion may be associated with subduction during the Middle(?) and Late Triassic. If the Imnaha intrusion is coeval with the Wild Sheep Creek Formation, it may be the intrusive equivalent of those volcanic rocks.

A coherent stratigraphic sequence is preserved for the Wild Sheep Creek, Doyle Creek, and Coon Hollow Formations, and their sedimentary and magmatic history can be reconstructed.

1. In the Middle and Late Triassic, dacite lavas and pyroclastic materials (lower volcanic facies of the Wild Sheep Creek Formation) erupted subaqueously along the flanks of a volcano within the Blue Mountains island arc. The basement rock on which these volcanic rocks formed is not exposed in the study area.

2. As volcanism evolved into more siliceous (more viscous) eruptions or as flows migrated to another position on the volcano, density currents redeposited pyroclastic debris (argillite-sandstone facies of the Wild Sheep Creek Formation) in channels within and above the lower volcanic facies of the Wild Sheep Creek Formation (fig. 2.10*A*). Eventually density current sedimentation ceased and low-energy shales and limestones were deposited.

3. Deposited directly on the argillites and sandstones were voluminous basaltic flows (upper volcanic facies of the Wild Sheep Creek Formation). Geochemical data from the Wild Sheep Creek Formation (fig. 2.11; tables 2.1, 2.2) indicates that these volcanic materials erupted as island-arc tholeiites and substantiates an island-arc genesis for the Wallowa terrane.

TABLE 2.2.—*Trace elements (in ppm) of Upper Triassic volcanic flows of the wild Sheep Creek Formation, and an Early Cretaceous pluton (Dry Creek stock), northeastern Oregon and western Idaho*

[Analysis: *, X-ray fluorescence; +, emission spectroscopy; <10, 10 ppm is lower limit of detection]

	Wild Sheep Creek Formation							Dry Creek stock	
Sample	G-7-8G	G-7-12B	G-7-19E	G-7-19K2	G-7-21F	G-7-22A	G-7-29F	G-7-18H	G-8-25C
Rb*	10	<10	25	<10	27	<10	12	18	<10
Sr*	500	530	300	190	400	380	72	1050	800
Zr*	50	58	44	100	80	40	140	140	97
Y*	13	16	13	23	27	<10	16	12	<10
Ba*	370	870	840	75	250	54	150	560	430
Co+	37	38	26	28	23	30	5.1	27	13
Cr+	45	51	61	100	<10	31	<10	62	22
Cu+	41	87	38	35	13	180	5.1	68	5.6
Ni+	34	28	36	35	6.7	22	4.1	41	12

Massive flows grade laterally into pillow lavas and, farther from the vent, pillow breccias. A change in the magma composition is indicated by the vertical transition from pyroxene basalt to hornblende basaltic andesite. The gabbroic part of the Imnaha intrusion may represent the intrusive equivalent of these volcanic rocks.

Topographic lows on the flanks of the volcano received volcaniclastic turbidites and debris flow sediments. The volcano was located to the southeast, and these sediments were shed toward the northwest. The Wallowa terrane has undergone approximately 66° of clockwise rotation since the Late Jurassic or Early Cretaceous (Wilson and Cox, 1980; Hillhouse and others, 1982; Vallier and Engebretson, 1984). Unfortunately, the amount and sense of rotation the Wallowa terrane has undergone before about 130 Ma is unknown, and therefore, the Late Triassic paleogeography cannot be corrected for tectonic rotation. Accordingly, all paleocurrent directions are given in present-day coordinates.

4. At least twice during the evolution of the volcanic island, fringing carbonate-platform environments formed (limestone facies of the Wild Sheep Creek Formation; fig. 2.10*B*). The presence of these platform environments substantiates paleomagnetic data for the Wallowa terrane that place it at a low paleolatitude—that is, 18° north or south of the Late Triassic equator (Hillhouse and others, 1982).

5. Periodically, volcaniclastic debris flows moved westward down the flanks of the volcano (sandstone-breccia facies of the Wild Sheep Creek Formation). These debris flows were deposited in a basin that eventually filled sufficiently for storm waves to rework the debris flows. Later, limestone was deposited over the debris flow deposits, and volcanic eruptions deposited tuff on the carbonate muds.

6. During the Karnian, epiclastic sediments of the Doyle Creek Formation were deposited in one or more oxygenated basins. The lack of lava flows and the abundance of lapilli and vitric tuffs suggest that either the eruptive center had moved farther away from the depositional basin(s) or that compositional changes in the magma had caused a transition to siliceous pyroclastic eruptions. Quartz diorite clasts in this formation may indicate uplifting of part of the Imnaha intrusion, which may, in turn, have been related to the emplacement of the gabbroic phase of the Imnaha intrusion.

7. There is no rock record of events that took place within the study area from the Karnian to the Oxfordian (approximately 62 m.y.). Elsewhere in the Wallowa terrane, thick carbonate-platform sequences were deposited during Norian time (Vallier, 1974; Vallier, 1977; Newton, 1986; Stanley, 1986). The platform carbonate rocks (Martin Bridge Limestone) grade into Upper Triassic to Lower Jurassic deep-water shales of the Hurwal Formation (Vallier, 1974; Vallier, 1977). The lack of volcanic material in the Martin Bridge Limestone suggests that volcanism had ceased by Norian time. By the Oxfordian, rocks in the study area had been tilted to the northwest and uplifted above sea level.

8. During the Oxfordian, sediments were being deposited over the eroded and tilted carbonate and volcanic rocks of the Wild Sheep Creek Formation in a nearshore and outer shelf environment (sandstone-conglomerate facies of the Wild Sheep Creek Formation; fig. 2.10*C*). The coastline trended roughly northeast-southwest. Carbonate and volcanic rocks of

the Wild Sheep Creek Formation and the quartz and hornblende diorites of the Imnaha intrusion were being eroded at this time. In the study area, no evidence of volcanism is found in the Callovian and Oxfordian Coon Hollow Formation. However, in the Pittsburg Landing area (southeast of the study area), volcanism occurred during Callovian time (White, D.L., and Vallier, chap. 3; White, J.D.L., chap. 4, both this volume).

9. The sea transgressed onto the landmass, and a submarine fan prograded to the northwest. A radiolarian chert and metasedimentary provenance was located to the south or southeast. A likely chert-metasedimentary provenance is the Permian to Late Triassic Baker terrane (T. Vallier, oral commun., 1986). Late Triassic radiolarians extracted from these cherts are similar to those found in the Baker terrane (Blome, written commun., 1987). The influx of sediments derived from this terrane may delimit the timing of the amalgamation of the Wallowa and Baker terranes to the Oxfordian. Parts of the Baker terrane are located south and southeast of the study area (Brooks and Vallier, 1978; Silberling and others, 1984) and correlate with the southeast paleocurrent directions for the chert-metasedimentary provenance in the flysch facies of the Coon Hollow Formation.

10. After deposition of the Coon Hollow Formation, hornblende diorite dikes and sills intruded the northern Wallowa terrane. These may be related to an extensional event at the time. Later, the terrane underwent northwest-southeast compression, which caused broad, open folds to develop. Also during the Late Jurassic, rocks of the Wallowa terrane were regionally metamorphosed to the greenschist facies (Hamilton, 1963).

11. During the Early Cretaceous (at approximately 139.5 Ma), a diorite stock and its associated dikes (the Dry Creek stock) shallowly intruded the northern Wallowa terrane (fig. 2.10*D*) and caused the contact metamorphism of the surrounding rocks. This stock has been grouped with the Late Jurassic to Early Cretaceous Wallowa batholith (Walker, 1979). Intrusive and contact relations of a satellite stock, the Cornucopia stock (Taubeneck, 1964), and the Wallowa batholith are similar to those of the Dry Creek stock.

Thayer and Brown (1964) suggested that the Wallowa batholith is related to the Idaho batholith.

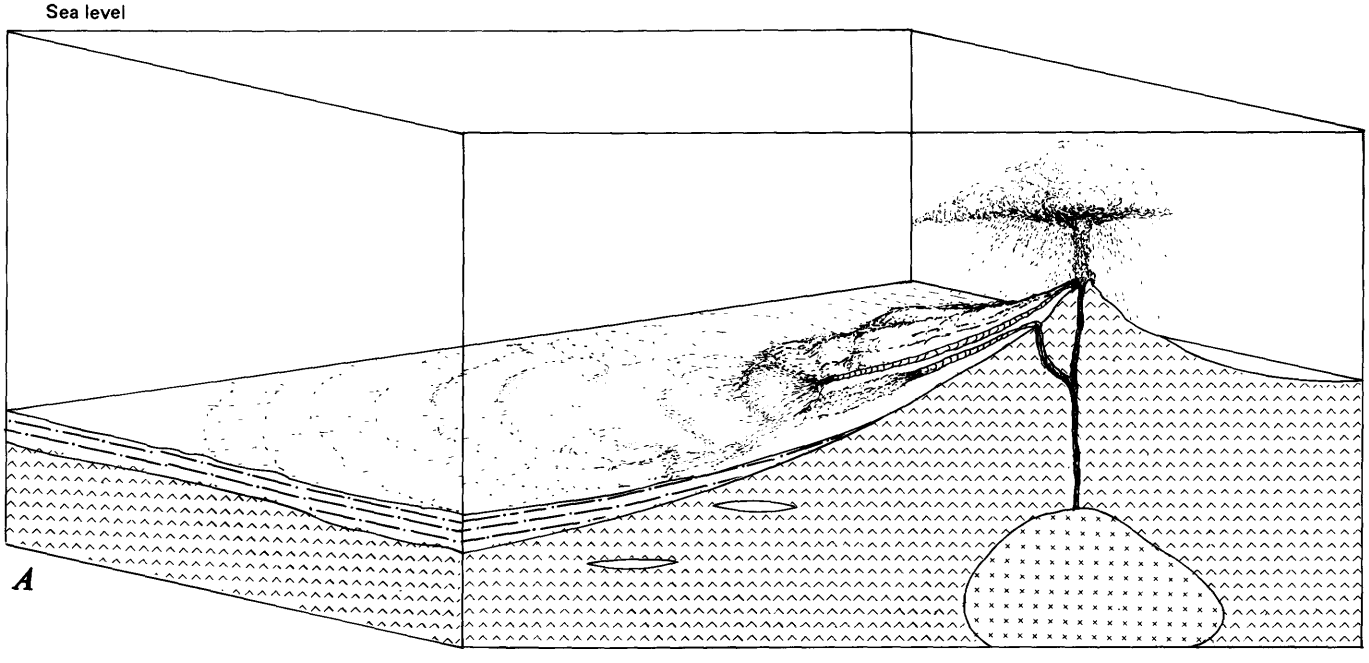

FIGURE 2.10.—Hypothetical reconstructions and present-day construction of northern Wallowa terrane, northern Oregon and western Idaho. *A*, Deposition of lower volcanic and argillite-sandstone facies of the Wild Sheep Creek Formation during Middle and Late Triassic. Channels (unpatterned units) within the lower volcanic facies and on the north flank are discussed in the text. Atop the argillite-sandstone facies is a small submarine fan. *B*, Deposition of upper volcanic and limestone facies of Wild Sheep Creek Formation during Late Triassic. Channels (unpatterned units) within lower volcanic facies are discussed in text. *C*, Deposition of sandstone-conglomerate and flysch facies of the Coon Hollow Formation during Middle and Late Jurassic. Channels (unpatterned units) within lower volcanic facies and flysch facies are discussed in text. Submarine fan atop flysch facies discussed in text. *D*, Present-day construction. Diagonal lines below the Columbia River Basalt Group south of Cottonwood Creek denote tilt of pre-Tertiary beds on the Idaho side of Snake River. Not to scale.

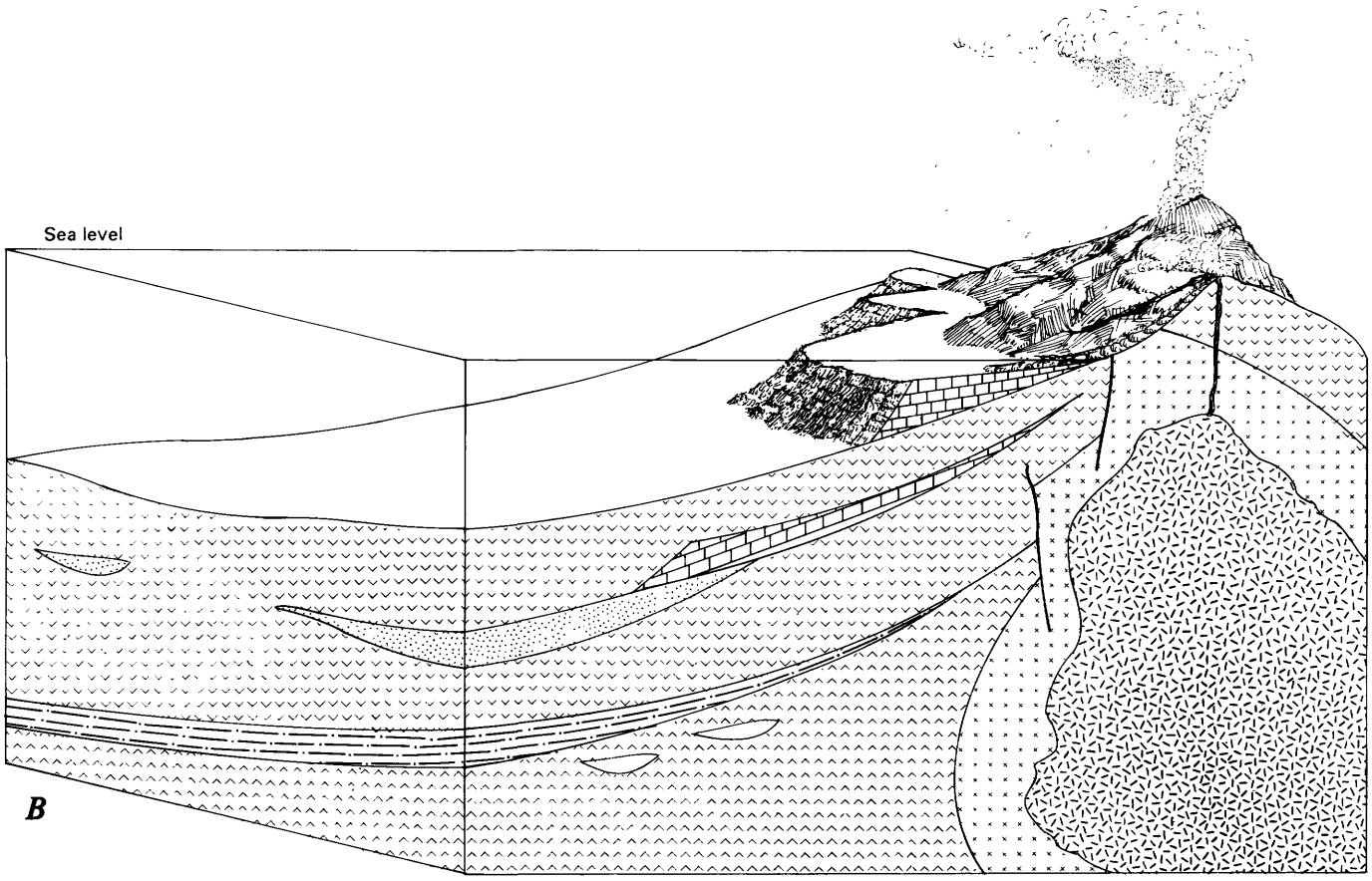

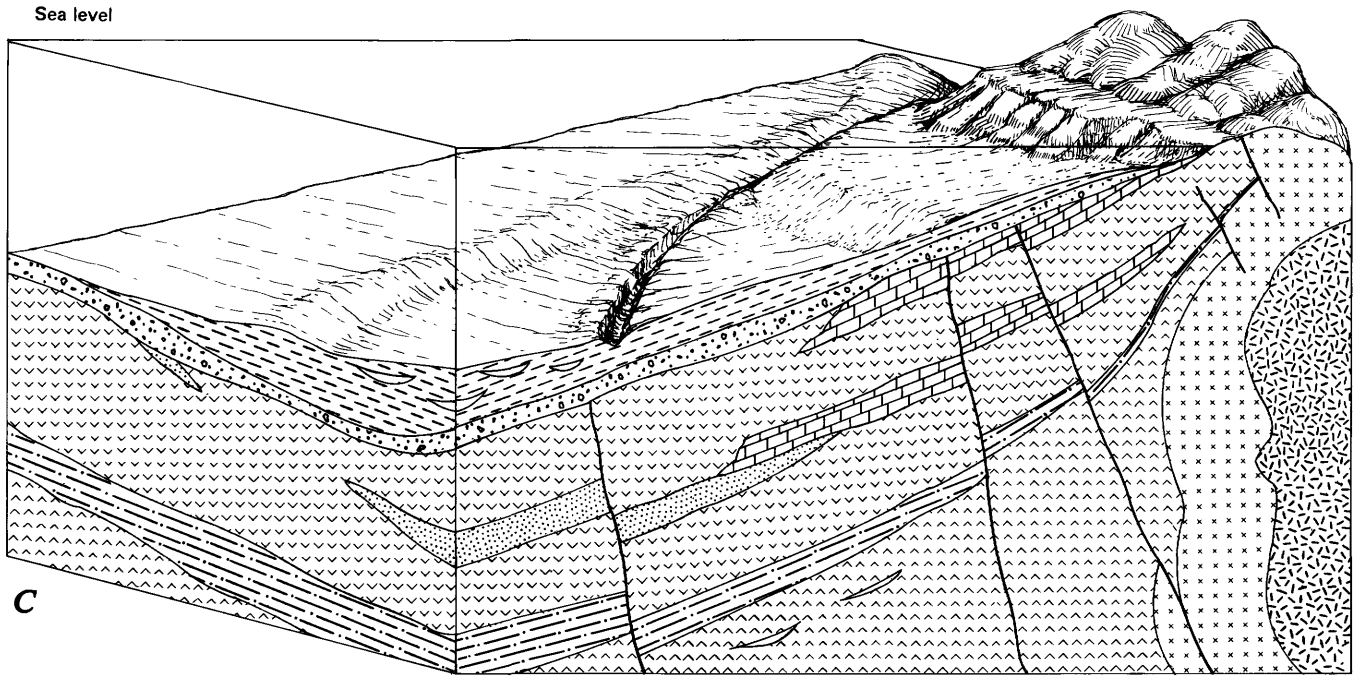

FIGURE 2.10.—Continued

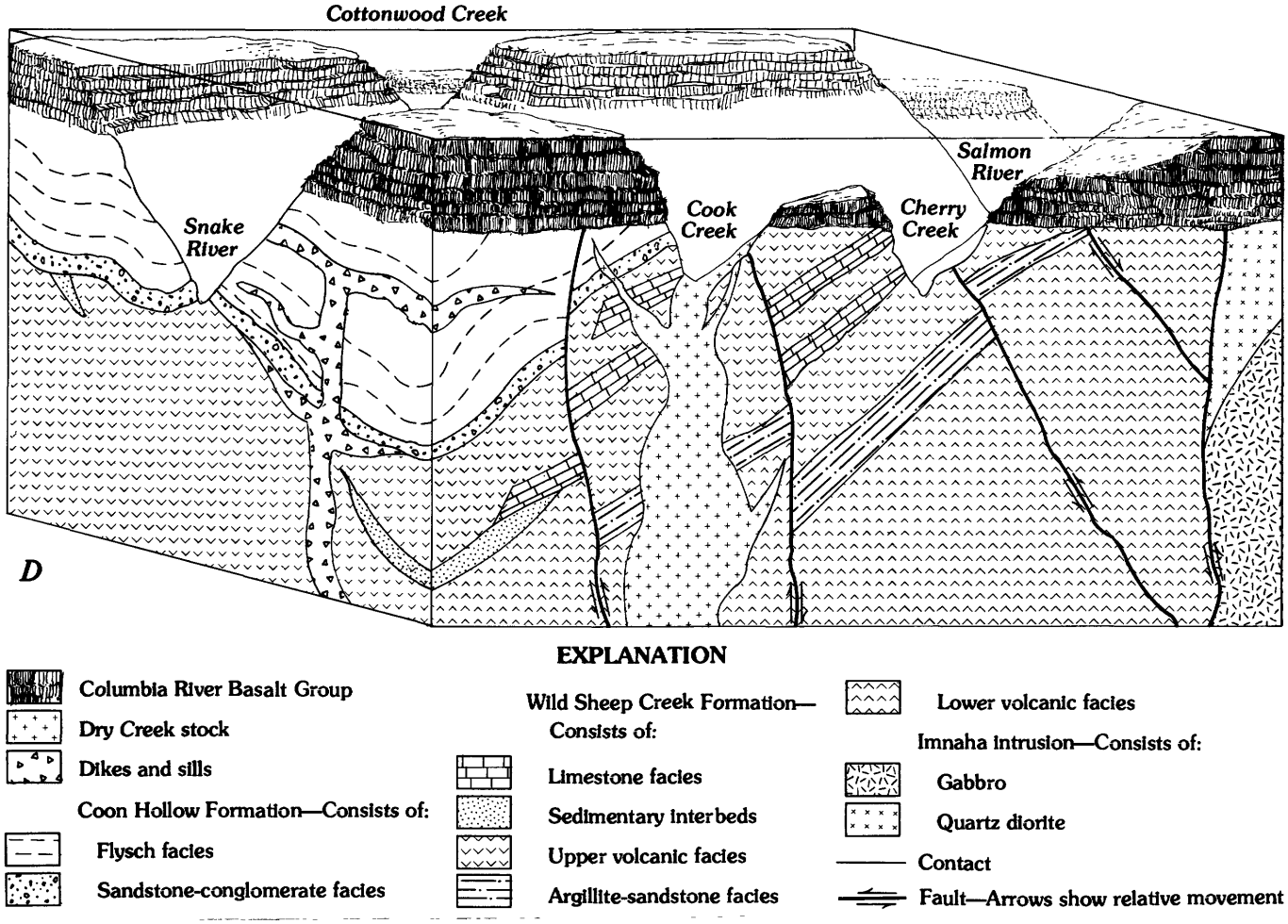

FIGURE 2.10.—Continued

However, the ages of the two batholiths are different; the Idaho batholith is between 75 and 100 Ma, and the Wallowa batholith is between 143 and 160 Ma (Armstrong and others, 1977). Although K-Ar ages increase near the western edge of the Idaho batholith (Armstrong and others, 1977), the age differences between the Wallowa and Idaho batholiths are significant enough to suggest that these batholiths represent two different intrusive phases (Vallier, written commun., 1987).

The Dry Creek stock may be associated with the Wallowa batholith and intruded the northern Wallowa terrane during the Early Cretaceous. This intrusion is not related to the younger Idaho batholith and may have originated during the initial collision of the Wallowa terrane with North America. Further evidence for a Late Jurassic to Early Cretaceous collisional event is the presence of chert and metasedimentary lithic fragments derived from the Baker terrane. The influx of Baker terrane detritus into the Late Jurassic depositional basin of the northern Wallowa terrane may indicate its uplift and erosion owing to the amalgamation and ini-

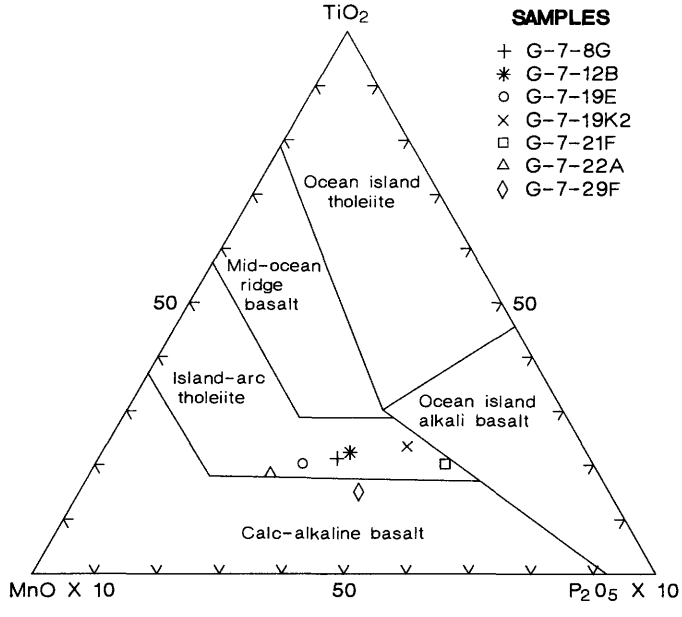

FIGURE 2.11.—TiO_2-MnO-P_2O_5 ternary diagram for samples collected from Wild Sheep Creek Formation in northern Wallowa terrane, northern Oregon and western Idaho.

tial collision of the Blue Mountains island arc to North America.

CONCLUSIONS

The pre-Tertiary rocks of the northern Wallowa terrane represent a small segment of an allochthonous terrane known as the Blue Mountains island arc (Vallier and Brooks, 1986). The rocks in the study area represent a part of a single volcanic island and associated basins within the Blue Mountains island-arc complex. This island arc formed at low latitudes in the eastern Pacific (Pessagno and Blome, 1986) or western Pacific (Vallier and Engebretson, 1984) during the Ladinian to Karnian (Middle to Late Triassic) and was accreted to North America by the mid-Cretaceous (Vallier, 1986).

The volcanic island shows two stages of volcanism—an older siliceous phase (lower volcanic facies of the Wild Sheep Creek Formation) and a younger mafic phase (upper volcanic facies of the Wild Sheep Creek Formation). The two volcanic facies are separated by eruption-generated turbidites of siliceous argillite and volcaniclastic sandstone. The upper volcanic facies shows a compositional change from basalt and basaltic andesite to siliceous pyroclastic eruptions, which were deposited as tuff in the Doyle Creek Formation. The two magmatic phases of the Wild Sheep Creek Formation may be reflected in the compositional zoning from older quartz diorite and diorite to younger gabbro in the Imnaha intrusion. The Imnaha intrusion may be a subduction-related pluton and is a likely parent-magma source for the Wild Sheep Creek Formation.

Volcaniclastic turbidites and debris flows (sandstone-breccia facies of the Wild Sheep Creek Formation) were shed into topographic lows along the flanks of the volcano. Carbonate platforms (limestone facies of the Wild Sheep Creek Formation) developed along the fringes of the island and provided an environment for a variety of nektonic and benthic organisms. The presence of carbonate platforms support the paleomagnetic data for a low paleolatitude for the Wallowa terrane during the Late Triassic.

The volcaniclastic Doyle Creek Formation was deposited in one or more oxygenated basins. Quartz diorite clasts within the formation suggest that part of the Imnaha intrusion had been uplifted and eroded by Karnian time, probably owing to the later emplacement of the gabbroic part of the Imnaha intrusion.

There is no record of Karnian to Oxfordian time in the study area. Elsewhere, thick accumulations of platform carbonate rocks (Martin Bridge Limestone) and deep-marine shales (Hurwal Formation) indicate subsidence of the Wallowa terrane during the Late Triassic and Early Jurassic. By Callovian time in the Pittsburg Landing area (White, D.L., and Vallier, chap. 3; White, J.D.L., chap. 4, both this volume), the Wallowa terrane was uplifted and tilted and the Coon Hollow Formation was deposited. In the northern Wallowa terrane, the Coon Hollow Formation was deposited during the Callovian and Oxfordian. In the study area, the Wild Sheep Creek Formation and the Imnaha intrusion were being eroded, and a nearshore to offshore, wave-dominated environment (sandstone-conglomerate facies of the Coon Hollow Formation) existed in the Cougar Rapids area. The shoreline trended approximately northeast-southwest, and the sea transgressed southeastward onto the terrane. With submergence of the terrane, a submarine fan (flysch facies of the Coon Hollow Formation) developed and prograded northwest. This fan had three sources: the Wild Sheep Creek Formation, the Imnaha intrusion, and a chert-metasedimentary source. The chert-metasedimentary source delimits the timing of the uplift and amalgamation of the Wallowa and Baker terranes to the Oxfordian, which agrees with the findings of other workers on the Jurassic sedimentary rocks of the Blue Mountains island arc (Blome and others, 1986; Imlay, 1986).

Late Jurassic extension allowed dikes and sills to intrude the northern Wallowa terrane, and it was followed by compression and regional metamorphism to the greenschist facies. During the Early Cretaceous, the Dry Creek stock intruded to shallow depths and caused contact metamorphism in the surrounding rocks. The diorite stock may be related to the granites of the Wallowa batholith and may have been generated by the initial accretion of the Blue Mountains island arc to the western margin of North America.

REFERENCES CITED

Abbott, P.L., and Peterson, G.L., 1978, Effects of abrasion durability of conglomerate clast populations: Examples from Cretaceous and Eocene conglomerate of the San Diego area, California: Journal of Sedimentary Petrology, v. 48, no. 1, p. 31–42.

Armstrong, R.L., Taubeneck, W.H., and Hales, P.O., 1977, Rb-Sr and K-Ar geochronometry of Mesozoic granitic rocks and their Sr isotopic composition, Oregon, Washington, and Idaho: Geological Society of America Bulletin, v. 88, no. 3, p. 387–411.

Balcer, D.E., 1980, 40Ar/39Ar ages and REE geochemistry of basement terranes in the Snake River Canyon, northeastern Oregon-western Idaho: Columbus, Ohio State University M.S. thesis, 111 p., unpublished.

Blome, C.D., 1984, Upper Triassic radiolaria and radiolarian zonation from western North America: Bulletin of American Paleontology, v. 85, no. 318, p. 1–88.

Blome, C.D., Jones, D.L., Murchey, B.L., and Liniecki, M., 1986, Geologic implications of radiolarian-bearing Paleozoic and Mesozoic rocks from the Blue Mountains province, eastern Oregon, *in* Vallier, T.L., and Brooks, H.C., eds., Geology of the Blue Mountains region of Oregon, Idaho, and Washington:

Geologic implications of Paleozoic and Mesozoic paleontology and biostratigraphy, Blue Mountains Province, Oregon and Idaho: U.S. Geological Survey Professional Paper 1435, p. 79–93.

Bouma, A.H., 1962, Sedimentology of some flysch deposits: A graphic approach to facies interpretation: Amsterdam, Elsevier, 168 p.

Bourgeois, J., 1980, A transgressive shelf sequence exhibiting hummocky stratification: The Cape Sebastian Sandstone (Upper Cretaceous), southwestern Oregon: Journal of Sedimentary Petrology, v. 50, no. 3, p. 681–702.

Brooks, H.C., and Vallier, T.L., 1978, Mesozoic rocks and tectonic evolution of eastern Oregon and western Idaho, *in* Howell, D.G., and McDougall, D.A., eds., Mesozoic paleogeography of Western United States: Pacific Section, Society of Economic Paleontologists and Mineralogists, (Pacific Coast Paleogeography Symposium 2): Los Angeles, p. 133–145.

Busby-Spera, C.J., 1984, The lower Mesozoic continental margin and marine intra-arc sedimentation at Mineral King, California, *in* Crouch, J.K., and Bachman, S.B., eds., Tectonics and Sedimentation along the California Margin: Society of Economic Paleontologists and Mineralogists, Pacific Section, Los Angeles, California, p. 135–156.

———1985, A sand-rich submarine fan in the lower Mesozoic Mineral King caldera complex, Sierra Nevada, California: Journal of Sedimentary Petrology, v. 55, no. 3, p. 376–391.

———1986, Depositional features of rhyolitic and andesitic volcaniclastic rocks of Mineral King submarine caldera complex, Sierra Nevada, California: Journal of Volcanology and Geothermal Research, v. 27, p. 43–76.

Dickinson, W.R., and Suczek, C.A., 1979, Plate tectonics and sandstone compositions: American Association of Petroleum Geologists Bulletin, v. 63, no. 12, p. 2164–2182.

Dimroth, E., Cousineau, P., Leduc, M., and Sanschagrim, Y., 1978, Structure and organization of Archean subaqueous basalt flows, Rouyn-Noranda area, Quebec, Canada: Canadian Journal of Earth Science, v. 15, no. 6, p. 902–918.

Dott, R.H., 1964, Wacke, graywacke, and matrix-what approach to immature sandstones classification?: Journal of Sedimentary Petrology, v. 34, no. 3, p. 625–632.

Fiske, R.S., and Matsuda, T., 1964, Submarine equivalents of ash flows in the Tokiwa Formation, Japan: American Journal of Science, v. 262, no. 1, p. 76–106.

Frey, R.W., and Pemberton, S.G., 1984, Trace fossil facies models, in Walker, R.G., ed., Facies Models (2d ed.): Geoscience Canada Reprint Series 1, p. 189–207.

Goldstrand, P.M., 1987, The Mesozoic stratigraphy, depositional environments, and tectonic evolution of the northern portion of the Wallowa terrane, northeastern Oregon and western Idaho: Bellingham, Western Washington University, M.S. thesis, 200 p., unpublished.

Hamilton, W., 1963, Metamorphism in the Riggins region, western Idaho: U.S. Geological Survey Professional Paper 436, 95 p.

Hillhouse, J.W., Grommé, C.S., and Vallier, T.L., 1982, Paleomagnetism and Mesozoic tectonics of the Seven Devils volcanic arc in northern Oregon: Journal of Geophysical Research, v. 89, no. B5, p. 4462–4477.

Howard, J.D., and Reineck, H.-E., 1981, Depositional facies of high-energy beach-to-offshore sequences: Comparison with low-energy sequence: American Association of Petroleum Geologists Bulletin, v. 65, no. 5, p. 807–830.

Hunter, R.E., and Clifton, H.E., 1982, Cyclic deposits and hummocky cross-stratification of probable storm origin in Upper Cretaceous rocks of Cape Sebastian area, southwestern Oregon: Journal of Sedimentary of Petrology, v. 52, no. 1, p. 127–144.

Imlay, R.W., 1986, Jurassic ammonites and biostratigraphy of eastern Oregon and western Idaho, *in* Vallier, T.L., and Brooks, H.C., eds., Geology of the Blue Mountains region of Oregon, Idaho, and Washington: Geologic implications of Paleozoic and Mesozoic paleontology and biostratigraphy, Blue Mountains province, Oregon and Idaho: U.S. Geological Survey Professional Paper 1435, p. 53–57.

Ingersoll, R.V., Bullard, T., Ford, R., Grimm, J., Pickle, J., and Sares, S., 1984, The effect of grain size on detrital modes: A test of the Gazzi-Dickinson point-counting method: Journal of Sedimentary Petrology, v. 54, no. 1, p. 103–116.

Jones, M.L., and Dennison, J.M., 1970, Oriented fossils as paleocurrent indicators of southern Appalachians: Journal of Sedimentary Petrology, v. 40, no. 2, p. 642–649.

Lajoie, J., 1976, Volcaniclastic rocks, *in* Walker, R.G. ed., Facies Models 15: Geoscience Conference 6, Ontario, no. 3, p. 129–139.

McBirney, A.R., 1984, Igneous Petrology: San Francisco, Freeman, Cooper, and Co., 362 p.

Milliman, J.D., 1974, Marine Carbonates (Part I): New York, Springer-Verlag, 375 p.

Mitchell, A.H.G., 1970, Facies of an early Miocene volcanic arc, Malekula Island, New Hebrides: Sedimentology, v. 14, no. 3, p. 201–243.

Morrison, R.F., 1963, The pre-Tertiary geology of the Snake River canyon between Cache Creek and Dug Bar, Oregon-Idaho boundary: Corvallis, Oregon State University, Ph.D. dissertation, 195 p., unpublished.

———1964, Upper Jurassic mudstone unit named in the Snake River Canyon, Oregon-Idaho boundary: Northwest Science, v. 38, p. 83–87.

Mutti, E., and Ricci-Lucchi, F., 1978, Turbidites of the northern Apennines: Introduction to facies analysis (translated by T.H. Nilsen): International Geology Review, v. 20, p. 125–166.

Newton, C.R., 1986, Late Triassic bivalves of the Martin Bridge Limestone, Hells Canyon, Oregon: Taphonomy, paleoecology, paleozoogeography, *in* Vallier, T.L., and Brooks, H.C., eds., Geology of the Blue Mountains region of Oregon, Idaho, and Washington: Geologic implications of Paleozoic and Mesozoic paleontology and biostratigraphy, Blue Mountains province, Oregon and Idaho: U.S. Geological Survey Professional Paper 1435, p. 7–22.

Pessagno, Emile A., Jr., and Blome, Charles D., 1986, Faunal affinities and tectonogenesis of Mesozoic rocks in the Blue Mountains Province of eastern Oregon and western Idaho, *in* Vallier, T.L., and Brooks, H.C., eds., Geology of the Blue Mountains region of Oregon, Idaho, and Washington: Geologic implications of Paleozoic and Mesozoic paleontology and biostratigraphy, Blue Mountains province, Oregon and Idaho: U.S. Geological Survey Professional Paper 1435, p. 65–78.

Pickerill, R.K., and Pajari, G.E. Jr., 1981, Resedimented volcaniclastics in Cormanville area, northeastern Newfoundland-depositional remnants of Early Paleozoic oceanic islands: Canadian Journal of Earth Science, v. 18, no. 1, p. 55–70.

Silberling, N.J., Jones, D.L., Blake, M.C., Jr., and Howell, D.G., 1984, Lithotectonic terrane map of the western conterminous United States, *in* Silberling, N.J., and Jones, D.L., eds., Lithotectonic terrane maps of the North American Cordillera: U.S. Geological Survey Open-File Report 84-523, pt. C, 43 p.

Stanley, G.D., Jr., 1986, Late Triassic coelenterate faunas of western Idaho and northeastern Oregon: Implications for biostratigraphy and paleogeography, *in* Vallier T.L., and Brooks, H.C., eds., Geology of the Blue Mountains region of Oregon, Idaho, and Washington: Geologic implications of Paleozoic and Mesozoic paleontology and biostratigraphy, Blue Mountains

province, Oregon and Idaho: U.S. Geological Survey Professional Paper 1435, p. 23–40.

Suczek, C.A., and Ingersoll, R.V., 1985, Petrology and provenance of Cenozoic sand from the Indus Cone and the Arabian Basin, DSDP sites 221, 222, and 224: Journal of Sedimentary Petrology, v. 55, no. 3, p. 340–346.

Tasse, N., Lajoie, J., and Dimroth, E., 1978, The anatomy and interpretation of an Archean volcaniclastic sequence, Noranda region, Quebec: Canadian Journal of Earth Science, v. 15, no. 6, p. 874–888.

Taubeneck, W.H., 1964, Cornucopia Stock, Wallowa Mountains, northeastern Oregon: field relationships: Geological Society of America Bulletin, v. 75, no. 11, p. 1093–1116.

Thayer, T.P., and Brown, C.E., 1964, Pre-Tertiary orogenic and plutonic intrusive activity in central and northeastern Oregon: Geological Society of America Bulletin, v. 75, no. 12, p. 1255–1262.

Vallier, T.L., 1974, A preliminary report on the geology of part of the Snake River canyon, Oregon and Idaho: Oregon Department of Geology and Mineral Industries Geological Map Series, GMS-6, 28 p.

———1977, The Permian and Triassic Seven Devils Group: U.S. Geological Survey Bulletin 1437, 58 p.

———1986, Tectonic implications of arc-axis (Wallowa terrane) and back-arc (Vancouver Island) volcanism in Triassic rocks of Wrangellia [abs.]: EOS (American Geophysical Union Transactions), v. 67, no. 44, p. 1233.

Vallier, T.L., and Brooks, H.C., 1986, Paleozoic and Mesozoic faunas of the Blue Mountains province: A review of their geologic implications and comments of papers in the volume, *in* Vallier, T.L., and Brooks, H.C., eds., Geology of the Blue Mountains region of Oregon, Idaho, and Washington: Geologic implications of Paleozoic and Mesozoic paleontology and biostratigraphy, Blue Mountains province, Oregon and Idaho: U.S. Geological Survey Professional Paper 1435, p. 1–6.

Vallier, T.L., and Engebretson, D.C., 1984, The Blue Mountains island arc of Oregon, Idaho, and Washington: An allochthonous coherent terrane from the ancestral western Pacific Ocean?, *in* Howell, D.G., and others, eds., Proceedings of the Circum-Pacific Terrane Conference: Stanford, Calif., Stanford University Publications in Earth Sciences, v. 18, p. 197–199.

Vallier, T.L., and Hooper, P., 1976, Geologic guide to Hells Canyon, Snake River [Oregon-Idaho]: Geological Society of America, Field Guide Book No. 5, 72d Annual Meeting, Cordilleran Section, 38 p.

Walker, G.W., 1979, Reconnaissance geologic map of the Oregon part of the Grangeville Quadrangle, Baker, Union, Umatilla, and Wallowa Counties, Oregon: U.S. Geological Survey Miscellaneous Investigations Series, Map I-1116.

Walker, N.W., 1986, U/Pb geochronologic and petrologic studies in the Blue Mountains terrane, northeastern Oregon and westernmost-central Idaho: Implications for pre-Tertiary tectonic evolution: Santa Barbara, University of California, Ph.D. dissertation, 224 p., unpublished.

White, D.L., 1974, Geology of the Pittsburg Landing-Big Canyon Creek area, Snake River canyon, Idaho and Oregon: Northwest Science, v. 48, no. 1, p. 72–79.

White, D.L., and Vallier, T.L., in press, Geologic evolution of the Pittsburg Landing area, Snake River canyon, Oregon and Idaho, *in* Vallier, T.L., and Brooks, H.C., eds., Geology of the Blue Mountains region of Oregen, Idaho, and Washington: petrology, stratigraphy, tectonics, and resources: U.S. Geological Survey Professional Paper 1438.

White, J.D.L., 1985, Intra-arc basin deposits, Wallowa terrane, western Idaho [abs.]: EOS (American Geophysical Union Transactions), v. 66, no. 46, p. 862–863.

Wilson, D., and Cox, A., 1980, Paleomagnetic evidence for tectonic rotation of Jurassic plutons in Blue Mountains, eastern Oregon: Journal of Geophysical Research, v. 85, p. 3681–3689.

Wilson, J.L., 1974, Characteristics of carbonate platform margins: American Association of Petroleum Geologists Bulletin, v. 58, no. 5, p. 810–824.

3. GEOLOGIC EVOLUTION OF THE PITTSBURG LANDING AREA, SNAKE RIVER CANYON, OREGON AND IDAHO

By DAVID L. WHITE[1] and TRACY L. VALLIER

CONTENTS

ABSTRACT

The Pittsburg Landing area in Idaho and Oregon consists of rocks of Pennsylvanian, Permian, Triassic, Jurassic, and Miocene age. Plutonic and metamorphic basement rocks of Pennsylvanian and Permian age are faulted over Triassic and Jurassic strata. Miocene basalt flows unconformably overlie the older rock units. The Quaternary record consists of unconsolidated landslide, terrace, and alluvial deposits.

Basement rocks in the Pittsburg Landing area are those of the Cougar Creek Complex. This rock unit is mostly of Permian age but includes some rocks as old as Pennsylvanian; it consists of a wide variety of igneous and metamorphic rocks, many of which have been mylonitized. These and lithologically similar rock units in the Wallowa terrane are crystalline basement to Middle and Upper Triassic strata.

The basal stratigraphic unit in the Pittsburg Landing area is the Middle Triassic Big Canyon Creek unit of the Wild Sheep Creek Formation. It consists mostly of basalt and basaltic andesite lava flows, many of them pillowed, volcanic breccia, tuff, conglomerate, sandstone, mudstone, and rare limestone. The Big Canyon Creek unit formed on the flanks of a submarine volcano. Unconformably(?) overlying the Big Canyon Creek unit is the Upper Triassic Kurry unit of the Doyle Creek Formation. It consists of volcanogenic sandstone, mudstone, tuff, and limestone that were deposited in a shallow-water, low-oxygen marine environment near a volcanic landmass. In places, submarine channels are filled with coarse breccia.

The Middle (Bajocian and Callovian) Jurassic Coon Hollow Formation unconformably overlies both the Wild Sheep Creek (Big Canyon Creek unit) and Doyle Creek (Kurry unit) Formations. The Coon Hollow Formation consists of a basal red tuff unit, an alluvial fan and deltaic conglomerate and sandstone unit, a marine sandstone and mudstone unit, a marine turbidite unit, and dikes and sills. The red tuff unit consists of partly welded to nonwelded ash-flow tuff, related pyroclastic and epiclastic sedimentary rocks, and conglomerate. The conglomerate and sandstone unit consists of conglomerate and sandstone that were deposited in a wide variety of subaerial settings including alluvial fan, deltaic, and braided stream environments. Fossil fern leaves and petrified wood fragments are common in the conglomerate and sandstone unit. The overlying sandstone and mudstone unit of the Coon Hollow Formation is a Middle (Bajocian) Jurassic marine deposit that transgressively overlapped the older units. The Middle (Callovian) Jurassic turbidite unit is in fault contact with the conglomerate and sandstone unit and with the Cougar Creek Complex; fossil ammonites indicate that it is the youngest (Callovian) sedimentary unit in the Coon Hollow Formation at Pittsburg Landing. Andesite porphyry and diabase sills and dikes intrude the Coon Hollow Formation in the Pittsburg Landing area.

Miocene flows of the Columbia River Basalt Group unconformably overlie the pre-Tertiary rocks. These flows were extruded onto a deeply dissected landscape that was carved by erosion during the Cretaceous and early Tertiary.

Faults and folds are common in the Pittsburg Landing area. Along the Klopton Creek thrust fault, beds of the Coon Hollow Formation are commonly overturned and, in places, are isoclinally folded. Most structures in the area parallel the Klopton Creek thrust fault. The Cougar Creek Complex was uplifted along the ancestral Klopton Creek fault in the Jurassic and served as a local source for sedimentary strata in the Coon Hollow Formation. This fault, reactivated after deposition of the Coon Hollow Formation, thrust the Cougar Creek Complex over the Triassic and Jurassic strata. Late(?) Miocene to Holocene uplift and erosion by the Snake River and its tributaries led to the cutting of the Snake River canyon.

INTRODUCTION

The Pittsburg Landing area in the Snake River canyon of Oregon and Idaho (fig. 3.1) is of regional

[1]Consultant, P.O. Box 124, Colton, Wash. 99113

geologic interest because of its unique stratigraphy and structure. The Pittsburg Landing area is referred to informally as that area where the Snake River canyon widens near lower Pittsburg Landing and upper Pittsburg Landing as shown on the USGS Grave Point 7 1/2 minute quadrangle map. On both sides of the Snake River Canyon in Idaho County, Idaho, and Wallowa County, Oregon, the approximately 65 km^2 area consists of rocks of Pennsylvanian, Permian, Middle and Late Triassic, Middle Jurassic, and early and middle Miocene age. As such, the rocks represent most rock units that are exposed in the Wallowa terrane (Silberling and others, 1984) of the Blue Mountains province. In this chapter, we describe the stratigraphy and structural geology of the area and interpret its geologic evolution in relation to the regional geology of the Blue Mountains province.

Wagner (1945) published the earliest geologic studies of the Pittsburg Landing area. Reconnaissance geologic maps that include the area were later published by Vallier (1968, 1974), White (1972), Vallier and Hooper (1976), and White (1985). Regional relations were discussed by White (1972), Vallier (1977), Vallier and others (1977), Vallier and Batiza (1978), and Brooks and Vallier (1978). This chapter complements the work of White (1985; chap. 4, this volume) and Vallier (in press).

Most fieldwork was completed in 1968, 1969, 1970, and 1971. Subsequent field studies have been carried out during short intervals since then with the latest in the summer of 1990. Field studies were complemented by thin-section investigations and some bulk-rock chemistry. Analytical methods for the chemical analyses are discussed by Vallier (in press).

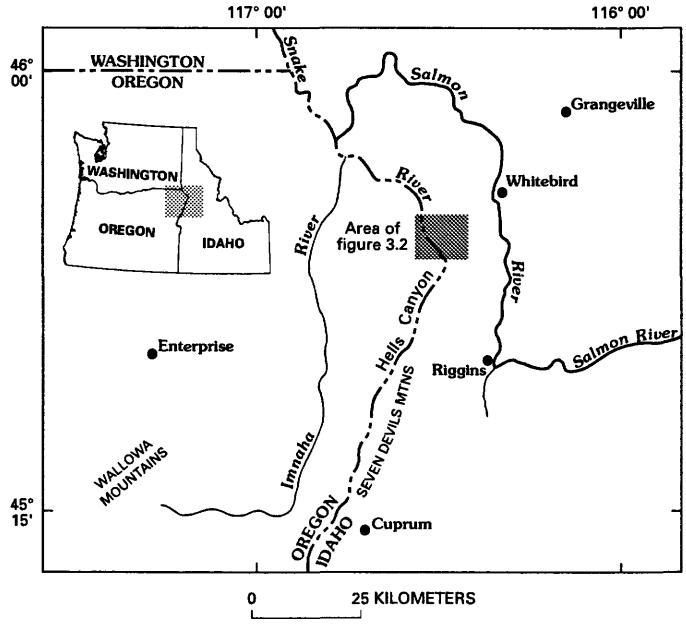

FIGURE 3.1.—Location map for the Pittsburg Landing area (stippled), Oregon and Idaho.

ACKNOWLEDGMENTS

We are grateful to many people for help with the collection of field data and for critical reviews. We particularly thank D. Fredley, R. Ozier, and J. Waldrip for assistance in the field during the 1969–1971 interval. Fossils were identified by S.R. Ash, R.W. Imlay, N.J. Silberling, and G.D. Stanley, Jr. We are grateful to H.C. Brooks, M.B. Underwood, N.W. Walker, J.D.L. White, and S.M. White who provided critical reviews. Susan Vath and Tau Rho Alpha helped with the illustrations.

REGIONAL GEOLOGY

Rocks of the Wallowa terrane (Silberling and others, 1984; Vallier, in press) are mostly Permian, Triassic, Jurassic, Cretaceous, and Miocene in age. Pennsylvanian rocks from the Cougar Creek Complex of Vallier (1968) were reported by Walker (1986). Pre-Tertiary rock types in the Wallowa terrane include those that are expected in an intraoceanic volcanic-arc setting, including basalt through rhyolite flow rocks, gabbro through granodiorite plutonic rocks, a broad assortment of volcaniclastic rocks (both pyroclastic and epiclastic), and limestone. The rocks have undergone variable amounts of metamorphism, mostly related to intrusive events that occurred somewhat episodically within the Early Permian, Middle and Late Triassic, and Late Jurassic to Early Cretaceous (Vallier, in press). In most of the Wallowa terrane, variably metamorphosed rocks are characterized by albite-epidote hornfels and greenschist-facies mineralogies (albite and oligoclase feldspars, epidote, chlorite, sphene, white mica, and quartz). Hornblende-, hornfels-, and amphibolite-facies mineralogies (amphibole, epidote, and andesine feldspar) are recognized in the Cougar Creek Complex and near large Jurassic to Cretaceous plutons.

The largest volume of stratified rocks within the Wallowa terrane occurs in the Lower Permian and Middle and Upper Triassic Seven Devils Group (Vallier, 1977). These rocks formed near the magmatic axis of an intraoceanic volcanic arc in the ancestral Pacific Ocean (Hillhouse and others, 1982; Vallier and Engebretson, 1984; Harbert and others, 1988;

Vallier, in press). Final accretion of the arc to the North American continent probably occurred in the mid-Cretaceous, about 118 to 100 Ma (Lund and Snee, 1988). According to Vallier (in press), accretion probably started much earlier.

Permian strata (mostly the Hunsaker Creek Formation) in the Seven Devils Group (Vallier, 1977) are predominantly silicic volcaniclastic rocks (mainly tuffs and tuffaceous sandstone and mudstone) with locally abundant conglomerate and breccia units. Volcanic flows are rare. These rocks are well exposed in the Snake River canyon near Homestead, Oregon, about 80 km south of the Pittsburg Landing area. Permian stratified and hypabyssal intrusive rocks were erupted from silicic volcanoes; at least two of the inferred eruptive centers are exposed in tributary canyons of the Snake River.

Middle (Ladinian) and Upper (Karnian) Triassic rocks of the Wild Sheep Creek Formation (Vallier, 1977) include abundant volcanic (flow) rocks and associated volcaniclastic breccia, sandstone, mudstone, and conglomerate. Pyroclastic strata are subordinate to epiclastic strata. Small limestone bodies are both lithofacies of the Wild Sheep Creek Formation and slide blocks (olistoliths). Igneous rocks in general are more mafic (mostly basalt and basaltic andesite) than the Permian rocks but include a complete range of compositions from basalt to rhyolite.

The uppermost part of the Seven Devils Group, which includes parts of the Doyle Creek Formation, and the correlative "Lower Sedimentary Series" of Prostka (1962) in the Wallowa Mountains were deposited both in shallow marine water and subaerially. In the Snake River canyon, a large part of the Doyle Creek Formation consists of lava flows and pyroclastic deposits; the rocks are more silicic than those of the Wild Sheep Creek Formation and contain abundant andesite and rhyolite. Quartz diorite and gabbro plutons were exposed during deposition of the Doyle Creek Formation and served as source rocks for some of the epiclastic conglomerate and sandstone. Parts of the Doyle Creek Formation in some areas probably interfinger with the upper parts of the Wild Sheep Creek Formation (Vallier, in press).

The Middle and Late Triassic volcanic arc was more complex, both structurally and petrologically, than originally reported (Vallier, 1977). Islands were composed not only of active volcanoes but also of older volcanic, plutonic, and sedimentary rocks, similar to the present-day geologic setting of the Aleutian island arc in the North Pacific Ocean (Scholl and others, 1983; Vallier and others, in press).

Unconformably overlying the Seven Devils Group at two places in Snake River canyon is the Martin Bridge Limestone of Norian age (Vallier, 1977). This unit is a shallow-water carbonate sequence that was deposited on eroded rocks of the volcanic arc after Triassic volcanism had ceased. Some reef facies have been recognized (Follo and Sevier, 1985; Follo, chap. 1, this volume). Many of the limestone and mudstone units of the Hurwal Formation in the Wallowa Mountains are deeper water facies equivalents of the Martin Bridge Limestone (Follo, chap. 1, this volume).

Middle and Upper Jurassic (Bajocian to Oxfordian) argillite, sandstone, and conglomerate beds of the Coon Hollow Formation unconformably overlie the Seven Devils Group; at Pittsburg Landing, Coon Hollow strata are Bajocian and Callovian in age, and along the Snake River canyon near the Oregon-Washington State line the Oxfordian stage is represented (Morrison, 1961, 1964; White, 1972; Vallier, 1977; Goldstrand, chap. 2, this volume). The present outcrops apparently were preserved in local grabens or half grabens that protected the strata from Cretaceous and early Tertiary subaerial erosion.

Major plutonism occurred in the Permian, Triassic, and Jurassic to Cretaceous throughout the Wallowa terrane of the Blue Mountains province (Vallier, in press). Some of the Cougar Creek Complex is of Pennsylvanian age (Walker, 1986), but the amount of plutonism represented is minor. The Permian and Triassic plutonic rocks are notably potassium poor and have tholeiitic affinities, whereas almost all of the later plutons of Jurassic to Cretaceous age are calc-alkaline (Vallier, in press). Some of the Permian and Triassic plutonic rocks are associated with igneous and metamorphic complexes; one of these complexes is exposed in the Snake River canyon just south of Pittsburg Landing (Cougar Creek Complex) and the other is exposed along the canyon near Oxbow, Oregon (Oxbow Complex of Vallier, 1967) about 90 km south of the Pittsburg Landing area. In the Pittsburg Landing area, the Cougar Creek Complex has been thrust faulted over Triassic and Jurassic stratified units. Plutonic rock types are mostly gabbro, norite, diabase, quartz diorite, and trondhjemite that have been variably mylonitized and metamorphosed. Dike zones that had protoliths of diabase, quartz keratophyre, and trondhjemite are mylonite and gneissic mylonite in several places within the complexes.

Unconformably overlying the pre-Tertiary rocks are lower and middle Miocene flows of the Columbia River Basalt Group. These flows were extruded onto a surface that had a regional relief of at least 500 m. Two units have been mapped (Ozier, 1971; Vallier and Hooper, 1976) in the Pittsburg Landing area, the (older) Imnaha Basalt and the (younger) Yakima Basalt Subgroup (Swanson and others, 1979).

Structures in the Snake River canyon and adjacent regions are predominantly high-angle faults and broad open folds. In most areas only one major deformation is recognized. In the Cougar Creek and Oxbow Complexes, however, two periods of deformation, and possibly three, are recognized. In those igneous and metamorphic complexes, primary igneous foliation and sedimentary bedding have been almost completely destroyed by a strong deformation that created a pronounced northeast-southwest mylonitic foliation. These mylonites occur in distinct linear zones within the complexes. A second deformation folded the mylonitic rocks; preliminary analyses of rocks a short distance south of the Pittsburg Landing area suggest that this deformation is related to movement along the Klopton Creek thrust fault.

GEOLOGY OF THE PITTSBURG LANDING AREA

GENERAL GEOLOGY

The layered rocks in the Pittsburg Landing area are predominantly of volcanic (flow) and volcaniclastic (pyroclastic and epiclastic) origin and consist of pillow lavas and massive lava flows, volcanic breccia, conglomerate, sandstone, and mudstone with subordinate amounts of limestone and welded tuff (figs. 3.2, 3.3). From oldest to youngest the sequence (fig. 3.3) is composed of the Middle Triassic (Ladinian) Big Canyon Creek unit of the Wild Sheep Creek Formation, which is overlain, probably unconformably, by the Upper Triassic (Karnian) Kurry unit of the Doyle Creek Formation. The Kurry unit is overlain unconformably by the Middle Jurassic Coon Hollow Formation. These pre-Tertiary rocks are in turn overlain unconformably by the Miocene Columbia River Basalt Group. Triassic and younger gabbro, diabase, basalt, and andesite porphyry sills and dikes, as well as dikes of the Columbia River Basalt Group intruded the layered sequence.

The Cougar Creek Complex was thrust over the Mesozoic stratified assemblage probably during the Late Jurassic and Early Cretaceous interval. Structural trends in the Pittsburg Landing area are predominantly N. 30° E. to N. 70° E. Maximum deformation occurs within the Cougar Creek Complex where some rocks are mylonitized. Folds are broad and open within the stratified sequences except along the Klopton Creek thrust fault (fig. 3.2), where rocks of the Coon Hollow Formation are both isoclinally folded and overturned. Faults throughout the area predominate over folds; most are steeply dipping normal and reverse faults.

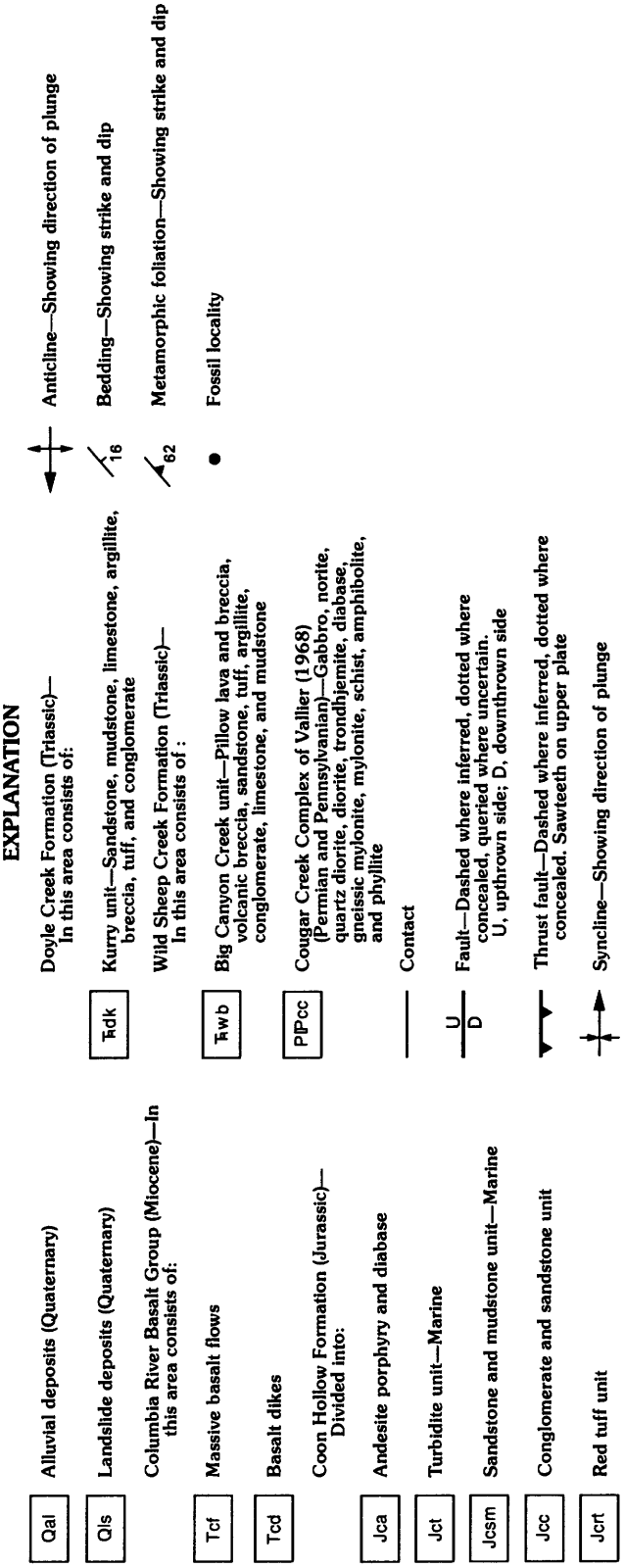

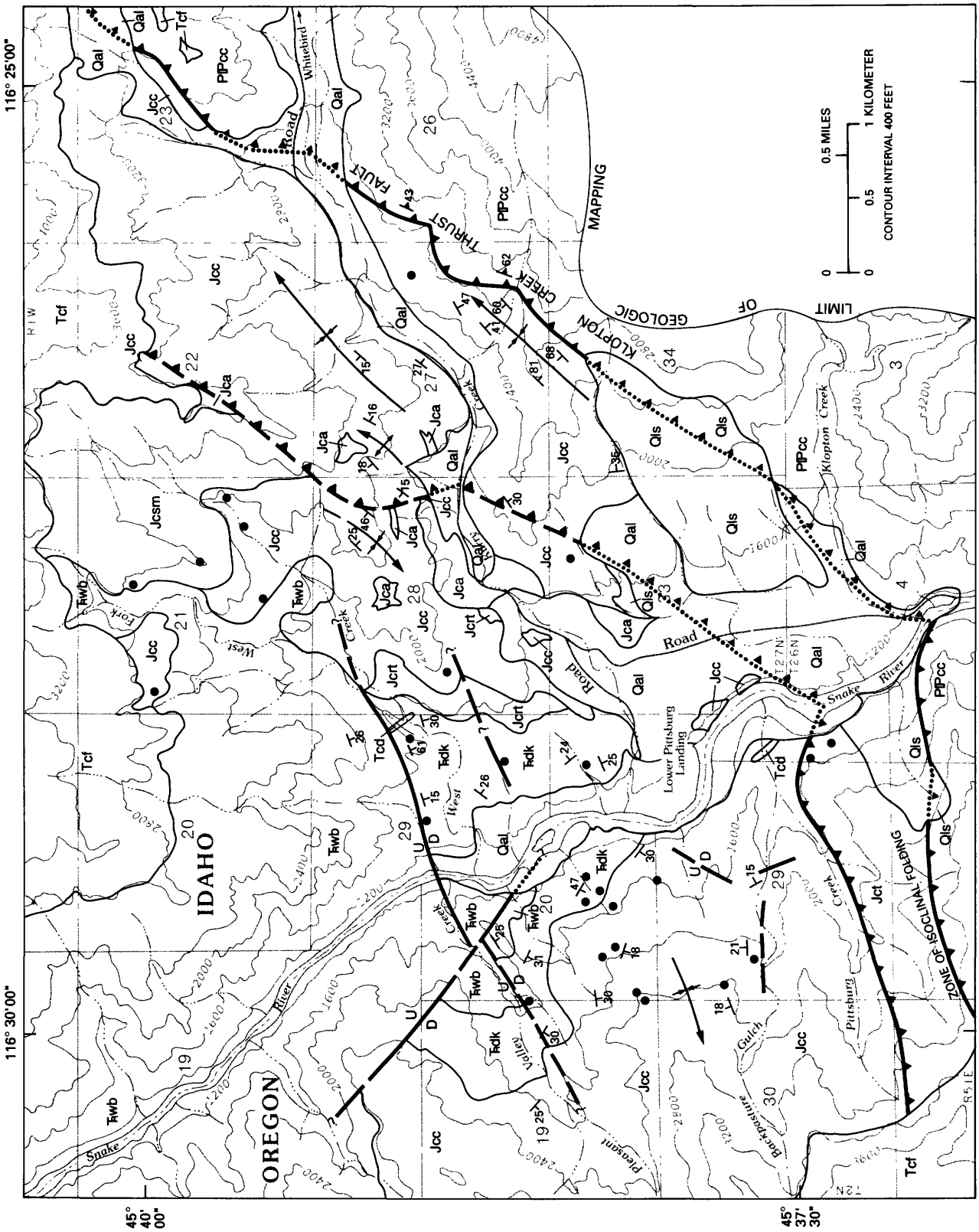

FIGURE 3.2.—Generalized geology of Pittsburg Landing area. Base from U.S. Geological Survey, 1:24,000 Grave Point quadrangle, 1963.

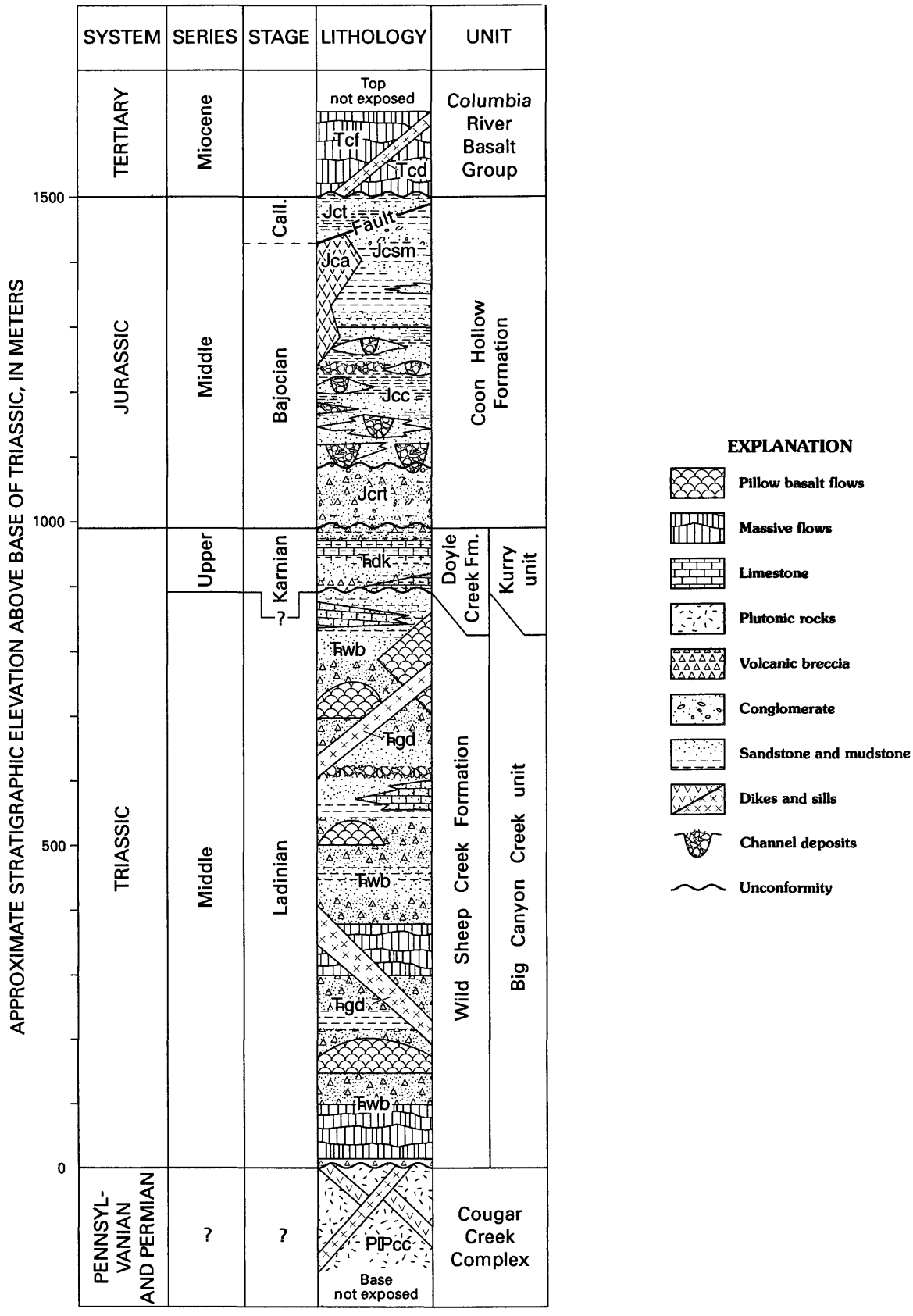

FIGURE 3.3.—Lithologic column for Pittsburg Landing area showing the major units. Map units shown in this figure include the Cougar Creek Complex of Vallier (1968) although contact with Triassic rocks is not exposed within study area. For explanation of map-unit symbols and lithologic descriptions, see figures 3.2 and 3.5. Call., Callovian.

BIG CANYON CREEK UNIT OF THE WILD SHEEP CREEK FORMATION

The Big Canyon Creek unit of the Wild Sheep Creek Formation derives its name from exposures located near Big Canyon Creek, which lies about 3 km north of the mapped area. The Big Canyon Creek unit is characterized by abundant pillow lava flows and pillow breccia, massive lava flows, and coarse-grained volcaniclastic rocks, which are intercalated with beds of tuff, mudstone, sandstone, conglomerate, and limestone. The abundant pillow lavas and pillow breccias distinguish the Big Canyon Creek unit from most of the remainder of the Wild Sheep Creek Formation in the Wallowa terrane, the rocks of which are dominated by coarse breccia units. The Big Canyon Creek unit is crudely graded with coarser grained strata and thicker flows and beds near the base of the sequence and thinner flows and finer grained beds near the top.

Volcanic (flow) rocks of the Big Canyon Creek unit consist of basalt, basaltic andesite, and rare andesite and dacite. Porphyritic textures are dominant. Colors range from reddish brown on weathered surfaces to black and greenish black on fresh surfaces. Plagioclase phenocrysts are pale green to white, range in length from 0.5 mm to 1.0 cm, and are set in a groundmass of intergranular, intersertal, and pilotaxitic textures. Plagioclase compositions range from labradorite to albite, depending on the intensity of metamorphism (White, 1972). Groundmass minerals are plagioclase (mostly albite), chlorite, epidote, white mica, calcite, sphene, and iron oxide minerals.

Pillow basalt flows and pillow basalt breccias are especially well exposed along both sides of the Snake River just north of the Pittsburg Landing mapped area. The pillows generally have maximum diameters of about 1 m although some flattened pillows are 2 m long. Pillow margins are rimmed by fine-grained alteration minerals (mostly chlorite and epidote) that replaced glassy selvages. Pillow interiors have mostly intersertal textures and contain irregularly shaped vesicles, some of which are filled with chlorite, epidote, and calcite.

Breccias in the Big Canyon Creek unit are of flow, pillow, epiclastic, and pyroclastic origins. The pyroclastic breccias characteristically are hydroclastic rocks that contain angular glass shards and monolithic clasts. The epiclastic breccias have polylithic clasts and are interlayered with sandstone and mudstone. Many of the breccias probably were mobilized as debris flows from oversteepened flanks of a submerged volcano.

In the northwest quarter of sec. 28 in Idaho near West Creek (fig. 3.2), a sequence of vertically graded tuff beds, 4 to 6 m thick, consists of alternating green and greenish-black layers of sand-sized grains. Thin sections show rock and mineral fragments separated by glass. The glass is palagonitic, but compared to tuff beds in other exposures of the Wild Sheep Creek Formation, it is surprisingly fresh. The repetitive character of the beds, their presence in marine strata, and the vertical coarse-to-fine grading indicate deposition from submarine turbidity currents. Rare lenses and pods of argillaceous limestone, 10 to 50 cm thick, alternate in places with sandstone, shale, and mudstone.

The lavas were erupted on the flanks of an island or a seamount. Explosive eruptions were common. Debris flows deposited thick breccia sequences on the insular and (or) seamount slopes, and limestone formed in shallow-water environments that were protected from terrigenous and volcanic debris. Many of the turbidite beds are distal deposits of the debris flows.

A fossil locality at Jones Creek, which lies about 5 km north of the map area, yielded *Daonella* sp. of Ladinian (late Middle Triassic) age (White, 1972); elsewhere in the Wallowa terrane *Daonella* are abundant in the Wild Sheep Creek Formation (Vallier, 1967, 1977). However, in a few areas the Wild Sheep Creek Formation contains Karnian (Late Triassic) ammonites (Vallier, 1977) and Karnian *Halobia* (Grant, 1980), but in the Pittsburg Landing area we believe that the Big Canyon Creek unit is Middle Triassic (Ladinian) in age.

KURRY UNIT OF THE DOYLE CREEK FORMATION

The Kurry Creek Member of the Doyle Creek Formation (Vallier, 1977) is herein abandoned because of its lithologic and geographic restrictions. The strata comprising the lower part of the Kurry Creek Member, which are here informally called the Kurry unit, are reassigned to the undivided Doyle Creek Formation. Rocks previously described as the upper part of the Kurry Creek Member (Vallier, 1977) are herein reassigned to the Coon Hollow Formation. The Kurry unit has been mapped at no other locality within the Wallowa terrane and apparently is restricted to outcrops in the Pittsburg Landing area.

The Kurry unit consists of thinly bedded tuffaceous sandstone and mudstone, argillaceous limestone, and tuff. It unconformably(?) overlies the Big Canyon Creek unit of the Wild Sheep Creek Formation. The Kurry unit is at least 100 m thick and is best exposed along the north side of West Creek between a point about 1 km upstream of its confluence with the Snake River in Idaho and across the river in the middle

drainage basin of Pleasant Valley Creek in Oregon (fig. 3.2). Thin-bedded tuffaceous and calcareous strata can be observed along the north side of Kurry Creek near the road that leads to lower Pittsburg Landing. Some sandstone beds contain small fossil plant fragments. Large wedge-shaped channel-fill deposits that crop out near the mouth of West Creek consist of debris that apparently was eroded from the Big Canyon Creek unit. Strata that filled these channels are mostly volcanic breccia and sandstone but also include a few large limestone boulders (1-2 m in diameter).

Fossils (*Halobia* and ammonite molds), recovered about 0.5 km south of the mouth of Pleasant Valley Creek (fig. 3.2) indicate that the rocks are of early Karnian age (N.J. Silberling, oral commun., 1985). The Kurry unit is regarded as a mappable local facies of the Doyle Creek Formation and is correlative with part of the "Lower Sedimentary Series" of the Wallowa Mountains (Smith and Allen, 1941; Prostka, 1962). Some of the Upper Triassic (Karnian) limestone-mudstone units in the Wild Sheep Creek Formation exposed along the Snake River canyon near the Washington-Oregon State boundary (Grant, 1980) about 50 km north of Pittsburg Landing may also be correlative with the Kurry unit. A closer study of these critical outcrops is required, however, before a correlation can be established.

The presence of the flat clam *Halobia* sp. and the absence of other benthic megafossils suggest a low-oxygen depositional environment. Strata of the Kurry unit apparently were deposited in a restricted shelf basin (or upper slope environment) that was protected from the deposition of coarse-grained debris except in channels. Some direct input of ash and lapilli occurred during volcanic eruptions.

COON HOLLOW FORMATION

We redescribe the lithology of the Coon Hollow Formation in the Pittsburg Landing area (Vallier, 1977) as a basal red tuff unit, an alluvial fan and deltaic conglomerate and sandstone unit, a marine sandstone and mudstone unit, a turbidite unit, and some small intrusive bodies.

In the Pittsburg Landing area, the Jurassic Coon Hollow Formation overlies the Triassic Big Canyon Creek unit of the Wild Sheep Creek Formation and the Kurry unit of the Doyle Creek Formation along an angular unconformity and is unconformably overlain by the Miocene Columbia River Basalt Group. The unconformity between the Kurry unit and the conglomerate and sandstone unit of the Coon Hollow Formation is well exposed along the Snake River just southwest of and across the river from the mouth of Kurry Creek (fig. 3.2). Rocks of the Coon Hollow Formation are truncated on the south and east by the Klopton Creek thrust fault (fig. 3.2). Rocks of the Cougar Creek Complex make up the hanging wall of the Klopton Creek thrust fault.

RED TUFF UNIT

Subaerial pyroclastic volcanism is indicated by the red tuff unit, the oldest strata of the Coon Hollow Formation. This rusty red, maroon, and gray rock unit is well exposed along a jeep trail just south of West Creek in Idaho along the west edge of sec. 28 (fig. 3.2), where it is about 50 m thick. The unit consists of tuff, conglomerate, and sandstone.

Tuff beds, for which the unit is named, are about 15 m thick and crop out near the jeep trail. A crystal-lithic welded tuff near the top of the tuff sequence is about 5 m thick and crops out with polygonal colonnades; it contains flattened and stretched pumice fragments. The remainder of the red tuff unit has mixed epiclastic rocks and nonwelded pyroclastic rocks. The unit was thinned by erosion before the overlying conglomerate and sandstone unit was deposited. Stream channels, later filled in with strata of the conglomerate and sandstone unit, cut downward into the red tuff unit and, in places, eroded completely through the red tuff unit and into the underlying Kurry unit. The irregular distribution of outcrops of the red tuff unit within the map area (fig. 3.2) and its absence directly across the Snake River in Oregon suggest that it was preserved locally because it had filled a depression in the ancient landscape and thereby escaped subsequent erosion.

The age of the red tuff unit is unknown, but because of similarities to the overlying conglomerate and sandstone unit, we infer that it is Bajocian (Middle Jurassic) or older. The source vent has not been located, but the presence of pyroclastic debris in the red tuff unit indicates that centers of silicic volcanism existed during the Middle Jurassic in the Wallowa terrane.

CONGLOMERATE AND SANDSTONE UNIT

The conglomerate and sandstone unit overlies the red tuff unit and unconformably overlies the Triassic strata. Stream channels of this unit, now filled with conglomerate and sandstone beds, cut the red tuff unit as well as the Big Canyon Creek and Kurry units. The conglomerate and sandstone unit is overlain conformably by marine strata of the sandstone

TABLE 3.1.—*Types and relative abundances of clasts in three conglomerate beds in conglomerate and sandstone unit of Jurassic Coon Hollow Formation*

Location	Total number of clasts counted per bed	Rock type of clast	Percent of total clasts
SW¼ NW¼ sec. 28	55	Volcanic (flow) rocks	38
		Volcaniclastic rocks	42
		Lithic tuff	10
		Fine-grained rocks of unknown lithology	10
SE¼ SE¼ sec. 28	46	Volcanic (flow) rocks	52
		Plutonic rocks	13
		Volcanogenic sandstone	11
		Fine-grained rocks of unknown lithology	24
NW¼ NW¼ sec. 28	41	Volcanic (flow) rocks	12
		Felsic igneous rocks	56
		Volcanogenic sandstone	10
		Fine-grained rocks of unknown lithology	22

and mudstone unit. The conglomerate and sandstone beds (White, chap. 4, this volume) are distinctive because of large variations in thickness over short distances, abrupt facies changes, abundant sedimentary structures, large ranges in sizes and shapes of clasts, and the presence of abundant fossil plants and petrified wood. The filled channels, as measured in their thalwegs, range in thickness from less than 1 to as much as 15 m. In places, steep crossbedding is evident in the channels. The conglomerate beds thin laterally and grade into sandier facies at greater distances from the thalwegs, where they represent point-bar and overbank deposits of braided streams (White, 1985, chap. 4, this volume). The lower part of the conglomerate and sandstone unit indicates abundant reworking of pyroclastic debris, probably derived from erosion of the red tuff unit. The conglomerate and sandstone unit is crudely graded vertically; it becomes finer grained and the percentage of conglomerate beds markedly decreases with greater stratigraphic elevation.

Clast diameters in conglomerates of the conglomerate and sandstone unit range from 1.5 cm to 1 m; the clasts are subrounded to well rounded and have a sphericity index of 0.3 to 0.7. The clasts consist predominantly of volcanic (flow), volcaniclastic, and plutonic rocks (table 3.1). Clast compositions vary from north to south; volcanic (flow)- and volcaniclastic-rock clasts are dominant in the north, whereas rare to common plutonic-rock clasts occur along with the more abundant volcanic-rock clasts in conglomerate south of Kurry Creek. Plutonic-rock clasts range in composition from gabbro to trondhjemite and reflect the wide range in composition of plutonic rocks in the adjacent Cougar Creek Complex (Vallier, in press).

Lithologic and bulk-rock chemical compositions (table 3.2) of selected clasts represent the range of 25 other clasts that were examined in thin section. Trace elements, particularly the rare-earth elements (table 3.3; fig. 3.4), indicate that the clasts were eroded from highly fractionated tholeiitic and calc-alkaline plutonic bodies. On the basis of physical and chemical data, it is apparent that the Cougar Creek Complex was at least one of the sources for the clasts. Such a source implies that the ancestral Klopton Creek fault or another nearby fault was active near the border of the basin during deposition of the conglomerate and sandstone unit (fig. 3.2).

In the middle part of the conglomerate and sandstone unit, the sandstone beds resemble cyclic deposits of sandy braided streams (White, chap. 4, this volume), probably a lower energy version of the coarse cyclic deposits from gravelly braided rivers (Miall, 1977). Sandstone and conglomerate are confined to widely separated channel-fill sequences in the upper parts of the conglomerate and sandstone unit. Tabular crossbedding is common.

The abundance of plant fossils in the conglomerate and sandstone unit is significant for the interpretation of its age and paleoenvironment. Some petrified

TABLE 3.2.—*Major- and minor-element oxides for plutonic-rock (diorite and quartz diorite) and dacite clasts from conglomerate in conglomerate and sandstone unit of Coon Hollow Formation, for diabase and andesite porphyry samples from irregular sills and dikes that intruded (and are herein considered part of) Coon Hollow Formation, and for welded tuff sample from red tuff unit of Coon Hollow Formation*

[Analyses are by X-ray fluorescence and wet-chemical methods; see Vallier (in press) for further discussion of sampling and analytical methods]

Clast type	Diorite	Quartz diorite		Dacite	Diabase	Andesite	Tuff
Sample	TP-13	TP-15	TP-18	Pl-4-83	V-1-85	T-68-16	V-11-85
Major- and minor-element oxides, in weight percent							
SiO_2	55.20	62.50	66.90	68.80	50.90	57.10	70.50
TiO_2	.78	1.37	1.14	.78	.88	.68	.41
Al_2O_3	21.50	13.60	15.00	14.70	15.30	16.90	11.60
Fe_2O_3	1.07	1.65	1.04	3.70	1.39	.91	1.02
FeO	1.40	1.90	2.90	1.08	6.43	3.90	3.82
MnO	.03	.11	.07	.04	.11	.06	.07
MgO	2.16	1.13	1.31	.95	6.16	4.02	1.46
CaO	7.90	6.23	2.30	2.33	5.90	4.15	2.45
Na_2O	5.61	5.73	5.50	5.09	4.90	6.54	3.58
K_2O	1.46	.37	.67	1.04	.32	.41	.14
P_2O_5	.30	.42	.30	.22	.20	.25	.06
H_2O^+	2.00	1.30	1.70	1.19	3.85	2.20	2.26
H_2O^-	.63	.34	.44	.54	.27	.48	.42
Total	100.06	99.75	99.68	100.06	100.14	99.40	99.87

tree trunks have diameters greater than 50 cm. Analyses of the fossil plants (Ash, 1991) indicate that the flora is dominated by the ferns with four taxa and conifers with four taxa. The ginkgoes are represented by several dozen specimens of one species. Seed ferns are very rare. The plant fossils identified (Ash, 1991, p. 29) include horsetails (*Neocalamites* sp.), lycopods (*Isoetites* n. sp.), ferns and fernlike foliage (*Phlebopteris* n. sp., *Dicksonia oregonesis*, *Adiantites* sp., and *Cladophlebis* sp.), seed ferns (*Sagenopteris* sp.), ginkgoes (*Ginkgo huttoni*), and conifers (*Podozamites* sp., *Pagiophyllum* sp., *Brachyphyllum* sp., and *Esembrioxylon* sp.). Furthermore, a few fragmentary imprints of cycadophyte leaves are present.

The Coon Hollow flora seems to correlate with some of the other Jurassic flora from suspect terranes of western North America (Ash, 1991). Unfortunately, fossil plants in the Coon Hollow Formation are not as age-diagnostic as marine fossils in the conformably overlying sandstone and mudstone unit, which probably are Bajocian (Middle Jurassic) in age.

Several environments are represented by the fossil flora from the conglomerate and sandstone unit (Ash, 1991), including moist habitats that occur along streams and lakes and drier environments of higher elevations. Some of the fragile ferns, for example, were preserved essentially in their growth positions whereas the petrified wood and the remains of conifers and ginkgoes were probably washed into the area from surrounding hills. Growth rings in petrified wood indicate well-pronounced seasons that typically occur in temperate climates. The temperate climate interpretation for these Bajocian rocks strengthens the conclusion of Pessagno and Blome (1986) that the Blue Mountains island arc had reached boreal latitudes by the Bathonian (next younger Jurassic Stage).

MARINE SANDSTONE AND MUDSTONE UNIT

The overlying marine sandstone and mudstone unit represents deposits laid down in a transgressive sea with subsequent deepening of the depositional basin. The sandstone and mudstone unit overlies both the conglomerate and sandstone unit of the Coon Hollow Formation and the Big Canyon Creek unit of the Wild Sheep Creek Formation as shown by outcrops in the northeast quarter of sec. 21 where shallow-water coral, pelecypod, and brachiopod fossils were collected directly above strata of the Big Canyon Creek unit (Stanley and Beauvais, 1990). Laterally, these fossil-bearing strata can be observed

TABLE 3.3.—*Trace elements of plutonic rock clasts from conglomerate in conglomerate and sandstone unit of Coon Hollow Formation and of andesite porphyry from dike or plug that intruded Coon Hollow Formation*

[Analyses by neutron activation unless otherwise noted; for discussion of methods, see Vallier (in press). Results in parts per million. ---, not determined, below detection limit, or too high coefficient of variation]

	Plutonic rock clasts			
Rock type-----	Diorite	Quartz diorite		Andesite
Sample---------	TP-13	TP-15	TP-18	T-68-16
Rb[1] ----------	40	---	19	23
Sr[1] ----------	317	154	238	505
Ba[1] ----------	231	92	138	280
Th ----------	.52	2.48	2.63	1.16
U ----------	.48	1.19	.90	.51
La ----------	4.7	13.10	9.5	11.5
Ce ----------	11.9	31.5	22.8	21.7
Sm ----------	2.8	8.4	---	2.7
Eu ----------	1.02	1.85	1.51	.73
Tm ----------	.30	.99	.60	.10
Yb ----------	2.35	6.95	4.79	.69
Lu ----------	.339	.894	.662	.110
Y[1] ----------	24	54	41	13
Zr[1] ----------	125	206	187	90
Hf ----------	3.56	7.04	6.19	1.9
Ta ----------	.21	.47	.38	.19
Nb[1] ----------	6	5	8	8
Co ----------	4.5	5.8	8.4	18
Cr ----------	4	2	5	113
Sc----------	17.6	14.9	21.0	13.4
Zn ----------	26	37	127	44

[1]Analysis by X-ray fluorescence.

overlying the conglomerate and sandstone unit, probably conformably.

Near the base of the sandstone and mudstone unit, sandstone is the dominant lithology, whereas at higher elevations mudstone is by far dominant. Carbonate concretions, some more than 30 cm in diameter, weather out of the mudstone. Hackly fracture characterizes the mudstone beds, and small fossil wood fragments and fossil leaves are common. Thickness of the unit is estimated to be about 100 m. The dark colors and abundance of fossil wood fragments and leaves suggest that the mudstone has a high organic carbon content. The absence of benthic fossils in all but the lowermost beds of the unit and the suspected high organic carbon content indicate a low-oxygen depositional environment.

Corals recovered from the lowermost part of the sandstone and mudstone unit are Middle Jurassic (Bajocian) in age and are the youngest shelly benthic fauna yet known from the Wallowa terrane (Stanley and Beauvais, 1990). Included in the coral faunas are *Coenastraea hyatti* (Wells) and a new species, *Thecomeandra vallieri*. The Bajocian age is assigned on the basis of *Coenastraea hyatti* (Wells), which is known from the Pryor Mountains of Montana, where it occurs with ammonites of middle and late Bajocian age (Imlay, 1980). Fossil bivalves from the unit include the following: *Pronoella uintahensis* Imlay; indeterminable pectinids, *Lima* sp. and *Inoceramus* sp.; *Myophorella (Promyophorella) montanaensis* (Meek); and *Platymya rockymontana* Imlay. The bivalves indicate a Middle Jurassic (Bajocian to early Callovian) age that is compatible with the Bajocian coral *Coenastraea hyatti* (Wells).

The well-documented age (Bajocian) of the marine sandstone and mudstone unit (Stanley and Beauvais, 1990) and its well-mapped transgressive basal contact indicate that the underlying units of the Coon Hollow Formation are Bajocian in age or older. We doubt if very much time elapsed between the subaerial accumulation of the alluvial fan, deltaic, and braided stream deposits of the conglomerate and sandstone unit and the deposition of the marine sandstone and mudstone unit. Apparently, a basin already was forming along the ridgetop of the arc during deposition of the subaerial conglomerate and sandstone unit. Further subsidence of the basin and transgression by the sea led to deposition of the sandstone and mudstone unit. Therefore, the red tuff unit, the conglomerate and sandstone unit, and the sandstone and mudstone unit presumably are all of Middle Jurassic (mostly Bajocian) age. The fauna in the sandstone and mudstone unit provide an apparent strong link with the

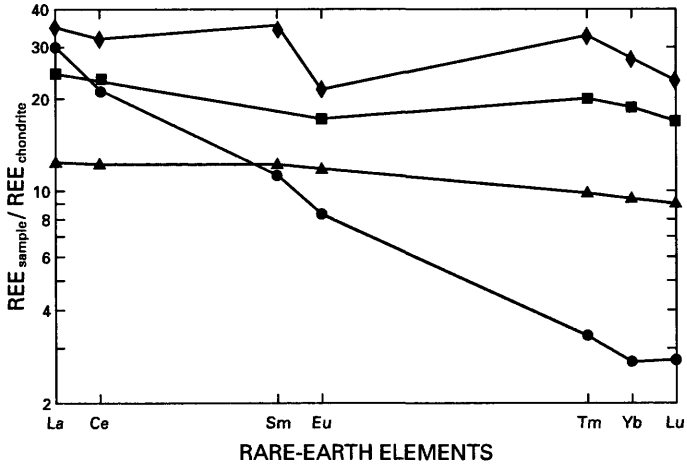

FIGURE 3.4.—Rare-earth element diagram for plutonic-rock clasts from conglomerate and sandstone unit of the Coon Hollow Formation and for an andesite clast from dike or plug that intruded the Coon Hollow. Diamond and square, quartz diorite samples TP-18 and TP-15, respectively; triangle, diorite sample TP-13; circle, andesite porphyry sample T-68-16. Normalizing values are from Masuda and others (1973): La, 0.378; Ce, 0.976; Sm, 0.230; Eu, 0.0866; Tm, 0.030; Yb, 0.249; Lu, 0.0387.

North American western interior fauna during the Bajocian (Stanley and Beauvais, 1990). These Coon Hollow fauna, however, are very different from fauna in correlative beds of most other suspect terranes along the west margin of North America and from Tethyan fauna in the older Triassic rocks. The Wallowa terrane was either attached or very close to the North American craton by Bajocian time (Stanley and Beauvais, 1990).

TURBIDITE UNIT

An enigmatic unit included in the Coon Hollow Formation is a turbidite sequence of sandstone and mudstone that occurs along the south edge of the Pittsburg Landing area in Oregon (fig. 3.2). This unit, referred to herein as the turbidite unit, is bounded by the Klopton Creek thrust fault on the south and an unnamed high-angle thrust fault on the north. The thrust faulting destroyed the original depositional contact between the turbidite unit and older units; possibly, the turbidite unit was transported several kilometers along the faults.

Thin-section analyses indicate that major components of the immature sandstone in the turbidite unit are angular to subrounded plagioclase, quartz, and volcanic rock fragments. Alteration products of white mica, chlorite, epidote, clay minerals, and zeolite (laumontite was identified by X-ray diffraction) indicate temperatures and pressures that were lower than those that affected Triassic rocks. Some sandstone beds are cemented by calcite; this characteristic suggests that a calcareous microfauna and (or) microflora were present before diagenesis (and metamorphism). Mudstone beds are dark brown to black on fresh surfaces and light-brown and gray on weathered surfaces. Ammonites from near the base of the turbidite unit include *Grossouvria*, *Lilloettia stantoni* Imlay and *Xenocephalites*. The presence of *Grossouvria* indicates a late Middle Jurassic (early Callovian) age (Imlay, 1981, 1986). Farther north in the Snake River canyon near the Oregon-Washington State line, at the type section for the Coon Hollow Formation, a sparse ammonite fauna is Late Jurassic (Oxfordian) in age (Imlay, 1981, 1986). The turbidite unit most likely is a deeper water deposit of the Coon Hollow Formation that resulted from continued subsidence of the ridgetop basin of the arc.

SMALL INTRUSIVE BODIES

Within the Coon Hollow Formation, andesite (keratophyre) porphyry and diabase dikes and sills intrude the sedimentary sequence. The two largest andesite porphyry exposures in the Pittsburg Landing area are in the southeast quarter of sec. 28 and the northwest quarter of sec. 33 (fig. 3.2). The intrusive contacts are sharp. That some of these intrusions occurred soon after deposition of some Coon Hollow beds is shown by soft-sediment deformation near intrusive contacts.

The andesite porphyries contain phenocrysts of plagioclase (replaced by albite) and mafic minerals (replaced by chlorite) set in a felty groundmass composed almost entirely of albite microlites and microcrystalline albite and quartz. Secondary minerals besides albite and chlorite are white mica and quartz. Diabase samples have coarse diabasic textures and consist of plagioclase, opaque minerals, and clinopyroxene (completely replaced by chlorite, epidote, and sphene). Some chlorite-filled interstices may have been glass prior to metamorphism.

Chemical analyses (tables 3.2, 3.3) of the andesite indicate that it is Na_2O enriched and has calc-alkaline affinities. The calc-alkaline characteristics, as shown by a low FeO_{total}/MgO value of about 1.2 and enriched light-rare-earth element values (fig. 3.4), are notably different from those of the mostly tholeiitic and transitional (tholeiitic to calc-alkaline) rocks of the Wild Sheep Creek and Doyle Creek Formations and more closely resemble the Jurassic to Cretaceous plutonic rocks of the Blue Mountains region (Vallier, in press).

DEPOSITIONAL AND TECTONIC ENVIRONMENTS

The Coon Hollow Formation was deposited in a subsiding basin during extensive uplift and erosion of the surrounding pre-Jurassic rocks. The depositional regime changed from dominantly pyroclastic and subaerial sedimentary (red tuff unit) to entirely subaerial sedimentary (alluvial fan, deltaic, and braided stream deposits of the conglomerate and sandstone unit) to transgressive marine sedimentary (sandstone and mudstone unit) to relatively deep basin sedimentary (turbidite unit). Modern analogs of the basin in which the Coon Hollow rocks evolved are the ridgetop or summit basins of the Aleutian island arc (Scholl and others, 1983, 1988) and the New Hebrides (Vanuatu) island arc (Carney and Macfarlane, 1980; Carney and others, 1985). The deposits at Pittsburg Landing are well preserved because during the long Cretaceous to early Tertiary time interval they were protected from erosion in a fault-bounded basin (Morrison, 1964; Brooks and Vallier, 1978; Imlay, 1981).

Strata correlative with the Coon Hollow Formation, in central and eastern Oregon (Dickinson and Thayer, 1978; Imlay, 1986), probably were deposited in an intra-arc basin (Vallier, in press). A series of interconnected (and possibly also isolated) basins apparently formed on the subsiding island-arc platform in the Late Triassic to Late Jurassic interval.

COLUMBIA RIVER BASALT GROUP

Flows of the Miocene Columbia River Basalt Group are essentially flat lying and overlie the pre-Tertiary sequence at Pittsburg Landing above an angular unconformity (Vallier, 1968; Ozier, 1971; White, 1972). Paleosols, rubbly baked zones, and opaline material including petrified wood developed locally along the contacts between the rocks of the Columbia River Basalt Group and the older pre-Tertiary rocks. Dikes in places cut the pre-Tertiary rocks; one about 10 m wide cuts the conglomerate and sandstone unit of the Coon Hollow Formation near the mouth of Pittsburg Creek (fig. 3.2).

In the Pittsburg Landing area, flows of both the Imnaha Basalt and the Grande Ronde Basalt (as defined by Hooper and Swanson, 1990) are exposed; the Grande Ronde Basalt is part of the Yakima Basalt Subgroup of Swanson and others (1979). The Columbia River Basalt Group was erupted between about 17.5 and 6.0 Ma (Hooper and Swanson, 1990) and the basalt flows in the Pittsburg Landing area are among the oldest, probably over 15 million years.

QUATERNARY DEPOSITS

The Quaternary deposits compose a wide range of landforms (fig. 3.2). Oldest deposits are those of a large landslide that heads along the Klopton Creek fault and covers the southern part of the Pittsburg Landing area in Idaho. The Bonneville flood (O'Connor, 1990) flattened the landslide debris and other older deposits, formed large sand bars, and deposited a thin veneer of boulders and cobbles on the flattened surfaces. Subsequently, present-day alluvial fans formed. A landslide in Oregon along the Klopton Creek thrust fault (fig. 3.2) formed either during or immediately after the Bonneville flood.

STRUCTURE

The major fault in the Pittsburg Landing area is the Klopton Creek thrust fault, which placed the Cougar Creek Complex over the Triassic and Jurassic stratified rocks. Another thrust fault parallels the Klopton Creek thrust fault and is well exposed along Pittsburg Creek in Oregon (fig. 3.2). This thrust fault probably continues into the upper drainage area of West Creek. The Klopton Creek thrust fault bounds the Cougar Creek Complex on the north and northwest (fig. 3.2). The fault contact is generally covered by Quaternary deposits. The fault line strikes about N. 30° E., similar to other pre-Tertiary structural trends, and the fault plane dips southeast about 30° (White, 1972). Displacement along the Klopton Creek thrust fault may be as much as several kilometers.

Other faults are mainly steeply dipping normal and reverse faults. Displacements range from a few meters to tens of meters. Their dominant strikes range from N. 30° E. to N. 70° E., generally parallel or subparallel to the major structural trends of the region.

The Cougar Creek Complex shows evidence for at least two deformations before it was propelled along the Klopton Creek thrust fault. That some movement began as early as Pennsylvanian or Early Permian time is indicated by the mylonites and gneissic mylonites that are crosscut by essentially undeformed Early Permian plutonic bodies (Vallier, in press). In places the mylonites are folded and faulted indicating a second deformation. A folded mylonite fabric near the Klopton Creek thrust fault suggests a third deformation.

Folds are well displayed in the sedimentary units at Pittsburg Landing. In the Coon Hollow Formation, broad and open folds have axes that trend N. 30° E. to N. 60° E. and the limbs generally have low dips; near the Klopton Creek thrust fault, folds are overturned and limbs dip steeply. Between the Klopton Creek thrust fault and the thrust fault that parallels Pittsburg Creek in Oregon (fig. 3.2), folds in the turbidite unit of the Coon Hollow Formation are isoclinal around nearly vertical to northward-verging axes. At least two periods of folding are recognized. Folds near and parallel or subparallel to the Klopton Creek thrust fault are youngest and related to movement along the fault. Folds that are not parallel and are some distance from the thrust fault developed prior to the thrust faulting and are oldest in the Pittsburg Landing area.

GEOLOGIC EVOLUTION

The geologic evolution of the Pittsburg Landing area is unique in the Blue Mountains region because of the extensive diversity and the wide range in rock ages. Rock types extend from metamorphosed and structurally deformed amphibolite and gneiss

through plutonic rocks of gabbro, quartz diorite, diabase, and keratophyre to sedimentary strata of pyroclastic, epiclastic, and biogenic origins that were deposited in both subaerial and marine environments. Ages of rocks range from as old as Pennsylvanian in the Cougar Creek Complex to as young as middle Miocene in the Columbia River Basalt Group. Upper Quaternary (including Holocene) sediments in the area record the latest parts of this geologic evolution.

We are not sure about the origin of the Cougar Creek Complex. Its volcanic arc affinities (Vallier, in press), variable metamorphic grade, and diverse structures suggest a long history before the Middle Triassic strata were deposited. The Cougar Creek Complex most likely represents mid-crustal igneous activity of a late Paleozoic (mostly Permian) volcanic arc.

Through late Middle and Late Triassic time, an intraoceanic volcanic arc developed on top of a preexisting (late Paleozoic, mostly Early Permian) volcanic arc. During accumulation of the Big Canyon Creek unit of the Wild Sheep Creek Formation (fig. 3.5*A*), volcanic and structural seamounts breached the water surface and formed islands. Basaltic volcanism

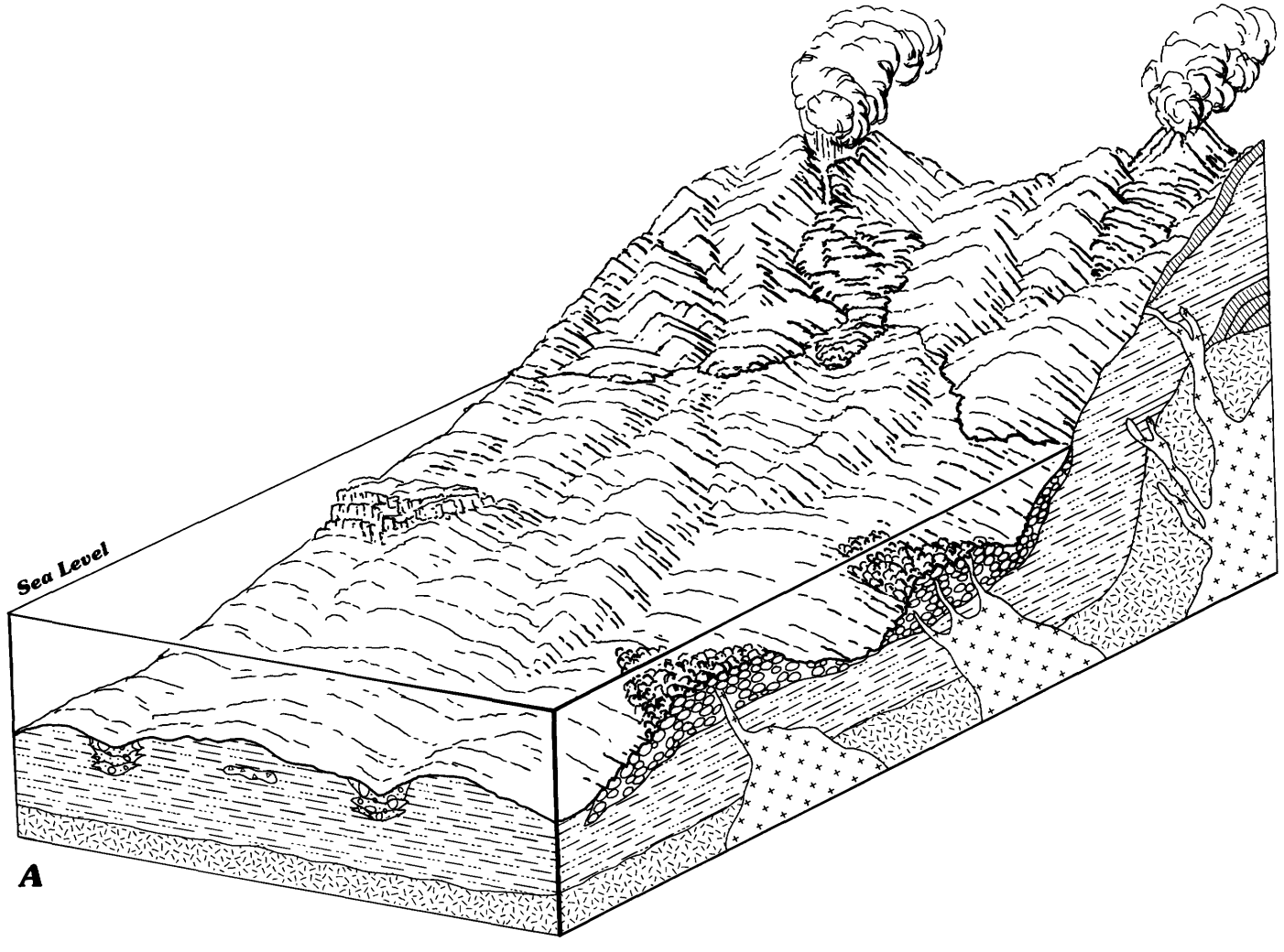

FIGURE 3.5.—Paleogeographic sketches showing rock units at Pittsburg Landing. *A*, Middle Triassic (Ladinian) volcano growth, erosion, and accumulation of the Big Canyon Creek unit of the Wild Sheep Creek Formation. *B*, Late Triassic (Karnian) erosion and subsidence; deposition of the Kurry unit of the Doyle Creek Formation; *C*, Middle Jurassic (Bajocian?) eruption and deposition of the red tuff unit of the Coon Hollow Formation. *D*, Middle Jurassic (Bajocian) development of alluvial fans, deltas, and shallow-marine transgressive facies of the conglomerate and sandstone unit of the Coon Hollow Formation and the sandstone and mudstone unit of the Coon Hollow Formation (The turbidite unit of the Coon Hollow Formation is not shown in these diagrams because the distance of its tectonic transport along thrust faults is not known). Explanation on page 69.

EXPLANATION
[for figures 3.5*A–D*]

Coon Hollow Formation (Jurassic)—Consists of:

- Andesite porphyry and diabase
- Sandstone and mudstone unit
- Conglomerate and sandstone unit
- Red tuff unit

Doyle Creek Formation (Triassic)—Consists of:
Kurry unit—Divided into:

- Tuffaceous sandstone and mudstone
- Argillaceous limestone
- Volcanic breccia and sandstone channel fills

Wild Sheep Creek Formation—Consists of:
Big Canyon Creek unit—Divided into:

- Massive lava flows
- Pillow basalt flows
- Pillow basalt breccia
- Conglomerate
- Breccia, sandstone, and tuff
- Gabbro and diabase dikes and sills (Triassic)
- Cougar Creek Complex
- Fault—Arrows show relative movement

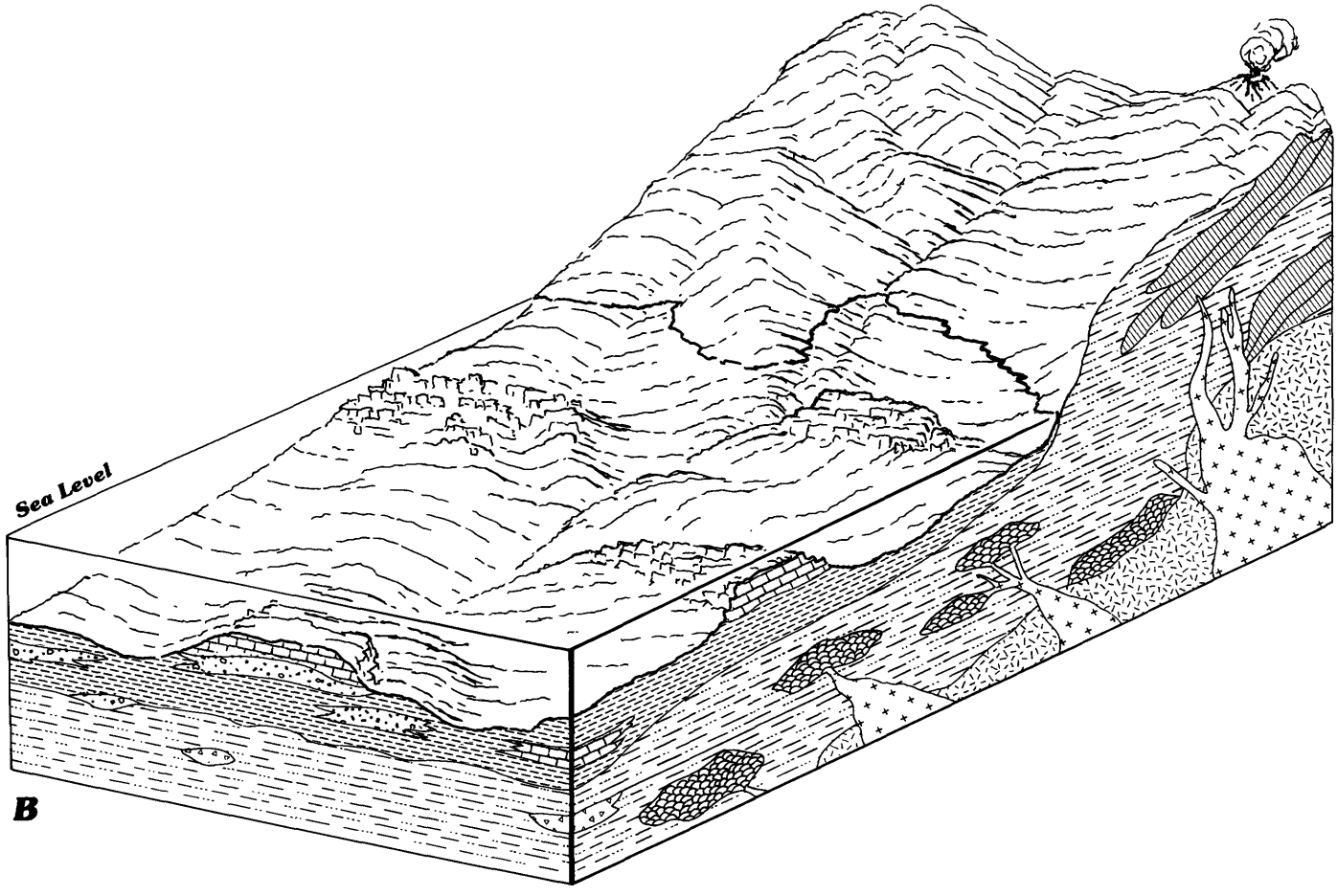

FIGURE 3.5.—Continued

was common and pillow basalt flows and breccias formed either when eruptions occurred on the sea floor or when lava flows reached the sea after subaerial eruptions. Also, epiclastic and pyroclastic detritus was shed from the volcanoes after they had grown to heights above sea level. As the volcanoes eroded and the landmass subsided (fig. 3.5*B*), tuff, sandstone, limestone, and mudstone of the Kurry unit (Doyle Creek Formation) were deposited in shallow-water shelf and (or) upper slope environments on top of the Big Canyon Creek unit (Wild Sheep Creek Formation).

During the Late Triassic to Middle Jurassic interval, uplift and erosion occurred. The Pittsburg Landing area apparently was a small part of an extensive region of large islands that shed sediments into multiple intra-arc basins that probably were connected (Dickinson and Thayer, 1978; Imlay, 1986). Subsequent to the erosional stage, most likely in the Middle Jurassic (Bajocian), a volcano erupted pyroclastic debris that formed much of the red tuff unit of the Coon Hollow Formation (fig. 3.5*C*). The development of alluvial fans and fan deltas, in addition to braided streams, resulted in the deposition of the overlying conglomerate and sandstone unit (fig. 3.5*D*); marine transgression led to the deposition of the sandstone and mudstone unit and a deepening basin resulted in the deposition of graded sandstone and mudstone

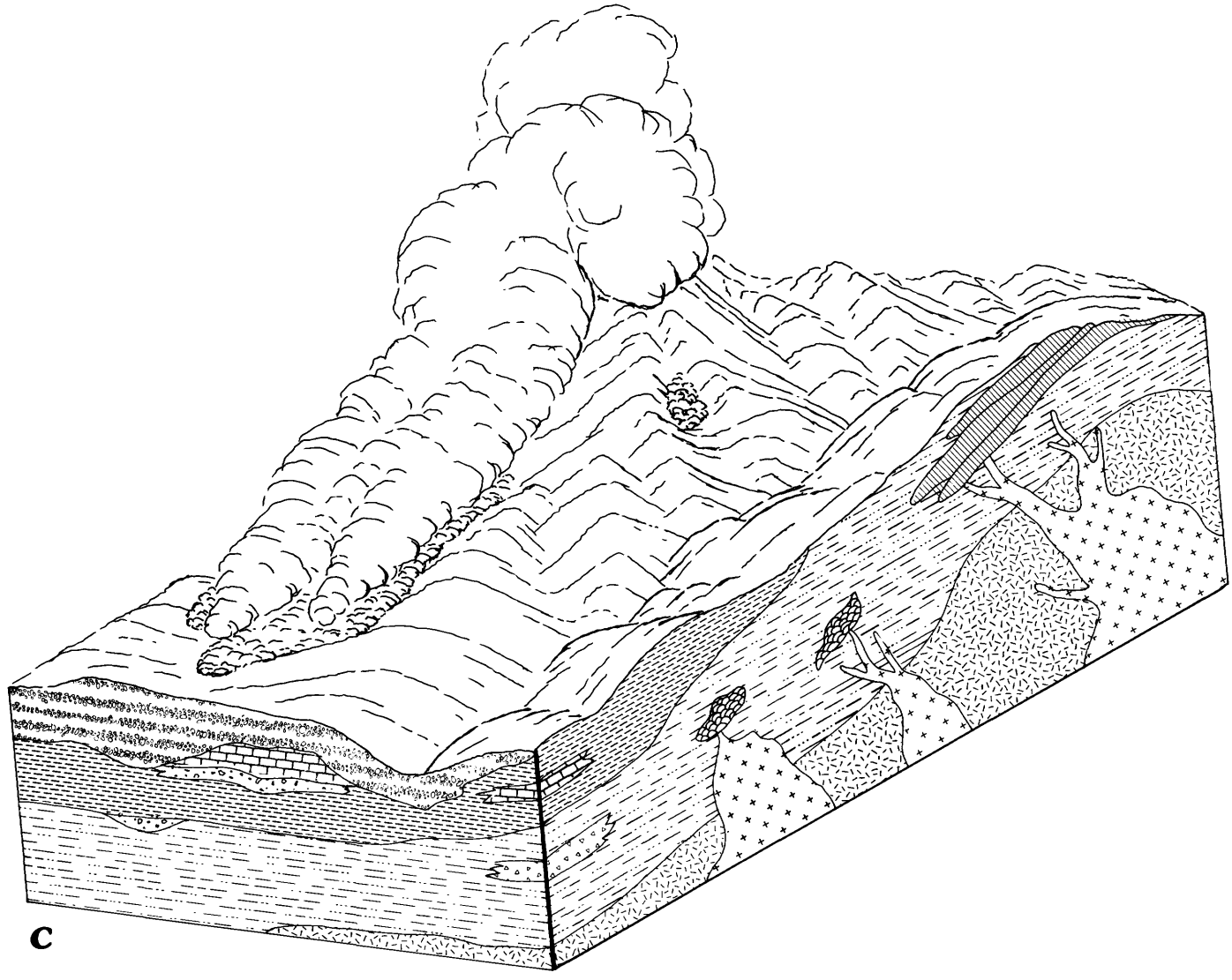

FIGURE 3.5.—Continued

beds of the turbidite unit. Dikes and sills of andesite porphyry and diabase intruded the older units of the Coon Hollow Formation; some of the andesite was intruded before the sediments were lithified.

Deformation, with attendant uplift and erosion, occurred between the Middle Jurassic and early Miocene, and the strongest deformation probably occurred in the Late Jurassic and Early Cretaceous. The Klopton Creek fault was active as a thrust during this interval; its movement may be related to the early stage of accretion of the Blue Mountains island arc to the North American craton (Vallier, in press).

Erosion continued until the early and middle Miocene, when voluminous basalt flows of the Columbia River Basalt Group were erupted. Broad regional uplift and erosion by the Snake River and its tributaries during the late Miocene, Pliocene, and Quaternary are responsible for the present topography. The deposits of landslides, alluvial fans, and floods accumulated during the late Quaternary (including the Holocene).

Thus, within the region, the evolution of the Pittsburg Landing area is unique. The diversity of rock types and abundance of fossils in the area have greatly aided our interpretations of the geologic history of the Blue Mountains region.

REFERENCES CITED

Ash, S.R., 1991, A new Jurassic flora from the Wallowa terrane in Hells Canyon, Oregon and Idaho: Oregon Geology, v. 53, no. 2, p.27–33.

Brooks, H.C., and Vallier, T.L., 1978, Mesozoic rocks and tectonic evolution of eastern Oregon and western Idaho, *in* Howell, D.G., and McDougall, K.A., eds., Mesozoic paleogeography of the Western United States (Pacific Coast Paleogeography Symposium 2): Los Angeles, Society of Economic Paleontologists and Mineralogists, Pacific Section, p. 133–146.

Carney, J.N., and Macfarlane, A., 1980, A sedimentary basin in the central New Hebrides arc, Symposium on Petroleum potential in island arcs, small ocean basins, submerged margins and related areas: United Nations Economic and Social Commission for Asia and the Pacific, Committee for Coordination of Joint Prospecting for mineral resources in south Pacific offshore areas (CCOP/SOPAC) Technical Bulletin, v. 3, p. 109–120.

Carney, J.N., Macfarlane, A., and Mallick, D.I.J., 1985, The Vanuatu island arc—An outline of the stratigraphy, structure, and

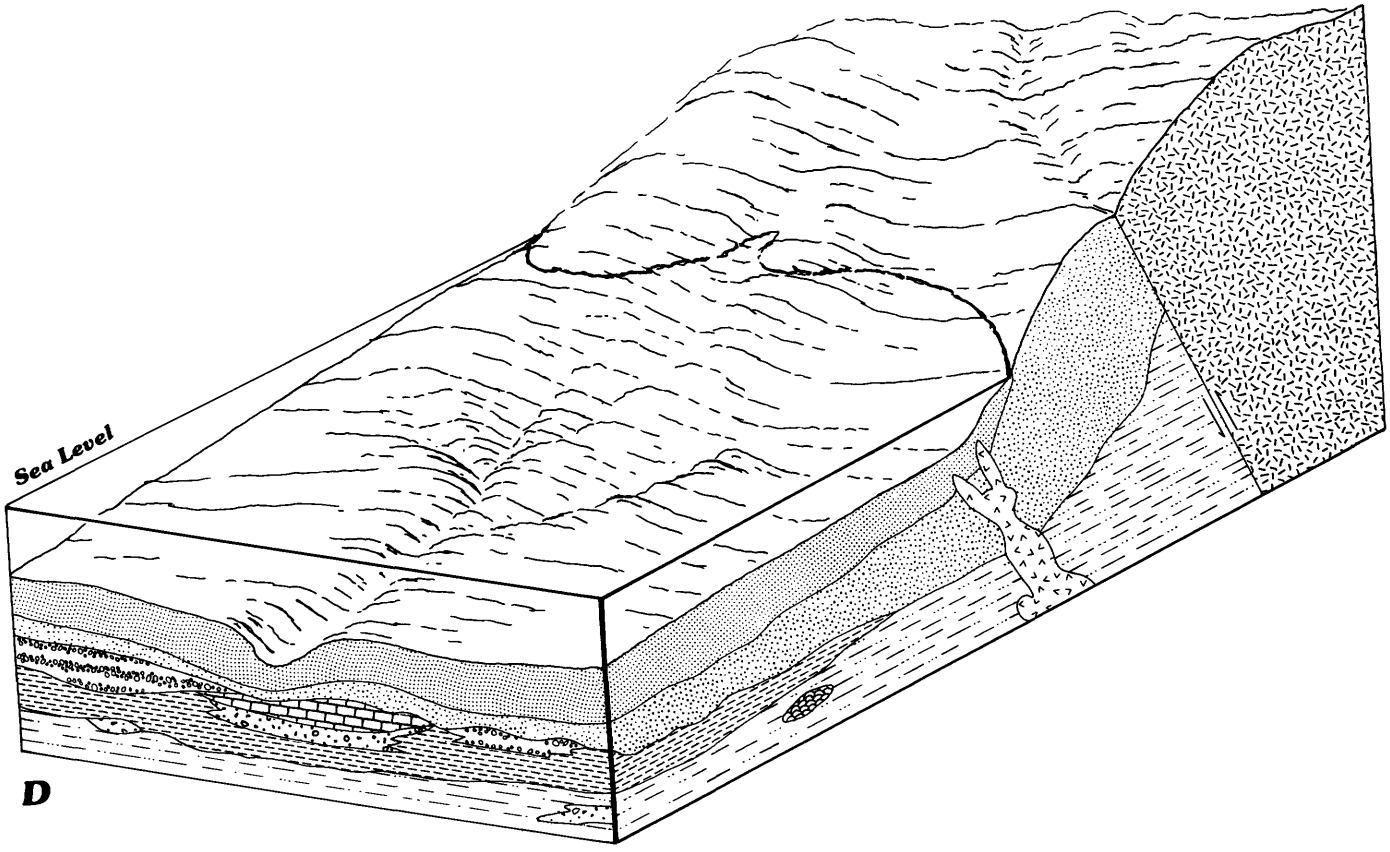

FIGURE 3.5.—Continued

petrology, *in* Nairn, A.E.M., Stehli, F.G., and Uyeda, S., eds., The ocean basins and margins—Vol. 7A, The Pacific Ocean: New York, Plenum Press, p. 685–718.

Dickinson, W.R., and Thayer, T.P., 1978, Paleogeographic and paleotectonic implications of Mesozoic stratigraphy and structure in the John Day inlier of central Oregon, in Howell, D.G., and McDougall, K.A., eds., Mesozoic paleogeography of the Western United States (Pacific Coast Paleogeography Symposium 2): Los Angeles, Society of Economic Paleontologists and Mineralogists, Pacific Section, p. 147–161.

Follo, M.F., and Sevier, R.S., 1985, Carbonate platform margin facies on an evolving suspect terrane—Wallowa Mountains, Oregon [abs.]: Geological Society of America, Abstracts with Programs, v. 17, no. 7, p. 584.

Grant, P.R., 1980, Limestone units within the Triassic Wild Sheep Creek Formation, Snake River canyon: Pullman, Washington State University, M.S. thesis, 103 p.

Harbert, W.P., Hillhouse, J.W., and Vallier, T.L., 1988, Leonardian paleolatitude of Wrangellia [abs.]: EOS (American Geophysical Union Transactions), v. 69, no. 44, p. 1169.

Hillhouse, J.W., Grommé, C.S., and Vallier, T.L., 1982, Paleomagnetism and Mesozoic tectonics of the Seven Devils volcanic arc, northeastern Oregon: Journal of Geophysical Research, v. 87, p. 3777–3794.

Hooper, P.R., and Swanson, D.A., 1990, The Columbia River Basalt Group and associated volcanic rocks of the Blue Mountains province, *in* Walker, G.W., ed., Geology of the Blue Mountains region of Oregon, Idaho, and Washington: Cenozoic Geology of the Blue Mountains region: U.S. Geological Survey Professional Paper 1437, p. 63–99

Imlay, R.W., 1980, Jurassic paleogeography of the conterminous United States in its continental setting: U.S. Geological Survey Professional Paper 1062, 134 p.

———1981, Jurassic (Bathonian and Callovian) ammonites in eastern Oregon and western Idaho: U.S. Geological Survey Professional Paper 1142, 24 p.

———1986, Jurassic ammonites and biostratigraphy of eastern Oregon and western Idaho, chap. 5, *in* Vallier, T.L., and Brooks, H.C., eds., Geology of the Blue Mountains region of Oregon, Idaho, and Washington: Geologic implications of Paleozoic and Mesozoic paleontology and biostratigraphy, Blue Mountains province, Oregon and Idaho: U.S. Geological Survey Professional Paper 1435, p. 53–57.

Lund, Karen, and Snee, L.W., 1988, Metamorphism, structural development, and age of the continent-island arc juncture in west-central Idaho, *in* Ernst, W.G., ed., Metamorphism and crustal evolution, western conterminous United States (Rubey Volume VII): Geological Society of America, p. 296–337.

Masuda, A., Nakamura, N., and Tanaki, T., 1973, Fine structures of mutually normalized rare-earth patterns of chondrites: Geochimica et Cosmochimica Acta, v. 37, p. 239–248.

Miall, A.D., 1977, A review of the braided-river depositional environment: Earth Science Reviews, v. 13, p. 1–62.

Morrison, R.F., 1961, Angular unconformity marks Triassic-Jurassic boundary in the Snake River area of northeastern Oregon: Ore Bin, v. 23, no. 11, p. 105–111.

———1964, Upper Jurassic mudstone unit named in the Snake River canyon, Oregon-Idaho boundary: Northwest Science, v. 38, p. 83–87.

O'Connor, Jim, 1990, Hydrology, hydraulics, and sediment transport of Pleistocene Lake Bonneville flooding on the Snake River, Idaho: Tucson, University of Arizona, Ph.D. dissertation, 192 p.

Ozier, R.L., 1971, The geology of the Tertiary-pre-Tertiary angular unconformity; McGraw Creek to the Grande Ronde river, Snake River canyon, Oregon and Washington: Terre Haute, Indiana State University, M.S. thesis, 86 p.

Pessagno, E.A., Jr., and Blome, C.D., 1986, Faunal affinities and tectonogenesis of Mesozoic rocks in the Blue Mountains province of eastern Oregon and western Idaho, *in* Vallier, T.L. and Brooks, H.C., eds., Geology of the Blue Mountains region of Oregon, Idaho, and Washington: Geologic implications of Paleozoic and Mesozoic paleontology and biostratigraphy, Blue Mountains province, Oregon and Idaho: U.S. Geological Survey Professional Paper 1435, p. 65–78.

Prostka, H.J., 1962, Geology of the Sparta quadrangle, Oregon: Oregon Department of Geology and Mineral Industries, Geologic Map GMS-1, one map sheet, scale 1:62,500.

Scholl, D.W., Vallier, T.L., and Stevenson, A.J., 1983, Arc, fore-arc, and trench sedimentation and tectonics—Amlia corridor of the Aleutian Ridge, *in* Watkins, J.S., and Drake, C.L., eds., Studies in continental-margin geology: American Association of Petroleum Geologists Memoir 34, p. 313–329.

———1988, Geologic evolution and petroleum potential of the Aleutian Ridge, *in* Scholl, D.W., Grantz, Arthur, and Vedder, J.G., eds., Continental margin of western North America and Alaska: Houston, Circum-Pacific Council for Energy and Mineral Resources Earth Science Series, v. 6, p. 123–156.

Silberling, N.J., Jones, D.L., Blake, M.C., and Howell, D.G., 1984, Lithotectonic terrane map of the western conterminous United States, Pt. C of Silberling, N.J., and Jones, D.L., eds., Lithotectonic terrane maps of the North American Cordillera: U.S. Geological Survey Open-File Report 84-523, 43 p.

Smith, W.D.P., and Allen, J.E., 1941, Geology and physiography of the northern Wallowa Mountains, Oregon: Oregon Department of Geology and Mineral Industries Bulletin 12, 65 p.

Stanley, G.D., Jr., and Beauvais, L.P., 1990, Middle Jurassic corals from the Wallowa terrane, west-central Idaho: Journal of Paleontology, v. 64, p. 352–362.

Swanson, D.A., Wright, T.L., Hooper, P.R., and Bentley, R.D., 1979, Revisions in stratigraphic nomenclature of the Columbia River Basalt Group: U.S. Geological Survey Bulletin 1457-G, p. 1–59.

Vallier, T.L., 1967, Geology of part of the Snake River canyon and adjacent areas in northeastern Oregon and western Idaho: Corvallis, Oregon State University, Ph.D. dissertation, 267 p.

———1968, Reconnaissance geology of the Snake River canyon between Granite Creek and Pittsburg Landing, Oregon and Idaho: Ore Bin, v. 30, p. 233–252.

———1974, A preliminary report on the geology of part of the Snake River canyon, Oregon and Idaho: Oregon Department of Geology and Mineral Industries Geological Map Series, GMS-6, 1 map sheet, 15 p. of text, scale 1:125,000.

———1977, The Permian and Triassic Seven Devils Group, western Idaho and northeastern Oregon: U.S. Geological Survey Bulletin 1437, 58 p.

———in press, Petrology of pre-Tertiary igneous rocks of the Blue Mountains province of Oregon, Idaho, and Washington: Implications for the geologic evolution of a complex island arc, *in* Vallier, T.L., and Brooks, H.C., eds., The geology of the Blue Mountains region of Oregon, Idaho, and Washington: Petrology and tectonic evolution of pre-Tertiary rocks: U.S. Geological Survey Professional Paper 1438.

Vallier, T.L., and Batiza, Rodey, 1978, Petrogenesis of spilite and keratophyre from a Permian and Triassic volcanic-arc terrane, eastern Oregon and western Idaho, U.S.A.: Canadian Journal of Earth Sciences, v. 15, p. 1356–1369.

Vallier, T.L., Brooks, H.C., and Thayer, T.P., 1977, Paleozoic rocks of eastern Oregon and western Idaho, *in* Stewart, J.H., Stevens, C.H., and Fritsche, A.E., eds., Paleozoic paleogeography of the Western United States (Pacific Coast Paleogeog-

raphy Symposium 1): Los Angeles, Society of Economic Paleontologists and Mineralogists Pacific Section, p. 455–466.

Vallier, T.L., and Engebretson, D.C., 1984, The Blue Mountains island arc of Oregon, Idaho, and Washington—An allochthonous terrane from the ancestral western Pacific Ocean?, *in* Howell, D.G., Jones, D.L., Cox, A.V., and Nur, A.M., eds., Circum-Pacific Terrane Conference, Stanford, Calif., 1983, Proceedings: Stanford University Publications in the Geological Sciences, v. 18, p. 197–199.

Vallier, T.L., and Hooper, P.R., 1976, Geologic guide to Hells Canyon, Snake River [Oregon-Idaho]: Geological Society of America Field Guidebook, Cordilleran Section Meeting, 38 p.

Vallier, T.L., Scholl, D.W., Fisher, M.A., Bruns, T., Wilson, F.H., von Huene, Roland, and Stevenson, A.J., in press, Geologic framework of the Aleutian arc, Alaska, *in* Plafker, George, and Berg, H.C., eds., Geology of Alaska, Vol. G-1 of The geology of North America: Boulder, Colo., Geological Society of America.

Wagner, W.R., 1945, Geological reconnaissance between the Snake and Salmon Rivers north of Riggins [Idaho]: Idaho Bureau of Mines and Geology Pamphlet 74, 16 p.

Walker, N.W., 1986, U-Pb geochronologic and petrologic studies in the Blue Mountains terrane, northeastern Oregon and westernmost-central Idaho—Implications for pre-Tertiary tectonic evolution: Santa Barbara, University of California, Ph.D. dissertation, 224 p.

White, D.L., 1972, The geology of the Pittsburg Landing area, Snake River canyon, Oregon-Idaho: Terre Haute, Indiana State University, M.S. thesis, 98 p.

White, J.D.L., 1985, The Doyle Creek Formation (Seven Devils Group), Pittsburg Landing, Idaho—A study of intra-arc sedimentation: Columbia, University of Missouri, M.S. thesis, 151 p.

4. INTRA-ARC BASIN DEPOSITS WITHIN THE WALLOWA TERRANE, PITTSBURG LANDING AREA, OREGON AND IDAHO

By JAMES D.L. WHITE[1]

CONTENTS

ABSTRACT

Triassic and Jurassic rocks exposed at Pittsburg Landing, Idaho, lie within the Wallowa terrane. Fluvial and marine sedimentary rocks of the Jurassic Coon Hollow Formation overlie a thick sequence of Triassic marine volcaniclastic rocks. Hydroclastic mass-flow breccia and pillow lava of the Triassic Big Canyon Creek unit of the Wild Sheep Creek Formation represent metamorphosed arc lava. Breccia highest in the sequence interfingers with thin-bedded, locally fossiliferous marine tuff (deposited by turbidity currents) and limey mudstone of the Kurry unit of the Doyle Creek Formation. Uplift, subaerial exposure, and erosion followed. Tuffaceous sandstone and conglomerate, shale, and silicic tuff of the Coon Hollow Formation were deposited above the resulting unconformity.

The lower fluvial sedimentary rocks unit of the Coon Hollow Formation contains framework conglomerate with poorly developed imbrication and planar bedding. Tuffaceous sandstone is commonly crossbedded and pebbly. Nonreworked ash-flow tuff is locally present. The conglomerate-sandstone couplets are laterally discontinuous and form multilateral, shallow channel-fill sequences. Deposition is attributed to braided fluvial processes. The upper fluvial sedimentary rocks unit of the Coon Hollow Formation consists of a stacked sandstone and mudstone sequence formed by more distal braided to meandering fluvial to deltaic-distributary streams. Lignite bands, fossil rootlets, and abundant plant fossils are present; these features suggest a locally swampy paleoenvironment. Strata of the uppermost part of this sequence indicate a return to low energy, mud-rich marine conditions that probably represent a gradual transgression over a muddy delta. The depositional sequence records initial sedimentation on a shoaling volcano (Big Canyon Creek unit) during the Late Triassic. Nonmarine deposits represent a retrogradational fluvial sequence, and renewed marine deposition is recorded near the top of the exposed Pittsburg Landing section. The entire sequence represents a complex history of intra-arc sedimentation.

INTRODUCTION

Rocks exposed at Pittsburg Landing, Idaho, (fig. 4.1) include the Big Canyon Creek unit of the Wild Sheep Creek Formation and the Kurry unit of the Doyle Creek Formation, both part of the Seven Devils Group (Vallier, 1977; White and Vallier, chap. 3, this volume). A second stage of deposition, of Jurassic age, is represented in alluvial and shallow marine lithofacies of the Jurassic Coon Hollow Formation (fig. 4.2). The age and character of these lithofacies provide important constraints on reconstructions of regional paleogeography (White and others, 1992), and they are described in some detail below. The succession represents part of a complex volcanic island-arc assemblage (Vallier, 1967; 1977; chap. 3, this volume), referred to as the Blue Mountains island arc (Vallier and Brooks, 1986).

The volcaniclastic rocks of the Seven Devils Group record the largely subaqueous growth of an oceanic

[1]Department of Geological Sciences, University of California, Santa Barbara, CA 93106-7160

island arc (Vallier, 1977). The Triassic rocks of the Group exposed at Pittsburg Landing are largely composed of hydroclastic breccias, tuffs, and pillow lavas. The uppermost Triassic rocks exposed include debris from subaerial volcanoes; the presence of such debris indicates that parts of the arc had shoaled by that time. Despite uncertainty about the specific structural sites in which this volcaniclastic debris was preserved, it was clearly deposited within the broader arc setting.

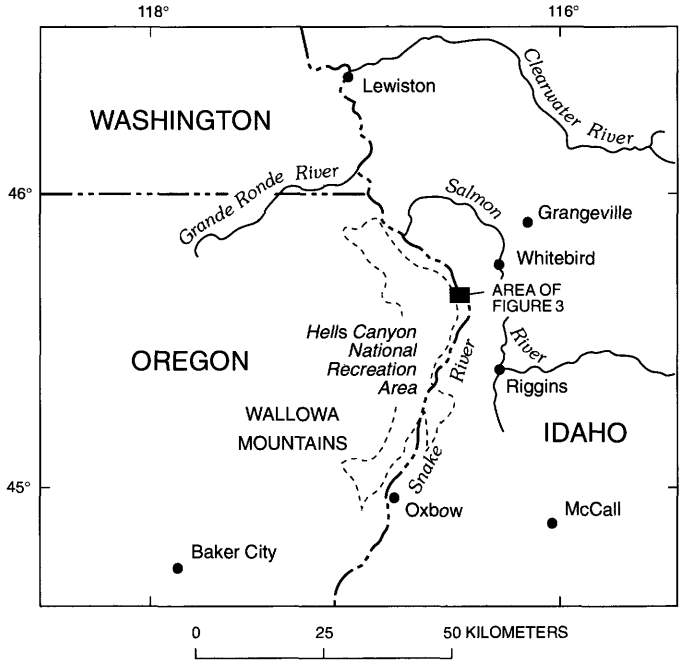

Figure 4.1.—Index map showing Pittsburg Landing area, Oregon and Idaho.

Pittsburg Landing alluvial and shallow marine deposits illustrate the importance of changes in fluvial depositional style driven by changes in available sediment type and amount. The lower fluvial unit at Pittsburg Landing probably formed when volcanic activity produced abundant coarse sediment and denuded slopes to induce braiding in a low-gradient, previously erosional, fluvial system. The brief progradational to retrogradational cycle recorded by the lower fluvial unit is ascribed to volcanic "sediment-loading" of a fluvial system. Further evolution of the system, subsequent to depletion of initially voluminous pyroclastic ejecta, was mediated by tectonic disturbances, changes in climate, or changes in base level.

ACKNOWLEDGMENTS

My work at Pittsburg Landing began in 1983 as a M.S. thesis project at the University of Missouri-Columbia (UMC), under the direction of M.B. Underwood (White, 1985). Tracy Vallier encouraged my work, and he has been unfailingly helpful throughout the project. Partial support for fieldwork was provided by a grant from Standard Oil Company (administered by the Department of Geology, UMC). Research grants from the Geological Society of America (#3239-83; #3518-85) funded the bulk of my fieldwork. On separate occasions, I was ably assisted in the field by my father, C.E. White, and by Craig Hall. Discussions in the field with Sam Johnson and C.J. Busby-Spera were helpful, as were those with R.V. Fisher at the University of California, Santa Barbara. Reviews by David White and Tracy Vallier improved the manuscript.

PURPOSE

Detailed aspects of the stratigraphy and sedimentology of the volcaniclastic deposits exposed at Pittsburg Landing are discussed herein. The rocks represent a mixture of subaerial and marine volcaniclastic deposits, intercalated with igneous flow and hypabyssal intrusive rocks emplaced at various times. Excellent exposures at Pittsburg Landing allow examination of complex facies and stratigraphic relations. Previous interpretations of Pittsburg Landing stratigraphy (Vallier, 1968; Vallier, 1974; White, 1972; Vallier, 1977) were hampered by the lack of appropriate sedimentation models.

Limited petrographic work and X-ray diffraction analysis supplemented fieldwork, which included lithofacies mapping, measurement of stratigraphic sections, collection of samples, and measurement of paleocurrent indicators. Low-angle imbrication is present in some conglomerate units, and although I took imbrication measurements, they are complicated by regional dips that are variable on a small scale as well as the thickness and nonplanar boundaries of the conglomerates. Petrographic criteria were used to confirm field identifications.

Lithofacies, or "facies" for brevity, are assemblages of rocks that share one or more specified characteristics. In studies dealing with clastic rocks, facies are generally defined on the basis of sedimentary structures within beds (for example, crossbedding or grading) formed by specific physical processes during deposition. Facies may be grouped into facies associations, which represent specific depositional environments characterized by certain depositional processes. Although lithofacies in a narrow sense are independent of depositional environment (because they represent specified physical processes), different facies and facies association shorthand terminologies (for example, the Bouma sequence) that

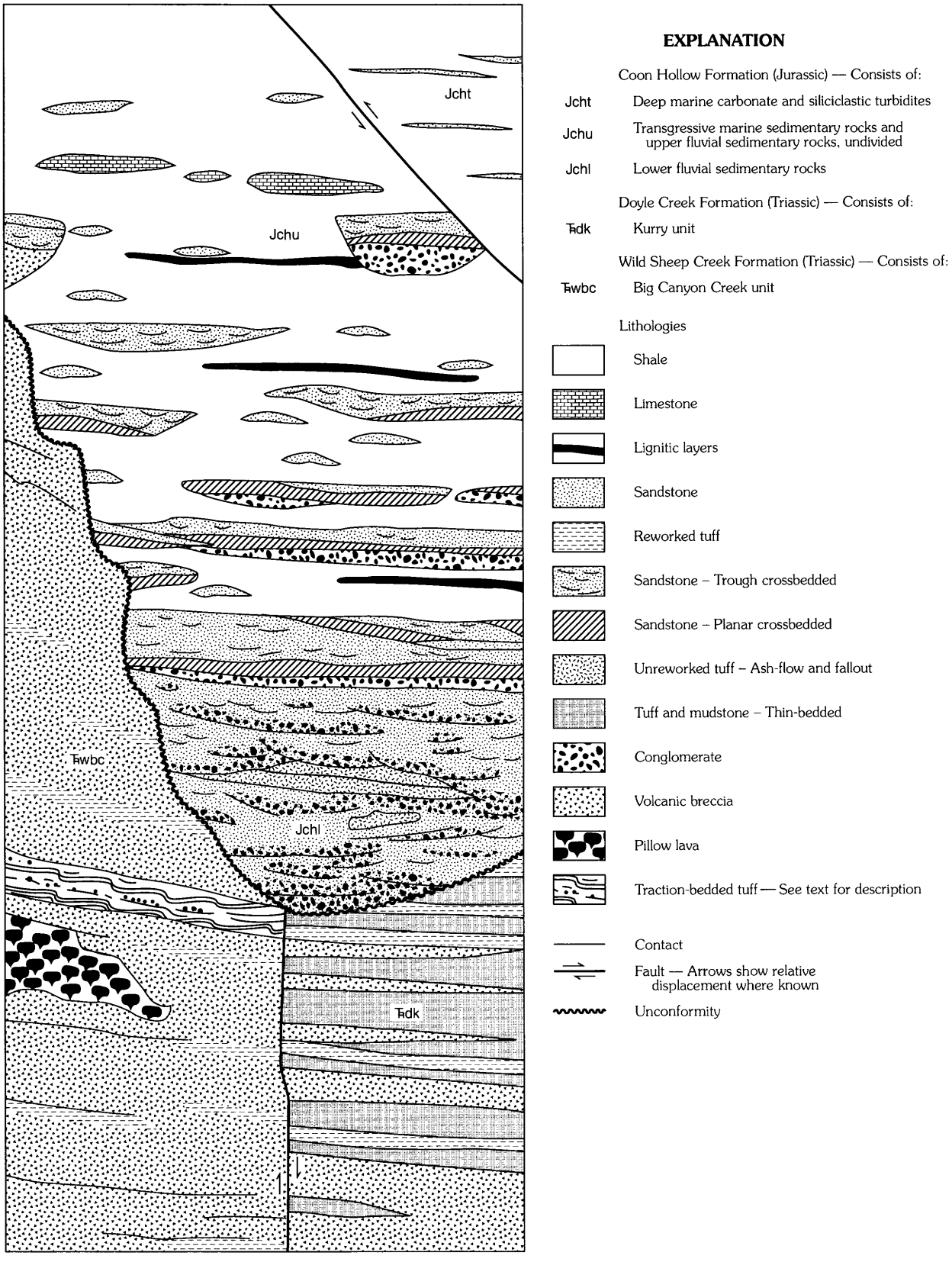

Figure 4.2.—Schematic diagram showing depositional features and stratigraphic relations of rocks in Pittsburg Landing area, Oregon and Idaho (see fig. 4.3A). Deep marine turbidites structurally overlie upper fluvial sedimentary rocks unit north of the Klopton Creek thrust fault on the Oregon side of the Snake River.

carry environmental connotations have been developed by various geologists.

Three overlapping facies terminologies are used herein. Rocks of the Big Canyon Creek unit are products of hydroclastic volcanic activity, and they are discussed using terminology drawn largely from Fisher and Schmincke (1984). The Kurry unit bears a marine fossil fauna and is accordingly discussed using terminology taken from Elliott (1978), whereas the fluvial sedimentary rocks have been described using the lithofacies codes of Miall (1977, 1978).

FIELD RELATIONS

The spatial relations among units provide information important for both facies interpretation and paleoenvironment reconstruction. The relations between the units exposed at Pittsburg Landing are shown in figure 4.3*A*. A simplified cross section from north to south across the map area is shown in figure 4.3*B*. The Ridgetop fault is postulated on the basis of an overly abrupt facies change.

The contact between the Kurry unit and the underlying Wild Sheep Creek Formation is conformable. An angular unconformity separates overlying alluvial deposits from the Kurry unit. A major zone of faulting, the Klopton Creek fault (White and Vallier, chap. 3, this volume), marks the southern boundary of the Pittsburg Landing area and separates older arc basement rocks to the south from layered rocks to the north. Within the Kurry unit, age control is provided by several species of ammonites and a species of *Halobia*. Jurassic plant fossils characterize the fluvial rocks of the Coon Hollow Formation, whereas the transgressive marine deposits of the Coon Hollow contain brackish-to-marine pelecypod fossils and some coral remains that are Bajocian in age (Stanley and Beauvais, 1990). A fault-bounded unit of carbonate and siliciclastic turbidites is exposed adjacent to the Klopton Creek thrust fault on the Oregon side of the Snake River. It contains Callovian ammonite fossils (Vallier, 1977) and represents a stratigraphically higher part of the Coon Hollow Formation that was structurally emplaced above the transgressive marine sedimentary rocks unit of the Coon Hollow Formation at Pittsburg Landing. This entire pre-Cenozoic section is overlain, above an angular unconformity, by the plateau basalts of the Columbia River Basalt Group.

The most important lithologic contact within the Pittsburg Landing area is the unconformity between the Kurry unit and fluvial sedimentary rocks of the Coon Hollow Formation. This unconformity is erosional, and the fluvial deposits fill rugged valleys or canyons. The lowermost of these fluvial sedimentary rocks are very poorly bedded, and the slight angular discordance between the Kurry unit and the fluvial sedimentary rocks is not immediately apparent in the field. An abrupt Late Triassic to Late Jurassic step in fossil ages indicates an episode of nondeposition and (or) erosion of about 40 million years prior to Coon Hollow deposition. In other parts of the Wallowa terrane, part of this time interval is represented by the Norian Martin Bridge Limestone, a unit deposited somewhat later than the Kurry unit during a phase of apparently widespread volcanic inactivity within the Blue Mountains island arc.

STRATIGRAPHY

BIG CANYON CREEK UNIT (OF THE WILD SHEEP CREEK FORMATION)

VOLCANIC BRECCIAS

The uppermost part of the Big Canyon Creek unit (informal unit of White and Vallier, chap. 3, this volume) of the Wild Sheep Creek Formation forms the lowest part of the section exposed at Pittsburg Landing. Near the mouth of West Creek, breccia of the Big Canyon Creek unit interfingers with thin- to thick-bedded tuff (fig. 4.4) that is presumably of marine origin on the basis of locally abundant fossils. Also present is well-developed spilitic pillow lava, with pillows as much as 2 m in diameter. Some parts of the Big Canyon Creek unit interfinger with coarser grained reworked tuff of phreatomagmatic origin.

The Big Canyon Creek unit of the Wild Sheep Creek Formation at Pittsburg Landing contains abundant hydroclastic breccia that apparently was produced by the secondary remobilization of hydroclastic debris. Hydroclastic products range from shards spalled off pillow lava rims and broken pillows to blocky, irregularly shaped, nonvesicular to poorly vesicular vitric fragments and syngenetic lithic fragments.

Important features of the Big Canyon Creek unit, which indicate its hydroclastic origin, include thick (1–3 m) bedding, mixed matrix and framework support, and essentially monolithic composition of large subangular, equidimensional clasts. Broken pillows and globular mini-pillows (10–30 cm) make up clasts in some zones, but in other zones the subequant clasts lack chilled margins and are of indeterminate origin (fig. 4.5). Coarse-sand to gravel-size matrix material is composed of volcanic rock fragments, blocky volcanic glass shards (now chloritized), and feldspar and pyroxene crystals. Less than 5 percent clay-size material is present in the matrix. Additional evidence for hydroclastic origin is the monolithic nature of the breccia clasts. As igneous bodies come into contact with water, hydroclastic fragmentation occurs and produces a mixture of blocky glass shards and

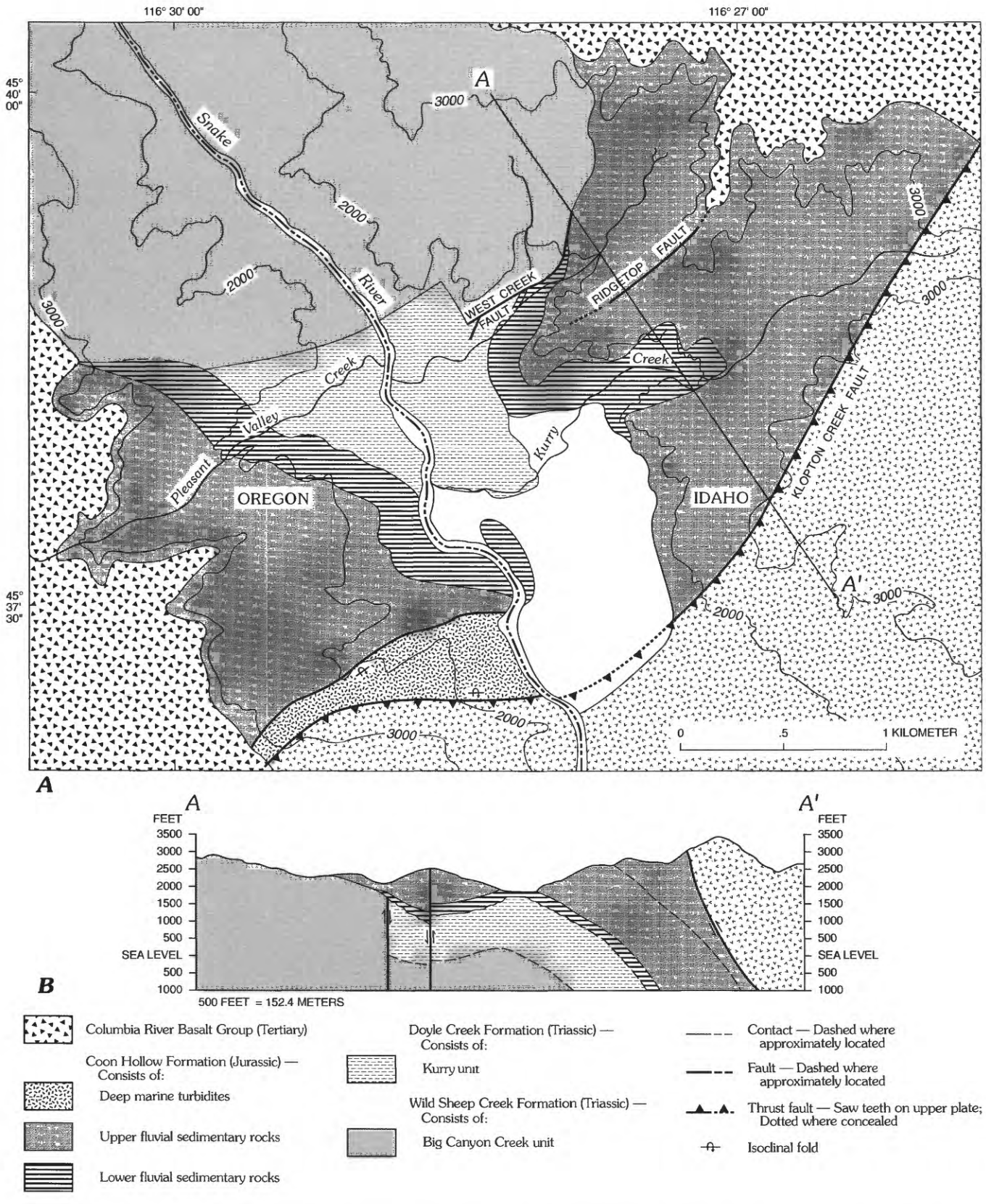

Figure 4.3.—Geologic map of Pittsburg Landing area, Oregon and Idaho, and accompanying cross section. *A*, Map showing geologic units. Contours in feet (Unpatterned areas are Quaternary alluvium). *B*, Simplified cross section (A-A') from north to south. Heavy black lines denote faults; arrows show relative movement. Dashed lines denote lithofacies boundaries.

larger clasts of single parentage that are either glassy or crystal-lithic. The combination of monolithic clasts and a blocky, lithic, and nonvesicular glass shard matrix support a hydroclastic origin for the breccia on petrographic grounds. The blocky character of the shards, along with the presence of abundant larger lithic fragments, indicates hydroclastic fragmentation by steam explosions; these characteristics suggest that the fragments were formed at shallow-water levels (<300 m), where steam explosions are possible (Fisher, 1984).

Although hydroclastic processes produced the breccia clasts, the rarity of lava pillows and flows within the unit suggests that much of the debris was remobilized. Very poor sorting, poorly defined bedding, low matrix-clay content and poorly developed reverse grading combined with bed thicknesses in the range of a meter or two suggest deposition from any or all of the cohesionless debris flow mechanisms cited by Postma (1986) and discussed at length by Lowe (1982). Cohesionless debris flows contain too little clay to provide the cohesive matrix characteristic of true debris flows, and they are supported by a combination of dispersive pressure (grain flow), upward flow of escaping pore fluids (fluidized flow), matrix strength (cohesive clays), and buoyancy of interstitial fluids (clays and water). Such flows are capable of moving down slopes of 9° or less, considerably shallower than the 18° required for grain-flow transport (Lowe, 1976).

Locally within the breccia sequence are lapilli tuffs; these tuffs have erosional bases, are matrix poor, and some are normally graded. They are associated with beds that lack large clasts and (or) have erosive bases. The association indicates that the material was probably deposited by high-concentration turbidity currents (Lowe, 1982).

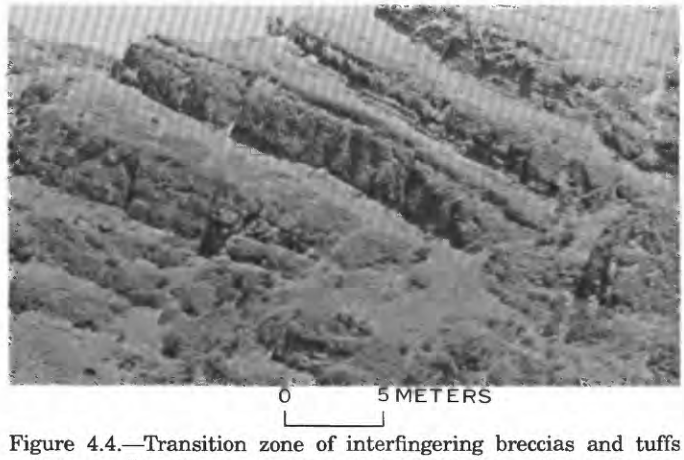

Figure 4.4.—Transition zone of interfingering breccias and tuffs between Big Canyon Creek unit (of Wild Sheep Creek Formation) and Kurry unit (of Doyle Creek Formation), Pittsburg Landing, Oregon and Idaho.

The very low shard vesicularity and abundant lithic fragments favor production of breccia clasts by hydroclastic fragmentation of partially cooled and degassed lava, as occurs when lava flows come into contact with water. Disaggregation of basaltic and andesitic lava flows and pillows, and subsequent downslope transport and resedimentation of the resultant debris piles, are the best explanations for the composition and characteristics of the breccia. The interbedded tuff is of both magmatic and phreatomagmatic origin, and it contains pumice in places. It may have erupted subaerially or in shallow (<500 m; Fisher, 1984) water, where vesiculation and steam explosions controlled fragmentation. There are abun-

Figure 4.5.—Hydroclastic breccia of Big Canyon Creek unit exposed at Pittsburg Landing, Oregon and Idaho. Contact between breccia and underlying tuff interval uneven on right because breccia gouged a few centimeters into tuff when deposited. Note matrix support and subequant, monolithologic clasts. Notebook is 20 cm tall.

dant syndepositional slump folds in tuff intercalated with the breccia. By correcting for the present regional dip, fold hinges with northward-dipping axial planes are obtained; the orientation of these folds indicates a south-facing paleoslope.

TRACTION-BEDDED TUFF

Well-bedded tuff forms an interval, about 10 m thick, within the hydroclastic breccia. In an area north of West Creek (fig. 4.3*A*), this tuff interval includes ripples, crossbeds, and dune-bearing beds. Other tuff beds within the interval are massive, reversely graded, or bear outsize clasts. The individual tuff beds were probably cohesive but not entirely lithified during breccia emplacement. Evidence for their cohesiveness is that the uppermost tuff beds are deformed, and the lower surface of the overlying breccia is uneven because the breccia gouged a few centimeters into the uppermost part of the tuff interval when it was deposited (fig. 4.5).

Bed forms in the tuff indicate they were deposited from traction carpets, which form by gravitational segregation and elutriation in high-concentration turbidity currents (Lowe, 1982; Fisher, 1983), and also by traction. Paleocurrent measurements from these tuff beds suggest downslope movement in the same transport direction as that measured in other parts of the Wild Sheep Creek Formation. The currents that produced these bed forms were probably sediment gravity flows, and the bed forms may represent an unusual case of traction bedding developed in the S_1 layer of high-concentration turbidites (Lowe, 1982).

The most common bed forms in the tuff interval are sandwaves that are commonly climbing and in many cases have preserved stoss-side laminations (fig. 4.6). Foreset beds are overturned in many instances. The overturned foresets probably resulted from shear at the base of subsequent flows. Other bed forms include ripples and foreset crossbedding. These traction bed forms were produced by fully turbulent, high-concentration flows that initially deposited part of their sediment load (in this case glass shards, volcanic lithic fragments, and plagioclase crystals) and subsequently produced bed forms through interaction with the remainder of the flow (S_1 beds, Lowe, 1982). Rare chute-and-pool structures formed under supercritical flow conditions (Fisher and Schmincke, 1984; Hand, 1974). High rates of deposition are indicated by the preservation of stoss-side sediments on many of the sand waves. Fine-grained beds may have been deposited from dilute ash clouds generated above high-concentration flows by gravitational segregation (Fisher, 1983).

Some large lithic blocks are present within the tuff interval. The blocks resemble ballistic ejecta, but the lack of impact pockets indicates transport of the clasts within high-concentration flows, at least immediately prior to deposition. The presence of smaller blocks concentrated at the tops of individual tuff beds without accompanying sag features (fig. 4.7) also supports the argument for clast transport within the

Figure 4.6.—Climbing sand wave in traction-bedded tuff of Big Canyon Creek unit (of Wild Sheep Creek Formation) that crops out near West Creek, Pittsburg Landing, western Idaho. Note preserved stoss side lamination. Pencil is 15 cm long.

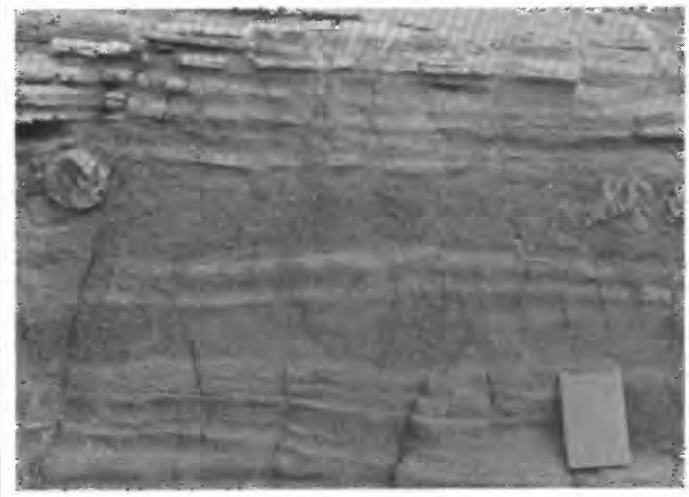

Figure 4.7.—Clasts near tops of beds in traction-bedded tuff of Big Canyon Creek unit (of Wild Sheep Creek Formation), exposed near West Creek, Pittsburg Landing, western Idaho. Deposition may have been from high-concentration laminar-flow layers at bases of high-concentration turbidity currents (see Lowe, 1982). Larger clasts rafted upward by dispersive pressure. Note pinch-and-swell of bedding. Notebook is 20 cm tall.

flows. Scarcity of the larger clasts reflects the size distribution of the clasts originally available for incorporation into the flow. As a result of elutriation and gravitational segregation, parts of the flows became highly concentrated dispersions of noncohesive particles. Mechanisms such as kinetic sieving (Middleton and Hampton, 1973), and (or) dispersive pressure (Bagnold, 1956) thus caused a concentration of the large lithic clasts near the tops of these flows, despite the greater size and density of the clasts. These beds correspond to the S_2 beds (traction carpet) of Lowe (1982).

This sequence of traction-bedded tuff contains no coarse hydroclastic breccia, and it may represent a period in which the hydroclastic fragmentation of gas-poor flows and pillows was interrupted by a period of explosive phreatomagmatic eruptions. The unabraded character of the fragments composing the tuff argues against segregation of tuffaceous material from the matrix of unsorted breccia during a period of volcanic quiescence. The tuff is enclosed within hydroclastic breccia, and both rock types were apparently deposited on the southern flank of a volcano.

KURRY UNIT (OF THE DOYLE CREEK FORMATION)

The Kurry unit locally bears marine fossils, and it includes tuff that is commonly interlayered with limey mudstone. Bedding thickness is variable, but beds of a few centimeters are characteristic (fig. 4.8). The lowest exposures of this unit are interfingered with hydroclastic breccia of the Big Canyon Creek unit of the Wild Sheep Creek Formation (fig. 4.4). The breccia is progressively less abundant upsection, and the uppermost part of the Kurry unit contains no breccia at all. A low-angle erosional unconformity separates the Kurry unit from overlying Jurassic deposits of the Coon Hollow Formation (White and Vallier, chap. 3, this volume).

The rocks of the Kurry unit form a fairly homogeneous section of thin-bedded limey mudstone and thin- to thick-bedded tuff. Limey mudstone containing mixtures of volcaniclastic silt in calcareous, clay-rich matrix is common in the lower part of the unit. Thin rip-up horizons are locally present, as are rare current ripples (some suggesting northerly currents). The marly limestone and fine-grained clastic rocks of the unit probably represent suspension deposits.

Tuff interbedded with the mudstone is increasingly abundant upsection. Some individual beds are coarse grained and have pronounced reverse grading. Rip ups of the limey mudstone are concentrated at the tops of these beds (fig. 4.9). Other beds are structureless or show subtle normal grading. This coarse-grained tuff was deposited by high-concentration sediment gravity flows, by density-modified grain flows (reversely graded), by high-concentration turbidity

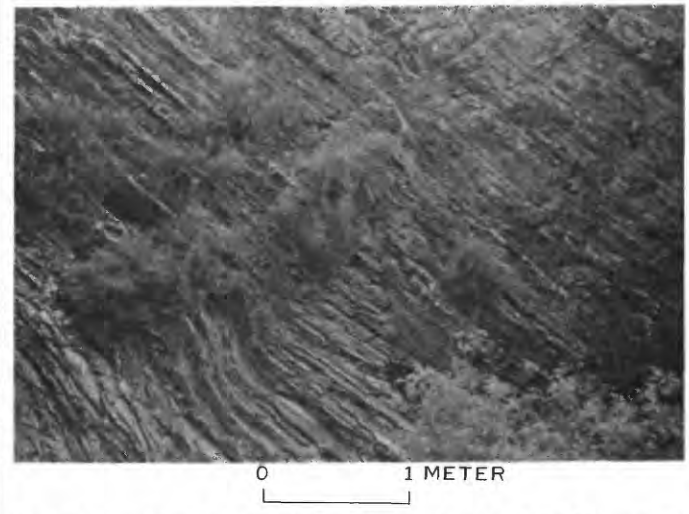

Figure 4.8.—Fossil-bearing tuffaceous sandstone of the Kurry unit of Doyle Creek Formation, exposed along West Creek, Pittsburg Landing, western Idaho. Individual beds are a few centimeters thick. Similar rocks make up much of the upper part of Kurry unit.

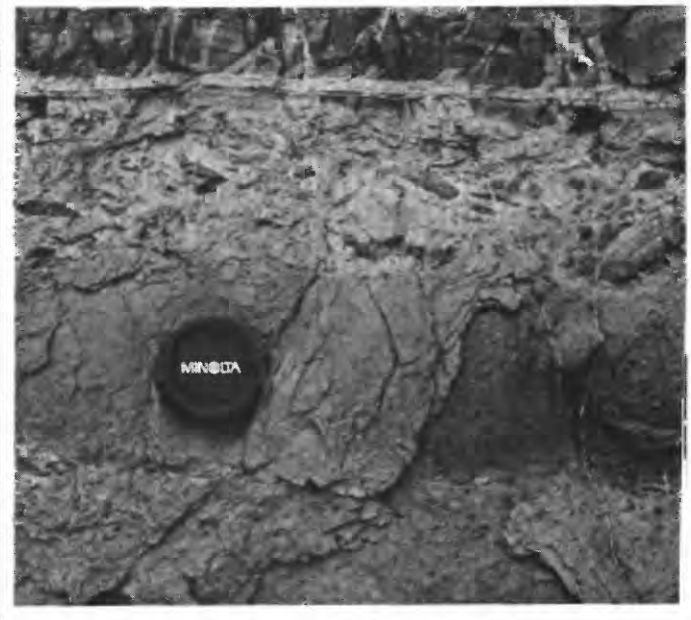

Figure 4.9.—Reversely graded tuff beds in Kurry unit of Doyle Creek Formation exposed along West Creek, Pittsburg Landing, western Idaho. Absence of wave-reworking features, in combination with such sediment gravity-flow deposits, indicates deposition of Kurry unit below storm-wave base. Lens cap is 49 mm in diameter.

currents, or by liquified flows (Lowe, 1982). The coarse beds are associated with very fine grained beds that may represent subaqueous fallout deposits.

High in the section, molds and casts of *Halobia* (Vallier, 1977), a Triassic pectinoid dysodont pelecypod (Moore and others, 1952), are common. The shells may have been redeposited by turbidity currents. Some beds littered with whole-shell casts are only a couple of shell widths thick, but the concavo-convex shells have a low settling velocity relative to more equant sand grains. The fossils' presence proves that marine conditions existed, as does the presence of ammonite molds (White and Vallier, chap. 3, this volume). The preservation of reversely graded tuff beds and the lack of wave-induced sedimentary structures suggest that the Kurry unit was deposited below fair-weather wave base by high- and low-concentration sediment gravity flows. The presence of plant fossils in some beds (White and Vallier, chap. 3, this volume) indicates that parts of the source terrane were subaerial. Sediment gravity flow deposits are rarely preserved above fair-weather wave base. Accordingly, the Kurry unit was probably deposited in the upper offshore zone or beyond. The upper offshore zone is characteristically bioturbated, parallel laminated, and consists of interbedded sand and mud (Elliot, 1978). Lower parts of the Kurry unit, particularly those parts interstratified with hydroclastic breccias, were probably deposited in similar settings. Depth to wave base on the shelves of island arcs varies with several factors including climate (stormy or calm), prevailing weather patterns, and irregularity of the coastline (for example, significant reentrants may be sheltered from the effects of storm waves).

COON HOLLOW FORMATION

LOWER FLUVIAL SEDIMENTARY ROCKS—BEDLOAD STREAM DEPOSITS

The lower fluvial sedimentary rocks unit consists of interlensing tuff, tuffaceous and volcanic-lithic sandstone and pebbly sandstone, conglomerate, and unreworked ash-flow tuff. It unconformably overlies the Kurry unit with a small angular discordance. The lowest part is very coarse (clasts as much as 70 cm in diameter and commonly 30 cm in diameter), whereas the upper boundary grades into the fine-grained strata of the upper fluvial sedimentary rocks unit. The lower and upper fluvial sedimentary rocks units form a generally fining upward sequence, with conglomerates becoming less abundant upsection.

Alternating strata of conglomerate, slope-forming sandstone, and tuff make up the lower fluvial sedimentary rocks unit. Shale is extremely rare, and siltstone is uncommon. Tuff and tuffaceous sandstone and conglomerate beds are abundant. Reworked pumice-gravel conglomerate beds (Stanley, 1978) are locally present.

Disorganized conglomerate, containing a variety of clast sizes from sand to boulders, characterizes the lower fluvial sedimentary rocks unit. Crude horizontal or subhorizontal bedding is generally present, and basal surfaces are typically erosive. In Miall's classification (1977, 1978), most of this conglomerate falls into the Gm (massive or crudely bedded gravel) facies, although rare matrix-supported conglomerate (facies Gms) is also present.

Sandstone generally overlies pebbly, commonly crossbedded, transitional sandstone-conglomerate intervals. Transitional sandstone and pebbly sandstone of this unit fall into the St and Sp facies, respectively, of Miall (1977). The admixture of pebbles and sand, both deposited simultaneously under tractive conditions, is common in systems where sediment concentrations are high, as in braided stream tracts of alluvial fans (Bluck, 1967).

There is abundant tuff, mostly reworked, within the unit. Unreworked tuff (red tuff unit of White and Vallier, chap. 3, this volume) is uncommon, but the presence of fallout and, especially, ash-flow tuff indicates close proximity of the area to an active volcano. Unreworked tuff was preserved when it deposited away from channels and thus escaped later erosion and reworking. Few such areas existed on the active braidplain at Pittsburg Landing and, therefore, reworked tuff is far more common.

The overall coarseness of this unit, combined with the abundance of traction-related sedimentary structures, argues for its deposition in a braided stream environment. Rounded clasts are reliable evidence for abrasion during stream transport. Incidental features such as fossilized logs (fig. 4.10) also lend support to this interpretation of depositional environment. Miall (1977, 1978) defined several braided stream facies assemblages. Strata of the lower fluvial sedimentary rocks unit most closely resemble those of Miall's (1977) Donjek-type streams because there are multiple conglomerate layers separated by finer grained deposits. There is too much sandy material to correspond to more gravelly Scott-type stream deposits, and the sequence is not dominated by debris flows, as is the Trollheim-type.

Donjek-type streams are the lowest average-energy conglomeratic braided stream described by Miall (1977). They are characterized by cyclicity, which produces multiple couplets of gravel and sand. Couplets are not vertical alternations of coarse and fine-grained

deposits, but they are instead multilateral channel fills that vary abruptly in texture both vertically and laterally. Multilateral channel-fill geometries are characteristic of fluvial systems with channels dominated by bedload (Galloway, 1981). Little overbank material is preserved in such systems.

Limited paleocurrent data (fig. 4.11) suggest that the lower and upper sedimentary rocks of the Coon Hollow Formation were deposited in a single stream system that transformed gradually from a relatively high energy braidplain to a lower energy meandering stream floodplain. Imbrication measurements from conglomerates of the lower fluvial sedimentary rocks unit indicate northward transport of sediments, as do numerous foreset and imbrication measurements from conglomerate and sandstone of the upper fluvial sedimentary rocks unit. If the strata of the lower unit were deposited on alluvial fans, paleocurrent indicators would likely be at high angles to those of the lower energy floodplain deposits that make up the upper unit.

UPPER FLUVIAL SEDIMENTARY ROCKS—MIXED-LOAD STREAM DEPOSITS

The upper fluvial sedimentary rocks unit gradationally overlies the lower fluvial sedimentary rocks unit. It is finer grained and consists of stacked sequences of conglomerate (absent locally), sandstone, and shale. Other characteristics distinguishing the upper unit from the lower unit include a smaller percentage of conglomerate, less volcanic ash (as tuff beds and within sandstones), abundant mudstone, and the presence of large-scale planar tabular crossbedding (facies Sp) in the upper unit. Together, these features support its deposition in a distal-braided to meandering fluvial system carrying sediment as both bedload and suspended load. Nearby volcanism ceased during deposition of the upper unit, and the proportion of clasts derived from the uplifted Cougar Creek Complex of Vallier (1968) to the south increased (White and Vallier, chap. 3, this volume).

Figure 4.10.—Coarse-grained braided stream deposits of the lower fluvial sedimentary rocks unit (of the Coon Hollow Formation) exposed south of Pleasant Valley Creek in northeastern Oregon. Note large fossilized log (arrow) near center of photograph.

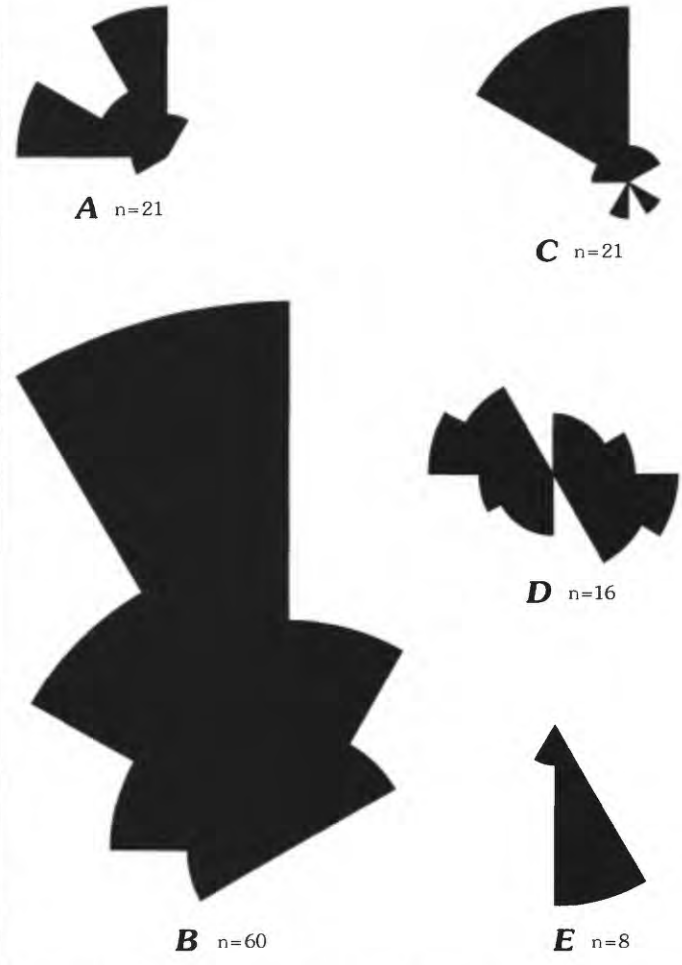

Figure 4.11.—Rose diagrams (radius, 30 units) showing paleocurrent data from strata at Pittsburg Landing, Oregon and Idaho. A, Indicator: foreset crossbedding measured at 2 locations in upper fluvial sedimentary rocks of Coon Hollow Formation. B, Indicator, pebble imbrication measured at 5 locations in upper fluvial sedimentary rocks of Coon Hollow Formation. C, Indicator: pebble imbrication measured at 2 locations in lower fluvial sedimentary rocks of Coon Hollow Formation. D, Indicator: wood fragments bimodal azimuth plot of data from 1 location in lower fluvial rocks of Coon Hollow Formation. E, Indicator: foreset crossbedding of sand waves at 1 location in traction-bedded tuff of Big Canyon Creek unit of Wild Sheep Creek Formation. n, number of measurements.

Conglomerate within the upper unit is less matrix rich than the conglomerate in the lower unit and commonly lies beneath well-developed beds of Sp sandstone. Basal layers containing large (about 10 cm) rip-up clasts are present locally. Disorganized conglomerate (facies Gm) is characterized by clast support, an erosive base, associated lenses of sandstone (facies Sh, St, and Sp of Miall, 1977, 1978), lateral variations in clast size, and imbrication. Gradational boundaries are common between conglomerate and overlying sandstone. Gravelly sandstone is less common in the upper unit than in the lower unit, and both conglomerate and pebbly sandstone are less common upsection. Some unusually coarse grained channel-filling amalgamates with very coarse, framework-supported cobble-boulder conglomerate at their bases are present high within the upper unit. These probably represent large valley-filling channel sequences with associated coarse-grained lag deposits.

The sandstone/shale ratio is nearly one in the lower part of the upper fluvial sedimentary rocks unit, and large-scale (> 1 m) planar-tabular crossbedding is common. Sandstone is characterized by large rip-up clasts of mudstone. Sets are from 1 to 3 m high and are repeated in places. Sp-facies units lie immediately above Gm-facies horizons in the lower part of the unit. In the upper parts of the unit, framework conglomerate is commonly absent, and Sp-facies sandstone overlies finer grained Fm-, Fr- and Fsc-facies deposits above a channeled base. Tuff and tuffaceous sandstone (facies Tr and St) are common in the lower part of the unit, but they are absent near its top. Facies St and Sp make up the largest part of the sandy channel deposits.

In the upper parts of the unit, the sandstone and mudstone are confined to widely separated, sheetlike (fig. 4.12) channel-fill sequences. Most mudstone is carbonate cemented, laminated, and breaks with a conchoidal fracture. Sandstone/shale ratios decrease markedly upsection to less than 1/10 in uppermost exposures of the unit. The shale commonly contains layers of charcoal and is locally seeded with subspherical limey nodules ranging from pea size up to 20 cm in diameter. Thin lignite layers and wood fragments are found in several locations within the fine-grained overbank deposits. Well-preserved fossil plants of various types, including ferns (*Dicksonia oregonensis*), conifers (*Pagiophyllum oregonensis*), and cycadophytes (*Pseudoctenis angustifolium*), are also present (Ash, 1991a, 1991b). Rootlet casts are locally preserved in thin horizons. Also present are thin (a few centimeters), laterally impersistent sandstone and siltstone beds that commonly show normal grading and are probably crevasse-splay and (or) levee deposits.

Of Miall's (1978) lithofacies assemblages, the lower beds of this unit most closely resemble the South Saskatchewan type, though the beds of the basal parts grade toward the Donjek type. The South Saskatchewan type records cyclic deposits of sandy braided streams, essentially a lower energy version of the gravelly cyclic deposits of the Donjek type. The amount of shale in the uppermost part of this unit may indicate that the fluvial system evolved into a meandering type late in its history.

Coarse-grained deposits of the upper fluvial sedimentary rocks unit are laterally continuous, and the distribution of the coarse layers is relatively simple. Multistory coarse-fine couplets, formed by stacked channel fills separated by overbank deposits, constitute the unit (fig. 4.12). The thickness of shaley deposits separating the sand bodies is greater upsection, and the thickness of individual sand bodies is concomitantly reduced. This type of sand-body geometry is developed in mixed bedload and suspended-load channels that carry coarse material in the bedload and finer materials in suspension (Galloway, 1981). Preserved deposits represent bank and bed accretion associated with higher sinuosity geometries, rather than the predominantly bed-accreted deposits of multilateral channel fills of braided streams. The lower and upper fluvial sedimentary rocks units make up a retrogradational sequence.

The most important distinctions between the units are differences in sand/shale ratios and sand-body

Figure 4.12.—Stacked sandstone and mudstone sequences that characterize the lower part of the upper fluvial sedimentary rocks unit of the Coon Hollow Formation. Photograph shows hillside above Kurry Creek, Pittsburg Landing, western Idaho. Outcrop face in foreground (arrow) is approximately 2 m high.

geometry. Coarse material is mostly confined to the lower part of this sequence, and the proportion of shale rises from nil near the base to well over 50 percent in the upper part of the sequence. Sand and gravel bodies are multilateral in the lower fluvial sedimentary rocks unit, and grade into multistory sand bodies in the upper fluvial sedimentary rocks unit. Virtually no overbank material was preserved. My mapping suggests that large valley-filling conglomerate and sandstone sequences occur within the upper fluvial sedimentary rocks unit, which resulted from stacked channel deposits filling paleovalleys.

TRANSGRESSIVE MARINE SEDIMENTARY ROCKS—ESTUARINE TO MARINE SHALE

The transgressive marine sedimentary rocks unit gradationally overlies the nonmarine shales of the upper part of the upper fluvial sedimentary rocks unit. The transition is obscure, and rocks of the transgressive unit are largely indistinguishable from shale-rich deposits of the upper fluvial sedimentary rocks unit. Fossil evidence, however, indicates a gradual invasion by seawater. Estuarine conditions are suggested by the presence of nonmarine clams (oral commun., Vallier, 1987) found locally in areas also containing abundant plant fossils. Higher in the transgressive unit, corals, including *Complexastrea* and *Stylina* (Stanley and Beauvais, 1990), are found. Within the marine shales, limey nodules are particularly abundant. Some areas of the transgressive unit contain small limestone lenses and beds. Rare conglomerates and sandstones are present within the shales.

The mudstone-dominated transgressive marine sequence was deposited in an organic-rich regime by suspension settling and low-energy overbank flows. The most likely depositional environments range from delta-plain to delta-front and pro-delta (nearshore marine). The conglomerates and sandstones probably represent distributary channel deposits of the low-elevation delta plain.

DEEP MARINE TURBIDITES

In the part of Pittsburg Landing just west of the Snake River in Oregon, carbonate and siliciclastic turbidites are folded into an isoclinal sequence, bounded to the south by the Klopton Creek fault, and overlying the marine transgressive sedimentary rocks above an unnamed fault to the north. Callovian ammonite fossils are present in the turbidites. These turbidites are correlated with strata of the Coon Hollow Formation exposed elsewhere in the Hells Canyon area (Vallier, 1977). This turbidite unit was structurally emplaced in the Pittsburg Landing area, and its relation to the other three units of the Coon Hollow Formation at Pittsburg Landing is not yet known.

DISCUSSION

PALEOGEOGRAPHY

There are two distinct phases to be accounted for in the reconstruction of Pittsburg Landing paleogeography. The Big Canyon Creek unit and Kurry unit were deposited in a Triassic island arc (Vallier, 1977). Separating these two units from the Jurassic Coon Hollow Formation is an unconformity representing a time interval of some 50 m.y.

Strata of the Big Canyon Creek unit are primarily hydroclastic volcanic deposits that were formed by the interaction of magma and seawater. The Kurry unit, gradationally overlying the Big Canyon Creek unit, is a mixed pyroclastic, hydroclastic, and biogenic deposit. The hydroclastic units formed on the slopes of an active volcano, as indicated by the presence of pillow lava. Constituents of the hydroclastic breccia and traction-bedded tuff appear to have undergone minimal transport.

The depth below sea level at which the hydroclastic breccia was deposited is not certain. A lack of current reworking, combined with its deposition from flows known to move over relatively steep slopes (approximately 9°, Lowe, 1976), favor deposition of the unit below storm-wave base. The flows could easily have moved down the steep flanks of a developing volcanic island. Also supporting deposition of the breccia below storm-wave base is the interfingering of the breccia with tuff of the Kurry unit.

The traction-bedded tuff enclosed within the hydroclastic breccia was deposited from south-moving flows (fig. 4.10) either during or subsequent to a period of phreatomagmatic eruptive activity. The vesicle-poor breccia, which forms most of the Big Canyon Creek unit, was probably produced by fragmentation of a largely degassed magma, most likely by fragmentation of effusive lava at the lava-seawater interface. The glassy, slightly vesicular character of the shards of the traction-bedded tuff suggests that they are the product of explosive fragmentation of almost crystal-free magma. At the time of fragmentation, the magma was beginning to vesiculate as it moved rapidly toward the surface within a volcanic vent.

Strata deposited atop those of the Kurry unit were subsequently removed by erosion, and the now over-

lying strata belong to the Coon Hollow Formation. The Coon Hollow Formation grades from largely pyroclastic rocks at its base to entirely epiclastic shales at the highest levels exposed at Pittsburg Landing. Although volcanism contributed material and influenced depositional style, the Coon Hollow strata were deposited by sedimentary processes. The transition between depositional styles within the formation is gradational. The uppermost shales were deposited subsequent to all active volcanism in the area.

During early Coon Hollow time, deposition occurred near an active volcano, near a coastline. The gradual transition upsection from alluvial to marine deposits is evidence for a coastal location, and the coarse-grained, unreworked fallout and ash-flow tuff in the lower fluvial sedimentary rocks unit suggests deposition near a volcano. Clasts derived from the Cougar Creek Complex, along with evidence of northward-flowing paleocurrents, indicate the presence of an emergent mass of arc-basement rocks to the south (White and Vallier, chap. 3, this volume). Mud-rich fluvial sedimentary deposits in the upper fluvial sedimentary rocks unit suggest that the Pittsburg Landing landmass was large enough to support a fairly well developed stream system. The cyclicity of fluvial deposits in the upper fluvial sedimentary rocks unit of the Coon Hollow Formation probably resulted from episodic uplift of the basement complex during the deposition of this part of the Coon Hollow Formation.

FLUVIAL TO MARINE SEDIMENTATION IN THE COON HOLLOW FORMATION

Most of the conglomerate, tuff and reworked tuff of the lower fluvial sedimentary rocks unit appear to have been "dumped onto" the erosional surface by extremely high sediment concentration streams. The onset of deposition above the erosional surface is probably related to renewed volcanism in the area, which apparently choked actively eroding (degrading) streams with volcanogenic debris.

The lower fluvial sedimentary rocks unit is rich in volcanogenic components. Remaining parts of the section form a simple retrogradational fluvial sequence, in which strata of the upper fluvial sedimentary rocks unit represent environments progressively more depleted in coarse-grained sediment at higher stratigraphic levels. The transgressive marine shales above the overbank shales were deposited as relative sea level rose and (or) as sediment supply was reduced; this rise in sea level resulted in submergence of the fluvial system as subsidence continued. Descriptions of braided outwash deposits from southeastern Alaska (Boothroyd and Nummedal, 1978) suggest that many of these changes could take place within a humid alluvial fan/delta setting. In the Alaskan systems they studied, proximal deposits are represented by longitudinal gravel bars and sheets, intermediate deposits by linguoid bar deposits, and distal deposits by marsh and swamp deposits associated with meandering streams. A retrogradational stacking of these deposits would be similar to the sequence observed at Pittsburg Landing. The change from proximal to distal deposits in Alaska is a simple function of distance from the sediment source (the toes of the glaciers). At Pittsburg Landing, the more distal upsection deposits thus seem to indicate source-area degradation and retreat (Heward, 1978).

In applying models developed in nonvolcanic areas to deposits associated with active volcanism, certain adjustments must be made. Most important is the ability of volcanoes to supply large amounts of coarse unconsolidated sediment over short periods of time, both by supplying ejecta and by removing plant cover that might otherwise inhibit dispersal of sediment from the volcanoes. Kuenzi and others (1979) concluded from examination of a fluvio-deltaic system in Guatemala that the addition of unconsolidated volcanic ejecta into a fluvial system can induce stream braiding independent of tectonic movement or changes in relative relief. Heward (1978) discussed possible vertical fining- and coarsening-upward megasequences in alluvial fan deposits in terms of tectonic uplift and fanhead entrenchment. Of the four megasequence models described, only scarp retreat and lowering of relief produce a fining-upward trend similar to that at Pittsburg Landing. In volcanic areas, progradation-retrogradation sequences can also be generated by addition and subsequent depletion of coarse-grained volcanic ejecta. Such volcanic sediment loading is likely reflected in the change from an erosional regime to the ash-rich, coarse-grained, aggradational depositional system represented by the lower fluvial sedimentary rocks unit. Depletion of this ejecta allowed subsequent development of the lower energy, cyclic depositional system of the upper fluvial sedimentary rocks unit.

CONCLUSIONS

The Triassic Big Canyon Creek unit (of the Wild Sheep Creek Formation) and the Kurry unit (of the Doyle Creek Formation), both of the Seven Devils Group, are composed of marine deposits of a former oceanic island arc now accreted to North America. The Jurassic Coon Hollow Formation overlies these Triassic rocks above an angular unconformity and

consists of volcanogenic and nonvolcanogenic fluvial deposits gradationally overlain by trans-gressive marine shales. A number of conclusions have been drawn about this area's geologic history. These are:

1. Volcanism occurred within and immediately north of Pittsburg Landing during Triassic time, as indicated by the pillow lava and hydroclastic breccia of the Big Canyon Creek unit. Strata of its upper part interfinger with marine-deposited tuff and mudstone of the Kurry unit.

2. Strata of the Coon Hollow Formation exposed at Pittsburg Landing are predominantly products of fluvial deposition. Evidence supporting fluvial deposition includes abundant traction deposition features, small lignitic seams, fossil rootlet horizons, and fossil plants. The lowermost deposits of this formation consist of ash-flow tuff and abundant stream-reworked tuff, and they grade upward in to less tuffaceous, finer grained fluvial deposits. These grade upward into marine rocks of Bajocian age (Stanley and Beauvais, 1990). The gradual transition from coarse-grained alluvial deposits through finer grained fluvial deposits into fine-grained marine rocks suggests deposition increasingly near sea level (base level) through time. Much of the sequence may have developed in a deltaic setting. Volcanism declined following emplacement of the ash-flow tuff in the lower fluvial sedimentary rocks unit, and there is little or no primary or reworked ash in the transgressive marine deposits that top the section. The lower fluvial sedimentary rocks unit (of the Coon Hollow Formation) was deposited by a system of gravelly, ash-choked braided streams. It fines upward into the upper fluvial sedimentary rocks unit that was deposited by more sandy braided streams in its lower part and possibly by meandering distributary systems in its upper part. The cyclic nature of the deposits of the upper unit is attributed to tectonism in the uplifted arc-basement source area to the south. The sequence may represent a retrogradational humid-region fan-delta sequence.

3. Gradationally overlying the upper fluvial sedimentary rocks unit is the transgressive marine sedimentary rocks unit (of the Coon Hollow Formation) that is made up of shales containing brackish-to-marine fossils.

4. The Coon Hollow Formation buries a substantial topography that developed during a period of emergence that followed shoaling of the arc, probably in Triassic time.

REFERENCES CITED

Ash, S.R., 1991a, A new Jurassic flora from the Wallowa terrane in Hells Canyon, Oregon and Idaho: Oregon Geology, v. 53, p. 27–34.

Ash, S.R., 1991b, A new Jurassic *Phlebopteris* (Plantae, Filicales) from the Wallowa terrane in the Snake River Canyon, Oregon and Idaho: Journal of Paleontology, v. 65, p. 322–328.

Bagnold, R.A., 1956, The flow of cohesionless grains in fluids: Philosophical Transactions of the Royal Society of London, Series A, v. 249, p. 235–297.

Bluck, B.J., 1967, Deposition of some Upper Old Red Sandstone conglomerates in the Clyde area: a study in the significance of bedding: Scottish Journal of Geology, v. 3, no. 2, p. 139–167.

Boothroyd, J.D., and Nummedal, D.,1978, Proglacial braided outwash: a model for humid alluvial-fan deposits, in Miall, A.D., ed., Fluvial sedimentology, Canadian Society of Petroleum Geologists Memoir No. 5, p. 641–668.

Elliott, T., 1978, Clastic shorelines, *in* Sedimentary Environments and Facies: Reading, H.G., ed., New York, Elsevier, p. 143–177.

Fisher, R.V., 1983, Flow transformations in sediment gravity flows: Geology, v. 11, no. 6, p. 273–274.

Fisher, R.V., 1984, Submarine volcaniclastic rocks in marginal basin geology: volcanic and associated sedimentary and tectonic processes, *in* Modern and Ancient Marginal Basins: Special Publication of the Geological Society of London, No. 16, p. 5–27.

Fisher, R.V., and Schmincke, H.-U., 1984, Pyroclastic Rocks. New York, Springer-Verlag, 472 p.

Galloway, W.E., 1981, Depositional architecture of Cenozoic Gulf Coastal Plain fluvial systems, *in* Ethridge, F.G., and Flores, R.M., eds., Recent and ancient nonmarine depositional environments: models for exploration: Special Publication No. 31, Society of Economic Paleontologists and Mineralogists, Tulsa, Okla., p. 127–156.

Hand, B.M., 1974, Supercritical flow in density currents: Journal of Sedimentary Petrology, v. 44, no. 5, p. 637–648.

Heward, A.P., 1978, Alluvial fan sequence and megasequence models, *in* Miall, A.D., ed., Fluvial Sedimentology, Canadian Society of Petroleum Geologists, Memoir No. 5, p. 669–702.

Kuenzi, W.D., Horst, O.H., and McGeehee, R.V., 1979, Effect of volcanic activity on fluvial-deltaic sedimentation in a modern arc-trench gap, southwestern Guatemala: Geological Society of America Bulletin, v. 90, no. 6, p. 827–838.

Lowe, D.R., 1982, Sediment gravity flows: II. Depositional models with special reference to the deposits of high-density turbidity currents: Journal of Sedimentary Petrology, v. 52, no. 3, p. 279–297.

Lowe, D.R., 1976, Subaqueous liquefied and fluidized sediment flows and their deposits: Sedimentology, v. 23, no. 3, p. 285–308.

Miall, A.D., 1977, A review of the braided-river depositional environment: Earth-Science Reviews, v. 13, no. 1, p. 1–62.

Miall, A.D., 1978, Lithofacies types and vertical profile models in braided river deposits: a summary, *in* Miall, A.D., ed., Fluvial Sedimentology: Canadian Society of Petroleum Geologists, Memoir No. 5, p. 597–604.

Middleton, G.V., and Hampton, M.A., 1973, Sediment gravity flows: mechanics of flow and deposition, *in* Turbidites and Deep Water Sedimentation: Society of Economic Paleontologists and Mineralogists, Short Course Notes No. 1, Anaheim, Calif., p. 1–38.

Moore, R.C., Lalicker, C.G., and Fischer, A.G., 1952, Invertebrate Fossils: New York, McGraw-Hill, 766 p.

Postma, G., 1986, Classification for sediment gravity-flow deposits based on flow conditions during sedimentation: Geology, v. 14, no. 4, p. 291–294.

Silberling, N.J., Jones, D.L., Blake, M.C., Jr., and Howell, D.G., 1984, Lithotectonic terrane map of the western coterminous

United States: U.S. Geological Survey Miscellaneous Field Studies, MF-1874-C, scale 1:2,500,000.

Stanley, D.J., 1978, Pumice gravels in the Riviere Claire, Martinique: selective sorting by fluvial processes: Sedimentary Geology, v. 21, no. 2, p. 161–168.

Stanley, G.D. Jr., and Beauvais, L., 1990, Middle Jurassic corals from the Wallowa terrane, west-central Idaho: Journal of Paleontology, v. 64, no. 2, p. 352–363.

Vallier, T.L., 1967, Geology of part of the Snake River Canyon and adjacent areas in northeastern Oregon and western Idaho: Corvallis, Oregon State University, Corvallis, Ph.D. dissertation, 267 p.

Vallier, T.L., 1968, Reconnaissance geology of the Snake River Canyon between Granite Creek and Pittsburg Landing, Oregon and Idaho: The Ore Bin, v. 30, no. 12, p. 233–252.

Vallier, T.L., 1974, A preliminary report on the geology of part of the Snake River Canyon, Oregon and Idaho: Oregon Department of Geology and Mineral Industries Geological Map Series, GMS-6, 15 p.

Vallier, T.L., 1977, The Permian and Triassic Seven Devils Group, western Idaho and northeastern Oregon: U.S. Geological Survey Bulletin 1437, 58 p.

Vallier, T.L., and Brooks, H.C., 1986, Geology of the Blue Mountains region of Oregon, Idaho, and Washington: Geologic implications of Paleozoic and Mesozoic paleontology and biostratigraphy, Blue Mountains province, Oregon and Idaho: U.S. Geological Survey Professional Paper 1435, 96 p.

White, D.L., 1972, The geology of the Pittsburg Landing area, Snake River Canyon, Oregon-Idaho: Terre Haute, Indiana State University, M.S. thesis, 98 p.

White, J.D.L., 1985, The Doyle Creek Formation (Seven Devils Group), Pittsburg Landing, Idaho: A study of intra-arc sedimentation Columbia, University of Missouri, M.S. thesis, 151 p.

White, J.D.L., White, D.L., Vallier, T.L., Stanley, G.D. Jr., and Ash, S.R., 1992, Mid-Jurassic strata link Wallowa, Olds Ferry, and Izee terranes in the accreted Blue Mountains island arc, northeastern Oregon: Geology, v. 20, p. 729–732.

5. PHYSIOGRAPHY OF THE SEVEN DEVILS MOUNTAINS AND ADJACENT HELLS CANYON OF THE SNAKE RIVER, IDAHO AND OREGON

By TAU RHO ALPHA and TRACY L. VALLIER

CONTENTS

ABSTRACT

Geomorphic processes that formed the landscapes in the Seven Devils Mountains and adjacent Hells Canyon of the Snake River are interpreted from regional geology and physiography. The intensely eroded landscapes can be distinctly shown in a physiographic diagram. That part of Hells Canyon shown on the physiographic diagram herein is deeper than the Grand Canyon of the Colorado River and is one of the deepest canyons in North America. The adjacent Seven Devils Mountains were carved by intense stream and glacial erosion.

The physiography developed during four large-scale Cenozoic events. First, early Tertiary erosion of the pre-Cenozoic rocks formed a westward-sloping low-relief surface with many streams that carried abundant coarse debris from central Idaho. Subsequently, several thousand feet of Miocene lavas buried the old erosion surface and created a high, nearly flat plateau. A third event is basin-and-range-type normal faulting that began after extrusion of the Miocene lavas and continues today. It produced large horsts and grabens that form the present mountain ranges and intermontane basins. The fourth event is the glaciation and attendant pluvial periods of the Pleistocene, which greatly intensified erosion. The Bonneville flood, which roared through Hells Canyon about 15,000 years ago, did not greatly modify the physiography of the region.

INTRODUCTION

The Snake River forms the boundary between Oregon and Idaho from near Ontario, Oregon, to the Oregon-Washington State line; from there to Lewiston, Idaho, it is the boundary between Washington and Idaho (fig. 5.1). Within that region, the river has carved a canyon that in places is deeper than the Grand Canyon of the Colorado River.

A particularly spectacular segment of the Snake River canyon, cut along the western edge of the Seven Devils Mountains of Idaho, is best shown in a physiographic diagram (fig. 5.2). This segment includes the most rugged part of the Snake River canyon (Ashworth, 1977), known as Hells Canyon (fig. 5.3). The exact extent of Hells Canyon proper is not agreed upon by those who study it and has not been adequately defined, but the segment of the Snake River canyon shown in figure 5.2 as part of Hells Canyon would not be disputed by anyone who has worked in the area. The adjacent Seven Devils Mountains are a rugged, intensely eroded, and glaciated ridge that locally separates the Snake River and the Salmon River (fig. 5.4).

The physiography of Hells Canyon and the adjacent Seven Devils Mountains are discussed herein. The regional geology and four large-scale events that contributed to the present-day landscape of this area are also discussed.

METHODS

The regional geology has been studied by T.L. Vallier during the past 25 years. The specific area shown in figure 5.2, however, was geologically mapped during parts of the summer field seasons of 1965, 1968, 1970, 1971, and 1986. Tau Rho Alpha visited Hells Canyon in 1986 and 1987 to interpret the landforms by sketching the landscape as well as recording it on camera.

An isometrograph (fig. 5.5) was used to construct the physiographic diagram (fig. 5.2) from portions of two 1957 edition U.S. Geological Survey 15-minute topographic quadrangles (Cuprum, Idaho-Oregon, and He Devil, Idaho-Oregon, both 1:62,500 scale). An oblique framework of contours was first compiled with the isometrograph using a constant viewing

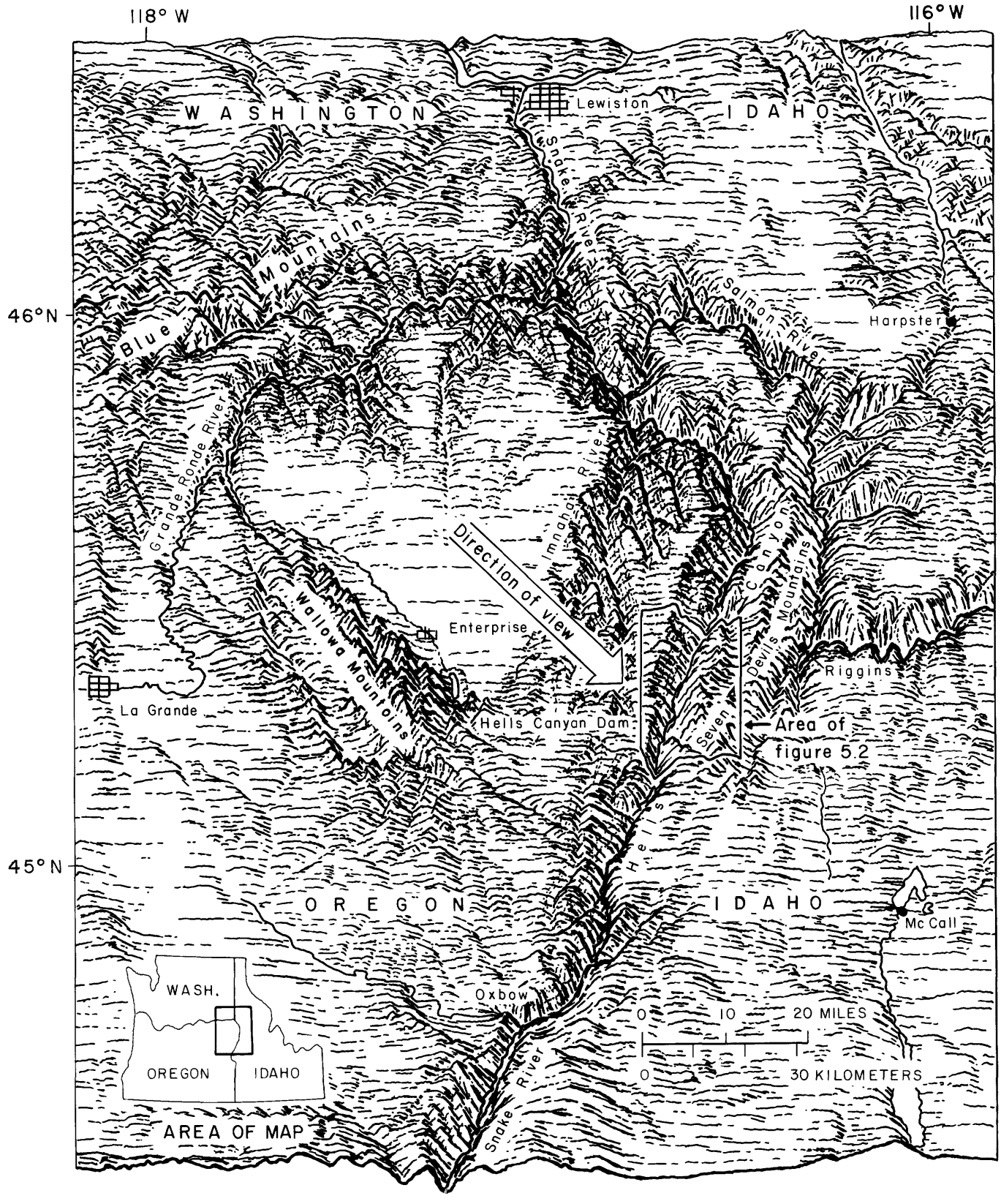

FIGURE 5.1.—Index map of eastern Oregon, western Idaho, and southeastern Washington showing most of Blue Mountains province.

angle of 30° from the horizon. This framework serves as a parallel perspective projection with a constant left-right scale and a constant scale parallel to the angle of view with no vertical exaggeration.

The contour framework was then interpreted on the basis of surface materials, what is known about geologic structure, and weathering characteristics of the Seven Devils Mountains and Hells Canyon area. The contours were interpreted as to shape, form, and surface materials. Shape relates to the outline of the landform; the outline or profile of the landform is the primary clue for the map reader's identification. Form is the volume or three-dimensionality of the landform. Surface material is the landform cover, whether solid rock or unconsolidated material such as alluvium.

Shape, form, and surface materials are depicted using formlines that are drawn parallel to the gradient of the slope. For example, slopes that make up Granite Creek (fig. 5.2, center) are very steep, and the formlines are nearly vertical to show that steepness. Near Granny Guard Station (fig. 5.2, lower left foreground), the top of the Columbia River plateau in Oregon, the formlines are horizontal, as there is little slope. Formlines represent variation in shape, as shown by the outline of Pyramid Peak (fig. 5.2, near the top), the horizontal surface of the plateau, and the steep, ragged, craggy bottom of Hells Canyon. Formlines consist of thick and thin lines such as those drawn along ridgelines near Granite Mountain (fig. 5.2, near center), which are straight on the ridgetop and curve off either side to portray

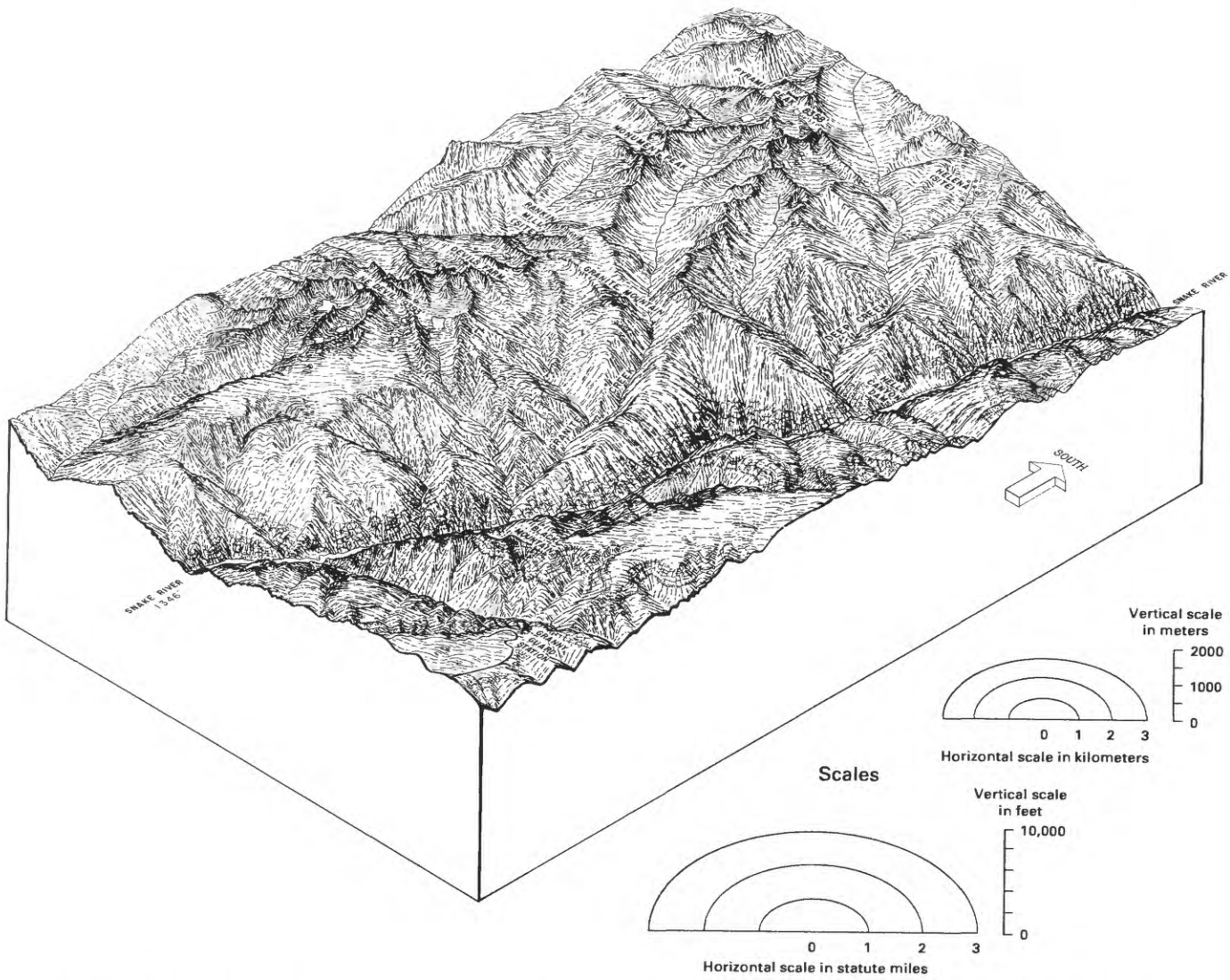

FIGURE 5.2.—Physiographic diagram (from Alpha and Austin, 1982) of Seven Devils Mountains and Hells Canyon, Idaho and Oregon.

the multilayered lava of the plateau. Relativity more space is used between the formlines that are composed of short thin lines and dots on some of the left-facing slopes of the ridges to represent reflecting light. Formlines also depict space by being either grouped together or spaced farther apart. The spacing of formlines helps denote shape in areas such as overlapping side canyons, and it helps convey form, as with left-facing (reflective) slopes. Space can also be used to portray the lack of texture of the surface material.

Formlines bring all the slopes, ridges, and canyons together to create a unified physiographic diagram without any visual breaks. Visual continuity is criti-

FIGURE 5.3.—Hells Canyon of Snake River in area between Hells Canyon Dam and Granite Creek. View is north toward Wild Sheep Creek.

cal to ensuring the individual parts create the whole physiographic diagram.

An elliptical scale is used to measure horizontal distance on this parallel-perspective physiographic diagram, (fig. 5.2). To use the elliptical scale, place a ruler on the diagram, note the number of units between the two points of interest, and then move the ruler to the zero point on the elliptical scale, keeping it parallel to its original alignment. Then read the distance from the elliptical scale.

Feet and miles, rather than meters and kilometers, are used in the text to designate heights and distances consistent with the contours, heights, and distances on the He-Devil and Cuprum topographic quadrangle

FIGURE 5.4.—Seven Devils Mountains viewed from north along Boise trail, which traverses ridge between Snake River and Salmon River drainages. Sheep Creek canyon in foreground.

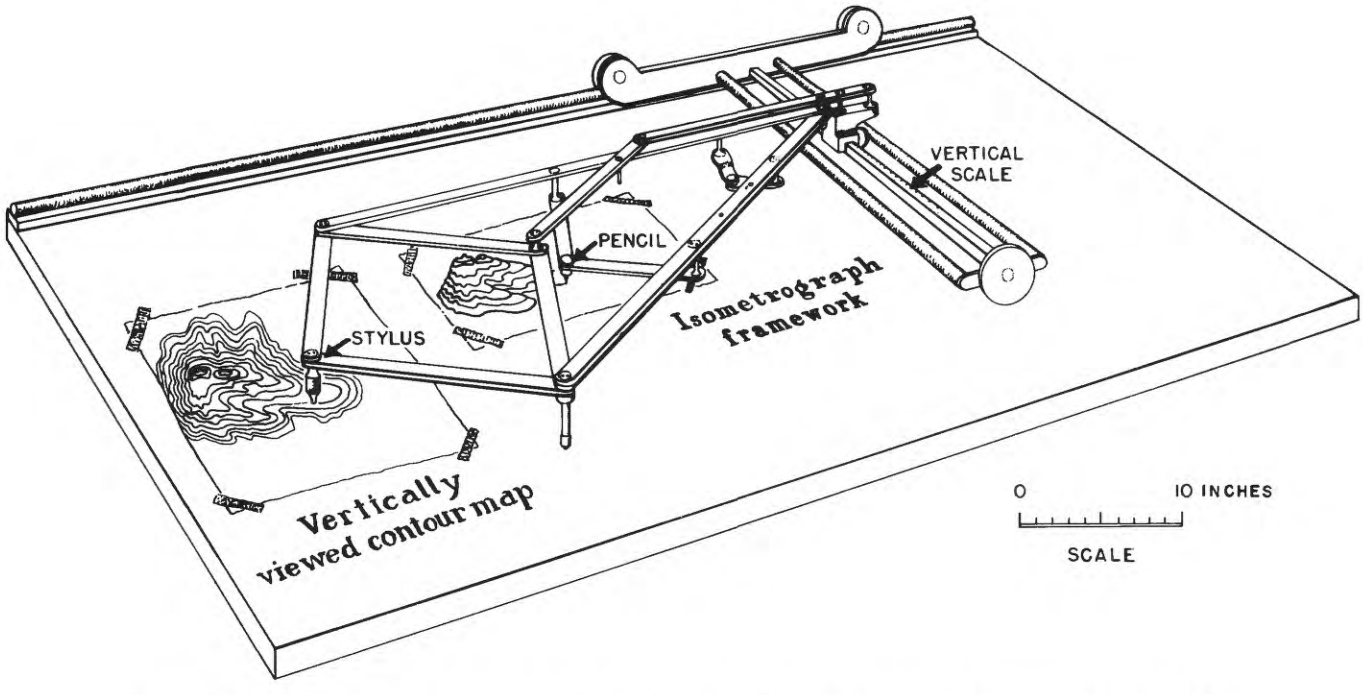

FIGURE 5.5—Isometrograph, the instrument used to develop the parallel perspective framework for figure 5.2.

maps that were used to construct this diagram, whereas metric units are used to quote of Bonneville flood discharge rates.

GEOLOGIC FRAMEWORK OF THE SEVEN DEVILS MOUNTAINS AND HELLS CANYON

The Seven Devils Mountains and Hells Canyon region is part of the Blue Mountains province (Fenneman, 1931). Pre-Tertiary rocks in the Blue Mountains province, particularly those of Permian and Triassic age, originated in an island arc (the Blue Mountains island arc) that developed in the ancestral Pacific and was accreted to the North American continent in the Early Cretaceous (Avé Lallemant, in press; Vallier, in press). The suture zone that marks this collision is exposed near Riggins, Idaho. The pre-Tertiary rocks were divided into five tectonostratigraphic terranes by Silberling and others (1984); the Seven Devils Mountains-Hells Canyon region is in the Wallowa terrane, which is part of the Permian and Triassic volcanic and plutonic axis (volcanic front) of the Blue Mountains island arc.

After accretion of the Blue Mountains island arc to North America, rocks of the mainly Late Cretaceous Idaho batholith were intruded into both the suture zone and the Precambrian rocks of the North American craton that lie farther east. Following extensive erosion, the pre-Tertiary rocks of the Blue Mountains province were buried by Miocene lava flows of the Columbia River Basalt Group, which were erupted onto a gently rolling upland having at least 1,500 to 2,000 ft (457-610 m) of relief in the Snake River canyon region shown in figure 5.1.

Those parts of the Seven Devils Mountains and Hells Canyon shown in figure 5.2 consist of Permian and Triassic volcanic rocks of the Seven Devils Group (Vallier, 1977, in press) and associated Permian and Triassic gabbro and quartz diorite plutons, overlying carbonate rocks and shales of the Upper Triassic Martin Bridge Limestone and Triassic(?) Lucile Slate, Late Jurassic and Early Cretaceous plutons of gabbro, quartz diorite, and granodiorite, and lava flows of the Miocene Columbia River Basalt Group (Vallier, 1974). Rocks of the Permian and Triassic Seven Devils Group are well exposed along a U.S. Forest Service trail that circles the Seven Devils Mountains; Triassic volcanic rocks are exposed along the northern and central parts, and Permian rocks crop out along the extreme southern reaches of the trail. Triassic volcanic rocks also crop out along most of the Snake River canyon walls in the area shown in figure 5.2. Rocks of a Cretaceous pluton cut Granite Creek about 1 mi (1.6 km) from its confluence with the Snake River and parallel it along the east side of the canyon. Rocks of a Permian pluton are exposed in the lower parts of Sheep Creek canyon. The extensive lava flows of the Columbia River Basalt Group are well exposed along the west side of the canyon.

Faults are abundant—dominant trends are northeast-southwest and north-south. In general, the older Mesozoic faults and folds trend northeast, whereas younger, latest Miocene to Holocene, normal faults trend north-south. In places, younger faults follow the older northeast trends. The oldest lava flows of the Columbia River Basalt Group are exposed in high parts of the Seven Devils Mountains; their presence indicates that the mountain range at one time was completely buried by the Miocene lava flows and that combined uplift along faults and erosion stripped away the volcanic cover.

PHYSIOGRAPHY OF HELLS CANYON AND THE SEVEN DEVILS MOUNTAINS

The regional physiography of the Blue Mountains province was discussed by Fenneman (1931) and Hunt (1974), and the physiography and geomorphology of specific parts of the Blue Mountains were described by Livingston (1928), Raisz (1945), Wheeler and Cook (1954), and Baldwin (1976).

The physiographic diagram (fig. 5.2) shows the most prominent landscape features. The Snake River has deeply incised the old plateau. From river level near the mouth of Granite Creek, at an elevation of less than 1,400 ft (427 m), 6 mi (9.6 km) eastward to the top of He Devil in the Seven Devils Mountains (fig. 5.6; elevation of 9,393 ft (2,863 m) the relief is about 8,000 ft. In places on the west side of Hells Canyon, dissected canyon walls rise precipitously more than 5,500 ft (1,676 m).

The direction of view of the physiographic diagram (fig. 5.2) is to the southeast, which places the west (Oregon) side of Hells Canyon in the foreground. The high features named on the map along the Oregon side of the canyon are Granny Guard Station of the Wallowa National Forest at 6,400 ft (1,950 m) and Black Mountain at an elevation of 6,862 ft (2,091 m). On the walls of the side canyons in that area, the multilayered lava flows of the Columbia River Basalt Group crop out. The lava flows are shown by horizontal lines, and the more resistant cliff-forming flows are depicted by vertical lines. At the bottom of the Snake River canyon, behind and to the left of Black Mountain, horizontal and crisscrossing lines represent the fractured volcanic and coarse volcaniclastic

sedimentary rocks of the Seven Devils Group and quartz diorite plutonic rocks. On the Idaho side near the river, Granite, Deep, and Sheep Creeks have V-shaped canyons. At higher elevations the glaciated Seven Devils Mountains are characterized by U-shaped stream canyons, cirques, tarns, arêtes, and horns (figs. 5.7, 5.8).

DISCUSSION

The geomorphology of the Snake River canyon and Seven Devils Mountains has not been adequately studied. Speculations concerning the canyon's history were presented by Livingston and Laney (1920), Livingston (1928), Wheeler and Cook (1954), and Vallier

FIGURE 5.6.—He Devil Mountain, Seven Devils Mountains, western Idaho. View from the south.

FIGURE 5.7.—Black Lake, one of several tarns in Seven Devils Mountains, western Idaho. View from the north.

(1967). The canyon's most recent history including the Bonneville flood was discussed by Malde (1968) and Jarrett and Malde (1987).

The Snake River canyon and Seven Devils Mountains are relatively young geomorphic features compared with the geologic history of the area. After extrusion of the approximately 17 to 6 (mostly about 17–14.5) million-year-old lava flows of the Columbia River Basalt Group, the region was uplifted, probably in the past 5 million years. Simultaneously with uplift, and probably within the past 2 million years (Wheeler and Cook, 1954), the Snake River incised downward through the Miocene lava flows and into the underlying pre-Tertiary volcanic and plutonic rocks. The river preferentially eroded its course along north- and northeast-trending normal faults that are associated with basin-and-range extension.

Four stages in the Cenozoic history of the region influenced the present morphology of the Snake River canyon and adjacent Seven Devils Mountains: (1) early and middle Tertiary erosion, (2) eruption of Miocene lava flows of the Columbia River Basalt Group, (3) latest Miocene to Holocene basin-and-range-type faulting with attendant uplift and subsidence, and (4) Pleistocene glaciation and associated pluvial events. The Bonneville flood, caused by the catastrophic draining of glacial Lake Bonneville near the end of the Pleistocene, swept through the canyon about 15,000 years ago.

In the first stage, early and middle Tertiary erosion formed a vast westward-sloping pediplain throughout western Idaho and eastern Oregon. Gravels and boulders deposited on the old erosion surface were derived locally as well as transported from long distances. Long-distance transport is indicated by locally abundant Precambrian(?) quartzite cobbles and boulders (from central Idaho?) that had been transported westward by streams. These quartzite cobbles and boulders, some as much as 38 cm in diameter, are present in several places along or near the contact between lava flows of the Columbia River Basalt Group and underlying pre-Tertiary rocks. It is apparent that high competency streams flowed in the area before the eroded landscape was buried by the Miocene lava flows.

Eruption of lava flows of the Columbia River Basalt Group was the second stage in the region's geomorphic evolution. Most of the flows were erupted in the middle Miocene, between about 17 and 14.5 million years ago, onto a landscape that had a regional relief in the Blue Mountains province of at least 1,500 to 2,000 ft (457-610 m). The volcanic activity formed an extensive high plateau.

A third stage was fault deformation that probably began in the latest Miocene about 5 or 6 million

FIGURE 5.8.—U-shaped upper reaches of Granite Creek canyon indicate intensity of Pleistocene glaciation in Seven Devils Mountains, western Idaho. Looking southeast from Granite Mountain.

years ago. This deformation continues and is largely responsible for the relief of the Seven Devils Mountains and other mountain ranges in the Blue Mountains province. Normal faults with hundreds (and in places, thousands) of feet of displacement uplifted large blocks that became deeply dissected mountain ranges. The Snake River cut downward along these mostly northeast- and north-trending faults through lava flows of the Columbia River Basalt Group and into the underlying pre-Tertiary rocks.

Pleistocene glaciation, and the attendant pluvial cycles, were the fourth stage in the geomorphic development of the region. The ruggedness and beauty of the Seven Devils Mountains (figs. 5.4, 5.7, and 5.8) were enhanced through erosion both by the glaciers and by high water runoff during glacial melting. Arêtes, cols, horns, cirques, tarns, moraines, and U-shaped valleys formed by these processes are common in the Seven Devils Mountains.

The most recent event in the history of the canyon was the Bonneville flood (Stearns, 1962; Malde, 1968; Jarrett and Malde, 1987), which swept through the Snake River canyon about 15,000 years ago. This flood did not greatly deepen or otherwise alter the appearance of the canyon in the region shown in figure 5.2. Farther north in the canyon (for example, near the mouth of Temperance Creek about 8 mi (or 13 km) south of Pittsburg Landing), high and broad river terraces indicate an extremely high water stage in the recent past. We believe these high terraces are the direct result of the Bonneville flood and that they formed when sediment was deposited in temporary lakes behind canyon constrictions, followed by downcutting through those sediments as the river flow decreased. Moreover, Bonneville flood deposits have been mapped along the Washington-Idaho State line near the junction of the Snake River and the Grande Ronde River (Hooper and others, 1985). According to Jarrett and Malde (1987), the discharge approached 1 million cubic meters per second and raised the height of the Snake River at least 130 m (425 ft) in constricted parts of the canyon. The high discharge probably contributed to the formation of some large landslides in the canyon, such as the one mapped south of Hells Canyon Dam at Big Bar (Vallier and Miller, 1974).

The rugged morphology of the Seven Devils Mountains and adjacent Hells Canyon of the Snake River is mostly the result of displacement along basin-and-range-type faults during the past 5 to 6 million years and intensive glacial and stream erosion during the Pleistocene Epoch. If uplift continues to outpace denudation, then the relief will increase in the future.

REFERENCES CITED

Alpha, T.R., and Austin, W.A., 1982, Physiographic diagram of the Seven Devils Mountains and Hells Canyon, Idaho and Oregon: U.S. Geological Survey Open-File Report 82-894, 1 sheet.

Alpha, T.R., Detterman, J.S., and Morely, J.M., 1988, Atlas of oblique maps: A collection of landform portrayals of selected areas of the world: U.S. Geological Survey Miscellaneous Investigations Series I-1799, 137 p.

Ashworth, William, 1977, Hells Canyon, the deepest gorge on Earth: New York, Hawthorn Books, 246 p.

Avé Lallemant, H.G., in press, Pre-Cretaceous tectonic evolution of the Blue Mountains province, northeastern Oregon, *in* Vallier, T.L., and Brooks, H.C., eds., Geology of the Blue Mountains region of Oregon, Idaho, and Washington: Petrology and Tectonic evolution of pre-Tertiary rocks of the Blue Mountains region: U.S. Geological Survey Professional Paper 1438.

Baldwin, E.M., 1976, Geology of Oregon: Dubuque, Iowa, Kendall-fflunt Publishing Co., 170 p.

Fenneman, N.M., 1931, Physiography of Western United States: New York, McGraw-Hill, 534 p.

Hooper, P.R., Webster, G.D., and Camp, V.E., 1985, Geologic map of the Clarkston 15-minute quadrangle, Washington and Idaho: State of Washington Department of Natural Resources, Geologic Map GM-31.

Hunt, C.B., 1974, Natural regions of the United States and Canada: San Francisco, W.H. Freeman, 725 p.

Jarrett, R.D., and Malde, H.E., 1987, Paleodischarge of the late Pleistocene Bonneville flood, Snake River, Idaho, computed from new evidence: Geological Society of America Bulletin, v. 99, no. 1, p. 127–134.

Livingston, D.C., 1928, Certain topographic features of northeastern Oregon and their relation to faulting: Journal of Geology, v. 36, no. 8, p. 694–708.

Livingston, D.C., and Laney, F.B., 1920, The copper deposits of the Seven Devils and adjacent districts (including Heath, Hornet Creek, Hoodoo, and Deer Creek): Idaho Bureau of Mines and Geology Pamphlet 13, 24 p.

Malde, H.S., 1968, The catastrophic late Pleistocene Bonneville flood on the Snake River plain, Idaho: U.S. Geological Survey Professional Paper 596, 52 p.

Raisz, Erwin, 1945, The Olympic-Wallowa lineament: American Journal of Science, v. 243-A, p. 479–485.

Silberling, N.J., Jones, D.L., Blake, M.C., and Howell, D.G., 1984, Lithotectonic terrane map of the western conterminous United States, *in* Silberling, N.J., and Jones, D.L., eds., Lithotectonic terrane maps of the North American Cordillera: U.S. Geological Survey Open-File Report 84-523, 106 p.

Stearns, Harold, 1962, Evidence of lake Bonneville flood along Snake River below Kin Hill, Idaho: Geological Society of America Bulletin, v. 73, no. 3, p. 385–387.

Vallier, T.L., 1967, Geology of part of the Snake River canyon and adjacent areas in northeastern Oregon and western Idaho: Corvallis, Oregon State University, Ph.D. dissertation, 267 p.

———1974, Preliminary report on the geology of part of the Snake River canyon: Oregon Department of Geology and Mineral Industries Map GMS-6, 1 sheet, 28 p.

———1977, The Permian and Triassic Seven Devils Group, western Idaho and northeastern Oregon: U.S. Geological Survey Bulletin 1437, 58 p.

———in press, Petrology of pre-Tertiary igneous rocks in the Blue Mountains province of Oregon, Idaho, and Washington, *in* Vallier, T.L., and Brooks, H.C., eds., Geology of the Blue Mountains region of Oregon, Idaho, and Washington:

Petrology and tectonic evolution of pre-Tertiary rocks of the Blue Mountain region: U.S. Geological Survey Professional Paper 1438.

Vallier, T.L., and Miller, V.C., 1974, Landslides in the Snake River canyon along the Oregon and Idaho boundary: Indiana State University Department of Geography and Geology, Professional Paper 5, p. 3–22.

Wheeler, H.E., and Cook, E.F., 1954, Structural and stratigraphic significance of the Snake River capture, Idaho-Oregon: Journal of Geology, v. 62, no. 6, p. 525–536.

6. GEOLOGY OF THE PECK MOUNTAIN MASSIVE SULFIDE PROSPECT, ADAMS COUNTY, IDAHO

By JOEL R. MANGHAM[1]

CONTENTS

ABSTRACT

In the Peck Mountain area of western Idaho is a window in the Columbia River Basalt Group through which rocks of the northern Huntington arc terrane are exposed. These consist of submarine felsic volcanic rocks underlain and overlain by intermediate volcanic and volcaniclastic rocks and cut by quartz diorite and quartz monzonite intrusions. The exposures of felsic rocks show a complete cross section of a submarine volcano. A quartz porphyry exogenous dome is exposed in the center, and is surrounded by a thick sequence of tuff and lava. The sequence of extrusive rocks progresses upward from aphyric tuff to quartz crystal tuff to quartz keratophyre flows; this progression suggests these rocks were erupted at different times from a single, progressively crystallizing magma chamber.

Throughout the volcanic pile are numerous exhalative rocks including sulfides, oxides, sulfates, and silica. In the north end of the window, a substantial thickness of pyrite and other exhalative rocks lies above a strongly altered footwall and below a thick sequence of unaltered keratophyre lava. Although economic ore has not been found, the geologic setting is similar to that of Kuroko massive sulfide deposits.

Quartz diorite intrusions in the felsic pile were accompanied by their own small hydrothermal systems. These intrusions may have scavenged copper and molybdenum from the volcanic host rocks to form quartz+molybdenite+chalcopyrite veins, which cut across the intrusions as well as the volcanic rocks.

[1]Route 7, Box 215, Charlottesville, VA 22901

INTRODUCTION

The Peck Mountain Prospect covers a 10 km^2 area, located about 200 km northwest of Boise, Idaho, or approximately 20 km northwest of Council, Idaho, on the Council-Bear-Cuprum Road. Peck Mountain is in the center of the prospect and is a small, isolated mountain immediately northeast of Cuddy Mountain, and due south of Seven Devils Mountains. Slopes in the prospect area are moderate, and the maximum local relief is 400 m.

ACKNOWLEDGMENTS

The current knowledge of Peck Mountain geology results from the cumulative work of several individuals. Roney Long and Donald Hudson first recognized and mapped the volcanogenic massive sulfide relations. Peter Kirwin, Cyrus Field, Howard Brooks, and Tracy Vallier all provided helpful constructive reviews of the manuscript. Field also introduced me to the geology of the Huntington arc terrane and freely supplied me with data he had on Peck Mountain geology. Finally, I would like to extend my appreciation to Conoco, Inc., Asarco, and Chevron Resources Company for their permission to publish this paper.

PREVIOUS WORK

Although numerous pits and short adits attest to an earlier recognition of the prospect's economic potential, the Peck Mountain area was first described as mineralized by Livingston and Laney (1920) and later, in more detail, by Livingston (1923). Other than a mention by Cook (1954) in a review of the Seven Devils Mining District, Peck Mountain received little

attention until 1964 when it was examined and staked by geologists from Bear Creek Mining Company during a regional stream-sediment sampling and mapping program. Numerous additional companies and geologists have examined the prospect since its rediscovery by Bear Creek Mining Company. Wracher (1969) mapped the rock units of this area. Noranda Mining Company briefly held the property, as did Asarco. All of these investigations concluded that the cause of hydrothermal mineralization near Peck Mountain is a porphyry copper system. In 1977, however, Asarco geologists started to examine the area for synvolcanic mineralization. Conoco acquired the property in 1978, and began a thorough evaluation of the volcanic stratigraphy and volcanogenic mineralization. I was involved with the project as an employee of Conoco between 1980 and 1982. Investigations during this period included detailed mapping, geochemical and geophysical surveys, and drilling.

GEOLOGIC SETTING

The Peck Mountain Prospect is part of a group of pre-Tertiary rocks exposed through a window in basalt of the Miocene Columbia River Basalt Group (fig. 6.1). The dominant lithologies exposed through this window are felsic submarine volcanic rocks, associated sedimentary rocks, and younger quartz diorite and porphyritic quartz monzonite intrusions. The volcanic rocks are at the northern tip of a belt of calc-alkaline rocks termed the Huntington arc terrane by Brooks (1979). To the north and west are exposures of the Wallowa-Seven Devils arc terrane of Brooks (1979), which is very similar in lithology and age to the Huntington arc terrane but probably separated by a large-scale regional structure. These ancient volcanic terranes host four known volcanogenic sulfide deposits and numerous other syngenetic sulfide occurrences. The so-called Wallowa-Seven Devils arc hosts the Iron Dyke and Red Ledge deposits (Juhas and others, 1980; Juhas and Gallagher, 1980) in rocks described by Vallier (1974) as belonging to the Permian Hunsaker Creek Formation. The age of the Peck Mountain volcanogenic mineralization is uncertain. Correlation with rocks at the south end of the Huntington arc terrane (Brooks and others, 1976) suggests a Triassic age, yet the rocks are similar to the Permian Hunsaker Creek Formation. More recently, Fifarek and others (1983) determined a sulfur isotope value of + 17.3 0/00 for massive bedded barite at Peck Mountain; this value suggests Late Jurassic deposition.

The intrusive rocks are also regionally extensive and are part of a belt of Late Permian (Brooks, oral commun., 1981) to Jurassic quartz diorite and quartz monzonite intrusions (Field and others, 1974) extending from Peck Mountain south through Cuddy Mountain and Hitt Mountain. Some of these southern intrusions were identified as the loci of hydrothermal mineralizing systems (Henricksen, 1974).

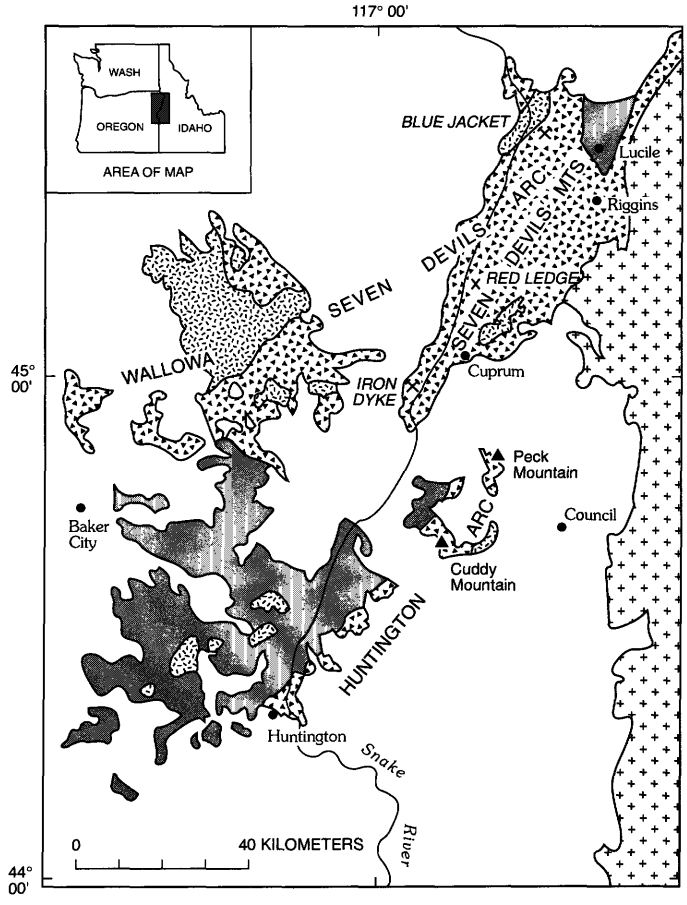

EXPLANATION

- Columbia River Basalt Group (Miocene)
- Idaho batholith (Cretaceous)
- Pluton (Mesozoic)
- Island-arc volcanic terrane (pre-Tertiary)
- Volcanic and sedimentary rock (pre-Tertiary)
- Contact
- Mine
- Prospect

FIGURE 6.1.—Regional geological map showing rock units of Peck Mountain and surrounding area, northeastern Oregon and western Idaho. Also shown are mines and prospects of the region. Modified from Brooks (1979).

GEOLOGY OF PRE-TERTIARY ROCKS AT PECK MOUNTAIN

VOLCANIC STRATIGRAPHY

The Peck Mountain area is underlain by an upright sequence of dominantly felsic volcanic and volcaniclastic rocks now homoclinally dipping between 45° and 88° northwest and striking northeast (fig. 6.2). Minor cross-faults strike northwest and offset units by as much as 100 m. As discussed below, the distinguishing features of these volcanic units are compositional or textural, and in most cases they are recognizable in hand samples. In the center of the felsic sequence, however, secondary mineralization and recrystallization are intense, and the distinguishing features are smaller and more subtle; therefore, they may need to be examined in thin section for positive identification. These subtle features include varying sizes and shapes of remnant quartz phenocrysts; remnant flattened pumice and flow foliation; or fine-grained, clastic groundmass of glass shards, quartz, and plagioclase.

The entire felsic sequence is underlain by green-gray intermediate volcanic and volcaniclastic rocks (not shown in fig. 6.2). These rocks generally lack quartz phenocrysts and differ from overlying rocks by being less siliceous and containing more sedimentary rocks. Although clearly part of a volcanic terrane, these rocks are interpreted as distal from any volcanic source.

Overlying the green intermediate volcanic rocks is a 1,200-m-thick tuffaceous unit that lacks phenocrysts. This aphyric tuff unit (unit at, fig. 6.2) extends along the entire length of the Peck Mountain window and is dominantly tuffaceous, as confirmed by the angular, broken nature of some of the smaller phenocrysts, remnants of flow foliation, and flattened pumice near the middle part and northern end of the window. Rocks in the extreme northern and southern ends of the window show evidence of reworking and sedimentary deposition, and they are probably a distal facies of the aphyric tuff. The outlying locations of this volcaniclastic part of the aphyric tuff suggest that the vent for this unit was nearer the middle part of the Peck Mountain window.

In the southern half of the window, the aphyric tuff is interlayered with discontinuous lenses of pyritic tuff (with 1–3 percent bedded pyrite), fine-grained green siltstone, quartz crystal tuff with local plagioclase phenocrysts, and a semimassive sulfide horizon composed of subequal amounts of pyrite and quartz+sericite groundmass.

A distinctive, 1- to 15-m-thick sulfide-bearing exhalative horizon overlies the aphyric tuff in the southern half of the window and may correlate with a massive sulfide horizon at the north end. This exhalative unit is divided into semimassive (< 50 percent sulfide) and massive (> 50 percent sulfide) facies (units ms and sms, fig. 6.2). The horizon can be further divided; both the extreme northern and southern exposures are magnetite-rich sulfides and silica, and the northern part also contains massive barite associated with massive pyrite. Other less continuous, disseminated sulfide horizons are present in both younger and older volcanic rocks; their presence suggests a long-lived hydrothermal system that coexisted with volcanism.

Overlying the main exhalative horizon is a 700-m-thick sequence of white quartz crystal tuff (unit qt, fig. 6.2) separated by a fault from possibly coeval gray keratophyre lava flows in the northern part of the prospect. The quartz crystal tuff has a matrix of quartz, clay, and sericite that is mineralogically similar to the underlying aphyric tuff except for the presence of quartz phenocrysts. In the center of the window, near Peck Mountain, are interbeds of coarse debris flows with sericitically altered tuff fragments in a detrital or, locally, a sulfide matrix. Fine-grained sediment is interbedded with the quartz crystal tuff in the southern end of the window. This facies change between coarse and fine sediment indicates a steep paleotopography near Peck Mountain and suggests that the vent for this unit was nearby.

The quartz crystal tuff has not been observed in outcrop or drill core at the northern end of the Peck Mountain window. In the same stratigraphic position is a 300-m-thick sequence of dark gray, fine-grained keratophyre (and minor quartz keratophyre) lava flows (unit k, fig. 6.2). The keratophyre is typically depleted in potassium and rich in sodium (table 6.1). This sequence overlies a 20- to 100-m-thick sequence of siliceous, exhalative, and tuffaceous rocks (unit ex, fig. 6.3), which in turn overlies the massive sulfide horizon. This dark keratophyre and exhalative sequence is separated from the quartz crystal tuff by a fault.

Overlying the quartz crystal tuff and dark keratophyre is a 500-m-thick extremely siliceous layer of tuff (unit st, fig. 6.3); it consists of 1 to 5 percent, 1 to 3 millimeter quartz phenocrysts in a white, quartz-rich quartz and sericite matrix. This unit locally contains as much as 10 percent pyrite. This siliceous tuff is interpreted to have been saturated with exhalative silica during or immediately after deposition.

The uppermost unit in the felsic sequence is a quartz keratophyre flow containing phenocrysts of quartz (5 percent) and albite (20 percent) and minor amounts of hornblende in a very fine grained matrix (unit qk, fig. 6.2). This unit extends from the northern end of the window, where it is locally brecciated, to a point about 700 m northwest of Peck Mountain,

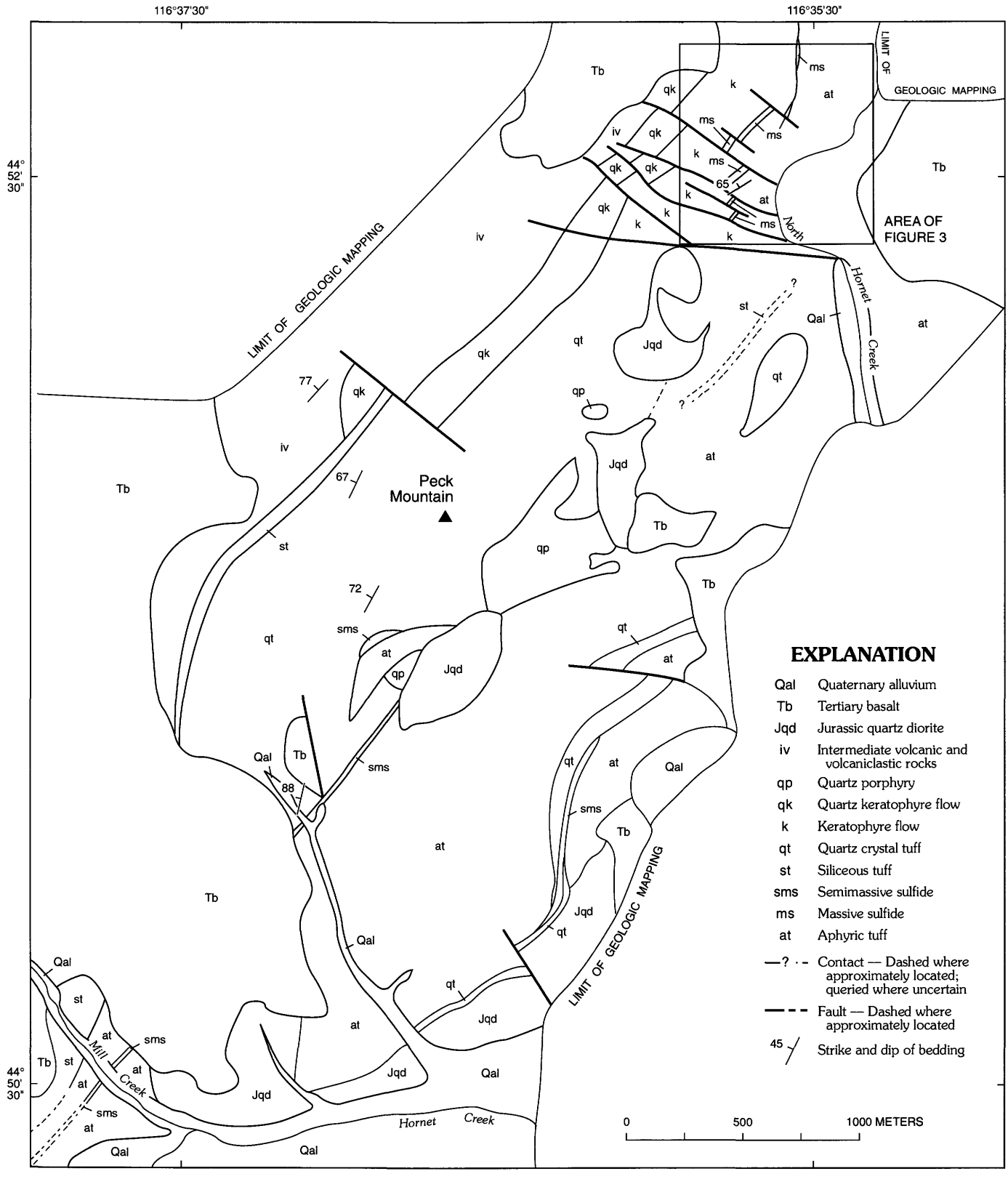

FIGURE 6.2.—Geologic map showing volcanic and volcaniclastic rocks of Peck Mountain area, western Idaho.

where it abruptly terminates. Although the flow is cut by faults at several locations along its strike, the termination does not appear to be faulted; thus it is interpreted as the depositional end of the flow.

Green to gray intermediate volcanic rocks and sedimentary rocks (unit iv, fig. 6.2) overlie the entire felsic sequence. The unit directly overlying the quartz keratophyre flow is a volcanic-pebble conglomerate.

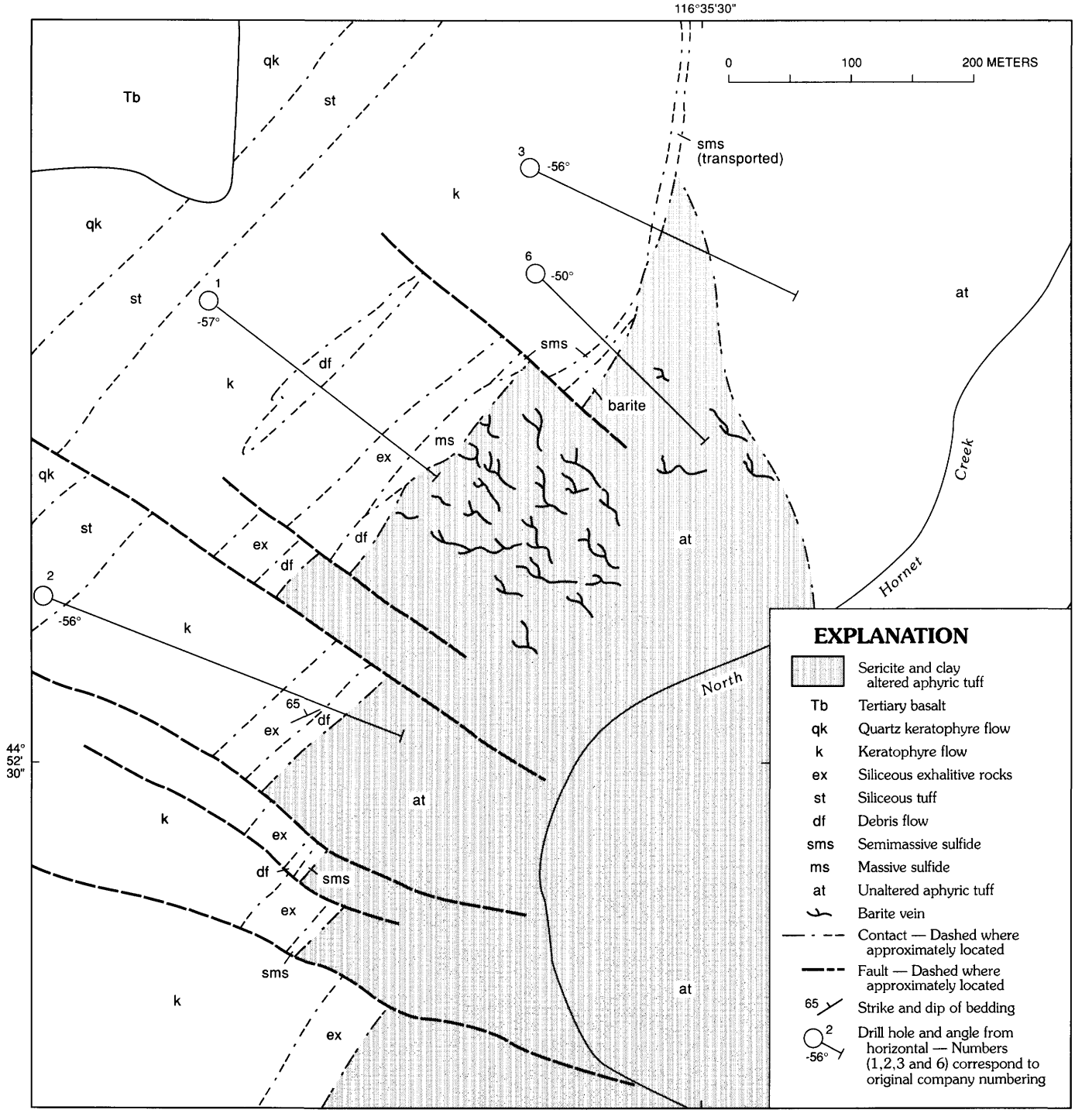

FIGURE 6.3.—Geologic map showing northern end of Peck Mountain window, western Idaho.

The thickness of these intermediate volcanic rocks is indeterminate because their uppermost part is covered by the Miocene Columbia River Basalt Group.

INTRUSIVE ROCKS

Located near the central area of the Peck Mountain window is an irregular quartz porphyry with 10 to 20 percent round, large (3- to 10-mm-diameter) quartz phenocrysts and 0 to 5 percent albite in a fine-grained, uniform quartz+sericite groundmass. This unit is interpreted to be an intrusion that occupies the vent for the felsic rocks of the window. It is probably an exogenous dome formed during deposition of the quartz crystal tuff.

The Peck Mountain volcanic sequence is intruded by stocks of fine-grained, equigranular quartz diorite. Drill holes and roadcuts show that the quartz diorite is more widespread than exposures would indicate because it easily weathers. The quartz diorite intrusions are aligned along a stratigraphic interval; their alignment suggests that the intrusions were emplaced while the country rocks were flat lying and that the depth of quartz diorite emplacement was controlled by lithostatic pressure.

Other intrusions of quartz diorite and porphyritic quartz monzonite occupy the stratigraphic basal part of the volcanic pile. These have not been mapped in detail, but they appear to be located along a constant stratigraphic level and thus, like the quartz diorite stocks, may have intruded prior to regional tilting.

The age of the Peck Mountain plutons remains uncertain. Field and others (1974) reported a K-Ar age from hornblende in the quartz diorite of 161±11 Ma. He cautions, however, that the age is anomalously young compared to similar rocks in the Huntington arc terrane and may have been affected by later metamorphism (Field, written commun., 1982).

METAMORPHISM

Contact metamorphism related to the intrusions of quartz diorite and quartz monzonite formed lithic assemblages dominated by hornblende-hornfels facies rocks. Later, regional metamorphism superimposed greenschist-facies metamorphism on the Peck Mountain rocks. The dominant assemblage consists of

muscovite+biotite+plagioclase±andalusite

formed during the initial intrusive period. It has been superimposed by

muscovite+epidote+chlorite

formed during later regional metamorphism. Excess SiO_2 is present as quartz throughout the entire felsic sequence.

ALTERATION

Hydrothermal alteration in the Peck Mountain area appears to have strongly affected only the felsic tuffaceous rocks and the quartz porphyry. Possible propyllitic alteration of the intermediate volcanic rocks and the felsic lava flows is indistinguishable from greenschist metamorphism. The quartz diorite intrusions are strongly altered only along vein selvages. The identification of altered felsic rocks is hindered by the similarity of quartz-sericite alteration to the metamorphic assemblages in these rocks. Because of these mineralogical similarities, alteration appears to be much more widespread than it is.

A distinct zone of hydrothermal alteration is present in the footwall rocks of the massive sulfide deposit in the northern end of the window. Mapping and sampling there has defined a zone of quartz, sericite, clay, pyrite, and barite alteration crisscrossed by abundant veins of barite. This intensely altered rock grades into less altered rock laterally and downsection (eastward), but alteration increases in intensity up-section (westward), toward the massive sulfide horizon. Above this horizon lies the exhalative horizon, which is moderately altered. Quartz-sericite alteration terminates abruptly at the contact between the exhalative horizon and overlying keratophyre.

Results from whole-rock analyses (table 6.1) indicate that the footwall alteration is zoned; that is, the central part is enriched in iron and potassium and depleted in calcium, sodium, and magnesium. The abrupt termination of the quartz-sericite alteration against overlying rocks, the presence of exhalative mineralization at and near this contact, and the apparent zoning of iron, calcium, sodium, and potassium are similar to features reported in Kuroko massive sulfide feeder zones (Lambert and Sato, 1974) and suggest that the alteration at Peck Mountain is also associated with a feeder zone. It should be noted, however, that the widespread barite, the depletion of magnesium, and the lack of (as yet undiscovered?) abundant copper veins in the altered zone is unusual and unlike most Kuroko deposits.

Examination of one particular quartz diorite intrusion showed a weak quartz-sericite alteration halo surrounding the intrusion. This alteration and the presence of mineralized veins (with quartz-sericite selvages), which crosscut several quartz diorite

TABLE 6.1.—*Major-oxide content (in weight percent) of representative samples of rock units at Peck Mountain prospect, Idaho*

[--, analyses not performed. *, reported as H_2O. LOI, loss on ignition]

Oxide	A	B	C	D	E	F
SiO_2	82.1	68.1	67.9	60.0	60.03	68.19
Al_2O_3	7.07	10.8	11.44	15.8	18.19	18.14
Fe_2O_3	4.28	11.7	9.10	10.8	2.22	2.52
FeO	--	--	--	--	--	.32
CaO	.07	.14	.47	4.00	6.61	.54
MgO	.14	1.47	3.11	1.31	2.37	.95
K_2O	1.81	2.29	2.48	.84	1.59	2.78
Na_2O	.31	.42	.66	4.91	4.21	3.35
MnO	.003	.072	.17	.16	.28	.02
P_2O_5	.017	.020	.019	.037	.18	.03
TiO_2	.165	.235	.35	.75	.48	.31
LOI	1.84	4.60	4.07	1.77	1.15*	3.22*
Total ---	97.80	99.84	99.77	100.38	97.31	100.37

A—Composite of 4 samples of weathered quartz-sericite altered aphyric tuff, from the surface, directly below massive sulfide horizon, and above drill hole 1.

B—Composite of 2 samples of quartz-sericite altered aphyric tuff from immediately below massive sulfide in drill hole 1 (proximal footwall alteration).

C—Composite of 4 samples of quartz-sericite altered aphyric tuff from below massive sulfide horizon, in drill holes 2, and 3 (distal footwall alteration).

D—Single sample of unaltered dark-gray keratophyre from drill hole 1, above the massive sulfide and other exhalative horizons.

E—Unaltered quartz diorite from the southern part of the Peck Mountain area (data from Wracher, 1969).

F—Quartz-sericite altered quartz diorite from the southern part of the Peck Mountain (data from Wracher, 1969).

stocks, indicate that these intrusions were accompanied by hydrothermal cells that resulted in alteration assemblages being superimposed on earlier volcanogenic alteration.

MINERALIZATION

Sulfide mineralization at Peck Mountain took place in two distinct periods—an early period of synvolcanic mineralization and a later period associated with the quartz diorite intrusions. Products of synvolcanic mineralization are present in numerous locations at the prospect as bedded or disseminated sulfide (mostly pyrite), pyrite clasts, and local sulfide-cemented debris flow deposits. The largest concentration of sulfide is present in the northern part of the window (fig. 6.3) and has been the target of several exploratory drill holes. There, the mineralized horizon is zoned both perpendicular and parallel to bedding. A longitudinal section in the plane of the drill holes is a cross section of the stratigraphy, and shows the mineral zonation (fig. 6.4). Perpendicular to bedding, in drill hole 1 (nearest the center of the massive sulfide), the mineralized horizon has a 17-m-thick massive sulfide body at its base; it consists of 95 percent pyrite, 5 percent barite, and minor amounts of sericite and chalcopyrite. The pyrite is weakly mineralized; it contains 1,600 ppm copper, 20 ppm lead, 100 ppm zinc, 7 ppm molybdenum, 3 ppm gold, 3 ppm silver, and 1.2 percent barium. Stratigraphically above the massive sulfide is approximately 65 m of siliceous exhalative rocks including siliceous tuff, debris flow deposits, and dolomitic rocks, all altered (most to quartz and sericite) and mineralized. Barium, copper, molybdenum, silver, and gold values are all less than in the underlying sulfide. Average values are approximately, 500 ppm barium, 200 ppm copper, 2 ppm molybdenum, 1 ppm silver, and trace amounts of gold. Lead and zinc values are higher—a

lead value of approximately 20 ppm was measured at the base of the siliceous exhalative rocks in drill hole 1. Also in drill hole 1, about 30 m stratigraphically up-section from the base of the exhalative rocks, a zinc value of 2,700 ppm was measured. The overlying keratophyre flow is unmineralized.

The siliceous exhalative rocks and the underlying massive sulfide thin parallel to bedding, toward the north, to less than 10 m in thickness within 250 m of drill hole 1. At this distal location, oxide and sulfate minerals (mostly magnetite and massive barite) are more abundant. Much of the horizon there appears to have been transported, as suggested by the broken and rounded clasts of tuff in an exhalative matrix. This disruption may also account for a lack of zoning perpendicular to bedding at this locality.

The thickness of the siliceous exhalative rocks and the tuffaceous debris flow deposits increases south of the center of the massive sulfide horizon. Outcrops and drill information are not conclusive but suggest that the massive sulfide pinches out against a southward-thickening wedge of debris flow material.

A longitudinal section through the drill holes, in the plane of the massive sulfide horizon (fig. 6.5)

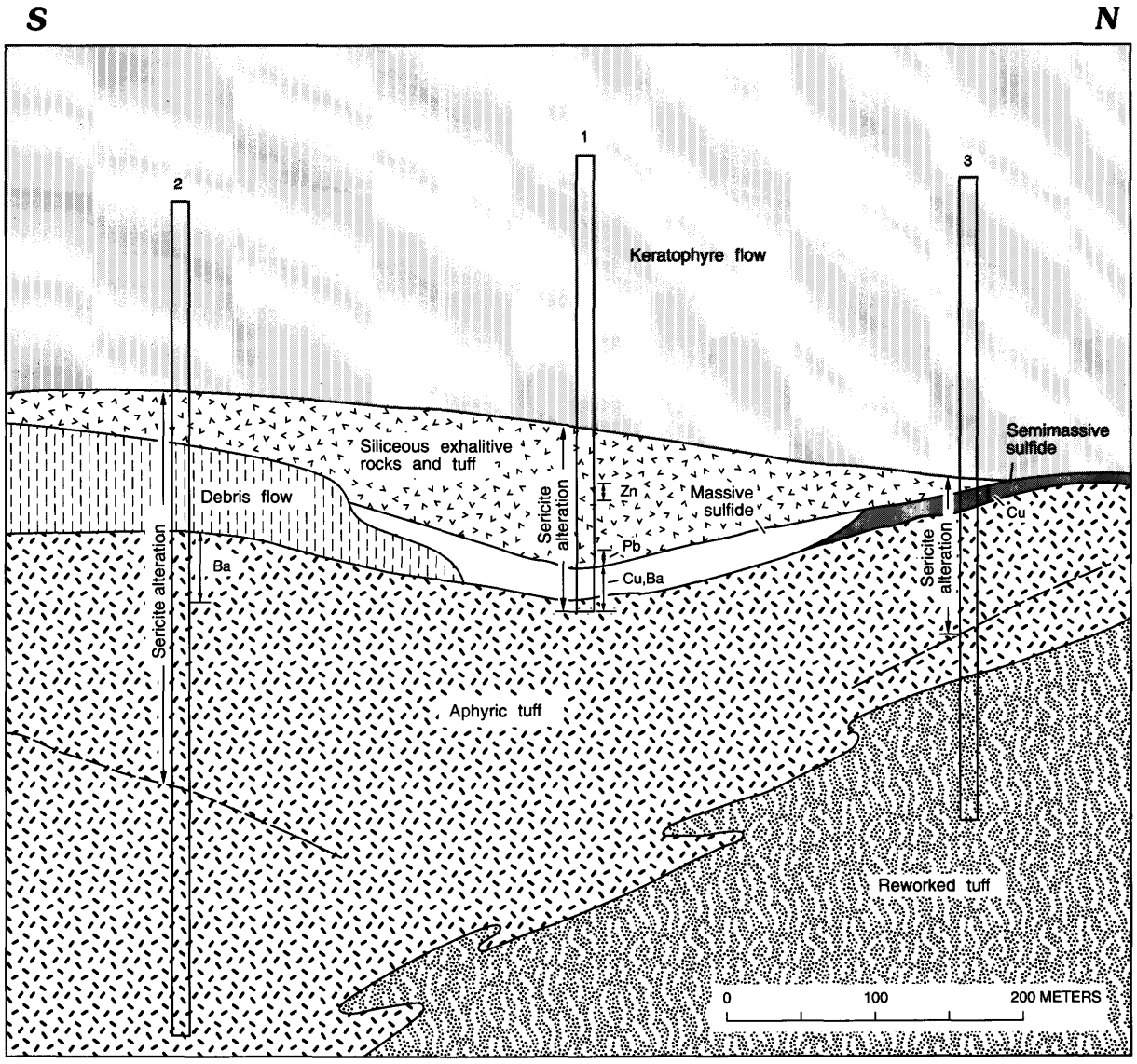

FIGURE 6.4.—Longitudinal cross section showing stratigraphy and mineral zonation in plane of drill holes 1–3 (fault restored), northern part of Peck Mountain, western Idaho. Element symbols represent locations of anomalous concentrations of the named elements. Vertical lines represent fault traces with displacement restored. Scale corresponds to depth and distance.

shows the different rock types present on the sea floor at the time of massive sulfide mineralization. The massive pyrite is in a basin, bounded to the southwest by a lahar deposit and to the northeast by a topographic basin edge. The massive barite appears to be a distal facies of the massive pyrite. Cutting through the massive barite and pyrite is a sulfide-bearing lahar deposit, which presumably flowed from an unknown sulfide-rich topographic high.

Associated with the quartz diorite intrusions are planar veins of quartz+pyrite+chalcopyrite±molybdenite with selvages of quartz and sericite. These mineralized veins cross volcanic rocks as well as the intrusions.

Soil samples were collected in a grid pattern over the entire prospect and analyzed for copper, zinc, molybdenum, and barium. The results were plotted on maps and contoured (figs. 6.6*A–D*). Molybdenum is anomalous over the quartz diorite intrusions and also at the massive sulfide at the north end of the window (fig. 6.6*A*). Copper has similar trends, although they are not as well defined (fig. 6.6*B*). Both zinc (fig. 6.6*C*) and barium (fig. 6.6*D*) are anomalous over the massive sulfide, but they are not anomalous elsewhere in the window. The distribution of these elements implies that they were concentrated during volcanogenic mineralization and the copper and molybdenum were scavenged during the intrusion of the quartz diorite bodies. The scavenged elements were concentrated and redeposited as part of the hydrothermal cells generated by the intrusive activity.

CONCLUSIONS

The felsic rocks exposed in the Peck Mountain window represent a cross section of a felsic submarine volcano. The volcanic sequence, from aphyric tuff to quartz crystal tuff through quartz keratophyre lava flow, records successive eruptions from an evolving magma chamber. The quartz porphyry is a remnant of the exogenous dome that formed during eruption of the quartz crystal tuff. Most of the massive sulfide and associated silica, oxide, and sulfate formed after the eruption of the aphyric tuff and possibly prior to the eruption of the quartz crystal tuff. The dark keratophyre flows at the north end of the window probably erupted from a separate volcanic vent. The locally great thicknesses and limited extent of the exhalative rocks-sulfide horizon suggest that these lithologies formed in a small basin.

The abundance of felsic tuff and the widespread, low-grade ore minerals present throughout the window indicates that Peck Mountain was the loci of violent phreatic eruptions during much of its mineralization history. The large volume of rock erupted during this period may have diluted the ore-bearing fluids and therefore inhibited the deposition of high concentrations of ore minerals. Also, the implied phreatic volcanism and the evidence of primary oxide and sulfate sea-floor mineralization suggest that the volcanism at Peck Mountain took place within a shallow sea.

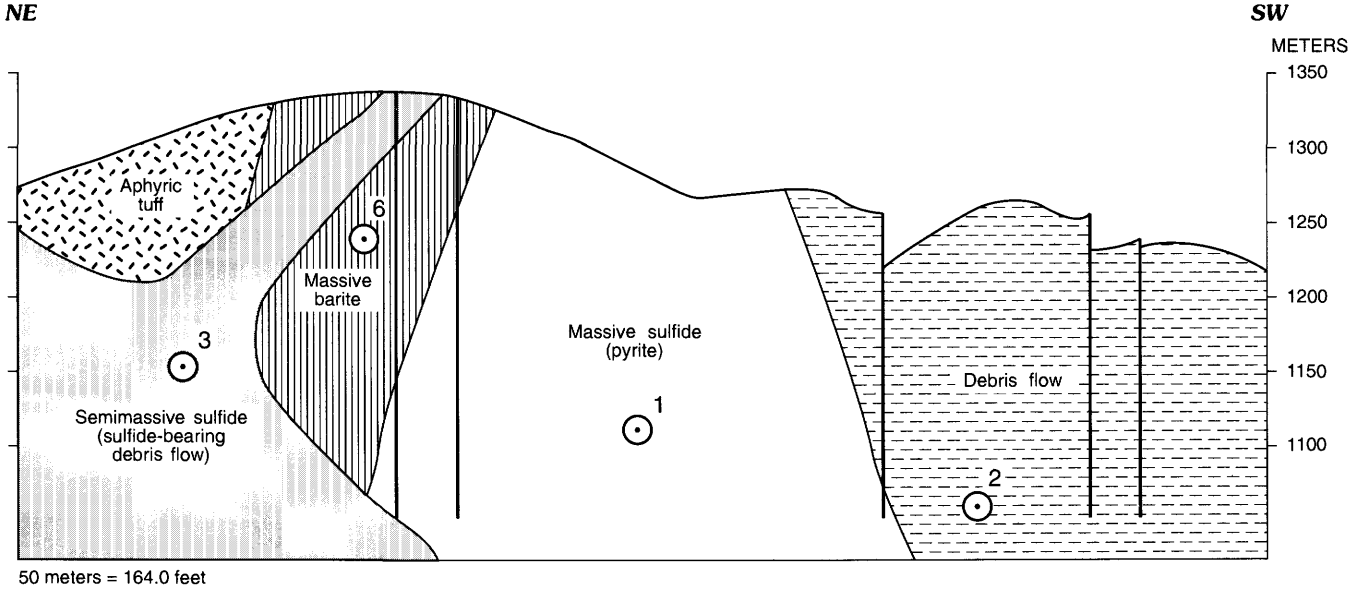

FIGURE 6.5.—Longitudinal cross section in the plane of the massive sulfide horizon (fault restored), northern part of Peck Mountain, western Idaho. Circles represent intersections of drill holes with the plane of the cross section. See figure 6.3 for location of drill holes.

The Peck Mountain deposit is similar to the deposits of the Japanese Kuroko district except for the apparent depletion of magnesium in footwall rocks and the apparent lack of economic ore. This lack of ore may simply be a function of a low exploration drilling density, however, and ore may yet be discovered at the prospect.

REFERENCES CITED

Brooks, H.C., McIntyre, J.R., and Walker, G.W., 1976, Geology of the Oregon part of the Baker 1° by 2° Quadrangle: Oregon Department of Geology and Mineral Industries Geologic Map Series GMS-7, scale 1:250,000.

Brooks, H.C., 1979, Plate tectonics and the geologic history of the Blue Mountains: Oregon Geology, v. 41, no. 5, p. 70–79.

Cook, E.F., 1954, Mining geology of the Seven Devils region: Idaho Bureau of Mines and Geology, Pamphlet 97, 22 p.

Field, C.W., Jones, M.B., and Bruce, W.R., 1974, Porphyry copper molybdenum deposits of the Pacific Northwest: Society of Mining Engineers of the American Institute of Mining Engineers, Transactions v. 255, p. 9–22.

Fifarek, R.H., Rye, R.O., and Field, C.W., 1983, Sulfur isotope geochemistry of the Red Ledge and other massive sulfide deposits of the Northwest [abs.]: Geological Society of America Abstracts with Programs, v. 15, no. 5, p. 372.

Henricksen, T.A., 1974, The geology and mineral deposits of the Mineral-Iron Mountain District, western Idaho: Corvallis, Oregon State University, Ph.D. dissertation.

Juhas, A.P., and Gallagher, T.P., 1980, Kuroko type mineralization at the Red Ledge deposit, Idaho: U.S. Geological Survey Open-File Report 81-355, 12 p.

Juhas, A.P., Freeman, P.S., and Fredericksen, R.S., 1980, Kuroko type copper-gold mineralization at the Iron Dyke Mine, Oregon: U.S. Geological Survey Open-File Report 81-355, 9 p.

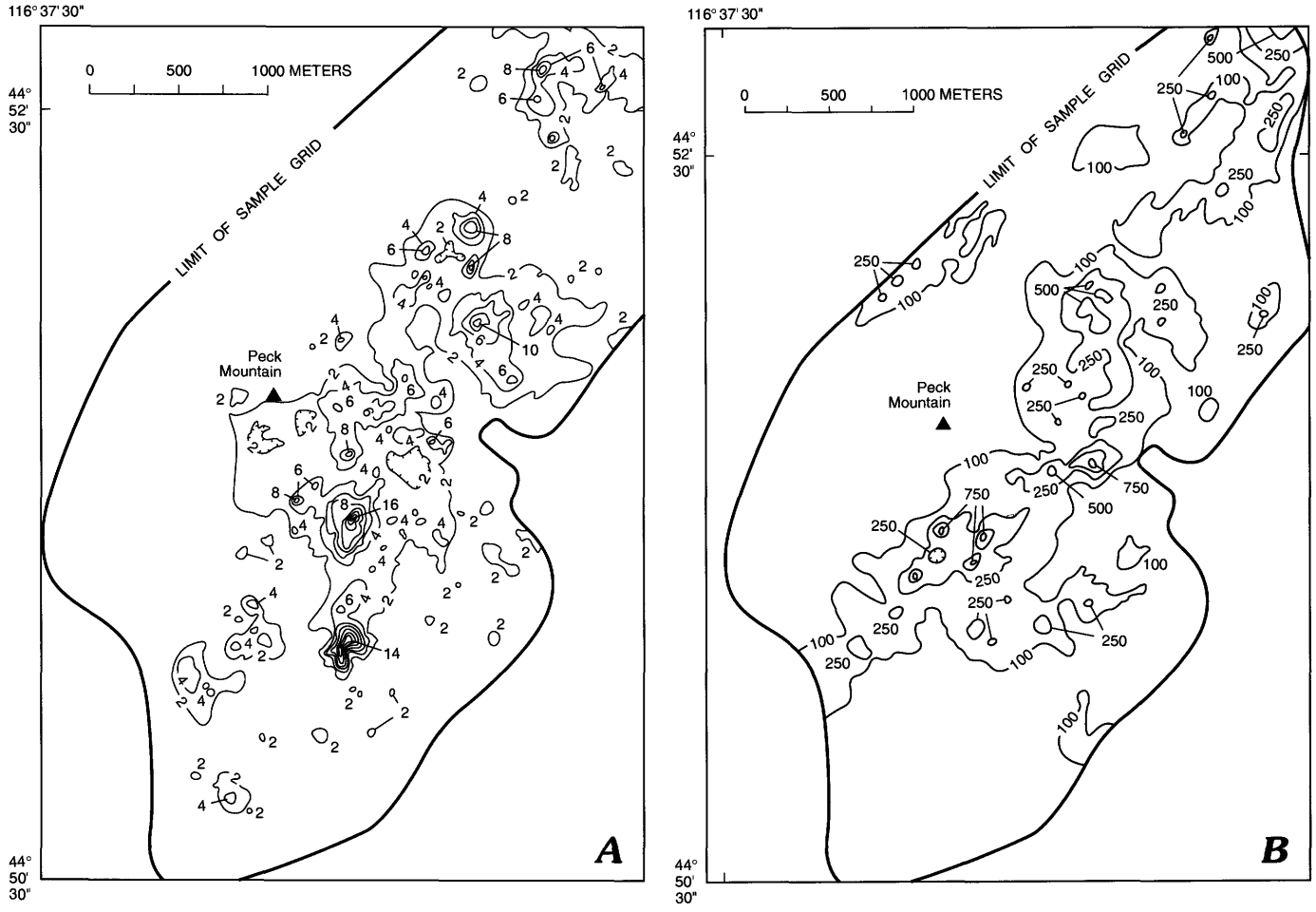

FIGURE 6.6.—Soil geochemistry at Peck Mountain, western Idaho. Maps cover same area shown in figure 6.2. Areas enclosed by hachured lines have element concentrations less than the contour value. *A*, Molybdenum concentration in parts per million. Contour interval, 2 ppm. *B*, Copper concentration in parts per million. Contour interval, 250 ppm. Extra contour at 100 ppm. *C*, Zinc concentration in parts per million. Contour interval, 100 ppm. *D*, Barium concentration in ppm. Contour interval, 100 ppm for values from 0 to 500 ppm. For values above 500 ppm, contour interval is 500 ppm. Note that soil sample grid for barium is smaller than that for other elements.

Lambert, I.B. and Sato, T., 1974, The Kuroko and associated ore deposits of Japan: A review of their features and metallogenesis: Economic Geology v. 69, p. 1215–1236.

Livingston, D.C. and Laney, F.B., 1920, The copper deposits of the Seven Devils and adjacent districts (including Heath, Hornet Creek, Hoodoo, and Deer Creek): Moscow, Idaho Bureau of Mines and Geology, Bulletin 1, 105 p.

Livingston, D.C., 1923, A geological reconnaissance of the Mineral and Cuddy Mountain Mining District, Washington and Adams Counties, Idaho: Moscow, Idaho Bureau of Mines and Geology, Pamphlet 13, 24 p.

Vallier, T.L., 1974, A preliminary report on the geology of part of the Snake River Canyon, Oregon and Idaho: Oregon Department of Geology and Mineral Industries Geologic Map Series GMS-6, 28 p.

Vallier, T.L., 1977, The Permian and Triassic Seven Devils Group, western Idaho and northeastern Oregon: U.S. Geological Survey Bulletin 1437, 58 p.

Wracher, D.A., 1969, The geology and mineralization of the Peck Mountain area, Hornet Quadrangle, Idaho: Corvallis, Oregon State University, M.S. thesis.

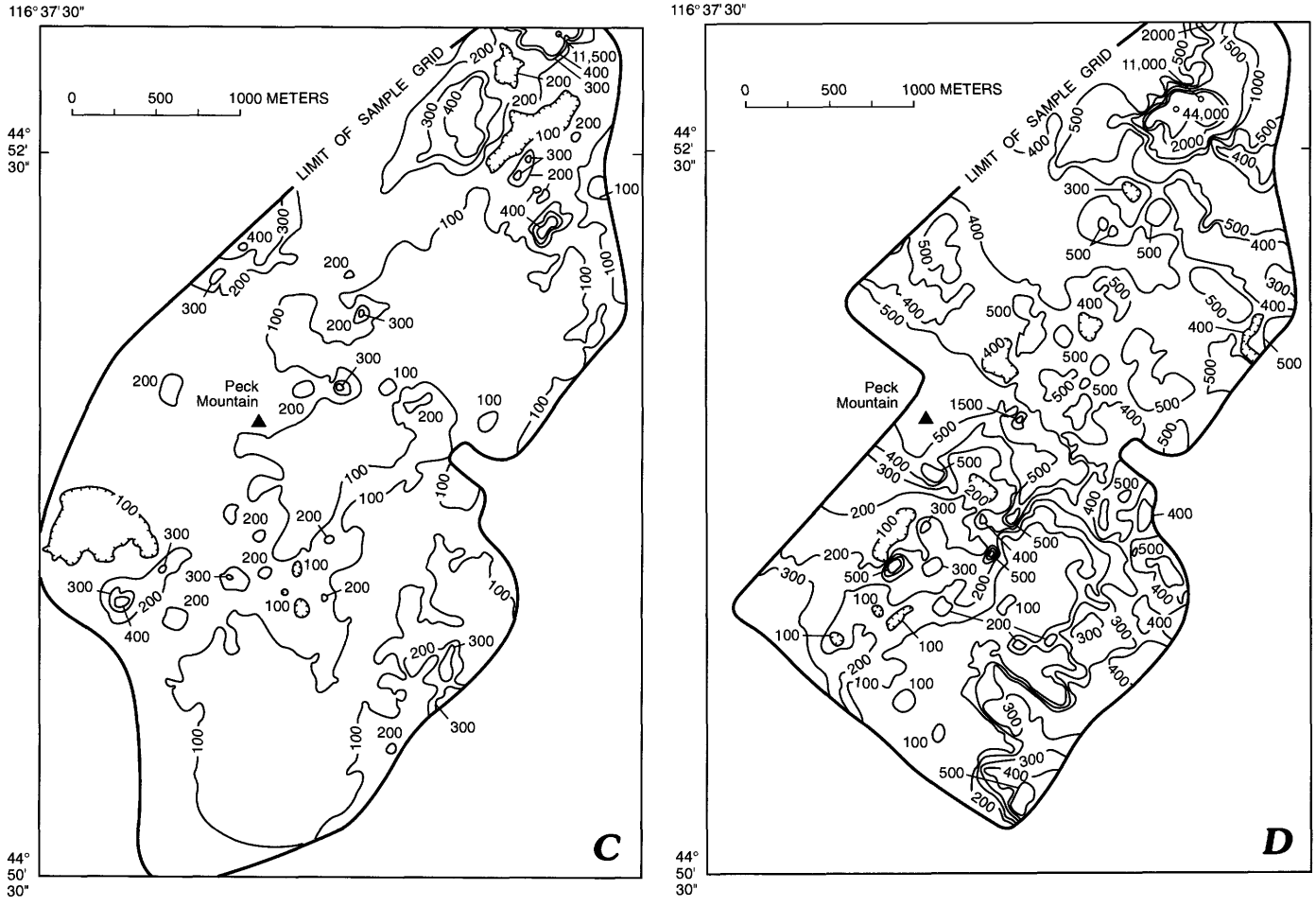

FIGURE 6.6.—Continued

7. GEOLOGY, MINERALIZATION, AND ALTERATION OF THE RED LEDGE VOLCANOGENIC MASSIVE SULFIDE DEPOSIT, WESTERN IDAHO

By RICHARD H. FIFAREK[1], ALLAN P. JUHAS[2], and CYRUS W. FIELD[3]

CONTENTS

ABSTRACT

The Red Ledge Zn-Cu-Ag prospect is a large volcanogenic exhalative deposit of island arc affinity and Early Permian age. It is hosted by basaltic and dacitic volcanic, volcaniclastic, and derivative epiclastic rocks that are correlative with the Hunsaker Creek Formation of the Seven Devils Group (Wallowa terrane). The deposit is genetically related to the Red Ledge rhyolite unit, a rhyodacite dome complex, and consists of three to four stacked sets of strata-bound stringer and stratiform massive sulfides that overlie a discordant zone of stockwork sulfides. Bodies of stringer sulfides are characterized by stringers and blebs of quartz-pyrite-barite-chalcopyrite-sphalerite that infill and partially replace beds of felsic breccia produced through the explosive disintegration of the dome. These mineralized breccias are overlain or flanked by layers of massive sulfide that typically grade from granular pyrite-quartz-chalcopyrite to laminated sphalerite-pyrite-barite±galena with increasing distance from the underlying stockwork zone. Thin units of hematite-barite exhalite, chloritic tuffaceous exhalite, and altered lava flows and sandstones interfinger with the mineralized felsic breccias. Stringer sulfide bodies total approximately 33 million metric tons and average 0.6 percent Zn, 0.3 percent Cu, 21.7 grams per metric ton (g/t) Ag, and 0.47 g/t Au, whereas the massive sulfide bodies total about 6 million metric tons and average 2.9 percent Zn, 0.9 percent Cu, 80.8 g/t Ag, and 0.9 g/t Au.

The underlying stockwork system crosscuts a >370-m section of volcaniclastic rocks adjacent to the dome and is comprised of three to four planar zones of veins that branch and expand upward to ultimately grade into stringer mineralization. Vein filling progressed from an early amethyst stage, through quartz-pyrite-chalcopyrite and barite±chalcopyrite±sphalerite stages, to a late carbonate±sulfide stage. The stockworks contain about 27 million metric tons of rock averaging 0.1 to 0.5 percent Zn, 0.3 percent Cu, 3.1 to 9.3 g/t Ag, and 0.31 g/t Au. Overall, the deposit is zoned from a Cu-rich core to a Zn-, Ag-, and Ba-enriched top and periphery.

Prograde alteration of host rocks resulted in a telescoped pattern of assemblages that grade upward and outward from a silicic zone proximal to the deposit, through sericite and sericite-chlorite zones, to a propylitic halo. If these zones advanced simultaneously outward from fluid conduits, then alteration proceeded in stages. Initial propylitization (of rhyodacite) involved an enrichment in MgO, CaO, H_2O^+, and CO_2, a depletion of K_2O and Na_2O, and the formation of minor chlorite, carbonate, and sericite. Subsequent overprinting by the sericite-chlorite assemblage produced gains in K_2O and H_2O^+, a loss and then a gain in SiO_2 accompanied by the antithetic behavior of MgO, and the nearly complete loss of CaO, Na_2O, and CO_2 during the total destruction of plagioclase feldspar and carbonate. Final sericitic and silicic alteration involved gains in SiO_2 and total Fe, a gain and then a loss of K_2O, and a loss of MgO, accompanying pyritization, sericitization, and late intense silicification. During all stages of alteration, TiO_2, Al_2O_3, and Zr were highly immobile.

Mineralization was part of a repeated sequence of magma intrusion, fault movement, phreatic and phreatomagmatic eruptions, and sulfide deposition. The hydrothermal fluids consisted of seawater that had chemically evolved during convection through and reaction with volcanic-arc rocks. Thus, components enriched in the deposit were either leached from the country rocks (for example, base metals, K, Fe, and Ba) or derived from seawater (for example, Mg, S, and CO_2).

Overall, the character and proposed origin of the Red Ledge deposit closely resemble those of the unmetamorphosed Kuroko (Japan) deposits of Tertiary age. However, the relatively large and well-developed stockwork system, abundance of stringer sulfides, and unusual size of the Red Ledge deposit are related to the large

[1] Department of Geology, Southern Illinois University, Carbondale, IL 62901.

[2] 4221 S. Yukon Way, Lakeside, CO 80235.

[3] Department of Geosciences, Oregon State University, Corvallis, OR 97331.

size of the associated dome complex and the cyclic deposition of sulfides following explosive volcanism. Accordingly, this deposit represents an important variant for exploration models of volcanogenic exhalative mineralization.

INTRODUCTION

Historically, many sulfide-rich prospects in the western Cordillera were regarded as magmatic hydrothermal deposits that formed after regional metamorphism and through the replacement of rocks along shear zones (schistose units) and fractures (see Livingston and Laney, 1920; Shenon, 1933; Kinkel and others, 1956). However, wide acceptance of the submarine exhalative theory of ore genesis during the 1960's and 1970's prompted a reevaluation of these occurrences. Consequently, many deposits, including the Red Ledge prospect, were reclassified and explored as volcanogenic massive sulfide deposits. According to this more recent theory, the strata-bound stringers and stratiform massive lenses of base-metal sulfides that characterize volcanogenic massive sulfide deposits are regarded as having precipitated on or near the sea floor from hydrothermal fluids that evolved from seawater. Moreover, the inclined orientation, sinuous form, mineral textures, and schistose host rocks of many of these deposits are now recognized as having been largely produced by metamorphism and deformation of the sulfide bodies and their chloritized or sericitized host rocks.

Numerous scientific investigations during the 1970's and 1980's have provided information on the geology and origin of specific volcanogenic massive sulfide deposits or districts in the western Cordillera (see Thompson and Panteleyev, 1976; Payne and others, 1980; Koski, 1981; Cramer, 1982; Derkey, 1982; Gronewold, 1983; Sorensen, 1983; Nold, 1983; Urabe and others, 1983; Høy and others, 1984; Reed, 1984; Skinner, 1985; Hitzman and others, 1986; Juras, 1987; Kuhns and Baitis, 1987; Wood, 1987; Eastoe and Nelson, 1988; Zierenberg and others, 1988; Gustin, 1990). However, several important features of these deposits and their formation require further elucidation: (1) the relationship of hydrothermal activity to specific tectonic and (or) magmatic events; (2) the distinctions and transitions between massive, strata-bound stringer, and stockwork (feeder) mineralization; (3) the principal mechanisms governing mineral deposition on and below the sea floor; (4) the factors that control size and grade of mineralization; and (5) the quantitative transfer of chemical components as a result of hydrothermal alteration.

The purpose of this investigation is to address these and other related questions through an integrated study of the geology and geochemistry of the Red Ledge prospect. This prospect is an unusually large Kuroko-like volcanogenic massive sulfide deposit that consists of strata-bound stringer, stratiform massive, and stockwork styles of mineralization (Juhas and Gallagher, 1981). The mineral assemblage for each of the three styles includes quartz, barite, and sulfides, whereas carbonate is found only in the stockwork type. Folding has rotated the deposit approximately 90° about a horizontal axis such that a complete cross section of the hydrothermal system is accessible through surface exposures and diamond drill cores. The fortuitous combination of mineralization types, mineral distributions, and accessibility facilitated the characterization of the fluids prior to venting and the geochemical effects associated with the mixing of seawater and hydrothermal fluids during venting. This chapter concerns the geologic setting, mineralization styles, alteration mineralogy and geochemistry, and genesis of the Red Ledge deposit. Results provided by this research, and by associated fluid-inclusion and stable-isotope studies (not reported herein), will enhance the understanding of volcanogenic massive sulfide deposits in the western Cordillera, allow for more specific comparisons with modern and ancient analogues elsewhere in the world, and aid in the refinement of exploration models.

ACKNOWLEDGMENTS

This study is based on part of the dissertation research of R.H. Fifarek. He gratefully acknowledges the encouragement and assistance he received from the coauthors of this chapter, C.W. Field and A.P. Juhas, and from R.G. Senechal, R.C. Long, T.L. Vallier, and K.J. Fifarek. Texasgulf Incorporated (former owners of the Red Ledge property) kindly allowed access to the property, drill core, and proprietary data. Financial support for the research was provided by Texasgulf Inc., the ASARCO Foundation, and U.S. Geological Survey. The authors thank M.A. Vice for her drafting services and H.C. Brooks, M.L. Ferns, T.L. Vallier, A.C. Eddy, and C. Donlin for their thorough and helpful reviews of previous versions of the manuscript.

GEOLOGY OF BLUE MOUNTAINS PROVINCE

The Red Ledge deposit is situated in one of numerous erosional inliers of Paleozoic and Mesozoic rocks that are present in the Blue Mountains geomorphic province of northeastern Oregon and western Idaho

(fig. 7.1). The pre-Tertiary rocks are exposed through an extensive cover of Cenozoic continental sedimentary and volcanic rocks along a northeast-trending belt of uplifts and incised rivers. To the east they are in contact with the Cretaceous to Eocene Idaho batholith and Precambrian and Paleozoic rocks of the North American craton.

The pre-Tertiary rocks of the Blue Mountains province form a large allochthonous terrane of island arc affinity, the Blue Mountains island arc, that was accreted to North America by Early Cretaceous time (Vallier, in press). Fossil types and ages indicate that the arc complex formed at low latitudes in the Pacific Ocean during Devonian through Early Jurassic time (Newton, 1986; Pessagno and Blome, 1986). A similar location is suggested by the paleomagnetic pole positions of Triassic volcanic rocks (Hillhouse and others, 1982). Apparently, the island arc was at the same approximate latitude as its North American site of accretion by the Middle Triassic and both the arc and craton moved collectively northward during the Early and Middle Jurassic (Vallier, in press).

The Blue Mountains island arc is composed of several major tectonostratigraphic terranes (see Vallier and others, 1977; Brooks and Vallier, 1978; Dickinson and Thayer, 1978; Brooks, 1979; Pessagno and Blome, 1986). Those recognized by Silberling and others (1984) consist of the Grindstone, Izee, Olds Ferry, Baker, and Wallowa terranes (fig. 7.1). Each terrane is metamorphosed, bounded by major faults or unconformities, and intruded by plutonic rocks of mostly intermediate composition. They represent a collage of variably deformed oceanic crustal and supracrustal rocks (Baker and Grindstone terranes), volcanic-arc assemblages (Wallowa and Olds Ferry terranes), and a flyschlike succession (Izee terrane). The Red Ledge and other volcanogenic massive sulfide deposits in the region are hosted exclusively by volcanic-arc rocks of the Wallowa and Olds Ferry terranes (fig. 7.1).

Radiometric age determinations of plutons in the Blue Mountains province suggest three major episodes of emplacement: (1) late Paleozoic and Triassic (mostly Wallowa and Baker terranes); (2) Late Triassic and Early Jurassic(?) (mostly Olds Ferry terrane); and (3) Late Jurassic and Early Cretaceous (all terranes except Grindstone) (Walker, 1986; Walker, in press; Vallier, in press). The oldest episode is represented by small, commonly metamorphosed, tholeiitic plutons, whereas the youngest episode consists of large, unmetamorphosed, calc-alkaline intrusions such as the Wallowa and Bald Mountain batholiths. The Late Triassic and Early Jurassic(?) plutons are generally tholeiitic and have field and petrographic characteristics similar to those of both other groups.

The pre-Tertiary rocks of the Blue Mountains province clearly record the development of a volcanic arc on oceanic crust and the subsequent accretion of this arc complex to the North American continent. However, many aspects of the evolution of this province have yet to be resolved. For example, the structural development of the region and its relationship to the process and timing of accretion are not well understood (Avé Lallemant, in press). Furthermore, Jones and others (1977, 1978) suggested that the Wallowa terrane is part of the Wrangellia superterrane that is discontinuously exposed along the coastline of British Columbia and in southeastern Alaska. This proposed association implies that the other terranes of the Blue Mountains province represent fragments of at least one other island arc complex. By contrast, Pessagno and Blome (1986) concluded that the province is part of a single arc complex and that it is related to the Nevadan terrane. Regional interpretations such as these have important implications for those reconnaissance exploration programs that utilize time-stratigraphic concepts to evaluate volcanogenic massive sulfide occurrences in the western Cordillera.

HELLS CANYON INLIER

The Red Ledge deposit is hosted by volcanic arc rocks in the Hells Canyon inlier of the Wallowa terrane. This assemblage is well exposed in Hells Canyon where a section 6,000 m thick has been divided into four formations that make up the Seven Devils Group (Vallier, 1977). The oldest units, the Windy Ridge Formation and Hunsaker Creek Formation, are Early Permian in age and consist of felsic volcanic and hypabyssal intrusive rocks and their epiclastic derivatives. The Windy Ridge Formation is dominated by lava flows and tuff and may represent a lithofacies of the lower Hunsaker Creek Formation, which is composed primarily of pyroclastic breccia, tuff, conglomerate, epiclastic breccia, sandstone, and siltstone (Vallier, in press). These units are overlain by the Wild Sheep Creek Formation and the Doyle Creek Formation, which are Middle and Late Triassic in age and principally composed of pyroclastic rocks, lava flows, hypabyssal intrusions, epiclastic rocks, and carbonate lenses. The Doyle Creek Formation was deposited in subaerial and shallow marine settings and is considered to be both a lithofacies equivalent and the overlying unit of the mostly marine Wild Sheep Creek Formation (Vallier, in press). Both formations contain rapid lithofacies changes, a small yet persistent component of plutonic debris, graded beds, pillow structures, and hematitic (oxidized) sections.

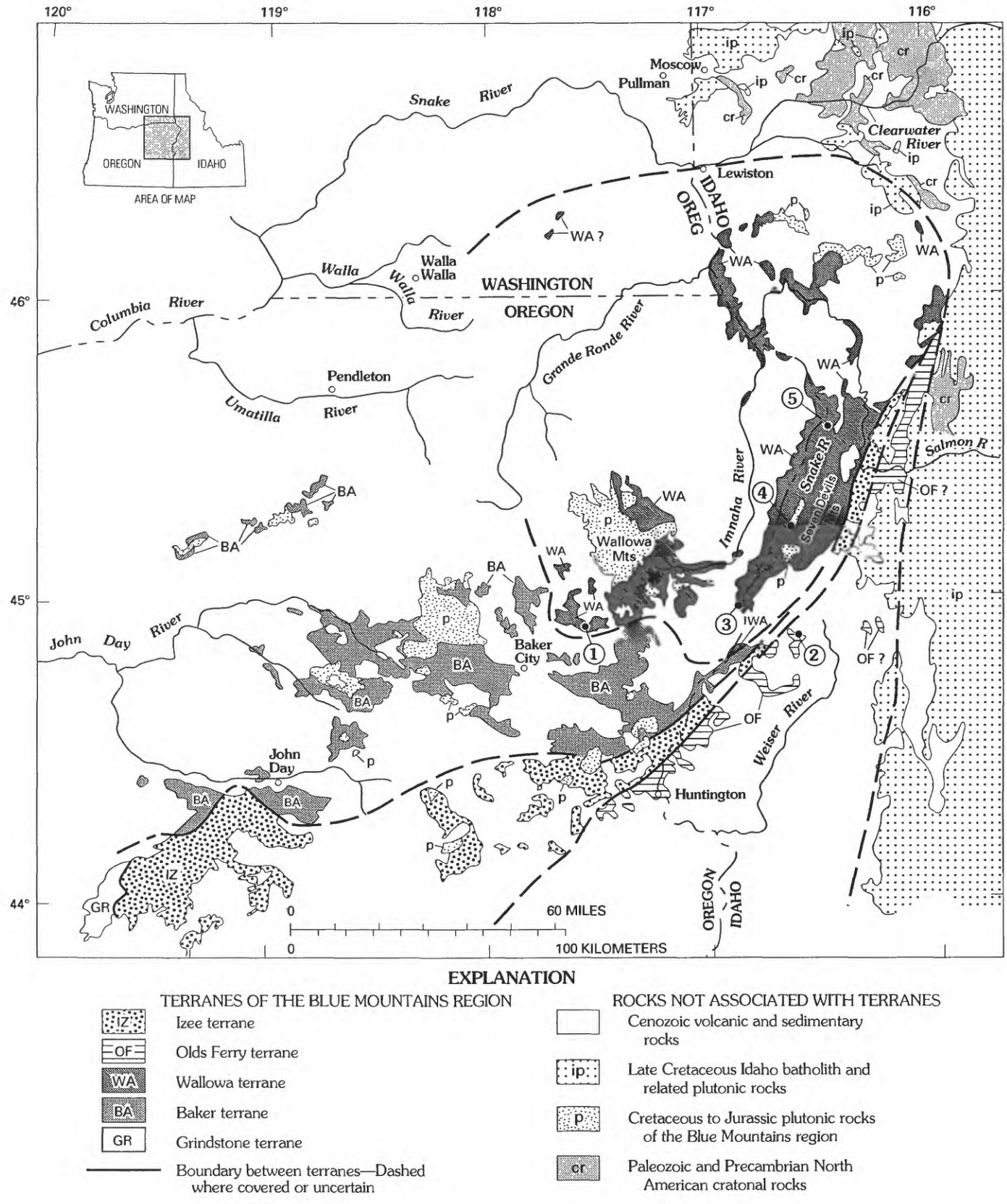

FIGURE 7.1.—Geology of the Blue Mountains province and the location of principal volcanogenic massive sulfide deposits (1, occurrences in the Keating district; 2, Peck Mountain; 3, Iron Dyke; 4, Red Ledge; 5, Blue Jacket). Modified from Vallier, in press.

Igneous rocks in the Seven Devils Group change from a bimodal assemblage of basalt and dacite or rhyolite in the Permian formations to dominantly basalt and andesite in the Triassic formations. Most belong to the island arc tholeiite magma series (Vallier, in press).

Rocks of the Seven Devils Group and the Red Ledge deposit have apparently undergone two episodes of metamorphism. The first episode commenced with deposition and burial of the oldest volcanogenic rocks and may have culminated in Late Triassic time with the intrusion of numerous small plutons. Mineral assemblages attributable to this regional metamorphic event are generally diagnostic of the greenschist facies and include secondary albite, chlorite, epidote, quartz, sphene, calcite, and prehnite (Vallier and Batiza, 1978). Experimental work involving amphibole-bearing assemblages (Liou and others, 1974; Winkler, 1976; Mottl and Holland, 1978) suggests that the presence of accessory actinolite and the absence of biotite in basalts of the Seven Devils Group indicate that the maximum temperature and pressure of metamorphism were 400 to 450 °C and 4 kb, respectively. A second episode of metamorphism is indicated by paleomagnetic data that, according to Hillhouse and others (1982), record a widespread but sporadically distributed thermochemical event associated with plutonism of Late Jurassic and Early Cretaceous age.

GEOLOGY OF THE RED LEDGE DEPOSIT

The Red Ledge prospect is a large Zn-Cu-Ag deposit of island arc volcanogenic massive sulfide affiliation. It is located in the Seven Devils mining district, Adams County, Idaho, about 193 km northwest of Boise and 3.2 km southeast of the Hells Canyon Dam on the Snake River. The deposit is exposed immediately east of Deep Creek in the south half of sec. 23, T. 22 N., R. 3 W. (lat 45°13'30" N., long 116°40'00" W.) between altitudes of 850 and 1,585 m. Mineralization resulted in an extensive stockwork system overlain by a capping of syngenetic stratiform and epigenetic strata-bound sulfides. The stockwork and capping sulfides are hosted by felsic volcaniclastic rocks that are part of a volcanic dome complex, known as the (informal) Red Ledge rhyolite unit. The dome intruded and is intercalated with a stratigraphic sequence of basaltic and dacitic volcanic rocks and their epiclastic derivatives. All rock types in and around the Red Ledge rhyolite unit were pervasively altered by hydrothermal fluids shortly after their deposition or emplacement. The Red Ledge deposit resembles many other volcanogenic massive sulfide deposits of various ages and locations around the world, but in this study it is primarily compared to the unmetamorphosed Kuroko deposits of Japan.

Rocks in the Red Ledge area have been variously regarded as Permian, Triassic, or Permian-Triassic in age (see Livingston and Laney, 1920; Long, 1975). However, on the basis of the discovery of a Permian brachiopod at the approximate stratigraphic position of the stratiform and strata-bound sulfides (T.L. Vallier, 1984, oral comm.) the sequence that hosts Red Ledge rhyolite unit is herein considered to be correlative with the Lower Permian Hunsaker Creek Formation. This paleontologic evidence, in addition to the sulfur isotopic composition of syngenetic barite from the deposit (Fifarek and others, 1983), implies that the syngenetic mineralization and associated epigenetic assemblages are also Early Permian in age.

Long (1975) reported a K-Ar age of 125±5 Ma for whole-rock hydrothermal sericite from the Red Ledge deposit. This age is similar to others obtained by the K-Ar method for samples from the Deep Creek stock, a dioritic pluton situated 5.6 km southeast of the Red Ledge deposit: 121 and 117±4 Ma on biotite and 127 and 137±4 Ma on hornblende (White, 1973; Armstrong and others, 1977). However, the radiometric age (Early Cretaceous) for the hydrothermal sericite is considerably younger than the stratigraphic age (Early Permian) for mineralization-alteration as inferred from the fossil evidence. Accordingly, the anomalously young age yielded by the hydrothermal sericite probably represents complete thermal resetting of the K-Ar systematics during Early Cretaceous plutonism in the region. If so, the thermal regime in the Red Ledge area must have exceeded the minimum argon blocking temperature of muscovite, or ~270 °C (Snee and others, 1988), during the second episode of metamorphism.

STRATIGRAPHIC UNITS

The rocks that host the Red Ledge rhyolite unit consist of a sequence of basaltic to dacitic tuffs, flows, volcanic breccias, and intercalated volcanogenic conglomerates, sandstones, and siltstones. These host rocks are grouped into four stratigraphic units: volcanogenic epiclastic rocks, felsic flows, felsic volcaniclastic rocks, and mafic to intermediate flows and clastic rocks (figs. 7.2 and 7.3). This sequence has been folded and rotated approximately 90° about a horizontal axis such that the stratigraphic units dip steeply and generally strike northeast. The sequence is overlain by Triassic volcanic and sedimentary

rocks, including redbeds and limestone lenses, exposed approximately 1 km northwest of the Red Ledge deposit.

About half of the stratigraphic sequence in the Red Ledge area is composed of lava flows (Long, 1975). Individual flows are generally massive but locally are

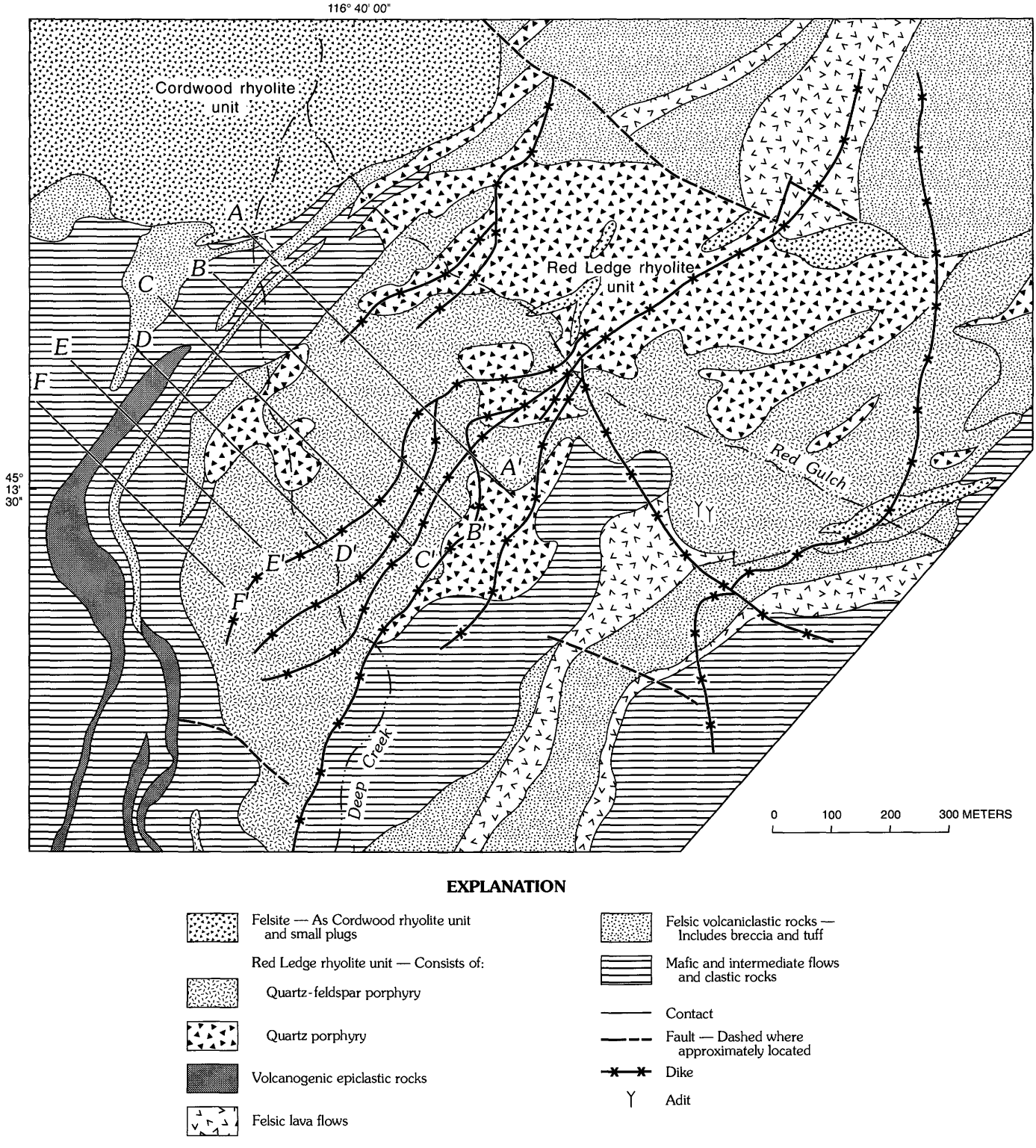

FIGURE 7.2.—Geology of Red Ledge massive sulfide deposit. Lines A-A' through F-F' correspond to cross sections shown in figure 7.3. Geology modified from Long (1975) and Texasgulf, Inc. (unpub. data, 1978).

characterized by columnar jointing or brecciated contacts. Mafic and intermediate lavas are gray green, dark reddish gray, or dusky red, the reddish hues resulting from pervasively disseminated hematite. These lavas commonly contain phenocrysts and microlites of plagioclase feldspar and locally contain vesicles that are partially or completely filled with calcite, chlorite, and quartz. Felsic flows are characterized by rounded (resorbed) phenocrysts of quartz and (or) a leucocratic groundmass of quartz and feldspar.

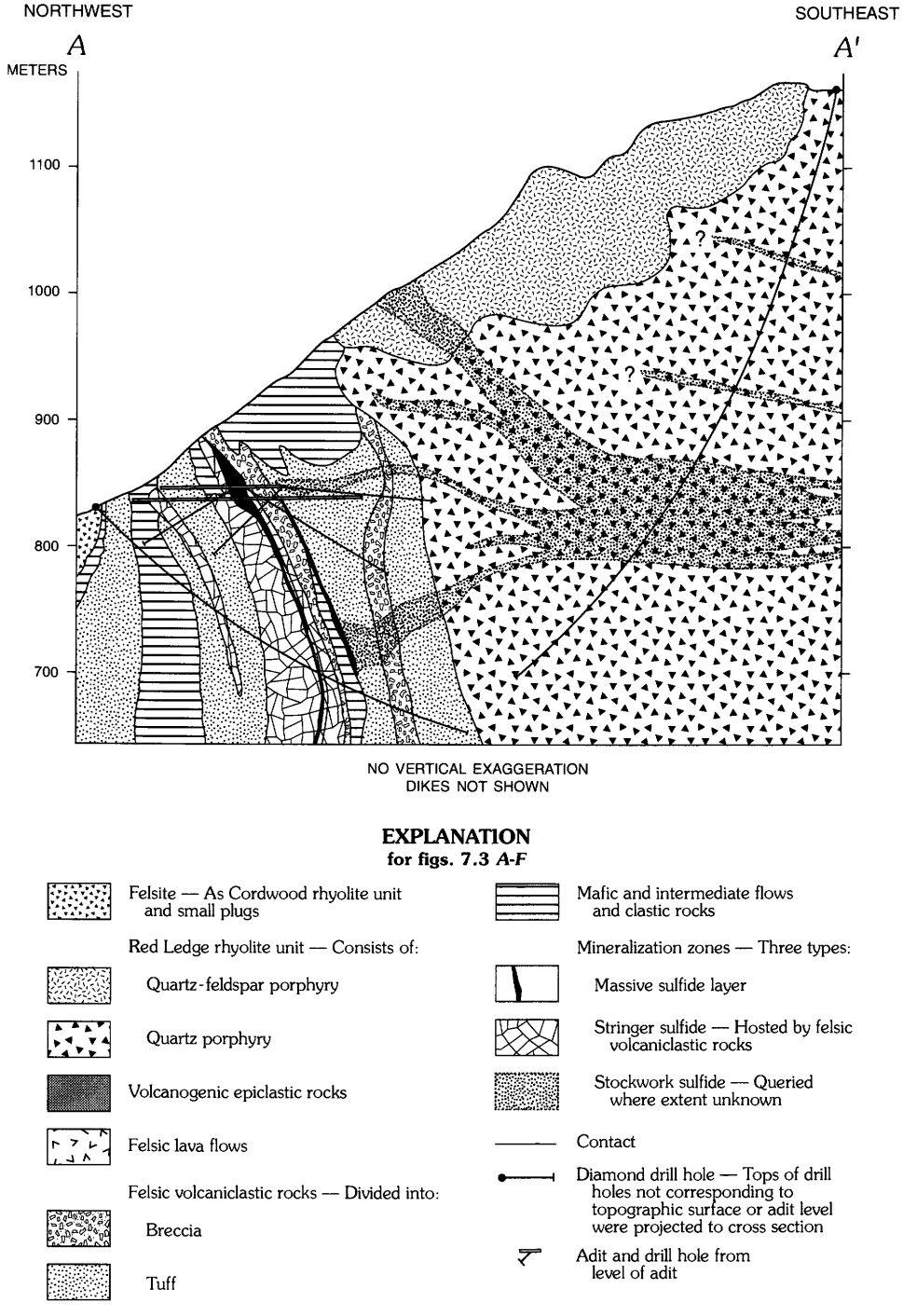

FIGURE 7.3.—Cross sections showing geology and mineralization of the Red Ledge massive sulfide deposit. Scale of cross sections does not match that of figure 7.2. Modified from Texasgulf, Inc. (1978).

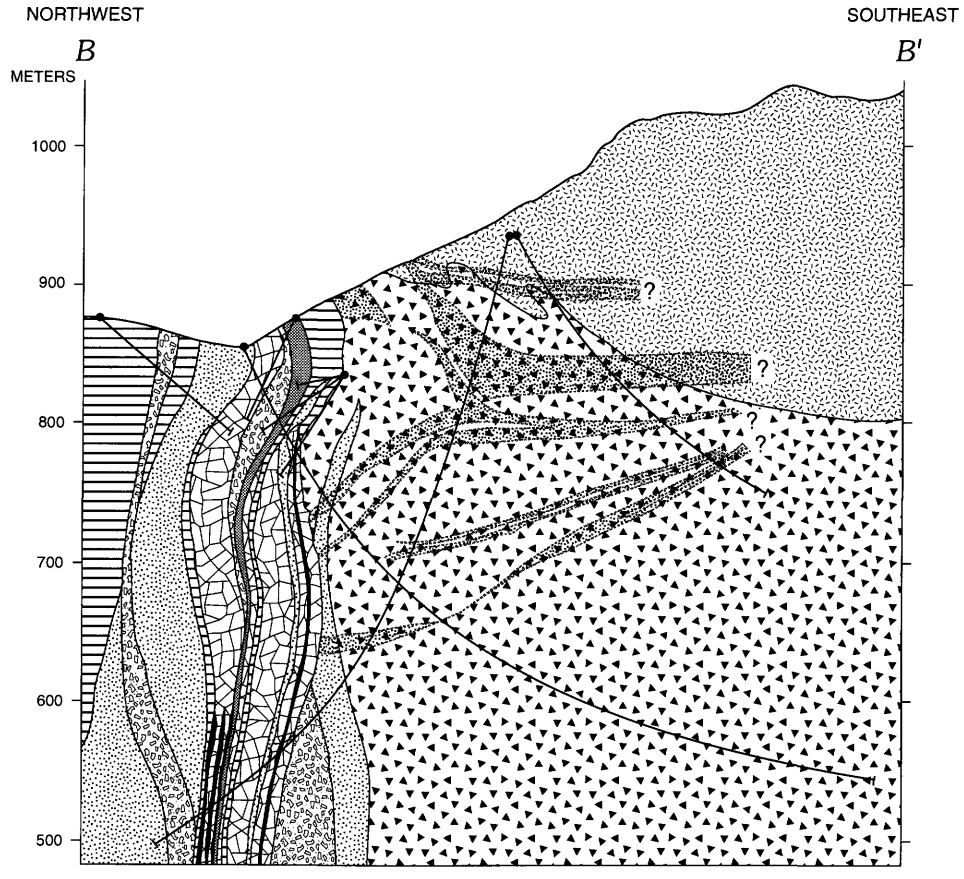

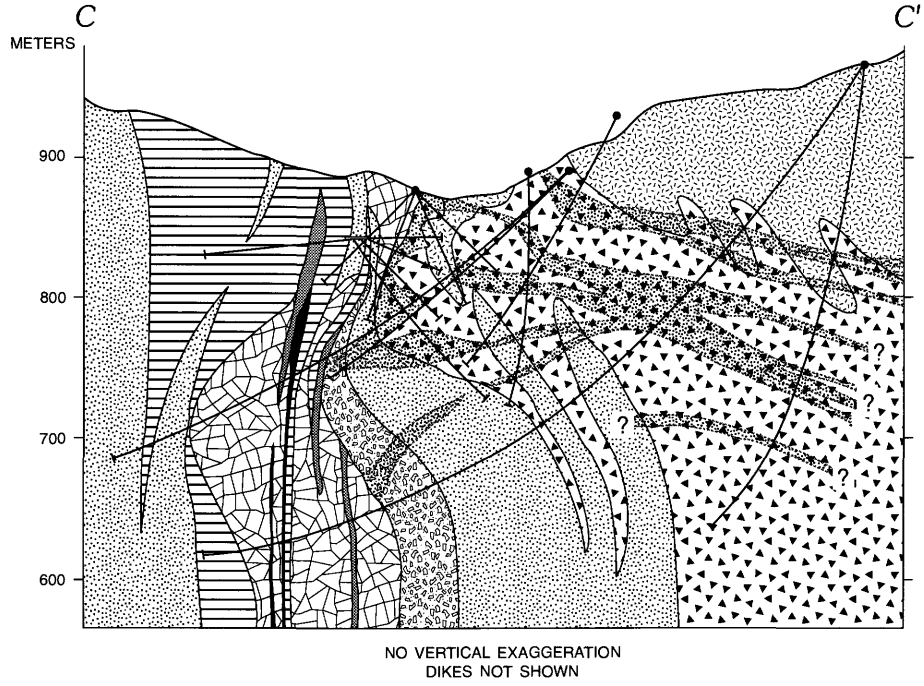

FIGURE 7.3.—Continued.

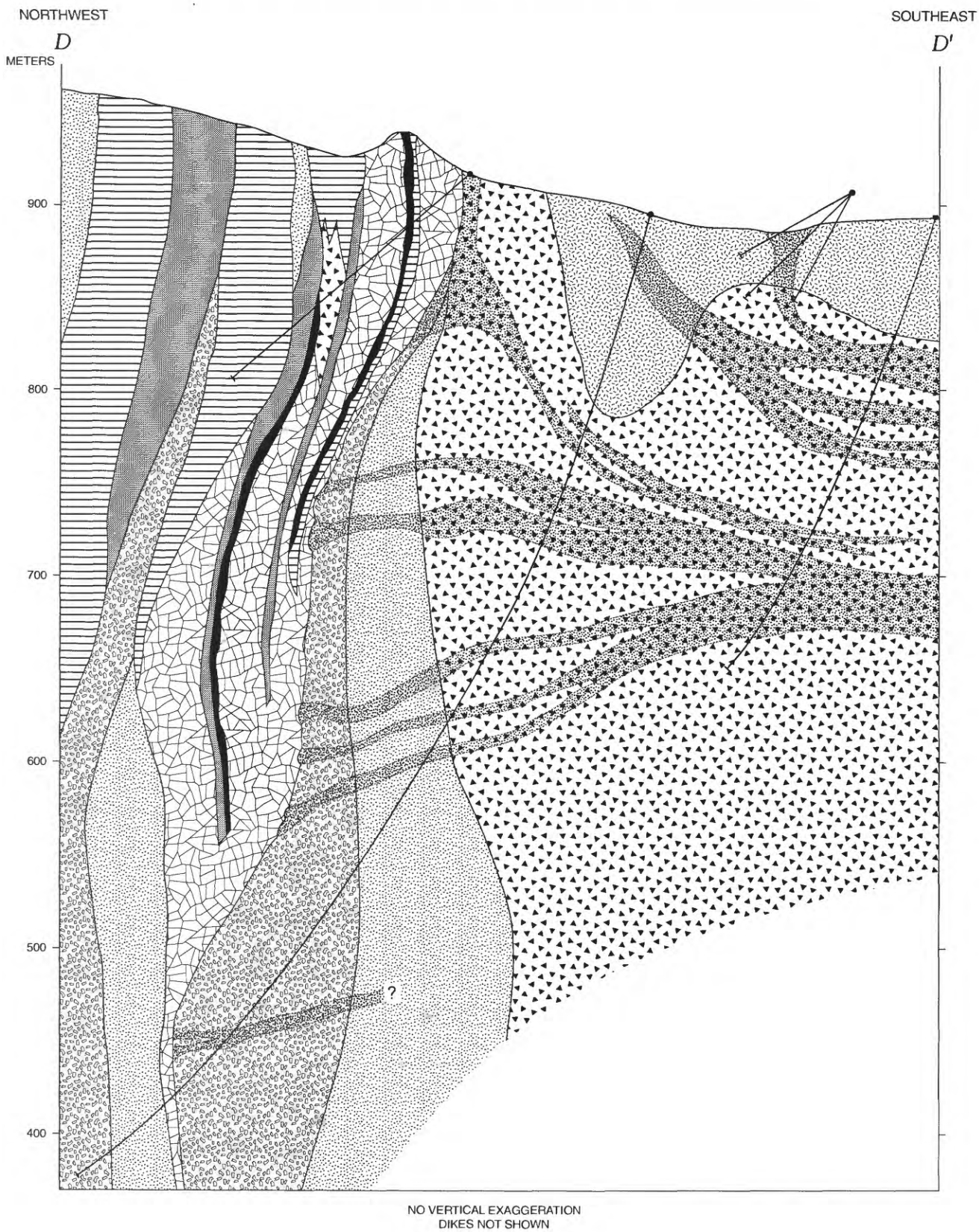

FIGURE 7.3.—Continued.

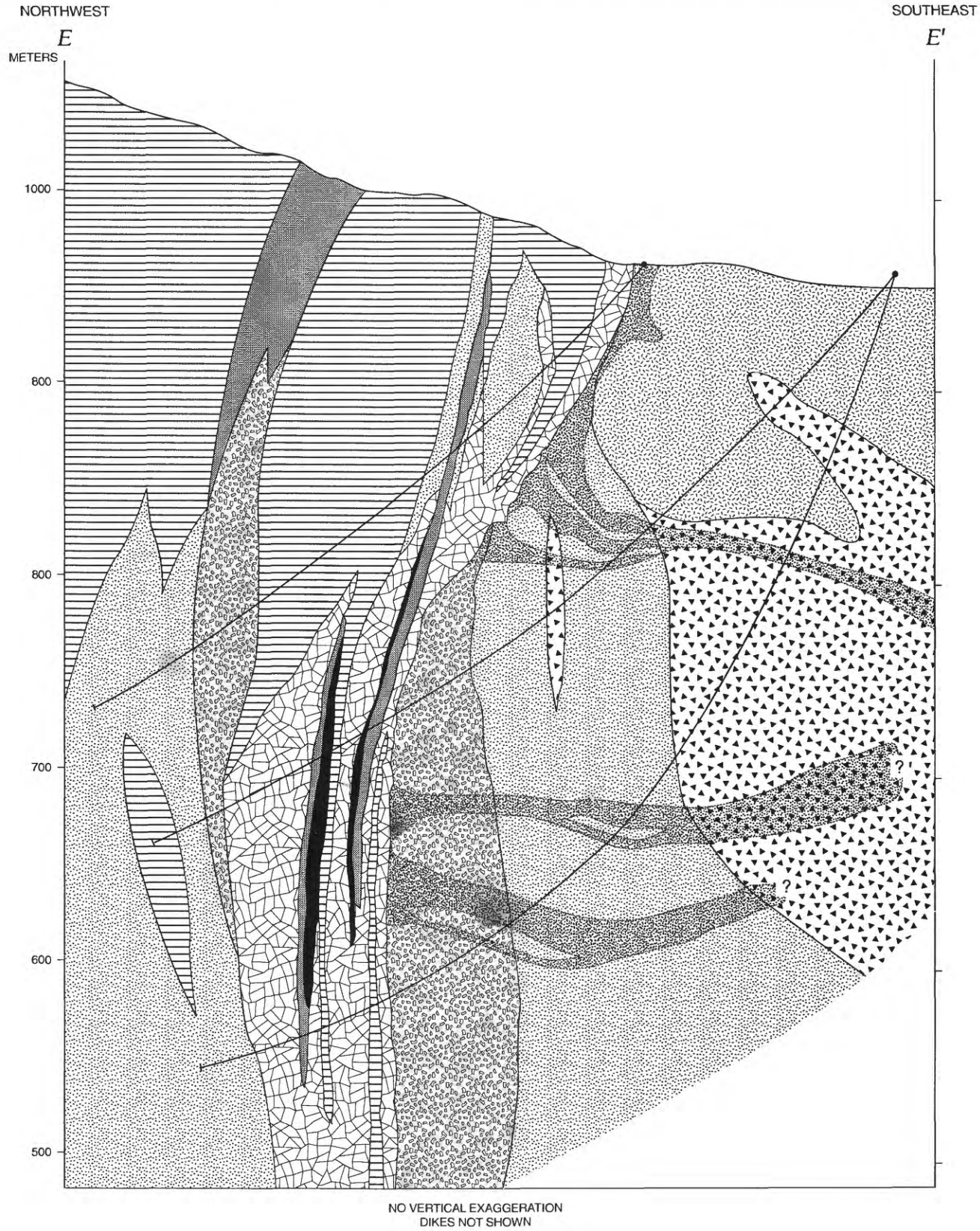

FIGURE 7.3.—Continued.

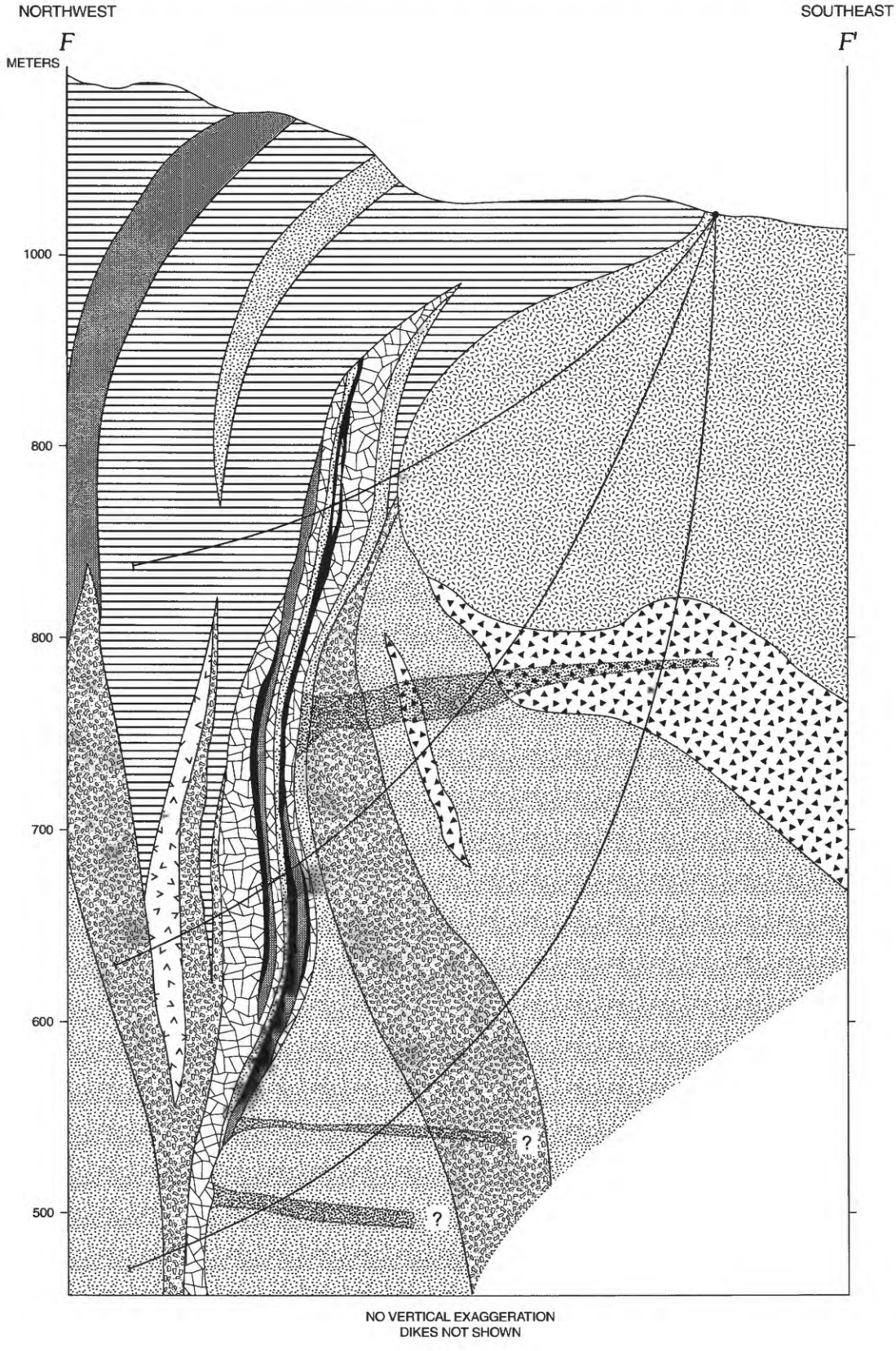

FIGURE 7.3.—Continued.

Tuffs of felsic composition commonly contain quartz eyes or xenocrysts of quartz set in a buff matrix, whereas those of intermediate composition contain crystals of plagioclase feldspar in a gray green to gray brown matrix. Most of the tuffs have a metamorphic foliation parallel to bedding, and some have lapilli-size clasts of volcanic and volcaniclastic rocks (fig. 7.4*A*). The volcanic breccias are composed of clasts (as much as 10 cm long) of mafic and felsic flows, felsic tuffs, and quartz-feldspar porphyry of the Red Ledge rhyolite unit (fig. 7.4*A*).

The volcanogenic siltstones, sandstones, and conglomerates are massive to faintly bedded or laminated and are composed of locally derived volcanic and volcaniclastic detritus (fig. 7.4*A*). A particularly distinctive epiclastic unit near the top of the stratigraphic interval that contains the strata-bound mineralization has the characteristics of a turbidite: graded bedding, moderate sorting, scour and fill, load cast, and flame structures. A few relatively mature quartz-rich sandstone beds are present in the section.

RED LEDGE RHYOLITE UNIT AND ASSOCIATED INTRUSIONS

The Red Ledge rhyolite unit is a volcanic dome complex of felsic composition that has both intrusive and extrusive components. Because of folding and rotation, this complex is exposed in cross section with the northwest margin representing the top of the dome. The surface expression of the complex is approximately 1,100 m long and 600 to 800 m wide, and it tapers eastward into a feeder dike that is at least 1,300 m long. The complex is generally discordant to the stratified country rocks near the base but becomes increasingly concordant and intercalated with the country rocks towards the top.

The Red Ledge rhyolite unit consists of irregular masses of quartz-feldspar porphyry and quartz porphyry (figs. 7.2 and 7.3). The quartz-feldspar porphyry is characterized by phenocrysts of subangular to rounded quartz, 1 to 4 mm in diameter, and tabular plagioclase feldspar, 1 to 4 mm in length (fig. 7.4*B*). Petrographic and chemical analysis of weakly altered samples of this rock type indicate that the plagioclase feldspar is andesine (An_{33-38}) and that the rock composition is rhyodacite (see "Petrography" and "Geochemistry" sections). Feldspars in intensely altered samples have been completely replaced by sericite and kaolinite.

The quartz porphyry contains quartz eyes but lacks feldspar phenocrysts or their altered remnants. It is typically brecciated and contains minor tuffaceous layers near the top of the complex that locally exhibit a eutaxitic structure indicating the probable former presence of collapsed pumice clasts and glass shards. Most of these fragmental rocks are intensely altered and veined. Therefore, it is probable that the quartz porphyry phase may, in part, represent the altered equivalent of the coextensive quartz-feldspar porphyry phase, as was suggested by Long (1975).

A large columnar-jointed body of felsite, called the (informal) Cordwood rhyolite unit, was emplaced into the stratigraphic section overlying the dome complex. Small plugs of felsite also intruded the quartz-feldspar and quartz porphyries of the complex. The felsite is characteristically light gray and homogeneous (fig. 7.4*B*) with sporadically distributed clots of chlorite and relict microphenocrysts of plagioclase feldspar. Although younger than the mineralization, the Cordwood rhyolite unit is pervasively altered to a quartz-sericite-calcite assemblage and is sparsely veined by calcite, quartz-calcite, and hematite. Its chemical composition is similar to that of the quartz-feldspar porphyry, thus it is regarded as altered rhyodacite.

Several porphyritic dikes crosscut all other rock types in the Red Ledge area (fig. 7.2). Phenocryst assemblages of the dikes are calcic plagioclase-augite, hornblende, and quartz-andesine (fig. 7.4*B*), which suggest rock compositions of basalt, andesite, and dacite or rhyodacite, respectively (Long, 1975).

MAGMATIC HISTORY

The various rock types present in the Red Ledge area and their distribution record the development of a vol-

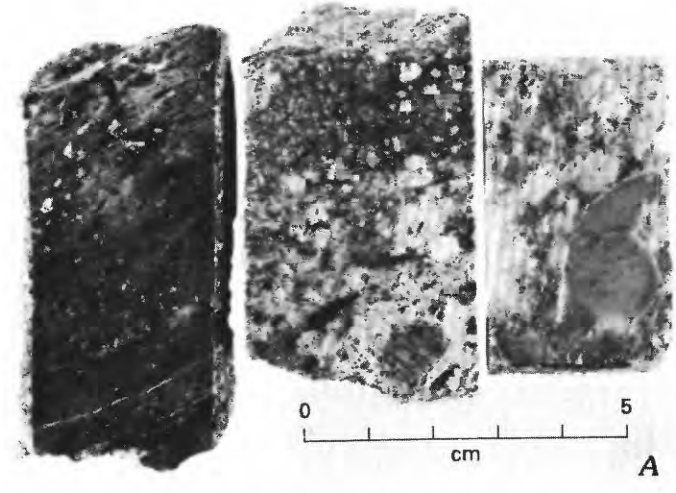

FIGURE 7.4.—Rocks representative of units associated with the Red Ledge deposit. *A*, Stratiform rocks: foliated quartz-eye tuff (left), volcanic breccia (center), and volcanogenic conglomerate (right). *B*, Intrusive rocks: weakly altered quartz-feldspar porphyry (upper left) of the Red Ledge rhyolite unit, felsite of the Cordwood rhyolite unit (right), and quartz-feldspar porphyry dike (lower left).

canic dome complex that formed on the sea floor through the repetitive formation and destruction of one or more domes around a volcanic vent. The geologic relationships (figs. 7.2 and 7.3) imply that the quartz-feldspar porphyry resulted both from the intrusion and extrusion of viscous rhyodacitic magma. Intrusive magma crystallized to form irregular plugs and dikes in an edifice of volcanic fragmental rocks, whereas extruded magma cooled to form stubby flows, domes, and possibly spires. Geologic relationships also suggest that the quartz porphyry breccia originated both by the mechanical disintegration of the dome and by explosive eruptions. The breccia that mantles the intrusive bodies (fig. 7.3) resulted from the fragmentation of quartz-feldspar porphyry by phreatic explosions, differential movement between semiconsolidated masses, and the spalling of domes and spires. Some of the felsic tuffs and breccias that form discrete stratigraphic units were produced by phreatomagmatic and magmatic eruptions. A thinning and (or) omission of these units near the inferred apex of the dome (see fig. 7.3*C* and 7.3*F*) indicate that the complex was a topographically positive feature during part of its development. Consequently, some fragmental material may have been transported to sites of deposition as rock slides, debris flows, and turbidity flows. All unconsolidated deposits of fragmental rocks were locally reworked by ocean currents and ubiquitously altered by hydrothermal fluids. The dome complex was eventually buried by felsic volcaniclastic rocks produced during a waning phase of steam explosions and magmatic eruptions, and by sediment and mafic lava flows derived from extraneous sources.

Permian magmatism in the Red Ledge area ended with the intrusion of felsite, primarily as the Cordwood rhyolite unit, followed by the intrusion of porphyry dikes.

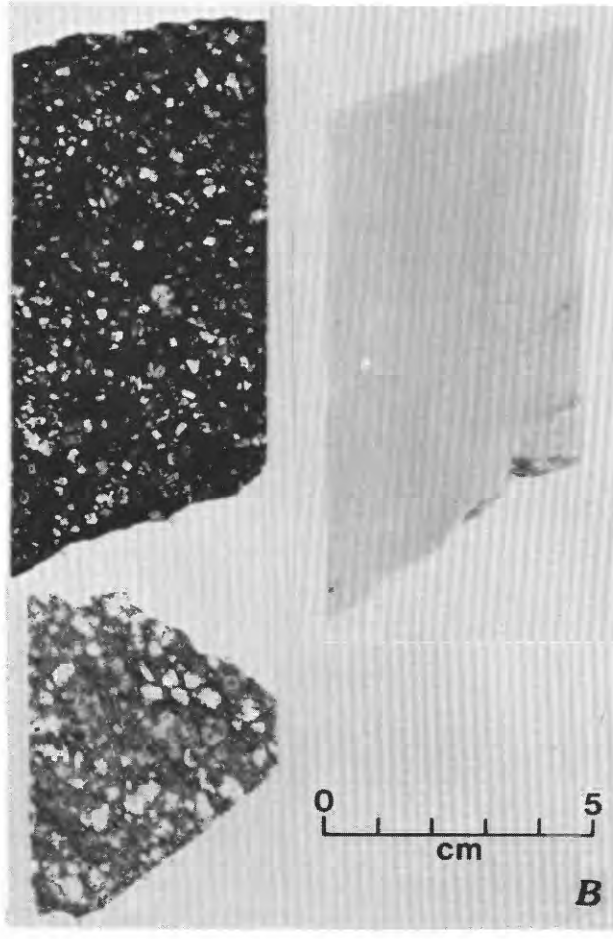

FIGURE 7.4.—Continued.

MINERALIZATION

The Red Ledge deposit consists of a steeply dipping zone of strata-bound stringer and stratiform massive sulfides and a subhorizontal discordant zone of stockwork sulfides (fig. 7.3). Regional tectonism has rotated the deposit approximately 90° around a horizontal axis. Thus, originally, the deposit had the overall configuration of a mushroom with the stringer and massive sulfide zone representing the cap, and the stockwork zone representing the stalk. Zones of stringer sulfides are hosted exclusively by felsic volcaniclastic units in the section of interfingering felsic and mafic to intermediate volcanic and sedimentary rocks that immediately overlies the Red Ledge rhyolite unit. The stockwork system largely occurs in felsic fragmental rocks that mantle the massive quartz-feldspar porphyry of the dome complex (fig. 7.3). Accordingly, these geologic features imply that the ore-forming process was genetically related to the waning, explosive phase of dome development.

GEOLOGIC CHARACTERISTICS

The capping zone of the deposit is grossly lenticular, measuring over 600 m long, about 460 m wide, and 120 m thick at the center. It largely consists of stringers, blebs, and disseminations of sulfides that infill and partially replace stratigraphic units of felsic breccia (fig. 7.5*A*). Hence, these "stringer" sulfides are strata-bound but epigenetic. Zones of stringer sulfides typically consist of microcrystalline quartz (50–85 percent), pyrite (10–35 percent), barite (3–20 percent), sphalerite (trace amounts to 10 percent), chalcopyrite (trace amounts to 5 percent), galena (0–1 percent), and tetrahedrite (<1 percent). Pervasive silicification

and sulfidation of the host breccias have obscured many primary lithologic and textural features. Nonetheless, it is evident that the breccia clasts are largely quartz-feldspar porphyry and quartz porphyry of the Red Ledge rhyolite unit. Veinlets confined to individual clasts and the local infilling and replacement of the breccias by late hematite-barite-chlorite±calcite indicate that these mineralized zones formed through multiple episodes of brecciation and hydrothermal precipitation.

Thin layers of exhalites, mafic flows, intermediate tuffs, and volcanic wackes interfinger with the felsic breccias that host stringer sulfides (figs. 7.2 and 7.3). The volcanic and sedimentary rocks are unmineralized but variably altered to propylitic, chlorite-sericite-clay, and chlorite-sericite assemblages. The exhalite units include beds and lenses of massive sulfide, hematite-barite-chlorite, and barite with sparsely disseminated pyrite. Thin stratigraphic intervals comprised of exhalites, tuffs, and (or) epiclastic units effectively separate the capping zone into three or four stacked sets of stringer sulfide zones and overlying massive sulfide layers. These relationships imply that sulfide precipitation was part of a cyclic repetition of specific tectonic, volcanic, and hydrothermal events.

The massive sulfide units occur as circular, lobate, and horseshoe-shaped stratiform bodies as much as 550 m in length and 25 m in thickness, although their average dimensions are appreciably smaller. They are variably composed of pyrite, sphalerite, chalcopyrite, barite, and quartz with minor amounts of galena, tetrahedrite, and chlorite, and local trace amounts of pyrrhotite and bismuthinite. Proximal occurrences centered over the stockwork zone generally consist of coarse-grained granular aggregates of pyrite, chalcopyrite, and quartz, whereas distal occurrences tend to be enriched in sphalerite, galena, and barite and have finely laminated textures (fig. 7.5*B*). Some examples of distal massive sulfides contain sparse, angular clasts of quartz-pyrite, barite, and hematite-quartz in a sphalerite-barite matrix (fig. 7.5*B*). Such occurrences suggest that previously consolidated exhalite and massive sulfides either were disaggregated explosively and the clasts fell into a sulfide-rich sediment or were fragmented and incorporated into a sulfide-rich matrix by slumping and debris flow mechanisms. Systematic vertical trends in mineralogy and texture between the stacked massive sulfide units have not been recognized.

Exhalite layers consisting of disseminated brick-red hematite in microcrystalline quartz, similar to the tetsusekiei layers of the Kuroko deposits (see Tsutsumi and Ohmoto, 1983), were not observed. However, the presence of rare tetsusekiei clasts (that is, the previously noted hematite-quartz clasts) embedded in a massive sulfide matrix suggests that one or more of these exhalite layers formed during the development of the deposit but were subsequently destroyed. Thin hematite-barite-chlorite layers, a possible variant of the tetsusekiei material, are locally interbedded with massive pyrite-barite layers (fig. 7.5*B*). The laminated

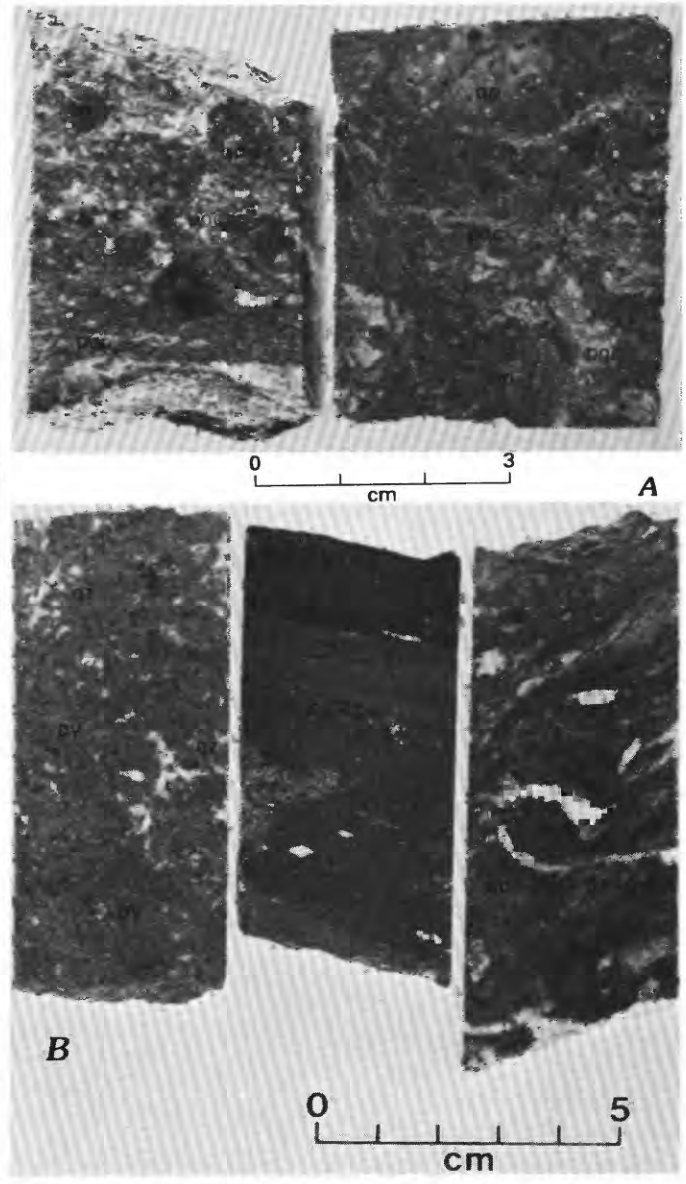

FIGURE 7.5.—Rocks of the capping mineralized zone. *A*, Stringers of pyrite+quartz±chalcopyrite (pqc) hosted by felsic breccias with quartz porphyry clasts (qp). *B*, Massive sulfide layers: proximal granular pyrite+quartz (left); distal laminated pyrite+barite interlayered with hematite+barite+chlorite (center); distal laminated sphalerite+pyrite+barite+galena with exotic clasts of pyrite+quartz (right). Abbreviations: ba, barite; ch, chlorite; cl, pyrite+quartz clasts; gn, galena; hm, hematite; pqc, pyrite+quartz±chalcopyrite, py, pyrite; qp, quartz-porphyry clasts; sp, sphalerite.

texture, sharp interdigitated contacts with the sulfides, and absence of boxwork-like features indicate that this hematitic assemblage is of exhalative origin rather than the product of sea-floor oxidation or recent weathering. It apparently represents the syngenetic counterpart of a mineralogically identical void filling found in areas of stringer sulfides.

The stockwork system stratigraphically underlies the mineralized capping and consists of distinct zones of anastomosing veins and veinlets separated by relatively barren wedge-shaped blocks of rock (fig. 7.3). A few relatively large zones typically make up the deeper part of the system, but these tend to branch and expand upward resulting in a greater density of narrower structures immediately below the mineralized capping. These high-level veins grade into and are indistinguishable from the overlying zones of stringer sulfides. Sparse veins of the later paragenetic stages crosscut strata-bound mineralization and the hanging-wall section of the deposit. The stockwork system, although not fully delimited by drilling, is exceptionally large for a Kuroko-type deposit: It measures over 370 m in length, averages about 150 m in width, and crosscuts at least 370 m of section.

The veins and veinlets consist primarily of quartz, pyrite, chalcopyrite, and lesser amounts of dolomite, sphalerite, barite, calcite, sericite, chlorite, gypsum, and anhydrite. The distribution of these mineral phases reveals a lateral and vertical zonation. Pyrite was the principal sulfide deposited at depths of 200 to 240 m below the contemporaneous sea floor (regarded as the stratigraphically lowest massive sulfide or equivalent sedimentary unit), whereas chalcopyrite predominates at depths of 80 to 150 m (Juhas and Gallagher, 1981). Sphalerite, barite, and dolomite were preferentially deposited at the top of the stockwork system, above and peripheral to the copper zone, although they are sporadically distributed to depths of 300 m. Quartz-anhydrite-pyrite, quartz-sphalerite-chalcopyrite, and quartz-carbonate veins locally crosscut zones of stringer and massive sulfides. The third assemblage is also found in hanging-wall rocks overlying the capping zone.

PARAGENETIC SEQUENCE

The paragenetic order of mineral deposition in the stockwork system was determined from crosscutting relationships and sequences of crustification in veins and vugs at both microscopic and megascopic scales. The paragenetic scheme is therefore a composite of observations made from numerous samples because individual samples portray only a part of the total depositional sequence.

Details of the paragenetic sequence in the stockwork system—prevein wallrock alteration followed by vein and vug filling—are shown in figure 7.6. Mineral deposition in veins and vugs is divided into stages 1 to 4, respectively dominated by amethyst, quartz and sulfides, barite, and carbonate; stages 2 and 4 are further subdivided into three substages. The principal alteration minerals are considered to have formed prior to and (or) contemporaneously with the earliest vein assemblages (stage 1 and substage 2A) because these early veins have irregular and diffuse contacts with silicified and sericitized wallrocks. In contrast, later veins are characterized by linear and sharp contacts and lack alteration selvages. Thus, they apparently formed after the rocks had achieved thermal and chemical equilibrium with the hydrothermal fluids.

In detail, the specific stages and substages of vein and vug filling are as follows:

Stage 1 (amethyst stage).—Amethyst forms the cores of quartz clots (as much as 2.5 cm in diameter) that are embedded in altered wallrocks or later stages of vein minerals (fig. 7.7). The clots grade outward from amethyst to growth-zoned, alternating white and purple (amethystine) quartz and then to white quartz.

Stage 2 (quartz-sulfide stage).—Vein filling consists chiefly of quartz, pyrite, and chalcopyrite. The sulfides, in amounts ranging from 10 to 80 percent of the vein, are present as granular aggregates in mottled white and gray quartz (substage 2A) and as crosscutting stringers associated with sericite, gray translucent quartz, and chlorite (substage 2B) (fig. 7.7). Coarsely crystalline, vuggy, white quartz with less than 5 percent sulfides characterizes substage 2C (fig. 7.7). Microscopic textures indicate that chalcopyrite is invariably later than pyrite.

Stage 3 (barite stage).—Barite is deposited as fine-grained masses in veinlets and as prismatic crystals lining vugs in earlier quartz (substages 2B and 2C). Barite is locally associated with minor sphalerite, pyrite, chalcopyrite, and dolomite.

Stage 4 (carbonate stage).—Carbonate in the form of coarsely crystalline pink to orange dolomite (substage 4A) partially or completely fills vugs and centerline cavities that may be lined with earlier drusy quartz and (or) barite (fig. 7.7). This dolomite is successively overgrown by botryoidal olive-brown dolomite (substage 4B) and accicular calcite (substage 4C).

A paragenetic sequence for stringer and massive sulfide mineralization was determined solely through the study of textures observed in polished sections. Pyrite is typically present as anhedral to subhedral crystals and rounded aggregates (fig. 7.8), and rarely

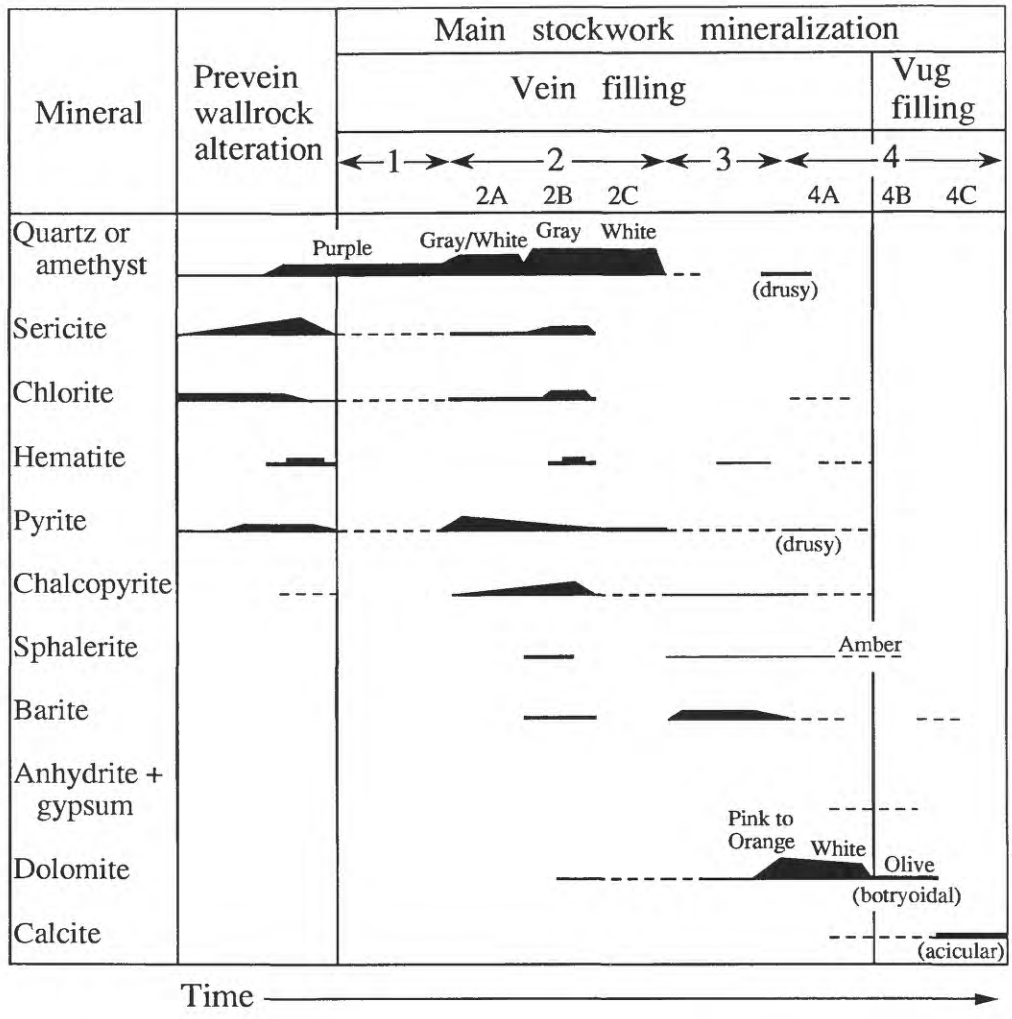

FIGURE 7.6.—Paragenetic sequence of vein and vug minerals of the stockwork zone of the Red Ledge deposit, Idaho, and their relationship to prevein alteration minerals of the wallrocks. 1, amethyst stage; 2, quartz+sulfide stage; 3, barite stage; 4, carbonate stage. 2A to 2C and 4A to 4C are substages of quartz+sulfide and carbonate stages, respectively. Profiles show relative abundance of minerals over time; dashed lines indicate sporadic occurrence in trace amounts.

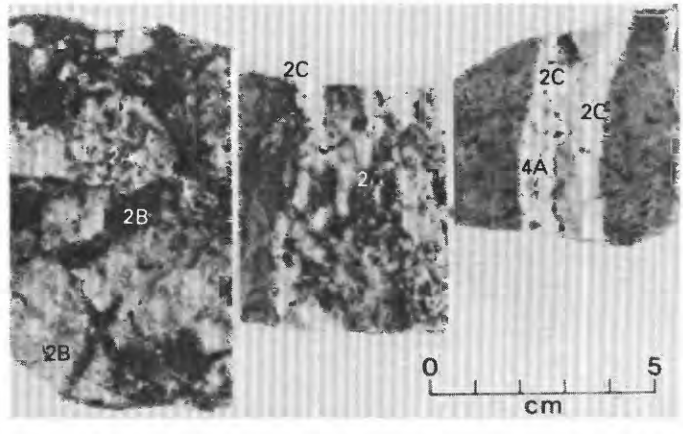

FIGURE 7.7.—Photomicrograph showing paragenetic relationships of vein mineralization, Red Ledge deposit, Idaho. Clots of amethyst (stage 1) and mottled white and gray quartz+pyrite (stage 2A) embedded in altered wallrock and cut by gray quartz+sericite+pyrite (stage 2B) (left); mottled white and gray quartz+pyrite±chalcopyrite (stage 2A) cut by white vuggy quartz (stage 2C) (center); white quartz+pyrite (stage 2C) with centerline vug filled by dolomite (stage 4A) (right).

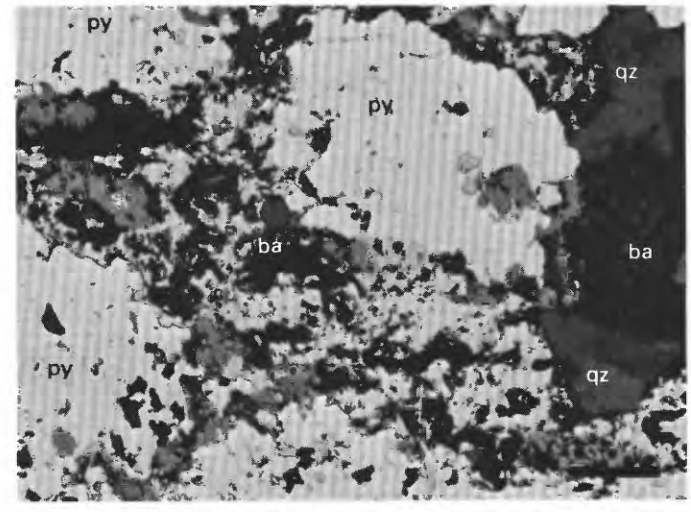

FIGURE 7.8.—Photomicrograph showing textures and paragenetic relationships of massive mineralization, Red Ledge deposit, Idaho. Pyrite (py), chalcopyrite (cp), sphalerite (sp), quartz (qz), and barite (ba). Bar is 0.1 mm long. Reflected light.

as clusters of small framboid aggregates. It is crosscut and replaced by all other sulfides (fig. 7.8). Galena and tetrahedrite are commonly associated, but the temporal relationship between these phases and the depositional order between sphalerite, chalcopyrite, and galena are ambiguous. Quartz is later than pyrite and locally replaces sphalerite and chalcopyrite. Barite deposition is also late in the paragenetic sequence and appears to overlap and supercede quartz deposition. Carbonate, a major vein phase, is absent in zones of stringer and massive sulfides.

Uncertainties remain as to the extent that the microscopic textures of the Red Ledge mineralization represent primary relationships or reflect secondary effects imposed by later metamorphism and deformation. During metamorphism, sulfides tend to rapidly equilibrate to ambient conditions and their primary features become modified (Barton and Skinner, 1967). Indeed, many of the petrographic features that characterize unmetamorphosed volcanogenic massive sulfide deposits—such as framboids, colloform banding, chalcopyrite disease, and sphalerite growth zones—have not been observed or are rare in the Red Ledge deposit. If formerly present or more abundant, they may have been largely destroyed during metamorphism. However, because petrographic criteria for intergranular equilibrium, as summarized by Vernon (1975) and Spry (1976), are also absent, metamorphic recrystallization was probably incomplete and restricted to local domains.

METAL GRADES AND VARIATIONS

The Red Ledge deposit contains approximately 39 million metric tons of stringer and massive sulfide bodies in the capping zone and about 27 million metric tons of stockwork sulfides. Four massive sulfide bodies total 6 million metric tons and collectively average 2.9 percent Zn, 0.9 percent Cu, 80.8 grams per metric ton Ag, and 0.9 grams per metric ton Au. Because of appreciable dilution by host rock, the 33 million metric tons of stringer sulfide bodies is typified by lower grades: 0.6 percent Zn, 0.3 percent Cu, 21.7 grams per metric ton Ag, and 0.47 grams per metric ton Au. The stockwork system averages 0.1 to 0.5 percent Zn, 0.3 percent Cu, 3.1 to 9.3 grams per metric ton Ag, and about 0.31 grams per metric ton Au.

Variations in the principal metals in the Red Ledge deposit are essentially a function of the distribution of a few sulfide minerals. Copper is contained primarily in chalcopyrite and shows a marked decrease upward and outward from the center of the stockwork system. It averages between 1 and 2 percent in the center of the stockwork zone, 0.6 percent near the top of the stockwork zone, and about 0.4 percent in the capping zone. Zinc is contained primarily in sphalerite and increases upward through the deposit. Drillhole intercepts average less than 0.1 percent Zn in the deep part of the stockwork zone, 0.5 percent in the upper part, and 1.0 percent in the capping zone. Lead values are related to the abundance of galena and average less than 0.1 percent in the capping zone. Silver concentrations are largely correlative with those of zinc, although some preliminary microprobe analyses indicate that silver is not a significant constituent of sphalerite. Most of the silver is presumably contained in tetrahedrite because silver minerals have not been identified in the Red Ledge deposit. Silver averages about 3.1 grams per metric ton deep in the stockwork system, 9.3 grams per metric ton near the top, and approximately 31.1 grams per metric ton in the capping zone. Gold averages about 0.31 grams per metric ton in the stockwork zone (as stated previously) relative to 0.53 grams per metric ton in the capping zone.

The overall variations of metal and mineral abundances in the Red Ledge deposit result in a Cu-rich core and a Zn-, Ag-, and Ba-enriched top and periphery. Such a zonation is characteristic of many volcanogenic massive sulfide deposits. Juhas and Gallagher (1981) reported that each of the three to four sets of stringer and massive sulfides have higher Zn/Cu and Ag/Au ratios near their hanging walls; these trends mimic those for the entire deposit. However, copper and gold in the capping mineralization tend to be concentrated in the upper part and zinc and silver concentrated in the lower part so that the Zn/Cu and Ag/Au ratios decrease upward through the sequence of stacked sets. Laterally, zinc and silver are relatively concentrated in the periphery and copper and gold in the center of the capping zone. Copper is also relatively concentrated within 60 m of the topographic surface as a result of supergene enrichment and the deposition of chalcocite, bornite, and covellite (Livingston and Laney, 1920).

HYDROTHERMAL ALTERATION

All rock types near the Red Ledge deposit were hydrothermally altered shortly after their deposition or emplacement. This event preceded, was contemporaneous with, and succeeded metallization and resulted in a zoned succession of alteration assemblages (fig. 7.9). These assemblages grade outward from a silicic zone, proximal to the deposit, through a phyllic zone, to a propylitic halo.

PETROGRAPHY

Silicification is prominent in rocks that host stockwork and stringer sulfides. In thin section, silicification is characterized by veinlets of quartz, replacement of the groundmass by microcrystalline quartz, and recrystallization and embayment of the margins of ellipsoidal quartz phenocrysts (quartz eyes). Pervasive wispy aggregates of sericite and veinlets, streaks, and disseminated euhedra of pyrite are also common in silicified rock. Barite as ragged crystals is typically part of this assemblage in zones of stringer sulfides but much less common in the stockwork system.

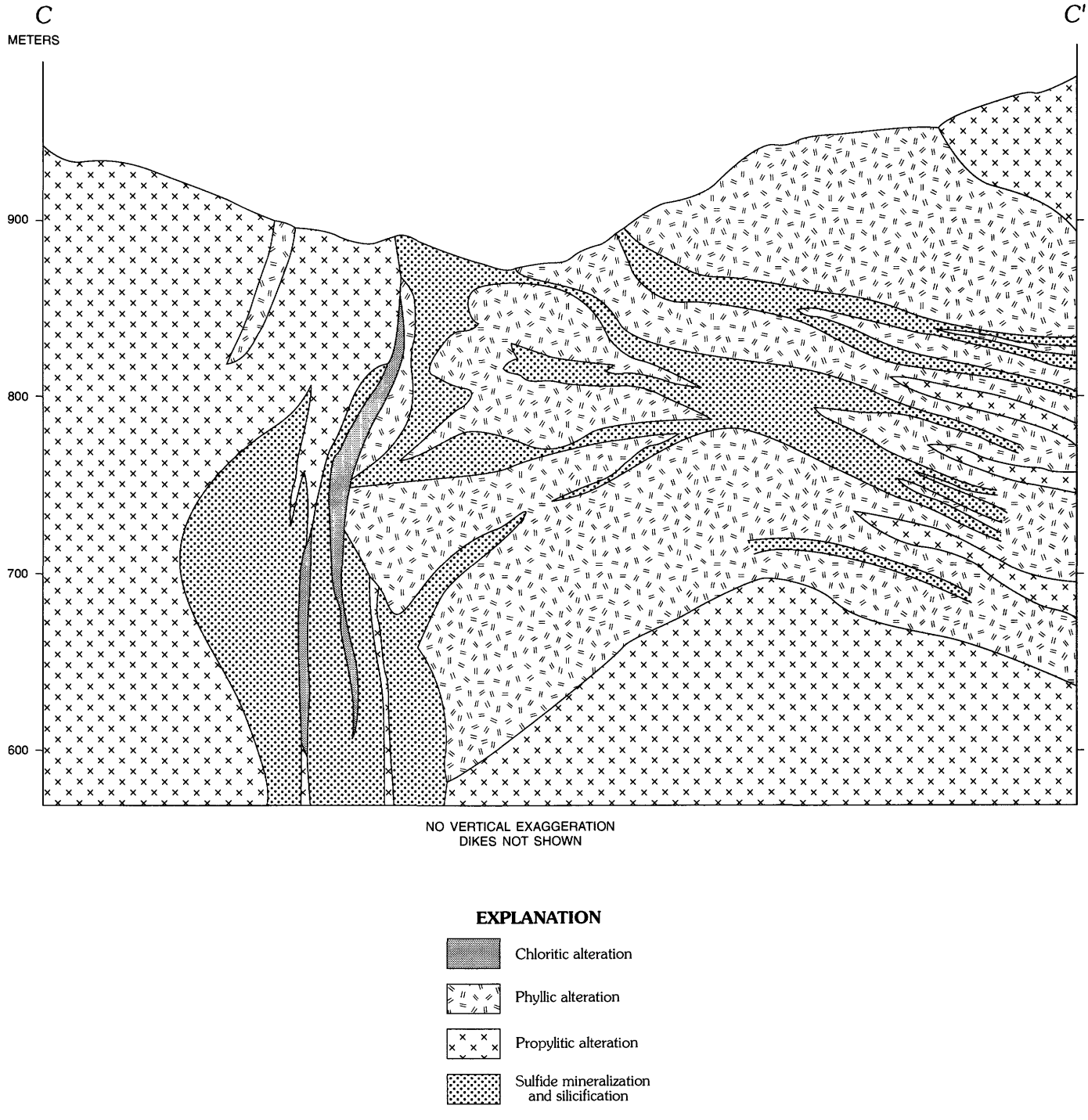

FIGURE 7.9.—Zonation of hydrothermal alteration assemblages along cross section C-C' of figure 7.3. Modified from Juhas and Gallagher (1981).

Phyllic alteration encases all silicified rocks and is particularly evident in rocks that host the mineralized capping and the upper part of the stockwork system. The phyllic zone is divided into an outer sericite-chlorite subzone, in which chlorite is a minor but persistent constituent, and an inner sericite subzone, where chlorite is generally absent.

Sericitic alteration in felsic rocks is characterized by 15 percent or more sericite, 3 to 10 percent pyrite, 0 to 5 percent clay minerals, and 0 to 4 percent barite. Chlorite, calcite, and relict plagioclase feldspar are notably absent. The sericite is pervasively disseminated in the groundmass, where it typically expresses a metamorphic foliation, and is present within small shears. It is also associated with quartz in aggregates completely replacing phenocrysts of plagioclase feldspar, in pressure shadows adjacent to quartz eyes and pyrite euhedra, and in recrystallization rinds on the quartz eyes (fig. 7.10*A*). Clay minerals are generally intergrown with sericite.

The sericite-chlorite alteration assemblage is transitional between the propylitic and sericitic assemblages with respect to its spatial distribution and mineralogy. It is characterized by 15 percent or more sericite, 2 to 12 percent chlorite, 1 to 10 percent pyrite, and variable amounts of sporadically distributed calcite. According to the optical criteria of Albee (1962), the chlorite is magnesian. Limited textural evidence indicates that the sericite partially replaced the chlorite. This apparent relationship implies that the sericitic assemblage may have formed at the expense of the sericite-chlorite assemblage and that the alteration zones grew outward over time in a manner similar to the development of vein selvages (see Meyer and Hemley, 1967). In mafic and intermediate rocks the sericite-chlorite alteration assemblage consists of subequal amounts of sericite, chlorite, and clay.

Propylitic alteration occurs in the country rocks both adjacent to and stratigraphically overlying the Red Ledge rhyolite unit. In felsic rocks, it is distinguished by 5 to 10 percent sericite, 5 to 15 percent calcite, 0 to 3 percent pyrite, 2 to 10 percent chlorite, and a variable amount of albite. In mafic to intermediate rocks it is characterized by 10 to 35 percent magnesian and ferromagnesian chlorite, 3 to 20 percent sericite, 5 to 15 percent calcite, 3 to 5 percent clay minerals, and 0 to 3 percent pyrite. Andesine phenocrysts that have been partially altered to albite, sericite, chlorite, and calcite are diagnostic of this propylitic assemblage (fig. 7.10*B*). The quartz-eye phenocrysts in the propylitically altered quartz-feldspar porphyry show less recrystallization and embayment than their counterparts in zones of more intense alteration; also, this porphyry contains small bipyramidal quartz phenocrysts. The outer margin of the propylitic zone grades into the mineralogically similar greenschist facies of regional metamorphism (see Vallier and Batiza, 1978, for metamorphic-mineral abundances). Propylitic alteration is distinguished by abundances of sericite and pyrite greater than 2 to 3 percent each and by the absence of epidote.

Zones of hydrothermal alteration associated with the unmetamorphosed Kuroko deposits generally are described as grading outward in succession through silica, sericite-chlorite, montmorillonite, and zeolite assemblages (Shirozu, 1974; Izawa and others, 1978; Date and others, 1983). The mineralogy, alteration

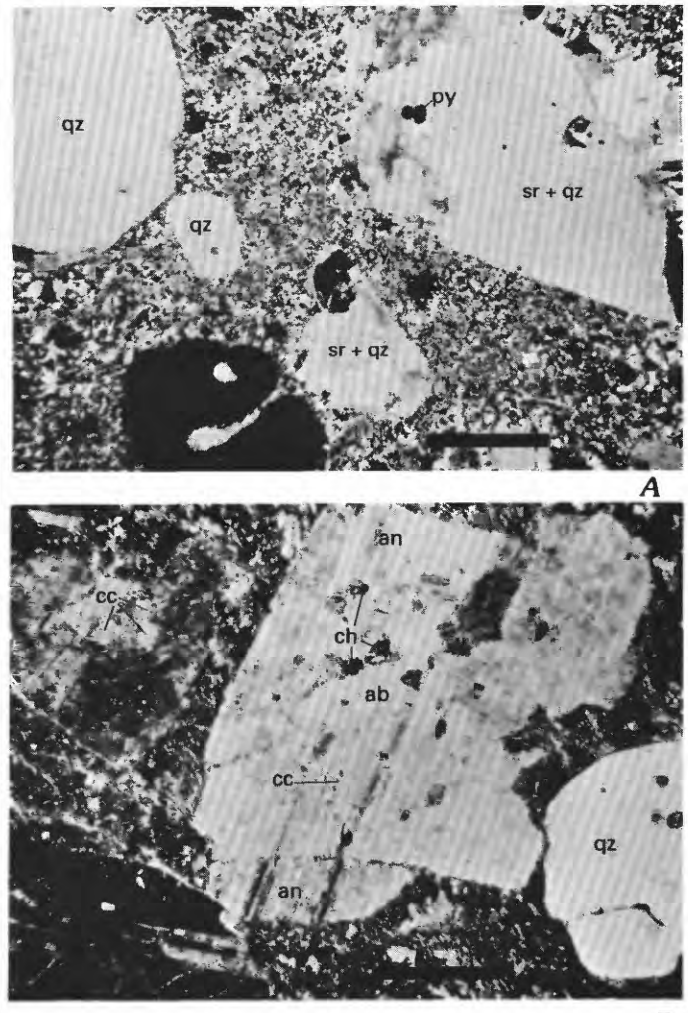

FIGURE 7.10.—Photomicrographs of altered quartz-feldspar porphyry samples of Red Ledge rhyolite unit. Crossed nicols. *A*, sericite type of phyllic alteration showing sericite(sr)+quartz(qz)+pyrite(py) aggregates (pseudomorphic after tabular plagioclase phenocrysts) and embayed and marginally recrystallized quartz (qz) phenocrysts. Black quartz crystal at lower left is at extinction. *B*, Propylitic assemblage with andesine (an) phenocrysts partially replaced by albite (ab), calcite (cc), and chlorite (ch). Bar is 1 mm long.

features of plagioclase feldspar, and relative distribution of the three inner assemblages closely resemble those of the silicic, phyllic, and propylitic assemblages, respectively, of the Red Ledge deposit. However, at the Red Ledge deposit clay minerals are not abundant in the propylitic zone, and a peripheral zone of zeolitic alteration has not been recognized. Zeolite and clay minerals, if originally present, were probably completely or partially destroyed during metamorphism to the greenschist facies.

Sporadically distributed alteration assemblages are present at the Red Ledge deposit. Hematitic alteration, characterized by disseminated hematite±calcite±barite, is found locally in the upper part of the stockwork system and in the overlying capping zone. It occurs as isolated patches and as selvages to hematite-barite-chlorite veins. Hematite of these mineralogical associations is distinct from the disseminated variety that forms irregular discordant zones in Permian and Triassic rocks and from another variety that forms the cement in some Triassic sandstones. The latter two types of hematite probably formed from oxidizing solutions produced during diagenesis of the sedimentary rocks and solidification of the volcanic rocks, whereas the hematite variously associated with calcite, barite, and chlorite formed from oxidizing solutions of hydrothermal origin.

Stratigraphic units characterized by abundant chlorite are spatially associated with some layers of massive sulfides. These rocks consist of generally predominant ferromagnesian chlorite, highly variable amounts of sericite, and subordinate quantities of hematite, barite, and quartz. They formed through the alteration of tuffaceous sediment to chlorite, sericite, and quartz and from the hydrothermal precipitation of hematite, barite, and quartz. These variable mixtures of altered rocks and chemical precipitates are interpreted as tuffaceous exhalites.

GEOCHEMISTRY

Representative samples of altered volcanic rocks in the Red Ledge area were analyzed for major, minor, and selected trace elements to geochemically characterize the different alteration assemblages and to establish the chemical, mass, and volume changes imposed by hydrothermal alteration. The mineralogy, alteration assemblages, and textural features of the samples analyzed are presented in table 7.1, and their chemical compositions and specific gravities are given in table 7.2. A qualitative evaluation of these mineralogical and geochemical data suggest that they reflect primary magmatic differences between the major rock types and (or) the influence of hydrothermal processes. The weakly altered (propylitized) felsic rocks are enriched in SiO_2 and depleted in TiO_2, FeO, and MgO relative to their mafic and intermediate counterparts; these differences are consistent with the more differentiated composition of the felsic rocks. Moreover, concentrations of K_2O and MgO apparently reflect the abundance of hydrothermal sericite and chlorite, respectively, in the altered felsic porphyries as well as primary differences between felsic and mafic rocks. By contrast, variations in Na_2O, CaO, and CO_2 concentrations are apparently related only to the hydrothermal effects of plagioclase feldspar replacement and calcite precipitation and not to igneous parentage. The tuffaceous exhalites are notable for their marked depletion in SiO_2 and enrichment in total iron, H_2O^+, and Ba relative to other rock types. The composition of the Cordwood rhyolite unit may reflect a slightly higher degree of magmatic differentiation than that of the quartz-feldspar porphyry of the Red Ledge domal complex.

MASS TRANSFER

The quantitative assessment of mass transfer (and volume changes) in an altered rock is possible if the composition of the protolith is known and if it can be demonstrated that at least one component was immobile or that constant volume (or mass) was maintained (Gresens, 1967). Unfortunately, unaltered and unmetamorphosed protoliths of the Red Ledge rock types are not available and a determination of constant volume would necessarily be based on qualitative textural criteria. Consequently, the evaluation of mass transfer was performed by establishing the least mobile components and estimating a protolith composition of the quartz-feldspar and quartz porphyries of the Red Ledge rhyolite unit. Restricting the evaluation to these closely related rock types minimized the effects of primary lithologic differences on chemical composition.

Gresens (1967) noted that the ratio of two immobile components in an altered rock will be the same as that for the parent rock even though the concentrations of both components may have varied due to changes in rock mass resulting from the addition or subtraction of mobile components. Immobile components will be diluted with a gain of rock mass and residually concentrated with a loss of rock mass and, therefore, exhibit a decrease and increase, respectively, in their concentrations reported as a fraction of the sample weight (weight percent or parts per million). Finlow-Bates and Stumpfl (1981) and MacLean and Kranidiotis (1987) pointed out that this relationship can be illustrated graphically (fig. 7.11*A*), where

TABLE 7.1.—*Mineralogy, alteration assemblages, and textures of geochemically analyzed host rocks, Red Ledge deposit, Idaho*

[Modal estimates in volume percent exclusive of veins; Tr, trace; --, not present. Phenocrysts: Qz, quartz; Pl, partially altered andesine. Secondary minerals: Qz+Ab, quartz+albite; Ch, chlorite; Cc, calcite; Sr, sericite; Ep, epidote group; Ba, barite; Py, pyrite; Cl, clay. Minor accessories include rutile, zircon, hematite. Alteration assemblages: CH, chloritic; PR propylitic; S, silicic; SC, sericite-chlorite; SR, sericite. Textures: A, amygdules of calcite, chlorite, quartz; F, weakly foliated; FM, Fe-Mg chlorite; M, Mg chlorite; MF, Mg-Fe chlorite; PS, pressure shadows of sericite or quartz around quartz phenocrysts and pyrite euhedra; S, minor shearing; V, veins of quartz±carbonate±gypsum, calcite, chlorite, sericite]

Sample number	Field number	Phenocrysts		Secondary minerals								Alteration assemblage	Textures
		Qz	Pl	Qz+Ab	Ch	Cc	Sr	Ep	Ba	Py	Cl		
Quartz-feldspar porphyry and quartz porphyry phases													
1	RL4-79	15	20	20	10	2	18	6	--	6	3	PR	F, M
2	TG20-570	25	25	23	2	5	10	--	--	--	3	PR	V, FM
3	TG13-597	20	25	30	6	15	5	--	--	1	1	PR	F, V, MF
4	TG14-472	12	5	55	2	13	10	--	--	3	2	PR	F, V
5	TG3-239	22	--	45	5	--	15	--	2	2	1	PR	V, S, PS, M
6	TG10-259	15	--	45	10	Tr	20	Tr	Tr	4	1	SC	F, V, M
7	TG17-182	20	--	50	5	--	15	2	--	7	--	SC	S, PS, M
8	TG10-639	25	--	35	7	--	25	--	--	5	--	SC	F, V, PS, M
9	TG16-130	10	--	70	3	Tr	14	--	--	3	--	SC	V, M
10	RL72-141*	20	--	45	--	--	30	--	1	3	--	SR	V
11	TG1-523	20	--	55	--	--	20	--	--	2	--	SR	F, V
12	TG7-45	15	--	60	--	--	15	--	3	7	--	S	V, PS
Felsic tuff													
13	TG5-1287	--	--	50	Tr	--	40	--	--	5	Tr	SR	F, PS, M
14	RLC2-500	--	--	70	--	--	30	--	--	1	Tr	SR	F, PS
15	TG2-1519	--	--	55	--	--	25	--	2	7	--	SR	F, V, S
Intermediate tuff													
16	TG1-1494	--	--	50	8	7	25	1	--	2	1	PR	M
Mafic flows													
17	RL2-81	--	12	15	20	35	10	--	--	--	4	PR	V, A, PS, M
18	TG10-1761	-	--	55	10	25	3	--	--	--	5	PR	A, V, FM
Tuffaceous exhalites													
19	TG9-1332	--	--	5	25	--	50	--	Tr	--	10	CH	FM
20	RL5-79	--	--	15	60	--	--	--	10	--	--	CH	FM
Cordwood rhyolite unit													
21	TG19-622	--	5	65	--	20	7	--	--	--	1	PR	F, V

*Sample collected by R.C. Long.

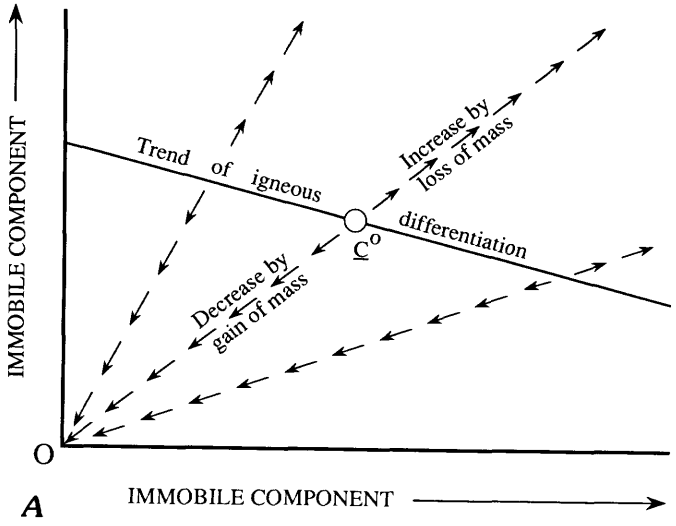

FIGURE 7.11.—Alteration trends of immobile and mobile chemical components (trends shown by dashed lines composed of arrows). *A*, Alteration trends of two immobile components that pass through primary compositions (such as *C*°) on igneous-differentiation trend and through origin (O) (modified from Finlow-Bates and Stumpfl, 1981; MacLean and Kranidiotis, 1987). Such trends are generated by an increase or decrease in concentrations (based on sample weight) of components as a result of net loss or gain, respectively, of rock mass due to mobility of other components. *B*, Possible trends for mobile-immobile pair (modified from MacLean and Kranidiotis, 1987): *C*°A or *C*°B by gain or loss, respectively, of mobile component at constant rock mass; *C*°D and *C*°E by the sympathetic gain or loss of a mobile component and rock mass; *C*°F and *C*°G by antithetic gain or loss of mobile component and rock mass; and *C*°BO and *C*°BH by loss of mobile component at constant mass followed by immobile behavior during gain or loss of rock mass. Figure continues on page 136.

TABLE 7.2.—*Major-, minor-, and trace-element compositions and specific gravities*

[See Table 7.1 for corresponding field numbers, mineralogy, and textures. Data for sample 10 from Long (1975). SG, specific gravity; Tr, trace; ---, not analyzed; <, below detection Sr, Y, Zr, and Nb determined by X-ray fluorescence spectroscopy. Most other trace-element abundances determined by induction-coupled plasma spectroscopy; Sc and Zn Analytical uncertainties for these values are reported by Baedecker and McKown (1987), Jackson and others (1987), Lichte and others (1987), and Taggart and others (1987)]

	Quartz-feldspar and quartz porphyries											
Sample number	1	2	3	4	5	6	7	8	9	10	11	12
	Major and minor oxides, in weight percent											
SiO_2	67.2	68.7	71.4	66.7	70.9	68.8	73.2	62.2	77.5	80.82	69.8	74.8
TiO_2	.50	.39	.39	.37	.49	.50	.39	.38	.30	.34	.39	.19
Al_2O_3	15.3	13.4	12.4	11.7	15.3	16.5	12.2	19.6	9.76	9.85	13.4	6.08
Fe_2O_3	1.93	1.20	.36	2.01	1.77	1.77	4.55	3.67	4.00	2.41	3.50	6.49
FeO	2.25	1.64	2.00	1.14	.92	.36	.20	.52	.49	.34	.54	.15
MnO	< .02	.19	.08	.12	.02	< .02	< .02	.04	.02	Tr	.05	< .01
MgO	3.22	.84	1.22	1.29	2.66	3.35	1.24	2.3	1.0	.07	1.4	.10
CaO	3.51	3.32	3.05	4.87	.20	.34	.23	.43	.20	.10	1.33	.04
Na_2O	1.90	3.95	3.94	1.65	.34	.58	.28	.43	.28	.41	.39	.20
K_2O	1.32	1.63	.90	2.27	3.34	2.70	2.45	4.73	2.18	1.74	3.30	1.38
P_2O_5	.10	.09	.08	.09	.12	.09	.09	.11	.04	.07	.09	< .02
H_2O+	2.40	1.25	1.42	1.30	2.74	3.25	2.01	2.93	1.68	2.94	1.97	.93
CO_2	.26	2.88	2.21	5.42	.03	< .01	< .01	.56	.16	---	1.74	.07
Total	99.91	99.48	99.45	98.93	98.83	98.27	96.87	97.90	97.61	99.09	97.90	90.46
	Trace elements, in parts per million											
Li	27	32	13	< 4	< 4	8	< 4	---	---	---	---	---
Ba	617	446	190	460	454	607	5,000	1,600	850	---	770	21,700
Rb	17	25	13	31	50	38	32	68	30	---	46	20
Sr	237	138	101	88	21	61	61	50	34	---	46	220
Sc	9	8	8	7	9	9	7	7.6	5.7	---	8.5	4.2
Y	22	24	21	23	26	29	18	26	14	---	14	14
Zr	201	169	177	175	213	246	173	190	130	---	170	85
V	53	46	32	41	47	44	36	32	30	---	44	39
Nb	6	6	7	6	7	6	6	< 10	<10	---	< 10	< 10
Mo	< 4	< 4	< 4	6	< 4	5	< 4	---	---	---	---	---
Cr	14	9	4	4	4	4	3	2	2	---	2	4
Co	7	5	5	9	6	7	5	5	11	---	8	15
Ni	< 4	5	4	< 4	< 4	< 4	< 4	< 2	3	---	< 2	9
Cu	23	27	48	23	290	36	170	93	1,960	135	2,930	885
Zn	70	50	50	< 40	120	150	50	150	135	10	53	5,240
Pb	20	10	< 8	8	< 8	15	< 8	18	11	20	10	36
Ga	17	12	16	16	19	15	14	---	---	---	---	---
As	< 20	< 20	< 20	< 20	< 20	< 20	< 20	---	---	---	---	---
SG	2.73	2.69	2.68	2.72	2.74	2.70	2.75	2.77	2.82	2.62	2.78	2.91

changes in rock mass cause the concentrations of two immobile components to deviate from primary values along a trend of constant positive slope that projects to the origin. Such a trend may be produced by a group of variably altered rocks derived from the same protolith. Alternatively, similar trends are generated if two mobile components were added to or extracted from such a group of altered rocks in constant proportion. However, this latter situation is generally fortuitous and particularly unlikely for components of dissimilar geochemical behavior.

MacLean and Kranidiotis (1987) also presented several possible alteration trends produced by plotting a mobile component against an immobile component

of host rocks, Red Ledge deposit, Idaho

limit shown; >, above detection limit shown. FeO determined by wet chemical methods; all other major oxides and Ba, Rb, for samples 8, 9, 11, 12, 13, and 14 determined by neutron activation analysis. Analyses performed at U.S. Geological Survey.

Felsic tuff		Intermediate tuff		Mafic flows		Tuffaceous exhalites		Cordwood rhyolite unit
13	14	15	16	17	18	19	20	21
Major and minor oxides, in weight percent—Continued								
59.5	73.2	72.6	60.4	45.4	49.9	35.9	26.9	74.3
.94	.45	.89	1.00	1.17	1.91	2.52	.65	.21
18.8	14.9	14.5	17.9	18.1	14.7	30.0	15.7	13.1
7.14	3.42	3.43	2.68	1.12	1.1	1.5	16.8	.65
.39	.03	.02	2.58	7.28	10.9	11.8	23.3	.61
.01	< .01	< .02	.13	.17	.21	.07	.09	.07
.88	.15	.12	3.48	8.55	4.16	4.09	3.64	.86
.28	.17	.24	.96	4.61	4.99	.81	.17	1.49
.39	.50	.63	.27	2.62	.42	1.97	.16	3.45
4.91	3.11	3.15	3.93	.87	1.24	2.32	.03	2.23
.16	.10	.18	.23	.23	.22	.43	.21	.08
2.72	1.96	1.86	3.68	5.76	5.01	7.08	7.30	.95
.76	.06	< .01	1.02	3.16	4.98	.09	.01	1.91
96.88	98.06	97.65	98.26	99.04	99.74	98.58	94.96	99.91
Trace elements, in parts per million—Continued								
---	---	< 4	< 4	53	57	59	58	< 4
1,100	830	1,280	1,700	1,310	1,570	3,990	> 23,500	216
62	44	35	60	16	19	41	34	25
45	74	149	41	134	48	256	762	100
24.7	10.0	8	23	36	45	60	7	< 4
25	10	18	40	21	31	33	9	30
120	125	166	124	90	104	158	119	140
191	40	69	210	280	450	540	92	5
< 10	< 10	7	10	9	8	12	5	9
---	---	6	6	< 4	< 4	< 4	12	< 4
15	3	< 2	28	470	11	480	11	< 2
31	7	18	25	37	38	31	130	< 2
13	3	< 4	7	150	15	92	28	< 4
35	49	66	54	52	17	7	29	< 2
53	18	< 40	60	60	100	< 40	< 40	< 40
8	24	15	9	18	29	57	10	< 8
---	---	15	20	23	19	32	<8	15
---	---	< 20	30	< 20	< 20	20	< 20	< 20
2.86	2.75	2.73	2.81	2.72	2.82	2.92	3.24	2.69

(fig. 7.11*B*). Several of these trends are depicted by the Red Ledge data. Regardless of whether one or both components are immobile, the alteration trends include or can be extrapolated to primary concentrations. Thus, the intersection of these alteration trends with a supposed igneous-differentiation trend can provide a means of estimating protolith compositions.

Binary plots involving the Al_2O_3, TiO_2, Zr, and Y concentrations of the altered quartz-feldspar and quartz porphyries show well-defined alteration trends of positive slope that project to points near the origin. Correlation coefficients and axis intercepts of regression lines for each trend are listed in table 7.3. The oxide TiO_2 is highly correlated ($r>0.95$) with Zr

in the sample suite and, if sample 8 is excluded because of its anomalous Al_2O_3 content (19.6 weight percent), both TiO_2 and Zr are highly correlated ($r>0.96$) with Al_2O_3. Therefore, it is probable that TiO_2, Zr, and Al_2O_3 were essentially immobile during the alteration of the quartz-feldspar and quartz porphyries and that variations in their concentrations are largely the result of the dilution or residual concentration accompanying the net addition or subtraction of other components, respectively.

Plots of the major oxides and Zr versus the immobile oxide TiO_2 for the quartz-feldspar and quartz porphyries reveal a generally consistent clustering of samples by alteration assemblage and three possible patterns of alteration trends (fig. 7.12). One pattern is exemplified by the plots of Al_2O_3 and Zr versus TiO_2 and, as noted previously, consists of a single well-defined trend of positive slope that projects to points near the origin (fig. 7.12*A*). This pattern indicates a high degree of component immobility. A second pattern is characterized by a trend of near-vertical orientation that intersects a trend of negative slope, as shown by the SiO_2 and Fe_2O_3* (total iron as Fe_2O_3) data (fig. 7.12*B*). The near-vertical trend implies that SiO_2 and Fe_2O_3* were added to or leached from some samples with little change in rock mass, whereas the trend of negative slope implies a sympathetic gain or loss of rock mass and SiO_2 and Fe_2O_3* for other samples. The third pattern is portrayed by plots of MgO, CaO, Na_2O, and K_2O versus TiO_2 and consists of a positively sloping trend that intersects one of near-vertical orientation (fig. 7.12*C*). The trend of positive slope for the MgO versus TiO_2 data does not project toward the origin and suggests an antithetic gain or loss of MgO and rock mass,

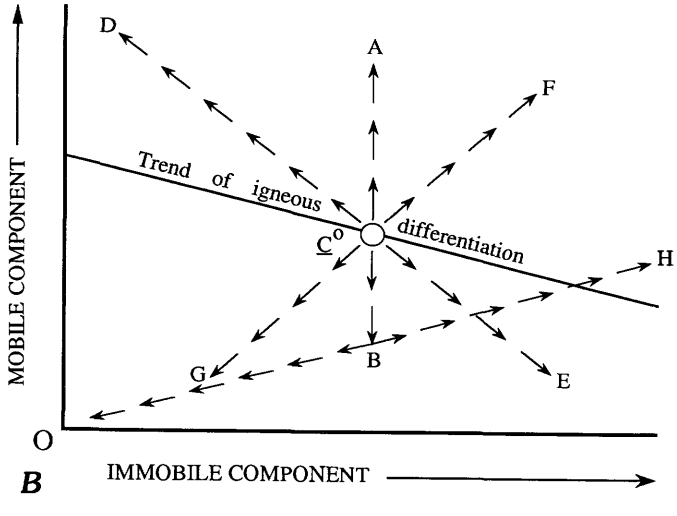

FIGURE 7.11.—Continued.

TABLE 7.3.—*Regression-line correlation coefficients and axis intercepts for paired immobile chemical components in quartz-feldspar and quartz porphyries of Red Ledge rhyolite unit*

[*r*, correlation coefficient; *x* and *y*, regression variables. Units for *y*-axis intercepts (*y* at $x = 0$): ppm, parts per million; wt pct, weight percent]

Components			
x	*y*	*r*	*y*(*x*=0)
TiO_2 -------	Zr ----------	.953	4.1 (ppm)
Al_2O_3 -----	Zr ----------	.842	44.3 (ppm)
Y ----------	Zr ----------	.818	40.3 (ppm)
TiO_2 -------	Al_2O_3 -----	.777	.9 (wt pct)
Al_2O_3 -----	Y ----------	.758	6.0 (ppm)
TiO_2 -------	[1]Al_2O_3 ----	.979	.08 (wt pct)
[1]Al_2O_3 ----	Zr ----------	.965	-2.4 (ppm)
[1]Al_2O_3 ----	Y ----------	.750	3.9 (ppm)

[1]Excluding sample 8 (see "Mass Transfer" section in text).

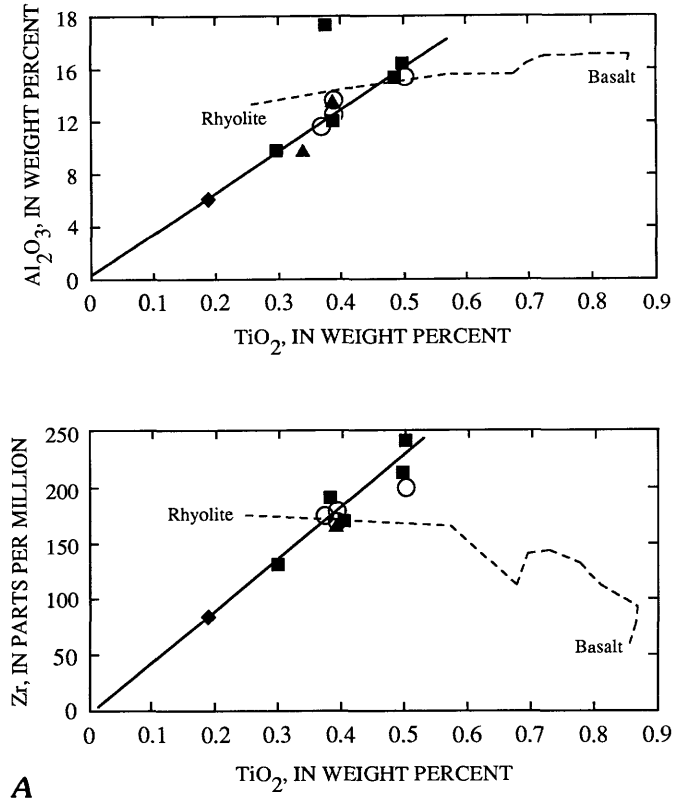

FIGURE 7.12.—Plots of major oxides and Zr versus TiO_2 showing alteration trends (solid lines) for altered quartz-feldspar and quartz porphyries of Red Ledge rhyolite unit: *A*, high degree of component immobility; *B*, component gain or loss with sympathetic change in rock mass; *C*, component immobility and (or) gain or loss with antithetic change in rock mass. Also shown are igneous-differentiation trends (dashed lines) for unaltered volcanic rocks from southwestern Pacific island arcs, based on data reported by Ewart (1979, 1982). Symbols for Red Ledge rocks indicate types of alteration assemblages: circle, propylitic; square, sericitic-chloritic; triangle, sericitic; and diamond, silicic. Fe_2O_3*, total Fe as Fe_2O_3.

whereas similar trends for CaO, Na_2O, and K_2O project to points near the origin and suggest that either these components were immobile or they varied antithetically with rock mass.

Basalt-rhyolite differentiation trends for unaltered island arc volcanic rocks in the southwestern Pacific are also shown in figure 7.12. These magmatic trendlines, based on data reported by Ewart (1979; 1982), represent low-K, calc-alkalic, and high-K volcanic rocks erupted in a variety of tectonic settings. They typically intersect the Red Ledge alteration trendlines near one of the data points representing propylitized quartz-feldspar porphyry (sample 2, table 7.1), which suggests that it is the least altered porphyry analyzed. Such an inference is supported by its mineralogy and its relatively distal sample locality. A comparison of the composition of this sample with that of a hypothetical protolith, estimated from the intersection of the magmatic and alteration trendlines shown in figure 7.12 and from reported data (Nockolds and others, 1978; Ewart, 1979; Byers and others, 1983), is presented in table 7.4. The abundances of SiO_2, TiO_2, Al_2O_3, Fe_2O_3*, Na_2O, and Zr in the hypothetical protolith are roughly similar to those in sample 2; protolith values range from 93 to

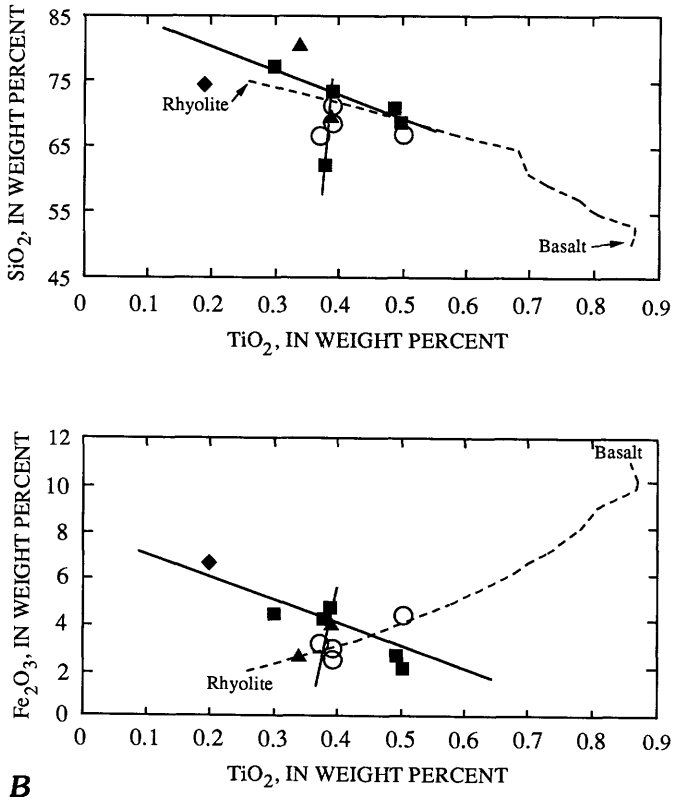

FIGURE 7.12.—Continued

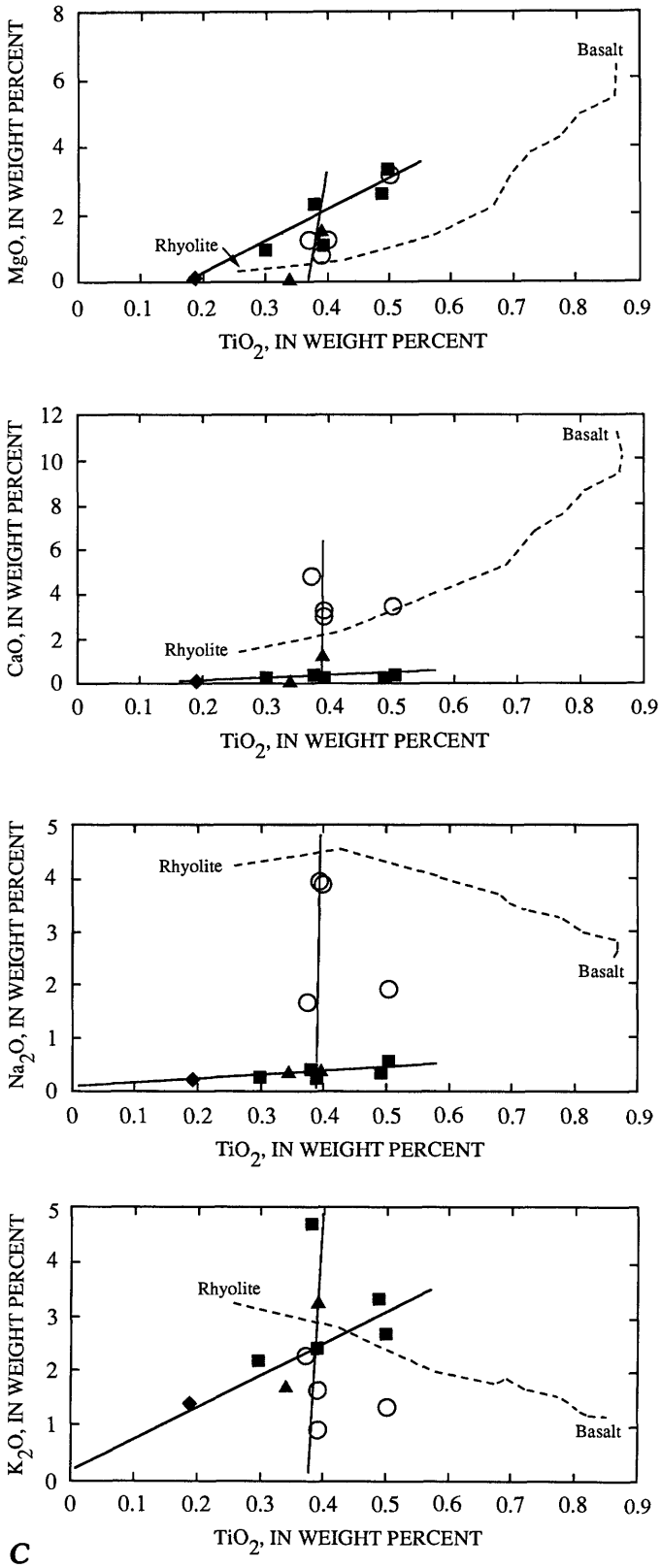

FIGURE 7.12.—Continued

TABLE 7.4.—*Compositions of hypothetical protolith and least altered sample of quartz-feldspar porphyry*

[Protolith values (normalized) estimated from intersection of igneous-differentiation trend and alteration trend lines in fig. 7.12 and from published data]

	Hypothetical protolith	[1]Quartz-feldspar porphyry
Major and minor oxides, in weight percent		
SiO_2	71.1	68.7
TiO_2	.39	.39
Al_2O_3	14.7	13.4
[2]Fe_2O_3	2.8	3.02
MnO	.10[3]	.19
MgO	.5	.84
CaO	2.1	3.32
Na_2O	4.5	3.95
K_2O	2.9	1.63
P_2O_5	.10[3]	.09
H_2O^+	.70[4]	1.25
CO_2	.10[5]	2.88
Total	99.99	99.66
Trace element, in parts per million		
Zr	172	169
Specific gravity		
	2.62[6]	2.69

[1]Sample 2, table 7.2.
[2]Total iron as Fe_2O_3.
[3]From Ewart (1979).
[4]From Nockolds and others (1978).
[5]From Byers and others (1983).
[6]From Longwell and others (1969).

114 percent of the sample 2 values. However, the abundances of MgO, CaO, H_2O^+, CO_2, and possibly MnO are significantly higher in sample 2 and must reflect, in part, the minor chloritization and carbonatization of this sample. Although weakly sericitized, sample 2 is apparently depleted in K_2O. This depletion might be the result of either the hydrothermal leaching of K_2O or an overestimate of its concentration in the protolith. However, an igneous trendline for low-K volcanic rocks from the southwestern Pacific island arcs does not intersect the K_2O alteration trendline, and using the trendlines for calc-alkalic and high-K volcanic rocks does not greatly change the estimated abundance of K_2O. Regardless of these uncertainties, the compositions of both sample 2 and the hypothetical protolith closely resemble that of calc-alkalic rhyodacite (68 to 73 percent SiO_2; <4 percent K_2O) from the southwestern Pacific islands (Ewart, 1979).

The mass gains and losses of components in samples of the Red Ledge rhyolite unit were calculated from the compositions of the altered rocks and hypothetical protolith by treating TiO_2 as an immobile component. The composition of the hypothetical protolith was used for these calculations because it resembles that of the least altered sample (sample 2, table 7.2) but does not reflect the geochemical effects of weak hydrothermal alteration. The mass of each component that would remain after the alteration of 100 g of rhyodacite protolith at constant TiO_2 was calculated, following the method of MacLean and Kranidiotis (1987), from the relationship:

$$M_i^a = (C_i^a / C_{TiO_2}^a) M_{TiO_2}^o \quad (1)$$

where M is the mass in grams and C is the concentration in weight percent of component i and TiO_2 for the protolith (o) and the altered rock (a). Note that the weight percent of a component in 100 g of protolith is equivalent to the amount of that component in grams. The results of these calculations for the major oxides and Zr and the final mass of the samples are presented in table 7.5. The relatively uniform abundances of Al_2O_3 and Zr in the samples (except sample 8) illustrate the general immobility of these components during alteration, whereas the variable abundances of all other components is indicative of chemical mobility. As a consequence of the mass transfer of most components, total rock mass also varies appreciably.

Estimates of the absolute gains and losses of major-oxide components in the quartz-feldspar and quartz porphyries were made by subtracting the component values for 100 g of hypothetical protolith (table 7.4) from the values for the altered rocks (table 7.5). The gains and losses in chemical components, total mass, and selected minerals for each sample are illustrated in figure 7.13. The samples in figure 7.13 are arranged by alteration assemblage, from propylitic (least altered) to silicic, and by the geochemical affinities suggested by the plotted data of figure 7.12. Accordingly, this illustration summarizes the lateral variations in mineralogy, rock mass, and geochemical fluxes with increasing proximity to the deposit. As noted previously, the variation of Al_2O_3 is minimal among the samples, except for sample 8, which shows a considerable (~37 percent) enrichment in Al_2O_3 relative to the hypothetical protolith. Predictably, variations in the absolute gains and losses of the most abundant component, silica, are closely matched by those in total rock mass. The transfer of other chemical components into or out of the porphyries may be expected to correlate with the distribution and relative abundance of specific minerals: MgO with chlorite, Fe_2O_3* with pyrite and chlorite,

TABLE 7.5.—*Abundance of chemical components in porphyries of Red Ledge rhyolite unit that would result from the alteration of 100 grams of hypothetical protolith at constant weight percent TiO_2*

[See table 7.1 for corresponding field numbers. Volume factor $=(\underline{C}^{o}_{TiO_2}/\underline{C}^{a}_{TiO_2})(\underline{SG}^{o}/\underline{SG})^{a}$, ratio of volume of altered rock (a) to volume of protolith (o). $\underline{C}_{TiO_2}$, concentration of TiO_2 in weight percent; SG, specific gravity. Tr, trace; ---, not analyzed; <, less than value shown]

Sample number	1	2	3	4	5	6	7	8	9	10	11	12
Major and minor oxides, in grams												
SiO_2	52.4	68.7	71.4	70.3	56.4	53.7	73.2	63.8	100.8	92.71	69.8	153.5
TiO_2	.39	.39	.39	.39	.39	.39	.39	.39	.39	.39	.39	.39
Al_2O_3	11.9	13.4	12.4	12.3	12.2	12.9	12.2	20.1	12.69	11.30	13.4	12.5
[1]Fe_2O_3	3.46	3.02	2.58	3.46	2.22	1.69	4.77	4.36	5.90	3.20	4.1	13.67
MnO	< .02	.19	.08	.13	.02	< .02	< .02	.04	.03	Tr	.05	< .02
MgO	2.51	.84	1.22	1.36	2.12	2.61	1.24	2.4	1.3	.08	1.4	.21
CaO	2.74	3.32	3.05	5.13	.16	.27	.23	.44	.26	.11	1.33	.08
Na_2O	1.48	3.95	3.94	1.74	.27	.45	.28	.44	.36	.47	.39	.41
K_2O	1.03	1.63	.90	2.39	2.66	2.11	2.45	4.85	2.83	2.00	3.30	2.83
P_2O_5	.08	.09	.08	.09	.10	.07	.09	.11	.05	.08	.09	< .04
H_2O^+	1.87	1.25	1.42	1.37	2.18	2.54	2.01	3.01	2.18	3.37	1.97	1.91
CO_2	.2	2.88	2.21	5.71	.02	< .01	< .01	.57	.21	—	1.74	.14
Total	78.08	99.66	99.67	104.37	78.74	76.76	96.89	100.51	127.00	113.71	97.96	185.70
Trace element, in parts per million												
Zr	157	169	177	184	170	192	173	195	169	—	170	174
Volume factor												
	0.75	0.97	0.98	1.05	0.76	0.76	0.95	0.97	1.21	1.15	0.94	1.85

[1] Total iron as Fe_2O_3.

K_2O with sericite, Na_2O with primary plagioclase feldspar, CaO with plagioclase feldspar and calcite, and CO_2 with calcite. Such general correlations are evident in the mineralogical and chemical data for the porphyries (fig. 7.13). Therefore, the mobility of most major oxide components was largely controlled by the formation or destruction of one or two minerals, which in turn can be expressed as a small number of alteration reactions.

Assuming that the alteration zones simultaneously advanced at their outer margins and retreated along their inner margins, then the rocks were sequentially altered in distinct stages. These stages, each characterized by a unique set of mineralogical and geochemical transformations, progressed from an initial propylitic stage, through sericite-chlorite and sericite stages, to a final stage of silicification. Thus, the general departure of the geochemical trends in figure 7.13 from the protolith composition represents the cumulative effect of as many as four stages of alteration, whereas the major inflections in the trends portray the relative geochemical variations between succeeding stages. Accordingly, an initial stage of alteration, represented by propylitized samples 2, 3, and 4, is characterized by minimal changes (<8 percent) in SiO_2 and Fe_2O_3*, increases in MgO (avg = 128 percent), CaO (avg = 83 percent), H_2O^+ (avg = 92 percent), and CO_2 (3500 percent), and decreases in Na_2O (avg = 29 percent) and K_2O (avg = 43 percent) relative to the hypothetical protolith. These enrichments and depletions are consistent with the partial chloritization, carbonatization, and sericitization (or illitization) of the plagioclase feldspar, groundmass, and perhaps a small amount of potassium feldspar (if originally present). Pertinent alteration reactions include the following:

$$\underset{\text{andesine}}{NaCaAl_3Si_5O_{16}} + 4(Mg,Fe)^{2+} + Fe^{3+} + 8H_2O \rightleftharpoons \underset{\text{chlorite}}{(Mg,Fe)_4^{2+}Fe^{3+}Al_3Si_2O_{10}(OH)_8} + \underset{\text{quartz}}{3SiO_2} + Na^+ + Ca^{2+} 8H^+ \quad (2)$$

and possibly

$$\underset{\text{K-feldspar}}{3KAlSi_3O_8} + 2H^+ \rightleftharpoons \underset{\text{sericite}}{KAl_3Si_3O_{10}(OH)_2} + \underset{\text{quartz}}{6SiO_2} + 2K^+. \quad (3)$$

Most of the Ca^{2+} ions released by reaction 2 were probably fixed in the calcite that replaced plagioclase

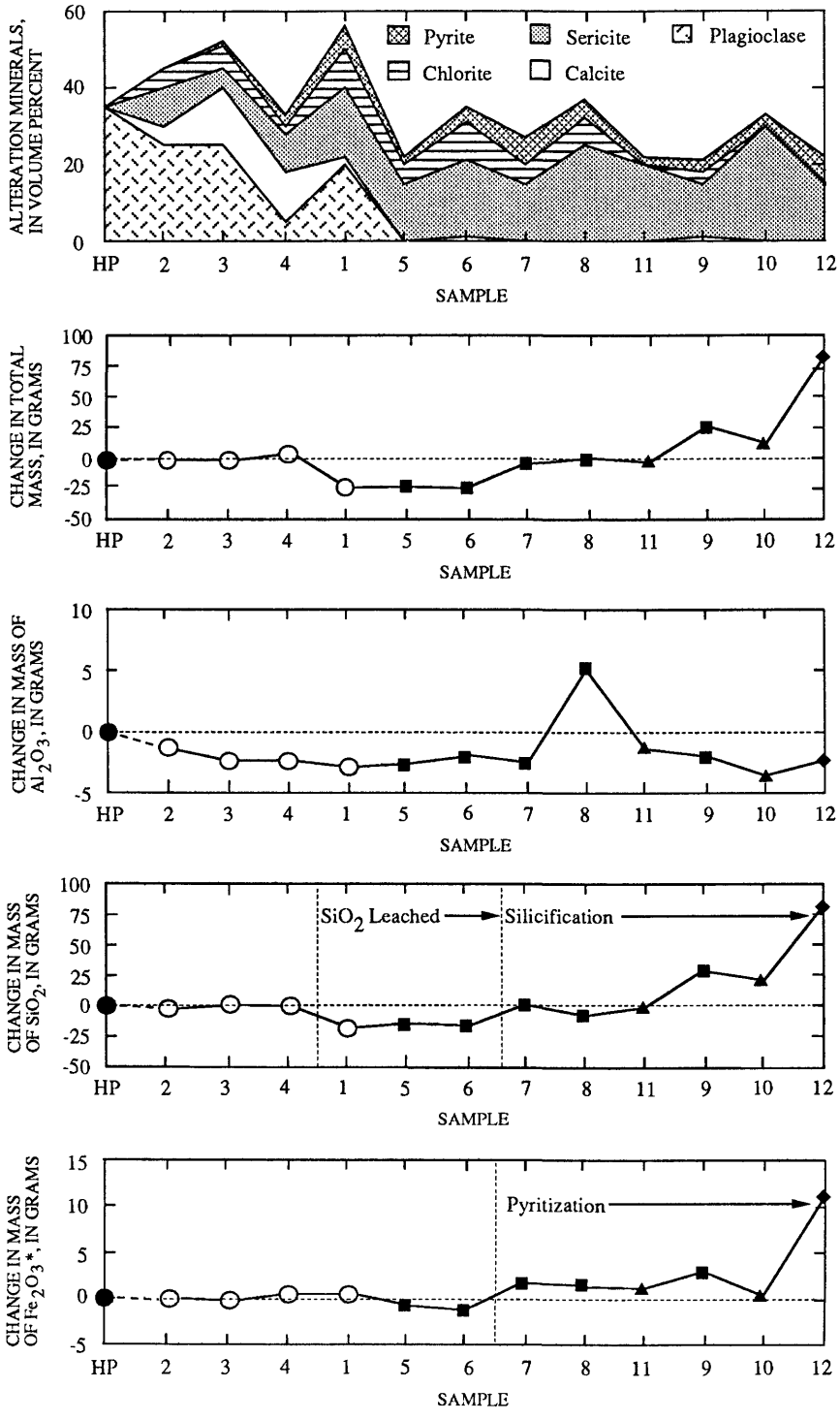

FIGURE 7.13.—Absolute gains and losses in grams of major oxides and of total mass for altered porphyries of Red Ledge rhyolite unit (samples 1–12) relative to 100 g of hypothetical protolith. Also shown (top, left) is relative abundance of some alteration minerals in samples. Samples are arranged by alteration assemblage, from propylitic (left) to silicic (right) and by coherency of geochemical behavior (see fig. 7.12). Solid circle represents hypothetical protolith (HP); dashed-line segment indicates supposed initial change in mass, and solid line represents successive mass changes for given component. For explanation of all other symbols see figure 7.12. Fe_2O_3*, total Fe as Fe_2O_3.

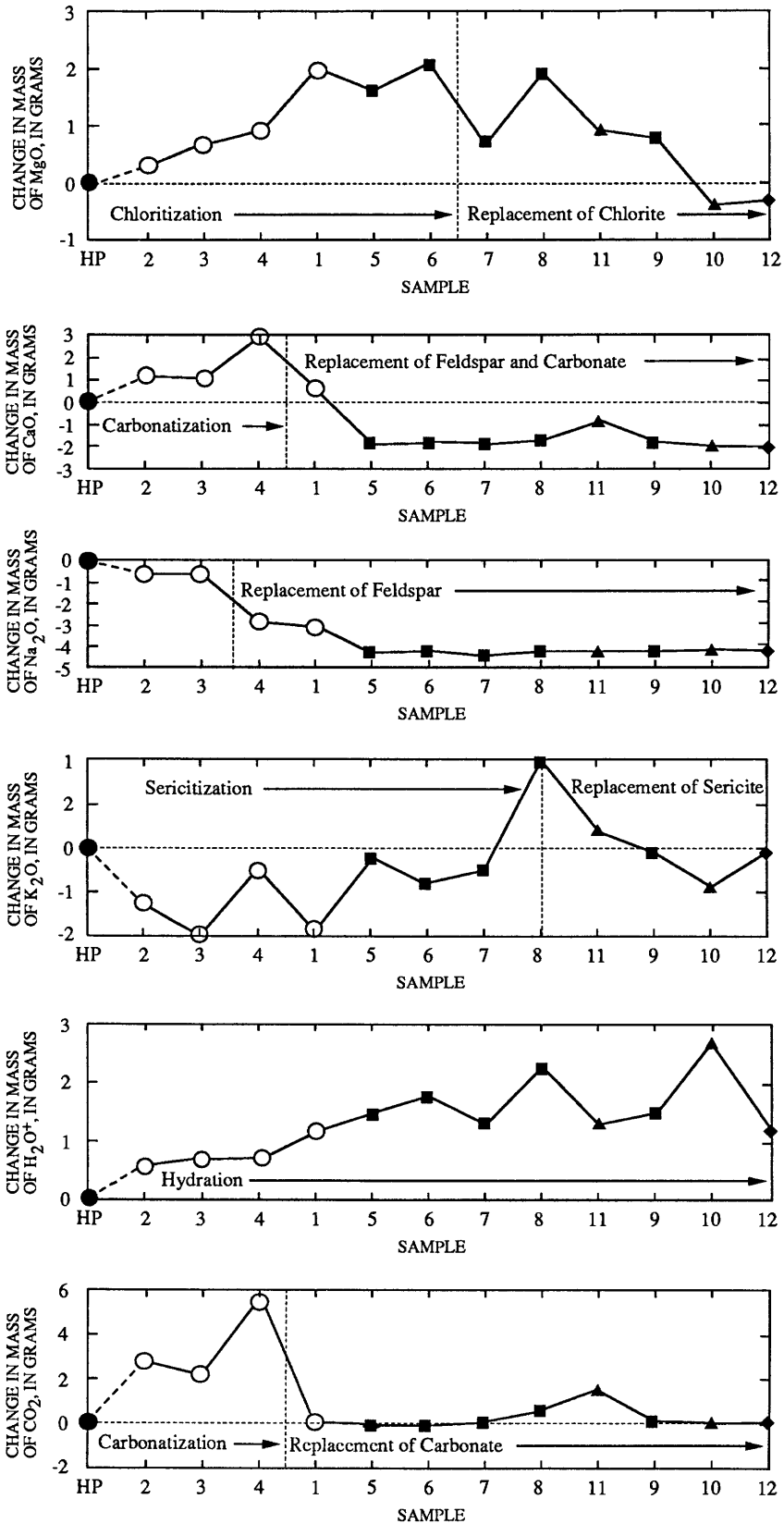

FIGURE 7.13.—Continued

feldspar and possibly in zeolites, and most of the released Na^+ ions were probably fixed in clays and zeolites. The K^+ ions generated by reaction 3 were removed in solution. Those components added to the rocks (MgO, CaO, H_2O^+, and CO_2) were derived from external sources and supplied to the reaction sites by the hydrothermal fluids. Apparently, the net mass loss accompanying mineral dissolution was essentially equal to the net mass gain accompanying mineral formation during propylitic alteration.

A succeeding stage of alteration is expressed by the general geochemical coherence of samples 1, 5 and 6 (fig. 7.13; fig. 7.12 at ~0.5 weight percent TiO_2) and apparently represents transformations that occurred in the outer part of the sericite-chlorite zone. This stage involved gains in MgO (avg = 111 percent), K_2O (18 percent), and H_2O^+ (avg = 63 percent), and losses of SiO_2 (avg = 23 percent) and Fe_2O_3* (avg = 19 percent) relative to the propylitic stage. Nearly all of the CaO, Na_2O, and CO_2 were removed from most of the rocks during this phase of alteration. Such geochemical transfers are largely consistent with the sericitization and continued chloritization of the host rocks and the total destruction of primary feldspar and secondary carbonate. Reaction equations 2 and 3 suggest that SiO_2 was released during alteration and precipitated as quartz. However, the net loss of SiO_2 indicated by the mass transfer calculations (fig. 7.13) implies that the formation of quartz was precluded.

A subsequent stage of alteration, characteristic of the inner part of the sericite-chlorite zone, is suggested by the plotted data for samples 7, 8, and 11 in figure 7.13. The compositions of these rocks shows the following changes relative to that of the rocks representing the preceding stage: an enrichment in SiO_2 (avg = 27 percent), Fe_2O_3* (avg = 79 percent), K_2O (avg = 83 percent), and H_2O^+ (avg = 6 percent), and a depletion in MgO (avg = 31 percent). Such gains and losses suggest that prograde alteration had proceeded to a stage of silicification, sericitization, pyritization, and the destruction of chlorite (at least the Mg-rich end member). Al_2O_3 was locally mobile (for example, in sample 8).

A final stage of alteration is inferred from the geochemistry of samples 9, 10, and 12, which are representative of the sericitic and silicic zones. These samples display an additional increase in SiO_2 (avg = 68 percent), Fe_2O_3* (avg = 72 percent), and H_2O^+ (avg = 7 percent), and an average depletion in MgO (avg = 68 percent) and K_2O (avg = 28 percent) to concentrations similar to or below that of the hypothetical rhyodacite protolith, respectively. The possible culmination of K_2O metasomatism after that of MgO metasomatism (fig. 7.13) suggests that some of the early formed chlorite in these rocks was later replaced by sericite—an inference supported by sparse paragenetic evidence. Replacement of chlorite by sericite may have taken place as follows:

$$2\underset{\text{chlorite}}{(Mg,Fe)_4^{2+}Fe^{3+}Al_3Si_3O_{10}(OH)_8} + 3Al^{3+} + 3Si(OH)_4 + 3K^+ + 2H^+ \rightleftharpoons 3\underset{\text{sericite}}{KAl_3Si_3O_{10}(OH)_2} + 8(Fe,Mg)^{2+} + 2Fe^{3+} + 12H_2O. \quad (4)$$

Note that this reaction consumes Al^{3+} and K^+ ions. These components possibly were derived from the conversion of sericite to quartz in host rocks undergoing silicification immediately adjacent to the hydrothermal conduits. The eventual conversion of sericite and all remaining chlorite to quartz would account for the late depletion in K_2O and MgO.

Clearly, the geochemical trends, as presented herein, are critically dependent on the assumed composition of the hypothetical protolith, immobility of TiO_2, and variability of primary TiO_2 concentrations. Analytical uncertainties for the component concentrations reported in table 7.2 are small (such as ±0.01 weight percent for TiO_2) relative to the chemical variations among the samples and thus have only a minor effect on the calculated results. The variability of TiO_2 in the protolith of the porphyries of the Red Ledge rhyolite unit is a potentially more significant problem but one that cannot be adequately assessed because of the lack of unaltered and unmetamorphosed rocks near the deposit.

The compositional similarity between the hypothetical protolith and the least altered of the porphyries (sample 2) suggests that the calculated results would not differ appreciably regardless of which one was used as a reference for comparison. If volatiles (CO_2 and H_2O^+) are excluded from the comparison, the principal differences in using sample 2 as the protolith are manifested in the calculated fluxes of MgO and K_2O; the magnitude of MgO enrichment and K_2O depletion would be diminished by 68 and 56 percent, respectively, whereas the magnitude of MgO depletion and K_2O enrichment would be commensurately enhanced by 68 and 56 percent, respectively. Nevertheless, the relative geochemical variations among the samples are nearly identical for either approximation of the protolith composition. Moreover, mass transfer calculations based on the conservation of volume, rather than TiO_2, result in grossly similar patterns of geochemical variations, even though the

calculated values for the gains and losses of most components differ appreciably from those plotted in figure 7.13. These comparisons strongly suggest that the geochemical trends and magnitudes of mass transfer proposed in this study primarily reflect the compositional differences among the porphyry samples, which, in turn, are largely the result of hydrothermal alteration.

VOLUME CHANGES

The considerable changes in rock mass that resulted from hydrothermal alteration at the Red Ledge deposit imply that the altered rocks also underwent considerable changes in volume. Using the established immobility of TiO_2 and specific gravities of the rocks, the change in volume for 100 g of hypothetical protolith can be calculated from the following relationship (modified after Gresens, 1967):

$$F_v = (C^o_{TiO_2}/C^a_{TiO_2})\,(SG^o/SG^a) \qquad (5)$$

where Fv is the volume factor or ratio of the volume of the altered rock (a) to that of the protolith (o), C_{TiO_2} is the concentration of TiO_2 in weight percent, and SG is the specific gravity. Note that when Fv>1, alteration resulted in a volume gain, whereas when Fv<1, alteration resulted in a volume loss. The calculated volume factors (Fv) for the Red Ledge rhyolite unit are presented in table 7.5. They were based on an assumed specific gravity of 2.62 for the hypothetical protolith. The results indicate that there was little volume change (3 percent loss to 5 percent gain) for propylitic samples 2, 3, and 4, a moderate volume reduction (24–25 percent) for propylitic sample 1 and sericitic-chloritic samples 5 and 6, a minor net volume reduction (3-6 percent) for sericitic-chloritic samples 7 and 8 and sericitic sample 11, a moderate net volume increase (15-21 percent) for sericitic-chloritic sample 9 and sericitic sample 10, and a large net volume increase (85 percent) for silicic sample 12. Although the accuracy of these values may be influenced by several uncertainties, particularly those regarding the protolith composition, it is likely that Fv values outside the range of 0.85 to 1.15 reflect the direction and magnitude of actual changes in rock volume.

The apparent changes in volume could have been produced by any of several possible mechanisms. For a given mass of rock (for example, 100 g), fracturing results in a decrease in specific gravity at a constant concentration (for example, weight percent) of an immobile component. Calculation of Fv by equation 5 would indicate the actual volume increase. Subsequent mineral deposition in the fractures would cause a proportionally antithetic change in specific gravity and concentration of an immobile component such that the calculated Fv would not vary further. The creation of secondary porosity by chemical processes, such as hydrothermal leaching or replacement, does not produce a change in the calculated volume factor, regardless of whether or not the voids were later filled. Most samples of the Red Ledge rhyolite unit have higher specific gravities than either the hypothetical protolith (assumed SG=2.62) or the least altered equivalent, sample 2 (SG=2.69). Consequently, the increases in volume and specific gravity inferred for some samples probably resulted from fracturing and the filling of fractures with minerals of relatively high density (for example, barite and sulfides). The large volume factors calculated for samples 9, 10, and 12 (table 7.5) imply that the abundance of fractures was generally greatest in the sericitized and silicified rocks proximal to mineralization.

Mechanisms that result in a reduction of volume, as implied for samples 1, 5, and 6 (table 7.5), are less certain. If these samples were characterized by primary porosities higher than that of an assumed protolith, then a collapse of the primary voids (such as by compaction) in these samples prior to alteration would result in specific gravities greater than that of the protolith. Because the concentrations of immobile components would not be affected by this mechanism, the calculated volume factors for these samples would be less than unity. By comparison, a collapse of secondary voids would result in a decrease of the Fv to values that approached, but were not less than, unity. Alternatively, the apparent volume reduction in these samples may be an artifact of different initial TiO_2 concentrations.

GENETIC MODEL

The available geologic and geochemical data on the Wallowa terrane, on the Hunsaker Creek Formation and host rocks, and on the mineralization of the Red Ledge area provide a basis for reconstructing the origin of the Red Ledge deposit. Rocks of the Hunsaker Creek Formation record an Early Permian (286-258 Ma) interval of subaerial and submarine bimodal explosive volcanism, reworking of volcanic detritus, and the localized development of volcanic domes. Volcanic activity and clastic deposition were punctuated by brief episodes of carbonate sedimentation. Such sequences are typical of oceanic back-arc tectonic settings, which in modern analogs are further characterized by block faulting, caldera formation,

and high heat flow. The combination of extensional tectonics, magmatism, and high heat flow are conducive to the formation of volcanogenic massive sulfide deposits (Kouda and Koide, 1978; Ohmoto, 1978; Scott, 1978).

The Red Ledge rhyolite unit represents a submarine dome complex of felsic composition that developed in and over a volcanic vent. Apparently, this area was near other active vents and offshore from a deeply eroded landmass (a continent?): The top part of the complex interfingers with extraneous volcanic rocks of largely mafic composition that include minor amounts of quartzose sandstone. The proximity of active vents may imply structural control by a deeply penetrating regional fault or fault zone. The dome grew by the repeated intrusion of sills and plugs, extrusion of stubby lava flows and small ash flows, and the accumulation of volcanic debris around the base of the dome. Mechanical breakdown of the dome was accomplished by differential movement between semiconsolidated masses, spalling of the dome and spires, phreatic explosions, and gravity slides. The constructive magmatic events are largely represented by the quartz-feldspar porphyry plugs and lava flows, whereas the destructive processes are manifested by the quartz porphyry breccias. Eventually the dome was buried by a sequence of interfingering felsic volcaniclastic rocks, mafic flows, and sedimentary rocks including a distinctive volcanic turbidite. Units in the lower part of this overlying sequence thin or pinch out near the apex of the dome. Magmatism in the Red Ledge area ended with the emplacement of the Cordwood rhyolite (felsite) unit and, subsequently, the porphyritic dikes.

The initiation of hydrothermal activity was centered on an area adjacent to and partially overlying the dome. Alteration preceded and overlapped the main interval of mineralization and, in the country rocks, produced prograde assemblages that grade upward and outward from a silicic zone proximal to the deposit, through sericitic and sericitic-chloritic zones, to a propylitic halo. These zones probably developed through the coalescence and expansion of alteration selvages that moved simultaneously away from fluid conduits by advancing at their outer margins and retreating along their inner margins. Accordingly, the altered rocks were affected by as many as four successive stages of mineralogical reactions. In the porphyries, the initial stage of propylitic alteration partially replaced plagioclase feldspar phenocrysts and groundmass with a secondary assemblage of sericite-albite-calcite-chlorite-pyrite±clay. Originally, zeolites may have been present and clays more abundant—as inferred from analogous Kuroko alteration assemblages. During subsequent greenschist facies metamorphism, the zeolites would have been destroyed and the clays greatly reduced in quantity. The succeeding sericitic-chloritic alteration converted all remaining primary feldspars and groundmass to an assemblage of sericite-chlorite-pyrite±clay. Sericitic alteration was produced by the conversion of chlorite to sericite and the formation of additional quantities of pyrite and minor clay. Silicification resulted in the precipitation of abundant quartz, partially as a replacement of sericite, the introduction of greater amounts of pyrite, and the formation of minor barite.

The sequential imposition of these mineralogical changes on the felsic rocks first involved gains in MgO, CaO, CO_2, and H_2O+ and a loss of K_2O and Na_2O during propylitic alteration. Propylitization was followed by a nearly complete loss of CaO, Na_2O, and CO_2, with the destruction of feldspar and carbonate, and a gain in K_2O and the culmination of MgO enrichment, with the formation of sericite and chlorite during sericitic-chloritic alteration. These reactions also resulted in a relative loss and then gain of SiO_2, Fe_2O_3*, and rock mass. With the successive sericitic- and silicic-alteration stages, first MgO and then K_2O were leached from the rock, whereas SiO_2 and total Fe commensurately increased. The mass transfer of these components occurred during the sequential replacement of chlorite by sericite and then sericite by quartz. The component H_2O+ increased while the components TiO_2, Al_2O_3, and Zr remained relatively immobile throughout prograde alteration.

The geochemical study of the Red Ledge host rocks suggests that hydrothermal alteration required a net gain of MgO, K_2O, H_2O+, and CO_2. Studies of experimental, natural, and theoretical seawater-rock interactions indicate that Si, Ca, K, Fe, Mn, Ba, Cu, Zn, and Ag are generally leached from and Mg added to rock reacted at temperatures of <100 to 500 °C and pressures of a few hundred bars (Mottl, 1983; Reed, 1983). Na is leached from reacted rock at water:rock ratios >10 and added to reacted rock at ratios <5 (Mottl, 1983). These results imply that many of the elements now enriched in the altered and mineralized rocks of the Red Ledge deposit were derived from the Hunsaker Creek Formation and older rocks during reactions with seawater. Convection of the seawater-hydrothermal fluids, initiated by magmatism in the Red Ledge area, supplied the chemical constituents to the site of the deposit which, in turn, formed the preserved mineral assemblages in response to the steep thermochemical gradients of the submarine hot-spring environment. Thus, of those components enriched in the Red Ledge deposit, it is likely that the hydrothermal fluids derived Ca, K, Si,

Ba, and many of the transition metals from the metamorphosed country rocks and Mg, SO_4, CO_2, and possibly some Ca directly from seawater.

The main period of hydrothermal mineralization was genetically related to the late stage development of the Red Ledge dome complex. This is particularly evident from the consistent and exclusive association of stringer sulfides with discrete beds of felsic breccia near the top of the complex. Such a relationship implies that mineralization was part of a general sequence of magmatic, tectonic, and hydrologic processes: (1) magma intrusion resulting in swelling and fracturing of the dome; (2) an explosion triggering event such as faulting which, in turn, caused dome failure (by landslides), the incursion of cold seawater into the dome, and possibly fluid boiling; (3) phreatic or phreatomagmatic explosions and deposition of felsic breccias and tuffs; and (4) initiation or rejuvenation of hydrothermal activity along fractures and in bedded breccias of the dome complex. Cyclic repetition of this sequence of events would account for the three or four stacked sets of stringer and massive sulfides. Each set originated through mineral precipitation in the permeable breccias blanketing the sea floor to form a strata-bound zone of stringer sulfides, and on the sea floor, particularly in depressions, to form an overlying or flanking massive sulfide layer. Cherty exhalite and tuffaceous exhalite were deposited during some cycles as the last, commonly distal, phase of mineral precipitation. The thin tuffs and sedimentary rocks that commonly overlie the sea floor precipitates record intervals of relatively quiet hydrothermal activity and dome development. The events leading to the formation of a mineralized set locally brecciated and veined previously formed sets. Explosive brecciation, in some instances, may have resulted from hydrothermal fluid overpressures generated by the sealing of the hydrothermal vent area with mineral-cemented volcaniclastic debris.

The stockwork system, consisting of three to four upward-branching en echelon zones of veins centered below the mineralized capping, represents the conduits along which the hydrothermal fluids ascended from depth to the sea floor. The fluids were expelled from several sites in an elongate, fault-controlled field of hot-spring vents (fig. 7.3). Each vein zone may have been produced by a discrete episode of fault movement and hydrothermal activity and may correspond to a set of stringer and massive sulfides. To tap the deeply convecting metal-rich fluids that were involved in mineralization, as discussed later, the fault movements must have been in response to regional stresses (for example, in a caldera setting). This hypothesis does not preclude the development of fractures by the compaction of porous volcaniclastic rocks around a rigid dome (see Reed, 1984), but it does minimize the importance of this mechanism to the mineralizing event.

Mineral deposition on and below the sea floor varied temporally and spatially in response to changing physical and chemical conditions during the ascent and venting of hydrothermal fluids. Stable-isotope data (Fifarek and others, 1984; Fifarek, 1985) suggest that the hydrothermal fluids evolved from seawater that had reacted with volcanic rocks during convection and then mixed with cooler and chemically more pristine seawater upon approaching the sea floor. A paragenetic trend in the $\delta^{18}O$ values of vein fluids is consistent with reaction at various temperatures and water-to-rock ratios (w/r): early fluids (~0 permil) at 250 to 275 °C and low w/r; intermediate fluids (4–6 permil) at ~450 °C and low w/r; and late fluids (0–1 permil) of weakly modified seawater at indeterminate temperature and high w/r. The ore-forming fluids of the intermediate stage apparently originated from deeply circulating seawater that had reacted with rocks at the temperature and w/r conditions most effective for leaching some metals, as inferred from experimental results (see Seyfried and Janecky, 1985). These fluids ascended to the site of the Red Ledge deposit and precipitated quartz, pyrite, and chalcopyrite in the center of the stockwork zone and near the vents on the sea floor. Conversely, barite, pyrite, sphalerite, galena, and tetrahedrite were deposited in more peripheral locations in both environments. Fifarek and others (1984) and Fifarek (1985) reported $\delta^{34}S$ values for sulfides (-0.6 to -9.5 permil) that support a derivation of sulfide sulfur by the inorganic reduction of Permian seawater sulfate ($\delta^{34}S$=10–12 permil). The $\delta^{34}S$ values of syngenetic barite (11.1–14.0 permil) imply a high component of seawater sulfate, whereas those of sulfates in stringer and vein mineralization (12.6–19.0 permil) suggest variable mixtures of seawater and hydrothermal sulfate. Similarly, the C and O isotopic compositions of the vein carbonates (-0.8 to -10.8 permil and 9.1 to 20.1 permil, respectively) suggest that carbonate formed from variable mixtures of seawater carbonate and hydrothermal carbon leached from the country rocks (Fifarek, 1985). These isotopic data indicate that the mixing of hydrothermal fluids and seawater at sites both below and above the sea floor was an important mechanism of mineral deposition.

The distribution and timing of deposition of these minerals is a function of the physiochemical conditions of the hydrothermal fluids as they relate to mineral solubilities, the kinetics of mineral precipitation, and the extent of chemical disequilibrium. Although a

detailed discussion of these parameters is beyond the scope of this study, the primary controls on mineral precipitation in volcanogenic massive sulfide deposits is briefly summarized from the relevant literature. Fluid-mineral equilibria indicate that the hydrothermal fluids were supersaturated with respect to both quartz and dolomite. However, the paucity of quartz in the massive sulfide layers of the Red Ledge deposit, relative to its predominance in the stockwork zone, is a consequence of a slow rate of precipitation from the vented fluids that were rapidly cooled to <250 °C (Reed, 1983). Quartz in massive sulfide zones characteristically occurs as a cement and apparently precipitated only after a thick, insulating sulfide-rich sediment had formed around the vents. The restriction of dolomite to veins also must be related to its slow rate of crystallization as well as to its retrograde solubility (Holland and Malinin, 1979). The deposition of barite is favored by decreasing temperatures (Holland and Malinin, 1979), particularly if cooling was produced by mixing with cold sulfate-rich seawater, as implied by the isotopic data. Such geochemical behavior may account for the generally peripheral distribution of barite in massive sulfides and its late appearance in the stockwork zone. Cooling was also the probable cause for the general distribution of sulfide minerals in the deposit. Sphalerite and galena, along with barite, most likely precipitated at cooler temperatures than did chalcopyrite. Moreover, with the accumulation of a sulfide mound and a rise in temperature at its base, chalcopyrite may then have replaced sphalerite and galena; such a paragenetic sequence would account for the encroachment of yellow ore on black ore, as proposed by Eldridge and others (1983) for the Kuroko deposits and as observed in black-smoker chimneys by Haymon and Kastner (1981) and Goldfarb and others (1983). Collectively, these primary controls account for the overall distribution of minerals in time and space and the zonation of economically important metals from a Cu core to a Zn-Pb±Ag periphery.

Soon after precipitation, the strata-bound sulfides were buried by volcanogenic and sedimentary rocks that effectively preserved the mineralization from sea-floor oxidation. Subsequently, the Cordwood rhyolite unit intruded this capping section and all rock types were propylitically altered by residual fluids related to the Red Ledge mineralization and (or) by fluids generated by emplacement of the felsite. A substantial thickness of Permian and Triassic volcanic-arc rocks were then deposited in the region. Burial resulted in the low-grade metamorphism of the Red Ledge deposit and the destruction of the presumed alteration halo of zeolite and clay minerals, recrystallization of some primary sulfide and silicate textures, and the modification of primary fluid inclusions. Accretion of the arc terrane to North America initiated an interval marked by intense deformation, low-grade metamorphism, uplift, intrusion of intermediate-composition plutons, and the complete resetting of the K-Ar systematics in sericite of the Red Ledge deposit as a consequence of heating to at least 270 °C. Flows of the Columbia River Basalt Group covered the area in the Miocene The present topography was created by block faulting, broad folding, and uplift accompanied by erosion.

In many respects, the geologic and geochemical features of the Red Ledge deposit and inferences about its origin are similar to those postulated in recent years for the Kuroko deposits. Major differences include the large size of the Red Ledge deposit, its metamorphic overprint, and its lack of bedded anhydrite. The size of this deposit appears to be the result of its association with a relatively large, composite felsic dome. That mineralization took place over an extended period is suggested by the presence of stacked sets of stringer and massive sulfides. Although this sequence of events may have resulted in abundant sulfide deposition, it was also economically deleterious in that metal grades for a significant part of the deposit were diminished by dilution with volcanic debris.

CONCLUSIONS

The major conclusions of this investigation regarding the character and origin of the Red Ledge deposit are summarized below:

1. The deposit formed on and immediately below the sea floor during Early Permian time in a volcanic-arc, probably back-arc, tectonic setting characterized by bimodal volcanism, extensional faulting, and high heat flow.
2. The deposit is characterized by three or four stacked sets of strata-bound stringer and stratiform massive sulfides that overlie a discordant zone of stockwork sulfides. Each set is associated with felsic volcaniclastic rocks produced by the explosive disintegration of a dome complex, and the stockwork mineralization occupies three to four en echelon fissures produced by movement along a fault system that controlled volcanism in the area. Metallization was in response to a repeated sequence of magma intrusion, rupturing of the dome by fault movement, phreatic and phreatomagmatic explosions, and hydrothermal activity. The character and proposed

origin of the Red Ledge deposit closely resemble those of the Kuroko deposits of Japan.

3. Mineral deposition in the stockwork zone temporally ranged from an amethyst quartz stage, through quartz-pyrite-chalcopyrite and barite±sphalerite±chalcopyrite stages, to a final carbonate±sulfide stage. In the stringer and massive sulfide zones, pyrite is early in the paragenetic sequence and is succeeded by other sulfides (chalcopyrite, sphalerite, and galena in uncertain order), quartz, and barite; carbonate is not associated with these stratabound sulfides. Superimposition of temporally and spatially distinct assemblages of sulfides and sulfates resulted in a zonation of metals from a Cu-rich core to a Zn-, Ag-, and Ba-enriched top and periphery.
4. Prograde alteration of the porphyry phases of the Red Ledge rhyolite unit resulted in a concentric and telescoped zonation of assemblages that grade outward from a silicic zone proximal to mineralization, through sericitic and sericitic-chloritic zones, to a propylitic halo. The mineralogy and relative position of these zones are similar to those reported for the unmetamorphosed Kuroko deposits except for the absence of an outermost zeolite assemblage, which, if originally present, was subsequently destroyed during regional metamorphism. The alteration assemblages most likely formed by simultaneously advancing along their outer margins and retreating along their inner margins away from fluid conduits. Thus, the rocks were sequentially altered in as many as four stages, each characterized by a different set of mineral reactions.
5. Geochemical data indicate that the altered porphyries were initially rhyodacitic in composition. The absolute quantities of TiO_2, Al_2O_3, and Zr in the porphyries remained relatively constant during alteration, whereas other components varied in mass with the imposition of each alteration assemblage. Propylitization resulted in an enrichment of MgO, CaO, H_2O+, and CO_2, and a depletion of K_2O and Na_2O. Sericitic-chloritic alteration produced additional gains in K_2O and H_2O+, the culmination of MgO enrichment, variable behavior of SiO_2, and the nearly complete loss of CaO, Na_2O, and CO_2. Finally, sericitic and silicic alteration involved relative gains in SiO_2 and total iron (as Fe_2O_3), a gain and then loss of K_2O, and the depletion of MgO. Both increases and decreases of rock volume were associated with these geochemical fluxes.
6. The hydrothermal fluids consisted of convected seawater that had been chemically modified during reactions with the country rocks. Those components enriched in the deposit were derived either from the country rocks by leaching (for example, Ca, K, Si, Ba, and metals) or from seawater (for example, Mg, S, and CO_2). Mineral deposition was initiated primarily by the thermal and chemical variations resulting from the mixing of hydrothermal fluids and seawater on and below the sea floor.
7. The deposit was eventually buried and metamorphosed to the greenschist facies, prior to the Late Triassic, and deformed, thermally metamorphosed at temperatures in excess of 270 °C, and uplifted during accretion of the volcanic arc to the North American craton by Early Cretaceous time. These events resulted in the rotation of the deposit approximately 90°, development of foliation and shear textures, recrystallization of sulfides and silicates, destruction of zeolite and some clay minerals in the altered host rocks, and the complete resetting of K-Ar systematics in hydrothermal sericite. The deposit was ultimately exhumed by erosion accompanying uplift of the region since Pliocene time.

REFERENCES CITED

Albee, A.L., 1962, Relationships between the mineral association, chemical composition, and physical properties of the chlorite series: American Mineralogist, v. 47, p. 851–870.

Armstrong, R.L., Taubeneck, W.H., and Hales, P.O., 1977, Rb-Sr and K-Ar geochronometry of Mesozoic granitic rocks and their Sr isotopic composition, Oregon, Washington, and Idaho: Geological Society of America Bulletin, v. 88, p. 397–411.

Avé Lallemant, H.G., in press, Pre-Cretaceous tectonic evolution of the Blue Mountains province, northeastern Oregon, *in* Vallier, T.L., and Brooks, H.C., eds., The Geology of the Blue Mountains region of Oregon, Idaho, and Washington: Petrology and tectonic evolution of pre-Tertiary rocks: U.S. Geological Survey Professional Paper 1438.

Baedecker, P.A., and McKown, D.M., 1987, Instrumental neutron activation analysis of geochemical samples, *in* Baedecker, P.A., ed., Methods for geochemical analysis: U.S. Geological Survey Bulletin 1770, p. H1–H14.

Barton, P.B., Jr., and Skinner, B.J., 1967, Sulfide mineral stabilities, *in* Barnes, H.L., ed., Geochemistry of hydrothermal ore deposits (1st ed.): New York, Holt, Rinehart, and Winston, p. 236–333.

Brooks, H.C., 1979, Plate tectonics and the geologic history of the Blue Mountains: Oregon Geology, v. 41, no. 5, p. 71–80.

Brooks, H.C., and Vallier, T.L., 1978, Mesozoic rocks and tectonic evolution of eastern Oregon and western Idaho, *in* Howell, D.G., and McDougall, K.A., eds., Mesozoic paleogeography of the Western United States (Pacific Coast Paleogeography Symposium 2): Los Angeles, Society of Economic Paleontologists and Mineralogists, Pacific Section, p. 133–146.

Byers, C.D., Muenow, D.W., and Garcia, M.O., 1983, Volatiles in basalts and andesites from the Galapagos spreading center, 85° to 86°W.: Geochimica et Cosmochimica Acta, v. 47, p. 1551–1558.

Cramer, R.S., 1982, Petrographic, fluid inclusion, and light stable isotope study of the Grey Eagle Cu-Au massive sulfide deposit, Siskiyou County, California: Davis, University of California, Master's thesis, 101 p.

Date, Jiro, Watanabe, Yoshihiro, and Saeki, Yuji, 1983, Zonal alteration around the Fukazawa Kuroko deposits, Akita Prefecture, northern Japan: Economic Geology Monograph 5, p. 365–386.

Derkey, R.E., 1982, Geology of the Silver Peak Mine, Douglas County, Oregon: Moscow, University of Idaho, Ph.D. dissertation, 188 p.

Dickinson, W.R., and Thayer, T.P., 1978, Paleogeographic and paleotectonic implications of Mesozoic stratigraphy and structure in the John Day inlier of central Oregon, *in* Howell, D.G., and McDougall, K.A., eds., Mesozoic paleogeography of the Western United States (Pacific Coast Paleogeography Symposium 2): Los Angeles, Society of Economic Paleontologists and Mineralogists, Pacific Section, p. 147–161.

Eastoe, C.J., and Nelson, S.E., 1988, A Permian Kuroko-type hydrothermal system, Afterthought-Ingot area, Shasta County, California: Lateral and vertical sections, and geochemical evolution: Economic Geology, v. 83, p. 588–605.

Eldridge, C.S., Barton, P.B., Jr., and Ohmoto, Hiroshi, 1983, Mineral textures and their bearing on formation of the Kuroko orebodies: Economic Geology Monograph 5, p. 241–281.

Ewart, Anthony, 1979, A review of the mineralogy and chemistry of Tertiary-Recent dacitic, latitic, rhyolitic, and related salic volcanic rocks, *in* Barker, Fred, ed., Trondhjemites, dacites, and related rocks: Amsterdam, Elsevier, p. 12–121.

———1982, The mineralogy and petrology of Tertiary-Recent orogenic volcanic rocks, with special reference to the andesitic-basaltic compositional range, *in* Thorpe, R.S., ed., Andesites—Orogenic andesites and related rocks, New York, John Wiley, p. 24–95.

Fifarek, R.H., 1985, Alteration geochemistry, fluid-inclusion, and stable-isotope study of the Red Ledge volcanogenic massive sulfide deposit, Idaho: Corvallis, Oregon State University, Ph.D. dissertation, 187 p.

Fifarek, R.H., Field, C.W., and Rye, R.O., 1984, Mineralization and isotopic geochemistry of the Red Ledge volcanogenic massive sulfide deposit, Idaho [abs.]: Geological Society of America Abstracts with Programs, v. 16, no. 6, p. 508.

Fifarek, R.H., Rye, R.O., and Field, C.W., 1983, Sulfur isotope geochemistry of the Red Ledge and other massive sulfide deposits of the Northwest [abs.]: Geological Society of America Abstracts with Programs, v. 15, no. 5, p. 372.

Finlow-Bates, Terry, and Stumpfl, E.F., 1981, The behavior of the so-called immobile elements in hydrothermally altered rocks associated with volcanogenic submarine-exhalative ore deposits: Mineralium Deposita, v. 16, p. 319–328.

Goldfarb, M.S., Converse, D.R., Holland, H.D., and Edmond, J.M., 1983, The genesis of hot-spring deposits on the East Pacific Rise, 21°N: Economic Geology Monograph 5, p. 184–197.

Gresens, R.L., 1967, Composition-volume relationships of metasomatism: Chemical Geology, v. 2, p. 47–55.

Gronewold, R.L., 1983, Trace and major element geochemistry of the Grey Eagle volcanogenic massive sulfide deposit, Siskiyou County, California: Davis, University of California, M.S. thesis, 154 p.

Gustin, M.M., 1990, Geology and geochemistry of the Bully Hill area of the East Shasta district, Shasta County, California: Tucson, University of Arizona, Ph.D. dissertation, 261 p.

Haymon, R.M., and Kastner, Miriam, 1981, Hot-spring deposits on the East Pacific Rise at 21°N—Preliminary description of mineralogy and genesis: Earth and Planetary Science Letters, v. 53, p. 363–381.

Hillhouse, J.W., Grommé, C.S., and Vallier, T.L., 1982, Paleomagnetism and Mesozoic tectonics of the Seven Devils volcanic arc in northeastern Oregon: Journal of Geophysical Research, v. 87, no. B5, p. 3777–3794.

Hitzman, M.W., Proffett, J.M., Jr., Schmidt, J.M., and Smith, T.E., 1986, Geology and mineralization of the Ambler District, northwestern Alaska: Economic Geology, v. 81, p. 1592–1618.

Holland, H.D., and Malinin, S.D., 1979, The solubility and occurrence of nonore minerals, *in* Barnes, H.L., ed., Geochemistry of hydrothermal ore deposits (2d ed.): New York, John Wiley, p. 461–508.

Høy, Trygve, Gibson, G., and Berg, N.W., 1984, Copper-zinc deposits associated with basic volcanism, Goldstream area, southeastern British Columbia: Economic Geology, v. 79, p. 789–814.

Izawa, Eiji, Yoshida, Tetsuo, and Saito, Ryo, 1978, Geochemical characteristics of hydrothermal alteration around the Fukazawa Kuroko deposit, Akita, Japan: Mining Geology, v. 28, p. 325–335.

Jackson, L.L., Brown, F.W., and Neil, S.T., 1987, Major and minor elements requiring individual determination, classical whole-rock analysis, and rapid rock analysis, *in* Baedecker, P.A., ed., Methods for geochemical analysis: U.S. Geological Survey Bulletin 1770, p. G1–G23.

Jones, D.L., Silberling, N.J., and Hillhouse, J.W., 1977, Wrangellia—A displaced terrane in northwestern North America: Canadian Journal of Earth Science, v. 14, p. 2565–2577.

———1978, Microplate tectonics of Alaska—Significance for the Mesozoic history of the Pacific Coast of North America, *in* Howell, D.G., and McDougall, K.A., eds., Mesozoic paleogeography of the Western United States (Pacific Coast Paleogeography Symposium 2): Los Angeles, Society of Economic Paleontologists and Mineralogists, Pacific Section, p. 71–74.

Juhas, A.P., and Gallagher, T.P., 1981, Kuroko-type mineralization at the Red Ledge deposit, Idaho, *in* Silberman, M.L., Field, C.W., and Berr, A.L., eds., Symposium on Mineral Deposits of the Pacific Northwest, 1980 Proceedings: U.S. Geological Survey Open-File Report 81-355, p. 223–235.

Juras, S.J., 1987, Geology of the polymetallic volcanogenic Buttle Lake camp, with emphasis on the Price Hillside, central Vancouver Island, British Columbia, Canada: Vancouver, University of British Columbia, Ph.D. dissertation, 279 p.

Kinkel, A.R., Jr., Hall, W.E., and Albers, J.P., 1956, Geology and base-metal deposits of West Shasta copper-zinc district, Shasta County, California: U.S. Geological Survey Professional Paper 285, 156 p.

Koski, R.A., 1981, Volcanogenic massive sulfide deposits in ocean-crust and island arc terranes, northwestern Klamath Mountains, Oregon and California, *in* Silberman, M.L., Field, C.W., and Berr, A.L., eds., Symposium on Mineral Deposits of the Pacific Northwest, 1980 Proceedings: U.S. Geological Survey Open-File Report 81-355, p. 197–212.

Kouda, Ryoichi, and Koide, Hitoshi, 1978, Ring structures, resurgent cauldron and ore deposits in the Hokuroku volcanic field, northern Akita, Japan: Mining Geology, v. 28, p. 233–244.

Kuhns, R.J., and Baitis, H.W., 1987, Preliminary study of the Turner-Albright Zn-Cu-Ag-Au-Co massive sulfide deposit, Josephine County, Oregon: Economic Geology, v. 81, p. 1362–1376.

Lichte, F.E., Golightly, D.W., and Lamothe, P.J., 1987, Inductively coupled plasma-atomic-emission spectrometry, *in* Baedecker, P.A., ed., Methods for geochemical analysis: U.S. Geological Survey Bulletin 1770, p. B1–B10.

Liou, J.G., Kuniyoshi, S., and Ito, K., 1974, Experimental studies of the phase relations between greenschist and amphibolite in a basaltic system: American Journal of Science, v. 274, p. 613–632.

Livingston, D.C., and Laney, F.B., 1920, The copper deposits of the Seven Devils and adjacent districts: Idaho Bureau of Mines and Geology Bulletin 1, p. 41–59.

Long, R.C., 1975, Geology and mineral deposits of the Red Ledge Mine area, Adams County, Idaho: Corvallis, Oregon State University, Master's thesis, 115 p.

Longwell, C.R., Flint, R.F., and Sanders, J.E., 1969, Physical geology: New York, John Wiley, 685 p.

MacLean, W.H., and Kranidiotis, P., 1987, Immobile elements as monitors of mass transfer in hydrothermal alteration: Phelps Dodge massive sulfide deposit, Matagami, Quebec: Economic Geology, v. 82, p. 951–962.

Meyer, Charles, and Hemley, J.J., 1967, Wallrock alteration, *in* Barnes, H.L., ed., Geochemistry of hydrothermal ore deposits (1st ed.): New York, Holt, Rinehart, and Winston, p. 166–235.

Mottl, M.J., 1983, Metabasalts, axial hot springs, and the structure of hydrothermal systems at mid-ocean ridges: Geological Society of America Bulletin, v. 94, p. 161–180.

Mottl, M.J., and Holland, H.D., 1978, Chemical exchange during hydrothermal alteration of basalt by seawater—Pt. I, Experimental results for major and minor components of seawater: Geochimica et Cosmochimica Acta, v. 42, p. 1103–1115.

Newton, C.R., 1986, Late Triassic bivalves of the Martin Bridge Limestone, Hells Canyon, Oregon—Taphonomy, paleoecology, paleozoogeography, *in* Vallier, T.L., and Brooks, H.C., eds., Geology of the Blue Mountains region of Oregon, Idaho, and Washington-Geologic implications of Paleozoic and Mesozoic paleontology and biostratigraphy, Blue Mountains province, Oregon and Idaho: U.S. Geological Survey Professional Paper 1435, p. 7–17.

Nockolds, S.R., Knox, R.W. O'B., and Chinner, G.A., 1978, Petrology for students: New York, Cambridge University Press, 435 p.

Nold, J.L., 1983, The Holden Mine—A metamorphosed volcanogenic deposit in the Cascade Range of Washington: Economic Geology, v. 78, p. 944–953.

Ohmoto, Hiroshi, 1978, Submarine calderas—A key to the formation of volcanogenic massive sulfide deposits: Mining Geology, v. 28, p. 219–232.

Payne, J.G., Bratt, J.A., and Stone, B.G., 1980, Deformed Mesozoic volcanogenic Cu-Zn sulfide deposits in the Britannia district, British Columbia: Economic Geology, v. 75, p. 700–721.

Pessagno, E.A., Jr., and Blome, C.D., 1986, Faunal affinities and tectonogenesis of Mesozoic rocks in the Blue Mountains province of eastern Oregon and western Idaho, *in* Vallier, T.L., and Brooks, H.C., eds., Geology of the Blue Mountains Region of Oregon, Idaho, and Washington-Geologic implications of Paleozoic and Mesozoic paleontology and biostratigraphy, Blue Mountains province, Oregon and Idaho: U.S. Geological Survey Professional Paper 1435, p. 65–78.

Reed, M.H., 1983, Seawater-basalt reaction and the origin of greenstones and related ore deposits: Economic Geology, v. 78, p. 466–485.

———1984, Geology, wallrock alteration, and massive sulfide mineralization in a portion of the West Shasta district: Economic Geology, v. 79, p. 1299–1318.

Scott, S.D., 1978, Structural control of the Kuroko deposits of the Hokuroku district, Japan: Mining Geology, v. 28, p. 301–312.

Seyfried, W.E., Jr., and Janecky, D.R., 1985, Heavy-metal and sulfur transport during subcritical and supercritical hydrothermal alteration of basalt—Influence of fluid pressure and basalt composition and crystallinity: Geochimica et Cosmochimica Acta, v. 49, p. 2545–2560.

Shenon, P.J., 1933, Copper deposits in the Squaw Creek and Silver Peak districts and at the Almeda Mine, southwestern Oregon, with notes on the Pennell and Farmer and Banfield prospects: U.S. Geological Survey Circular 2, 35 p.

Shirozu, Haruo, 1974, Clay minerals in altered wallrocks of the Kuroko-type deposits: Society of Mining Geologists of Japan Special Issue 6, p. 303–310.

Silberling, N.J., Jones, D.L., Blake, M.C., Jr., and Howell, D.G., 1984, Lithotectonic terrane map of the western conterminous United States, *in* Silberling, N.J., and Jones, D.L., eds., Lithotectonic terrane maps of the North American Cordillera: U.S. Geological Survey Open-File Report 84-523, p. C1–C43.

Skinner, B.J., ed., 1985, A special issue devoted to massive sulfide deposits, West Shasta district, California: Economic Geology, v. 80, no. 8, p. 2067–2254.

Snee, L.W., Sutter, J.F., and Kelly, W.C., 1988, Thermochronology of economic mineral deposits—Dating the stages of mineralization at Panasqueira, Portugal, by high-precision $^{40}Ar/^{39}Ar$ age-spectrum dating techniques on muscovite: Economic Geology, v. 83, p. 335–354.

Sorensen, M.R., 1983, The Queen of Bronze copper deposit, southwestern Oregon: Eugene, University of Oregon, M.S. thesis, 205 p.

Spry, Alan, 1976, Metamorphic textures (3d ed.): New York, Pergamon Press, 350 p.

Taggart, J.E., Jr., Lindsay, J.R., Scott, B.A., Vivit, D.V., Bartel, A.J., and Stewart, K.C., 1987, Analysis of geological materials by wavelength-dispersive X-ray fluorescence spectrometry, in Baedecker, P.A., ed., Methods for geochemical analysis: U.S. Geological Survey Bulletin 1770, p. E1–E19.

Thompson, R.I., and Panteleyev, Andrejs, 1976, Strata-bound mineral deposits of the Canadian Cordillera, *in* Wolf, K.H., ed., Handbook of strata-bound and stratiform ore deposits—Pt. II, Regional studies and specific deposits: New York, Elsevier, p. 37–108.

Tsutsumi, Makoto, and Ohmoto, Hiroshi, 1983, A preliminary oxygen isotope study of tetsusekiei ores associated with the Kuroko deposits in the Hokuroku District, Japan, *in* Ohmoto, Hiroshi, and Skinner, B.J., eds., The Kuroko and related volcanogenic massive sulfide deposits: Economic Geology Monograph 5, p. 433–438.

Urabe, Tetsuro, Scott, S.D., and Hattori, Keiko, 1983, A comparison of footwall-rock alteration and geothermal systems beneath some Japanese and Canadian volcanogenic massive sulfide deposits, *in* Ohmoto, Hiroshi, and Skinner, B.J., eds., The Kuroko and related volcanogenic massive sulfide deposits: Economic Geology Monograph 5, p. 345–364.

Vallier, T.L., 1977, The Permian and Triassic Seven Devils Group, western Idaho and northeastern Oregon: U.S. Geological Survey Bulletin 1437, 58 p.

———in press, Petrology of pre-Tertiary igneous rocks of the Blue Mountains province of Oregon, Idaho, and Washington—Implications for the geologic evolution of a complex island arc, *in* Vallier, T.L., and Brooks, H.C., eds., The Geology of the Blue Mountains region of Oregon, Idaho, and Washington: Petrology and tectonic evolution of pre-Tertiary rocks: U.S. Geological Survey Professional Paper 1438.

Vallier, T.L., and Batiza, Rodey, 1978, Petrogenesis of spilite and keratophyre from a Permian and Triassic volcanic-arc terrane, eastern Oregon and western Idaho, U.S.A.: Canadian Journal of Earth Science, v. 15, p. 1356–1369.

Vallier, T.L., Brooks, H.C., and Thayer, T.P., 1977, Paleozoic rocks of eastern Oregon and western Idaho *in* Stewart, J.H., Stevens, C.H., and Gritsche, A.E., eds., Paleozoic paleogeography of the

Western United States (Pacific Coast Paleogeography Symposium 1): Los Angeles, Society of Economic Paleontologists and Mineralogists, Pacific Section, p. 455–466.

Vernon, R.H., 1975, Metamorphic processes, reactions, and microstructure development: New York, John Wiley, 243 p.

Walker, N.W., 1986, U-Pb geochronologic and petrologic studies in the Blue Mountains terranes, northeastern Oregon and westernmost-central Idaho—Implications for pre-Tertiary tectonic evolution: Santa Barbara, University of California, Ph.D. dissertation, 224 p.

———in press, Tectonic implications of U-Pb zircon ages for the Canyon Mountain complex, Sparta complex, and related plutonic rocks of the Baker terrane, northeastern Oregon, *in* Vallier, T.L., and Brooks, H.C., eds., The Geology of the Blue Mountains region of Oregon, Idaho, and Washington: Petrology and tectonic evolution of pre-Tertiary rocks: U.S. Geological Survey Professional Paper 1438.

White, W.H., 1973, Flow structure and form of the Deep Creek stock, southern Seven Devils Mountains, Idaho: Geological Society of America Bulletin, v. 84, p. 199–210.

Winkler, H.G.F., 1976, Petrogenesis of metamorphic rocks (4th ed.): New York, Springer-Verlag, 334 p.

Wood, R.A., 1987, Geology and geochemistry of the Almeda mine, Josephine County, Oregon: Los Angeles, California State University, M.S. thesis, 237 p.

Zierenberg, R.A., Shanks, W.C., III, Seyfried, W.E., Koski, R.A., and Strickler, M.D., 1988, Mineralization, alteration, and hydrothermal metamorphism of the ophiolite-hosted Turner-Albright sulfide deposit, southwestern Oregon: Journal of Geophysical Research, v. 93, p. 4657–4674.

8. GEOLOGY OF THE IRON DYKE MINE AND SURROUNDING PERMIAN HUNSAKER CREEK FORMATION

By STEVEN D. BUSSEY[1] AND P. JAMES LEANDERSON[2]

CONTENTS

ABSTRACT

The copper-gold Iron Dyke massive sulfide deposit is located in the Wallowa terrane of eastern Oregon and western Idaho and formed during Permian tholeiitic volcanism in the Blue Mountains island arc. Stratigraphically, the deposit is located within the upper part of the Hunsaker Creek Formation, at the top of a local accumulation of low-K felsic lavas and tuffs, and is overlain by a thick sequence of epiclastic sedimentary rocks including conglomerate, sandstone, siltstone, and limestone. The Hunsaker Creek Formation was deposited in shallow water, in a basin adjacent to a volcanically active and subaerially eroding island arc. Rapidly changing sediment sources and synvolcanic tectonism resulted in the widespread formation of local unconformities. Felsic lavas and hypabyssal intrusions near the Iron Dyke Mine differentiated in a shallow magma chamber, which may have supplied the heat to drive the mineralizing hydrothermal system.

The shallow depths at which the deposit formed resulted in low confining pressure of the water column on the hydrothermal system; this low confining pressure permitted explosive hydrothermal activity, which formed multigeneration breccias dominated by vein-material fragments. Penetration of cool seawater into the upper parts of the deposit resulted in mixing below the sea floor, cooling, and deposition of metals from the hydrothermal fluids. These processes produced a deposit dominated by stockwork and epithermal veins.

Uplift of the deposit shortly after its formation lead to catastrophic collapse of the upper part of the stockwork and the formation of a submarine debris flow, rich in mineralized fragments, which came to rest adjacent to the uplifted stockwork. Continued sedimentation buried the mineralized fragments and prevented them from being destroyed by oxidation on the sea floor.

ACKNOWLEDGMENTS

This study was condensed and revised from a doctoral dissertation by S.D. Bussey. Financial support was provided by the Fogarty Fellowship, the Coulter Scholarship, and the Geology Department of the Colorado School of Mines. Special thanks go to Tom Nash of the U.S. Geological Survey in Denver for taking an interest in this study. We thank Stuart Havenstrite and the management of Silver King Mines, Inc., for access to drill core and underground workings, as well as field support during the summers of 1984, 1985, and 1986. Reviews by Tracy Vallier, Mark Ferns, and Richard Fifarek greatly improved the original manuscript.

INTRODUCTION

The Permian section of the Wallowa island-arc terrane in western Idaho and eastern Oregon is host to several volcanogenic massive sulfide deposits, including the Iron Dyke Mine, a Cu-Au deposit located in the upper part of the Hunsaker Creek Formation. The mine lies just south of Hells Canyon on the west

[1]Western Mining Corp., 240 South Rock Blvd., Suite 137, Reno, NV 89502
[2] P.O. Box 1492, Jeddah, Saudi Arabia

side of the Snake River near Oxbow, Oregon (fig. 8.1). It was discovered in 1897, reached peak production during World War I, and continued operating at peak production through the early 1920's. Low copper prices forced the mine to shut down in 1928 but by then it had become Oregon's top copper producer. The Butler Ore Company attempted unsuccessfully to reopen the mine in the early 1940's. Texasgulf, Inc., began exploration in the Hells Canyon region in the early 1970's and recognized the volcanogenic origin of the deposit. In 1979, Texasgulf, Inc., purchased the property and entered into an agreement with Silver King Mines, Inc., to mine and mill the ore. Silver King Mines acquired the mine from Texasgulf in 1983 and has operated it intermittently since then.

From 1910 to 1928, the total recorded production from the Iron Dyke Mine was 34,967 troy oz Au, 258,489 troy oz Ag, and 14,417,920 lb Cu (Brooks and Ramp, 1968). Since 1979, exploration by Texasgulf and Silver King Mines has resulted in the discovery of additional reserves that average 2.5 percent Cu, 0.25 troy oz Au/ton, and 0.5 troy oz Ag/ton (B.E. Wise, written commun., 1983). From 1979 to early 1981, about 50,000 tons of ore was mined (Mark Ferns, Oregon Department of Geology and Mineral Industries, written commun., 1987) and an additional

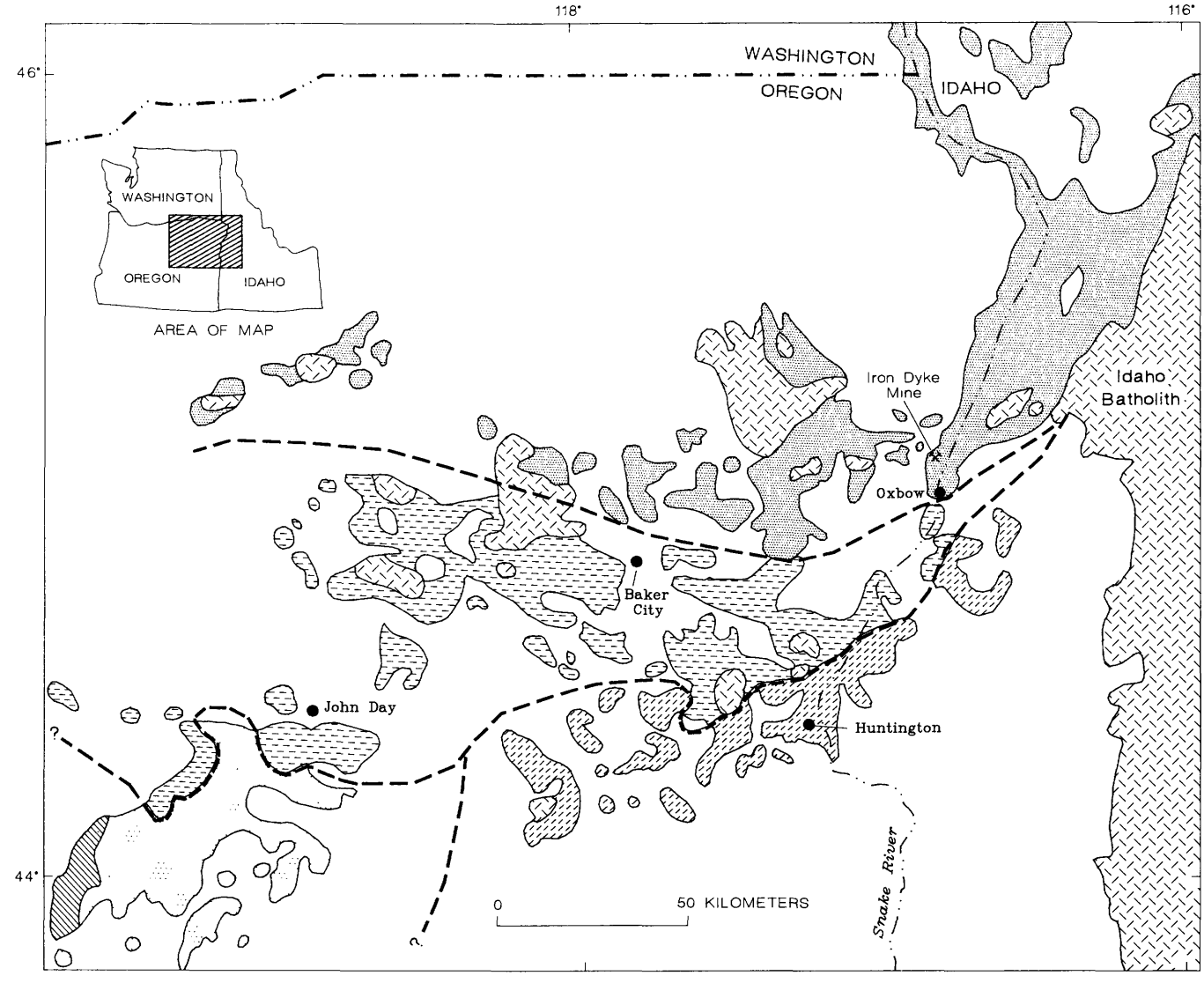

FIGURE 8.1.—Index map showing location of study area in eastern Oregon, western Idaho, and southeastern Washington. Dashed lines show boundaries of the Wallowa, Baker, Izee, and Olds Ferry terranes that make up the Blue Mountains province (Silberling and others, 1984). Queried where location uncertain.

6,000 tons produced in 1984. There was little or no production in 1982, 1983, or 1984 (Mark Ferns, written commun., 1987). The Silver King Mines, Inc., annual report for 1987 states that 12,000 tons of ore grading 0.3 troy oz Au/ton and 3 percent Cu were taken from the mine in 1986 and 1987.

REGIONAL GEOLOGY

The Blue Mountains province (Silberling and others, 1984) of eastern Oregon and western Idaho is one of the oldest and most inland of the accreted land masses in the North American Cordillera. The five terranes (fig. 8.1), which make up the Blue Mountains province were amalgamated about 160 Ma (Goldstrand, 1987) and accreted to the continent by 120 Ma (Sutter and others, 1984). The Blue Mountains province was rotated 60° clockwise sometime after its initial docking but prior to Eocene time (Wilson and Cox, 1980).

Early Permian subduction formed the Wallowa terrane, an oceanic island-arc sequence, which consists of a late Paleozoic basement complex of metamorphosed oceanic-arc-generated rocks overlain and intruded by Lower Permian(?) and Lower Permian and Middle and Upper Triassic mafic to felsic volcanic rocks of the Seven Devils Group (Vallier, 1967, 1977; Walker, 1983; LeAnderson and Richey, 1986). The volcanic section is overlain by the Triassic(?) Lucile Slate and Upper Triassic Martin Bridge Limestone and the Upper Triassic and Lower Jurassic Hurwal Formation (Smith and Allen, 1941; Hamilton, 1963; Vallier, 1977; Lund and others, 1983; LeAnderson and Richey, 1986; Orr, 1986). Unconformably overlying the Triassic(?) and Lower Jurassic rocks is the Middle and Upper Jurassic Coon Hollow Formation (Morrison, 1961, 1964; Vallier, 1977; Imlay, 1986; Goldstrand, 1987; Vallier and others, 1987).

The Grindstone terrane consists of a small exposure in the southwesternmost part of the Blue Mountains province. It consists of structurally chaotic, lenticular-shaped blocks of silicic metavolcanic rock, volcaniclastic graywacke, radiolarian chert, argillite, limestone, and sandstone (Vallier and others, 1977; Blome, 1988). The overall lithologic association and structural juxtaposition of the blocks suggest that this terrane represents a subduction complex (Dickinson and Thayer, 1978) related to the Baker terrane.

South and east of the Wallowa terrane is the Baker terrane, a melange that contains arc-related and oceanic-rock assemblages, serpentinite-matrix melange, and ophiolite complexes (Dickinson, 1979; Mullen and Sarawitz, 1983; Morris and Wardlaw, 1986). Fossils of Devonian age indicate that rocks in the Baker terrane, along with those in the Grindstone terrane, are the oldest in the Blue Mountains province. The two terranes probably represent a forearc suite that formed at the same time as the Wallowa terrane (Mullen, 1985; Bishop, 1988).

The Olds Ferry terrane is another oceanic island-arc sequence that formed as a result of Middle to Late Triassic subduction and consists of mafic to felsic lavas dominated by andesite with associated volcaniclastic and minor amounts of clastic sedimentary rocks and limestone (Brooks and Vallier, 1978). The volcanic sequence is overlain by the Lower to Middle Jurassic Weatherby Formation of Brooks (1979a), which consists of volcanic wacke and siltstone, conglomerate with minor amounts of limestone, gypsum, and tuffaceous sedimentary rock (Brooks, 1979b).

The Izee terrane consists of a thick sequence of Upper Triassic to Upper Jurassic sandstone with rare andesite and basaltic volcanic rock that lies between the Baker and Olds Ferry terranes (Brooks, 1979a; Mullen and Sarawitz, 1983; Imlay, 1986). This sequence was deposited beginning in the Late Triassic (Dickinson, 1979) in a basin underlain by melange and is correlative in age with the Triassic sedimentary rocks that overlie the volcanic part of the Wallowa terrane.

The northeastern margin of the Wallowa terrane is in contact with the border zone of the Idaho batholith. Where studied in detail (Onasch, 1987; Bonnichsen, 1987), the border zone is described as extremely complex with multiple stages of metamorphism as well as thrusting and complicated stratigraphy. Lithologies include schist, amphibolite, and peridotite that apparently represent metamorphosed parts of

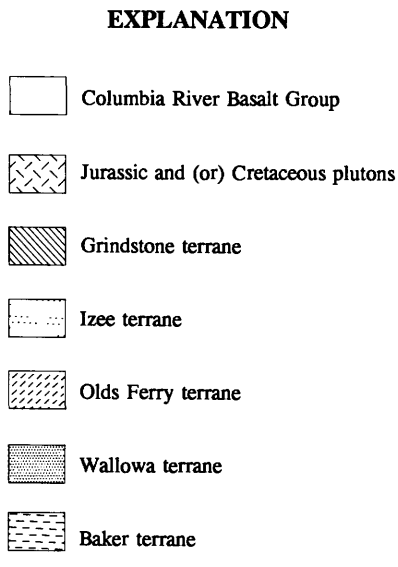

FIGURE 8.1.—Continued.

the Blue Mountains province (Mann and Vallier, 1987; Bonnichsen, 1987).

Of the other well-documented terranes in the Pacific Northwest, the Wrangellia terrane is most similar to the Wallowa terrane in age, stratigraphy, and latitude of formation (Jones and others, 1977). However, recent detailed geologic investigations revealed differences in the composition of the volcanic rocks and differences in paleontological affinity (Sarawitz, 1983; Silberling, 1983; Stanley, 1986) between the two terranes. Pessango and Blome (1986) felt that the tectonostratigraphic relations among the terranes in the Blue Mountains province are clearer if the Wrangellia terrane is not included. In fact, they pointed out that the megafossil assemblages suggested a closer relation of the Blue Mountains province to their so-called Nevadian complex of California and western Nevada than to the Wrangellia terrane. Hillhouse and others (1982) suggested that the Wallowa terrane formed north of the Wrangellia terrane and north of the paleoequator. This hypothesis is in agreement with the calculated positions of the Wrangellia and the Wallowa terranes based on paleomagnetic data (Debiche and others, 1987; Harbert and Vallier, 1988).

GEOLOGY OF THE WALLOWA TERRANE

REGIONAL STRUCTURE

The Wallowa terrane was deformed in three separate episodes. The oldest episode is Permian to Triassic in age and is related to formation of the Blue Mountains island arc. It probably represents synvolcanic faulting and sea-floor burial metamorphism that took place throughout the island-arc volcanism. In Middle Jurassic time, all of the rocks were folded (Avé Lallemant, 1983) and those below the Triassic Martin Bridge Limestone were metamorphosed to the greenschist or amphibolite facies. The third episode of deformation and metamorphism began about 120 Ma and continued to 93 Ma during accretion of the Blue Mountains province to North America. It included intrusion of several early phases of the Idaho batholith into, and metamorphism of, the Riggins Group, followed by thrusting of the Riggins Group over the Wallowa terrane (Onasch, 1987). The effects in the Wallowa terrane were largely confined to the Triassic(?) Lucile Slate and Triassic Martin Bridge Limestone on the east side of the province.

STRATIGRAPHY

The Wallowa terrane consists of, in ascending order, a basement complex, the Seven Devils Group of volcanic arc-related rocks, and Triassic and Jurassic sedimentary rocks. Rocks of the Wallowa terrane are unconformably overlain by flows of the Columbia River Basalt Group. The basement complex of the Wallowa terrane is exposed in several locations along the Snake River in Hells Canyon (Vallier, 1974, 1977; LeAnderson and Richey, 1986; Walker, 1986). It consists of migmatitic and amphibolitic gneiss, gabbroic and trondhjemitic intrusions, and zones of sheeted dikes, all of which are cut by northeast-trending mylonitic shear zones. The migmatitic gneiss is the oldest unit in the terrane, and has a discordant U-Pb age of 309 Ma (Walker, 1983, 1986). Walker concluded that the protolith of the gneiss was plutonic and is the remnant of Late Pennsylvanian oceanic crustal rocks that underlie the Wallowa terrane. A U-Pb age of 249 Ma (Walker, 1986) and a ^{40}Ar-^{39}Ar age of 214 Ma (Phelps, 1979) on the dikes delimit formation of the mylonite to between the latest Permian and Late Triassic time (Walker, 1986).

The Seven Devils Group (Vallier, 1977) makes up the volcanic section of the Wallowa terrane. It is divided into four formations, which are (in ascending order) the Permian(?) Windy Ridge, Permian Hunsaker Creek, Triassic Wild Sheep Creek, and Triassic Doyle Creek Formations. The Lower Permian(?) Windy Ridge Formation is a sequence of weakly metamorphosed silicic volcanic flow and volcaniclastic rocks exposed along the Snake River near Oxbow, Oregon (Vallier, 1977). Several small exposures are also located just north of Oxbow on the Oregon side of the river. The base of the Windy Ridge Formation is not exposed but lower parts of it are sheared, and it appears to be in tectonic contact with the Oxbow Complex. The contact with the overlying Hunsaker Creek Formation is sharp and marked by a thin, discontinuous layer of volcanic sandstone. Along the Snake River, the two formations are separated by a high-angle fault. Vallier (1977) estimated the total thickness of the Windy Ridge Formation to be 500 m. The presence of the Windy Ridge Formation only in this area suggests it may represent a local felsic volcanic center located below the Hunsaker Creek Formation.

Overlying the Windy Ridge Formation is the Lower Permian Hunsaker Creek Formation, a 2,500- to 3,500-m-thick sequence of weakly metamorphosed epiclastic, volcaniclastic, and volcanic rocks (Vallier, 1977). The formation is exposed along the Snake River canyon for 15 km north of Oxbow (fig. 8.2). Less accessible exposures of the unit are present on the east side of the Snake River north of Cuprum for 50 km. LeAnderson and Richey (1986) mapped what they believe are lithic equivalents of the Windy Ridge and Hunsaker Creek Formations overlying exposures

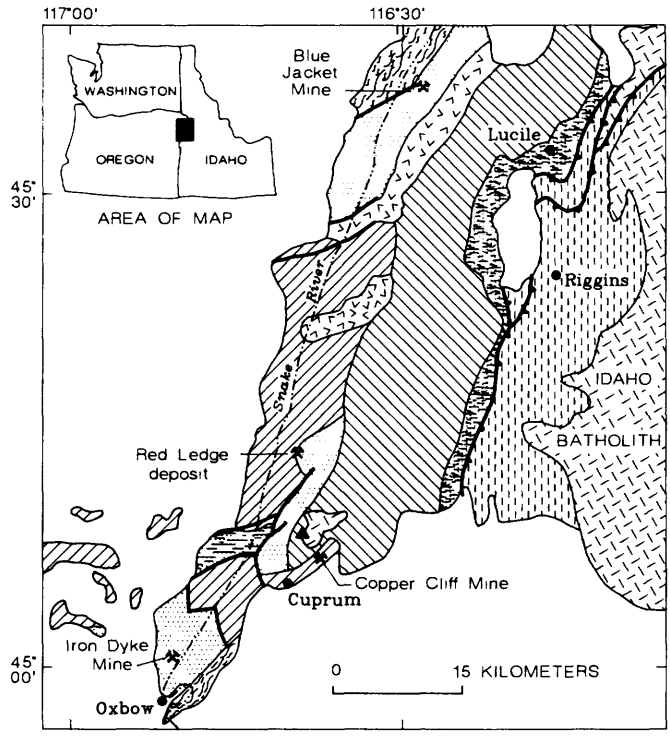

of the basement complex along the Snake River near the Blue Jacket Mine (fig. 8.2).

The Hunsaker Creek Formation differs from the Windy Ridge Formation in that it contains abundant sedimentary rocks such as conglomerate, sandstone, and limestone in addition to basaltic, dacitic, and rhyolitic lava, tuff, and breccia. The abundance of epiclastic sedimentary rocks increases upward and is characteristic of the Hunsaker Creek Formation throughout the Snake River canyon near Oxbow. Volcanic rocks of Permian(?) age around the Blue Jacket Mine (LeAnderson and Richey, 1986) are different from the Hunsaker Creek Formation in the Oxbow area in that they consist of abundant andesitic volcanic rocks and rare sedimentary rocks.

The Middle and Upper Triassic Wild Sheep Creek Formation (Vallier, 1977) is a thick sequence of weakly metamorphosed Triassic basalt, basaltic andesite, andesite flows, volcaniclastic rocks, graywacke, argillite, and limestone. It is widely exposed in the Snake River canyon and Seven Devils Mountains (fig. 8.2). Vallier (1977) recognized three units within the Wild Sheep Creek Formation. These are a lower unit that consists mainly of andesitic volcaniclastic rocks, a middle unit that consists mostly of massive and pillow basaltic lavas with beds of basaltic tuff and thick beds of coarse breccia, and an upper unit of argillite, sandstone, limestone, and volcaniclastic rocks. Conglomerate and graywacke are present throughout the formation and epiclastic rocks dominate over pyroclastic rocks.

Conformably overlying the Wild Sheep Creek Formation (fig. 8.2) is the Upper Triassic Doyle Creek Formation (Vallier, 1977). The Doyle Creek Formation consists of basaltic to rhyolitic lava, pyroclastic rock, and conglomerate, sandstone, siltstone, argillite, arkosic wacke, and graywacke. The formation has a distinctive red color, which helps to distinguish it from the Wild Sheep Creek Formation and which led Vallier (1977) to suggest it was deposited in a shallow, well-oxygenated marine environment.

The Seven Devils Group has not been mapped in detail north of Cuprum nor throughout the Seven Devils Mountains. The distribution of the Hunsaker Creek, Wild Sheep Creek, and Doyle Creek Formations in this area is not known and is shown on figure

◀ FIGURE 8.2.—Geologic map of Hells Canyon region showing distribution of rock units that make up the Wallowa terrane and location of mineral deposits and mines discussed in text (modified from Livingston and Laney, 1920; Vallier, 1974, 1967; Brooks and Vallier, 1978; LeAnderson and Richey, 1985; and Onasch, 1987).

8.2 as undifferentiated Permian and Triassic volcanic rocks of the Seven Devils Group.

Stratigraphically above the Seven Devils Group are the Upper Triassic Martin Bridge Limestone (fig. 8.2) and the Triassic(?) Lucile Slate. The stratigraphic relation between the Lucile Slate and the Martin Bridge Limestone has been complicated by thrust faulting and the presence of similar shales and limestones in the volcanic section. The Lucile Slate has been at least partially correlated with the Hurwal Formation in Oregon, which shows a facies relation with the Martin Bridge Limestone and which was deposited on Martin Bridge strata when the volcanic platform was submerged.

An unconformity separates the pre-Tertiary rocks from the basalts of the Miocene Columbia River Basalt Group and can be seen along much of the Snake River from Oxbow and north to the Washington border. Beds of boulders and cobbles mark the unconformity surface. Vallier (1977) identified a lower and upper unit within the basalts exposed in Hells Canyon. The lower unit is composed of porphyritic basalt, which apparently accumulated only in low areas and filled topographic depressions. Its thickness ranges from 200 to a maximum of 450 m (Vallier, 1977). The upper unit is well exposed throughout the Hells Canyon region and, unlike the lower unit, caps the old topography. It has a maximum thickness of about 900 m (Vallier, 1977). Small feeder dikes, which cut the pre-Tertiary rocks, are also common along the Snake River north of Oxbow.

DEPOSITIONAL ENVIRONMENT

The pre-Tertiary rocks in the Snake River canyon are the remnants of old island-arc systems that formed in the paleo-Pacific. The Permian strata represent the oldest arc rocks in the terrane and were deposited on a complex of deformed and metamorphosed arc-basement rocks. The silicic nature of the volcanic rocks indicates that subduction of oceanic crust and differentiation of the orogenic magmas were well underway in Permian time. The abundance of clastic sedimentary rocks in the Hunsaker Creek Formation suggests that it was deposited in a basin very near the magmatic arc. Coarse clastic debris containing rounded cobbles and boulders of many lithologies indicates subaerial erosion of the arc. The period of erosion lasted 15 to 25 m.y. and culminated in another great outpouring of volcanic rocks in Triassic time. Volcanism during the Triassic was dominated by andesite and basaltic andesite. By the time the Martin Bridge Limestone and Lucile Slate were being deposited, volcanic activity was greatly reduced and the volcanic section had been faulted into a series of platforms and basins.

MINERAL DEPOSITS

A variety of mineral deposits are present in the Blue Mountains province but the two most important types are volcanogenic massive sulfide deposits in the Permian Hunsaker Creek Formation and skarn deposits associated with Jurassic felsic plutons that contain assimilated blocks of limestone, presumably derived from the Martin Bridge Limestone. The volcanogenic deposits include the Iron Dyke just north of Oxbow, Oregon, the Red Ledge 2 km east of the Hells Canyon Dam, and the Blue Jacket located 32 km northwest of Lucile, Idaho (fig. 8.2). The Iron Dyke and Red Ledge deposits are present within the Permian Hunsaker Creek Formation, whereas the Blue Jacket deposit is present in rocks of probable Permian age. Both the Blue Jacket and the Red Ledge are Cu-Zn-Ag massive sulfide deposits but the Iron Dyke is a volcanogenic Cu-Au stockwork deposit with epithermal characteristics and only minor amounts of massive sulfide. The Red Ledge deposit is similar to the Iron Dyke, however, in that it also has a well-developed epithermal-like quartz stockwork preserved stratigraphically beneath a massive sulfide body. Numerous smaller volcanogenic prospects are present throughout the Permian section. The volcanogenic deposits were mined principally for Cu, Zn, Ag, and Au. Ore minerals include chalcopyrite, sphalerite, tetrahedrite, acanthite, and native gold in a gangue of quartz, pyrite, chlorite, hematite, barite, and calcite.

The Copper Cliff Mine, about 2 km northeast of Cuprum, Idaho (fig. 8.2), is a Cu-Ag deposit localized within the Triassic Doyle Creek Formation. Ore minerals are bornite and chalcopyrite disseminated in meta-andesite (Morganti, 1972). The deposit has many similarities to Jurassic to mid-Cretaceous aged volcanic and volcano-sedimentary rock-hosted copper deposits known as manto-type deposits in northern and central Chile and may have formed in a manner similar to sediment-hosted stratiform copper deposits.

Contact metamorphic skarn deposits (Lindgren, 1899) formed as a result of intrusion of Jurassic quartz diorite stocks into the Martin Bridge Limestone 4 km northeast of Cuprum, Idaho (fig. 8.2). The skarn deposits were mined principally for Cu, Mo, Fe, and W, but they also contained significant amounts Au, Ag, and Pb. Ore minerals include chalcopyrite, bornite, chalcocite, galena, magnetite, molybdenite, and scheelite in a gangue of quartz, garnet, epidote, various calc-silicates, spinels, and scapolite (Snyder, 1973).

TABLE 8.1.—*Source, depositional environment, and mode of transport for seven facies of the Permian volcanic section from Oxbow, Oregon, to the Iron Dyke Mine*

Facies	Environment	Source	Mode of transport
		Gravity-transported facies	
Siltstone	Marine: below wave base.	Subaerial volcanic rocks, nearshore marine deposits.	Turbidity currents.
Sandstone	Marine: below wave base marine deposits.	Subaerial volcanic rocks; nearshore.	Turbidity currents.
Conglomerate	Marine: below wave base.	Subaerial volcanic rocks; nearshore marine deposits.	Subaerial or submarine cold lahars, turbidity currents?
Limestone	Marine: below wave base.	Fore-reef talus, growing reef?	Submarine calcareous mudflows.
		Pyroclastic and volcanic facies	
Tuff	Marine: below wave base.	Subaerial or submarine pyroclastic eruptions.	Wind, ocean currents, gravity settling, submarine pyroclastic flows.
Tuffaceous conglomerate.	Marine: below wave base.	Subaerial or submarine pyroclastic eruptions.	Gravity settling, submarine lahar, submarine pyroclastic flows.
Volcanic lava and breccia.	Marine: below wave base.	Volcanic intrusions or flows.	Flowing lava, flowing breccias.

STRATIGRAPHY OF THE SNAKE RIVER CANYON FROM OXBOW, OREGON, TO THE IRON DYKE MINE

The stratigraphic section from Oxbow, Oregon, to the Iron Dyke Mine consists of (in ascending order) the late Paleozoic to Triassic basement complex of Vallier (1967), Permian(?) Windy Ridge Formation, Permian Hunsaker Creek Formation, Triassic Wild Sheep Creek Formation, and Tertiary Columbia River Basalt Group. The basement complex was described by Vallier (1967, 1974, 1977) and Walker (1986). The Wild Sheep Creek Formation, exposed in a small downdropped fault block just north of the Iron Dyke Mine, and the Columbia River Basalt Group, which caps the pre-Tertiary rocks near the mine were described by Vallier (1967, 1974, 1977).

The following discussion of facies refers only to the Windy Ridge and Hunsaker Creek Formations. Seven facies can be identified within the Permian volcanic rocks shown on figure 8.3 on the basis of lithology and sedimentary structures. The association of one facies with another allows depositional environments to be deduced where one facies alone is not sufficient. The facies described herein are analogous to the facies described by Mitchell (1970) in his detailed study of the volcanogenic sediments exposed on Malekula Island in the New Hebrides island arc. The seven facies are divided into two genetic groups—gravity-transported facies and pyroclastic-volcanic facies. Gravity-transported facies are siltstone, sandstone, conglomerate, and limestone. Pyroclastic-volcanic facies are tuff, tuffaceous conglomerate, and volcanic lava and breccia. Table 8.1 summarizes the facies and gives the possible environment of deposition, source, and mode of transport for each. All were deposited in a marine environment below the level where they could be reworked by wave action.

Felsic flows, mafic flows, and mafic intrusions generally decrease upward in the section (Bussey, 1988); this phenomenon suggests that either igneous activity was decreasing with time or that the volcanic center was shifting away from this part of the arc. The large percentage of felsic flow material in the lower part of the section is part of the Windy Ridge Formation. The gravity-transported facies (siltstone, sandstone, conglomerate, and limestone) all increase in abundance upward in the section, which reflects the increased role of weathering and erosion in transporting material off the exposed parts of the arc. Felsic

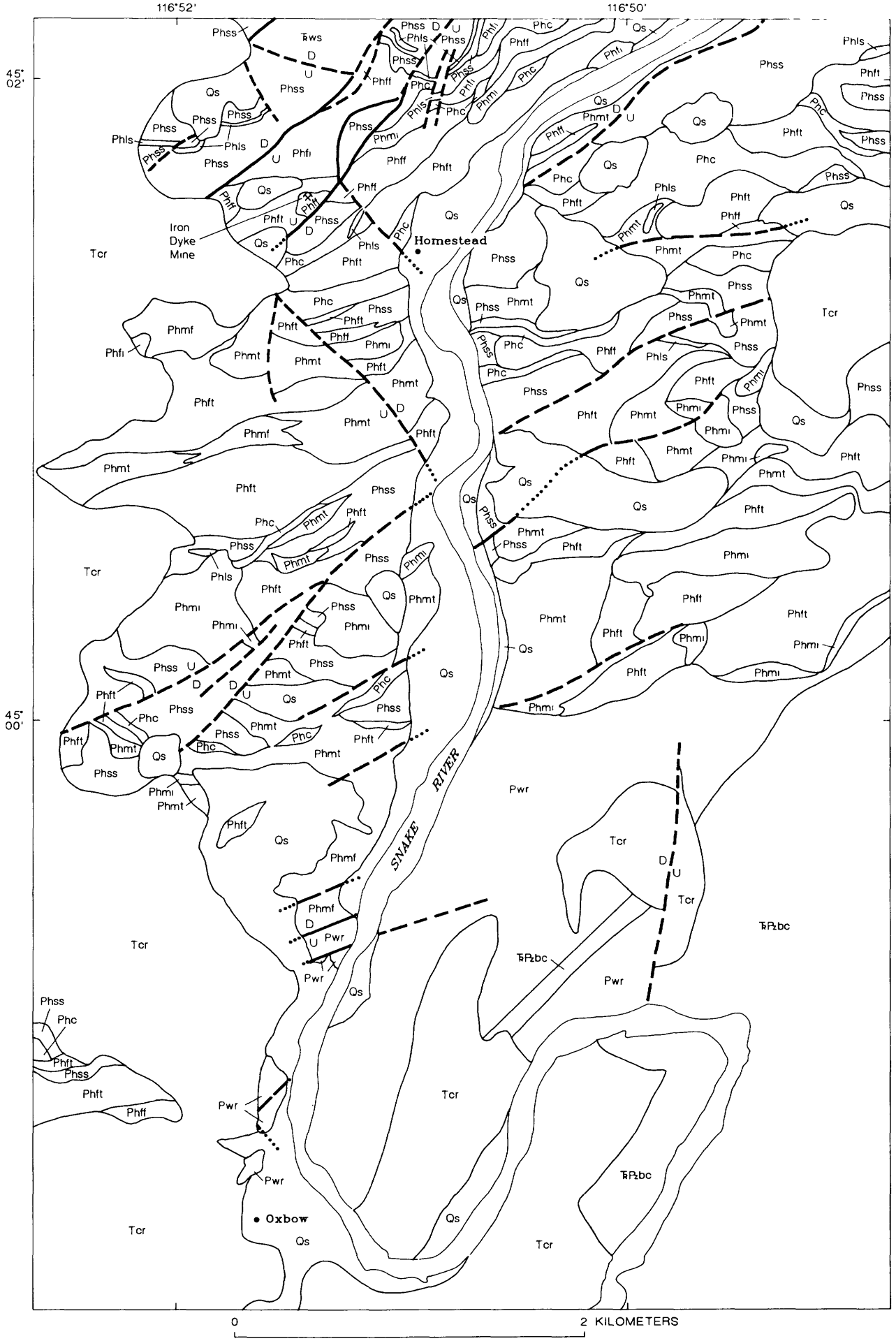
116°52'
116°50'
45°
02'
45°
00'
Homestead
Iron
Dyke
Mine
Oxbow
SNAKE RIVER
Qs
Phss
Phls
Phft
Phff
Phfi
Phmf
Phmt
Phmi
Phc
Pnc
Tcr
Pwr
TPzbc
D
U
0
2 KILOMETERS

tuffs predominate over mafic tuffs in the area shown in figure 8.3 and show a general increase upward in the section. The mafic tuff facies is most abundant in the middle part of the section whereas mafic flows are less common in the middle and lower parts of the section and decrease in abundance upward.

The conglomerates of the Hunsaker Creek Formation correspond to the submarine canyon and inner fan regions of Walker's (1978) fan model. On modern fans, the conglomeratic mass-flow material is confined to the fan channels and is surrounded by more laterally extensive levee and interchannel materials (Howell and Normark, 1982). The thick northeast-trending sequence of conglomerates that is exposed from northeast of the Iron Dyke Mine to the northeast corner of the map area shown in figure 8.3 may represent a large filled channel. The basic fan model of Walker (1978) is not completely applicable to the rocks of the Hunsaker Creek Formation because of the large amount of pyroclastic materials present.

EXPLANATION

Qs	Surficial deposits (Quaternary)—Alluvium, landslides, and terrace deposits; as mapped, also includes covered areas
Tcr	Columbia River Basalt Group (Miocene)—Older flows correlative with Picture Gorge Basalt and younger flows correlative with Yakima Basalt
₮ws	Wild Sheep Creek Formation (Triassic)—Argillite, volcaniclastic rocks, limestone, and basalt
	Hunsaker Creek Formation (Permian)—Divided into:
Phmi	Mafic intrusions—Dikes, sills, and irregular stocks composed of gabbro, diabase, and porphyritic basalt
Phfi	Felsic intrusions—Dikes, sills, and stocks composed of porphyritic dacite and rhyolite; often autobrecciated
Phss	Sandstone and siltstone—Planar, waved, and crossbedded sandstone and siltstone; rare climbing ripples present; massive; volcanic in origin
Phls	Limestone—Clastic limestone with brachiopod and crinoid fossil fragments, volcanic clasts, and quartz and feldspar grains
Phc	Conglomerate—Composed of rounded to angular clasts as much as 1 m in diameter; most are cobble size; felsic volcanic clasts dominate
Phft	Felsic tuff—Crystal-lithic lapilli to pumice lapilli tuff; in part, may be sedimentary in origin
Phmt	Mafic tuff—Lithic lapilli tuff; in part, may be sedimentary in origin
Phff	Felsic flow—Lenticular-shaped flow; associated with monolithic breccia; may be brecciated
Phmf	Mafic flow—Massive, brecciated, and pillow-breccia flows; amygdaloidal
Pwr	Windy Ridge Formation (Permian?)—Rhyolite flows and rhyolite tuff breccia
₮₱zbc	Basement complex (Triassic and Paleozoic)—Includes metamorphosed gabbro and basalt; quartz diorite, diorite, albite granite intrusive rocks; mylonite, gneissic mylonite, and amphibolite schist
———	Contact
U / D	Fault—Dashed where approximately located; dotted where inferred; D denotes downthrown block; U denotes upthrown block

FIGURE 8.3.—Detailed geologic map of Snake River canyon from Oxbow, Oregon, to the Iron Dyke mine.

During an eruption, these materials are not necessarily transported to deep water in submarine canyons like clastic sediments. Instead, they will be transported to deep water by gravity flow movement down the volcano flank. Thus, epiclastic materials accumulated by fluvial processes may be spatially separate from volcanically derived materials, or at least they will be deposited in distinct units that may be interbedded with the volcanic materials. This type of depositional system appears to have existed during deposition of the Hunsaker Creek Formation.

Vallier (1967) recognized lateral lithofacies changes within the Hunsaker Creek Formation which indicate that water depths were shallower to the west. Clast size, abundance, and sorting of conglomerates increase toward the west. North to northeast paleocurrent directions measured by Vallier (1967) also indicate that the subaerial part of the arc was present to the west. The subaerially exposed parts of the arc must have been extensive enough to produce epiclastic materials such as rounded boulders and cobbles. In addition, they must have been sufficiently uplifted and eroded to expose plutonic rocks. Fringing reefs must have been present to supply the materials for the clastic limestone deposits. Igneous activity, which occurred during deposition, resulted in dikes, sills, and flows being intruded into and extruded on top of the unconsolidated sediments. The abundance of pyroclastic and coarse-grained epiclastic materials preserved in the area shown in figure 8.3 suggests that this part of the Hunsaker Creek Formation formed along the flank of a volcano within the Blue Mountains island arc.

The asymmetric distribution of plutonic rocks of the basement complex exposed at Oxbow and volcanic rocks of the Hunsaker Creek and Windy Ridge Formations (fig. 8.3) gives rise to a paleogeographic reconstruction (fig. 8.4) of asymmetric subsidence and preservation of the flank of a volcano in an island-arc complex (Francis, 1983). The felsic plutonic rocks of the basement complex at Oxbow are similar in composition to the volcanic rocks of the Hunsaker Creek and Windy Ridge Formations and are the right age to be their subvolcanic feeders (Walker, 1986). However, the presence of a zone of intense shearing with strike-slip motion, which separates the plutonic and volcanic rocks, precludes a direct correlation between the two lithic groups.

GEOLOGY OF THE IRON DYKE MINE

LOCAL GEOLOGY

Although several geologists studied the rocks around the Iron Dyke Mine during its early development (Lindgren, 1901; Swartley, 1914), the local geology was first mapped by Vallier (1967) and Vallier and Brooks (1970). It was later mapped in detail by R.S. Fredrickson (written commun., 1977), Juhas and others, (1980), Stevens (1981), and B.E. Wise (written commun., 1983).

In the mine area, the rocks have been folded into a series of northeast-southwest trending anticlines and

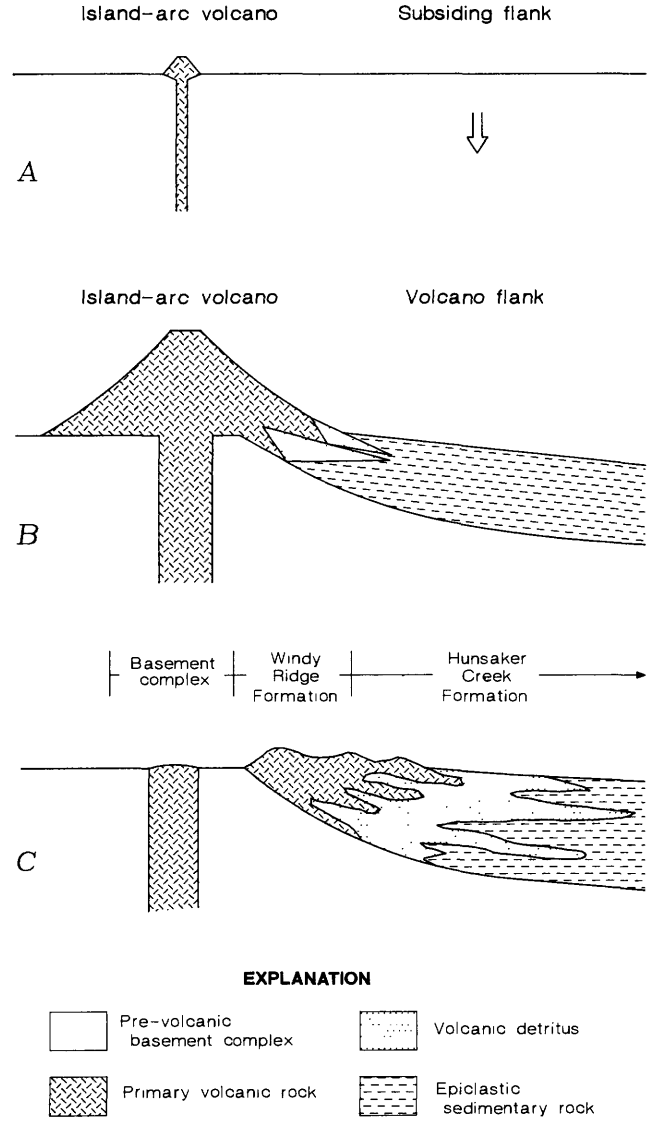

FIGURE 8.4.—Schematic diagrams (modified from Francis, 1983) showing sequence of asymmetric preservation of a volcano flank by local subsidence. *A*, Initial island-arc volcano; *B*, Growth by eruption of volcano accompanied by flank subsidence and sediment accumulation; *C*, Post-volcanic erosion removed all but part of volcano flank and some overlying sedimentary rocks. Depositional environments for late Paleozoic basement complex, Windy Ridge Formation, and Hunsaker Creek Formation also shown.

synclines (fig 8.5). The informally named Stewart syncline is the most prominent structure on the mine property and plunges 20° to 30° northeast (R.S. Fredrickson, written commun., 1977). The youngest strata exposed in the axis of the syncline is a sequence of volcanic sandstone and siltstone. The informally named Copper Giant anticline is a broad fold northwest of the Stewart syncline and both bedded volcaniclastic tuff and rhyolite flow are exposed along its axis.

Both the Stewart syncline and Copper Giant anticline are bounded by northeast-southwest-trending, vertical to steeply dipping faults that show normal displacement. The Glory Hole fault zone, which separates the Stewart syncline and Copper Giant anticline, is a complex series of closely spaced normal faults that dip steeply southeast. The northwest side of the Copper Giant anticline is bounded by another fault that dips steeply west and has normal displacement of at least 300 m (L. Smith, written commun., 1981). Stevens (1981) identified a second fault set trending northwest-southeast that cut and displaced the northeast-southwest-trending fault system. These faults are typically sharp with very little gouge, near vertical, and have normal displacements of 10 to 50 m.

The lowermost rocks in the mine area consist of a sequence of predominantly intermediate to mafic tholeiitic volcanic and pyroclastic rocks with interbedded lenses of coarse conglomerate and volcanic sandstone. Exposures often contain vesicular zones with irregularly shaped fragments that suggest pillow breccia. Mafic pyroclastic rocks are heterolithic but rarely contain felsic volcanic material. Fragments range in size from ash to blocks, and lapilli is the dominant size. Pyroclastic rocks dominated by lapilli usually contain very little ash and are tightly packed with white calcite and quartz cement. Felsic, quartz-bearing pumiceous lapilli tuffs are interbedded with increasing frequency toward the top of the sequence, which grades into an overlying sequence composed of felsic volcaniclastic tuff.

The felsic volcaniclastic tuff consists of coarse-grained lapilli tuff with abundant lithic fragments, pumice, and crystals. At the base of the sequence is a massive pumice breccia that contains pumice blocks as much as 20 cm in length. Elongate pumice fragments and rare block- to lapilli-sized fragments of mafic lava and breccia show subparallel alignment. The top of this sequence is characterized by finer grained dacitic or rhyolitic crystal-pumice-lithic lapilli tuffs. In places these tuffs contain large irregular swirls and lenses of well-indurated tuff or lava as much as 10 m in length. These features are similar to those described in subaqueous rhyolitic flows by Dimroth and others (1979) from both Archean and Pleistocene volcanic complexes. Such features suggest a progression from explosive pyroclastic volcanism to more quiet effusion of rhyolitic lava.

Overlying the sequence of felsic volcaniclastic tuff is a series of discontinuous low-K flows (Bussey, 1988), informally designated as the Iron Dyke rhyolite unit. These flows are related to the effusive volcanic rocks that occur in the uppermost part of the felsic volcaniclastic tuff. They are fine grained and porphyritic with 1- to 3-mm plagioclase phenocrysts and rare quartz phenocrysts that are usually rounded and partially resorbed. Columnar jointing and flow layering developed locally.

A thick sequence of heterolithic conglomerate overlies the Iron Dyke rhyolite unit. This sequence thickens to the southeast, away from the Glory Hole fault zone, and includes a lens of fossiliferous limestone. In the mine area, detailed stratigraphic analysis of this sequence from drill core revealed a distinct unit rich in mineralized fragments (Stevens, 1981), informally referred to as the Iron Dyke lahar unit (B.E. Wise, written commun., 1983).

The youngest strata in the mine area is a sequence of volcanic sandstones that overlies the conglomerates. Thin beds of normally graded volcanic debris, interlayered with the sandstones, often contain cobble-size clasts of volcanic material. Pyrite framboids are present in dark-gray sandstone-siltstone layers. The finer grained parts of the sequence show evidence of soft-sediment deformation and bioturbation. Also interlayered with the sandstones are several fine-grained felsic lavas.

Dikes and sills of autobrecciated dacite are also common near the mine. They are characterized by finely disseminated hematite, which gives them a dark red color. A sill of hematitic dacite is present at depth in the Stewart syncline where it has intruded the conglomerates. Sills and plugs of low-K rhyolite porphyry present in the footwall rocks could be the subvolcanic equivalents of the felsic volcaniclastic tuffs, which are mineralogically similar (Bussey, 1988). They are commonly bleached and in places contain disseminated pyrite. Plugs, dikes, and sills of gabbro, diabase, dacite, and rhyolite are common in the Hunsaker Creek Formation near the Iron Dyke Mine (fig. 8.3). A small dike of unaltered gabbro is exposed in the mine and several drill holes in this area intersect small unaltered gabbro bodies, which are calc-alkaline.

MINERALIZATION AND ALTERATION

Mineralization at the Iron Dyke Mine can be divided into two fundamental styles, which are spatially

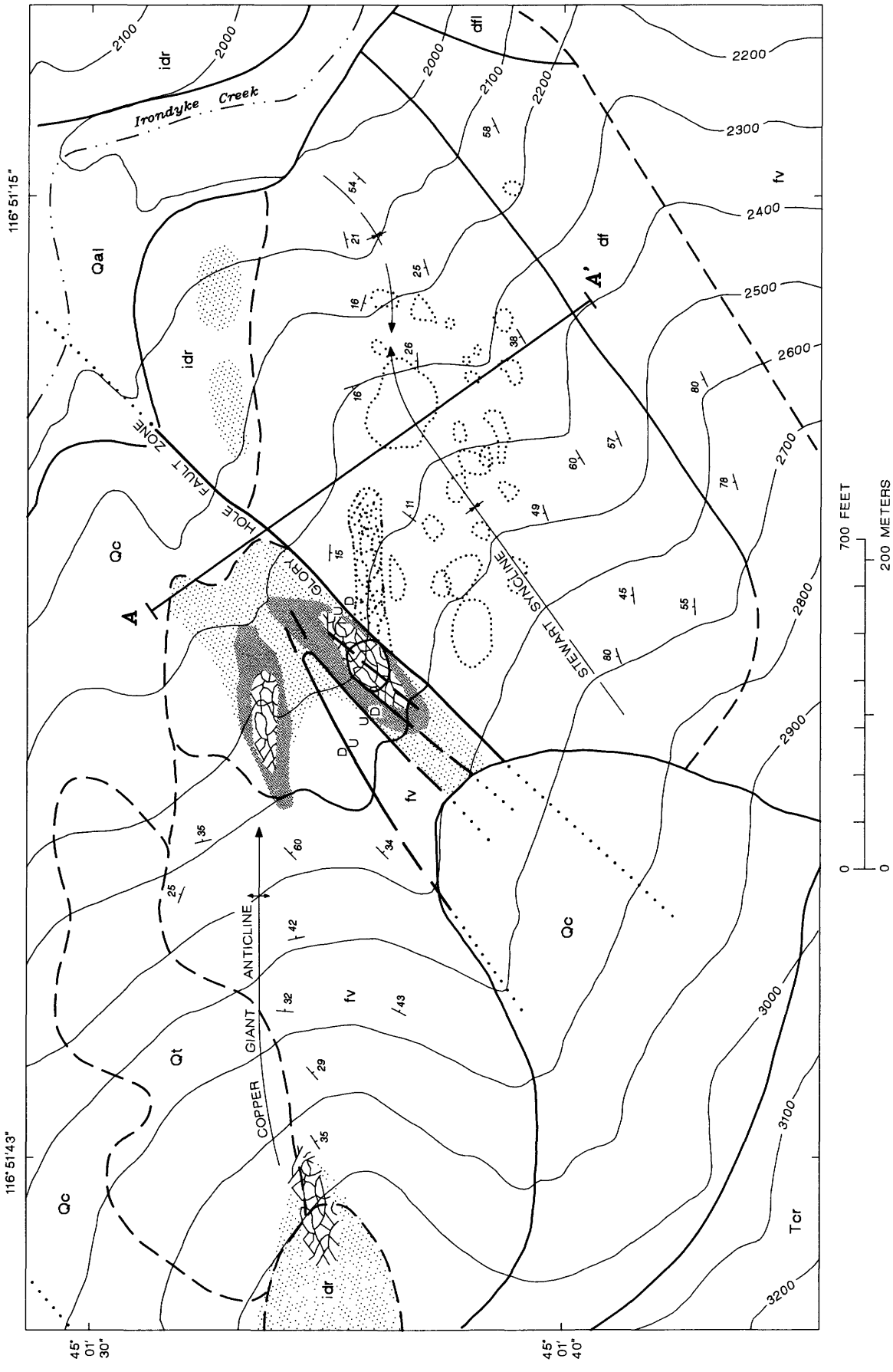

FIGURE 8.5.—Geologic map of Iron Dyke Mine area (modified from B.E. Wise, written commun., 1983). Mined and inferred mineralized fragments at depth in Stewart syncline and stoped parts of stockwork projected to surface. Contour interval, 100 ft.

and morphologically distinct (figs. 8.5 and 8.6). Immediately northwest of the Glory Hole fault zone, quartz-pyrite-chalcopyrite veins and associated alteration form a pipe-like stockwork that cuts through the Iron Dyke rhyolite unit and the underlying sequence of felsic volcaniclastic tuff (Bussey and LeAnderson, 1986). Southeast of the Glory Hole fault zone, mineralized fragments and clasts are present in the Iron Dyke lahar unit (Stevens, 1981). The fragments range in size from pebbles to enormous boulders and consist of mineralized stockwork as well as other types of mineralization.

EXPLANATION
[for figures 8.5 and 8.6]

Qal	Alluvium (Quaternary)
Qc	Cover deposit (Quaternary)
Qt	Talus (Quaternary)
Tcr	Columbia River Basalt Group (Miocene)
	Permian Strata
fi	Felsic intrusions
ss	Sedimentary sequence
df	Debris flow sequence—Locally divided into:
idl	Iron Dyke lahar unit
dfl	Limestone
idr	Iron Dyke rhyolite unit
fv	Felsic volcaniclastic sequence
———	Contact—Dashed where approximately located
———	Fault—Dashed where approximately located; dotted where inferred; D denotes downthrown block; U denotes upthrown block
	Chloritic altered area
	Sericitic altered area
	Exposed stockwork
	Stoped stockwork—Projected to surface
	Ore fragment in Iron Dyke lahar unit—Dotted where projected to surface
15	Strike and dip of bedding
	Anticline—Showing direction of plunge; dashed where approximately located
	Syncline—Showing direction of plunge; dashed where approximately located

FIGURE 8.5.—Continued.

QUARTZ-SULFIDE VEINS

Overall, the exposed stockwork has a roughly oval shape, 100 by 70 m, that is elongate in a northeast-southwest direction (fig. 8.5). Two distinct stockwork bodies are present: one is adjacent and parallel to the Glory Hole fault zone; the other lies along the axis of the Copper Giant anticline and is elongate in the same direction. Veins typically range in width from a few millimeters to 10 cm, and a few are up to a meter in width. R.S. Fredrickson (written commun., 1977) noted that individual veins strike north-northwest to northeast and dip steeply west. The center of the stockwork shows the greatest variation in vein orientation with north-south being the most common. Along the northern edge of the stockwork, most veins strike northwest and dip steeply southwest.

The original near-surface workings caved in and subsided to form a small glory hole. Early mining stoped a lenticular body within the vein system, as much as 2 m wide, that plunged 60° east and extended to a depth of 125 m below the glory hole (Swartley, 1914). High-grade ore from this body reportedly contained 15 to 20 percent copper (Lindgren, 1901). About 130 m below the glory hole, mineralized stockwork is truncated by the Glory Hole fault zone.

Another quartz-sulfide stockwork is located about 350 m west of the glory hole. Mineralization and alteration were similar to those that formed the glory hole stockwork but this stockwork is smaller and much less extensive. Quartz veining, widespread silicification, and alteration are also present along the ridge between the two stockworks, defining an east-west trending mineralized zone coincident with the axis of the Copper Giant anticline. The northeast trend of the Glory Hole fault zone is parallel to regional folding and faulting associated with Jurassic deformation across the eastern part of the Blue Mountains province, and accordingly the Glory Hole fault zone is probably much younger than the mineralization.

In addition to chalcopyrite and pyrite, the stockwork exposed in the glory hole also contains minor amounts of sphalerite and galena along with traces of tetrahedrite, bornite, and gold. Individual veins (figs. 8.7 and 8.8) cut sericitically altered wall rocks and are surrounded by dark-green chloritic halos. Most veins have crustiform banding of quartz, chalcopyrite, and pyrite. The veins contain late, euhedral quartz in vugs and open cavities. Many large veins have banded quartz-chalcopyrite-pyrite margins and central brecciated bodies containing euhedral quartz, vein fragments, chalcopyrite, and pyrite in a siliceous matrix (fig. 8.9).

The recognition of metal zoning in the stockwork is hampered by the inaccessibility of the old workings and a lack of drill-core data from the stockwork.

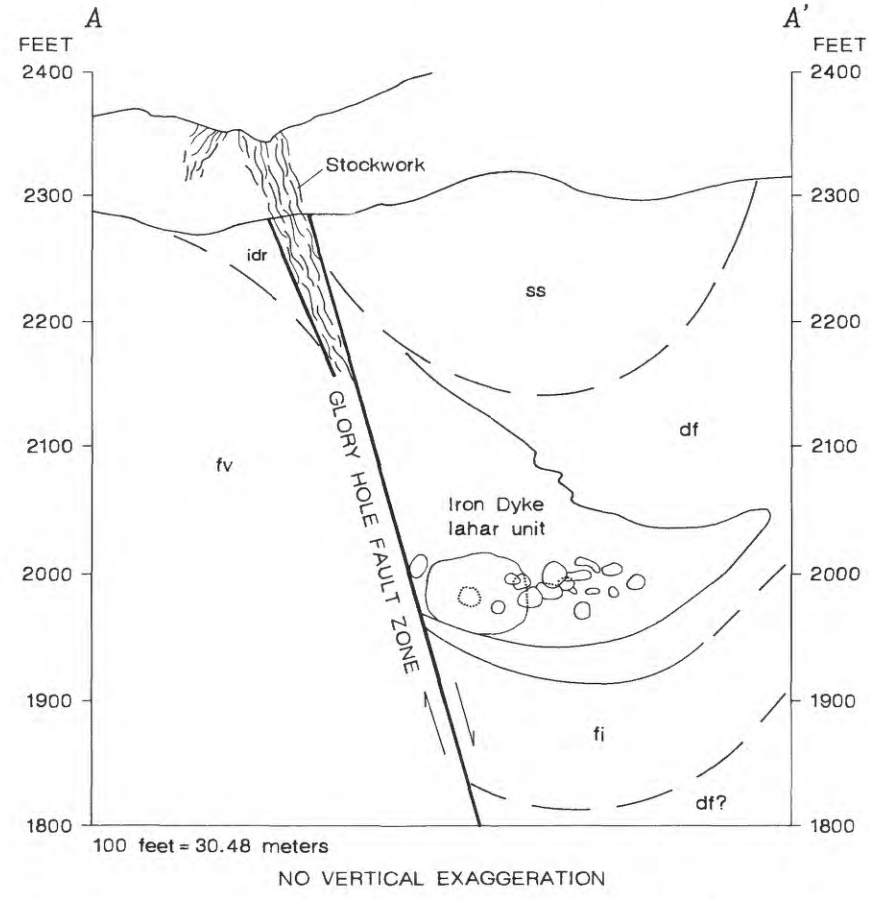

FIGURE 8.6.—Geologic cross section through Iron Dyke Mine area. Location of cross section shown on figure 8.5. The stockwork, 122 m to the south, is projected onto plane of cross section. Unit symbols same as in figure 8.5. Arrows denote movement along fault zone.

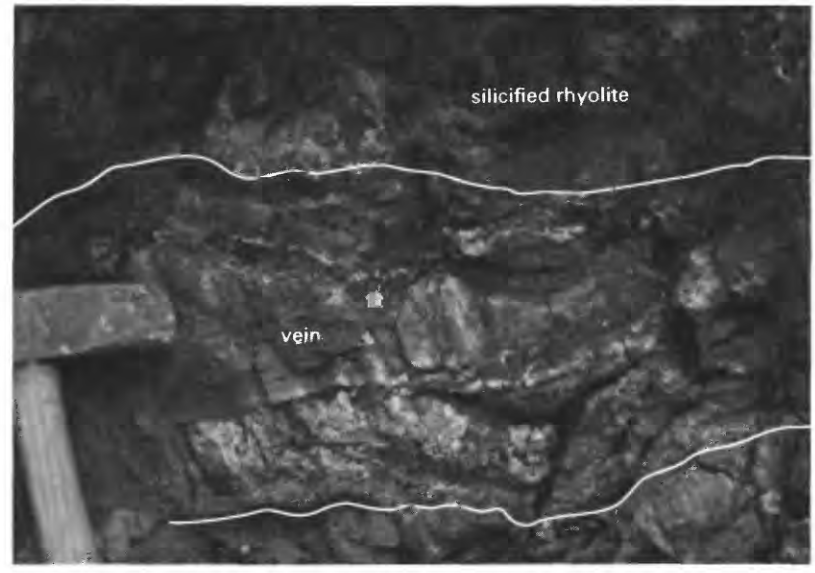

FIGURE 8.7.—Quartz-pyrite-chalcopyrite vein with well-developed crustiform banding cutting altered and silicified Iron Dyke rhyolite unit in glory hole, Iron Dyke Mine. Field of view is 40 cm.

From the data available, zoning appears to be poorly developed. Drill core from the stockwork suggests that the ratio of sphalerite and galena to pyrite and chalcopyrite increases upward and outward.

A broad area of footwall alteration is centered on the stockwork and consists of a central chloritic and silicified zone confined to the stockwork. An outer sericitic envelope in the upper part of the stockwork can be found discontinuously over an area 300 by 1,000 m that is elongated in a northeast-southwest direction (fig. 8.5). In the chloritic zone, dark-green chlorite forms narrow halos around veins (fig. 8.8) and is pervasive where the vein density is high. Chlorite, quartz, pyrite, leucoxene, and minor amounts of sericite are the most abundant minerals in the chlorite zone. The transition from the chloritic zone to the sericitic envelope encompasses several tens of centimeters in the upper part of the stockwork but is wider at greater depths. In the deepest part of the stockwork, sericitic alteration is absent and the chloritic zone grades into the regional greenschist facies assemblage. Sericite and quartz are the dominant minerals in the sericitic zone, although minor amounts of chlorite are commonly intergrown with the sericite (Stevens, 1981). Sericitic alteration of vein walls is associated with early mineralization, although it is usually overprinted and obscured by chloritic alteration associated with later mineralization (see fig. 8.14 and the "Paragenesis" section for a discussion of the stages of mineralization). Disseminated pyrite euhedra are also common especially near quartz-sulfide veins. The outer margin of the sericitic zone is gradational over several centimeters to dark red Iron Dyke rhyolite that contains hematite, barite-filled fractures, and barite rosettes as much as 5 mm in diameter.

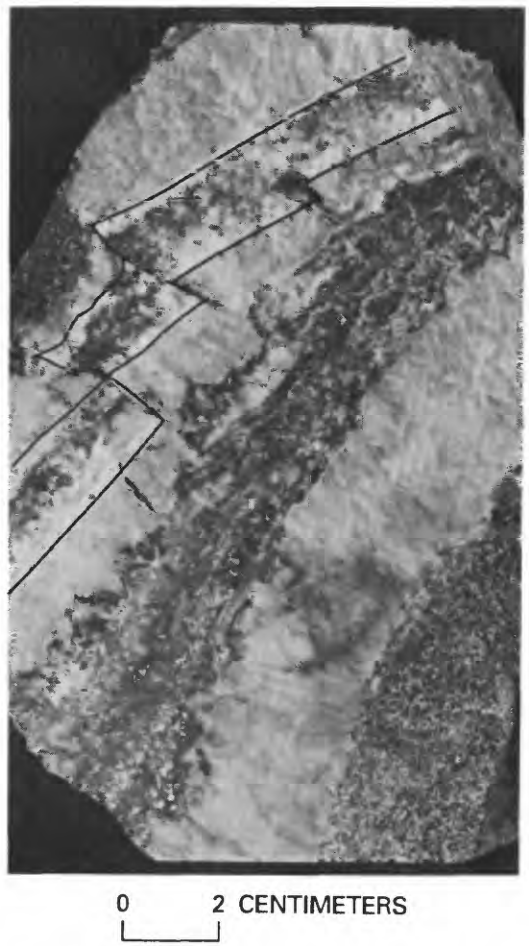

FIGURE 8.8.—Quartz-pyrite-chalcopyrite vein from glory hole, Iron Dyke Mine, showing two episodes of vein formation. Euhedral quartz formed comb-textured linings along walls of vein, which was then brecciated. Quartz, pyrite, chalcopyrite, chlorite, and hematite were deposited later in cross cutting veins.

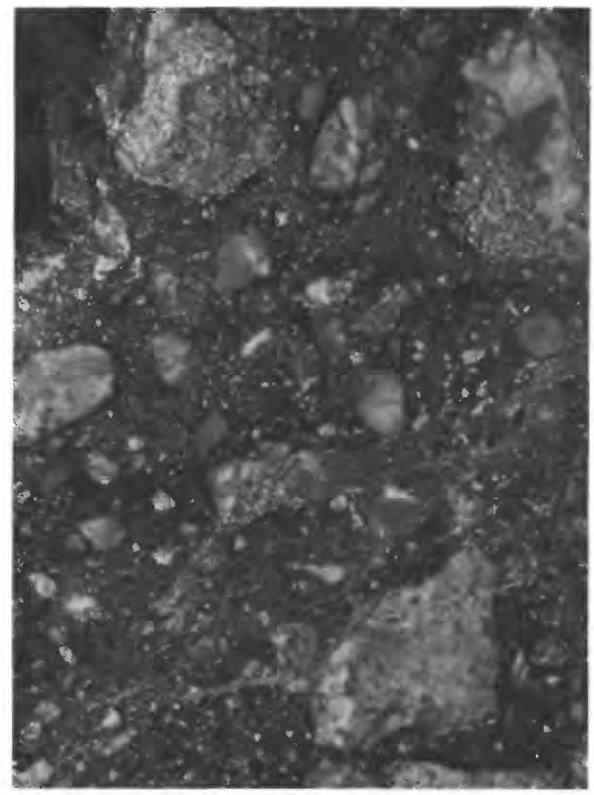

FIGURE 8.9.—Fragment of quartz-pyrite-chalcopyrite breccia from Iron Dyke lahar unit. Breccia is identical to that found cutting banded quartz-pyrite-chalcopyrite veins in glory hole.

MINERALIZED FRAGMENTS IN THE IRON DYKE LAHAR UNIT

The Iron Dyke lahar unit (fig. 8.6) is the heterolithic fragmental unit interbedded with conglomerates of the debris-flow sequence of Stevens (1981) and B.E. Wise (written commun., 1983). Exposures of Iron Dyke lahar in the mine workings are coarse grained, angular to rounded fragments ranging in size from pebble to boulder in a chloritic, tuffaceous, sandy matrix that often contains trace amounts of disseminated pyrite (B.E. Wise, written commun., 1983). Fragments constitute 65 to 90 percent of the unit and include sedimentary, volcaniclastic, and mafic to felsic flow rocks. The lahar reaches a maximum thickness of 90 m in the northwest limb of the Stewart syncline near the Glory Hole fault zone (B.E. Wise, written commun., 1983) and abruptly thins to the southeast. Fragment size and abundance decrease to the southeast.

The most distinguishing characteristic of the Iron Dyke lahar unit is that it contains a significant percentage of altered and mineralized fragments. The most recent and much past production was from these mineralized stockwork fragments, which are typically silicified and consist primarily of quartz, pyrite, and chalcopyrite (fig. 8.10). In addition to the stockwork fragments, other types of mineralized fragments, which are not found in the glory hole area, are also present in the lahar. These include massive sphalerite, massive chalcopyrite-pyrite, chalcopyrite-pyrite-chlorite breccia, two types of hematitic quartz breccia, and massive hematitic barite (table 8.2). Although present in only minor amounts, these other fragments are found throughout the Iron Dyke lahar along with the mineralized stockwork fragments.

The size and distribution of known fragments and their spatial relation to the glory hole stockwork ore body are shown in figures 8.5 and 8.6. Some fragments of mineralized stockwork are unusually large and range from a few meters to 50 m in diameter (Stevens, 1981). They are angular in shape and have sharp contacts with the lahar.

These other (nonstockwork) mineralized fragments (table 8.2) have important implications for the genesis of the deposit. Bedded massive sulfide has not been found in place, but several fragments from the Iron Dyke lahar unit bear a strong resemblance to massive sulfide ores from well-preserved deposits. Massive chalcopyrite-pyrite fragments have clastic textures of rounded chalcopyrite-pyrite grains in a matrix of chalcopyrite and pyrite. They are usually massive, but one sample has a clastic texture with graded bedding (fig. 8.11). Chalcopyrite-pyrite-chlorite breccias are texturally similar to the massive chalcopyrite-pyrite previously described, but they consist of elongate, rounded clasts of chalcopyrite-pyrite-chlorite and clasts of dark green to black chlorite as much as 3 cm in length (fig. 8.12). The long axes of these clasts are subparallel and define a layering within the samples.

Hematitic quartz breccia fragments are common in the Iron Dyke lahar unit, but they are not present in the exposed stockwork. The breccias can be divided into two types: those that contain chlorite, native gold, and oxidized vein material and those that do not. The first type (type I, table 8.2) consists of bright-red hematitic chert with delicate laminations in a red, siliceous, hematitic matrix containing minor amounts of barite and pyrite. Fragments range from angular to round and are usually less than 5 cm across. Pyrite-quartz fragments without hematite are also common.

The second type of breccia (type II, table 8.2) contains fragments of quartz and hematite, as much as 5 cm in diameter, but only traces of pyrite and chalcopyrite in a matrix of quartz, chlorite and minor amounts of carbonate (fig. 8.13). Fragments of chlo-

FIGURE 8.10.—Chalcopyrite-pyrite-quartz stockwork fragment from Iron Dyke lahar unit, Iron Dyke Mine.

TABLE 8.2.—*Textures and preferred genesis of nonstockwork mineralized fragments from the Iron Dyke lahar unit, Iron Dyke Mine, Homestead, Oregon*

Fragment type (Relative abundance in Iron Dyke lahar unit)	Texture	Deposits where similar textures are described (Preferred genesis)
Massive sphalerite (Rare)	Crude compositional layering; anhedral to euhedral grains; colloform banding, framboidal grains; very fine grained; dominated by sphalerite, but also includes pyrite, barite, galena, chalcopyrite, tetrahedrite, acanthite, and gold. (see figs. 8.15, 8.16, 8.17, 8.22).	Kuroko deposits, Japan;[1] Buchans deposits, Newfoundland. [2, 3] (Accumulation of sulfide mounds on the sea floor).
Massive chalcopyrite-pyrite (Rare)	Massive with irregular framboidal aggregates of chalcopyrite and pyrite, and anhedral to euhedral pyrite as much as 3 mm in diameter, in a matrix of very fine grained pyrite, chalcopyrite, and quartz. (see figs. 8.11, 8.19, 8.20).	Kuroko deposits, Japan;[1] Buchans deposits, Newfoundland, [2, 3] Prince Lyell, Tasmania.[4] (Basal parts of sulfide mounds that accumulate on the sea floor.)
Chalcopyrite-pyrite-chlorite breccia (Minor)	Fragments consist of chalcopyrite-pyrite-chlorite, as long as 3 cm, with porous colloform pyrite aggregates partially replaced by chalcopyrite; crude alignment of elongate fragments; rare silicified country rock fragments also present. (see figs. 8.12, 8.20).	No known equivalents; most similar to Prince Lyell, Tasmania.[4] (Altered fragmental rocks immediately below massive ore horizon; modified by deformation.)
Hematitic (type I) quartz breccia (Common)	Quartz with finely disseminated hematite (jasper); small (less than 0.02 mm) pyrite grains common, especially in less hematitic parts; large pyrite fragments replaced by quartz and hematite along crystallographic planes; often brecciated with jasper matrix; some fragments thinly laminated. (see fig. 8.11 (vein cutting massive cp-py)).	Kuroko deposits—tetsusekiei.[5] (Late and (or) distal exhalative mineralization, which forms stratiform-bedded lenses, breccia, and veins.)
Hematitic (type II) quartz-chlorite breccia. (Common)	Consists of partially to completely oxidized vein fragments in siliceous hematitic matrix; chalcopyrite, pyrite, bornite, and chlorite common, also chalcocite, digenite, and covellite after chalcopyrite; fragments rounded to angular, as much as 10 cm in diameter; morphologically identical to siliceous breccias in stockwork. (see figs. 8.13, 8.23, 8.24, 8.25, 8.26).	No known equivalents; most similar to Prince Lyell, Tasmania.[4] (Altered fragmental rocks at contact between upper hematite dominated alteration and lower chlorite dominated alteration.)
Massive hematitic barite (Common)	Euhedral to anhedral barite crystals, as long as 1 cm, in matrix of hematite; usually massive but may be cut by vein-like bodies of lighter colored barite; matrix 0 to 15 percent pyrite, sphalerite rare.	Buchans deposits;[2] Mount Lyell (The Blow), Tasmania;[4] Red Ledge, Idaho.[6] (Late and (or) distal exhalative mineralization, which forms stratiform lenses.)

[1]Eldridge and others, 1983.
[2]Thurlow and Swanson, 1981.
[3]Strong, 1981.
[4]Walshe and Solomon, 1981.
[5]Kalogeropoulos and Scott, 1983.
[6]Bussey, unpub. data, 1984.

rite as much as 1 mm in diameter are present in the matrix, and chlorite later filled in spaces between 0.5 mm euhedral quartz grains in the matrix. The matrix makes up 10 to 15 percent of the breccia, which is mostly clast supported. Larger fragments are slightly rounded whereas small fragments are round to angular. These breccias are economically important in that they often contain very small grains (10 to 30 microns) of gold disseminated in hematite and chlorite.

Fragments composed wholly of barite and hematite are present throughout the Iron Dyke lahar unit. The fragments tend to be well rounded and much smaller than the sulfide-bearing fragments. The barite in these fragments is typically pink to red in color, owing to finely disseminated hematite, and ranges in grain size from fine to very coarse. The coarse-grained barite crystals are as long as 1 cm, are often broken, and are enclosed in a matrix of massive hematite. Pyrite and sphalerite are not common, but they

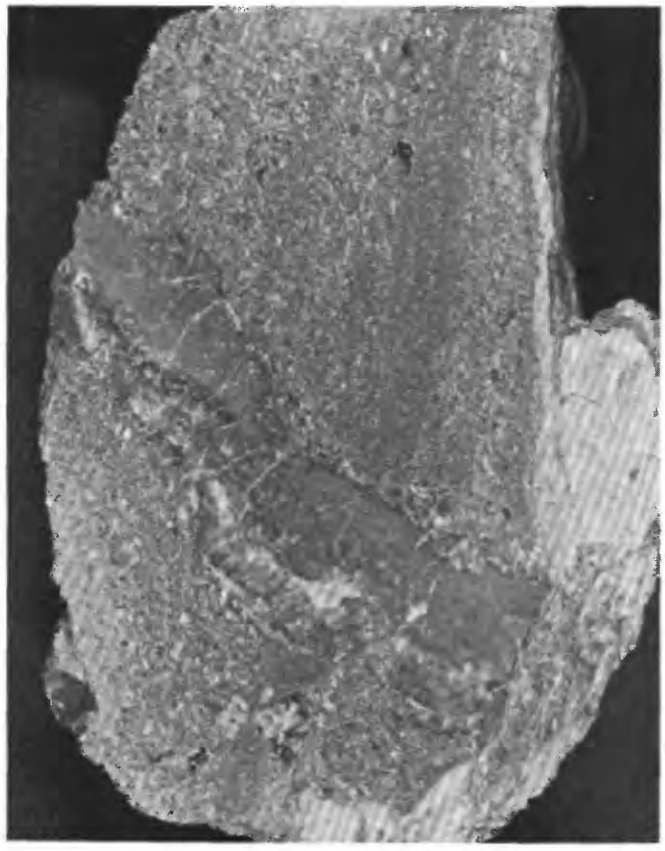

◀ FIGURE 8.11.—Chalcopyrite-pyrite fragment from Iron Dyke lahar unit, Iron Dyke Mine. Note size-graded layers of sulfide and minor amounts of silicified fragments. Sample is cut by hematitic quartz vein.

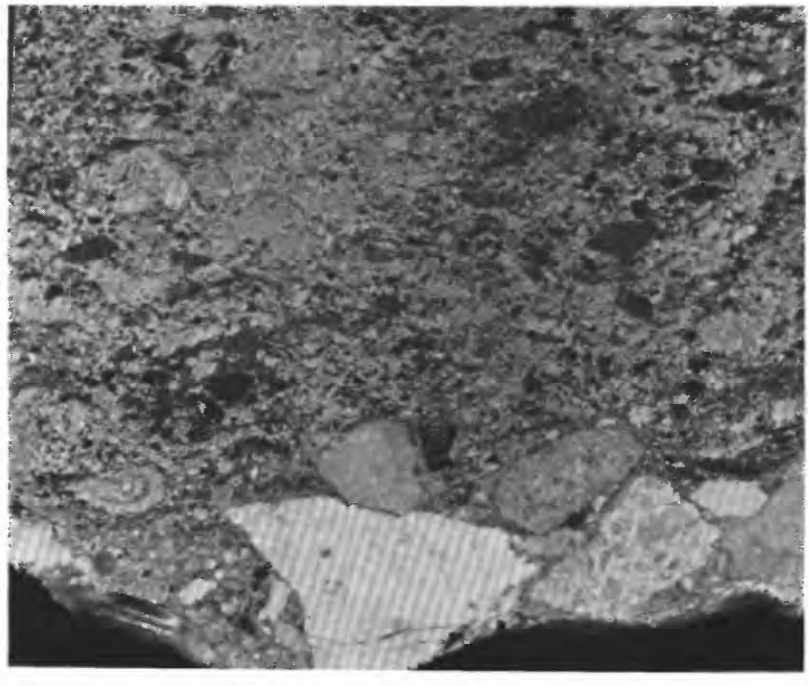

◀ FIGURE 8.12.—Chalcopyrite-pyrite-chlorite breccia fragment from Iron Dyke lahar unit, Iron Dyke Mine. Note elongate clasts define layering. Light-colored clasts at bottom of sample are part of Iron Dyke lahar unit.

are present in some barite-rich fragments that do not contain much hematite.

PARAGENESIS

Samples representing as many different types of mineralization as possible were taken from the dumps, accessible workings, and drill core and examined in reflected light. Ore minerals, in decreasing order of abundance, are pyrite, chalcopyrite, sphalerite, galena, tetrahedrite, bornite, acanthite, chalcocite, covellite, digenite, and native gold. Gangue minerals, in decreasing order of abundance, are quartz, chlorite, sericite, hematite, barite, goethite, and calcite. A petrogenetic study of the ore samples and their textures revealed that mineralization can be divided into a six-stage paragenetic sequence (fig. 8.14).

Fine-grained colloform and botryoidal pyrite in quartz veins of the stockwork and siliceous chalcopyrite-pyrite breccias are characteristic of stage 1 mineralization. Stage 1 pyrite affected by processes of later stages is recrystallized to a coarser grain size and is often euhedral, with only remnants of stage 1 textures preserved. Every sample examined contains early variety pyrite; the widespread distribution of this early variety pyrite indicates that stage 1 mineralization was widespread and affected the entire deposit. Sericitic alteration of wall rocks is also associated with stage 1 mineralization.

Sphalerite, galena, and tetrahedrite characterize stage 2 and are best developed in sphalerite-rich veins from the periphery of the stockwork and in massive sphalerite fragments found in the Iron Dyke lahar unit. In these veins, which can be as wide as 10 cm, sphalerite is present as anhedral grains, as long as 3 mm. Individual sphalerite grains occur in clusters, which are cut by white quartz veinlets. Chalcopyrite disease and blebs of chalcopyrite, as long as 5 microns, are elongate along crystal planes in sphalerite and are more abundant around quartz veinlets. Galena is present in fractures within coarser grained anhedral to euhedral pyrite. Tetrahedrite forms irregularly shaped patches, as much as 0.06 mm in diameter, within sphalerite. In chalcopyrite-rich veins, tetrahedrite occurs in trace amounts as 0.02-mm grains in chalcopyrite and is often associated with similar-sized sphalerite grains. Sericitic alteration of wall rocks is also associated with stage 2 mineralization. One massive sphalerite fragment from the Iron Dyke lahar unit is mineralogically and texturally similar to massive black ore described at the Kuroko massive sulfide deposits in Japan (Yui and Ishitoya, 1983; Eldridge and others, 1983). The fragment is crudely banded owing to mineralogic variations into sphalerite and chalcopyrite bands in a barite-rich matrix (fig. 8.15). Much of the fragment consists of colloform and framboidal intergrowths of sulfides (fig. 8.16), but there are zones of anhedral to euhedral intergrowths (fig. 8.17).

Replacement textures of earlier sulfides by chalcopyrite characterize stage 3. Earlier formed pyrite, now recrystallized to coarse anhedral to euhedral

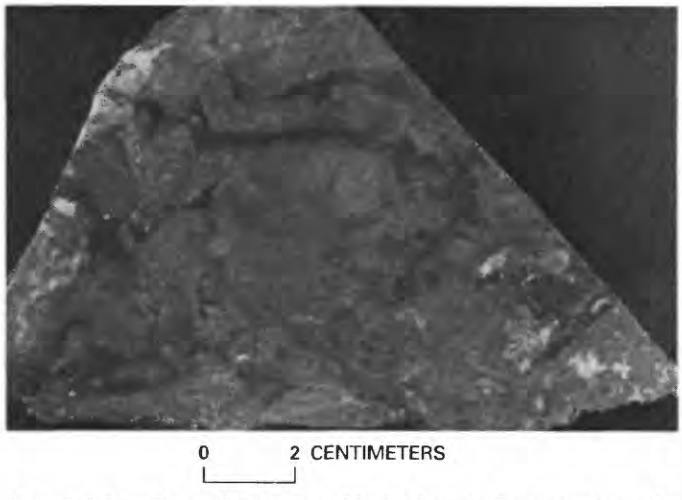

FIGURE 8.13.—Hematitic quartz-chlorite breccia fragment from the Iron Dyke lahar unit, Iron Dyke Mine. Breccia consists of hematitic vein and wall rock material in quartz and chlorite matrix.

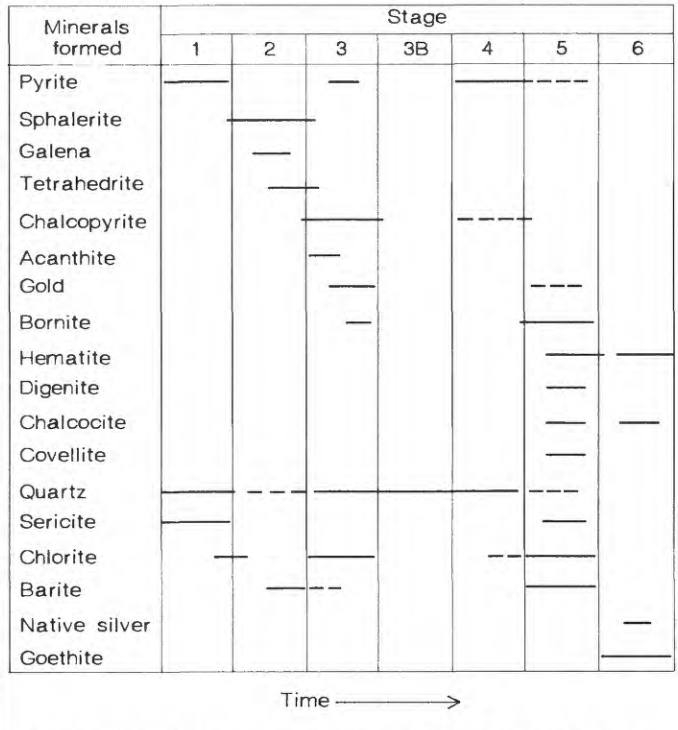

FIGURE 8.14.—Paragenetic sequence of minerals identified at the Iron Dyke Mine, near Oxbow, Oregon.

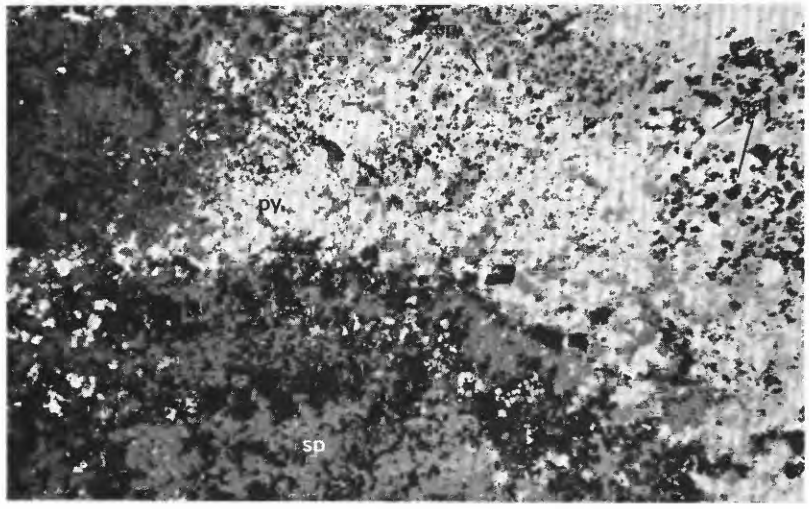

FIGURE 8.15.—Crude compositional layering in a massive sphalerite fragment from the Iron Dyke lahar unit. cp, chalcopyrite; ga, galena; py, pyrite; sp, sphalerite. Field of view is 3.5 mm. Reflected light.

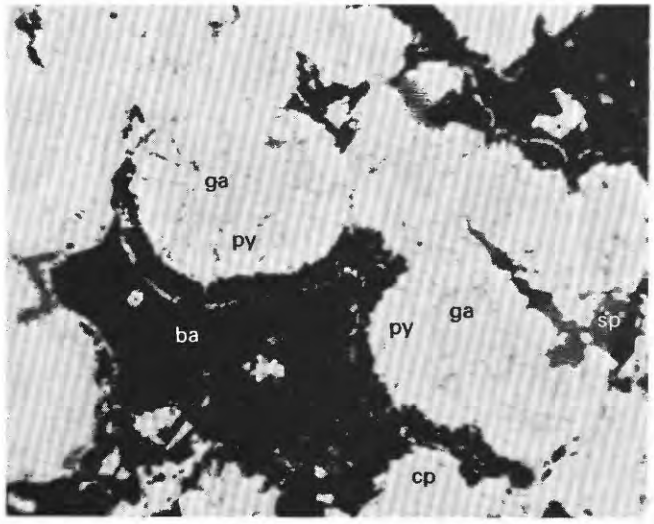

FIGURE 8.16.—Colloform intergrowth of galena (ga) and pyrite (py), which has been partially replaced by chalcopyrite (cp), sphalerite (sp), and barite (ba), in a massive sphalerite fragment. Field of view is 0.55 mm. Reflected light.

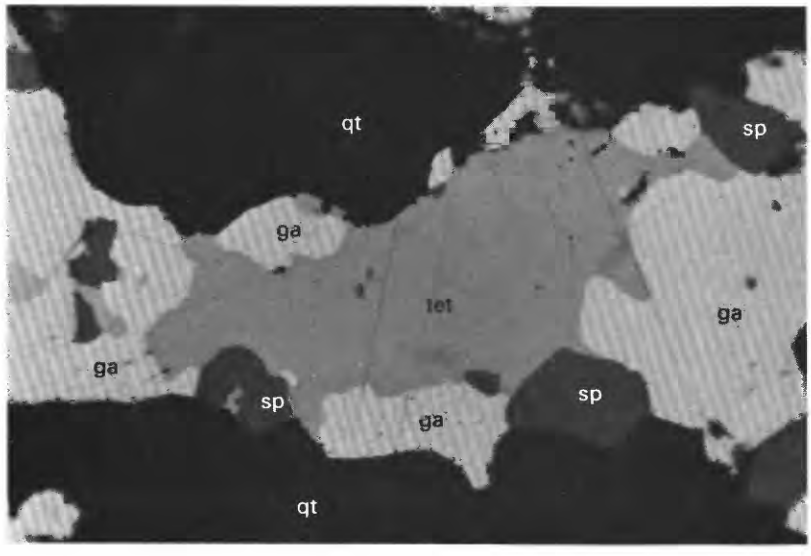

FIGURE 8.17.—Anhedral and euhedral intergrowth of sphalerite (sp), galena (ga), tetrahedrite (tet), and quartz (qt) in a massive sphalerite fragment from Iron Dyke lahar unit, Iron Dyke Mine. Field of view is 0.55. Reflected light.

grains, contains chalcopyrite along fractures and crystallographic planes. The extent of replacement ranges from fracture filling to nearly complete replacement of the entire grain (fig. 8.18). Chalcopyrite is present along growth zones in colloform pyrite, and it surrounds colloform pyrite grains (fig. 8.19). In samples containing early fine-grained colloform and botryoidal sulfides, chalcopyrite cuts across banding and completely encloses rounded grains of pyrite and galena. Chalcopyrite also occurs with chlorite as round grains in the center of early pyrite framboids (fig. 8.20). This texture is analogous to the "bullet hole texture" described by Howe (1985, p. 2115) from deposits in the West Shasta Mining District in northern California. In chalcopyrite-rich samples, 50-micron thick crustiform bands of fine-grained pyrite line quartz- and chalcopyrite-filled vugs. Chalcopyrite disease, described by Eldridge and others (1983) in ores of the Kuroko deposits, Japan, is well developed in stage 2 sphalerite-rich veins where they are cut by stage 3 quartz-chalcopyrite veins.

Trace amounts of bornite and economically important gold and acanthite are associated with chalcopyrite in stage 3. Bornite is present as round blebs as much as 50 microns in size in coarse-grained pyrite, commonly in association with chalcopyrite. Gold is present as white to yellow grains up to 50 microns in size in pyrite, chalcopyrite, sphalerite, and galena, but it is most common in pyrite and chalcopyrite where it occurs as blebs and fracture fillings (fig. 8.21). Gold is assigned to stage 3 but may have formed as extremely fine grained disseminations in earlier deposited sulfides and recrystallized into microscopically visible grains during deposition of stage

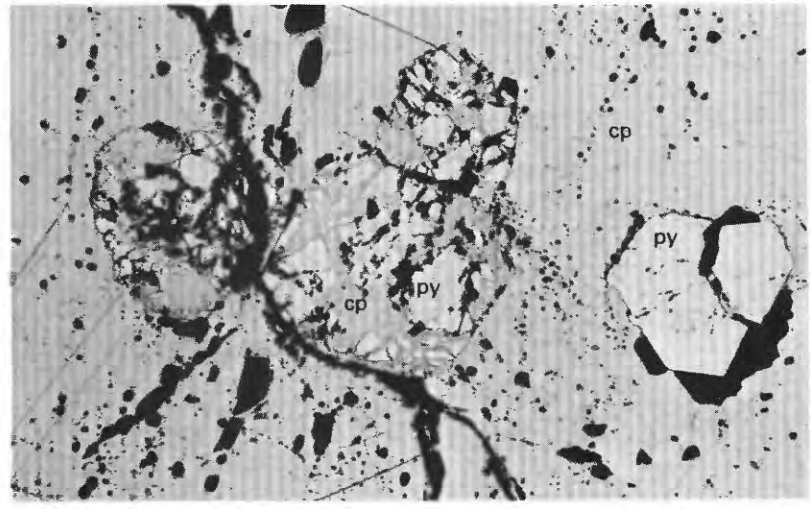

► FIGURE 8.18.—Variable replacement of euhedral pyrite (py) by chalcopyrite (cp) in chalcopyrite-pyrite stockwork sample. Pyrite grains on left are almost completely replaced, pyrite on right is still mostly intact. Field of view is 1.1 mm. Reflected light.

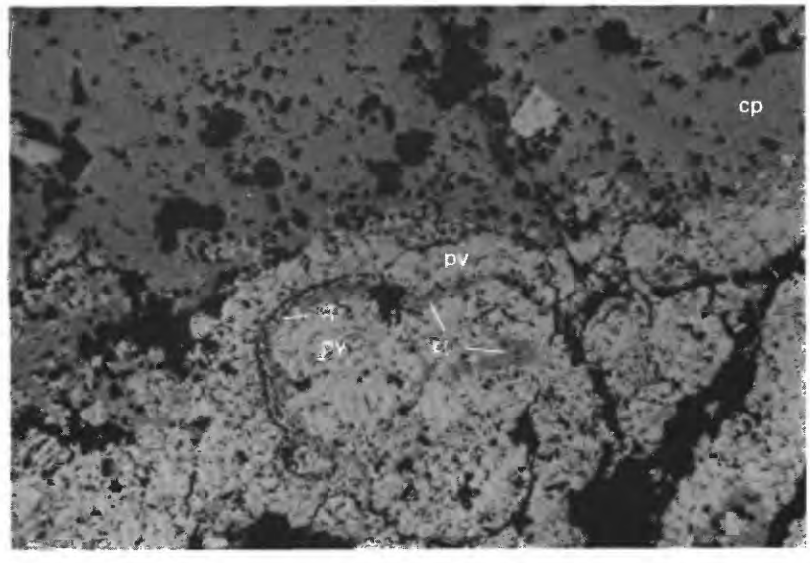

► FIGURE 8.19.—Replacement of colloform pyrite (py) by chalcopyrite (cp) in a massive chalcopyrite-pyrite fragment from the Iron Dyke lahar unit, Iron Dyke Mine. Field of view is 1.1 mm. Reflected light.

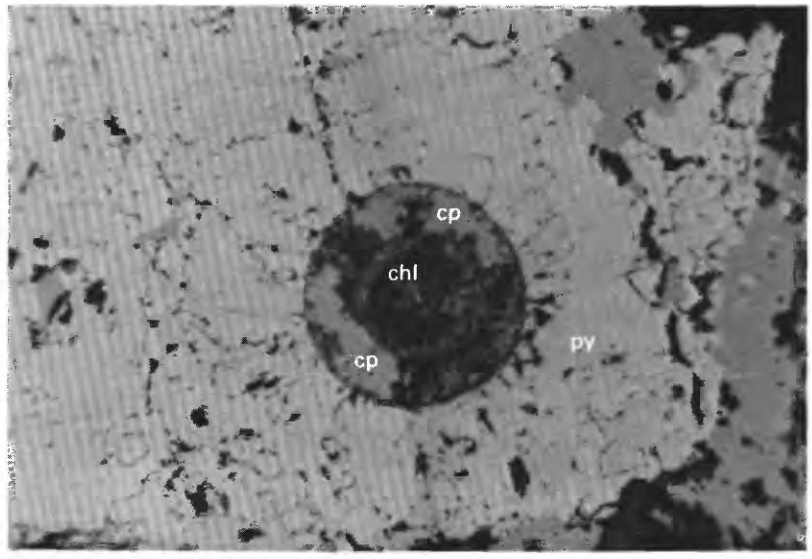

FIGURE 8.20.—Chalcopyrite (cp) and chlorite (chl) replacement of a pyrite (py) framboid in a massive chalcopyrite-pyrite fragment from Iron Dyke lahar unit, Iron Dyke Mine. Field of view is 0.55 mm. Reflected light.

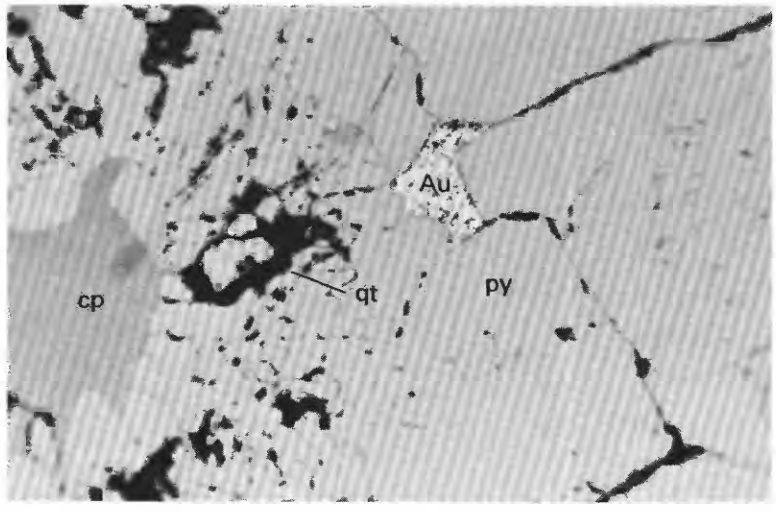

FIGURE 8.21.—Anhedral pyrite (py) replaced by chalcopyrite (cp) and gold (Au), in a chalcopyrite-pyrite-quartz (qt) stockwork fragment from Iron Dyke lahar unit, Iron Dyke Mine. Field of view is 0.23 mm. Reflected light.

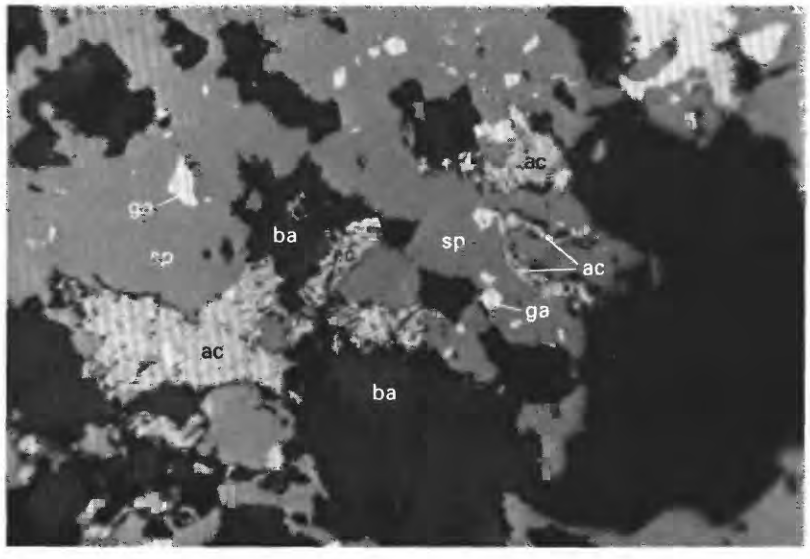

FIGURE 8.22.—Irregular acanthite (ac) grain replacing sphalerite (sp), galena (ga), and barite (ba) in a massive sphalerite fragment from Iron Dyke lahar unit, Iron Dyke Mine. Field of view is 0.23 mm. Reflected light.

3 minerals. Acanthite forms ragged, gray, cryptocrystalline masses as much as 100 microns in length and is usually associated with galena. It was one of the last minerals to form during stage 3. It rims vugs and cavities and forms irregular vein-like bodies (fig. 8.22) that cut across layering. Pervasive chloritic alteration of the wall rock is associated with stage 3 and often overprints earlier sericitic alteration.

Stage 3B refers to late euhedral quartz that fills vugs and cavities in quartz-sulfide veins formed during stages 1–3. Stage 3B quartz also forms late barren veins that cut earlier quartz-sulfide veins, and it forms comb-textured linings along the walls of late veins whose interiors contain quartz, pyrite, chalcopyrite, hematite, and chlorite deposited during stage 4 (see fig. 8.8).

The textures of stage 4 are restricted to the siliceous chalcopyrite-pyrite breccias, described in the "Quartz-Sulfide Veins" section, which form vein or pipe-like bodies within the stockwork and contain earlier mineralized fragments and altered country rock with variable proportions of a fine-grained quartz matrix. The breccias consist of variably altered fragments and very little siliceous matrix, and they range in composition from highly siliceous to sulfidic. Fragments of earlier comb-quartz veins and crustiform-banded quartz-sulfide veins are common. The fine-grained quartz matrix often contains disseminated 50- to 70-micron-size chalcopyrite-pyrite framboids. Fragments of altered country rock within the breccias show evidence of at least three earlier episodes of brecciation. Fragments are angular to subangular and as much as 10 cm in diameter. The best examples of siliceous breccia are found as fragments in the Iron Dyke lahar unit (see fig. 8.9), but the fragments are identical to the siliceous breccias that cut through the exposed stockwork.

Minerals and textures of stage 5 are restricted to hematitic siliceous breccias, described in the "Mineralized Fragments in the Iron Dyke Lahar Unit" section, which are present only in the Iron Dyke lahar unit. Bornite of this stage surrounds, and occupies fractures within, chalcopyrite (fig. 8.23). Bornite, in turn, is cut by veinlets of digenite less than 5 microns thick. Where digenite veinlets cut chalcopyrite, they are separated from the chalcopyrite by halos of bornite. Digenite also forms irregularly shaped grains as much as 0.50 mm in diameter. Large grains of bornite may contain chalcocite in a roughly cubic network of fine veinlets or lamellae in the center of the grain (fig. 8.24). These same grains may also be surrounded by a thin rim of chalcopyrite with short chalcopyrite lamellae that extend into the bornite in a crude basket weave texture. Hematite in the breccia fragments is present as massive hematite and as very fine hematite disseminated in quartz. In transmitted light, opaque hematite masses fill the centers of euhedral-comb quartz veins. Hematite is most abundant along vein structures that terminate at the fragment margins. Less-abundant hematite colors veins and breccias reddish. Disseminated grains of chalcopyrite, specular hematite, and corroded pyrite are also present. Gold is present as grains less than 20 microns in size. It is found in both

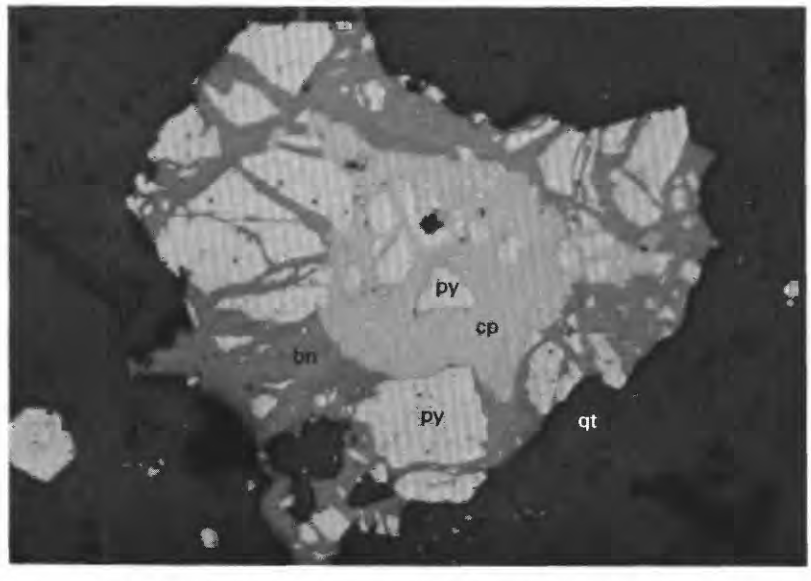

FIGURE 8.23.—Bornite (bn) replacement of chalcopyrite (cp) in hematitic quartz-chlorite breccia fragment from Iron Dyke lahar unit, Iron Dyke Mine. py, pyrite; qt, quartz. Field of view is 0.55 mm. Reflected light.

the hematitic and nonhematitic parts of the breccia, but it is most abundant in the hematitic parts, often in association with massive hematite (fig. 8.25). Clusters of gold grains are often enclosed within chlorite grains (fig. 8.26).

Weathered samples collected from the exposed stockwork show the development of stage 6 colloform banded hematite and goethite with rare grains of native silver and gold. Azurite, malachite, and chalcocite form rare surface crusts several millimeters thick on some of the largest exposed veins.

FLUID INCLUSIONS

The abundance of veins with comb quartz and crustiform banding of quartz and sulfides prompted a fluid-inclusion study of the deposit (Bussey, 1988). Vein samples were collected from exposed stockwork, from drill cores cutting through the stockwork at depth, and from fragments of stockwork in the Iron Dyke lahar unit. Uncertainties in temperature measurements are generally less than ±5°C for filling temperatures and ±0.1°C for freezing-temperature determinations. A summary of the filling temperature and salinity data is shown in figure 8.27. The uniform paragenetic sequence of stages 1–3 found in all samples of the deposit indicates that most minerals were deposited under increasing thermal conditions, culminating with chalcopyrite during stage 3 at 300°C. Following stage 3, fluid temperatures dropped to 150°C during the deposition of late barren quartz of stage 3B. No fluid inclusions are associated with stage 4, but the presence of pyrite-chalcopyrite framboids within the siliceous breccia matrix suggests rapid deposition of sulfides.

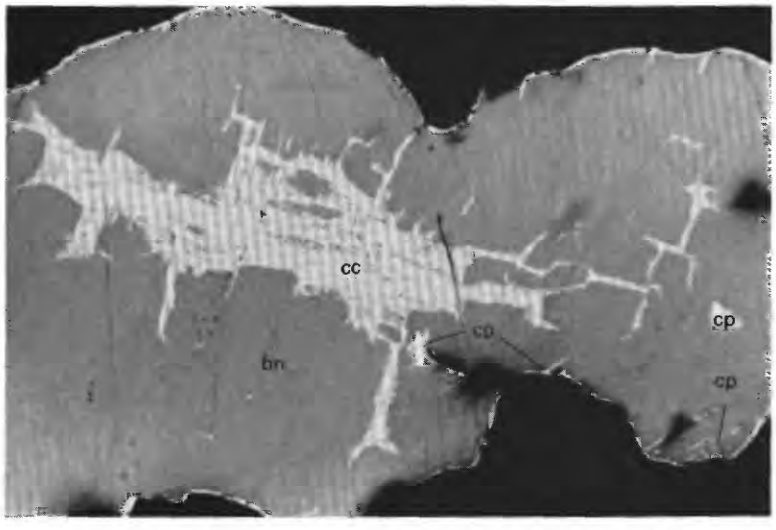

◄ FIGURE 8.24.—Bornite (bn) being replaced by chalcocite (cc) in a grid pattern in the center of grain in a hematitic quartz-chlorite breccia fragment from Iron Dyke lahar unit, Iron Dyke Mine. Chalcopyrite (cp) forms the rim around grain with lamellae extending inward. Field of view is 0.55 mm. Reflected light.

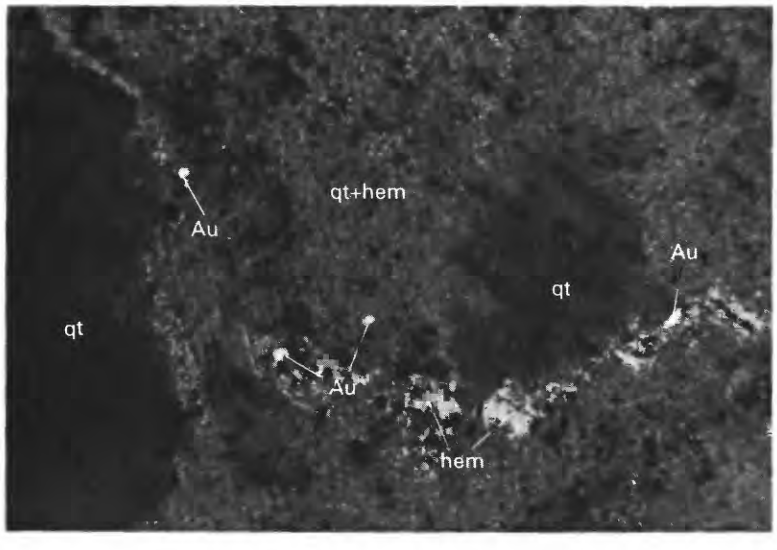

◄ FIGURE 8.25.—Hematitic quartz (qt+hem), cut by vein-like mass of hematite (hem), containing three grains of gold (Au). From hematitic quartz-chlorite breccia fragment in Iron Dyke lahar unit, Iron Dyke Mine. Field of view is 0.23 mm. Reflected light.

No evidence was found to indicate the fluids were boiling in any of the samples studied. However, the highly brecciated nature of the stockwork and the surrounding Iron Dyke rhyolite unit suggest that explosive hydrothermal activity may have played an important role in the formation of the Iron Dyke deposit. If the hydrothermal fluids were a mixture of NaCl and pure water at 300°C, a salinity of 10 weight percent NaCl (fig. 8.27) would require a minimum water depth of 800 m to prevent boiling. However, a small amount of CO_2 in solution would lower the boiling temperature of the fluid considerably and accordingly increase the minimum depth of seawater required to prevent boiling. If the fluid contained 0.2 molal CO_2 (average for Kuroko stockwork ore, Pisutha-Arnond and Ohmoto, 1983) and 10 equivalent weight percent NaCl, the minimum depth would be 1,100 m.

RECONSTRUCTION OF THE DEPOSIT

Silicification and quartz veining along the axis of the Copper Giant anticline and the location of the two stockworks along this trend suggest the anticline was a controlling structure during mineralization. The northeast-trending Glory Hole fault zone is probably a Jurassic structure, but the location of the Iron Dyke stockwork at the intersection of the Copper

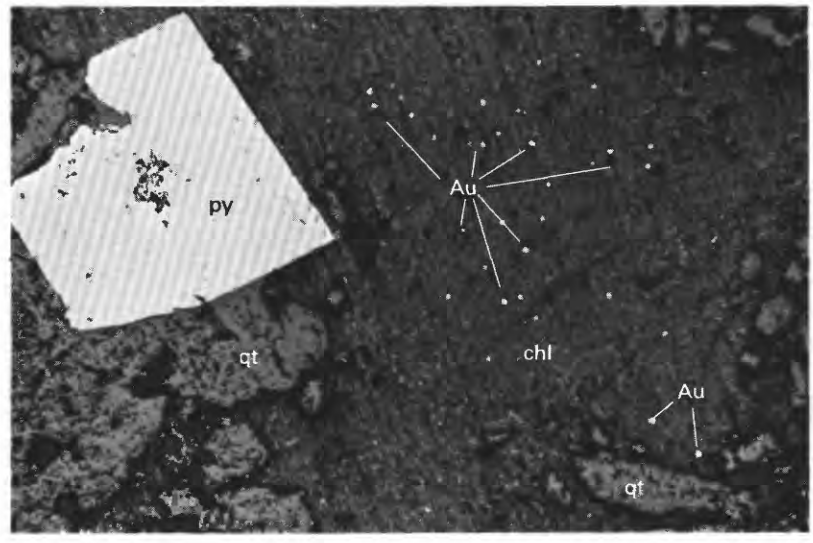

► FIGURE 8.26.—Chlorite (chl) in matrix of hematitic quartz-chlorite breccia fragment from the Iron Dyke lahar unit, Iron Dyke Mine, containing numerous small grains of gold (Au). Field of view is 0.55 mm. pr, pyrite; qt, quartz. Reflected light.

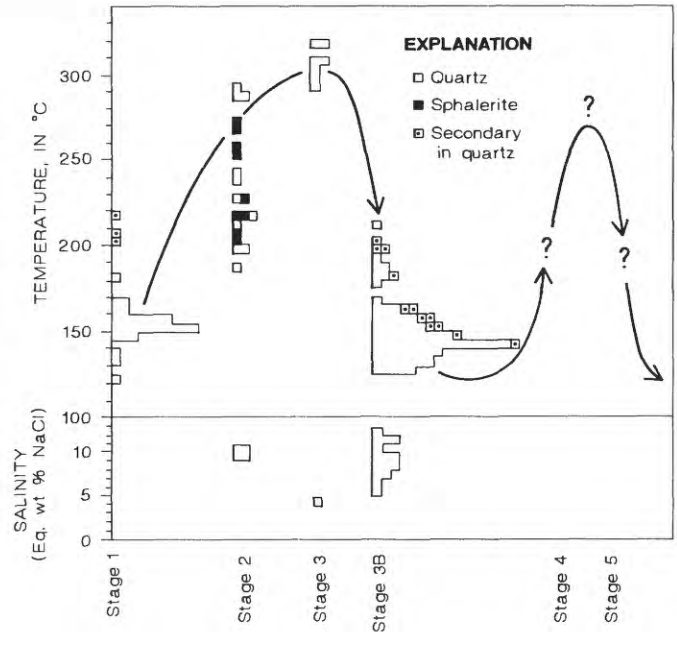

► FIGURE 8.27.—Filling temperature and salinity data for 118 primary and 15 secondary inclusions in quartz and sphalerite from 10 samples. Suggested increase in temperature of fluid evolution path (line with arrows) in stages 4 and 5 is based on mineralogic data because no inclusions were formed during those stages.

Giant anticline and the Glory Hole fault zone suggests that the Glory Hole fault zone may represent a structural zone that has been active since the Early Permian.

Four observations support the interpretation that the stockwork fragments in the Iron Dyke lahar unit were derived from the stockwork exposed at the glory hole. These are:

1. The intimate spatial association between the stockwork exposed in the glory hole and the Iron Dyke lahar unit.
2. Rapid decrease in thickness of the lahar away from the exposed stockwork.
3. The decrease in size and abundance of mineralized fragments with distance from the exposed stockwork.
4. The extremely large size of some stockwork fragments in the Iron Dyke lahar unit.

Furthermore, the presence of nonstockwork mineralized fragments in the Iron Dyke lahar unit suggests that these fragments represent mineralization that formed vertically above the exposed stockwork.

The mineralized Iron Dyke lahar unit was possibly a stratiform stringer zone, as originally suggested by Juhas and others (1980), that was broken into individual fragments during folding of the Stewart syncline. Mining of the deposit, however, revealed that fragments were completely separated from one another by varying thicknesses of unaltered debris-flow material. Whereas some fragments are surrounded by thin clay gouge zones (Stevens, 1981), others clearly are not. In addition, fragments with distinctively different mineral assemblages are juxtaposed throughout the Iron Dyke lahar unit.

Another possibility is that individual ore fragments formed in place as nodules, similar to those described by Steefel (1987) at the Johnson River Prospect in Alaska. However, fragments in the Iron Dyke lahar unit show no evidence of concentric growth. On the contrary, veins in the stockwork fragments are abruptly truncated at fragment margins. Also, fragments (of variable alteration) are not concentrically altered around the margin of the fragment, as would be expected if the alteration had occurred in place.

The morphology of the Iron Dyke deposit strongly resembles that of deposits in the Buchans area in central Newfoundland where three related types of ore are present: stockwork ore, in-situ ore, and mechanically transported fragmental ore (Thurlow and Swanson, 1981). Two of these types, stockwork ore and mechanically transported fragmental ore, are present at the Iron Dyke Mine. In addition, many of the transported ore fragments at the Iron Dyke are fragments of in-situ massive ore. The preservation of delicate framboidal textures suggests some of the ores were protected from recrystallization owing to later high-temperature fluids. The clastic textures of massive ore fragments indicate reworking of an accumulating sulfide mound by explosive hydrothermal discharge or sea-floor weathering causing fragmentation and slumping of part of the sulfide mound away from its vent area.

Examples of slumped sulfide material have been described from the axial zone of the Escanaba Trough in the southern Gorda Ridge, off the northern California coast (Zierenberg and others, 1986; Morton and others, 1986). Sulfide deposits in the Escanaba Trough have formed along the base of small, uplifted hills and mark original syndepositional faults along which uplift occurred. Some of the largest deposits are exposed on steep slopes near the base of the uplifted hills. Individual deposits, which are mounds tens of meters wide and several meters high, are surrounded by sulfide talus aprons formed by disintegration and collapse of sulfide chimneys. Many of the deposits are in the process of being buried by turbiditic siltstones and slump deposits from the steep slopes of the uplifted hills. These examples appear to be modern analogs of the processes envisaged at the Iron Dyke Mine.

The Iron Dyke deposit, as it now exists, represents a part of what must have been a much more extensive mineralized area. Faulting and erosion have dismembered the deposit to such a degree that its original morphology is no longer apparent. The lowermost part of the reconstructed deposit is represented by the stockwork now exposed in the glory hole. The stockwork continued upward and breccia was more abundant in the upward part. Massive and transported sulfides accumulated below the vent area and formed a sulfide talus apron similar to that in the Escanaba Trough. Similarly, massive hematitic barite formed around the vent, probably on top of, and laterally beyond the massive sulfides.

Stockwork fragments subjected to apparently highly oxygenated conditions in the upper parts of the hydrothermal system are represented by the type II hematite-quartz-chlorite breccia. Highly oxygenated conditions are also indicated by the abundance of massive barite fragments and pervasive hematite in the surrounding rhyolite flows.

GENESIS OF THE DEPOSIT

All the rocks of the Hunsaker Creek Formation have been affected by sea-floor burial metamorphism and weak regional greenschist facies metamorphism. The extent to which this has modified the original

textures of the deposit is unknown. However, the preservation of delicate fine-grained textures identical to those found in the unmetamorphosed Kuroko deposits (Eldridge and others, 1983; Ishihara, 1974) suggests that the metamorphic effects are minor. The textures and mineralogy, descriptions of which are taken mainly from veins in the stockwork, probably accurately represent the depositional history of the Iron Dyke deposit.

Evidence from fluid inclusions indicates that in stages 1–3 minerals were deposited under waxing conditions in a thermally intensifying hydrothermal system. These conditions are similar to those in which the Kuroko deposits formed (Pisutha-Arnond and Ohmoto, 1983). Additional chalcopyrite mineralization in stage 4, separated from stage 3 by intervening low-temperature quartz veins (stage 3B), indicates that the hydrothermal system underwent at least two pulses of high-temperature fluid discharge. The second period of chalcopyrite deposition (stage 4) is associated with brecciation of previously formed veins.

Explosive activity in the discharge vent is the most likely cause of brecciation. Widespread silicification, which formed a cap over the discharge site, sealed the upper part of the system allowing accumulation of rising hot fluid and a corresponding build up of pressure beneath the cap. When the confining pressure of the cap was exceeded, explosive hydrothermal activity occurred.

The type II hematite-quartz-chlorite breccia contains the assemblage of bornite, chalcocite, covellite, and digenite, which is characteristic of supergene processes. The breccias are present only as fragments in the Iron Dyke lahar unit and probably represent mineralization that took place in the upper part of the deposit. The origin of the secondary copper minerals of stage 5 is not readily apparent. A similar assemblage of copper minerals is described at the North Lyell and Crown Lyell volcanic-hosted deposits in western Tasmania. Walshe and Solomon (1981) suggested that bornite and chalcopyrite were deposited by late-stage fluids circulating within the upper part of the system. They suspect these fluids were oxidized, acidic, and copper-enriched owing to leaching of preexisting pyrite-chalcopyrite mineralized areas. Leaching probably also formed the stage 5 secondary copper minerals at the Iron Dyke deposit.

SUMMARY AND CONCLUSIONS

The Cu-Au Iron Dyke Mine was formed during Permian tholeiitic volcanism in the Blue Mountains island arc. Stratigraphically, the deposit is situated within the upper part of the Hunsaker Creek Formation, at the top of a local accumulation of low-K felsic lavas and tuffs, and is overlain by a thick sequence of epiclastic sedimentary rocks including conglomerate, sandstone, siltstone, and limestone. The Hunsaker Creek Formation was deposited in a basin adjacent to a volcanically active and subaerially eroding island arc. Rapidly changing sediment sources and synvolcanic tectonism resulted in the widespread formation of local unconformities. Felsic lavas and hypabyssal intrusions near the mine differentiated in a shallow magma chamber that probably supplied the heat to drive the hydrothermal mineralizing system.

The epiclastic facies overlying the deposit indicate deposition by debris flows and turbidites in a submarine fan environment adjacent to a subaerial volcanic arc. Shallow-water-facies rocks of the Hunsaker Creek Formation are present 11 kilometers to the west of the present-day mine area (Vallier, 1967). Assuming a moderately steep arc slope of 7° (Sigurdsson and others, 1980), water depths in the study area would have been only about 1,400 meters which compares favorably to the 1,100-meter minimum depth of formation calculated from fluid-inclusion data.

The development of the deposit is shown in a series of schematic diagrams (fig. 8.28*A–D*). Paleogeographic reconstruction of the Iron Dyke area suggests a high-energy environment of active volcanism, rugged topography, and rapid deposition of reworked immature volcanic debris. Following the extrusion of the Iron Dyke rhyolite unit, hydrothermal activity along an east-west-trending fracture zone resulted in widespread alteration, brecciation, and silicification of the Iron Dyke rhyolite unit and the underlying sequence of felsic volcaniclastic tuff. Penetration of cool seawater into the upper parts of the fracture zone promoted circulation below the sea floor of heated and evolved fluids with fluid mixing, cooling, and deposition of metals from the hydrothermal fluids (fig. 8.28*A*). This may explain why the Iron Dyke deposit is dominated by ore consisting of stockworks and epithermal-like crustiform veins. It is also consistent with the argument that the hematitic quartz breccias, which contain oxidized vein fragments, formed in the upper parts of the deposit.

Normal movement along the fracture system created a fault scarp that uplifted part of the deposit (fig. 8.28*B*). When the scarp became unstable, it slumped, disrupted the uplifted part of the deposit, and formed the Iron Dyke lahar unit (fig. 8.28*C*). Continued sedimentation buried the lahar with coarse conglomerates and associated fine-grained sediments. Additional faulting and folding occurred during accretion of the Blue Mountains island arc to the North American

craton. It was during this time that movement on the Glory Hole fault zone brought the stratigraphically higher Iron Dyke lahar unit into fault contact with the stockwork mineralization (fig. 8.28*D*). Erosion has removed mineralization that must have extended above the level of the stockwork now exposed in the area of the Glory Hole fault zone.

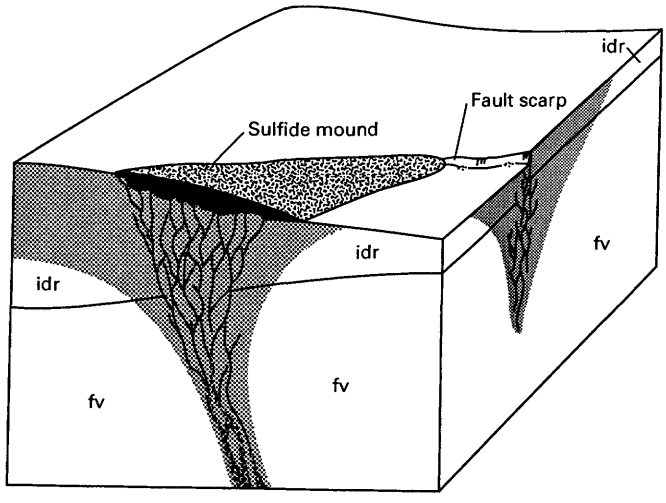

A

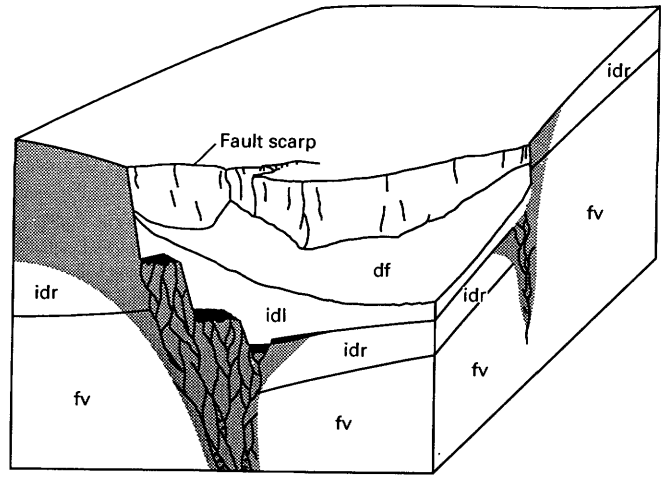

B

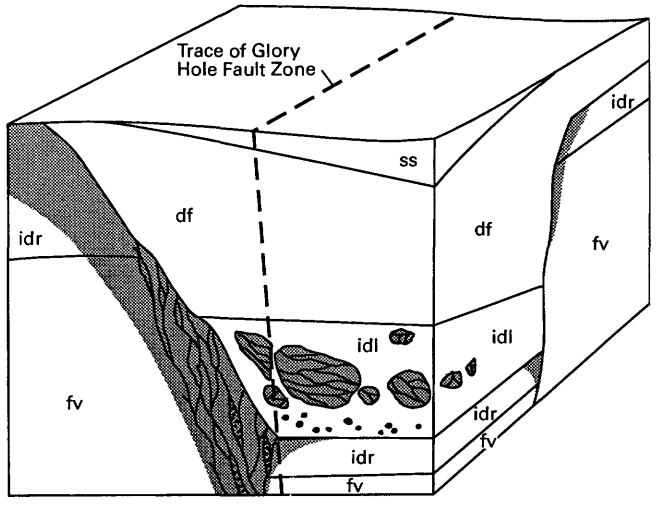

C

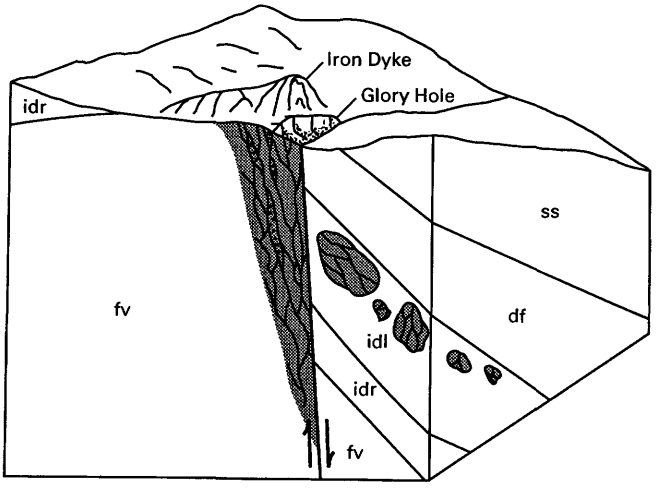

D

EXPLANATION

ss	Sedimentary sequence
df	Debris flow sequence
idl	Iron Dyke lahar unit
idr	Iron Dyke rhyolite unit
fv	Felsic volcaniclastic sequence
———	Contact
———	Fault—Arrows show relative movement
	Stockwork or stockwork fragment—Dotted pattern within stockwork denotes brecciated area
	Sulfide mound
	Area of alteration

FIGURE 8.28.—Schematic diagram showing geologic history of Iron Dyke deposit, near Oxbow, Oregon. Black pattern denotes sulfide mound in cross section. *A*, Initial hydrothermal activity and formation of sulfide mound. *B*, Movement along the stockwork fracture zone caused slumping of sulfide mound and formation of clastic sulfide lenses. *C*, Continued uplift and collapse of the stockwork formed Iron Dyke lahar unit, which was later buried by fine-grained sediments. *D*, Present configuration following movement along Glory Hole fault zone as well as Tertiary erosion.

Their preservation had a profound effect on the economic value of the mine, because mineralized fragments in the Iron Dyke lahar unit have accounted for about 60 percent of the total recorded production.

REFERENCES CITED

Avé Lallemant, H.G., 1983, The kinematic insignificance of mineral lineations in Late Jurassic thrust and fold belt in eastern Oregon, U.S.A.: Tectonophysics, v. 100, no. 1–3, p. 389–404.

Bishop, Ellen Morris, 1988, Igneous petrology of the Baker melange terrane and the Canyon Mountain complex [abs.]: Geological Society of America, Abstracts with Programs, v. 20, no. 6, p. 407.

Blome, C.D., 1988, Paleontologic and tectonic significance of the Grindstone terrane, east-central Oregon [abs.]: Geological Society of America, Abstracts with Programs, v. 20, no. 3, p. 144.

Bonnichsen, Bill, 1987, Pre-Cenozoic geology of the West Mountain-Council Mountain-New Meadows area, west-central Idaho, *in* Vallier, T.L., and Brooks, H.C., eds., Geology of the Blue Mountains region of Oregon, Idaho, and Washington: The Idaho batholith and its border zone: U.S. Geological Survey Professional Paper 1436, p. 151–170.

Brooks, H.C., 1979a, Geologic map of the Huntington and part of the Olds Ferry quadrangles, Baker and Malheur Counties, Oregon: Oregon Department of Geology and Mineral Industries, Geologic Map Series, GMS-13.

Brooks, H.C., 1979b, Plate tectonics and geologic history of the Blue Mountains: Oregon Geology, v. 41, no. 5, p. 71–80.

Brooks, H.C., and Ramp, Len, 1968, Gold and silver in Oregon: Oregon Department of Geology and Mineral Industries, Bulletin 61, 337 p.

Brooks, H.C., and Vallier, T.L., 1978, Mesozoic rocks and tectonic evolution of eastern Oregon and western Idaho, *in* Howell, D.G., and McDougall, K.A., eds., Mesozoic Paleogeography of the Western United States, (Pacific Coast Paleogeography Symposium 2): Los Angeles, Society of Economic Paleontologists and Mineralogists, Pacific Section, p. 133–145.

Bussey, S.D., 1988, Geology of the Iron Dyke copper-gold massive sulfide deposit and its relationship to facies of the Permian Hunsaker Creek Formation, Snake River canyon, Oregon and Idaho: Golden, Colorado School of Mines, Ph.D. dissertation, 202 p.

Bussey, S.D., and LeAnderson, James, 1986, Epithermal mineralization at the Iron Dyke massive sulfide deposit, N.E. Oregon: Geological Society of America, Rocky Mountain Section, Abstracts with Program, v. 18, no. 5, p. 344.

Debiche, M.G., Cox, Allen, and Engebretson, David, 1987, The motion of allochthonous terranes across the north Pacific basin: Geological Society of America Special Paper 207, 49 p.

Dickinson, W.R., 1979, Mesozoic forearc basin in central Oregon: Geology, v. 7, no. 4, p. 166–170.

Dickinson, W.R., and Thayer, T.P., 1978, Paleogeographic and paleotectonic implications of Mesozoic stratigraphy and structure in the John Day inlier of central Oregon, *in* Howell, D.G., and McDougall, K.A., eds., Mesozoic Paleogeography of the Western United States, (Pacific Coast Paleogeography Symposium 2): Los Angeles, Society of Economic Paleontologists and Mineralogists, Pacific Section, p. 147–161.

Dimroth, E., Cousineau, P., Leduc, M., Sanschagrin, Y., and Provost, G., 1979, Flow mechanisms of Archean subaqueous basalt and rhyolite flows, *in* Current Research, Part A: Geological Survey of Canada, Paper 79-1A, p. 207–211.

Eldridge, C.S., Barton, P.B., and Ohmoto, Hiroshi, 1983, Mineral textures and their bearing on formation of the Kuroko orebodies, *in* Ohmoto, Hiroshi, and Skinner, B.J., eds., The Kuroko and Related Volcanogenic Massive Sulfide Deposits: Economic Geology Monograph 5, p. 241–281.

Francis, E.H., 1983, Magma and sediment—II: Problems of interpreting paleovolcanics buried in the stratigraphic column: Journal of the Geological Society of London, v. 140, p. 165–183.

Goldstrand, P.M., 1987, Depositional environments of the Coon Hollow Formation, Wallowa terrane, N.E. Oregon and W. Idaho [abs.]: Geological Society of America, Abstracts with Programs, v. 19, no. 6, p. 382.

Hamilton, W.B., 1963, Metamorphism in the Riggins region, western Idaho: U.S. Geological Survey Professional Paper 436, 95 p.

Harbert, William, and Vallier, Tracy, 1988, Determination of Leonardian paleolatitude of Wrangellia: EOS (American Geophysical Union, Transactions), v. 69, no. 16, p. 339.

Hillhouse, J.W., Gromme, C.S., and Vallier, T.L., 1982, Geomagnetism and Mesozoic tectonics of the Seven Devils volcanic arc in northeastern Oregon: Geophysical Research, v. 87, no. B5, p. 3777–3794.

Howe, S.S., 1985, Mineralogy, textures, and relative age relationships of massive sulfide ore in the West Shasta district, California: Economic Geology, v. 80, no. 8, p. 2114–2127.

Howell, D.G., and Normark, W.R., 1982, Sedimentology of submarine fans, *in* Scholle, P.A., and Spearing, Darwin, eds., Sandstone Depositional Environments: Tulsa, Okla., American Association of Petroleum Geologists, p. 365–404.

Imlay, R.W., 1986, Jurassic ammonites and biostratigraphy of eastern Oregon and western Idaho, *in* Vallier, T.L., and Brooks, H.C., eds., Geology of the Blue Mountains Region of Oregon, Idaho, and Washington: Geologic implications of Paleozoic and Mesozoic paleontology and biostratigraphy, Blue Mountains province, Oregon and Idaho: U.S. Geological Survey Professional Paper 1435, p. 53–58.

Ishihara, Shunso, ed., 1974, Geology of Kuroko deposits: Society of Mining Geologists Japan, Special Issue 6, 435 p.

Jones, D.L., Silberling, N.J., and Hillhouse, J.W., 1977, Wrangellia—A displaced terrane in northwestern North America: Canadian Journal of Earth Sciences, v. 14, no. 11, p. 2565–2577.

Juhas, A.P., Freeman, P.S., and Fredrickson, R.S., 1980, Kuroko type copper-gold mineralization at the Iron Dyke Mine, Oregon: Proceedings of the Symposium of Mineral Deposits of the Pacific Northwest: U.S. Geological Survey Open-File Report 81-355, p. 236–245.

Kalogeropoulos, S.I., and Scott, S.D., 1983, Mineralogy and geochemistry of tuffaceous exhalites (tetsusekiei) of the Fukazawa Mine, Hokuroko district, Japan, *in* Ohmoto, H., and Skinner, B.J., eds., The Kuroko and Related Volcanogenic Massive Sulfide Deposits: Economic Geology Monograph 5, p. 412–432.

LeAnderson, P.J., and Richey, Scott, 1986, Geology of the Wallowa-Seven Devils volcanic (island) arc terrane between the Snake and Salmon rivers near Lucile, Idaho: Part 1, Stratigraphy, structure, and metamorphism: U.S. Geological Survey Open-File Report 85-0611, 30 p.

Lindgren, Waldemar, 1899, The copper deposits of the Seven Devils mining district, Idaho: Mining and Science Press, v. 78, p. 125.

Lindgren, Waldemar, 1901, The gold belt of the Blue Mountains of Oregon: U.S. Geological Survey Annual Report, 22nd, p. 560–576.

Livingston, D.C., and Laney, F.B., 1920, The copper deposits of the Seven Devils and adjacent districts (including Heath, Horney Creek, Hoodoo, and Deer Creek): Idaho Bureau of Mines and Geology, Bulletin 1, 105 p.

Lund, Karen, Scholten, Robert, and McCollough, W.F., 1983, Consequences of interfingering lithologies in the Seven Devils island arc [abs.]: Geological Society of America, Abstracts with Programs, v. 15, no. 15, p. 284.

Mann, G.M., and Vallier, T.L., 1987, Geology of the Wildhorse River area, western Idaho: Telescoped terranes of the Blue Mountains province [abs.]: Geological Society of America, Abstracts with Programs, v. 19, no. 5, p. 318.

Mitchell, A.H.G., 1970, Facies of an early Miocene volcanic arc, Malekula Island, New Hebrides: Sedimentology, v. 14, no. 3–4, p. 201–243.

Morganti, J.M., 1972, Geology and ore deposits of the Cuprum area, Seven Devils district, Idaho: Pullman, Washington State University, M.S. thesis, 153 p.

Morris, E.M., and Wardlaw, B.R., 1986, Conodont ages for limestones of eastern Oregon and their implications for pre-Tertiary melange terranes, *in* Vallier, T.L., and Brooks, H.C., eds., Geology of the Blue Mountains region of Oregon, Idaho, and Washington: Geologic implications of Paleozoic and Mesozoic paleontology and biostratigraphy, Blue Mountains province, Oregon and Idaho: U.S. Geological Survey Professional Paper 1435, p. 53–58.

Morrison, R.F., 1961, Angular unconformity marks Triassic–Jurassic boundary in Snake River area of northeastern Oregon: Ore Bin, v. 23, no. 11, p. 105–111.

Morrison, R.F., 1964, Upper Jurassic mudstone unit named in Snake River canyon, Oregon-Idaho boundary: Northwest Science, v. 38, no. 3, p. 83–87.

Morton, J.L., Holmes, M.L., Normark, W.R., Ross, S.L., and Lyle, Mitchell, 1986, Sedimentary setting of massive sulfide deposits, Escanaba Trough, offshore northern California: EOS (American Geophysical Union, Transactions), v. 67, no. 44, p. 1282.

Mullen, E.D., 1985, Petrologic character of Permian and Triassic greenstones from the Melange terrane of eastern Oregon and their implications for terrane origin: Geology, v. 13, no. 2, p. 131–134.

Mullen, E.D., and Sarawitz, D.M., 1983, Paleozoic and Triassic terranes of the Blue Mountains, northeast Oregon: Discussion and field trip guide, Part 1. A new consideration of old problems: Oregon Geology, v. 45, no. 6, p. 65–68.

Onasch, C.M., 1987, Temporal and spatial relations between folding, intrusion, metamorphism, and thrust faulting in the Riggins area, west-central Idaho, *in* Vallier, T.L., and Brooks, H.C., eds., Geology of the Blue Mountains region of Oregon, Idaho, and Washington: The Idaho batholith and its border zone: U.S. Geological Survey Professional Paper 1436, p. 139–150.

Orr, W.N., 1986, A Norian (Late Triassic) icthyosaur from the Martin Bridge Limestone, Wallowa Mountains, Oregon, *in* Vallier, T.L., and Brooks, H.C., eds., Geology of the Blue Mountains region of Oregon, Idaho, and Washington: Geologic implications of Paleozoic and Mesozoic paleontology and biostratigraphy, Blue Mountains province, Oregon and Idaho: U.S. Geological Survey Professional Paper 1435, p. 41–52.

Pessango, E.A., and Blome, C.D., 1986, Faunal affinities and tectonogenesis of Mesozoic rocks in the Blue Mountains province of eastern Oregon and western Idaho, *in* Vallier, T.L., and Brooks, H.C., eds., Geology of the Blue Mountains region of Oregon, Idaho, and Washington: Geologic implications of Paleozoic and Mesozoic paleontology and biostratigraphy, Blue Mountains province, Oregon and Idaho: U.S. Geological Survey Professional Paper 1435, p. 65–78.

Phelps, D.W., 1979, Petrology, geochemistry, and the origin of the Sparta quartz diorite-trondhjemite complex, northeastern Oregon, *in* Barker, F., ed., Trondhjemites, dacites, and related rocks: Amsterdam, Elsevier, p. 549–579.

Pisutha-Arnond, Visut, and Ohmoto, Hiroshi, 1983, Thermal history, and chemical and isotopic compositions of the ore-forming fluids responsible for the Kuroko massive sulfide deposits in the Hokuroko district of Japan, *in* Ohmoto, H., and Skinner, B.J., eds., The Kuroko and Related Volcanogenic Massive Sulfide Deposits: Economic Geology Monograph 5, p. 523–558.

Sarawitz, Daniel, 1983, Seven Devils terrane: Is it really a piece of Wrangellia?: Geology, v. 11, no. 11, p. 634–637.

Sigurdsson, H., Sparks, R.S.J., Carey, S.N., and Huang, T.C., 1980, Volcanogenic sedimentation in the Lesser Antilles arc: Journal of Geology, v. 88, no. 5, p. 523–540.

Silberling, N.J., 1983, Stratigraphic comparison of the Wallowa and Huntington terranes, northeast Oregon [abs.]: Geological Society of America, Abstracts with Programs, v. 15, no. 5, p. 372.

Silberling, N.J., Jones, D.L., Blake, M.C., Jr., and Howell, D.G., 1984, Lithotectonic terrane maps of the North American Cordillera: U.S. Geological Survey Open-File Report 84-523, 43 p.

Smith, W.D., and Allen, J.E., 1941, Geology and physiography of the northern Wallowa Mountains, Oregon: Oregon Department of Geology and Mineral Industries, Bulletin 12, 64 p.

Snyder, K.D., 1973, Geochemical orientation survey in the Seven Devils mining district: Moscow, University of Idaho, M.S. thesis, 84 p.

Stanley, G.D., Jr., 1986, Late Triassic coelenterate faunas of western Idaho and northeastern Oregon: Implications for biostratigraphy and paleogeography, *in* Vallier, T.L., and Brooks, H.C., eds., Geology of the Blue Mountains region of Oregon, Idaho, and Washington: Geologic implications of Paleozoic and Mesozoic paleontology and biostratigraphy, Blue Mountains province, Oregon and Idaho: U.S. Geological Survey Professional Paper 1435, p. 23–40.

Steefel, C.I., 1987, The Johnson River prospect, Alaska: Gold-rich seafloor mineralization from the Jurassic: Economic Geology, v. 82, no. 4, p. 894–914.

Stevens, M.G., 1981, Geology of the Iron Dyke Mine, Homestead, Oregon: Salt Lake City, University of Utah, M.S. thesis, 78 p.

Strong, D.F., 1981, Notes on ore mineralogy of the Buchans district, *in* Swanson, E.A., Strong, D.F., and Thurlow, J.G., eds., The Buchans Orebodies: Fifty Years of Geology and Mining: Geological Association of Canada, Special Paper 22, p. 141–160.

Swartley, A.M., 1914, Ore deposits in northeastern Oregon: Oregon Bureau of Mines and Geology of Mineral Resources., v. 1, no. 8, 229 p.

Sutter, J.F., Snee, L.W., and Lund, Karen, 1984, Metamorphic, plutonic, and uplift history of a continent-island arc suture zone, west-central Idaho [abs.]: Geological Society of America, Abstracts with Programs, v. 16, no. 6, p.670–671.

Thurlow, J.G., and Swanson, E.A., 1981, Geology and ore deposits of the Buchans area, central Newfoundland, *in* Swanson, E.A., Strong, D.F., and Thurlow, J.G., eds., The Buchans Orebodies: Fifty Years of Geology and Mining: Geological Association of Canada, Special Paper 22, p. 113–142.

Vallier, T.L., 1967, Geology of part of the Snake River canyon and adjacent areas in northeastern Oregon and western Idaho: Corvallis, Oregon State University, Ph.D. dissertation, 267 p.

Vallier, T.L., 1974, A preliminary report of the geology of part of the Snake River canyon, Oregon and Idaho: Oregon Department of Geology and Mineral Industries, Geological Map Series, GMS-6, 1 map sheet, 15 p. of text, scale 1:125,000.

Vallier, T.L., 1977, The Permian and Triassic Seven Devils group, western Idaho and northeastern Oregon: U.S. Geological Survey Bulletin 1437, 58 p.

Vallier, T.L., and Brooks, H.C., 1970, Geology and copper deposits of the Homestead area, Oregon and Idaho: Ore Bin, v. 32, no. 3, p. 37–57.

Vallier, T.L., Brooks, H.C., and Thayer, T.P., 1977, Paleozoic rocks of eastern Oregon and western Idaho, *in* Stewart, J.H., Stevens, C.H., and Fritsche, A.E., eds., Paleozoic paleogeography of the Western United States (Pacific Coast Paleogeography Symposium 1): Los Angeles, Society of Economic Paleontologists and Mineralogists, Pacific Section, p. 455–465.

Vallier, T.L., White, D.L., White, J.D.L., Ash, S.R., Stanley, G.D., and Jones, David, 1987, Jurassic rocks in Hells Canyon, Oregon and Idaho: Volcanism, extension, and sedimentation in the Blue Mountains island arc [abs.]: Geological Society of America, Abstracts with Programs, v. 19, no. 5, p. 339–340.

Walker, N.W., 1983, Pre-Tertiary tectonic evolution of northeastern Oregon and west-central Idaho: Constraints based on U/Pb ages of zircons [abs.]: Geological Society of America, Abstracts with Programs, v. 15, no. 5, p. 371.

Walker, N.W., 1986, U/Pb geochronological and petrologic studies in the Blue Mountains terrane, northeastern Oregon and westernmost-central Idaho: Implications for pre-Tertiary tectonic evolution: Santa Barbara, University of California, Ph.D. dissertation, 214 p.

Walker, R.G., 1978, Deep-water sandstone facies and ancient submarine fans: models for exploration for stratigraphic traps: American Association of Petroleum Geologists Bulletin, v. 62, no. 6, p. 932–966.

Walshe, J.L., and Solomon, M., 1981, An investigation into the environment of formation of the volcanic-hosted Mt. Lyell copper deposits using geology, mineralogy, stable isotopes, and a six-component chlorite solid solution model: Economic Geology, v. 76, no. 2, p. 246–284.

Wilson, D., and Cox, A., 1980, Paleomagnetic evidence for tectonic rotation of Jurassic plutons in the Blue Mountains, eastern Oregon: Journal of Geophysical Research, v. 85, no. B7, p. 3681–3689.

Yui, Shunzo, and Ishitoya, Kimihide, 1983, Some textures of the ores from the Ezuri Kuroko deposits, Akita Prefecture, Japan, *in* Ohmoto, H., and Skinner, B.J., eds., The Kuroko and Related Volcanogenic Massive Sulfide Deposits: Economic Geology Monograph 5, p. 224–230.

Zierenberg, R.A., Koski, R.A., Shanks, W.C., and Rosenbauer, R.J., 1986, Form and composition of sediment-hosted sulfide-sulfate deposits, Escanaba Trough, southern Gorda Ridge: EOS (American Geophysical Union, Transactions), v. 67, no. 44, p. 1282.

9. THE ENVIRONMENTAL AND TECTONIC SIGNIFICANCE OF TWO COEVAL PERMIAN RADIOLARIAN-SPONGE ASSOCIATIONS IN EASTERN OREGON

By BENITA L. MURCHEY and DAVID L. JONES[1]

CONTENTS

ABSTRACT

Two Permian radiolarian-sponge spicule associations can be quantitatively distinguished in Permian chert and siliceous argillite of the structurally complex Paleozoic and Mesozoic accreted terranes of eastern Oregon. The two associations appear to be tectonically juxtaposed. In the Grindstone terrane (Grindstone-Twelvemile melange of Dickinson and Thayer, 1978), radiolarians belonging to the superfamily Ruzhencevispongacea outnumber radiolarians belonging to the superfamily Albaillellacea, and sponge spicules commonly make up more than 10 percent of the siliceous microfossil populations. In the Baker terrane (central melange of Dickinson and Thayer, 1978), albaillellacid radiolarians are more abundant than ruzhencevispongacid radiolarians, and sponge spicules make up less than 10 percent of the microfossil faunas. Coeval Leonardian, Guadalupian, and post(?)-Guadalupian chert and siliceous argillite are present in many other accreted terranes in the western Cordillera of North America. Permian faunas in the Grindstone terrane are quantitatively similar to those in the Golconda and Black Rock terranes of Nevada and the Eastern Klamath and Northern Sierra terranes of California. Permian faunas in the Baker terrane are quantitatively similar to those in the North Fork and Hayfork terranes of California and the San Juan and Hozameen terranes of Washington.

We present a depositional model for the paleoenvironments of the two associations. We consider the population compositions to be controlled by water depth and distance from a shallow-water platform. In our model, populations with abundant ruzhencevispongacid radiolarians and abundant sponge spicules (Grindstone terrane type) were deposited on or near topographic highs such as continental margins, subsided volcanic arcs, and subsided carbonate platforms; populations with abundant albaillellacid radiolarians but few sponge spicules (Baker terrane type) represent deeper or more open ocean assemblages. The model can be used to infer the original depositional setting of rocks within structurally complex areas such as eastern Oregon and can provide evidence for tectonic juxtaposition.

[1]Department of Geology, University of California at Berkeley, CA 94720

INTRODUCTION

The Blue Mountains province of eastern Oregon and western Idaho is a complex of Paleozoic and Mesozoic accreted terranes (Blome and others, 1986). Three Paleozoic terranes have been distinguished in eastern Oregon and have been characterized as "shelf, oceanic, and volcanic arc as distinguished by their probable original geologic settings" (Vallier and others, 1977). Shelf terrane rocks are essentially equivalent to the Grindstone-Twelvemile melange of Dickinson and Thayer (1978) and to the Grindstone lithotectonic terrane of Silberling and others (1987). The oceanic terrane is equivalent to the dismembered oceanic crust terrane of Brooks and Vallier (1978), to most of the central melange terrane of Dickinson and Thayer (1978), and to the Baker terrane of Silberling and others (1987). The volcanic-arc terrane includes the Wallowa terrane of Silberling and others (1987) (Wallowa Mountains-Seven Devils Mountains volcanic-arc terrane of Brooks and Vallier, 1978) and the Olds Ferry terrane of Silberling and others (1987) (Juniper Mountain-Cuddy Mountain volcanic-arc terrane of Brooks and Vallier, 1978). Herein, the terrane designations of Silberling and others (1987) are used. Two of the terranes, the Grindstone and the Baker (fig. 9.1), contain bedded chert and siliceous argillite with Permian radiolarian and sponge-spicule faunas.

No Permian siliceous microfossils have been recovered from either the Wallowa terrane or the Olds Ferry terrane, although rich Permian radiolarian and sponge faunas are present in the Wrangellia terrane of Alaska and British Columbia, a possible disjunct equivalent of the Wallowa terrane (Jones and others, 1977).

The Grindstone terrane is a disrupted assemblage of upper Paleozoic (Devonian to Lower Permian) limestone, sandstone, and conglomerate (Merriam and Berthiaume, 1943; Kleweno and Jeffords, 1962) and Lower Permian to Lower Triassic chert (Wardlaw and Jones, 1980; Blome and others, 1986). The Lower Permian (Leonardian) Coyote Butte Formation is a partly arkosic limestone that contains fusulinids similar to those in the Black Rock terrane (fig. 9.1) in Nevada and the Eastern Klamath terrane (fig. 9.1) in California (Wardlaw and others, 1982). The Grindstone terrane lacks thick volcaniclastic units characteristic of Upper Permian sequences (Nosoni and Dekkas Formations of Coogan (1960) and the basal part of the Pit Formation) in the Eastern Klamath terrane. The Permian bedded chert is apparently not in depositional contact with the Coyote Butte Formation or any other older unit.

The Baker terrane is a structurally complex, disrupted association of igneous ophiolitic rocks (ultramafic, mafic, plagiogranitic rocks, tuff, and pillow basalt, including the Canyon Mountain Complex); marine sedimentary rocks (Elkhorn Ridge Argillite, including radiolarian chert and argillite associated with pillow basalt and tuff, and shallow marine limestone blocks); and metasedimentary and metavolcanic rocks (Burnt River Schist including quartz phyllite, phyllitic quartzite, pelitic phyllite, metachert, marble, greenschist, and greenstone) (Gilluly, 1937; Dickinson and Thayer, 1978; Brooks and Vallier, 1978). The chert and argillite contain Permian and Triassic radiolarians (Blome and others, 1986), and the shallow-marine limestone pods contain Carboniferous and Permian conodonts, megafossils, and fusulinids (Vallier and others, 1977, Brooks and Vallier, 1978). Permian fusulinid faunas from the limestones have both Tethyan and North American affinities, although the two faunas are not found together. Rocks of the Baker terrane are structurally dismembered, and the original stratigraphic and geographic relations between the rocks are unknown.

Permian siliceous microfossil faunas in the Grindstone and Baker terranes have different population characteristics. We have attempted to find useful criteria for distinguishing the populations and to determine which population characteristics may be environmentally controlled.

All samples studied are from allochthonous terranes lying west of the belt of clastic rocks and shallow marine limestones that extends through central Nevada and marks the westernmost margin of autochthonous Permian rocks in the conterminous United States (Stevens, 1977). The paleogeographic relations of the allochthonous terranes with one another and with coeval autochthonous rocks on the continent are uncertain. Temporal, environmental, and paleobiogeographic correlations have been used with varying degrees of success for constructing tectonic and paleogeographic models. The quantitative comparison of siliceous microfossil faunas presented in this paper gives paleogeographers another comparative tool.

In the following discussion of the allochthonous Permian siliceous rocks in the western United States, we consider the units within the context of their lithotectonic terranes. Lithotectonic or tectonostratigraphic terranes are fault-bounded entities distinguished from adjacent rocks by a distinctive geologic history. Displacement of terranes from their sites of origin may be hundreds of kilometers or merely tens of kilometers (Jones and others, 1983). The samples in this study came from terranes shown in figure 9.1, which is based on the terrane map of Silberling and others (1987).

ACKNOWLEDGMENTS

We thank C.D. Blome for permitting us to examine his processed rock residues from the Grindstone and Baker terranes. We also thank D. Harwood, P. Irwin, N. Mortimer, L. Fraticelli, L. Henderson, J. Whetten, L. Tennyson, and L. Kanter for providing us with whole rock samples from various localities. David G. Howell, Howard C. Brooks, and Tracy L. Vallier kindly reviewed the manuscript.

RADIOLARIANS AND SPONGES: ENVIRONMENTAL CONTROLS

The principal fossil components of Permian siliceous fine-grained rocks in the western Cordillera, including eastern Oregon terranes, are radiolarians and siliceous sponge spicules. In modern oceans, accumulation of siliceous biogenic sediments reflects biologic fertility of surface waters coupled with dissolution of calcium carbonate at depth. Areas in which siliceous biogenic sediments are accumulating today include marginal basins and high-productivity zones along the equator and at high latitudes.

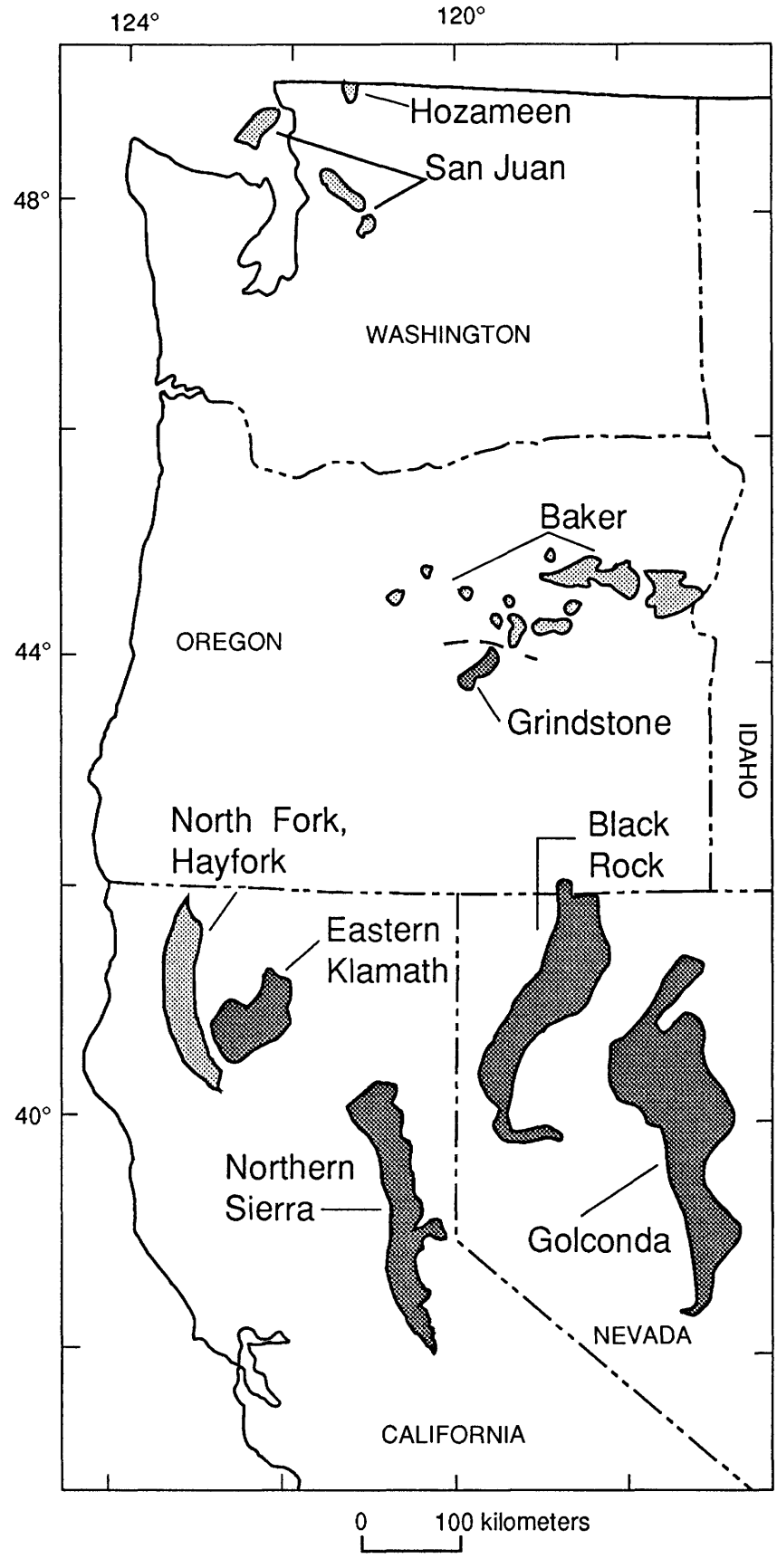

FIGURE 9.1.—Index map showing assignment of outcrops to lithotectonic terranes in eastern Oregon and surrounding states. Dashed line in Oregon denotes approximate boundary between Baker and Grindstone terranes. Dark gray pattern denotes presence of association A faunas within terrane. Light gray pattern denotes presence of association B faunas within terrane. See text for discussion.

Radiolarians are marine planktonic organisms found in all modern oceans. The polycystines are the only radiolarian group preserved in the fossil record because they secrete tests of biogenic opal. Radiolarians can live at all depths in the water column but are most abundant in the upper few hundred meters (Petrushevskaya, 1971). Radiolarians are rare in many marine deposits owing to dilution by large quantities of terrigenous material, although they may be abundant in surface waters above the depositional site (Kling, 1978). In marginal basins with low rates of terrigenous dilution and favorable chemical conditions, radiolarian-rich sediments can accumulate in water depths of less than 500 m. The composition of radiolarian assemblages in the modern oceans is largely controlled by water mass and circulation patterns. Some forms are particularly abundant in cold northern waters or in upwelling zones, whereas others are characteristic of equatorial waters (Casey, 1971; Petrushevskaya, 1971; Renz, 1976).

During Permian time, radiolarians were the most abundant test-forming microplankton. Planktonic foraminifers, diatoms, silicoflagellates, and calcareous nannoplankton did not appear in the fossil record until Mesozoic time. Permian radiolarian faunas in North America are preserved in calcareous or siliceous sedimentary rocks of marginal basins such as the Delaware Basin of Texas (Ormiston and Babcock, 1979) and in allochthonous siliceous strata accreted to the western margin of the continent. Prior to this study, no one had quantitatively compared Paleozoic radiolarian populations on a regional scale. However, Murchey and Jones (1983) noted a difference in diversity between Permian radiolarian faunas in northern (central and northern Alaska) and southern (southern Alaska and western conterminous United States) North America.

The distribution of living sponges is controlled by environmental conditions at the sediment-water interface. Their density on the sea-floor is limited by food and nutrient availability. Other parameters controlling density are substrate conditions, turbidity, and energy regime. Although some modern siliceous sponges can live at great depths, they are most abundant near topographic highs such as reefs (Rützler, 1978). In a living reef, such as the Belize barrier reef, sponges are more abundant and diverse in the deeper part of the inner forereef (spur and groove zones, 4 to 12 m) and on the outer forereef (12 to 60 m) than in the high-energy reef zones. In the Belize reef, sponge spicules are the primary component of particulate silica in reef and forereef sediments (Rützler and Macintyre, 1978). Sponge-spicule mats 2 m thick and more are reported from the nutrient-rich Ross Ice Shelf region of Antarctica (Koltun, 1968; Dayton and others, 1974). Significant sponge-spicule deposits are, however, much less common in modern seas than diatom or radiolarian oozes.

After a siliceous sponge dies, the spicules forming its internal skeleton generally dissociate. Density flows and bottom currents may transport and redeposit these spicules. Siliceous sponge spicules can become concentrated by differential dissolution rates between carbonate fossils and siliceous fossils, especially below the carbonate-compensation depth or in organic-rich sediments.

The original geographic relations between the depositional sites of Permian radiolarian- and sponge-bearing strata off the west coast of North America have been largely obscured by tectonic processes. The Delaware Basin in Texas, however, is an undisrupted Permian continental margin basin whose faunas contain both siliceous sponge spicules and radiolarians. Finks (1960) described two groups of sponge faunas in the Permian strata of the Delaware Basin. Shallow marine deposits of shelf, bank, and reef are dominated by calcareous sponges and also contain a subordinate number of siliceous sponges, whereas dark, bituminous basinal limestones contain only siliceous sponges, including abundant hexactinellids. In most strata, the sponges are present only as isolated spicules. Whole or partial sponge skeletons have been found in a few basinal localities where the rocks may represent distal reef talus and reef-flank facies. The siliceous hexactinellids and most of the siliceous demosponges (including lithistids) probably lived in quiet, deep water in well-aerated zones on reef flanks and basin floors. Throughout Paleozoic time, the siliceous demosponges and hexactinellids dominated quiet-water environments (Finks, 1970; Wiedenmayer, 1980). Radiolarians are associated with disaggregated sponge spicules in the thin-bedded basinal limestones of the Delaware Basin (Ormiston and Babcock, 1979).

METHODS

We compared population characteristics of Leonardian, Guadalupian, and post(?)-Guadalupian siliceous microfossil faunas from eastern Oregon (Grindstone and Baker terranes) with those from Nevada (Golconda and Black Rock terranes), California (Eastern Klamath, Northern Sierra, North Fork, and Hayfork terranes), and Washington (San Juan and Hozameen terranes). Permian radiolarian assemblages in eastern Oregon and elsewhere in the western Cordillera (Murchey, 1990; Murchey and Jones, 1992; Blome

and Reed, 1992) generally can be correlated with the zones of Ishiga (1986). Key radiolarian taxa in each sample (where present) are shown in table 9.1. Blome and others (1986) list taxa for individual samples from Oregon.

Siliceous rocks were etched with hydrofluoric acid using a modified version of the technique described by Pessagno and Newport (1972). The 63- to 180-micrometer-size fraction of residues from the third or fourth acid etching was used for population counts. The residue was strewn on a microfossil tray and each fossil lying along a line or lines was noted. Fifty to 100 radiolarians and sponge spicules were counted to determine the percentage of the two groups in the assemblage. When possible, the count was extended until 100 radiolarians were counted. The relative abundances of the following three radiolarian groups were determined:

(A) Albaillellacea (Deflandre, 1952)—Holdsworth and Jones (1980) and Ishiga (1986) have based their Paleozoic zonation schemes on this fossil group. Permian genera include *Pseudoalbaillella, Imotoella, Parafollicucullus, Follicucullus*, and *Neoalbaillella*.

(B) Ruzhencevispongacea (Kozur, 1980; following the usage of Kozur and Mostler, 1989)—Multirayed (stauraxon) radiolarians (Latentifistulidea of Nazarov and Ormiston, 1983) are very abundant in some Permian assemblages.

(C) Spheroidal spumellarians (mostly Entactinaria)—Spheroidal Permian radiolarians are currently less used for biostratigraphy than other forms, but are commonly the most abundant group of Permian radiolarians.

We used data from 67 samples in our comparisons. The U.S. Geological Survey radiolarian sample accession numbers for each sample in this study are listed in table 9.1 along with population count results and key radiolarian taxa. A locality map for the Oregon samples is included in Blome and others (1986). Locality data for most of the other samples were published in the following: Whetten and others (1978), Miller and others (1982), Irwin and others (1982), Stewart and others (1986), Murchey (1989), and Harwood and Murchey (1990). Twelve faunas in Oregon were counted (9 in the Grindstone terrane and 3 in the Baker terrane). Nineteen faunas in Nevada were counted (15 in the Golconda terrane and 4 in the Black Rock terrane). Sixteen faunas in California were counted (4 in the Eastern Klamath terrane, 23 in the North Fork or Hayfork terranes, and 3 in the Northern Sierra terrane). Six faunas in Washington were counted (3 in the Hozameen terrane and 3 in the San Juan terrane).

POPULATION COUNT RESULTS

The results from the population counts are given in table 9.1 and shown graphically in figures 9.2 and 9.3. The graphic representations on the triangular diagrams reveal two distinct faunal associations. In association A, sponge spicules are abundant (ranging from 3 percent to 100 percent, and they generally make up more than 10 percent of the population) and ruzhencevispongacid radiolarians are more abundant than the albaillellacids. Spheroidal radiolarians are particularly abundant in association A and make up more than 90 percent of the radiolarian populations in about half the samples. In association B, sponge spicules make up less than 10 percent of the faunas (most commonly less than 3 percent) and albaillellacid radiolarians are more abundant than ruzhencevispongacid forms. Spheroidal radiolarians are somewhat less abundant than in association A, and they make up more than 90 percent of the radiolarian populations in less than one third of the association B faunas.

GEOGRAPHIC DISTRIBUTION OF MICROFOSSIL ASSOCIATIONS

Faunal associations A and B appear to have distinct geographic distributions (fig. 9.1). Terranes having association A faunas, including the Golconda, Black Rock, Eastern Klamath, Northern Sierra, and Grindstone terranes, lie to the south and east of terranes having association B faunas, including the North Fork, Hayfork, San Juan, Hozameen, and Baker terranes.

TERRANES WITH ASSOCIATION A FAUNAS

Comparison of the terranes characterized by these two biofacies reveals other patterns. The southeastern terranes with association A populations have some common elements. Limestone is a significant component of each of these terranes, in addition to chert or siliceous argillite. Tuff and volcaniclastic rocks also form significant parts of the Eastern Klamath, Northern Sierra, and Black Rock terranes, but they are less common in the Grindstone terrane and rare in the Golconda terrane. Continent-derived clastic rocks form a large part of the Golconda terrane.

The Havallah sequence and related rocks in the Golconda terrane of central Nevada (fig. 9.1) is a structurally complex assemblage of deep marine sedimentary and igneous rocks spanning the Late Devonian to Permian (Stewart and others, 1977, 1986; Miller and others, 1982, 1984; Murchey, 1989, 1990). These

TABLE 9.1.—*Microfossil content of samples, in percent, from tectonostratigraphic terranes of the western Cordillera including the Grindstone and Baker terranes of eastern Oregon*

[Sample numbers are U.S. Geological Survey sample accession numbers; field numbers given in parentheses below sample numbers; <, less than; *data on fig. 9.2; ‡, data on fig. 9.3; -, not present or very rare]

Sample number	Collector	Sponge spicules	Radiolarian population			Key fossils
			Spheroidal	Albaillellacea	Ruzhencevi-spongacea	
Grindstone terrane						
4578* (82CB101A)	Blome ------	5	99	<1	<1	*Entactinia* sp.
4579* (82CB101B)	Blome ------	53	99	<1	<1	*Entactinia* sp.
4593*‡ (82CB105C)	Blome ------	4	80	6	14	*Deflandrella* sp.
4606*‡ (82CB108B)	Blome ------	25	96	1	3	*Albaillella levis*
4611*‡ (82CB109)	Blome ------	98	48	<1	52	*Hegleria* sp. [1]
4610*‡ (82CB109B)	Blome ------	60	83	1	16	*Deflandrella* sp.
4618* (82CB113)	Blome ------	86	99	<1	<1	*Entactinia* sp.
4592*‡ (82CB105B)	Blome ------	4	29	31	40	*Parafollicucullus fusiformis*, *P. globosus*
4622*‡ (82CB115)	Blome ------	22	92	<1	8	*Neoalbaillella* sp. aff. *N. grypus*
Baker terrane						
4602*‡ (82CB107A)	Blome ------	4	92	8	<1	*Follicucullus scholasticus*
4603*‡ (82CB107B)	Blome ------	<1	93	4	3	*Follicucullus scholasticus*, *F. ventricosus*
4706*‡ (82CB117)	Blome ------	0	97	3	<1	*Follicucullus scholasticus*, *F. ventricosus*
Golconda terrane						
O196* (77JN12)	Jones -------	1	99	<1	<1	*Follicucullus scholasticus*, *F. ventricosus*, and *Parafollicucullus fusiformis*
8437*‡ (82PM16y)	Murchey —	36	44	<1	56	*Pseudoalbaillella* sp.
8438* (82PM16x)	Murchey —	60	99	<1	<1	*Pseudoalbaillella* sp., *Hegleria* sp.
8439*‡ (82PM18)	Murchey —	52	92	<1	8	*Deflandrella* sp.
8440‡ (82PM19)	Murchey —	100	-	-	-	None
8441*‡ (82PM20)	Murchey —	95	96	<1	4	*Pseudoalbaillella scalprata*
8442 (82PM21)	Murchey —	100	-	-	-	None
4241*‡ (83MY177)	Murchey —	11	88	10	2	*Pseudoalbaillella* sp. aff., *P. scalprata*, and *Parafollicucullus globosus*

TABLE 9.1.—*Microfossil content of samples, in percent, from tectonostratigraphic terranes of the western Cordillera including the Grindstone and Baker terranes of eastern Oregon*—Continued

[Sample numbers are U.S. Geological Survey sample accession numbers; field numbers given in parentheses below sample numbers; <, less than; *data on fig. 9.2; ‡, data on fig. 9.3; -, not present or very rare]

Sample number	Collector	Sponge spicules	Radiolarian population			Key fossils
			Spheroidal	Albaillellacea	Ruzhencevi-spongacea	
Golconda terrane—Continued						
8443*‡ (83MY330)	Murchey —	50	94	1	5	*Deflandrella* sp.
8444*‡ (83MY342)	Murchey —	40	84	1	9	*Pseudoalbaillella scalprata*
8445*‡ (83MY352)	Murchey —	60	74	<1	26	*Pseudoalbaillella scalprata*
4233*‡ (83MY167b)	Murchey —	51	87	2	11	*Pseudoalbaillella scalprata*
4236‡ (83MY173)	Murchey —	100	-	-	-	None
4235*‡ (83MY171)	Murchey —	23	88	3	9	*Pseudoalbaillella* sp. aff. *P. globosa*
1884*‡ (LK61R)	Kanter -----	48	97	<1	3	*Pseudoalbaillella scalprata*
Black Rock terrane						
3559* (82MQR5)	Murchey —	1	99	1	<1	*Imotoella levis*
3558*‡ (82MQR4)	Murchey —	46	94	<1	6	*Hegleria* sp.
3557*‡ (82MQR3)	Murchey —	10	93	2	5	*Imotoella levis*
3555A*‡ (82MQR1A)	Murchey —	42	97	<1	3	*Hegleria* sp.
Northern Sierra terrane						
6652*‡ (GV854)	Harwood -	78	80	<1	20	*Pseudoalbaillella scalprata*
6654*‡ (GV8551A)	Harwood -	40	84	3	13	*Pseudoalbaillella scalprata*
6652*‡ (GV8549)	Harwood -	70	80	<1	20	*Pseudoalbaillella scalprata*
North Fork or Hayfork terrane						
3800*‡ (83MY089A)	Murchey —	40	62	12	26	*Pseudoalbaillella globosa*
3801*‡ (83MY089B)	Murchey —	6	55	37	8	*Pseudoalbaillella* sp.
3802*‡ (83MY090)	Murchey —	30	93	4	3	*Hegleria* sp., *Quinqueremis robusta*
3803*‡ (83MY091)	Murchey —	30	85	10	5	*Pseudoalbaillella* sp. aff. *P. scalprata*
3804*‡ (83MY092)	Murchey —	16	25	55	20	*Parafollicucullus globosus*, *Follicucullus monacanthus*

TABLE 9.1.—*Microfossil content of samples, in percent, from tectonostratigraphic terranes of the western Cordillera including the Grindstone and Baker terranes of eastern Oregon*—Continued

[Sample numbers are U.S. Geological Survey sample accession numbers; field numbers given in parentheses below sample numbers; <, less than; *data on fig. 9.2; ‡, data on fig. 9.3; -, not present or very rare]

Sample number	Collector	Sponge spicules	Radiolarian population			Key fossils
			Spheroidal	Albaillellacea	Ruzhencevi-spongacea	
North Fork or Hayfork terrane—Continued						
3806*‡ (83MY094X)	Murchey —	12	72	28	<1	*Follicucullus ventricosus*
3807*‡ (83MY095A)	Murchey —	6	59	37	4	*Follicucullus ventricosus, F. scholasticus*
3810*‡ (83MY097)	Murchey —	2	46	54	<1	*Follicucullus ventricosus , F. scholasticus*
3811*‡ (83MY098)	Murchey —	14	58	36	6	*Follicucullus ventricosus , F. monacanthus*
3814*‡ (83MY101)	Murchey —	4	82	10	8	*Follicucullus scholasticus*
3815*‡ (83MY102)	Murchey —	10	42	50	8	*Follicucullus scholasticus, F. ventricosus*
1733*‡ (I58-80)	Irwin -------	<1	98	2	<1	*Neoalbaillella* sp., *Imotoella levis*
1960*‡ (I94A-80)	Irwin -------	1	80	14	6	*Pseudoalbaillella fusiformis*
1250*‡ (I17A-80)	Irwin -------	<1	75	25	<1	*Follicucullus scholasticus*
2620*‡ (I26-81)	Irwin -------	<1	66	32	2	*Follicucullus scholasticus*
1744*‡ (I67B-80)	Irwin -------	2	88	10	2	*Neoalbaillella* sp., *Imotoella levis , Follicucullus ventricosus*
4880*‡ (NM504)	Mortimer –	<1	25	75	<1	*Follicucullus* sp.
4882*‡ (NM510)	Mortimer –	1	83	9	8	*Follicucullus scholasticus, F. ventricosus*
4886*‡ (NM512)	Mortimer –	<1	39	60	1	*Follicucullus* scholasticus, *F. ventricosus,*
4887*‡ (NM513)	Mortimer –	<1	68	42	<1	*Follicucullus scholasticus, Pseudoalbaillella* sp.
4889*‡ (NM515)	Mortimer –	1	73	26	1	*Follicucullus ventricosus*
4890*‡ (NM516)	Mortimer –	<1	40	56	4	*Follicucullus ventricosus*
4891* (NM517)	Mortimer –	<1	58	37	5	*Follicucullus scholasticus*

TABLE 9.1.—*Microfossil content of samples, in percent, from tectonostratigraphic terranes of the western Cordillera including the Grindstone and Baker terranes of eastern Oregon*—Continued

[Sample numbers are U.S. Geological Survey sample accession numbers; field numbers given in parentheses below sample numbers; <, less than; *data on fig. 9.2; ‡, data on fig. 9.3; -, not present or very rare]

Sample number	Collector	Sponge spicules	Radiolarian population			Key fossils
			Spheroidal	Albaillellacea	Ruzhencevi-spongacea	
Eastern Klamath terrane						
3868‡ (FR100)	Fraticelli -	100	-	-	-	latentifistulids
3871‡ (FR103)	Fraticelli -	100	-	-	-	latentifistulids
1281* (LH3)	Henderson	3	99	<1	1	latentifistulids
1282* (LH45)	Henderson	4	99	<1	<1	*Hegleria* sp.
San Juan terrane						
O499*‡ (W78-34)	Whetten —	9	67	29	4	*Parafollicucullus globosus*, Pa. aff. *P. fusiformis*
O136*‡ (W77-55h)	Whetten —	<1	80	20	<1	*Follicucullus* ventricusus
O136*‡ (W77-55i)	Whetten —	8	97	1	2	*Follicucullus* sp.
Hozameen terrane						
1435*‡ (T234a)	Tennyson -	2	97	3	<1	*Follicucullus scholasticus*, *F. ventricosus*
1436*‡ (T234b)	Tennyson -	1	20	67	13	*Follicucullus scholasticus*
1437*‡ (T234C)	Tennyson -	<1	51	45	4	*Follicucullus ventricosus*

[1] Only 25 radiolarians counted.

[2] Six percent total radiolarians belong to genus *Circulaforma*.

rocks include bedded chert, argillite, basalt, chert-pebble conglomerate, and silty limestone turbidites of the Havallah sequence (Silberling and Roberts, 1962). Most of our samples from the Golconda terrane were collected in the Willow Creek area near Antler Peak in the Galena Range (south of the town of Battle Mountain) where moderately well preserved radiolarian and sponge faunas are present in red, green, and purple siliceous argillite in the structurally lowest part of the Havallah sequence (Murchey, 1990). Radiolarians in these faunas are diverse and ruzhencevispongacid forms generally outnumber albaillellacids by a factor of three or more. Sponge spicules make up 10 to 100 percent of the microfossils in the siliceous argillite. The spicule faunas of the siliceous argillite are diverse and include hexactines, pentactines, paraclavules, hemidiscs, lithistid desmas, anadiaenes, anatriaenes, protriaenes, calthrops, and strongyles. Locally the argillite is interbedded with silicified sponge-spicule turbidites (dominantly large oxeas, strongyles, and rhax spicules) and sandstones. Farther west in the Antler Peak area and in Hoffman Canyon of the Tobin Range (south of Winnemucca), silty radiolarian- and sponge-bearing chert and argillite is intercalated with Permian silty and sandy limestone turbidites rich in sponge spicules (Stewart and others, 1986; Murchey, 1990). In the Hoffman Canyon lithologies, the sponge spicules are commonly current oriented and, along with silt

and conodonts, show vertical size grading. Both the sponge spicule-bearing chert turbidites of the Willow Creek area and the sponge-rich silty limestone turbidites of Hoffman Canyon have abundant deep-water trace fossils such as *Lophoctinium* (Roberts, 1964; Stewart and others, 1977). Permian chert and argillite of the Havallah sequence in the sampled areas probably formed along a continental margin because these lithologies are interbedded with continent-derived clastic rocks. The size and the tectonic setting of the basin in which the Havallah sequence was deposited have been debated. Most models postulate a basin (either small or large) lying between the continent and an east- or west-facing island arc (Burchfiel and Davis, 1972, 1975; Miller and others, 1984; Snyder and Bruekner, 1983; Speed, 1977).

The Black Rock terrane of northwestern Nevada and southeastern Oregon (fig. 9.1) (Silberling and others, 1987) includes upper Paleozoic to Middle Triassic oceanic basin and island-arc rocks that crop out in isolated localities. Also within this terrane are the pre-Tertiary rocks in the southwestern Bilk Creek Mountains, which lie east of Denio, Nev., and trend southeast, near Quinn River Crossing (Ketner and Wardlaw, 1981; Jones, 1990). Lithologic units in the Bilk Creek Mountains include Permian(?) chert arenite, Lower Permian volcanic rocks, intrusive rocks, graywacke, fossiliferous Lower Permian cherty limestone, fossiliferous Upper Permian dolomite, Upper Permian radiolarian-sponge-spicule chert, and Middle Triassic tuffaceous shale and tuff. Permian limestone in the Bilk Creek Mountains contains fusulinids and brachiopods reported to be similar to those of the McCloud Limestone of the Eastern Klamath terrane in California (Skinner and Wilde, 1965; Ketner and Wardlaw, 1981) and to those of the Coyote Butte Formation of the Grindstone terrane in Oregon (Ketner and Wardlaw, 1981; Wardlaw and others, 1982). Ketner and Wardlaw (1981) subdivided the Quinn River Crossing area into four structural blocks separated by thrust faults. In their uppermost structural block, approximately 10 m of gray and black bedded chert conformably overlies ferruginous dolomite containing Late Permian brachiopods. The chert unit contains thick (150 cm or more) resistant beds as well as thinner, argillaceous beds that may be tuffaceous. Siliceous microfossils include both radiolarians and abundant sponge spicules (as much as 46 percent of the total population). The radiolarian taxa have been listed by Jones (1990). Sponge spicules and silicified

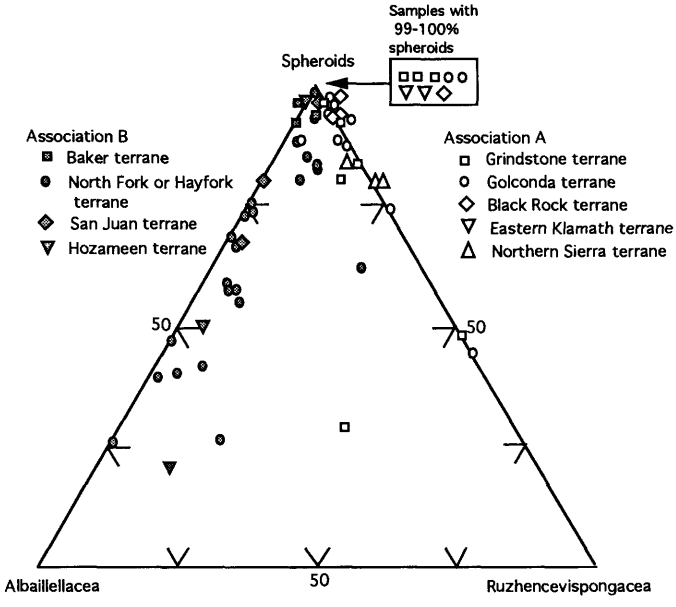

FIGURE 9.2.—Ternary diagram showing relative abundance of spheroidal, albaillellacid, and ruzhencevispongacid radiolarians in Permian faunas from ten tectonostratigraphic terranes in the western United States (63- to 180-micrometer size fraction of acid residue). Data points from terranes having predominantly association A faunas (abundant sponge spicules; high ratio of ruzhencevispongacids to albaillellacids) shown by open symbols. Data points from terranes having predominantly association B faunas (few sponge spicules, low ratio of ruzhencevispongacids to albaillellacids) shown by shaded symbols.

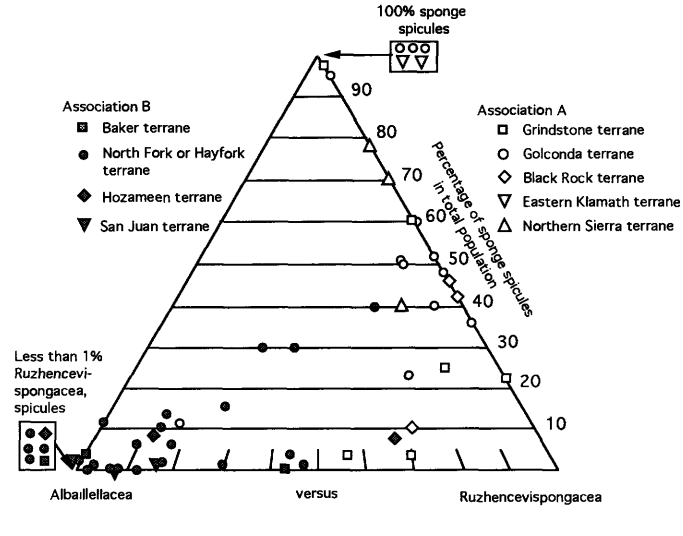

FIGURE 9.3.—Modified X-Y diagram showing ratio of ruzhencevispongacids to albaillellacids (horizontal axis) versus percentage of sponge spicules in total microfossil population (vertical axis) for Permian faunas from ten tectonostratigraphic terranes in the western United States (63- to 180- micrometer size fraction of acid residue). Data points from terranes having predominantly association A faunas (abundant sponge spicules; high ratio of ruzhencevispongacids to albaillellacids) shown by open symbols. Data points from terranes having predominantly association B faunas (few sponge spicules, low ratio of ruzhencevispongacids to albaillellacids) shown by shaded symbols.

brachiopod(?) spines are current oriented in the thick chert beds. Sponge spicules are dominantly monaxon and oxyhexactine. Ruzhencevispongacid radiolarians are generally more abundant than albaillellacids by a factor of three or more. Tuffaceous chert, shale, argillite, and sandstone, which contain late Early(?) and Middle Triassic pelecypods and ammonites (N.J. Silberling, 1979, oral commun. cited in Ketner and Wardlaw, 1981; N.J. Silberling, 1988, personal commun. cited in Jones, 1990), overlie the Permian chert. Assuming that the apparently conformable contact between Upper Permian dolomite and overlying Upper Permian chert is depositional, then the stratigraphic sequence in this structural unit may be interpreted as an arc-related succession deposited on a subsiding platform.

The Eastern Klamath terrane in northern California (fig. 9.1) consists of a homoclinal east-dipping sequence of Devonian to Middle Jurassic island-arc volcanic and intercalated sedimentary rocks. Permian rocks include the Wolfcampian to upper Leonardian McCloud Limestone (Skinner and Wilde, 1965), the Guadalupian Nosoni Formation (Skinner and Wilde, 1965), the Upper Permian Dekkas Formation (Coogan, 1960), and the Upper Permian and Triassic Pit Formation (Silberling and Jones, 1982). The shallow-water McCloud Limestone is the reference for fusulinids and corals of the eastern Klamath faunal province of Stevens (1977). Tuff breccia and conglomerate, volcaniclastic rocks, and scattered chert beds characterize the 270- to 1,850-m-thick Nosoni Formation (Skinner and Wilde, 1965). The overlying Dekkas is a thick (1,150 m) sequence of tuffaceous sedimentary rocks, andesitic tuff breccia, basalt, and minor amounts of chert, mudstone, and shale. A chert sample included in this study from the Dekkas contains large sponge spicules but no radiolarians. Elsewhere in the Dekkas, however, radiolarians are locally present (Noble and Renne, 1990). The basal beds of the Pit Formation are spiculitic chert that contains Permian radiolarians at outcrops on Nosoni Creek, a tributary to the Pit River (Silberling and Jones, 1982), and near Lake Shasta (approximately 15 km north of Redding). Radiolarian faunas, when present, contain spheroidal forms and a few ruzhencevispongacid forms but lack albaillellacids.

The Northern Sierra terrane in eastern California (fig. 9.1) is an isolated remnant of a late Paleozoic and Mesozoic arc and arc-related basins. Permian radiolarians and sponge spicules were recovered from the Reeve Formation in this terrane (Murchey and others, 1986; Harwood and Murchey, 1990). The Reeve Formation is primarily a volcanic and volcaniclastic rock unit that includes lenses of red siliceous argillite with siliceous microfossil faunas. Sponge spicules are abundant (40 to 78 percent of the total population) and include hexactines, birotules, anadiaenes, anatriaenes, strongyles, and oxeas. Ruzhencevispongacid radiolarians are more abundant than albaillellacids by a factor of four or more.

The Grindstone terrane of eastern Oregon (fig. 9.1) is similar in several respects to the other terranes characterized by the radiolarian-sponge faunas of association A. It is dominantly Paleozoic in age and contains a significant amount of Permian limestone. The Permian fusulinids in the Grindstone have been assigned to the same biogeographic province as those in the Eastern Klamath and Black Rock terranes. Finally, like the other terranes having faunas of association A, the Grindstone lacks the ophiolitic plutonic rocks characteristic of the northwestern terranes having faunas of association B. Diverse populations of sponge spicules make up 4 to 98 percent (median is 25 percent) of the total siliceous microfossils in the study samples. In radiolarian faunas with less than 99 percent spheroids, ruzhencevispongacids commonly outnumber albaillellacids by a factor of two or more.

TERRANES WITH ASSOCIATION B FAUNAS

The northwestern terranes with association B populations are primarily melange units characterized by blocks of metamorphic rocks, mafic and ultramafic igneous rocks, bedded chert, and minor amounts of limestone and marble (some of which have Tethyan-affinity fusulinids). Although these terranes contain some upper Paleozoic rocks, these rocks are subordinate to Mesozoic rocks.

In the Klamath Mountains of northern California, the east-dipping Trinity ultramafic sheet and the central metamorphic belt separate the Eastern Klamath terrane (association A populations) from the arcuate east-dipping terranes of the western Klamath belt (Irwin, 1977), including the North Fork, Hayfork, and Rattlesnake Creek terranes (Irwin, 1972). The North Fork and Hayfork terranes (fig. 9.1) have Permian chert with association B siliceous microfossil populations.

The western part of the North Fork terrane contains serpentinized ultramafic rocks, gabbro, diabase, basalt, and red chert (Irwin, 1977). Structurally higher rocks to the east include bedded chert, argillite, siliceous tuff, chert-pebble conglomerate, basalt, and minor amounts of upper Paleozoic limestone. Radiolarian faunas from the fine-grained sedimentary rocks in this terrane range in age from Permian (Leonardian) to Jurassic (Irwin and others, 1982). Permian siliceous assemblages in the North Fork terrane and presumed North Fork on strike to the north contain a

low ratio of sponge spicules to radiolarians (0 to 40 percent, but generally less than 10 percent, sponge spicules). The low-diversity sponge faunas contain small monaxons and a few oxyhexactines. Albaillellacid radiolarians are more abundant than ruzhencevispongacid forms in 21 of 22 samples. In some samples, albaillellacids are closely packed and current oriented.

The Hayfork terrane structurally underlies the North Fork terrane along an east-dipping fault. The western part of the terrane is a Middle Jurassic volcanic-arc unit (meta-andesite and volcaniclastic sedimentary rocks) whereas the eastern part consists of chert and argillite, sandstone, conglomerate, and limestone (including blocks with Tethyan-affinity fusulinids) (Irwin, 1977; Wright, 1982). Radiolarians range from Permian (one locality) to Jurassic, but most are Late Triassic in age (Irwin and others, 1982).

Two melange terranes in northeastern Washington, the San Juan and Hozameen terranes (fig. 9.1), contain Permian chert. The San Juan terrane consists of deformed chert and argillite as well as greenstone, metagraywacke, metaconglomerate, marble, and ultramafic rocks. The marble contains fusulinids with Tethyan affinities (Danner, 1977, p. 500). Chert in the Roche Harbor subterrane of Whetten and others (1978) ranges from Mississippian to Jurassic in age. Albaillellacids greatly outnumber ruzhencevispongacids in two of three samples and sponge spicules make up less than 10 percent of the total microfossils in all three samples.

The Hozameen terrane consists of structurally disrupted and metamorphosed chert of Permian to Jurassic age, argillite, basalt, minor amounts of carbonate rocks, and alpine-type ultramafic rocks (Tennyson and others, 1982). Permian albaillellacid radiolarians outnumber ruzhencevispongacids by a factor of five or more in the three study samples. Sponge spicules make up 2 percent or less of the microfossil fauna in the samples.

Like the other terranes with association B populations, the Baker terrane of eastern Oregon (fig. 9.1) is a melange with mafic and ultramafic igneous rocks, metamorphic rocks including blueschist and serpentinite, Permian and Triassic chert, and upper Paleozoic limestone (some with Tethyan-affinity fusulinids). Permian siliceous microfossil faunas from the Baker terrane contain abundant albaillellacids, mostly *Follicucullus* and *Ishigaconus* spp., and less than 5 percent sponge spicules.

The geologic processes that formed the melanges characterizing the northwestern terranes (those with association B faunas) destroyed the depositional relations between sedimentary units within these terranes. The presence of dismembered ophiolites, coupled with the absence of large volumes of carbonate rocks, continent-derived clastic rocks, or arc-related tuffs, flows, and volcaniclastic rocks, suggests that a marine environment far from any shallow platform was the most likely depositional site for the siliceous strata in these terranes.

CONCLUSIONS

The distribution pattern of the two faunal associations provides some clues as to the reasons for their differences. The association A populations occur in terranes that were once part of arcs, arc-related basins, and (or) continental margin basins, whereas association B populations occur in terranes that were once part of deep, open-ocean basins.

We interpret the abundant sponge spicules in association A as an indication of proximity to a platform or reef-slope environment. This view is consistent with the presently known distribution patterns of sponges. Abundant sponge spicules in sediments may also indicate high productivity and silica availability associated with upwelling along the eastern margins of the Pacific Ocean during Permian time (Murchey and Jones, 1992). The higher diversity of sponge spicules in association A populations as compared to those of association B indicates higher diversity of whole sponges at or near the depositional sites of association A populations.

The northwestern terranes (those with association B faunas) have a lower ratio of sponge spicules to radiolarians in Permian siliceous rocks than the southeastern terranes (those with association A faunas). In addition, sponge-spicule faunas in the northwestern terranes are less diverse and consist of smaller spicules than those in the southeastern terranes. Monaxon and oxyhexactine spicules are the only commonly found spicule types. There is no evidence for great turbidity, poorly oxygenated bottom waters, or other environmental conditions inimical to the growth of sponges in the sediments of the northwestern terranes. Therefore, we believe that the low sponge-spicule values indicate sedimentation in deep basins far from shallow topographic features from which abundant spicules could be redeposited, or seaward from a sediment trap such as a trench.

The explanations for the geographic differences in the abundances of ruzhencevispongacid radiolarians versus albaillellacid radiolarians are somewhat speculative. The association A radiolarian faunas, in addition to having a high ratio of ruzhencevispongacids to albaillellacids, are generally more diverse (in total numbers of species) than correlative association B

faunas. The composition of fossil radiolarian populations are controlled by their living distribution patterns, their preferential dissolution in the water column and, after burial, their diagenetic and metamorphic histories.

Sponge spicules are commonly more resistant to dissolution than radiolarians, and the solid-walled albaillellacids are probably more resistant to dissolution than the more delicate ruzhencevispongacids. If dissolution were the only parameter controlling the associations, then one would expect a direct correlation between sponge-spicule abundance and albaillellacid abundance rather than the inverse correlation that we actually find.

Siliceous microfossil faunas from the northwestern terranes (those with association B faunas) are generally more coarsely crystalline than those from the southeastern terranes (those with association A faunas) and this is probably a result of metamorphic history. However, the close packing and current orientation of the radiolarians in many of the northwestern terrane samples lead us to believe that the major regional differences in radiolarian populations were present before burial.

By process of elimination, the most probable explanation for the different ratios of ruzhencevispongacids to albaillellacids in the two microfossil associations is an environmentally controlled initial difference between the Permian radiolarian populations near arcs and continental margins and those in the open ocean. As with sponge-spicule abundance and diversity, high productivity and nutrient availability related to upwelling may be related to the high radiolarian diversity and the high ratio of ruzhencevispongacids to albaillellacids in association A faunas. Additionally, albaillellacids may tend to inhabit deeper water than the ruzhencevispongacids.

We have developed a depositional model for the distribution of faunal associations A and B (fig. 9.4). In this model there is a lateral faunal gradation from shallow-marine carbonate fossil assemblages to sponge-spicule faunas to association A to association B as the depositional site increases in depth, distance from platform, and distance from a high productivity zone. We propose that a similar vertical sequence is produced as a platform subsides.

That we often see sharp geographic and structural boundaries between faunal associations A and B rather than transitional zones may be a result of tectonic events. In our interpretation, accretionary processes juxtaposed siliceous microfossil faunas from platform-proximal continent- or arc-related environments (association A) with microfossil faunas from more platform-distal environments (association B).

The ability to determine paleoenvironments by quantitative comparisons of Permian radiolarian and sponge-spicule populations has direct practical applications in regions such as the Blue Mountains province of eastern Oregon and western Idaho where the original geographic relations between rock units have been obscured by tectonic processes. We interpret the two distinct Permian radiolarian-sponge associations in eastern Oregon as representing two different depositional environments. The association A faunas of the Grindstone terrane were deposited in a platform-proximal environment, probably adjacent to an island arc. Analogous Permian sequences are known in the Eastern Klamath, Northern Sierra, and Black Rock terranes. Such an interpretation is consistent with the lithologic association of chert and argillite of the Grindstone terrane with upper Paleozoic shallow marine carbonate and clastic rocks, an association that may be a sedimentary (olistostromal) melange (Blome and Nestell, 1991). The association B faunas of the Baker terrane were deposited in a deeper, platform-distal environment. The tectonic setting could have been on an oceanic plate. This interpretation is consistent with the association of chert and argillite with ophiolitic plutonic rocks and pillow basalt in the Baker terrane, although contacts there are tectonic.

Our analysis supports the interpretation of Morris and Wardlaw (1986) that the sedimentary rocks of

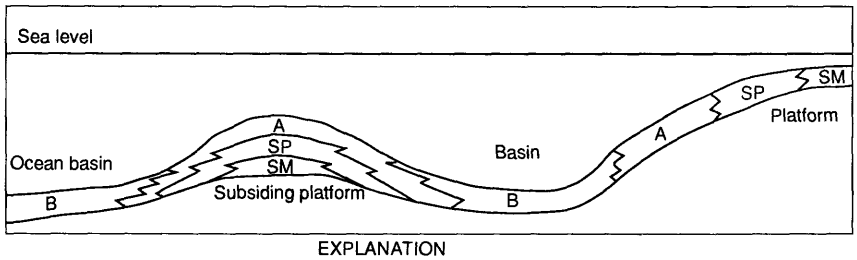

FIGURE 9.4.—Depositional model for distribution of radiolarians and siliceous sponge spicules in Permian rocks of the western United States. Radiolarians are present in faunal associations A and B. In association A faunas, ruzhencevispongacid radiolarians are more abundant than albaillellacid radiolarians and sponge spicules make up more than 10 percent of siliceous fossils. In association B faunas, albaillellacid radiolarians are more abundant than ruzhencevispongacid radiolarians and sponge spicules make up less than 10 percent of the siliceous fossils. See text for discussion of population count methods.

eastern Oregon can be generally divided into an arc-related assemblage associated with North American-affinity fusulinids and an oceanic assemblage associated with Tethyan-affinity fusulinids. In their analysis, primarily of carbonate rocks, these two assemblages are distributed across the boundary between the Baker and Grindstone terranes. In our study we did not find evidence that faunal associations A or B cross terrane boundaries in eastern Oregon, but further collection of data is encouraged.

REFERENCES CITED

Blome, C.D., Jones, D.L., Murchey, B.L., and Lienecki, M., 1986, Geologic implications of radiolarian-bearing Paleozoic and Mesozoic rocks from the Blue Mountain province, eastern Oregon, *in* Vallier, T.L., and Brooks, H.C., eds., Geology of the Blue Mountains region of Oregon, Idaho, and Washington: Geologic implications of Paleozoic and Mesozoic Paleontology and Biostratigraphy, Blue Mountains province, Oregon and Idaho: U.S. Geological Survey Professional Paper 1435, p. 79–93.

Blome, C.D., and Nestell, M.K., 1991, Evolution of a Permo-Triassic sedimentary melange, Grindstone terrane, east-central Oregon: Geological Society of America Bulletin, v. 103, no. 10, p. 1280–1296.

Blome, C.D., and Reed, K.M., 1992, Permian and Early(?) Triassic radiolarian faunas from the Grindstone terrane, Central Oregon: Journal of Paleontology, v. 66, no. 3, p. 351–383.

Brooks, H.C., and Vallier, T.L., 1978, Mesozoic rocks and tectonic evolution of eastern Oregon and western Idaho, *in* Howell, D.G., and McDougall, K.A., eds., Mesozoic paleogeography of the Western United States (Pacific Coast Paleogeography Symposium 2): Los Angeles, Society of Economic Paleontologists and Mineralogists, Pacific Section, p. 133–146.

Burchfiel, B.D., and Davis, G.A., 1972, Structural framework and evolution of the southern part of the Cordilleran orogen, Western United States: American Journal of Science, v. 272, no. 2, p. 97–118.

———1975, Nature and controls of Cordilleran orogenesis, Western United States: Extensions of an earlier synthesis: American Journal of Science, v. 275A, p. 363–396.

Casey, R.E., 1971, Radiolarians as indicators of past and present water masses, *in* Funnell, B.M., and Riedel, W.R., eds., The Micropaleontology of Oceans: London, Cambridge University Press, p. 331–341.

Coogan, A.H., 1960, Stratigraphy and paleontology of the Permian Nosoni and Dekkas Formations (Bollibokka Group): University of California Publications, Department of Geological Science Bulletin, v. 36, p. 243–316.

Danner, W.R., 1977, Paleozoic rocks of northwestern Washington and adjacent parts of British Columbia, *in* Stewart, J.H., Stevens, C.H., and Fritsche, A.E., eds., Paleozoic paleogeography of the Western United States (Pacific Coast Paleogeography Symposium 1): Los Angeles, Society of Economic Paleontologists and Mineralogists, Pacific Section, p. 481–502.

Dayton, P.K., Robilliard, G.A., Paine, R.T., and Dayton, B., 1974, Biological accommodation in the benthic community at McMurdo Sound, Antarctica: Ecological Monographs 44, p. 105–128.

Deflandre, Georges, 1952, *Albaillella* nov. gen., Radiolaire fossile du Carbonifere inferieur, type d'une lignee aberrante eteinte: Academie des Sciences Comptes Rendus, Paris, v. 234, p. 872–874.

Dickinson, W.R., and Thayer, T.P., 1978, Paleogeographic and paleotectonic implications of Mesozoic stratigraphy and structure in the John Day Inlier of central Oregon, *in* Howell, D.G., and McDougall, K.A., eds., Mesozoic paleogeography of the Western United States (Pacific Coast Paleogeography Symposium 2): Los Angeles, Society of Economic Paleontologists and Mineralogists, Pacific Section, p. 147–162.

Diller, J.S., 1908, Geology of the Taylorsville region, California: U.S. Geological Survey Bulletin 353, 128 p.

Finks, R.M., 1960, Late Paleozoic sponge faunas of the Texas region, *in* The siliceous sponges: American Museum of Natural History Bulletin 120, art. 1, 160 p.

———1970, The evolution and ecologic history of sponges during Paleozoic times, *in* Fry, W.G., ed., The biology of the Porifera: Symposia Zoological Society of London, No. 25, Academic Press, London, p. 3–22.

Gilluly, James, 1937, Geology and mineral resources of the Baker quadrangle, Oregon: U.S. Geological Survey Bulletin 879, 119 p.

Harwood, D.S., and Murchey, B.L., 1990, Biostratigraphic, tectonic, and paleogeographic ties between upper Paleozoic volcanic basinal rocks in the Northern Sierra terrane, California and the Havallah sequence, Nevada, *in* Harwood, D.S., and Miller, M.M., eds., Paleozoic and Early Mesozoic Paleogeographic Relations: Sierra Nevada, Klamath Mountains, and Related Terranes: Geological Society of America Special Paper 255, p. 157–217.

Holdsworth, B.K., 1969, Namurian Radiolaria of the genus *Ceratoikiscum* from Staffordshire and Derbyshire, England: Micropaleontology, v. 15, no. 2, p. 221–229.

Holdsworth, B.K., and Jones, D.L., 1980, Preliminary radiolarian zonation for Late Devonian through Permian time: Geology, v. 8, no. 6, p. 281–285.

Irwin, W.P., 1972, Terranes of the western Paleozoic and Triassic belt in the southern Klamath Mountains, California: U.S. Geological Survey Professional Paper 800-C, p. C103–C111.

———1977, Review of Paleozoic rocks of the Klamath Mountains, *in* Stewart, J.H., Stevens, C.H., and Fritsche, A.E., eds., Paleozoic paleogeography of the Western United States (Pacific Coast Paleogeography Symposium 1): Los Angeles, Society of Economic Paleontologists and Mineralogists, Pacific Section, p. 441–454.

Irwin, W.P., Jones, D.L., and Blome, C.D., 1982, Map showing sampled radiolarian localities in the western Paleozoic and Triassic belt, Klamath Mountains, California: U.S. Geological Survey Miscellaneous Field Studies Map MF-1399, scale 1:250,000.

Ishiga, Hiroaki, 1986, Late Carboniferous and Permian radiolarian biostratigraphy of southwest Japan: Journal of Geosciences, Osaka City University, v. 29, p. 89–100.

Jones, A.E., 1990, Geology and tectonic significance of terranes near Quinn River Crossing, Nevada, *in* Harwood, D.S., and Miller, M.M., eds., Paleozoic and Early Mesozoic Paleogeographic Relations: Sierra Nevada, Klamath Mountains, and related terranes: Geological Society of America Special Paper 255, p. 239–254.

Jones, D.L., Howell, D.G., Coney, P.J., and Monger, J.W.H., 1983, Recognition, character, and analysis of tectonostratigraphic terranes in western North America, *in* Hashimoto, M., and Uyeda, S., eds., Accretion Tectonics in the circum-Pacific Regions: Tokyo, Terra Scientific, p. 21–35.

Jones, D.L., Silberling, N.J., and Hillhouse, J., 1977, Wrangellia—A displaced terrane in northwestern North America: Canadian Journal of Earth Science, v. 14, no. 11, p. 2565–2577.

Ketner, K.B., and Wardlaw, B.R., 1981, Permian and Triassic rocks near Quinn River Crossing, Humboldt County, Nevada: Geology, v. 9, no. 3, p. 123–126.

Kleweno, W.P., Jr., and Jeffords, R.M., 1962, Devonian rocks in the Suplee area of central Oregon: Geological Society of America Special Paper 68, p. 34.

Kling, S.A., 1978, Radiolaria, *in* Haq, B.U., and Boersma, A., eds., Introduction to Marine Micropaleontology: New York, Elsevier, p. 203–244.

Koltun, V.M., 1968, Spicules of sponges as an element of the bottom sediments of the Antarctic, *in* Symposium on Antarctic Oceanography, Santiago, Chile, 1966, Proceedings: Cambridge, Scott Polar Research Institute, p. 121–123.

Kozur, Heinz, 1980, Ruzhencevispongidae, eine neue Spumellaria-Familie aus dem oberen Kungurian (Leonardian) und Sakmarian des Vorurals: Geologisch-Palaontologische Mitteilungen Innsbruck, v. 10, no. 4, p. 235–242.

Kozur, Heinz, and Mostler, Helfried, 1989, Radiolarien un Schwammskleren aus dem Unterperm des Vorurals: Geologisch-Palaontologische Mitteilungen Innsbruck, Sonderband 2, p. 147–275.

McMath, V.E., 1958, The geology of the Taylorsville area, Plumas County, California: Los Angeles, University of California, Ph.D. dissertation, 199 p.

———1966, Geology of the Taylorsville area, northern Sierra Nevada, *in* Geology of northern California: California Division of Mines and Geology Bulletin 190, p. 173–183.

Merriam, C.W., and Berthiaume, S.A., 1943, Late Paleozoic formations of central Oregon: Geological Society of America Bulletin, v. 54, no. 2, p. 145–171.

Miller, E.L., Kanter, L.R., LaRue, D.K., Turner, R.J., Murchey, B.L., and Jones, D.L., 1982, Structural fabric of the Paleozoic Golconda allochthon, Antler Peak quadrangle, Nevada: Progressive deformation of an oceanic sedimentary assemblage: Journal of Geophysical Research, v. 87, no. B5, p. 3795–3804.

Miller, E.L., Holdsworth, B.K., Whiteford, W.B., and Rodgers, D., 1984, Stratigraphy and structure of the Schoonover sequence, northeastern Nevada: Implications for Paleozoic plate-margin tectonics: Geological Society of America Bulletin, v. 95, no. 9, p. 1063–1076.

Morris, E.M., and Wardlaw, B.R., 1986, Conodont ages for limestones of eastern Oregon and their implication for pre-Tertiary melange terranes, *in* Vallier, T.L., and Brooks, H.C., eds., Geology of the Blue Mountains region of Oregon, Idaho, and Washington: Geologic Implications of Paleozoic and Mesozoic Paleontology and Biostratigraphy, Blue Mountains province, Oregon and Idaho: U.S. Geological Survey Professional Paper 1435, p. 59–63.

Murchey, B.L., 1989, Late Paleozoic siliceous basins of the western Cordillera of North America (Nevada, California, Mexico, and Alaska): Three studies using radiolarians and sponge spicules for biostratigraphic, paleobathymetric, and tectonic analyses: Santa Cruz, University of California, Ph.D. dissertation, 189 p.

Murchey, B.L., 1990, Age and depositional setting of siliceous sediments in the upper Paleozoic Havallah sequence near Battle Mountain, Nevada: Implications for the paleogeography and structural evolution of the western margin of North America, *in* Harwood, D.S., and Miller, M.M., eds., Paleozoic and Early Mesozoic paleogeographic relations: Sierra Nevada, Klamath Mountains, and related terranes: Geological Society of America Special Paper 255, p. 137–155.

Murchey, B.L., and Jones, D.L, 1983, Tectonic and paleobiologic significance of Permian radiolarian distribution in Circum-Pacific region [abs.]: American Association of Petroleum Geologists Bulletin, v. 67, no. 3, p. 522.

———1992, A mid-Permian chert event: widespread deposition of biogenic siliceous sediments in coastal, island arc and oceanic basins. Palaeogeography, Palaeoclimatology, Palaeoecology, v. 96, p. 161–174.

Murchey, B.L., Harwood, D.S., and Jones, D.L., 1986, Correlative chert sequences from the northern Sierra Nevada and Havallah sequence, Nevada [abs.]: Geological Society of America, Pacific Section, Abstracts with Programs, v. 18, p. 162.

Nazarov, B.B., and Ormiston, A.R., 1983, A new superfamily of stauraxon polycystine Radiolaria from the late Paleozoic of the Soviet Union and North America: Senckenbergiana Lethaea, v. 64, 363–379, 1 pl.

Noble, Paula, and Renne, P.R., 1990, Paleoenvironmental and biostratigraphic significance of siliceous microfossils from Permo-Triassic rocks of the Redding section, eastern Klamath Mountains, California: Marine Micropaleontology, v. 15, p. 379–391.

Ormiston, A.R., and Babcock, L.C., 1979, *Follicucullus*, new radiolarian genus from the Guadalupian Lamar Limestone of the Delaware Basin: Journal of Paleontology, v. 53, no. 2, p. 328–334.

Pessagno, E.A., Jr., and Newport, R.L., 1972, A technique for extracting Radiolaria from radiolarian cherts: Micropaleontology, v. 18, no. 2, p. 231–324.

Petrushevskaya, M.G., 1971, Spumellarian and nassellarian Radiolaria in the plankton and bottom sediments of the Central Pacific, *in* Funnell, B.M., and Riedel, W.R., eds., The Micropaleontology of Oceans: London, Cambridge University Press, p. 309–317.

Renz, G.W., 1976, The distribution and ecology of Radiolaria in the Central Pacific plankton and surface sediments: Scripps Institute of Oceanography Bulletin, v. 22, p. 267 p.

Roberts, R.J., 1964, Stratigraphy and structure of the Antler Peak quadrangle, Humboldt and Lander Counties, Nevada: U.S. Geological Survey Professional Paper 459-A, p A1–A93.

Rützler, Klaus, 1978, Sponges in coral reefs, *in* Stoddart, D.R. and Johannes, R.E., eds., Coral Reefs: Research Methods: Paris, United Nations Educational, Scientific, and Cultural Organization, p. 299–313.

Rützler, Klaus, and Macintyre, I.G., 1978, Siliceous sponge spicules in coral reef sediments: Marine Biology, v. 49, no. 2, p. 147–159.

Silberling, N.J., and Roberts, R.J., 1962, Pre-Tertiary stratigraphy and structure of northwestern Nevada: Geological Society America Special Paper 72, 58 p.

Silberling, N.J., and Jones, D.L., 1982, Tectonic significance of Permian-Triassic strata in northwestern Nevada and northern California [abs.]: Geological Society of America, Abstracts with Programs, v. 14, p. 234.

Silberling, N.J., Jones, D.L., Blake, M.C., and Howell, D.G., 1987, Lithotectonic terrane map of the western conterminous United States: U.S. Geological Survey Miscellaneous Field Studies Map MF-1874-C, scale 1:2,500,000.

Skinner, J.W., and Wilde, G.L., 1965, Permian biostratigraphy and fusulinid faunas of the Shasta Lake area, northern California: University of Kansas Paleontological Contributions, Protozoa, art. 6, 98 p.

Snyder, W.S., and Bruekner, H.K., 1983, Tectonic evolution of the Golconda allochthon, Nevada: problems and perspectives, *in* Stevens, C.H., ed., Pre-Jurassic rocks in western North America suspect terranes: Society of Economic Paleontologists and Mineralogists, Pacific Section, p. 103–123.

Speed, R.G., 1977, An appraisal of the Pablo Formation of presumed late Paleozoic age, central Nevada, *in* Stewart, J.H., Stevens, C.H., and Fritsche, A.E., eds., Paleozoic paleogeography of the Western United States (Pacific Coast Paleogeography Symposium 1): Los Angeles, Society of Economic Paleontologists and Mineralogists, Pacific Section, p. 315–324.

Stevens, C.H., 1977, Permian depositional provinces and tectonics, western United States, *in* Stewart, J.H., Stevens, C.H., and

Fritsche, A.E., eds., Paleozoic paleogeography of the Western United States (Pacific Coast Paleogeography Symposium 1): Los Angeles, Society of Economic Paleontologists and Mineralogists, Pacific Section, p. 113–135.

Stewart, J.H., MacMillan, J.R., Nichols, K.M., Stevens, C.H., 1977, Deep-water Upper Paleozoic rocks in north-central Nevada—A study of the type area of the Havallah Formation, *in* Stewart, J.H., Stevens, C.H., and Fritsche, A.E., Paleozoic paleogeography of the Western United States (Pacific Coast Paleogeography Symposium 1): Los Angeles, Society of Economic and Paleontologists and Mineralogists, Pacific Section, p. 337–348.

Stewart, J.H., Murchey, B.L., Jones, D.L., and Wardlaw, B.R., 1986, Paleontologic evidence for complex interlayering of Mississippian to Permian deep-water rocks of the Golconda allochthon in Tobin Range, north-central Nevada: Geological Society of America Bulletin, v. 97, no. 9, p. 1122–1132.

Tennyson, M.E., Jones, D.L., and Murchey, B.L., 1982, Age and nature of chert and mafic rocks of the Hozameen Group, North Cascade Range, Washington [abs.]: Geological Society of America Abstracts with Programs, v. 14, p. 239.

Vallier, T.L., Brooks, H.C., and Thayer, T.P., 1977, Paleozoic rocks of eastern Oregon and western Idaho, *in* Stewart, J.H., Stevens, C.H., and Fritsche, A.E., eds., Paleozoic paleogeography of the western United States (Pacific Coast Paleogeography Symposium 1): Los Angeles, Society of Economic Paleontologists and Mineralogists, Pacific Section, p. 455–466.

Wardlaw, B.R., and Jones, D.L., 1980, Triassic conodonts from eugeosynclinal rocks of western North America and their tectonic significance: Revista Italiana di Paleontologia e Stratigrafica, v. 85, p. 895–908.

Wardlaw, B.R., Nestell, M.K., and Dutro, J.T., Jr., 1982, Biostratigraphy and structural setting of the Permian Coyote Butte Formation of central Oregon: Geology, v. 10, no. 1, p. 13–16.

Whetten, J.T., Jones, D.L., Cowan, D.S., and Zartman, R.E, 1978, Ages of Mesozoic terranes in the San Juan Islands, Washington, *in* Howell, D.G., and McDougall, K.A., eds., Mesozoic paleogeography of the Western United States (Pacific Coast Paleogeography Symposium 2): Los Angeles, Society of Economic Paleontologists and Mineralogists, Pacific Section, p. 117–132.

Wiedenmayer, Felix, 1980, Ecology of siliceous sponges, *in* Hartman, W.D., Wendt, J.W., and Wiedenmayer, Felix, eds., Living and fossil sponges, Notes for a short course: Sedimenta, v. 8, p. 113–168.

Wright, J.E., 1982, Permo-Triassic accretionary subduction complex, southwestern Klamath Mountains, northern California: Journal of Geophysical Research, v. 87, no. B-5, p. 3805–3818.

☆ U.S. GOVERNMENT PRINTING OFFICE: 1993–583–048/80006

SELECTED SERIES OF U.S. GEOLOGICAL SURVEY PUBLICATIONS

Periodicals

Earthquakes & Volcanoes (issued bimonthly).
Preliminary Determination of Epicenters (issued monthly).

Technical Books and Reports

Professional Papers are mainly comprehensive scientific reports of wide and lasting interest and importance to professional scientists and engineers. Included are reports on the results of resource studies and of topographic, hydrologic, and geologic investigations. They also include collections of related papers addressing different aspects of a single scientific topic.

Bulletins contain significant data and interpretations that are of lasting scientific interest but are generally more limited in scope or geographic coverage than Professional Papers. They include the results of resource studies and of geologic and topographic investigations, as well as collections of short papers related to a specific topic.

Water-Supply Papers are comprehensive reports that present significant interpretive results of hydrologic investigations of wide interest to professional geologists, hydrologists, and engineers. The series covers investigations in all phases of hydrology, including hydrogeology, availability of water, quality of water, and use of water.

Circulars present administrative information or important scientific information of wide popular interest in a format designed for distribution at no cost to the public. Information is usually of short-term interest.

Water-Resource Investigations Reports are papers of an interpretive nature made available to the public outside the formal USGS publications series. Copies are reproduced on request unlike formal USGS publications, and they are also available for public inspection at depositories indicated in USGS catalogs.

Open-File Reports include unpublished manuscript reports, maps, and other material that are made available for public consultation at depositories. They are a nonpermanent form of publication that may be cited in other publications as sources of information.

Maps

Geologic Quadrangle Maps are multicolor geologic maps on topographic bases in 7 1/2- or 15-minute quadrangle formats (scales mainly 1:24,000 or 1:62,500) showing bedrock, surficial, or engineering geology. Maps generally include brief texts; some maps include structure and columnar sections only.

Geophysical Investigations Maps are on topographic or planimetric bases at various scales; they show results of surveys using geophysical techniques, such as gravity, magnetic, seismic, or radioactivity, which reflect subsurface structures that are of economic or geologic significance. Many maps include correlations with the geology.

Miscellaneous Investigations Series Maps are on planimetric or topographic bases of regular and irregular areas at various scales; they present a wide variety of format and subject matter. The series also includes 7 1/2-minute quadrangle photogeologic maps on planimetric bases that show geology as interpreted from aerial photographs. Series also includes maps of Mars and the Moon.

Coal Investigations Maps are geologic maps on topographic or planimetric bases at various scales showing bedrock or surficial geology, stratigraphy, and structural relations in certain coal-resource areas.

Oil and Gas Investigations Charts show stratigraphic information for certain oil and gas fields and other areas having petroleum potential.

Miscellaneous Field Studies Maps are multicolor or black-and-white maps on topographic or planimetric bases on quadrangle or irregular areas at various scales. Pre-1971 maps show bedrock geology in relation to specific mining or mineral-deposit problems; post-1971 maps are primarily black-and-white maps on various subjects, such as environmental studies or wilderness mineral investigations.

Hydrologic Investigations Atlases are multicolor or black-and-white maps on topographic or planimetric bases presenting a wide range of geohydrologic data of both regular and irregular areas; principal scale is 1:24,000, and regional studies are at 1:250,000 scale or smaller.

Catalogs

Permanent catalogs, as well as some others, giving comprehensive listings of U.S. Geological Survey publications are available under the conditions indicated below from the U.S. Geological Survey, Books and Open-File Reports Sales, Federal Center, Box 25286, Denver, CO 80225. (See latest Price and Availability List.)

"Publications of the Geological Survey, 1879-1961" may be purchased by mail and over the counter in paperback book form and as a set of microfiche.

"Publications of the Geological Survey, 1962-1970" may be purchased by mail and over the counter in paperback book form and as a set of microfiche.

"Publications of the Geological Survey, 1971-1981" may be purchased by mail and over the counter in paperback book form (two volumes, publications listing and index) and as a set of microfiche.

Supplements for 1982, 1983, 1984, 1985, 1986, and for subsequent years since the last permanent catalog may be purchased by mail and over the counter in paperback book form.

State catalogs, "List of U.S. Geological Survey Geologic and Water-Supply Reports and Maps For (State)," may be purchased by mail and over the counter in paperback booklet form only.

"Price and Availability List of U.S. Geological Survey Publications," issued annually, is available free of charge in paperback booklet form only.

Selected copies of a monthly catalog "New Publications of the U.S. Geological Survey" are available free of charge by mail or may be obtained over the counter in paperback booklet form only. Those wishing a free subscription to the monthly catalog "New Publications of the U.S. Geological Survey" should write to the U.S. Geological Survey, 582 National Center, Reston, VA 22092.

Note.—Prices of Government publications listed in older catalogs, announcements, and publications may be incorrect. Therefore, the prices charged may differ from the prices in catalogs, announcements, and publications.


U.S. DEPARTMENT OF THE INTERIOR
MARCH 3, 1849